Bruno Yaron · Ishai Dror
Brian Berkowitz

# Soil-Subsurface Change

## Chemical Pollutant Impacts

Soil-Subsurface Change

Bruno Yaron · Ishai Dror · Brian Berkowitz

# Soil-Subsurface Change

## Chemical Pollutant Impacts

🦄 Springer

Bruno Yaron
Ishai Dror
Brian Berkowitz
Weizmann Institute of Science
Department of Environmental Sciences
and Energy Research
Rehovot
Israel
ybyaron@gmail.com
ishai.dror@weizmann.ac.il
brian.berkowitz@weizmann.ac.il

*To our parents,*
                 *Leontine (z"l) and Iosef (z"l),*
                 *Tamar and David,*
                 *Sheila (z"l) and Norbert (z"l)*
*. . .with our eternal love and respect.*

# Preface

The soil layer and the subsurface region below it are two interrelated natural bodies that comprise the earth's upper layer from land surface to aquifers. In general, it is considered that the structure and properties of the soil–subsurface system are the result of natural processes occurring over geological timescales, formed as a result of rock weathering under various climatic and biotic regimes. Despite the fact that the soil–subsurface has in many cases been affected by human impact, anthropogenic factors in defining the actual matrix and properties of the soil–subsurface system have been largely neglected.

More specifically, in modern society, the natural soil–subsurface system has been exposed to considerable amounts of chemical contaminants, added both intentionally and by accident. The fate of chemical contaminants in the soil–subsurface system has been the subject of an enormous number of experimental studies, designed to quantify their retention, transport, and persistence. The reversibility of chemical interactions between contaminants and the soil–subsurface system has been studied frequently, and in a variety of cases, irreversible pollutant retention has been reported. However, the effect of chemical pollutants on the soil–subsurface matrix and properties has been essentially neglected.

In this book, we draw attention to a new perspective, namely irreversible changes in the pristine soil–subsurface system following chemical pollution. By integrating the results available in the literature, reporting on various cases of interactions between chemical pollutants and soil, we observe that contaminants may lead to the formation of a new soil–subsurface regime characterized by a matrix and properties different than those of the pristine regime. In contrast to the geological timescales controlling natural changes of the matrix and properties of the soil–subsurface system, the timescale associated with chemical pollutant induced changes is far shorter and extends over a "human lifetime scale". The many examples resembled in the present book confirm that chemical contamination should be considered as an additional factor in the formation of a contemporary soil–subsurface regime with a different matrix and properties than those of the pristine system.

After an introductory part (Chaps. 1–4), we describe irreversible contaminant induced changes in the matrix of isolated mineral and organic constituents that form the soil–subsurface system. For this purpose, we group the examples selected from the literature according to contaminant induced changes resulting from exchange (Chap. 5) and binding (Chap. 6) processes. However, contaminant effects on soil–subsurface properties are a result of changes occurring in natural bodies, where the various constituents are not isolated but appear together as organo-mineral complexes. Chapter 7 discusses contaminant induced changes occurring in chemical and physical characteristics of the soil–subsurface system, as well as in the fluid transmission properties of this system.

In support of our analysis, we relied on research findings presented in a large number of papers, selected from the vast number of available publications. Many other research results of equal value could have been used to illustrate contaminant induced changes to the soil–subsurface matrix and properties, showing that anthropogenic chemicals may become a factor in contemporary soil–subsurface metagenesis.

We hope that the present book, written for the use of soil scientists, hydrologists, and geochemists, will be helpful in shaping their approach to chemical induced changes in the soil–subsurface system. Our thesis on irreversible changes, and formation of a new, contemporary soil–subsurface regime following chemical disposal, should be considered in preventing, controlling, and developing new technologies for a sustainable soil–subsurface system exploitation and management.

Rehovot, Israel                                         Bruno Yaron, Ishai Dror, Brian Berkowitz
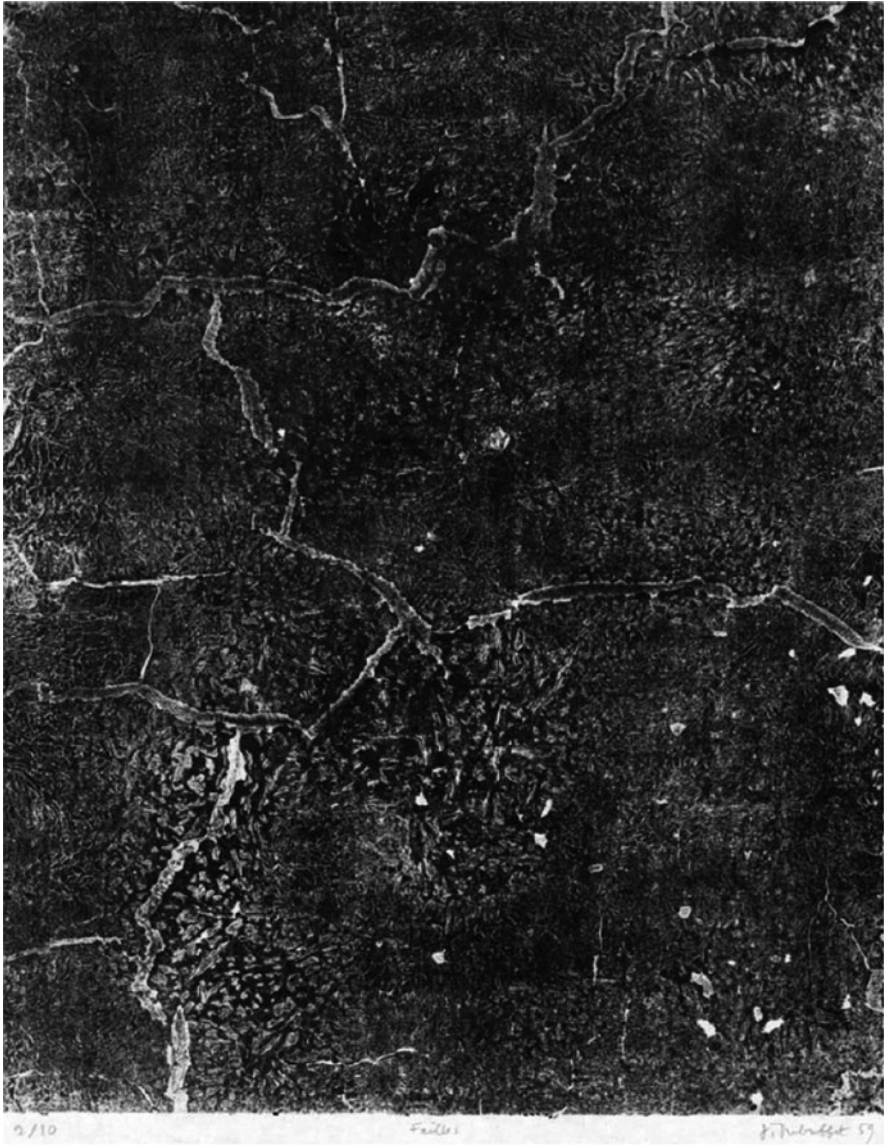
**Fractureted soils by Dubuffet[*] (1959)**

This black and white lithograph is part of a series of oil paintings and lithographs inspired from the soil and subsurface morphology.

---

[*][Jean Dubuffet (1901–1985) "Failles" in "Les Phenomenes-VII,Territories," Plate 12, Cat. Rais. Webel 523]

# Contents

# Chapter 1
# Chemical Pollutants as a Factor of Soil–Subsurface Irreversible Transformation: An Introductory Discussion

## 1.1 Raison d'être

The literature contains a very broad spectrum of research results that deal with anthropogenically induced, contaminant–soil–subsurface interactions. Most of these studies focus on transport, retention, and persistence of chemical pollutants, as well as on potential remediation of polluted systems. Changes in the soil–subsurface matrix and properties are usually treated as "perturbations" that disappear by natural processes or by specific remediation procedures. However, in addition to their environmental toxicity, chemical pollutants may cause – under specific conditions – significant, long-term changes in both the matrix and the properties of the soil–subsurface system.

While reviewing a large number of research papers on contaminant interactions in the soil–subsurface geosystem, during preparation of our book "Contaminant Geochemistry" (Berkowitz et al. 2008), we observed that in addition to targeting topics on soil–subsurface contamination and remediation, a number of research results reveal data confirming contaminant-induced (over "lifetime" scales) changes in soil–subsurface matrix and properties. In a recent paper (Yaron et al. 2008), we used some of these published data to outline the transformation of soil–subsurface matrix and properties following exposure to chemical contaminants. We also considered that chemical contamination, under specific conditions, may even become a *forming factor* of new soil–subsurface regimes. In this case, the uncontaminated soil and subsurface matrix may serve as parent material for a new formation (Yaron et al. 2009, 2010). In this book, we argue that soil–subsurface systems formed under natural environmental conditions over "geological" time may be transformed irreversibly, by exposure to chemical pollutants, into new systems with different matrix structure and properties. Thus, chemical pollutants are a significant factor in the formation and modification of contemporary soil–subsurface systems.

## 1.2  Soil–Subsurface Region as Part of the Critical Zone

The soil and the subsurface region below it are two interrelated natural bodies that comprise the earth's upper layer from land surface to aquifers; this region is also known as the "Critical Zone" (CZ). The ratios among these phases fluctuate as a function of environmental conditions, and the subsurface water content value ranges from air-dried to completely water saturated. Because the soil–subsurface water content is controlled by rainfall, irrigation, evaporation, and depth to the groundwater, a vertical water gradient always exists.

The CZ is a complex mixture of air, water, biota, organic matter, and earth materials (Brantley et al. 2007). In the CZ, the soil–subsurface region lies at an atmospheric–hydrological interface, coupling with biota to form a feed-through reactor (Prestrud Anderson et al. 2007). Under natural conditions in this reactor, fluids are supplied through precipitation, with the upper boundary being influenced by biological and physical processes occurring under aerobic and anaerobic environments.

Natural interactions between biota and earth materials in the Critical Zone were discussed in a series of papers on physico-chemical and biogeochemical processes by Prestrud Anderson et al. (2007), Brantley et al. (2007), Amundson et al. (2007), and Chorover et al. (2007). Natural equilibria of the Critical Zone are disturbed, however, by the huge amounts of toxic chemicals that are (directly or indirectly) released or disposed of onto the land surface, and then transported through the soil layer, vadose zone, and deeper into the groundwater by precipitation and/or irrigation. The matrix and properties of the soil–subsurface solid phase may be altered as these chemicals migrate. The extent of changes to the soil–subsurface system induced by chemical pollutants is controlled by their physico-chemical behavior, as well as microbial activity, in the CZ environment.

Organic contaminants, for example, may have negative or positive effects on biota, and consequently on contaminant persistence or natural attenuation in the CZ environment. Natural biodegradation of organic contaminants will decrease when these compounds have a direct toxic effect on biota, decreasing biological activity. In such cases, contaminant persistence in the soil–subsurface system will increase. On the contrary, when the organic contaminant acts as a source of energy for natural biota, contaminant degradation will occur together with metabolite formation. This biologically induced, persistence-transformation process clearly affects the potential impact of contaminants and their metabolites on irreversible changes in the soil–subsurface matrix and properties.

Natural organic compounds found in the CZ may in some cases serve as ligands for inorganic contaminants such as heavy metals, by forming organometallic complexes. These compounds may be retained or transported within the CZ in a different manner than the original heavy metal species. However, under different CZ conditions, the organometallic complexes can be biodegraded by natural microbial populations.

## 1.3   Human Impact on Soil Formation

Over the years, the structure and properties of the soil–subsurface system have been considered to be the result of natural processes occurring over geological time scales, under various climatic conditions. The soil is the thin layer on the earth's surface in contact with the atmosphere, which is the repository of living vegetation, microbiological populations, and their debris. The constitution of the subsurface region is controlled by the rock stratigraphy and mineralogy, weathering intensity, fluvial deposition, and glaciation processes. There is a feedback mechanism between the soil layer and the subsurface region: the subsurface region serves as parent material for soil, and once formed, the soil affects the properties and matrix of the subsurface.

The soil–subsurface system comprises multiple scales ranging from atomic to field scales. Bertsch and Hunter (1998) illustrate (Fig. 1.1) the various scales of interest required to examine the interaction between the soil–subsurface solid and liquid phases and products of anthropogenic origin under specific environmental conditions. The solid phase of the soil–subsurface system comprises both nano-sized materials and larger size particles which react differently with incoming chemical contaminants of anthropogenic origin. These reactions – which occur mainly at a molecular scale – may under specific conditions lead to irreversible modification of the soil and subsurface matrix and properties.

Until the nineteenth century, soil formation was related strictly to the degradation of geological material, due to weathering processes, at the land–water–air–atmosphere interface. It was only in the late nineteenth century that Dokuceaev (1860, 1899) in Russia, and in the beginning of the twentieth century that Hilgard (1906) and Marbut (1928) in the USA, reached the conclusion that soil is a living body formed under various natural processes and specific forming factors that involve geological (parent) material, climate, topography, biota, and time. Later on, in his book entitled "The
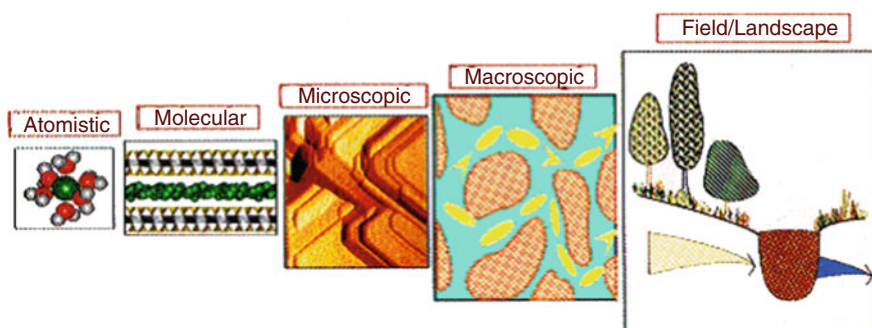


**Fig. 1.1**  Illustration of the various spatial scales relevant to the soil–subsurface system (Bertsch and Hunter 1998). Copyright 1998, Soil Science Society of America. Reprinted with permission

Factors of Soil Formation," Jenny (1941) integrated the functional nature of environmental influences on soil by defining the clorpt equation:

$$s = f(cl, o, r, p, t)...,$$

where s is the soil and other variants represent, respectively, climate (cl), organisms (o), surface relief (r), parent material (p), and time ($t$).

The Dokuceaev–Jenny factorial conception in soil genesis remained a basic philosophy for subsequent developments of soil formation modeling (e.g., Jenny 1961, 1980; Yaalon 1975; Johnson and Hole 1994; Phillips 1993, 1998; Ryzhova 1996; Bockheim et al. 2005). At the beginning of this century, Chadwick and Chorover (2001) referred to pedogenesis as a biogeochemical process constrained by thermodynamics but still maintaining large flexibility as a result of multiple reaction kinetics and a spatially heterogeneous matrix. These authors considered that from a thermodynamics perspective, the chemistry of pedogenesis is characterized by a number of thresholds controlled by time and, mainly, by natural environmental factors.

In the past, the human factor as a soil modifier was not incorporated into soil formation theories or into general conceptual models. From Dokuceaev (1883) to Jenny (1941, 1961), soil-forming factors referred only to natural "virgin" soils formed under natural environments over geological time scales. The formation processes altered by human intervention were considered to be deviations from the normal soil type which is reversed over time by natural attenuation processes or as a result of remediation techniques. Human impacts on soil matrix and properties became a topic of interest only in the second part of the last century. For example, effects of human agricultural practices on soil properties were discussed by Edelman (1954) and Jacks (1956). Analysis of the effects of bio-vegetative changes and crop cultivation on the soil profile morphology was the main focus of the papers published by Damaska and Nemecek (1964), Liberoth (1962), and Manil (1963). An overall view of human impacts on soil formation as a result of agricultural and municipal activity was presented by Bidwell and Hole (1965), who identified about 40 possible human-induced soil changes grouped according to the classical soil-forming factors theory. It may be seen, for example, that watershed management and even planning are integral components of soil formation, in addition to hunting, gathering, and cultivation. Each of the mentioned anthropogenic actions, whether independently or in combination, may lead to changes in initial soil characteristics.

For the first time, Yaalon and Yaron (1966) proposed that human-induced changes in soil-forming processes should be considered as an integral, independent factor to be added to the five recognized natural forming factors. In contrast to the natural factors, the rate of change of human-induced processes is relatively rapid, and the fundamental properties of soils acquired under the influence of the environmental soil formers are changed quantitatively within a short time. Yaalon and Yaron (1966) considered these changes as an additional factor within a new reference system where the natural soil serves as parent material and an initial state for the newly formed soil. The differences between the rate of impact on soil

characteristics of anthropogenic and natural environmental factors support the view that anthropogenic changes to the soil matrix and properties are an additional, independent soil-forming factor. Yaalon and Yaron (1966) suggested that human-induced processes leading to the formation of new soils be called *metapedogenesis*. These processes may be described by the function

$$s_2 = f(s_1, m_1, m_2, m_3, ...),$$

where $s_2$ is the new human-induced formed soil, $s_1$ is the initial state soil, and $m_1$, $m_2$, $m_3$,... are metapedogenetic factors (e.g., topographical, hydrological, chemical, or mechanical) acting singly or in combination. Selected examples of soil changes due to metapedogenetic processes are presented in Table 1.1.

   Amundson and Jenny (1991) considered the role of humans in soil formation, stating that anthropogenic factors are contained implicitly in the organism factor from the clorpt equation; human effects on the time scale and rate of soil–subsurface modification have been recognized subsequently (e.g., Rozanov 1990; Dudal et al. 2002; Richter 2007; Brantley 2008). The anthropogenic factor as an independent "sixth factor of soil formation," where human impact "occurs across all natural soils not as deviation but part of the genetic soil type," is discussed by Dudal et al. (2002). He introduced the notion of "anthropogenic soils" comprising human-induced changes, such as soil class, soil horizon, parent material, and landform, with consequences for soil classification and nomenclature (Dudal 2004). Recently, in a comprehensive paper on human transformation of the earth's soil, Richter (2007) distinguished between contemporary and historic influences, supporting the approach of Yaalon and Yaron (1966). He suggested that the rapid change of the ecosystem on a time scale of decades be considered as a basis for defining metagenesis of new contemporary soils having natural soils as the parent material. The human influence on soil–subsurface modification was, however, reduced mainly to physically and mechanically induced changes, with the effects of chemical pollutants being neglected almost entirely.

## 1.4   Chemical Pollutant-Induced Irreversible Changes to the Soil–Subsurface System

Potential interrelated pathways for exposure of the soil–subsurface system to chemical contamination, which may lead to soil–subsurface transformation, are depicted in Fig. 1.2. Chemical contaminants added to the land surface as agrochemicals and industrial and municipal products may be transported through the subsurface and to the groundwater zone in the form of dissolved solutes, adsorbed on colloidal materials or as immiscible-with-water liquids. The fate of these chemicals is affected by the soil–subsurface environment; existing research has been devoted mainly to this aspect. However, often chemical contaminants

**Table 1.1** Soil formation resulting from metapedogenetic processes. Reprinted from Yaalon DH, Yaron B (1966) Framework for man-made soil changes – an outline of metapedogenesis. Soil Sci 102:272–278. Copyright 1966 with permission of Wolters Kluwer Health

| Manipulation | Principal processes observed in the soil | Soil formation | |
|---|---|---|---|
| | | Initial soil | Resulting soil |
| *Topographical features* | | | |
| Terracing or land leveling | Reduction of erosion, human content increase; rejuvenation of pedogenetic processes, catenary slope differentiation altered | Lathosohe terra rossa (Litbic rhodustalfs) | Terra rossa (Rhodustalfs) |
| | | Rendzina (Rendolls) | Brown rendzina (Rendolls) |
| Dam construction on flood plains | Stopping of sedimentation and leaching, water table rise, salt accumulation. | Alluvial soil (Entisola) | Solonchak (Natrustont) |
| *Hydrological factors* | | | |
| Drainage, lowering of water table | Improved oxidation, structure formation, permeability change | Pseudogley (Aqualfs) | Parabraunerde (Udalfs) |
| Planting of wind breaks | Change of moisture regime; base saturation altered; carbonate leaching | Chernozem (Ustolls) | Leached chernozem (Altalfs) |
| Flooding of paddy fields | Hydromorphic water regime, reduced oxidation, gleying | Alluvium (Entisols) | Gley (Aquopts) |
| *Chemical factors* | | | |
| Irrigation with sodic water | Adsorption of sodium, structural degradation, decrease in permeability | Brunizem or Chestnut (Udolls) | Solonetz (Natrustalfs) |
| *Clay marling or warping* | Textural change in upper horizons, moisture regime change, base saturation altered | Regosol (Entisols) | Brown earth (Inceptisols) |
| *Cultivation and cropping factors* | | | |
| Deforestation and plowing in temperature areas | Mixing or upper horizons, change in pH, retardations of podsolization | Podsol (Spodosols) | Acid brown forest (orthrepts) |
| | | Leasive; gray-brown podsolic (Alfisols) | Brown earth (Ustalfs) |
| Deforestation and shifting cultivation in tropical areas | Erosion, dehydration of iron oxides | Lstosol, ferrallitic soils (Oxisols) | Ferrallitic crusts (Aerox) |
| Over-grazing | Destruction of natural vegetation; erosion of surface horizons, reduction in infiltration | Various mountain soils (Ustent, Udents) | Lithosols, calcareous grusts |

The table is not exhaustive but lists only selected examples, well documented in the literature, which show the variegated effect of the metapediogenetic processes in transforming soils
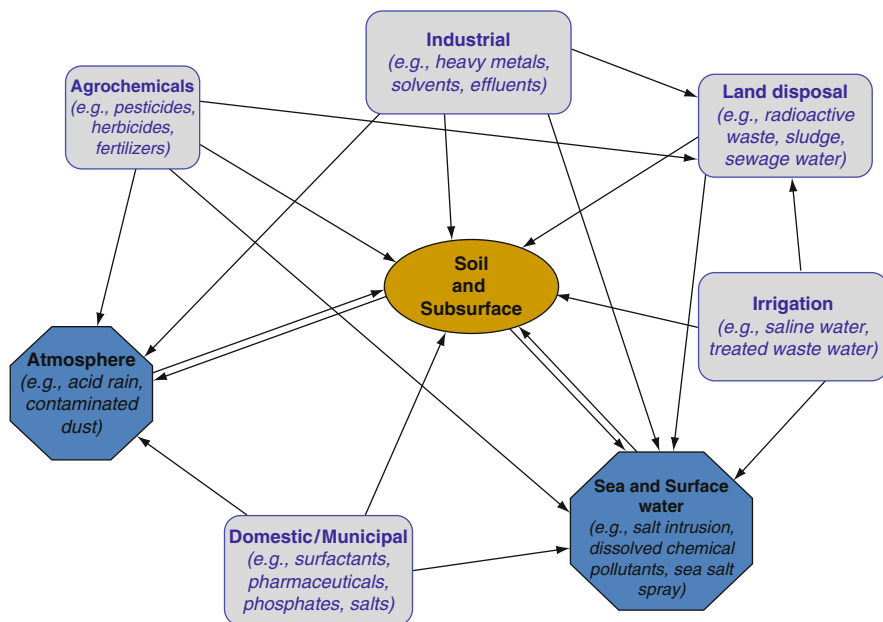
**Fig. 1.2** Potential interrelated pathways for soil–subsurface chemical contamination

**Table 1.2** Selected chemical contaminant-induced, potential irreversible changes in the soil and subsurface matrix and properties

| Aqueous phase | | Solid phase | |
|---|---|---|---|
| Solution composition | Solution properties | Matrix configuration | Matrix properties |
| Ionic composition | Acidity | Surface charge | Infiltration rate |
| Organic ligands | Alkalinity | Surface area | Hydraulic conductivity |
| Heavy metals | Dissolution capacity | Organic matter configuration | Retention capacity |
| Organic contaminants | Redox potential | Clay redistribution with depth | Hydration status |
| Radionuclides | Turbidity | Porosity | Rheological properties |
| Colloids, polyelectrolytes | Surface tension | Aggregation status | Water repellency |

induce alteration of the soil–subsurface matrix and in many cases may lead to their irreversible change. The possible irreversible changes in the matrix and properties of the soil and subsurface natural system, as result of anthropogenic chemical contamination, are presented in Table 1.2.

In our era, termed the "Anthropocene Age" (Crutzen 2002; Zalasiewicz et al. 2010, 2011), when humans have come to rival nature in their impact on the global environment, we must consider chemical contamination as a major factor acting on

the modification of natural soil–subsurface systems. As the soil–subsurface domain is an open thermodynamic system, it will never return to its initial state following exposure to chemical contamination, and new soils with different matrix and properties will be formed by changing the existing natural system.

As mentioned at the beginning of this chapter, existing data on the influence of chemical pollutants on soil–subsurface matrix and properties were obtained as "by-products" in published studies that focused on the effects of the soil–subsurface environment on the retention, transport, and persistence of contaminants. These results are used in support of our arguments that contaminants induce changes in the soil–subsurface matrix and properties, and that anthropogenic chemicals act as forming factors in shaping the contemporary soil–subsurface regimes.

# References

Amundson R, Jenny H (1991) The place of humans in state factor theory of ecosystems and their soils. Soil Sci 151:99–109

Amundson R, Richter DD, Humphreys GS, Jobbágy EG, Gaillardet J (2007) Coupling between biota and earth materials in the critical zone. Elements 3:327–332

Berkowitz B, Dror I, Yaron B (2008) Contaminant geochemistry. Springer, Heidelberg

Bertsch PM, Hunter DB (1998) Elucidating fundamental mechanisms in soil and environmental chemistry: The role of advanced analytical, spectroscopic, and microscopic methods. In: Huang PM, Sparks DL, Boyd SA (eds) Future prospects for soil chemistry. SSSA Special Publ 55, Madison, WI, pp 103–122

Bidwell OW, Hole FD (1965) Man as a factor of soil formation. Soil Sci 96:65–72

Bockheim JG, Gennadiev AN, Hammer RD, Tandarich JP (2005) Historical development of key conception in pedology. Geoderma 124:23–36

Brantley SL (2008) Understanding soil time. Science 321:1454–1455

Brantley SL, Goldhaber MB, Ragnarsdottir VK (2007) Crossing disciplines and scales to understand the critical zone. Elements 3:307–314

Chadwick OA, Chorover J (2001) The chemistry of pedogenetic thresholds. Geoderma 100:321–353

Chorover J, Kretzschmar R, Garcia-Pichel F, Sparks DL (2007) Soil biogeochemical processes within the critical zone. Elements 3:321–326

Crutzen PJ (2002) Geology of mankind. Nature 415:23

Damaska J, Nemecek J (1964) Contribution to the problem of genesis and fertility in Czechoslovakia. Rostlina Vyroba 5–6:540–555

Dokuceaev VV (1860) Russian Chernozen. In: Selected works of VV Dokuceaev vol 1 1948, English translation. Jerusalem

Dokuceaev VV (1883) Russian Chernozem. Israel Program for Scientific Translation, Jerusalem

Dokuceaev VV (1899) A contribution to the theory of natural zones: horizontal and vertical soil zones. Mayor's Office Press, St. Petersburg (in Russian)

Dudal R (2004) The sixth factor of soil formation. International conference on soil classification 2004, Petrozavodsk, Russia, 3–5 August, 2004

Dudal R, Nachtergaele F, Purnell M (2002) The human factor of soil formation. Symposium 18, vol II, paper 93. Transactions 17th World Congress of Soil Science, Bangkok

Edelman CH (1954) L'importance de la pedologie pour la production agricole. Trans Int Cong Soil Sci, Leopoldville 1:1–12

Hilgard EW (1906) Soils: their formation, properties, composition and relation to climate and plant growth in the humid and arid regions. Macmillan, NY

Jacks GV (1956) The influence of man on soil fertility. Adv Sci 50:137–145

Jenny H (1941) Factors of soil formation. McGraw-Hill, NY

Jenny H (1961) Derivation of state factor equations of soils and ecosystems. Soil Sci Soc Am Proc 25:385–388

Jenny H (1980) The soil resources, origin and behavior. Springer, NY

Johnson DL, Hole FD (1994) Soil formation theory: a summary of its principal impacts on geography, geomorphology, soil geomorphology, quaternary geology and paleopedology. In: Factors of soil formation. Soil Sci Soc Am Spec Pub 33, Madison, WI, pp 111–114

Liberoth I (1962) The effect of cultivation on soil formation in the loess region of Saxony. Albrecht- Thear- Arch 6:3–30

Manil G (1963) Profile chimique, solum biodynamique et aute characteristque ecologique du profil pedologique. Science du Sol 31–47

Marbut CF (1928) A scheme for soil classification. Proc First Int Congr Soil Sci IV:1–31; Metapedogenesis. Soil Sci 102:272–277; reprinted in Soil Sci (1996) 171:S154–S159

Phillips JD (1993) Stability implication of the state factor model of soils as a nonlinear dynamical system. Geoderma 58:1–15

Phillips JD (1998) On the relations between complex systems and the factorial model of soil formation. Geoderma 86:1–21

Prestrud Anderson S, von Blanckenburg F, White AF (2007) Physical and chemical controls on the critical zone. Elements 3:315–319

Richter DD (2007) Humanity's transformation of Earth's soil: Pedology's new frontier. Soil Sci 172:957–967

Rozanov BG (1990) Impact on evolution of soils under various ecological conditions of the world. Transaction of the Kyoto 14th IUSS Congress, Plenary Lectures Volume 1 pp 53–63

Ryzhova JM (1996) Analysis of the feedback effects of ecosystem produced by changes in carbon-cycling parameters using mathematical models. Eurasian Soil Sci 28:44–53 (translated)

Yaalon DH (1975) Conceptual model in pedogenesis: can soil-forming function be solved? Geoderma 14:189–205

Yaalon DH, Yaron B (1966) Framework for man-made soil changes – an outline of metapedogenesis. Soil Sci 102:272–278

Yaron B, Dror I, Berkowitz B (2008) Contaminant-induced irreversible changes in properties of the soil-vadose-aquifer zone: an overview. Chemosphere 71:1409–1421

Yaron B, Dror I, Berkowitz B (2009) Chemical contaminants as a factor of soil-subsurface metagenesis. Int Union Soil Sci (IUSS) Bull 15:11–12

Yaron B, Dror I, Berkowitz B (2010) Contaminant geochemistry – a new perspective. Naturwissenschaften 97:1–17

Zalasiewicz J, Williams M, Steffen W, Crutzen P (2010) The new world of the Anthropocene. Environ Sci Technol 44:228–231

Zalasiewicz J, Williams M, Haywood A, Ellis M (2011) The Anthropocene: a new epoch of geological time? Phil Trans R Soc A 369:835–841

# Chapter 2
# Soil–Subsurface Interrelated Matrix

The soil–subsurface regime comprises two distinct, interacting phases which may be affected by anthropogenic chemicals: the *solid phase*, formed by mineral and organic constituents in various states of evolution, and the *liquid phase*, including the water retained in the soil–subsurface pores and in the aquifer. The impact of anthropogenic chemicals on the soil–subsurface system may lead to irreversible changes in the solid phase matrix and properties, as well as to alteration of the liquid phase chemical composition. In this chapter, we provide a basic overview of soil–subsurface system characteristics as formed under natural environmental conditions; the reader is referred to the literature for detailed information.

## 2.1 Soil and Subsurface Solid Phase

The soil and subsurface solid matrix consists generally of a heterogeneous, friable material with aggregates and fractures of various sizes exhibiting a large range of porosity. The soil solid matrix comprises a mineral phase originating directly from rock weathering and subsurface earth materials, as well as an organic matter phase obtained from the decomposition of earth vegetative cover or from microbial populations. Components of the soil organic phase may be transported into the subsurface as dissolved solutes, colloidal materials, or suspended particles in the leaching water coating the mineral phase or precipitating as minor organic deposits. The subsurface solid matrix contains a mineral phase resulting mainly from direct weathering processes of the local geological material, from wind- and alluvial-induced redeposition of earth materials originating from other geological systems, and/or from precipitation of salts and other inorganic components found in incoming waters.

## 2.1.1  The Mineral Phase

The minerals formed by inorganic processes are naturally occurring homogeneous solids with a definite chemical composition and ordered atomic arrangements. Minerals with the same chemical composition may have different crystal structure, and vice versa. The most common chemical elements in the earth's crust, together with their crustal average, mole fractions, ionic radius, and volume, are presented in Table 2.1.

Based on their dominant anion or anionic group, Hurlbut and Klein (1977) grouped the minerals into the following classes: native elements, sulfides, sulfosalts, oxides and hydroxides, halides, carbonates, nitrates, borates, phosphates, sulfates, tungstates, and silicates. The minerals in the soil and subsurface system may also be classified as primary or secondary minerals. Primary minerals originate at high temperature mainly from igneous or metamorphic rocks, and rarely from sedimentary rocks. Secondary minerals are formed at low-temperature reactions by weathering of sedimentary rocks (Jackson 1964). Below, we discuss specific matrix properties of these minerals, which control their potential interactions with anthropogenic chemical compounds.

### 2.1.1.1  Silicates
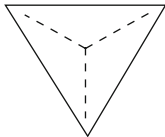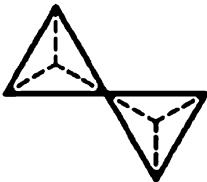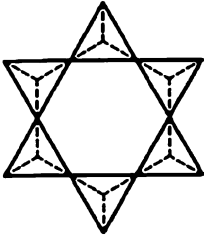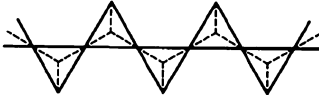
Silicates include a group forming about 90% of the earth's crust, comprising both primary and secondary minerals. The fundamental unit of the silicate tetrahedron consists of four $O^{2-}$ ions coordinated to one $Si^{4+}$ at the center. An $O^{2-}$ ion is shared by individual tetrahedra to form various complex structures such as sorosilicates (double), cyclosilicates (ring), inosilicates (single or double chains), phyllosilicates (sheets), or tectosilicates (three dimensional). The various arrangements of silica minerals are presented in Table 2.2.

**Table 2.1**  The 12 most common elements in the earth's crust (after Hurlbut and Klein 1977)

| Element | Crustal average (G kg$^{-1}$) | Mole fraction | Ionic radius (Nm) | Volume (%) |
|---|---|---|---|---|
| $O^{2-}$ | 466.0 | 0.6057 | 0.140 | 89.84 |
| $Si^{4+}$ | 277.2 | 0.2052 | 0.039 | 2.37 |
| $Al^{3+}$ | 81.3 | 0.0627 | 0.051 | 1.24 |
| $Fe^{2+}$ | 50.0 | 0.0186 | 0.074 | 0.79 |
| $Mg^{2+}$ | 20.9 | 0.0179 | 0.066 | 0.60 |
| $Ca^{2+}$ | 36.3 | 0.0188 | 0.099 | 1.39 |
| $Na^{+}$ | 28.3 | 0.0256 | 0.097 | 1.84 |
| $K^{+}$ | 25.9 | 0.0138 | 0.133 | 1.84 |
| $Ti^{++}$ | 4.4 | 0.0019 | 0.068 | 0.08 |
| $H^{+}$ | 1.4 | 0.0288 | † | † |
| $Mn^{4+}$ | 0.9 | 0.0003 | 0.060 | 0.01 |
| $P^{5+}$ | 1.0 | 0.0007 | 0.035 | 0.01 |
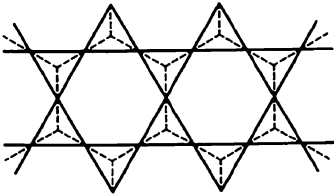
†undetermined

**Table 2.2** Classification of silicate minerals (after Schulze 1989; Allen and Fanning 1983; Hurlbut and Klein 1977)

| Silicate class | Unit composition and arrangement of $SiO_4$ tetrahedra | Mineral | Ideal formula |
|---|---|---|---|
| Nesosilicates $(SO_4)^{4-}$ | | Olivine | $(Mg, Fe)_2SiO_4$ |
| | | Forsterite | $Mg_2SiO_4$ |
| | | Fayarite | $Fe_2SiO_4$ |
| | | Zircon | $ZrSiO_4$ |
| | | Sphene | $CaTiO(SiO_4)$ |
| | | Topaz | $Al_2SiO_4(F, OH)_2$ |
| | | Garnets | $X_3Y_2(SiO_4)_3$ where $X = Ca, Mg, Fe^{2+}, Mn^{2+}$ $Y = Al, Fe^{3+}, Cr^{3+}$ |
| | | Andalusite | $Al_2SiO_5$ |
| | | Silimanite | $Al_2SiO_5$ |
| | | Kyanite | $Fe_2Al_9O_6(SiO_4)_4 (O, OH)_2$ |
| | | Staurolite | $Ca2(Al,Fe)Al_2O (SiO_4)(Si_2O_7) (OH)$ |
| Sorosilicates $(Si_2O_7)^{6-}$ | | Epidote | $Ca_2(Al,Fe)Al_2O (SiO_4)(Si_2O_7) (OH)$ |
| Cyclosilicates $(Si_6O_{18})^{12-}$ | | Berlyl | $Be_8Al_2(Si_6O_{18})$ |
| | | Tourmaline | $(Na,Ca)(Li,Mg,Al) (Al, Fe, Mn)_6 (BO_3)_3(Si_6O_{18}) (OH)$ |
| Inosilicates (single chains) $(SiO_3)^{2-}$ | | Pyroxenes | |
| | | Augite | $(Ca,Na)(Mg,Fe,Al) (Si,Al)_2O_6$ |
| | | Enstatite | $MgSiO_3$ |
| | | Hypersthene | $(Mg,Fe)SiO_3$ |
| | | Diopside | $CaMgSi_2O_6$ |
| | | Hedenbergit | $CaFeSi_2O_6$ |
| | | Pyroxenoids | |
| | | Wollastonite | $MnSiO_3$ |
| | | Rhodonite | $MnSiO_3$ |

(continued)

**Table 2.2** (continued)

| Silicate class | Unit composition and arrangement of SiO$_4$ tetrahedra | Mineral | Ideal formula |
|---|---|---|---|
| Inosilicates (double chains) $(Si_4O_{11})^{6-}$ | | Amphiboles Hornblende | $(Ca,Na)_{2-3}(Mg,Fe, Al)_5Si_6 (Si,Al)_2O_{22}(OH)_2$ |
| | | Tremolite | $Ca_2Mg_5Si_8O_{22}(OH)_2$ |
| | | Actinolite | $Ca_2(Mg,Fe)_5 Si_8O_{22}(OH)_2$ |
| | | Cummingtonite | $(Mg,Fe)_7Si_8O_{22} (OH)_2$ |
| | | Grunerite | $Fe_7Si_8O_{22}(OH)_2$ |

Silica minerals may be altered by physical weathering, forming secondary or altered primary minerals which form clay materials. As a consequence, the two predominant minerals in soils and subsurface are quartz (a silica mineral) and clay. The ratio (wt./wt.) of these two minerals defines the physical and surface properties of the earth materials. Below we present briefly the characteristics of these two major minerals that define the matrix and properties of the soil–subsurface system.

### 2.1.1.2 Quartz

Quartz, a silicate mineral, is one of the most abundant minerals in the soil–subsurface solid phase. In the soil and subsurface environment, quartz is found generally in sand and silt fractions, the amount of silicate mineral being determined by the parent material and the degree of weathering. Quartz is a primary mineral when crystallized from magma, and a secondary mineral (neoformed quartz) created in situ under specific temperature and pressure.

Common trace elements in quartz are Al, Ti, Fe, Na, Li, K, Mg, and Ca. Aluminum tends to be the most frequent element in quartz, substituting for Si in the crystal structure (Dennen 1966). In soil and subsurface systems, quartz may be altered in situ by chemicals and by physical weathering. Quartz is generally found in these systems in the form of anhedral grains (Fig. 2.1a), exhibiting also a variety of granular forms (Fig. 2.1b, c) and rarely prismatic forms, with the prism terminated by a set of rhombohedral faces (Fig. 2.1d). Quartz yields a characteristic X-ray pattern with well-defined peaks exhibiting a d-spacing ranging between 0.426 and 1.181 nm (Dress et al. 1989). The infrared (IR) absorption band is at 692 cm$^{-1}$, with two strong doublets at 798 and 780 cm$^{-1}$, as well as at 390 and 370 cm$^{-1}$ (Chester and Green 1968).

The silica tetrahedron in quartz is almost symmetrical and has a Si–O distance of 0.16 nm. Quartz has a spiral network structure consisting of silica tetrahedra around z-axis (Wilding et al. 1989). Each tetrahedron is repeated in the network by a rotation of 120° and a translation of c/3 (Fig. 2.2). The dense packing of the crystal structure and the high activation energy required to alter the Si–O–Si bond contribute to the high stability of quartz (Stober 1967). The specific gravity of quartz

**Fig. 2.1** Scanning electron microscope images of various quartz grains (after Drees et al. 1989). Copyright 1989, Soil Science Society of America. Reprinted with permission
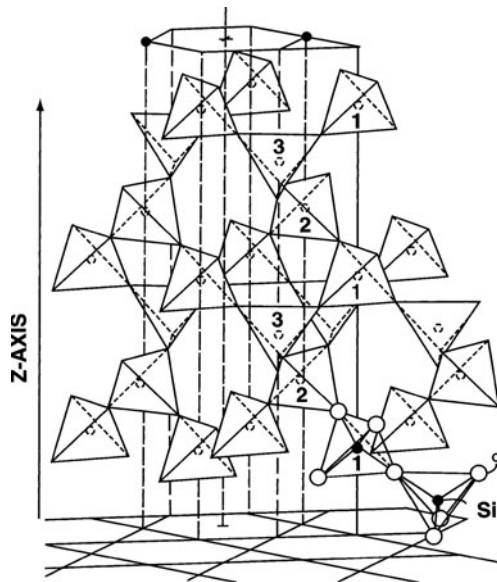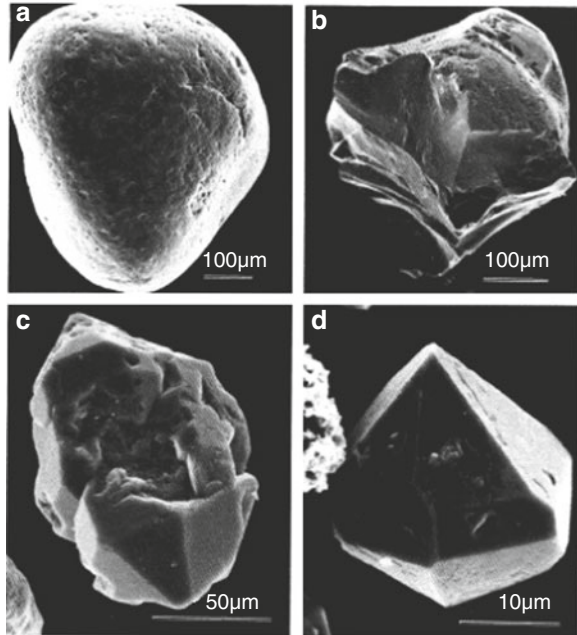




**Fig. 2.2** The structure of quartz (Drees et al. 1989). Copyright 1989, Soil Science Society of America. Reprinted with permission

ranges between 2.65 g mL$^{-1}$ in macrocrystalline varieties and 2.60 g mL$^{-1}$ in cryptocrystalline varieties (Frondel 1962; Katz et al. 1970). Substitution of Al by Si in quartz leads to a decrease in its specific gravity. Quartz minerals may exhibit

cleavage parallel to lattice planes, especially along planes where Si–O bonds are broken (Margolis and Krinsley 1974).

### 2.1.1.3   Clay Minerals

Clay minerals are the major natural nanomaterials in the soil–subsurface system, which interact with almost all of the contaminants introduced into the environment by humans. While the fraction of clay minerals in the soil–subsurface system is often relatively low, even small percentages of clay have a critical effect on the transport and fate of chemical contaminants, due to large active surface areas which substantially exceed those of other components.

Most soil and subsurface clays are a mixture of one or more aluminosilicate clays with minute amounts of iron oxides and hydroxides, quartz and feldspar, oxides and hydroxides of aluminum and manganese, and carbonates (especially calcite). Many clay minerals have a layer structure in which the atoms within layers are strongly bonded to each other; the bonding between layers is weaker. The layers in different kinds of clays are structurally similar. However, different layers can fit together to form stable structures common among interstratified clay minerals. Bailey et al. (1971) define layer silicates as continuous, two-dimensional tetrahedral sheets of composition $Z_2O_5$ in which individual tetrahedra are linked to neighboring tetrahedra by sharing three corners each when Z is the tetrahedrally coordinating cation of $Si^{4+}$ or $Al^{3+}$. Tetrahedral sheets are linked in the unit structure to octahedral sheets, groups of coordinated cations or individual cations. As a function of their external or internal surface characteristics, clays interact differently with organic or inorganic contaminants.

The clay solid phase is characterized by a net charge on the solid phase that is in contact with the liquid or gaseous phase. These charged surfaces usually are faced by one or more layers of counter ions having a net charge separate from the surface charge. The adsorption of charged solute on the mineral solid phase surface is subject to both chemical binding forces and an electric field at the interface, and is controlled by electrochemical properties.

We focus our discussion below on the characterization of two major groups of clay minerals: *kaolinite*, with a 1:1 layered structured aluminosilicate and a surface area ranging from 6 to 36 $m^2\ g^{-1}$, and *smectites*, with a 2:1 silicate layer and a total (internal and external) surface area of about 800 $m^2\ g^{-1}$ (Schofield and Samson 1954; Borchard 1989).

*Kaolinite* is composed of unit layers, each consisting of one silica tetrahedral sheet and one alumina octahedral sheet bound together in a common sheet with shared oxygens (Grim 1962). The units are stacked one above the other in the *c*-axis direction. The classical schematic diagram (Gruner 1932) of a kaolinite unit layer is reproduced in Fig. 2.3. Refinements of the kaolinite structural diagram were developed later (e.g., Brindley and MacEvan 1953; Dixon 1989), but we consider the original Gruner representation to remain valid for didactic purposes.
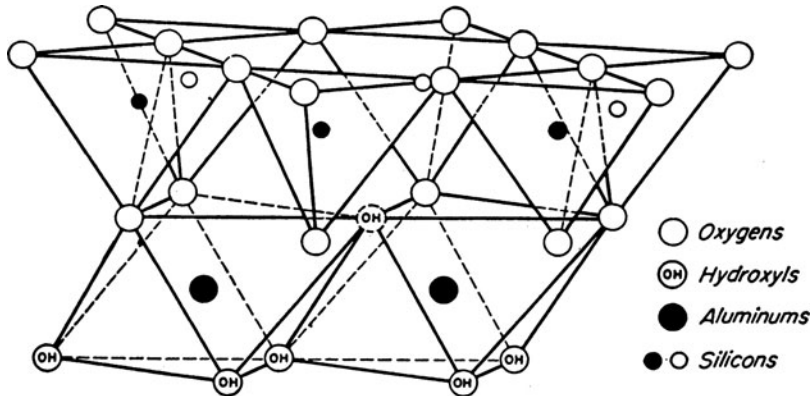
**Fig. 2.3**  Structure of kaolinite (after Gruner 1932)

Summarizing the structural properties of kaolinite, Dixon (1989) noted that the composed tetrahedral and octahedral sheets form a 0.7-nm layer in a triclinic unit cell. Two-thirds of the octahedral positions are occupied by Si and Al, which are located in two rows parallel to the *x*-axis. Every third row of the octahedral sheet is vacant. The surface plane of octahedral anions and a third layer of the inner plane are built up by hydroxyl (OH) groups. The surface hydroxyls bond through their hydrogens to the oxygen sheet of the bordering layer.

The kaolinite structure exhibits covalent sharing of H which leads to conceptualization of the presence of two inner surface hydroxyls perpendicular to the layer bonded to the O of an adjacent layer (Giese 1982). As a result of polarization of the Si–O and O–H groups, the surface oxygen and proton plane become negatively or positively charged. Electrostatic attraction and van der Waals forces determine the stacking of kaolinite unit layers. Kaolinite exhibits a very low cation exchange capacity, in general lower than 1 $cmol_c$ $kg^{-1}$ (Schofield and Samson 1953) at pH = 7 (Lim et al. 1980). The positive charge on kaolinite occurs on the edges of the plates which become positive by acceptance of $H^+$ in the acid pH range (Schofield and Samson 1953).

Morphological characteristics of kaolinite crystals from the clay fraction of some Brazilian soils as related by Melo et al. (2001) are reproduced in Fig. 2.4. As a function of type of soil, kaolinite crystals are hexagonal exhibiting either six euhedral faces or otherwise an anhedral form. The dominant forms of the soil clay fraction kaolinite are elongated and rounded with relatively lower proportion of hexagonal particles. These findings are in accordance with a previous observation of Sings and Gilkes (1990) showing that the hexagonal form is found commonly in kaolin deposits but rarely in weathered soils.

Kaolinite surface charge is heterogeneous because different reactions occur on a variety of distinct crystallographic sites. Brady et al. (1996) showed, for example, that the pH-dependent, multi-site surface charge on kaolinite is explained by proton donor–acceptor reactions occurring simultaneously on Si and Al sites exposed on basal planes and edges.
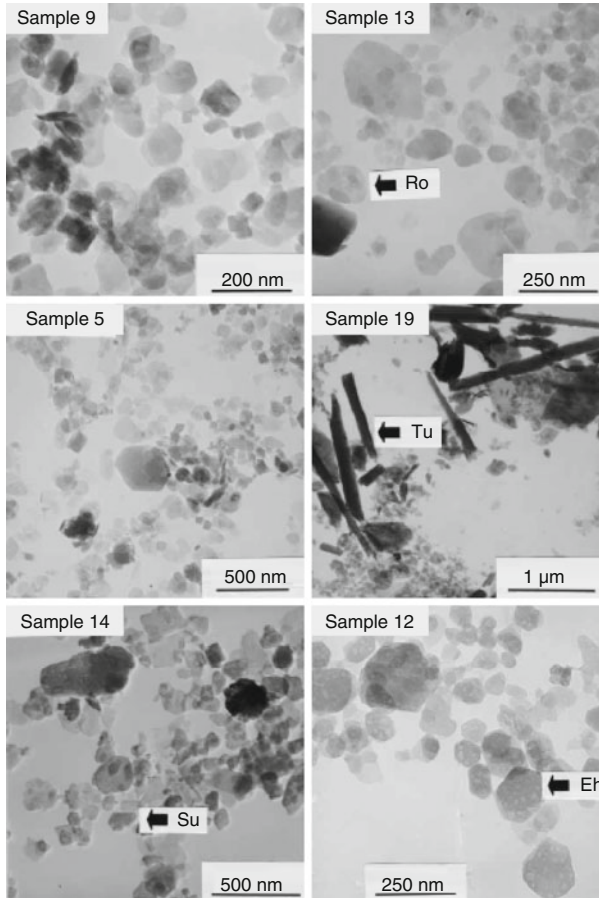
**Fig. 2.4** Transmission electron microscope (TEM) micrographs of kaolinite from the clay fraction of some representative Brazilian soils showing a wide range of crystal morphologies and size. Various morphologies are indicated: *Ro* rounded, *Su* subeuhedral faces, *Eh* euhedral, and *Tu* tubular (after Melo et al. 2001). Copyright 2001, Soil Science Society of America. Reprinted with permission

*Smectites* are clay minerals with an expanding nature, a negative charge, and a large total surface area. These properties are of major importance in controlling the fate of chemical contaminants in the soil–subsurface system by affecting their retention, transport, and persistence. The idealized structure of a smectite clay mineral as depicted by Kaviratna et al. (1996) is presented in Fig. 2.5. The oxyanion layer consists of two inverted silicate tetrahedral sheets sharing their oxygens with an octahedral sheet. The 2:1 relation between the tetrahedral and octahedral sheets within a layer accounts for classification of these clays as 2:1 phyllosilicates. The layer charge originates from the substitution of octahedral $Al^{3+}$ by $Mg^{2+}$. In a unit cell formed from 20 oxygens and four

**Fig. 2.5** Idealized structure
of a smectite clay mineral.
*Large circles*, oxygen atoms;
*small circles*, hydroxyl
groups. Silicon and
sometimes aluminum
normally occupy tetrahedral
positions in the oxygen frame
work. Aluminum,
magnesium, iron, or lithium
may occupy octahedral sites.
Exchange cations and water
occupy the interlayer region
(after Kaviratna et al. 1996).
Reprinted from Kaviratna PD,
Pinnavaia TJ, Schroeder PA,
Dielectric properties of
smectites clay. J Phys Chem
Solids 57:1897–1906,
Copyright (1996), with
permission from Elsevier
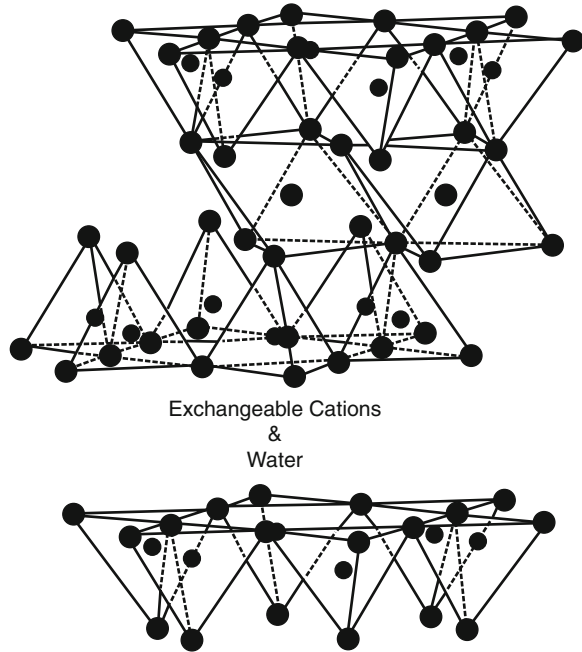


Exchangeable Cations
&
Water

hydroxyl groups, there are eight tetrahedral sites and six octahedral sites, along with
four cavities surrounded by a six-membered oxygen ring on the surface.

The montmorillonite and beidellite minerals, which are the most common
smectites in the earth, contain significant amounts of tetrahedral Al and octahedral
Fe. A detailed description of smectite structure and properties is given by Borchard
(1989). Montmorillonite ($Si_4Al_{3.5} Mg_{0.5}$) with a cation exchange capacity of
135 $cmol_c$ $kg^{-1}$ has an octahedral sheet that shares oxygen atoms between two
tetrahedral sheets, with cationic substitution occurring in the tetrahedral and octahe-
dral sheets. The layer charge originates from the substitution of octahedral $Al^{3+}$ by
$Mg^{2+}$. In a unit cell formed from 20 oxygens and four hydroxyl groups, there are eight
tetrahedral sites and six octahedral sites along with four cavities surrounded by a six-
membered oxygen ring on the surface.

The expanding characteristics of smectites are affected by the nature of adsorbed
ions and molecules. The interlayer cations are replaced when the clay is wetted with an
electrolyte solution, affecting the interlayer spacing. The hydration water of the
interlayer exchangeable cation forms the first water layer followed by an additional
water layer held with less energy (Barshad 1960). According to Barrer and Jones
(1970), layer charge and the type of cations in galleries of clay determine the extent of
water adsorption, thereby controlling the swelling of the gallery region. The dielectric
properties of smectites are controlled by their water content and saturating cation.
Kaviratna et al. (1996) report that, in general, the dielectric constant of a smectite
changes slowly as the first monolayer of adsorbed water builds up in the clay galleries.
Water loading beyond the first monolayer causes the dielectric constant to rise rapidly

to very high values. Environmental temperature may affect the mineral hydration status. Smectite loses pore water below 110°C, adsorbed water below 300°C, and OH water at a temperature above 300°C. Borchard (1989) reported on the effect of saturating cations on the basal spacing of smectites (a mixture of montmorillonite and beidellite from a Californian soil) using XRD measurements. All magnesium-saturated smectites give a peak corresponding to a d-spacing of 1.5 nm at 54% relative humidity, while potassium-saturated smectites give a peak corresponding to a d-spacing of 1.25 nm at the same moisture content. These differences are explained by variations in the hydration status of the saturating ions. When smectites are kept at 0% relative humidity after 110°C heating, they yield a peak corresponding to a d-spacing of 1.0 nm. Simultaneous morphological observation by HRTEM and chemical analysis by AEM (EDS) techniques provide a comprehensive, nanoscale level understanding of smectite interlayer configuration and composition.

TEM images (Yaron-Marcovich et al. 2005) show the morphology of a sodium montmorillonite along with the corresponding selected area electron diffraction (SAED) pattern (Fig. 2.6). At lower magnification, crystalline aggregates composed of relatively small, thin, flake-like, and pointed nanoscale silicate particles (about 10–50 nm wide and 50–400 nm long) with no obvious orientation are visible. The interlayer compositional variation of the same smectite clay sample, determined by X-ray energy dispersive spectroscopy (EDS), shows that the nanoparticles are of similar composition containing Na, K, Al, Mg, and O.
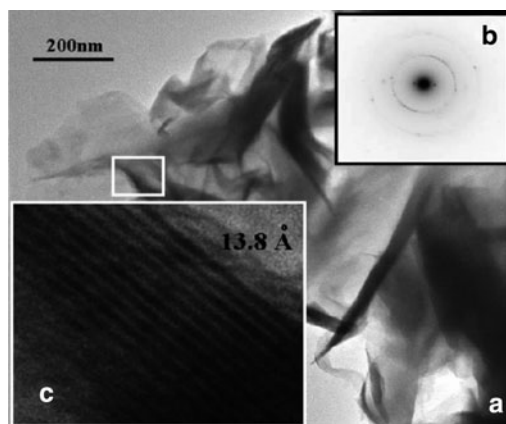


**Fig. 2.6** TEM images of Na-montmorillonite particles: (**a**) low-magnification TEM image showing a typical crystalline aggregate; (**b**) the corresponding SAED pattern: note the 001 diffraction spots corresponding to the planes parallel to the e-beam; the calculated spacing is 13.83 Å; (**c**) high-resolution TEM image of a particle attached to the edge of the aggregate (white frame in (**a**)) exhibiting the layered structure; the measured lattice spacing (13.8 Å) is in agreement with calculations from the SAED in (**b**) (Yaron-Marcovich et al. 2005). Reprinted with permission from Yaron-Marcovich D, Chen Y, Nir S, Prost R (2005) High resolution electron microscopy structural studies of organo-clay nanocomposites. Environ Sci Technol 39:1231–1239. Copyright 2005 American Chemical Society

Infrared analysis of smectite provides additional information on its structural properties. Silicate minerals have strong Si–O bands near 600 and 1,000 cm$^{-1}$ which can be affected by substitution of Si atoms by Al atoms. The OH banding vibrations produce the adsorption characteristics of the octahedral sheet. When Al is present, the absorption is near 920 cm$^{-1}$ and when only Fe is present, the absorption is near 820 cm$^{-1}$. A mixture of Al, Fe, and Mg leads to intermediate values. Hydroxyl adsorption is in the 3,000–3,800 cm$^{-1}$ region. Farmer and Russel (1967) showed that this band appears to broaden as a result of Al substitution by Si in tetrahedral sheets and reflects the type of saturating cation and the hydration status in the interlayer space. The surface oxygen atoms are weak electron donors and form weak hydrogen bonds. As a consequence and as a result of their association with exchangeable cations, water molecules on the smectite surface are more acidic than the interlayer water (Borchard 1989).

Of particular interest for chemical transport into a predominantly smectite medium is the shrink–swell property of the clay material. The swelling properties of smectites are explained by two different concepts. The first one, developed by Sposito (1973), shows that smectite swelling is caused by the hydration and mobility of the cations, which in turn balance the negative charge of the layer silicates. The second concept, presented by Low (1981), emphasizes the direct interaction of water molecules with the silicate surface. Both viewpoints fit the common observation that smectite swells in a high hydration environment and at low electrolyte concentrations, and shrinks when water is lost and salt is added to the bulk solution.

A mixture of intercalating clays may be found in the soil–subsurface medium. Interstratification of kaolinite and smectite has been reported in some cases (e.g., Herbillon et al. 1981; Yerima et al. 1985). This fact is reflected in a XRD spacing of about 0.8 nm (Dixon 1989) or in HRTEM micrographs (Fig. 2.7).

Environmentally induced processes occurring in the subsurface (e.g., leaching and acidification) may induce weathering processes and structural changes in natural clays. For example, in soils with low organic matter, moderate leaching and a pH of about 5 cause smectites to be transformed into pedogenetic chlorites (Barnhisel and Bertsch 1989). Laboratory studies proved a direct transformation of smectites into kaolinite during intense weathering. Under natural environmental conditions, the transformation of smectite to kaolinite, in the presence of iron oxide, may occur under enhancement of drainage conditions during landscape evolution. In the case of sedimentary environments (Morgan et al. 1979) and of well-drained red–black soils (Herbillon et al. 1981), the transformation may proceed through an intermediate step consisting of interstratified kaolinite–smectite.

### 2.1.1.4 Minerals Other Than Silicates

In addition to quartz and clay minerals, the subsurface contains a variety of minerals (e.g., oxides and carbonates) which may react with organic and inorganic contaminants. Gilkes (1990), summarizing the properties of the metal oxides
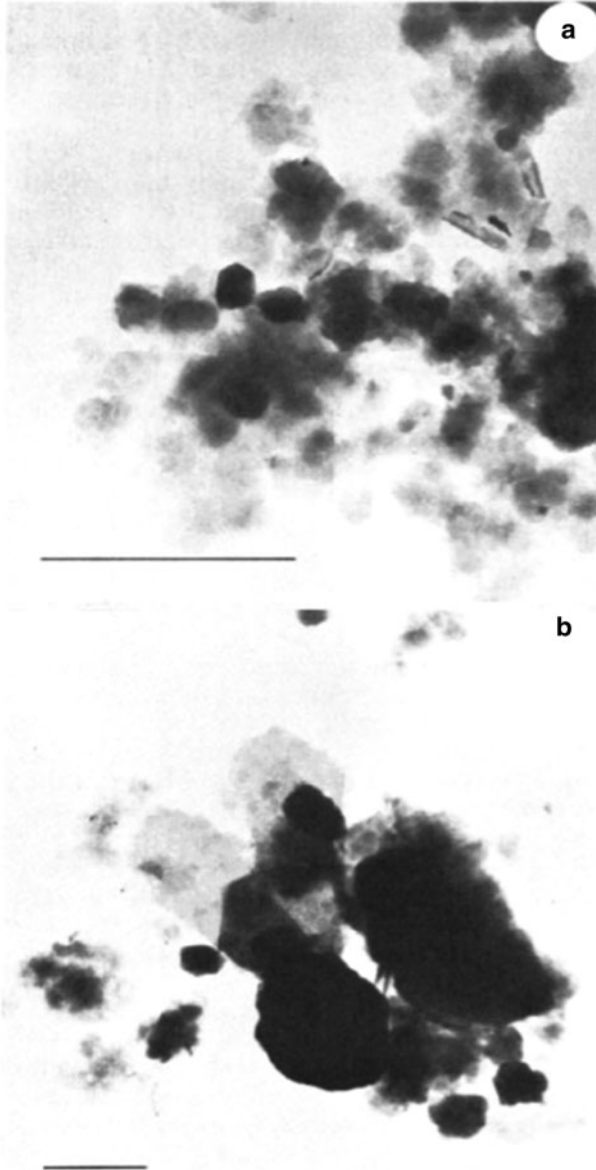
**Fig. 2.7** Transmission electron micrographs of (**a**) fine (<0.2 μm) and (**b**) coarse (2–0.2 μm) clay from the Atiocoyo pedon (horizon 2A2) showing subrounded and hexagonal shapes characteristic of interstratified kaolinite–smectite. Each *bar* represents 0.5 μm (after Yerima et al. 1985). Copyright 1985, Soil Science Society of America. Reprinted with permission

in earth materials, states that iron oxides (e.g., hematite $\acute{\alpha}$-$Fe_2O_3$, maghemite $\beta$-$Fe_2O_3$, goethite $\alpha$-FeOOH, and lepidocrocite $\beta$-FeOOH) are common constituents with crystals that vary greatly in size, shape, and surface morphology. The surface of

iron oxides in the subsurface environment is often hydroxylated either structurally or through hydration of iron atoms. Crystals of the aluminum oxides that commonly occur (e.g., gibbsite and boehmite) are small but often larger than the associated iron oxides. Other oxide minerals are less abundant than iron and aluminum oxides, but because of their very small crystal sizes and large surface areas, they may affect very significantly the geochemical properties of the subsurface and their interaction with chemicals. For example, the various manganese oxides that can be found in the subsurface can occur as very small (about 10 nm), structurally disordered crystals. Similarly, titanium oxides (rutile, anatase, $TiO_2$) and even corundum, a rare pyrogenic mineral, occur within the clay fraction as approximately 30-nm crystals. The ability of iron and certain other metal ions to undergo redox reactions further increases the role of metal oxides in the activity of the solid phase.

Other major components found in the subsurface include significant quantities of relatively high surface area, soluble calcium carbonate ($CaCO_3$), and calcium sulfate ($CaSO_4$). It is difficult to estimate the contribution of amorphous materials (e.g., allophane or imogolite) to the surface activity of earth materials. Amorphous materials often coat crystal minerals, which may further affect interaction of these minerals with contaminants.

## 2.1.2 The Organic Phase

The natural organic matter in the soil solid phase is "a heterogeneous mixture composed largely of products resulting from microbial and chemical transformations of organic debris" (Hayes and Swift 1978) disposed on land surface. Stevenson (1994) regards the soil organic matter in the solid phase as a mixture of vegetation litter, microbial biomass light fractions, and stabilized decomposed natural organic materials named *humus*. The transformation process of natural organic matter into humus is called humification. Humic substances include a series of relatively high molecular weight yellow- to black-colored substances formed in secondary synthesis reactions (Stevenson 1994). Major components of the soil organic matter and their definition are presented in Table 2.3.

Although humus – comprising the humic substances and other organic non-humic components – forms a minor part of the total solid phase, it is of major importance in defining the surface properties of the solid phase and has an enormous impact on the retention and persistence of anthropogenic chemicals reaching the land surface. In the soil–subsurface system, humus may be found as a free organic fraction or coating the mineral constituents of the solid phase. The main mass of natural organic materials is deposited in the soil layer and the soil offers optimum conditions for the humification process. However, organic matter may also be transported from the soil as suspended particles into the subsurface porous medium or even into the groundwater region.

**Table 2.3** Definition and characterization of soil organic matter. Reprinted from Stevenson FJ (1994) Humus Chemistry, 2nd edn. Wiley, New York. Copyright 1994 with permission of John Wiley and Sons

| Term | Definition |
|------|-----------|
| Litter | Macroorganic matter (e.g., plant residues) that lies on the soil surface |
| Light fraction | Undecayed plant and animal tissues and their partial decomposition products that occur within the soil proper and that can be recovered by flotation with a liquid of high density |
| Soil biomass | Organic matter present as live microbial tissue |
| Humus | Total of the organic compounds in soil exclusive of undecayed plant and animal tissues, their "partial decomposition" products, and the soil biomass |
| Soil organic matter | Same as humus |
| Humic substances | A series of relatively high molecular weight, yellow- to black-colored substances formed by secondary synthesis reactions. The term is used as a generic name to describe the colored material or its fractions obtained on the basis of solubility characteristics. These materials are distinctive to the soil (or sediment) environment in that they are dissimilar to the biopolymers of microorganisms and higher plants (including lignin) |
| Non-humic substances | Compounds belonging to known classes of biochemistry, such as amino acids, carbohydrates, fats, waxes, resins, and organic acids. Humus probably contains most, if not all, of the biochemical compounds synthesized by living organisms |
| Humin | The alkali-insoluble fraction of soil organic matter or humus |
| Humic acid | The dark-colored organic material that can be extracted from soil by dilute alkali and other reagents and that is insoluble in dilute acid |
| Hymatomelanic acid | Alcohol-soluble portion of humic acid |
| Fulvic acid | Fraction of soil organic matter that is soluble in both alkali and acid |
| Generic fulvic acid | Pigmented material in the fulvic acid fraction |

### 2.1.2.1 Genesis and Structure

In general, the genesis of soil organic matter may be described by two major pathways of humus formation: (1) biologically induced degradation of dead plant tissue, involving the modification of lignine, suberine, and cutine (Hatcher and Spiker 1988; Clapp et al. 2005), and (2) abiotic synthesis process (Stevenson 1994; Essington 2004). However, Wershaw (2000) in his work on "Humic Substances – In Search of a Paradigm" stated that 100 years of research has not advanced knowledge on the structure of humic acids. Moreover, based on a large overview of humic substances, Burdon (2001) reached the conclusion that there is insufficient biological or chemical information to define their structure in the soil environment.

Numerous structures have been proposed for humic substances in the past, based mainly on speculative or "in vogue" research results over the years. A basic structure for the modeling of humic substances was the preliminary concept of a two-dimensional representation of humic acid (Schulten and Schnitzer 1993, 1997). Another model, which embraces the concept of molecular association based on ordered aggregates of amphiphiles – compounds with hydrophobic stretches and charged or

polar center – is based on the assumption of acidic functionality of the altered plant molecular functions (Wershaw 1986, 1993). The humic molecules are held together by hydrophobic bonding, charge transfer, and H-bonding interactions (Piccolo 2001). Models were also developed on the basis of analytical and spectroscopic data associated with computer calculations (e.g., Jansen et al. 1996; Bailey et al. 1971). Schulten (2001) improved this model (Schulten and Schnitzer 1993, 1997) by trapping biological substances such as sugars and peptides, thus developing different models for terrestrial humic acids, soil organic matter, and dissolved organic matter.

Because organic matter is such an important component of soil, development of models to describe subsurface behavior now incorporates chemical interaction studies, molecular mechanism calculations, structural modeling, and geometry optimization. A reevaluation of molecular structure of humic substances based on data obtained primarily from nuclear magnetic resonance spectroscopy, X-ray absorption near-edge structure spectroscopy, electrospray ionization-mass spectrometry, and pyrolysis studies was presented by Sutton and Sposito (2005). The authors consider that "humic substances are collections of diverse, relatively low molecular mass components forming dynamic associations stabilized by hydrophobic interactions and hydrogen bonds." These associations are capable of organizing into micellar structures in suitable aqueous environments.

Humic components display contrasting molecular motion behavior and may be spatially segregated on a scale of nanometers. Within this structural context, these components comprise any molecules closely associated with a humic substance. Sutton and Sposito (2005) consider that biomolecules which bind strongly within humic fractions are by definition humic components. Kleber et al. (2007), continuing the assumptions of Wershaw et al. (1996), Piccolo (2001), and Sutton and Sposito (2005), showed that soil organic matter consists of organic molecular fragments of varying degrees of amphiphilicity or surfactant-like properties. The organic fragments and mineral surfaces arrange themselves in structures that maximize entropy, a fact that suggests the formation of a layered mineral–organic association. Kleber et al. (2007) suggest that the soil organic matter sorbs to mineral surfaces in a discrete zonal sequence where a contact zone, a hydrophobic zone, and a kinetic zone (Fig. 2.8) are involved.

In the *contact zone*, amphiphilic fragments accumulate on charged surfaces through electrostatic interactions, directing hydrophobic portions outward toward the polar aqueous solution. The *zone of hydrophobic interactions* expresses the hydrophobic region. This region is the result of entropically driven shielding of the hydrophobic portions of adsorbed organic molecules from the polar aqueous phase by a second layer of amphiphilic molecules.

Progression from model structures to molecular structures of natural organic matter (NOM) components was discussed by Leenheer et al. (2003). Based on the hypothesis that humification processes occur as extensive condensation/oxidative coupling, reactions were developed in the previous NOM models as macromolecular random coil shapes. Ulterior molecular models were developed on the basis of analytical evidence showing that NOM is an aggregate of small molecules. The progression from NOM model structure to molecular structure, however, requires better analytical and instrumental techniques. Because the genesis of component molecules of humic substances is still not known, the best indication of their nature
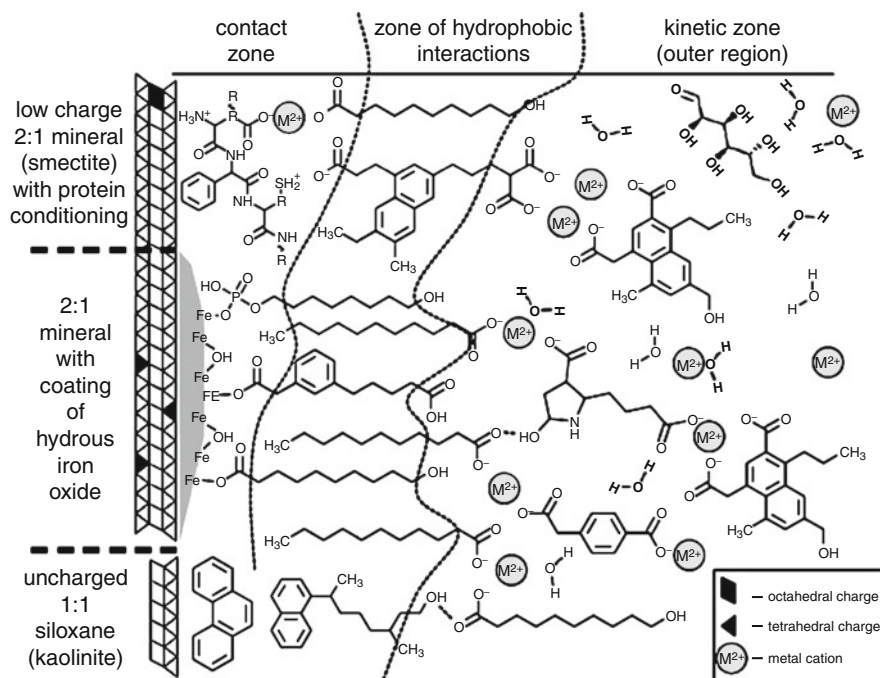
**Fig. 2.8** The zonal model of organo-mineral interactions (after Kleber et al. 2007)

is the identification of the degradation products using various advanced techniques (e.g., NMR, FTIR, and Raman spectroscopy).

*Humic components* include humic acid (soluble in alkaline solution, insoluble in acid solution), fulvic acid (soluble in aqueous media at any pH), hymatomelamic acid (alcohol-soluble part of humic acid), and humin (insoluble in alkaline solution at any pH value). Humin is a major component of the soil humic fraction, representing more than 50% of the organic carbon of soil (Kononova 1966). It should be noted, however, that this fractionation of soil organic matter does not lead to a pure compound; each named fraction consists of a very complicated heterogeneous mixture of organic substances. For example, biomolecules which are not part of humic substances may precipitate at pH 1 or 2 with the humic acid (Hayes and Malcom 2001), and more polar compounds with fulvic acids.

Dark-colored pigments extracted from earth materials are produced as a result of multiple reactions, the major pathway being through condensation reactions involving polyphenols and quinones. According to Stevenson (1994), polyphenols derived from lignin are synthesized by microorganisms and enzymatically converted to quinines, which subsequently undergo self-condensation or combine with amino compounds to form N-containing polymers. The number of molecules involved in this process, as well as the number of ways in which they combine, is almost unlimited, explaining the heterogeneity of humic materials.

The major atoms comprising humic materials are C (50–60%) and O (30–35%). Fulvic acid has lower carbon and higher oxygen contents. The percentage of hydrogen (H) and nitrogen (N) in fulvic acid varies between 2 and 6%, and that of sulfur (S) varies from 0 to 2%. The various fractions of humic substances obtained on the basis of solubility characteristics are part of a heterogeneous mixture of organic molecules, which originate from different earth materials and locations and might have molecular weights ranging from several hundred to several hundred thousand. Humic acids have an average molecular weight of the order 10,000–50,000, and a typical fulvic acid has a molecular weight in the range of 500–7,000.

The humic fraction in the soil represents a colloidal complex including long-chain molecules or two- or three-dimensional cross-linked molecules whose size and shape in solution are controlled by the pH and the presence of neutral salts. Under neutral or slightly alkaline conditions, these molecules are in an expanded state as a result of the repulsion of the charged acidic groups, whereas at a low pH and high salt concentration, molecular aggregation occurs due to charge reduction. These large organic molecules may exhibit hydrophobic properties, which govern their interaction with nonionic solutes.

*Nonhumic components of humus* include the organic components of the humus – originating from plants and microorganisms – which are insoluble in aqueous acidic or basic media. Clapp et al. (2005) show that this group may include the following organic compounds:

– *Polysaccharides*, with origins in plants and microorganisms, are important components of the soil organic matter with major environmental impact
– *Peptides and proteins*, which may comprise amino acids, amino groups, amino sugars, or nucleic acid derivates and many other N-containing compounds
– *Tannins* are the fourth in order of abundance in terrestrial plants after cellulose, hemicelluloses, and lignins. In soils, organic matter occurs as hydrolyzable tannins. Because the ester linkages of the hydrolyzable tannins are readily cleaved by esterases, tannins are assumed to have a limited persistence in the soil environment
– *Lipids* including fats, waxes, and natural hydrocarbons are naturally occurring compounds that produce fatty acids when hydrolyzed. In the soil environment, they form strong associations with humic acids and humin components
– *Glomalin*, a glue contributing to soil aggregation, is produced by mycorrhizal fungi
– *Black carbon*, or char, is a term to describe forms of pyrogenic carbon produced by incomplete combustion of organic substances

### 2.1.2.2 Stabilization of Soil Organic Matter

Studies of stabilization and destabilization of soil organic matter may provide some understanding of the effects of anthropogenic chemicals on natural soil constituents. Soil organic matter can be (a) physically stabilized or protected from decomposition

through microaggregation, (b) associated with salt and clay particles, and
(c) biochemically stabilized through the formation of recalcitrant compounds (Six
et al. 2002). The largest proportion of carbon input into stable soil organic matter pools
was found in microaggregates (Kong et al. 2005). The formation of organo-mineral
microaggregates (20–250 μm) is hypothesized to result from interactions of polyva-
lent metals and organic ligands with mineral surfaces, the nature and binding strength
being controlled by the surface area of the mineral (Guggenberger and Keiser 2003).
Occlusion of organic debris by the clay minerals was suggested as an additional type
of organo-mineral formation (e.g., Tisdall and Oades 1982; Jastrow 1996).

   A more recent study on spatial distribution of organic carbon in free stable
microaggregates (Lehman and Solomon 2007) shows no discernible gradient between
the interior and exterior of aggregates. Carbon distribution maps in three soils,
obtained by near-edge X-ray absorption fine structure (NEXAFS) spectroscopy, are
presented in Fig. 2.9a, b. These results suggest – at least for the soils studied – that
microaggregate formation is initiated mainly by accumulation of organics on clay
particle surfaces and not by occlusion of organic debris by clay minerals.
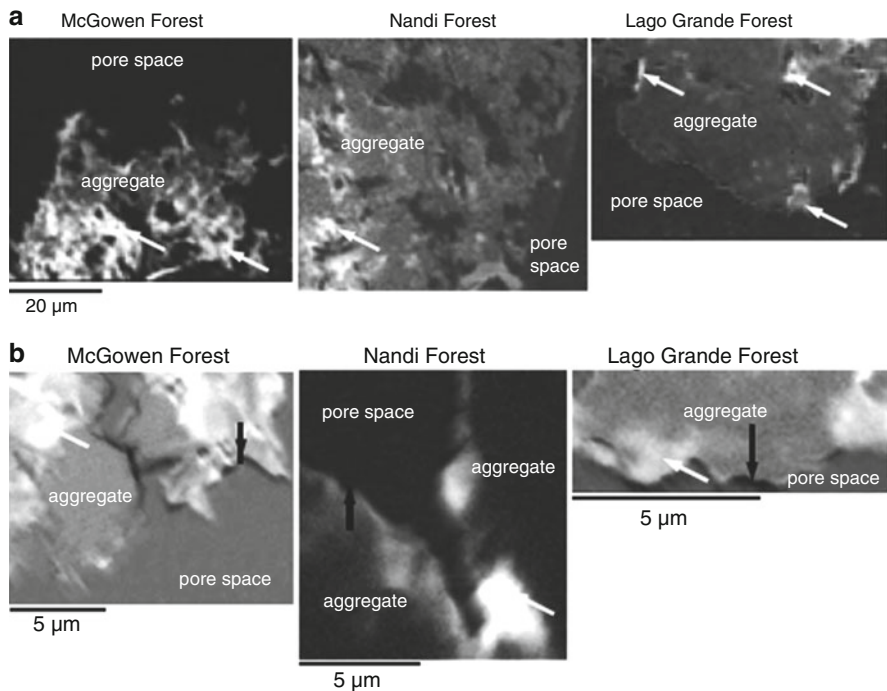


**Fig. 2.9** Carbon distribution in three different soils using C (1 s) NEXAFS (0.5-μm resolution)
(**a**) in free stable microaggregates; *white arrows* point at regions of high C content shown as *white
areas* (**b**) near microaggregate surfaces; *white arrows* point at regions of high C content shown
as white areas; *black arrows* point at *dark areas* of high absorbance consisting of clay coatings
(after Lehman and Solomon 2007)

## 2.2   Soil and Subsurface Liquid Phase

Within the soil–subsurface system, two liquid phases can be defined. One region, containing *near solid phase water*, has a composition controlled mainly by the properties of the surrounding surfaces. The second region, containing *free water*, has a composition affected by lithogenic and biogenic processes, the amount and quality of incoming water, and climatic changes reflected in drying/rewetting or freezing/thawing of subsurface water. The subsurface liquid phase is generally an open system and its composition is a result of dynamic transformations of dissolved constituents over a range of reaction time scales. At any particular time, the liquid phase is an electrolyte solution, potentially containing a broad spectrum of inorganic and organic ions and non-ionized molecules.

The composition of the subsurface liquid phase varies over time mainly due to recharge with rainwater, recharge with irrigation water, or the fluctuation of the water table (groundwater) level. In addition, anthropogenic chemicals discarded on the land surface as beneficial ingredients or hazard materials may change the natural quality of both near-surface and free soil and subsurface water.

### 2.2.1   Structure of the Water Molecule

The $H_2O$ molecule has a dipolar character with a high negative charge density near the oxygen atom and a high positive charge density near the protons. Horne (1969) showed that the electron cloud of the angular water molecule results from the hybridization of electrons in two bonding orbitals between the O and the two H atoms. This specific character strongly influences the interaction of water with the solid and air phases in the soil–subsurface system.

The local structure of water has been compared to ordinary hexagonal ice structures and calculated spectra. Synchrotron X-ray measurements have led to contrasting opinions regarding the H-bond coordination environment in liquid water. Wernet et al. (2004) used this technique, together with X-ray Raman scattering, to probe the molecular arrangement in the first coordination shell of liquid water. Most molecules in liquid water are in two hydrogen-bonded configurations, with one strong donor and one strong acceptor hydrogen bond, in contrast to the four hydrogen-bonded tetrahedral structures specific to ice. Heating water to $90°C$ causes about 10% of the molecules to change from tetrahedral environments to a two hydrogen-bonded configuration.

Water is a dynamic liquid where H-bonds are continuously broken and reformed. Wernet et al. (2004) showed that water, probed on the sub-femtosecond time scale, consists mainly of structures with two strong H-bonds, implying that most molecules are arranged in strongly H-bonded chains, or in rings embedded in a disordered cluster network connected mainly by weak H-bonds. These results are consistent with neutron and X-ray diffraction data, and confirm the theoretical

model of Weinhold (1998); this model considers an asymmetric H-bonding pattern in agreement with general quantum mechanical principles underlying H-bonding.

### 2.2.2  Near Solid Phase Water

Water molecules that are oriented preferentially with the polar axis perpendicular to the solid surface, in the vicinity of a solid surface, are considered "*near solid phase water*." When the net surface charge of the polar phase is negative, the hydration occurs through one hydrogen of water, forming a hydrogen bond with specific atoms at the boundary of the polar surface in such a way that the second hydrogen can still form a hydrogen bond with another water molecule outside the primary hydration level. In contact with a nonpolar solid, water molecules are oriented such that the positive hydrogen points into the bulk solution (Yariv and Cross 1979).

A water molecule exhibits a series of spatial arrangements with great irregularity as it moves through a bulk liquid phase. Unlike a solid, which has a well-defined structure, the liquid phase has instantaneous structures comprised of molecules in highly irregular arrangements. Stillinger (1980) conceives of liquid water as consisting of macroscopically connected random networks of hydrogen bonds with frequent, strained and broken bonds that continually undergo topological reformation. The water properties arise from competition among relatively bulky means of connecting molecules into local patterns, characterized by strong bonds and nearly tetrahedral angles, and more compact arrangements characterized by more strain and bond linkage.

The presence of an electrolyte introduces a localized perturbation of the "tetrahedral configuration." This perturbation derives from several sequences. Near the ion, water molecules are dominated by a dense electromagnetic field, resulting in the formation of the primary solvation shell. In the next zone, called the secondary solvation shell, water molecules interact weakly with the ion. An example of such behavior of an electrolyte solution near a clay surface was discussed by Sposito (1984). It was shown that the primary solvation shell of a monovalent cation contains between three and six water molecules that exchange relatively rapidly with the surrounding bulk liquid. A secondary solvation shell, if it exists, is very weakly developed. The primary solvation shell of a bivalent cation contains between six and eight water molecules that exchange rapidly with the surrounding bulk liquid. A secondary solvation shell containing about 15 water molecules develops as the cation concentration decreases, and it also moves with the cation as a unit.

The presently accepted description of the energy characteristics of the liquid phase is based on the concept of matrix and osmotic potentials. Matrix potential is due to the attraction of water to the solid matrix, while the osmotic potential is due to the presence of solute in the subsurface water. Water may bond to the soil and subsurface matrix by a combination of adhesive forces described by Koorevar et al. (1983): (1) adhesive forces – binding between the solid phase and water molecules, (2) cohesive forces – binding between water molecules, and (3) osmotic forces – binding due to gradients in

chemical potentials in electric double layer. Water binding properties of the solid phase matrix can be described by its thermodynamic properties (Slayter 1967). Water bound to the matrix is less able to work than free water, hence it has lost energy.

The configuration of near solid phase water can be altered in close proximity to the phyllosilicate. The siloxane surface influences the character of the water due to the nature of the charge distribution and of the complexes formed between the cation and the surface functional groups. Both the type of charge and the degree of charge localization, as well as the valence and size of the complexed cations, control the characteristics of the water molecules near the surface. Clay minerals with their own surface properties affect the near-surface water in different ways. The adsorbed water in the case of kaolinite consists only of water molecules ("pure" water), whereas water adsorbed on a smectite-type mineral is an aqueous solution due to the presence of exchangeable cations on the 2:1 layer silicate.

Sposito (1989) noted the generally accepted description that the spatial extent of adsorbed water on a phyllosilicate surface is about 1.0 nm (2–3 layers of water molecules) from the basal plane of the clay mineral. The interlayer water of clay minerals is structurally different from bulk liquid water or water in aqueous solution (Sposito and Prost 1982), and chemical reactions in this region are affected by a perturbed water structure. Another ability of the interlayer water is to diffuse widely over surface oxygens (e.g., smectites); a strong hydrogen bonding to the layer is not essential. The same patterns also follow when the cation is large and univalent. Under these conditions, a much less polar liquid can completely replace the interlayer water (Farmer 1978). Water is retained on oxides and hydroxides of aluminum and iron through the hydroxyl groups; it can also involve oxide bridges and water coordinated with structural cations. Retention of water on organic surfaces occurs also at a molecular level. Farmer (1978) stated that the principal polar sites where water adsorption occurs are likely to include carboxyl groups, e.g., phenolic and alcoholic groups, oxides, amines, aldehydes, and esters. Ionized carboxyilic groups and their associated cations are likely to have the greatest affinity for aqueous solutes. It should be recalled that in addition to polar sites, organic surfaces exhibit important hydrophobic regions which are involved largely in the retention of toxic organic chemicals.

### 2.2.3   Soil and Subsurface Solution

The soil and subsurface solution refers here to free water in the soil and subsurface porous medium, having a composition affected by the interaction between the incoming water and the resident solid and gaseous phases. The solution composition is determined under a dynamic partitioning between rain or irrigation water transported from the land surface and natural biological and vegetative processes. The chemical composition of the soil and subsurface solution at a given time is the end product of all the reactions to which the liquid water has been exposed. Because of the diversity in physicochemical properties of the solid phase, as well as changes

in the amount of water in the subsurface as result of natural and human influences, it is difficult to provide generalizations regarding the chemical composition of the soil and subsurface solution.

The thermodynamic properties of soil and subsurface solutions are expressed in terms of a single-species solution activity coefficient for each molecular constituent. The composition should, however, be considered on the basis of molecular speciation in the aqueous solution, which in turn is related to biological uptake exchange reactions and transport through the subsurface.

Soil and subsurface solutions may be delineated in terms of the following main characteristics:

*Acidity–alkalinity* of the solution, measured as pH, is affected by the quality of the incoming water (generally acidic for rain, and neutral or alkaline for irrigation and effluents) and buffered by the environmental system. *Salinity*, or total salt concentration, is usually expressed in terms of total dissolved solids (TDS) or as electrical conductivity (EC) of the solution. The major fractions of anions are comprised of $Cl^-$, $SO_4^{2-}$, and $NO_3^-$, while the common cations are $Ca^{2+}$, $Mg^{2+}$, $Na^+$, and $K^+$. The composition of the subsurface solution varies between the composition of water entering the system and that of the solution in equilibrium with the solid phase.

*Trace elements* of natural or anthropogenic origin, such as alkali and cationic materials, transition metals, nonmetals, and heavy metals, are inorganic elements that may also be found in subsurface solutions. The presence and concentrations of typical trace elements can differ significantly from one region to another. However as an indication, Table 2.4 shows representative trace element concentrations as reported by Sauvé et al. (2000). The properties of the soil–subsurface environment play an important role in metal solubility in soil and subsurface solutions. Adsorption is the most significant mechanism for distributing trace elements between the solid and liquid phases in the subsurface.

*Organic ligands* originate from humic substances, root exudates, or microbial enzymatic products. In soil and subsurface solutions, they may cause complexation of inorganic trace elements, which influences the equilibrium status between solid and

**Table 2.4** Range of trace elements observed for certain soil solution concentrations as estimated from the data compiled by Sauvé et al. (2000). Reprinted with permission from Sauvé S, Hendershot W, Allen HE (2000) Solid-solution partitioning of metals in contaminated soils: Dependence on pH, total metal burden, and organic matter. Environ Sci Tehnol 34:1125–1131. Copyright 2000 American Chemical Society

| Element | Soil solution ($\mu g\ L^{-1}$) |
| --- | --- |
| As | 0.5–60,000 |
| Cd | 0.01–5,000 |
| Cr | 2–500 |
| Cu | 5–10,000 |
| Ni | 0.5–5,000 |
| Pb | 0.5–500 |
| Se | 1–100,000 |
| Zn | 1–100,000 |

aqueous phases and affects their concentration in the subsurface solution. For example, humic acids in the soil and subsurface solution (1) are less aromatic and more highly oxidized than those that are components of solid humic substances, (2) have very few sugars and amino acids, and (3) are sterically protected from enzymatic attack in their humic association (Clapp et al. 2005). The organic trace compounds of natural or anthropogenic origin in soil and subsurface solutions are controlled by the nature and properties of subsurface colloids, the chemical and physicochemical characteristics of the organic molecules, and the nature of the environmental system.

*Seasonal changes* in soil and subsurface composition occur as result of climatic fluctuations and anthropogenic impacts. Soil drying and rewetting or freezing and thawing may affect soil and subsurface composition. The volume of solution in the subsurface, under partially saturated conditions, varies with the physical properties of the medium. In the soil layer, the composition of the soil solution fluctuates as a result of evapotranspiration or addition of water by rain or irrigation to the system. Changes in the solution concentration and composition, as well as the rate of change, are controlled by the buffer properties of the solid phase. Walworth (1992) note significant variability in the concentration of various parameters of soil solution composition, including EC, pH, $NH_4$, Ca, K, Mg, Na Cl, F, $NO_3$, and $SO_4$. Seasonal changes in the soil moisture content affect the ionic concentration, speciation, and activity of the soil solution (Wolt 1994).

Dyer et al. (2008) showed that the characteristics of soils control the effect of soil moisture on soil solution concentration; soil solution was extracted from a variable-charge soil (oxisols) and from several permanent-charge soils (vertisols) at moisture content potential ranging from $-5$ to $-230$ kPa. For the vertisols, a decrease in moisture content resulted in a proportionate increase in the soil solution ionic strength at a rate similar to that expected from a solution without any solid phase interaction. In contrast, the ionic strength of the soil solutions in oxisols remained constant as the soil moisture content decreased, and was associated with a decrease in the total amount of cations in the soil solution at lower moisture content.

### 2.2.4  Aquifers and Groundwater

An aquifer is defined as a saturated geological unit that can transmit significant quantities of water under ordinary hydraulic gradients. Aquifers form the region below the vadose zone where the solid phase is in contact with a flowing groundwater phase and where a local chemical equilibrium between the solid and aqueous phases has a tendency to be reached. Within the context of aquifers, an aquitard is defined as a less permeable geological unit that has the potential to store water in significant quantities. In addition to geological controls of an aquifer, groundwater composition is affected by properties of recharge water, which originates from the initial incoming water constituents.

The lithology, stratigraphy, and structure of a geological system control the nature and distribution of aquifers. Lithology includes the mineral composition,

grain size, and grain aggregation of the sediments or rocks; stratigraphy defines the relation among the lenses, beds, and formations of geological sediments; and structural features describe the geometry of the geological system resulting from deformation.

According to their origins, aquifer materials may be classified as deposits of various origins, and as sedimentary or metamorphic rocks. Aquifers of fluvial origin are characterized by alluvial deposits composed of particles of gravel, silt, and clay of various sizes that are not bound or hardened by mineral cement, pressure, or temperature. The topography controls the deposition of sediments and their spatial redistribution as a function of their textural properties. Aeolian deposits consisting of sand or silt are more homogeneous in comparison to fluvial deposits. Glacial deposits including glacial till and glaciofluvial and glaciolacustrine sediment forms are also components of aquifers. The type and origin of sediments affect their permeability, which in turn controls the water transmission potential of aquifers.

Sedimentary rocks, consisting mostly of sandstones and carbonates, are bodies of major hydrological significance. Sandstone comprises about 25% of the sedimentary rocks, originating from environmental depositions (e.g., floodplain, deltaic and marine shoreline), which are characterized by cementing materials like quartz, calcite, and clays in various stages of alteration (Freeze and Cherry 1979). Porosity of sandstone in extreme cases can be as low as 1%, compared to that of sands that reach only as low as 30%. The relationship between porosity and permeability for various grain sizes shows that an increase in porosity of a few percent generally corresponds to a large increase in permeability (Chilingar 1963).

Carbonate rocks consist mostly of calcite and dolomite with minor amounts of clay. The porosity of carbonate rocks ranges from 20 to 50%, but in contrast to sandstones, it tends to decrease with depth. Often carbonate rocks are fractured, providing a permeability that is much greater than the primary one. In some cases, initial small-scale fractures in calcite and dolomite are enlarged by dissolution during groundwater flow, leading to an increase in rock permeability with time. Igneous and metamorphic rocks, which exhibit a low porosity generally smaller than 2%, are characterized by a minute permeability. As result of changes in stress conditions occurring during geological periods, wide fractures are formed which lead to a substantial increase in the permeability of igneous and crystalline metamorphic rocks. Dissolution of siliceous rocks increases the widths of fractures and consequently increases their permeability. However, the permeability of crystalline rocks usually decreases with depth.

*Groundwater composition* is controlled by chemical and biochemical interactions with the geological materials through which water flows, as well as by the chemistry of incoming water. Because inorganic components dissolved in groundwater are mainly in an ionic form, groundwater may be considered an electrolyte solution with a conductance ranging from tens of microsiemens (a value close to that of rain water) to hundreds of thousands of microsiemens (for brines in sedimentary basins). Dissolved inorganic constituents are grouped in three classes: major constituents, with concentrations greater than 5 mg L$^{-1}$; minor constituents with a concentration

**Table 2.5** Dissolved inorganic substances in groundwater (modified from Freeze and Cherry 1979). Reprinted with permission

| Category | Components |
| --- | --- |
| Major constituents (greater than 5 mg $L^{-1}$) | Bicarbonate, calcium, carbonic acid, chloride, magnesium, silicon, sodium, sulfate |
| Minor constituents (0.1–10.0 mg $L^{-1}$) | Boron, carbonate, fluoride, iron, nitrate, potassium, strontium |
| Selected trace constituents (less than 0.1 mg $L^{-1}$) | Aluminum, arsenic, barium, bromide, cadmium, chromium, cobalt, copper, gold, iodide, lead, lithium, manganese, molybdenum, nickel, phosphate, radium, selenium, silver, tin, titanium, uranium, vanadium, zinc, zirconium |

between 0.01 and 5.0 mg $L^{-1}$; and trace constituents having a concentration of less than 0.01 mg $L^{-1}$. Table 2.5 gives examples of constituents included in these groups.

Organic contaminants may be found in groundwater in dissolved forms, associated with ligands or adsorbed on colloidal materials. Natural products such as humic and fulvic acids have a low aqueous solubility but may serve as ligands for inorganic trace components. The majority of organic pollutants – including petroleum hydrocarbons, solvents and toxic organic chemicals of industrial origin known as nonaqueous phase liquids (NAPLs) – exhibit a limited solubility in aqueous solutions, with usually very low concentrations. However, it should be recognized that even low solubility limits (and the corresponding concentration) are usually several orders of magnitude higher than the maximal allowable concentrations for potable water. As a consequence, NAPLs as a mixture or as individual components can be found in groundwater in concentrations exceeding concentrations stipulated by environmental protection agencies. In addition, inorganic polymers, various natural ligands (e.g., bio-exudates), or surfactants may also serve as mediators that shuttle organic pollutants toward groundwater via the vadose zone.

Groundwater may contain dissolved gases as a result of exposure to the surface environment prior to water infiltration, contact with the subsurface gaseous phase, and gas produced biologically below the water table. The most important dissolved gas in groundwater is $CO_2$.

# References

Allen BL, Fanning DS (1983) Composition and soil genesis. In: Wilding EP (ed) Pedogenesis and soil taxonomy: I concepts and interactions. Elsevier, New York

Bailey SW, Brindley GW, Johns WD, Martin RT, Ross M (1971) Clay mineral society report on nomenclature committee 1969–1970. Clay Clay Miner 19:132–133

Barnhisel RL, Bertsch PM (1989) Chloride and hydroxy-interlayered vermiculite and smectite. In: Dixon JB, Weeds SB (eds) Minerals in soils. SSSA, Madison, WI, pp 730–789

Barrer RM, Jones DL (1970) Chemistry of soil minerals 8. Synthesis and properties of fluorhectorites. J Chem Soc A: 1531–1537

Barshad I (1960) Thermodynamics of water adsorption and desorption on montmorillonite. Clays Clay Miner 8:84–101

Borchard G (1989) In: Dixon JB, Weeds SB (eds) Minerals in soils. SSSA, Madison, WI, pp 675–728

Brady PV, Cygan RT, Nagy KL (1996) Molecular controls of kaolinite surface charge. J Colloid Interf Sci 183:356–364

Brindley GW, MacEvan DMC (1953) Structural aspects of the mineralogy of clays and related silicates. In: Green AT, Stewart GH (eds) A Symposium. The British Ceramic Society, Stoke on Trent, UK, pp 15–59

Burdon J (2001) Are the traditional concepts of the structure of humic substances realistic? Soil Sci 199:752–769

Chester R, Green RN (1968) The infrared determination of quartz in sediments and sedimentary rocks. Chem Geol 3:199–212

Chilingar GV (1963) Relationship between porosity, permeability and grain size distribution of sands and sandstones. Proc inter Sedimentol Congr, Amsterdam

Clapp CE, Hayes MHB, Simpson AJ, Kingery WL (2005) Chemistry of soil organic matter. In: Tabatabai MA, Sparks DL (eds) Chemical processes in soils. SSSA Book Series, Madison WI, pp 1–150

Dennen WH (1966) Stoichiometric substitution in natural quartz. Geochim Cosmochim Acta 30:1235–1241

Dixon JB (1989) Kaoline and serpentine group minerals. In: Dixon JB, Weeds SB (eds) Minerals in soils. SSSA, Madison, WI, pp 468–527

Drees LR, Wilding LP, Smeck NE, Senkayi AL (1989) Silica in soils, quartz and disordered silica polymorphs. In: Dixon JB, Weeds SB (eds) Minerals in soil environments. 2nd ed, SSSA Book Series 1, Madison, WI, pp 913–974

Dyer CL, Kopittke PM, Sheldon AR, Memzies NW (2008) Influence of soil moisture content on soil solution composition. Soil Sci Soc Am J 72:355–361

Essington ME (2004) Soil and water chemistry: an integrative approach. CRC, Boca Raton, FL

Farmer VC (1978) Water on partial surfaces. In: Greenland DJ, Hayes NHB (eds) The chemistry of soil constituents. Wiley, NY, pp 405–449

Farmer VC, Russel HD (1967) Infrared absorption spectrometry in clay studies. Clay Clay Miner 15:121–142

Freeze RA, Cherry JA (1979) Groundwater. Prentice Hall, Engelwood Cliffs, NJ

Frondel C (1962) Dana's system of mineralogy. III Silica minerals. Wiley, New York

Giese RF Jr (1982) Theoretical studies of the kaolin minerals: electrostatic calculation. Bull Mineral 105:417–424

Gilkes RY (1990) Mineralogical insights into soil productivity: An anatomical perspective. In: Proc 14th Congress of Soil Sci, Kyoto, Japan Trans Plenary Papers. pp 63:73

Grim RE (1962) Clay mineralogy. Science 135:890–898

Gruner JW (1932) Crystal structure of kaolinite. Z Kristallogr 83:75–88

Guggenberger G, Keiser K (2003) Dissolved organic matter in soil: challenging the paradigm of sorptive preservation. Geoderma 113:293–310

Hatcher PG, Spiker EC (1988) Selective degradation of plant biomolecules. In: Frimel FH, Christman RF (eds) Humic substances and their role in the environment. Wiley, Chichester, UK, pp 59–74

Hayes MHB, Malcom RL (2001) Consideration of composition and aspects of the structure of humic substances. In: Clapp CE, Hayes MHB, Senesi N, Bloom PR, Jardine PM (eds) Humic substances and chemical contaminants. SSSA, Madison, WI, pp 1–39

Hayes MHB, Swift RR (1978) The chemistry of soil organic colloids. In: Greenland DJ, Hayes MHB (eds) The chemistry of soil constituents. Wiley, Chichester, UK, pp 170–320

Herbillon AJ, Frankart R, Vielvoye L (1981) An occurrence of interstratified kaolinite-smectite minerals in a red-black soil toposequence. Clay Miner 16:195–201

Horne RE (1969) Marine chemistry. Wiley, NY

Hurlbut CS, Klein C (1977) Manual of mineralogy. Wiley, New York

Jackson ML (1964) Chemical composition of soils. In: Bear FE (ed) Chemistry of the soil, 2nd edn. Van Nostrand-Reinhold, New York, pp 71–141

Jansen S, Malaty AM, Nabara S, Johnson E, Ghabbour E, Davies G, Vanum JM (1996) Structural modeling in humic acids. Mater Sci Eng C4:175–179

Jastrow JD (1996) Soil aggregate formation and accrual of particulate and mineral associated organic matter. Soil Biol Biochem 28:665–676

Katz MYA, Katz MM, Rasskazov AA (1970) Mineral studies in the gravitation gradient field 2. Changes of quartz and density due to natural and experimental "maturation". Sedimentology 15:161–177

Kaviratna PD, Pinnavaia TJ, Schroeder PA (1996) Dielectric properties of smectite clays. J Phys Chem Solids 57:1897–1906

Kleber M, Sollins P, Sutton RA (2007) A conceptual model of organo mineral interactions in soils: self assembly of organic molecular fragments in multilayered structure on mineral surfaces. Biogeochemistry 85:9–24

Kong AYY, Six J, Bryant DC, Denison RF, Kessel C (2005) The relationship between carbon input, aggregation and soil organic carbon stabilization in sustainable cropping systems. Soil Sci Soc Am J 69:1078–1085

Kononova MM (1966) Soil organic matter: its nature, its role in soil formation and fertility, 2nd edn. Pergamon, Oxford, UK

Koorevar P, Menelik G, Dirksen C (1983) Elements of soil physics, developments in soil science #13. Elsevier, Amsterdam

Leenheer JA, Nanny MA, McIntyre C (2003) Terpenoids as major precursors of dissolved organic matter in landfill leachates, surface water, and groundwater. Environ Sci Technol 37:2323–2331

Lehman KJ, Solomon D (2007) Organic matter stabilization in soil microaggregates: implications from spatial heterogeneity of organic carbon contents and carbon forms. Biogeochemistry 85:45–57

Lim CH, Jackson ML, Koons RD, Helmke PA (1980) Kaolons: sources of differences in cation-exchange capacities and cesium retention. Clays Clay Miner 28:223–229

Low PF (1981) The swelling of clay: III dissociation of exchangeable cations. Soil Sci Soc Am J 45:1074–1078

Margolis SV, Krinsley DH (1974) Processes of formation and environmental occurrence of microfeatures on detrital quartz grains. Am J Sci 274:449–464

Melo VF, Singh B, Schaefer CEGR, Novais RF, Fontes MPF (2001) Chemical and mineralogical properties of kaolinite-rich Brazilian Soils. Soil Sci Soc Am J 65:1324–1333

Morgan DJ, Highley DE, Bland DJ (1979) A montmorillonite, kaolinite association in the Lower Cretaceous of south-west England. In: Mortaland M, Farmer VC (eds) Proc Int Clay Conf. Pergamon, Oxford, pp 301–310

Piccolo A (2001) The supramolecular structure of humic substances. Soil Sci 166:810–832

Sauvé S, Hendershot W, Allen HE (2000) Solid-solution partitioning of metals in contaminated soils: dependence on pH, total metal burden, and organic matter. Environ Sci Technol 34:1125–1131

Schofield RK, Samson HR (1953) The deflocculation of kaolinite suspension and the accompanying change-over from positive to negative chloride adsorption. Clay Miner Bull 2:45–51

Schofield RK, Samson HR (1954) Flocculation of kaolinite due to the attraction of oppositely charged crystal faces. Discuss Faraday Soc 18:135–145

Schulten HR (2001) models of humic structure :association of humic acids and organic matter in soils and water. In: Clapp CE, Hayes MHB, Senesi N, Bloom PR, Jardine PM (eds) Humic substances and chemical contaminants. SSSA, Madison, WI, pp 73–88

Schulten HR, Schnitzer M (1993) A state of the art: structural concept for humic substances. Naturwissenschaften 80:29–30

Schulten HR, Schnitzer M (1997) Chemical model structures for soil organic matter and solid. Soil Sci 162:115–130

Schulze DG (1989) An introduction to soil mineralogy. In: Dixon JB, Weed SB (eds) Minerals in soil environments. SSSA Book Series 1, Madison, WI

Six J, Connant RT, Paul EA, Paustian K (2002) Stabilization mechanism of soil organic matter: implication for C-saturation of soils. Plant Soil 241:155–176

Slayter RO (1967) Plant-water relationships. Academic, London, p 366

Sposito G (1973) Volume changes in swelling soils. Soil Sci 115:315–320

Sposito G (1984) The surface chemistry of soils. Oxford University Press, New York

Sposito G (1989) The chemistry of soils. Oxford University Press, New York

Sposito G, Prost R (1982) Structure of water on smectites. Chem Rev 82:553–573

Stevenson FJ (1994) Humus chemistry, 2nd edn. Wiley, New York

Stillinger FH (1980) Water revisited. Science 209:451–453

Stober W (1967) Formation of silicic acid in aqueous suspension of different silica modification. In: Goulded RF (ed) Equilibrium concepts in natural water systems. Adv Chem Ser 67:161–172

Sutton R, Sposito G (2005) Molecular structure in soil humic substances: the new view. Environ Sci Technol 39:9009–9011

Tisdall JM, Oades JM (1982) Organic matter and water stable aggregates in soil. J Soil Sci 33:141–163

Walworth JL (1992) Soil drying and rewetting or freezing and thawing affects soil solution composition. Soil Sci Soc Am J 56:433–437

Weinhold F (1998) Quantum cluster equilibrium theory of liquids: illustrative application to water. J Chem Phys 109:373–384

Wernet P, Nordlund D, Bergman U, Cavalleri M, Odelius M, Ogasawara H, Naslund LA, Hirsh TK, Ojamae L, Glazel P, Petterson LGM, Nilsson A (2004) The structure of the first coordination shell in liquid water. Science 304:995–999

Wershaw RL (1986) A new model for humic materials and the interaction with hydrophobic chemicals in soil-water or sediment-water. J Contam Hydrol 1:29–45

Wershaw RL (1993) Model for humus in soils and sediments. Environ Sci Tech 27:814–816

Wershaw RL (2000) The study of humic substances – In search of a paradigm. In: Ghabbour EA, Devies G (eds) Humic substances, versatile components of plants, soil and water. Royal Soc Chem Cambridge, Cambridge, UK, pp 1–7

Wershaw RL, Llaguno EC, Leenheer JA (1996) Mechanism of formation of humus coatings on mineral surfaces 3. Composition of adsorbed organic acids from compost leachate on alumina by solid-state (13) CNMR. Coll Surf A-Physicochem Eng Aspects 108:213–223

Wilding LP, Smeck NE, Drees LR (1989) Silica in soils. In: Dixon JB, Weeds SB (eds) Minerals in soils. SSSA, Madison WI, pp 471–553

Wolt JD (1994) Soil solution chemistry; application to environmental science and agriculture. Wiley, New York

Yariv S, Cross H (1979) Geochemistry of colloid systems. Springer, Heidelberg

Yaron-Marcovich D, Chen Y, Nir S, Prost R (2005) High resolution electron microscopy structural studied of organo-clay nanocomposites. Environ Sci Technol 39:1231–1239

Yerima BPK, Calhoun FG, Senkayi AL, Dixon JB (1985) Occurrence of interstratified kaolinite-smectite in El Salvador vertisols. Soil Sci Soc Am J 49:462–466

# Chapter 3
# Properties and Behavior of Selected Inorganic and Organometallic Contaminants

## 3.1 Introductory Comments

We discuss the potential sources, properties, and chemistry of several major groups of contaminants found in the soil–subsurface environment. Usually, the release of contaminants to the environment originates from anthropogenic processes. Even when the contaminants are naturally occurring species, human intervention or changes in natural conditions are often involved in the development of pollution. Furthermore, many contaminants are relatively persistent and may, therefore, be found in the soil–subsurface environment long after their actual release.

The massive industrial development that has improved quality of life and influenced the world over the last two centuries has also had a profound impact on the amounts and types of compounds released to the soil–subsurface environment. Over this period, many thousands of new materials have been produced, used, stored, transported, and subsequently discarded. In parallel, the understanding that many compounds may be toxic or hazardous to ecological systems, in general, and to humans, in particular, has gradually evolved during the last 50 years. This understanding is dependent largely on complex analytical capabilities: environmental samples contain very low concentration of target substance(s), and such samples often contain large amounts of interfering compounds.

In addition to release of contaminants, there are many anthropogenic factors that generate processes which can irreversibly change soil and subsurface properties. Some examples are acid rain, which leaches several soil microelements, increased salinity of soil due to changes in irrigation practice and overpumping of groundwater, and changes to soil acidity (or alkalinity). These processes can be of large scale and very influential in terms of their impact on the soil–subsurface environment.

The following sections discuss only a small portion of the potential contaminants that belong to each group; we have attempted to choose representative materials that provide a broad view of the subject. Finally, it should be mentioned that because other aspects of chemical interactions and transport of such substances in the soil–subsurface environment are discussed in other parts of this book, we focus

here mainly on the sources of potential pollution and properties that make these compounds contaminants.

## 3.2   Nitrogen Forms

Nitrogen is a key building block in all living forms; it is an essential element in many fundamental cell components such as proteins, DNA, RNA and vitamins, as well as hormones and enzymes. Nitrogen is an extremely versatile element, existing in both inorganic and organic forms as well as in many different oxidation states. Nitrogen gas constitutes almost 80% of the atmosphere and is, therefore, present almost everywhere. However, nitrogen gas is not available for use by most organisms. For plants and animals to be able to use nitrogen, $N_2$ gas must first be converted to a more chemically available form, such as ammonium ($NH_4^+$), nitrate ($NO_3^-$), or organic nitrogen (e.g., urea ($NH_3)_2CO$). Furthermore, higher organisms (e.g., animals) cannot use these simple forms of nitrogen, such as nitrate and ammonium, and require even more complex forms, such as amino acids and nucleic acids.

Some of the relevant properties of nitrate and nitrite ions are given in Table 3.1. The nitrate ion ($NO_3^-$) is a stable form and although chemically unreactive, it can be reduced by microbial activity. The nitrite ion ($NO_2^-$) contains nitrogen in a relatively unstable oxidation state. Chemical and biological processes can further reduce nitrite to various compounds or oxidize it to nitrate.

To sustain the food needs of the world's growing population, it is essential to maintain modern agriculture, which in turn is dependent on a constant supply of nitrogen fertilizers that support enhanced agricultural production. Currently, the main technology for the "fixation" of atmospheric nitrogen is the *Haber–Bosch method*, which was developed in Germany between 1908 and 1910, and is now the primary process in the production of over 99% of nitrogen fertilizer materials (Alan 2004). Nitrogen fertilizers have been produced and applied in very large amounts to field crops around the world for several decades; in the years 1980, 1990, and 2000, for example, the world "fixed" N production by the Haber–Bosch process, in amounts that increased from 59,290 KT, to 76,320 KT, to 85,130 KT, respectively

Fixed nitrogen in the subsurface results from many processes and is applied in many forms and materials. Fixation by rhizobium–legume combinations or by free-living organisms adds N directly to the crop or the soil organic forms. Animal

**Table 3.1** Physicochemical properties of nitrate and nitrite (ICAIR Life Systems, Inc. 1987)

| Property | Nitrate | Nitrite |
|---|---|---|
| Acid | Conjugate base of strong acid $HNO_3$; $pK_a = -1.3$ | Conjugate base of weak acid $HNO_2$; $pK_a = 3.4$ |
| Salts | Very soluble in water | Very soluble in water |
| Reactivity | Unreactive | Reactive; Oxidizes antioxidants, $Fe^{2+}$ of hemoglobin (Hb) to $Fe^{3+}$, and primary amines; nitrosates several amines and amides |

manure, sewage sludge, crop residues, and roots add organic nitrogen materials, which are then mineralized to give ammonium, which is further transformed to nitrate. Other possible sources of nitrogen formed in the environment include wastewater treatment, and oxidation of nitrogenous waste products in human and animal excreta, including septic tanks. Nitrite can also be formed chemically in distribution pipes by *Nitrosomonas* bacteria, during stagnation of nitrate-containing and oxygen-poor drinking water in galvanized steel pipes, or if chloramination is used to provide a residual disinfectant and the process is not sufficiently well controlled. Because plants often cannot utilize all of the nitrogen applied to agricultural fields, some is left in the soil and can leach into the groundwater (Pratt and Jury 1984). In addition, some of the applied nitrogen does not infiltrate the soil, and is washed away in the form of runoff, flowing into surface waters such as streams and rivers.

In soil, fertilizers containing inorganic nitrogen and wastes containing organic nitrogen are first decomposed to give ammonia, which is then oxidized to nitrite and nitrate. The nitrate is taken up by plants during their growth and used in the synthesis of organic nitrogenous compounds. Surplus nitrate moves readily with the groundwater (van Duijvenboden and Matthijsen 1989; EPA 1987).

Under aerobic conditions, nitrate percolates in large quantities into groundwater systems because of the small extent to which denitrification or degradation occurs. Under anaerobic conditions, nitrate may be denitrified or degraded almost completely to nitrogen. The presence of high or low water tables, the amount of rainwater, the presence of other organic material, and other physicochemical properties are also important in determining the fate of nitrate in soil (van Duijvenboden and Loch 1983). In surface water, nitrification and denitrification may occur, depending on temperature and pH. The uptake of nitrate by plants, however, is responsible for most of the nitrate reduction in surface water.

Nitrogen compounds are also formed in the atmosphere, by lightning, or discharged into it from industrial processes, motor vehicles, and intensive agriculture. Nitrate is present in air primarily as nitric acid and inorganic aerosols, as well as nitrate radicals and organic gases or aerosols. These are removed by wet and dry deposition.

Concentrations of nitrate in rainwater of up to 5 mg $L^{-1}$ have been observed in industrial areas (van Duijvenboden and Matthijsen 1989). In rural areas, concentrations are somewhat lower. The nitrate concentration in surface water is normally low (0–18 mg $L^{-1}$), but can reach high levels as a result of agricultural runoff, refuse dump runoff, or contamination with human or animal wastes. The concentration often fluctuates with the season and may increase when, for example, a river is fed by nitrate-rich aquifers. Nitrate concentrations have gradually increased in many European countries over the last few decades and have in some cases doubled over the past 20 years. In the United Kingdom, for example, an average annual increase of 0.7 mg $L^{-1}$ has been observed in some rivers (Young and Morgan-Jones 1980).

The natural nitrate concentration in groundwater, under aerobic conditions, is a few milligrams per liter and depends strongly on soil type and the geological situation. In the USA, naturally occurring levels do not exceed 4–9 mg $L^{-1}$ for nitrate and 0.3 mg $L^{-1}$ for nitrite (EPA 1987). As a result of agricultural activities, however, the

nitrate concentration can easily reach several hundred milligrams per liter (WHO 1985). For example, concentrations of up to 1,500 mg $L^{-1}$ were found in groundwater in an agricultural area of India (Jacks and Sharma 1983). In the USA, nitrates are present in most surface water and groundwater supplies at levels below 4 mg $L^{-1}$, with levels exceeding 20 mg $L^{-1}$ in about 3% of surface waters and 6% of groundwater. In 1986, a nitrate concentration of 44 mg $L^{-1}$ (10 mg of nitrate nitrogen per liter) was exceeded in 40 surface water and 568 groundwater supplies. Nitrite levels were not surveyed but were expected to be much lower than 3.3 mg $L^{-1}$ (EPA 1987).

The increasing use of artificial fertilizers, the disposal of wastes (particularly from animal farming), and changes in land use are the main factors responsible for the progressive increase in nitrate levels in groundwater supplies over the last 20 years. In Denmark and the Netherlands, for example, nitrate concentrations are increasing by 0.2–1.3 mg $L^{-1}$ per year in some areas (WHO 1985). Because of the delay in the response of groundwater to changes in soil, some endangered aquifers have not yet shown the increase expected from the increased use of nitrogen fertilizer or manure. Once the nitrate reaches these aquifers, they will remain contaminated for decades, even if there is a substantial reduction in the nitrate loading of the surface.

In most countries, nitrate levels in drinking water derived from surface water do not exceed 10 mg $L^{-1}$. In some areas, however, concentrations are higher as a result of runoff and the discharge of sewage effluents and certain industrial wastes. In 15 European countries, the percentage of the population exposed to nitrate levels in drinking water above 50 mg $L^{-1}$ ranges from 0.5 to 10% (ECETOC 1988; WHO 1985); this corresponds to nearly ten million people.

Nitrogen is also released in the form of nitrite. For example, sodium nitrite is used as a food preservative, especially in cured meats. Chloramination may give rise to the formation of nitrite within the distribution system, and the concentration of nitrite may increase as the water moves toward the extremities of the system.

## 3.3 Phosphorus Forms

Phosphorus is one of the inorganic macronutrients in all known forms of life. Inorganic phosphorus in the form of phosphate ($PO_4^{3-}$) plays a major role in vital biological molecules, such as DNA and RNA. Living cells also utilize phosphate to transport cellular energy via adenosine triphosphate (ATP). Phospholipids are the main structural components of all cellular membranes. Calcium phosphate salts are used by animals to stiffen their bones, and adequate phosphorus supplies are necessary for seed and root formation.

The principal phosphorus forms in the subsurface are Ca-phosphate, adsorbed phosphates, occluded phosphates, and organic phosphate (Mengel 1985; Lindsay 1979). The principal phosphate mineral is apatite (or fluorapatite), $Ca_{10}(PO_4)_6(OH, F)_2$. Secondary minerals include silica, silicates, and carbonates, generally as calcite or dolomite. Usually, these minerals are utilized as a raw material source for the

production of phosphorus fertilizers. Many soils in their natural state are low in readily available P. For example, typical levels of phosphorus in subsurface solutions of unfertilized soils range from 0.001 to 0.1 mg $L^{-1}$ P (Hook 1983). Therefore, intensive agricultural activity requires fertilization to achieve maximum possible yields. Application of phosphorus to soil as fertilizer, manure, or effluents results in an immediate rise in the concentration of utilizable phosphorus. It was once thought that P was completely immobile in soil, and therefore farmers were encouraged to increase phosphate fertilizer application without fear that P applied in excess of crop requirements would be lost from the soil profile. The P cycle in the soil–subsurface environment is depicted in Fig. 3.1.

Phosphorus persistence is related to the soil–subsurface system properties. Phosphorus loss from soils occurs mainly through crop removal, runoff, and leaching. The uptake of phosphorus by agricultural crops, for example, varies greatly (i.e., 10–100 kg $ha^{-1}$ $year^{-1}$). While subsurface pathways can be significant in P transfer to water, especially in soils with low P retention properties and/or significant preferential flow pathways, it is reasonably well established that, in most watersheds, P export occurs mainly in overland flow. Soils that have been used heavily for agricultural crops are often deficient in phosphorus, as are acidic sandy and granitic soils. In landscaped urban soils, however, phosphorus is rarely deficient and the misapplication of this element can have serious repercussions on plants, the soil environment, and adjoining watersheds.
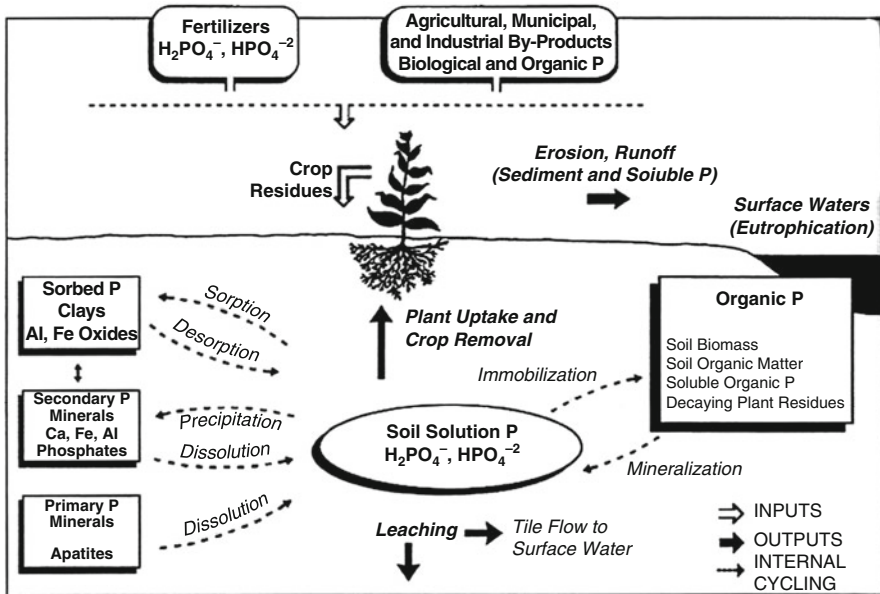


**Fig. 3.1** The soil P cycle: an overview of the physical, chemical, and microbiological processes controlling the availability of P to plants, and P transport in runoff or leaching waters (after Pierzynski et al. 2000)

Often in aquatic systems, an excess of phosphorus may cause eutrophication. Eutrophication has been linked to many aspects of water quality degradation, including fish kills, loss of biodiversity and recreational uses of waters, and the onset of harmful algal blooms that can pose a threat to human health (Burkholder et al. 1999). Phosphorus losses from agricultural production systems are known to contribute to accelerated eutrophication of natural waters (Toor et al. 2003; Sims et al. 1998). This is especially true in areas with intensive animal farming, where repeated manure applications have led to excessive accumulation of P in soils. Substantial evidence exists to show that higher P concentrations in soils can result in increased P losses to natural waters (Sharpley and Tunney 2000; Sims et al. 1998).

Organic compounds of phosphorus form a wide class of materials, some of which are extremely toxic. Fluorophosphate esters are among the most potent neurotoxins known. A wide range of organophosphorus compounds are employed for their toxicity to certain organisms, such as pesticides (herbicides, insecticides, and fungicides), and developed as nerve agents in weapons. In contrast, most inorganic phosphates are relatively nontoxic and essential nutrients.

## 3.4   Radionuclides

Radionuclides are present in the environment both as naturally occurring species and as anthropogenic substances. Emission of ionizing radiation during the decay of active atoms is the main contamination route for this group of pollutants: this radiation can disrupt atoms, creating positive ions and negative electrons, and cause biological harm. Exposure to large radiation doses can be fatal to humans, while lower doses cause mainly elevated cancer risks (Shaw 2005; Zhu and Shaw 2000; Stannard 1973). Ionizing radiation may be emitted in the process of natural decay of some unstable nuclei or following excitation of atoms and their nuclei in nuclear reactors, cyclotrons, X-ray machines, or other instruments.

The exposure to ionizing radiation from natural sources is continuous and unavoidable. For most individuals, this exposure exceeds that from all human-made sources combined (UNSCEAR 2000a). The two main contributors to natural radiation exposures are high-energy cosmic ray particles incident on the earth's atmosphere and radioactive nuclides that originate in the earth's crust and are present everywhere in the environment, including the human body itself.

Naturally occurring radionuclides of terrestrial origin (also called *primordial radionuclides*) are present in various degrees in all media in the environment. Only the radionuclides with half-lives comparable to the age of the earth, and their decay products, exist in significant quantities in these materials. Irradiation of the human body from external sources is mainly by gamma radiation from radionuclides in the $^{238}U$ and $^{232}Th$ series and from $^{40}K$. These radionuclides are also present in the body and irradiate the various organs with alpha and beta particles, as well as gamma rays. Some other terrestrial radionuclides, including those of the $^{235}U$ series, $^{87}Rb$, $^{138}La$,

$^{147}$Sm, and $^{176}$Lu, exist in nature but at such low levels that their contributions to the dose in humans are small.

Exposure from terrestrial radionuclides present at trace levels in all soils is specific and related to the types of rock from which the soils originate. Higher radiation levels are associated with igneous rocks, such as granite, and lower levels with sedimentary rocks. There are exceptions, however, as some shales and phosphate rocks have relatively high contents of radionuclides. Radon and its short-lived decay products in the atmosphere are the most important contributors to human exposure from natural sources.

The main human-made contribution to exposure of the world's population has come from the testing of nuclear weapons in the atmosphere, from 1945 to 1980 (UNSCEAR 2000b). Each nuclear test resulted in unrestrained release into the environment of substantial quantities of radioactive materials, which were dispersed widely in the atmosphere and deposited everywhere on the earth's surface. Underground testing caused exposures beyond the test sites only if radioactive gases leaked or were vented. Most underground tests had much lower yields than atmospheric tests, and it usually was possible to contain the debris. Underground tests were conducted at the rate of 50 or more per year from 1962 to 1990. During the time when nuclear weapon arsenals were being expanded, especially in the earlier years (1945–1960), radionuclide releases exposed local populations downwind or downstream of nuclear installations. At the time, there was little recognition of exposure potentials, and monitoring of releases was limited. More recent controls on the military fuel cycle have now diminished exposures to very low levels.

Several industries process or utilize large volumes of raw materials containing natural radionuclides. Discharges from these industrial plants to air and water and the use of by-products and waste materials may contribute to enhanced exposure of the general public. A list of radionuclides responsible for most environmental concerns is given in Table 3.2. Estimated maximum exposures arise from phosphoric acid production, mineral sand processing industries, and coal-fired power stations. Except in the case of accidents or at sites where wastes have accumulated, causing localized areas to be contaminated to significant levels, no other practices result in important exposures of radionuclides released into the environment. Estimates of releases of isotopes produced and used in industrial and medical applications are being reviewed, but these seem to be associated with rather insignificant levels of exposure.

**Table 3.2** Characteristics of major radionuclides that occur in soil (after Zhu and Shaw 2000). Reprinted from Zhu YG, Shaw G, Soil contamination with radionuclides and potential remediation. Chemosphere 41:121–128, Copyright (2000), with permission from Elsevier

| Isotope | Half-life (year) | Principal radiation | Main occurrence |
|---------|------------------|---------------------|-----------------|
| $^{14}$C | $5.7 \times 10^3$ | $\beta^-$ | Natural and nuclear reactor |
| $^{40}$K | $1.3 \times 10^9$ | $\beta^-$ | Natural |
| $^{90}$Sr | 28 | $\beta^-$ | Nuclear reactor |
| $^{134}$Cs | 2 | $\beta^-$, $\gamma$ | Nuclear reactor |
| $^{137}$Cs | 30 | $\beta^-$, $\gamma$ | Nuclear reactor |
| $^{239}$Pu | $2.4 \times 10^4$ | $\alpha$, X-rays | X-rays, nuclear reactor |

When accidents occur, environmental contamination and exposures may become significant. The accident at the Chernobyl (Russia) and that recently at the Fukushima Daiichi (Japan) nuclear power plants are notable examples. Exposures were the highest in the local areas surrounding the reactors, but low-level exposures could be estimated for the European region and for the entire northern hemisphere in the Chernobyl case. In the first year following the accident, the highest regionally averaged annual doses in Europe, outside the former Union of Soviet Socialist Republics, were less than 50% of the natural background dose. Subsequent exposures decreased rapidly.

## 3.5   Heavy Metals and Metalloids

The term *heavy metal* refers to any metallic chemical element that has a relatively high density (usually specific density of more than 5 g mL$^{-1}$) and is toxic or poisonous at low concentrations. Examples of heavy metals include arsenic (As), cadmium (Cd), chromium (Cr), mercury (Hg), lead (Pb), and thallium (Tl). The sources, uses, and environmental effects of several exemplary specific metals are discussed briefly here.

Heavy metals are natural components of the earth's crust. They cannot be degraded or destroyed. To a small extent, they generally enter human and animal bodies via food, drinking water, and air due to natural processes. However, exposure to increasingly higher amounts of pollutants from this group usually is due to technological progress that, in many cases, is linked to the ability to extract and process metals. Therefore, already several thousands of years ago, polluted zones were identified and some effects of metal poisoning were known during the period when methods for use of metals were being developed (Jarup 2003; Maskall and Thornton 1998; Nariagu 1996).

In trace amounts, some heavy metals (e.g., copper, nickel, selenium, and zinc) are essential to all organisms, to accomplish specific catalytic functions. However, at levels exceeding these requirements, all metals can disturb metabolism by binding nonspecifically to biomolecules and inflicting oxidative damage, due to their ability to catalyze redox reactions. This can result in the deactivation of essential enzymatic reactions, damage to cellular structures (especially membranes), and DNA modification (mutagenesis). In humans, exposure to high levels of metals can cause acute toxicity symptoms, while long-term exposure to lower levels can trigger allergies and even cancers.

## 3.5.1   *Arsenic and Arsenic Compounds*

Arsenic is considered a metalloid (have both metallic and nonmetallic properties) and is widely distributed in the earth's crust. It occurs in trace quantities in all rock,

soil, water, and air (WHO 2001). Under reducing conditions, arsenite (As(III)) is the dominant form, while arsenate (As(V)) generally is the stable form in oxygenated environments. Arsenic salts exhibit a wide range of solubilities, depending on pH and the ionic environment.

The average subsurface abundance of arsenic is 5–10 mg kg$^{-1}$ (Han et al. 2003), and it is present in more than 200 mineral species. Approximately 60% of natural arsenic minerals are arsenates, 20% sulfides and sulfosalts, and the rest are arsenides, arsenites, oxides, alloys, and polymorphs of elemental arsenic. Inorganic arsenic of geological origin is found in groundwater used as drinking water in several parts of the world, especially in the Bengal Basin. Organic arsenic compounds are found mainly in marine organisms.

Kumaresan and Riyazuddin (2001) reviewed the speciation of arsenic and noted that because As forms anions in solution, it does not form complexes with simple anions like $Cl^-$ and $SO_4^{2-}$ as do cationic metals. Rather, anionic arsenic complexes behave like ligands in water. Kumaresan and Riyazuddin (2001) note also that arsenic forms bond with organic sulfur, nitrogen, and carbon. As(III) reacts with sulfur and sulfydryl groups such as cystine, organic dithiols, proteins, and enzymes, but it does not react with amine groups or organics with reduced nitrogen constituents. On the contrary, As(V) reacts with reduced nitrogen groups such as amines, but not sulfydryl groups. Carbon forms organoarsenicals with both the trivalent and pentavalent forms. The complexation of arsenic (III and V) by dissolved organic matter in natural environments prevents sorption and coprecipitation with solid phase organics and inorganics; essentially, it increases the mobility of arsenic in aquatic systems and in the soil. The methylation of arsenic (mostly biological process) is important because of the extremely toxic products that result. Also, this process transfers arsenic from sediments back to the water column in aquatic systems, increasing arsenic mobility in the environment. Biotransformation of arsenic can produce highly volatile compounds such as arsine ($AsH_3$), dimethylarsine ($HAs(CH_3)_2$), and trimethylarsine ($As(CH_3)_3$). The biological cycle of arsenic in air, water, and sediment is shown in Fig. 3.2.

Mining, smelting of nonferrous metals, and burning of fossil fuels are the major industrial processes that contribute to anthropogenic arsenic contamination of air, water, and soil. Use of chromated copper arsenate (CCA) for wood preservation is still in widespread use in many countries and was used heavily during the latter half of the twentieth century as a structural and outdoor building material, where there was a risk of rot or insect infestation in untreated timber. Lead arsenate was used, well into the twentieth century, as a pesticide on fruit trees, and copper arsenate has even been recorded in the nineteenth century as a coloring agent in sweets.

Arsines released from microbial sources in soils or sediments undergo oxidation in the air, reconverting the arsenic to non-volatile forms, which settle back to the ground. Dissolved forms of arsenic in the water column include arsenate, arsenite, methylarsonic acid (MMA), and dimethylarsinic acid (DMA). Some arsenic species have an affinity for clay mineral surfaces and organic matter, and this can affect their environmental behavior. There is a potential for arsenic release when there is fluctuation in Eh, pH, soluble arsenic concentration, and sediment organic content.
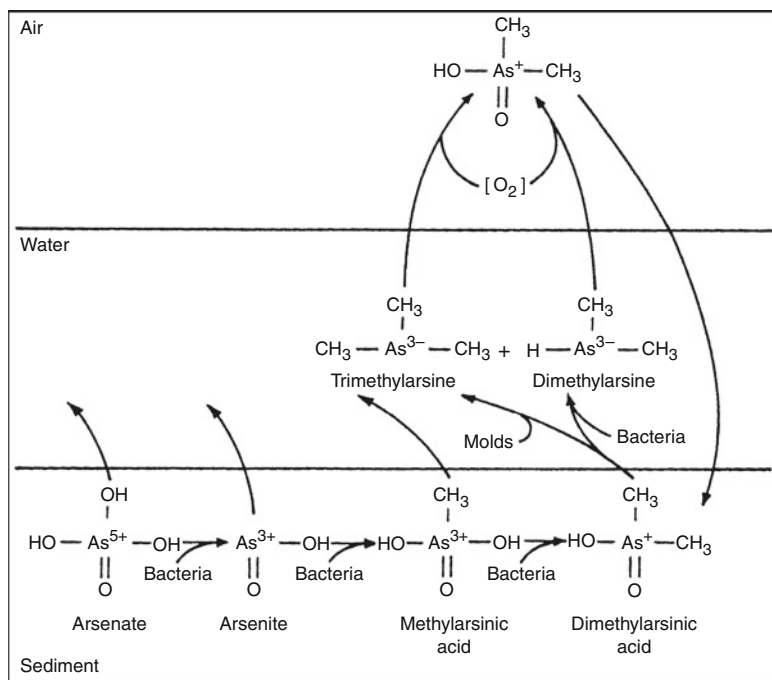
**Fig. 3.2** Biological cycle of arsenic after (Kumaresan and Riyazuddin 2001). Reprinted with permission

Many arsenic compounds tend to adsorb to soils, and leaching usually results in transportation over only short distances in soil. Three major modes of arsenic biotransformation have been found to occur in the environment: redox transformation between arsenite and arsenate, reduction and methylation of arsenic, and biosynthesis of organo-arsenic compounds. Arsenic levels in groundwater average about $1$–$2\ \mu g\ L^{-1}$ except in areas with volcanic rock and sulfide mineral deposits, where arsenic levels can range up to $3\ mg\ L^{-1}$. Naturally elevated levels of arsenic in soils may be associated with geological substrata such as sulfide ores. Anthropogenically contaminated soils can have concentrations of arsenic up to several grams per 100 mL.

## 3.5.2   Cadmium

Cadmium is found naturally deep in the subsurface in zinc, lead, and copper ores, and in coal, shales, and other fossil fuels; it is also released during volcanic activity. These deposits can serve as sources to ground and surface waters, especially when in contact with soft, acidic waters. Chloride, nitrate, and sulfate salts of cadmium are soluble, and sorption to soils is pH dependent (increasing with alkalinity). Cadmium found in

association with carbonate minerals, precipitated as stable solid compounds, or coprecipitated with hydrous iron oxides is less likely to be mobilized by resuspension of sediments or biological activity. Cadmium absorbed to mineral surfaces (e.g., clay) or organic materials is more easily bioaccumulated or released in a dissolved state when sediments are disturbed, such as during flooding.

Roughly 15,000 t of cadmium is produced worldwide each year (McMurray and Tainer 2003). It is produced as an inevitable by-product of zinc, lead, and copper refining and smelting, because these combined metals occur naturally within the raw ore. The most significant uses of cadmium are metal plating and coating for corrosion protection in alloys and electronic compounds, and in nickel/cadmium batteries. Additional uses for cadmium are in pigments and stabilizers for PVC. Cadmium is also present as an impurity in several products, including phosphate fertilizers, detergents, and refined petroleum products (EPA 2005a; Jarup 2003). Industrial contamination of topsoil is likely the major source of human exposure, via uptake into food plants and tobacco (Hayes 1997).

As with all cationic metals, the chemistry of cadmium in the soil environment is to a great extent controlled by pH. The EPA (1999) reports that under acidic conditions, cadmium solubility increases and very little adsorption of cadmium by soil colloids, hydrous oxides, and organic matter takes place. At pH values greater than 6, cadmium is adsorbed by the soil solid phase or is precipitated, and the concentrations of dissolved cadmium are greatly reduced. Cadmium forms soluble complexes with inorganic and organic ligands, in particular with chloride ions. The formation of these complexes increases cadmium mobility in soils (McLean and Bledsoe 1992). Adriano et al. (2005) suggested that in general, chloride can be expected to form a soluble complex with $Cd^{2+}$ as $CdCl^{+}$, thereby decreasing the adsorption of $Cd^{2+}$ to soil particles. In contrast to inorganic ligand ions, $Cd^{2+}$ adsorption by kaolinite, a variable-charge mineral, can be enhanced by the presence of organic matter via the formation of an adsorbed organic layer on the clay surface (Adriano et al. 2005).

Both toxicity and bioavailability of cadmium are influenced by soil characteristics (ECB 2005). Soil characteristics influence cadmium sorption and therefore its bioavailability and toxicity (ECB 2005). Cadmium mobility and bioavailability are higher in noncalcareous soils than in calcareous soils (ATSDR 1999). Liming of soil raises the pH, increasing cadmium adsorption to the soil and reducing bioavailability (ATSDR 1999). A general trend emerges that toxicity increases in soil when mobility of cadmium is higher, i.e., soil toxicity increases as soil pH or soil organic matter decreases. However, exceptions to this trend have also been found (ECB 2005).

Cadmium may be adsorbed by clay minerals, carbonates, or hydrous oxides of iron and manganese, or may be precipitated as cadmium carbonate, hydroxide, and phosphate (EPA 1999). Evidence suggests that adsorption mechanisms may be the primary source of cadmium removal from soils. In soils and sediments polluted with metal wastes, the greatest percentage of total cadmium was associated with the exchangeable fraction. Cadmium concentrations have been shown to be limited by cadmium carbonate in neutral and alkaline soils (EPA 1999).

### 3.5.3   Chromium

Chromium(III) occurs naturally in the environment and is an essential nutrient. Chromium(VI) and chromium(0) are generally produced by industrial processes. Chromium exists in small quantities throughout the environment. Chromite ore ($FeCr_2O_4$) is the most important commercial ore and usually is associated with ultramafic and serpentine rocks. Chromium is also associated with other ore bodies (e.g., uranium and phosphorites) and may be found in tailings and other wastes from these mining operations. Acid mine drainage can make chromium available to the environment. In air, chromium compounds are present mostly as fine dust particles, which eventually settle over land and water. Chromium can attach strongly to soil, and only a small amount can dissolve in water and move deeper in the soil to underground water.

Chromium and its compounds are used in refractories, drilling muds, electroplating cleaning agents, catalytic manufacture, and production of chromic acid and specialty chemicals. The metal chromium, which is the chromium(0) form, is used for making steel. Chromium(VI) and chromium(III) are used for chrome plating, dyes and pigments, leather tanning, and wood preserving. Chromium enters the air, water, and soil mostly in the chromium(III) and chromium(VI) forms. The key to these uses is that under typical environmental and biological conditions of pH and oxidation–reduction potential, the most stable form of chromium is the trivalent oxide. This form has very low solubility and low reactivity, resulting in low mobility in the environment and low toxicity in living organisms. However, the stable and generally nontoxic trivalent form of chromium can be transformed (oxidized) in the environment to chromate ($CrO_4$) and dichromate ($Cr_2O_7$) anions, which are mobile and toxic. Hexavalent chromium anions are the predominant form of dissolved chromium in waters that are alkaline and mildly oxidizing. While hexavalent chromium contamination is generally associated with industrial activity, it can occur naturally.

Chromium(VI) exists in solution as monomeric ions $H_2CrO_4$, $HCrO_4^-$ (bichromate), and $CrO_4^{2-}$ (chromate), or as the dimeric ion $Cr_2O_7^{2-}$ (bichromate). The monomeric species imparts a yellow color to the water when the Cr(VI) concentration is greater than 1 mg $L^{-1}$. Water that contains high levels of $Cr_2O_3$ has an orange color. The monomeric chromate species are related through a series of acid dissociation reactions

$$H_2CrO_4 \rightleftharpoons HCrO_4^- + H^+$$
$$HCrO_4^- \rightleftharpoons CrO_4^{2-} + H^+$$
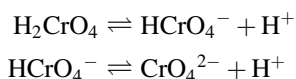
with pK values of $-0.86$ and $6.51$, respectively (Allison et al. 1990). Bichromate is the result of the polymerization of monomeric bichromate ions to form the dimer $Cr_2O_7^{2-}$

$$HCrO_4^- + HCrO_4^- \rightleftharpoons Cr_2O_7^{2-} + H_2O$$
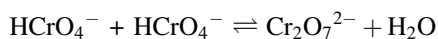
where pK is $-1.54$ (Allison et al. 1990). The relative concentration of each of these species depends on both the pH of the contaminated water and the total concentration of Cr(VI).

Under slightly acidic to alkaline conditions, Cr(III) can precipitate as an amorphous chromium hydroxide. Amorphous $Cr(OH)_3$ can crystallize as $Cr(OH)_3 \cdot 3H_2O$ or $Cr_2O_3$ (eskolaite) under different conditions. In the presence of Fe(III), trivalent chromium can precipitate as a solid solution. If the pH within the contaminant plume is between 5 and 12, the aqueous concentration of Cr(III) will be less than 1 μmol/L (<0.05 mg $L^{-1}$). Several mineral phases that contain Cr(VI) may be present at chromium contaminated sites. Palmer and Wittbrodt (1990) identified $PbCrO_4$ (crocoite), $PbCrO_4 \cdot H_2O$ (iranite), and $K_2CrO_4$ (tarapacaite) in chromium sludge from a hardchrome plating facility. $CaCrO_4$ was found at a seepage face in a drainage ditch where there was high evaporation. Most of the contaminated groundwater was at equilibrium with $BaCrO_4$ (hashemite). $BaCrO_4$ forms a complete solid solution with $BaSO_4$.

Cr(VI) is a strong oxidant and is reduced in the presence of electron donors. Electron donors commonly found in soils include aqueous Fe(II), ferrous iron minerals, reduced sulfur, and soil organic matter. The reduction of Cr(VI) is very fast on the time scales of interest for most environmental problems, with the reaction reaching completion in less than 5 min even in the presence of dissolved oxygen. Numerous minerals in geologic materials contain ferrous iron that is potentially available for the reduction of hexavalent chromium.

The major reaction of chromium species in the soil–water environment is given in Fig. 3.3. Here, the starting point of the cycle is Cr(VI) because of its environmental importance. Cr(VI) is relatively mobile in the subsurface because it forms anionic species. Although Cr(VI) is not retained by negatively charged colloids in soils, it is sorbed on many hydrous oxides (Fendorf 1995). Cr(VI) can also undergo reduction by organic matter (soluble and insoluble), Fe(II), and sulfides. Reduced Cr is typically bound by a variety of ligands in soil solutions, which render it insoluble, immobile, and unreactive. However, ligands such as citrate can mobilize Cr(III) and deliver it to $MnO_2$ surfaces where both the organic ligand and Cr become oxidized (Avudainayagam et al. 2003).

### 3.5.4   Lead

Lead is a bluish-white lustrous metal. It is very soft, highly malleable, ductile, and a relatively poor conductor of electricity. It is very resistant to corrosion but tarnishes upon exposure to air. It is one of the oldest metals used by humans and has been used widely since 5,000 BC; lead was known to the ancient Egyptians and Babylonians. The Romans used lead for pipes and in solder. The element has four naturally occurring stable isotopes, three of which result from the decay of naturally occurring radioactive elements (thorium and uranium). Although lead is seldom found uncombined in nature, its compounds are distributed widely throughout the world, principally in the ores galena (a lead sulfide ore), cerussite ($PbCO_3$), and anglesite ($PbSO_4$).
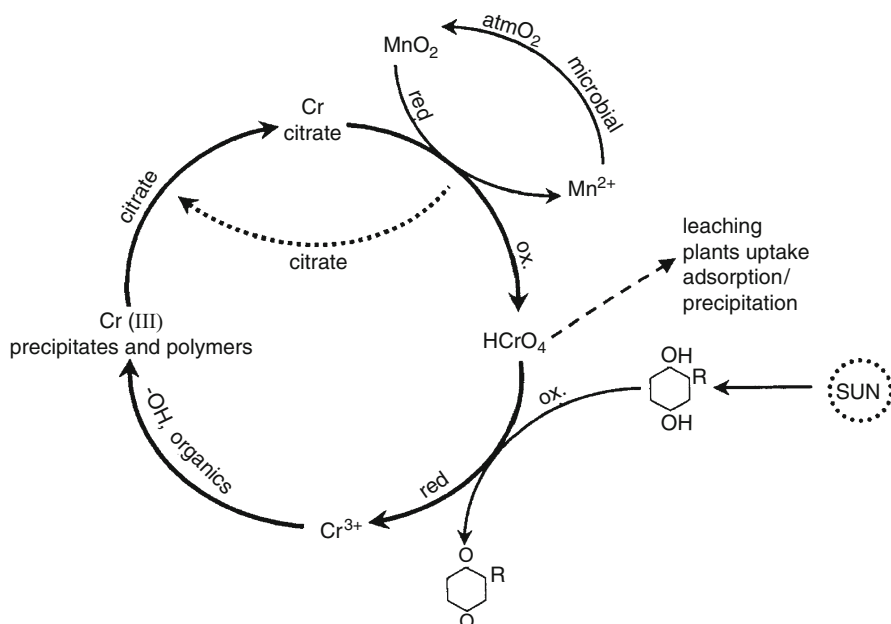
**Fig. 3.3** Chromium cycle in soil and water (after Avudainayagam et al. 2003)

To date, the single most important commercial use of lead is in the manufacture of lead–acid storage batteries. However, for much of the twentieth century, the most important environmental source of Pb was gasoline combustion. It is also used in alloys, such as fusible metals, antifriction metals, and solder. Lead foil is made with lead alloys. Lead is used for covering cables and as a lining for laboratory sinks, tanks, and the "chambers" in the lead-chamber process for the manufacture of sulfuric acid. It is used extensively in plumbing. Because it has excellent vibration-dampening characteristics, lead is often used to support heavy machinery.

Contamination of lead in groundwater originates from the dissolution of lead from soil and the earth's crust. Lead particulate from the combustion of leaded gasoline and ore smelting can contaminate local surface water by surface runoff. Lead itself is only of minor content in the earth's crust. A wide distribution of lead in sedimentary rock and soils has been reported, with an average lead content of 10 mg kg$^{-1}$ (10 ppm) in topsoil, and a range of 7–12.5 ppm in sedimentary rock (EPA 1992). In soils, lead is generally present in the form of carbonates and hydroxide complexes. Strong absorption by soil and complexion by humus can further limit the lead concentrations in surface waters and groundwater.

The primary mechanisms of Pb attenuation in soil include adsorption by soil mineral surfaces, complexation on organic matter molecules, and precipitation as an insoluble Pb hydroxide. Pb (II) and Fe(II) in natural aquatic environments have similar affinities to complex with ligands (because of similar electronegativity and covalent index), and thus they show similar patterns of species distribution (Turner

et al. 1981). The dissolution or precipitation of Fe (oxy)hydroxides can release or sorb Pb. In soils, dissolution of Fe (oxy)hydroxides is generally promoted by reducing Fe(III) to Fe(II), which is sensitive to soil redox status (Lindsay 1979; Gotoh and Patrick 1974). Under oxidizing conditions, Fe (oxy)hydroxides tend to immobilize Pb (Gambrell et al. 1980), whereas under reducing conditions they dissolve to release Pb (Gambrell 1994). Interactions with soil organic carbon, especially dissolved organic carbon (DOC), are an important factor controlling Pb in soil (Dorr and Munnich 1991; Laxen 1985; Davis 1984). DOC functions as a ligand to complex with Pb, which increases its solubility (Davis and Leckie 1978). When the DOC is sorbed to Fe (oxy)hydroxides, via ligand exchange or hydrophobic interaction (Murphy and Zachara 1995), Pb solubility decreases.

Lead is often thought to be immobile in soils because of its low solubility and a strong affinity to soil particles (Yin et al. 2010; Hu et al. 2008). However, several studies have suggested that Pb adsorbed on colloids in the soil solution may be transported to the deeper layers of the subsurface system (Newman et al. 1993; Denaix et al. 2001; Citeau et al. 2003). With large specific surface area and abundant surface functional groups, soil colloids have a strong ability to adsorb various chemical species including heavy metals. Physicochemical perturbations such as reduction in ionic strength, increase in solution pH, and increase in flow velocity may favor the release of colloids and colloid-borne metals in soils. Increases in solution pH enhance release of both colloidal and dissolved Pb. At low pH, the release of organic colloids may dominate Pb transport in soils.

### 3.5.5 Nickel

Nickel is a silver-white, lustrous, hard, malleable, ductile, ferromagnetic metal that is relatively resistant to corrosion and is a fair conductor of heat and electricity. Nickel is a ubiquitous trace metal that occurs in soil, water, and air, and in the biosphere. The average content in the earth's crust is about 0.008%. Nickel ore deposits are accumulations of nickel sulfide minerals (mostly pentlandite) and laterites. Nickel exists in five major forms: elemental nickel and its alloys; inorganic, water-soluble compounds (e.g., nickel chloride, nickel sulfate, and nickel nitrate); inorganic, water-insoluble compounds (e.g., nickel carbonate, nickel sulfide, and nickel oxide); organic, water-insoluble compounds; and nickel carbonyl $Ni(CO)_4$.

Nickel is used mostly for the production of stainless steel and other nickel alloys with high corrosion and temperature resistance. Nickel alloys and nickel platings are used in vehicles, processing machinery, armaments, tools, electrical equipment, household appliances, and coins. Nickel compounds are also used as catalysts and pigments, and in batteries.

Nickel, which is emitted into the environment from both natural and human-made sources, is circulated throughout all environmental compartments by means of chemical and physical processes and is biologically transported by living organisms. Nickel enters groundwater and surface waters from erosion and

dissolution of rocks and soils, as well as from biological cycles, atmospheric fallout, industrial processes, and waste disposal. Nickel leached from dump sites can contribute to nickel contamination of an aquifer, with potential ecotoxicity. Acid rain has a tendency to mobilize nickel from soil and increase nickel concentrations in groundwater, leading eventually to increased uptake and possible toxicity in microorganisms, plants, and animals. Depending on the soil type, nickel may exhibit a high mobility within the soil profile, finally reaching groundwater, rivers, and lakes. Terrestrial plants take up nickel from soil, primarily via the roots. The amount of nickel uptake from soil depends on various geochemical and physical parameters, including soil type, soil pH and humidity, the organic matter content of the soil, and the concentration of extractable nickel.

Nickel can interact with soil components in two major ways: cation exchange at the permanently negative sites on the clay fraction (outer-sphere complexes), and by forming complexes with specific functional groups (mainly Fe, Mn, and Al hydrous oxide and organic matter). It has been shown that Ni has lower affinities for soil colloids and is generally considered to be a weakly bonded and rather mobile metal under acidic conditions (Atanassova 1999) compared to other metals such as Cu, Pb, and Hg. Studies reported that cation exchange is the major sorption mechanism for Ni. Adsorption of Ni is related to several factors, including charge to radius ratio, electronegativity, softness parameter, and first hydrolysis constant (Antoniadis and Tsadilas 2007; Tsang and Lo 2006; Sposito 1984). On the contrary, the reaction of Ni with soil minerals is related to metal-ion hydrolysis in studies of specific sorption.

## 3.6  Nanosized Materials

Engineered nanomaterials are usually described as inorganic materials of high uniformity, with at least one critical dimension below 100 nm. This group of substances has received considerable attention recently as the basis for the current and next "scientific revolution." In this framework, nanomaterials are expected to be incorporated in a wide range of applications, from medicine and cosmetics to new construction materials and industrial process, and to many more applications in all areas of technological development (e.g., Dror et al. 2005; Nurmi et al. 2005; McKenzie and Hutchison 2004; Mohanty et al. 2003).

However, these possibilities also bring new threats that must be considered and monitored. Nanomaterials magnify and stimulate properties that, at larger scales, are in many cases of minor importance. Below 100 nm – the upper limit of the nanomaterial range – the surface area to mass ratio and the proportion of total number of atoms at the surface of a structure are large enough that surface properties become very significant. This can alter chemical reactivity, thermal and electrical conductivity, and tensile strength of known substances (Owen and Depledge 2005). Additional physicochemical properties of engineered nanomaterials include specific chemical composition (e.g., purity, crystallinity, and electronic properties), surface structure (e.g., surface reactivity, surface groups, and inorganic or organic coatings), solubility,

shape, and aggregation (Nel et al. 2006). Furthermore, when the size of a structure is 10–30 nm, it approaches certain physical length scales, such as the electron mean free path and the electron wavelength, resulting in quantum-size effects that alter the electronic structure of the particle (Nurmi et al. 2005; Wang and Herron 1991; Brus 1986). These changes modify optical, magnetic, and electrical behavior.

The desired size-related properties of nanomaterials also raise major concerns: the same characteristics that make these substances so appealing may have negative health and environmental impacts. Recent studies (e.g., Balbus et al. 2005; Royal Society 2004; Colvin 2003) state that the data collected to date are inadequate to provide full risk assessments, but substantial reason for concern exists and should be further investigated.

At this point, there is very limited knowledge about the transport and fluxes of nanoparticles in the natural environment (Klaine et al. 2008). Colvin (2003) suggested that if engineered nanomaterial applications develop as projected, increasing concentrations of nanomaterials in the soil–subsurface system present the most significant exposure avenues for environmental risk. Release to the environment, either by accident or by approved and regulated discharge of effluents and waste water, may result in direct exposure of humans to nanoparticles via ingestion or inhalation of airborne (Dowling 2004; Moore 2002, 2006; Warheit 2004; Brigger et al. 2002) or water aerosols, skin contact, and direct ingestion of contaminated drinking water or particles adsorbed on vegetables or other foodstuffs (Daughton 2004; Howard 2004; Moore 2006).
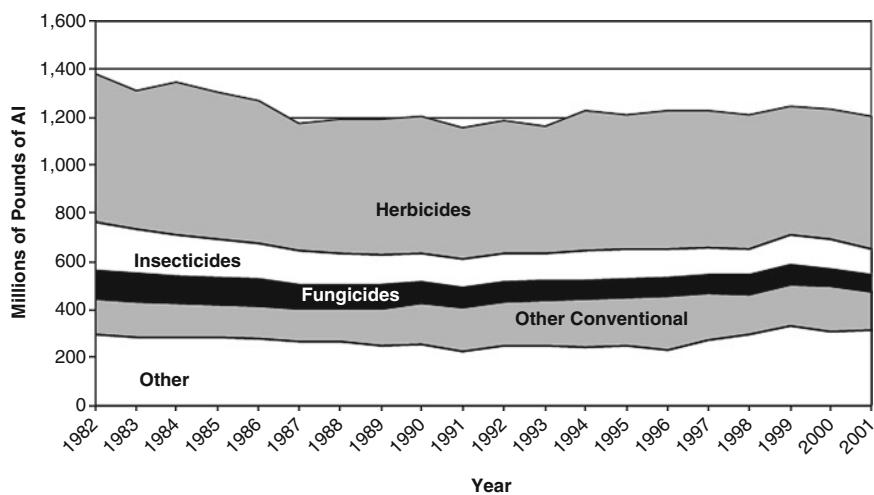
## 3.7   Pesticides

Pesticides are substances, or mixtures of substances, intended to prevent, destroy, repel, or mitigate any pest. The term *pest* includes insects, plant pathogens, weeds, mollusks, birds, mammals, fish, nematodes (roundworms), and microbes that compete with humans for food, destroy property, spread or are a vector for disease, or are a nuisance (EPA 2006). Pests have attacked and destroyed crops, and pesticides have been developed, as long as agriculture has been practiced. Some historical examples include selection of seed from resistant plants in Neolithic times (~7000 BC; Ordish 2007), sulfur dusting by the Sumerians (~2500 BC), and over 800 recipes in the Ebers' Papyrus, the oldest known medical document (dated around 1550 BC), which describes recognizable substances that were used as poisons and pesticides. More recently, during the fifteenth century, arsenic, mercury, and lead were used to fight pests. The first book to deal with pests in a scientific way was John Curtis's *Farm Insects*, published in 1860, but massive production and application of pesticides only began around World War II. The major development at that time was the discovery of the insecticidal properties of DDT by P. H. Müller in 1942, who received the Nobel Prize (medicine) for his discovery in 1948.

From this point on, many millions of tons of active ingredients have been released intentionally each year to the environment, spreading around the globe.

An illustration of the amounts of active-ingredient pesticides applied can be seen in Fig. 3.4, where total annual amounts used in the USA surpass billion of pounds for the period from 1982 to 2001.

In contrast to all other groups of contaminants mentioned in this chapter, pesticides are released to the environment in staggering quantities, even though they are designed to suppress normal biological growth of different pests. Pesticides are formulated specifically to be toxic to living organisms and, as such, are usually hazardous to humans. In fact, most pesticides used today are acutely toxic to humans, causing poisonings and deaths every year. The toxicity, transport, fate, chemical and physical properties, environmental impact, and many more aspects of pesticides, their metabolites, and adjuvants ("inert ingredients") have been studied extensively for many decades now and numerous publications are available (e.g., Barbash 2003; Matthews 2006; Milne 1995; Briggs 1992).
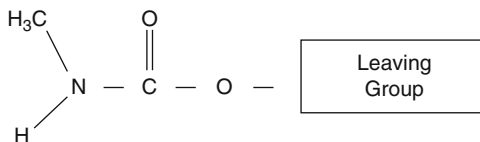
Pesticides and their degradation products are a major potential source of contamination for users, bystanders, and manufacturing workers during storage, transport, and during or after use. Exposure routes include direct intake of pesticide residues through, for example, ingestion of pesticides adsorbed on crops or dissolved in water, and indirect paths such as, for example, intake of pesticides or their degradation products that were concentrated in the food chain, or by intake of other environmental mediators. In some cases, pesticides have synergistic effects with other contaminants, thus increasing overall toxicity. Pesticides are found virtually everywhere in the soil–subsurface environment, in varying amounts. These residues and their degradation products are toxic to many components of the ecological system, either by being lethal to certain living forms or by changing environmental conditions which in turn alter and usually decrease biodiversity.



**Fig. 3.4** Annual amount of pesticide active ingredient used in the USA by pesticide type, 1982–2001; estimates are for all market sectors (from EPA 2004)

Usually, only a small fraction of the applied amounts of pesticides reach the target organism: the majority is distributed to the air, soil, and water. Upon such release, many nontarget organisms can be impacted severely.

Official lists of pesticides contain over 1,500 substances (Wood 2006). Pesticides are divided into several major groups (e.g., herbicides, fungicides, and insecticides), which are subdivided into chemical or other classes (e.g., chloroacetanilide herbicides or auxins). These compounds can be arranged according to their toxicity (WHO 2005), chemical structure, and/or activity. Here, we briefly discuss only few of the more common groups of pesticides; interested readers should consult the references mentioned above as a primary source of more detailed information.

### 3.7.1  Organophosphates

The general chemical structure of organophosphate pesticides is shown in Fig. 3.5. The functional group R is usually either ethyl or methyl. Pesticides with double-bonded sulfur moieties are organothiophosphates but are converted to organophosphates in the liver. Phosphonate contains an alkyl (R-) in place of one alkoxy group (RO). The "leaving group" is the principal metabolite for a specific identification.

Acute pesticide poisonings frequently involve organophosphate pesticides; these pesticides were originally derived from chemical warfare agents developed during World War II. Some common organophosphates include chlorpyrifos, diazinon, azinphos-methyl, malathion, parathion, and methyl-parathion, all of which apparently share a common mechanism of cholinesterase inhibition and cause similar symptoms. Organophosphates poison insects and mammals primarily by phosphorylation of the acetylcholinesterase enzyme (AChE) at nerve endings. The result is a loss of available AChE so that the affected organ becomes over-stimulated by the excess acetylcholine (ACh, the impulse-transmitting substance) in the nerve ending. The enzyme is critical to normal control of nerve impulse transmission from nerve fibers to smooth and skeletal muscle cells, glandular cells, and autonomic ganglia, as well as within the central nervous system.

### 3.7.2  N-methyl Carbamates

The general chemical structure of N-methyl carbamate is shown in Fig. 3.6. Common N-methyl carbamates include aldicarb, carbofuran, methiocarb, oxamyl, and



**Fig. 3.5**  General structure of organophosphate pesticides

**Fig. 3.6** General structure of
*N*-methyl carbamates



carbaryl. *N*-methyl carbamates share with organophosphates the capacity to inhibit cholinesterase enzymes and, therefore, share similar symptomatology during acute and chronic exposures.

The *N*-methyl carbamate esters cause reversible carbamylation of the AChE, allowing accumulation of acetylcholine, the neuromediator substance, at parasympathetic neuroeffector junctions (muscarinic effects), at skeletal muscle myoneural junctions and autonomic ganglia (nicotinic effects), and in the brain (CNS effects). The carbamyl–acetylcholinesterase combination dissociates more readily than the phosphoryl–acetylcholinesterase complex produced by organophosphate compounds. This property has several important consequences: (1) it tends to limit the duration of *N*-methyl carbamate poisoning, (2) it accounts for the greater span between symptom-producing and lethal doses than in most organophosphate compounds, and (3) it frequently invalidates the measurement of blood cholinesterase activity as a diagnostic index of poisoning. *N*-methyl carbamates are absorbed by inhalation and ingestion, and somewhat by skin penetration, although the latter tends to be a less toxic route.

## 3.7.3  *Triazines*

Triazine and their metabolites are a group of closely related herbicides used widely in agriculture and urban sites; they are inhibitors of electron transport in photosynthesis. As a family, their chemical structures are heterocyclic, composed of carbon and nitrogen in their rings. Most, except for metribuzin, are symmetrical with their altering carbon and nitrogen atoms. Herbicide members in this family include atrazine, hexazinone, metribuzin, prometon, prometryn, simazine, and the degradates DACT, DEA, and DIA. Atrazine is used widely in corn production and is estimated to have been the most often-used pesticide in the USA during the late 1990s. Its toxic effects may include disruption of ovarian function, generation of mammary (breast) tumors in animals, and interference with the binding of steroid hormones and the breakdown pathway of estrogen (Bradlow et al. 1995; Cooper et al. 1989; Danzo 1997). Some uses of atrazine are classified as restricted because of ground and surface water concerns. Many of the triazines show acute and chronic toxicities at low concentrations (Letterman 1999; Montgomery 1993), and they are generally known or are suspected to be carcinogenic, mutagenic, and/or teratogenic (Newman 1995; Letterman 1999; Montgomery 1993; C&EN 2002). There is also evidence (Reeder et al. 1998; Renner 2002; Tavera-Mendoza et al. 2002a, b) implicating specific triazines and/or their degradation products as endocrine disruptors and teratogens in amphibians.

### 3.7.4 Organochlorines

Organochlorine insecticides (e.g., DDT, aldrin, dieldrin, heptachlor, mirex, chlordecone, and chlordane) were used commonly in the past, but many have been removed from the market due to their health and environmental effects and their persistence. However, insecticides of this group are in some cases found in soils as persistent residues or still used as active ingredients in various pest control products, such as gamma hexachlorocyclohexane (lindane). Lindane is also used as the active agent in the medicine Kwell®, used for human ectoparasitic disease, although it has been associated with acute neurological toxicity either from ingestion or in persons treated for scabies or lice. The chemical structures of some of the organochlorine insecticides are given in Fig. 3.7. These compounds are characterized by cyclic structures, a relatively large number of chlorine atoms on the molecule, and low volatility. As a result, they are usually resistant to natural degradation processes and thus stable for very long periods after release into the environment.

Organochlorines are absorbed in the body through ingestion, inhalation, and across the skin. These substances tend to concentrate in fatty tissues following exposure. There has been considerable interest recently in the interaction of organochlorines with endocrine receptors, particularly estrogen and androgen receptors.

### 3.7.5 Paraquat and Diquat

Paraquat (1,1′-dimethyl-4,4′-bipyridinium dichloride) is a nonselective contact herbicide. It is used almost exclusively as a dichloride salt and is usually formulated to contain surfactants. Both its herbicidal and toxicological properties are
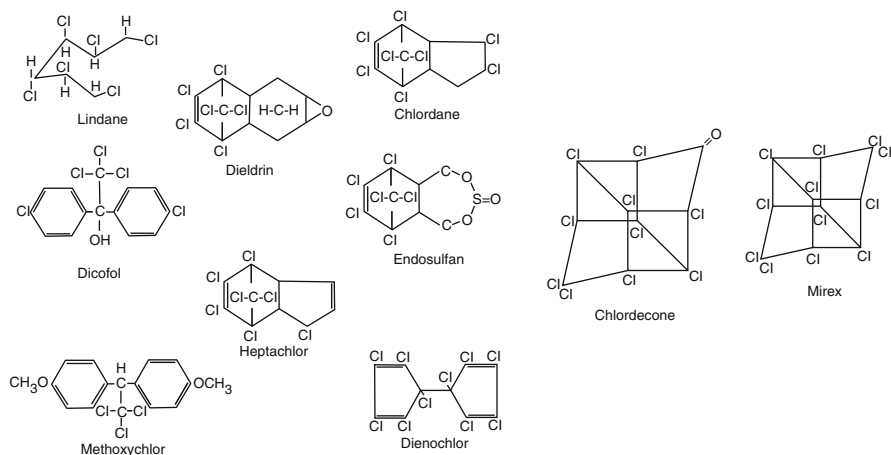


**Fig. 3.7** Chemical structures of some organochlorine insecticides

Diquat dibromide                 Paraquat dichloride
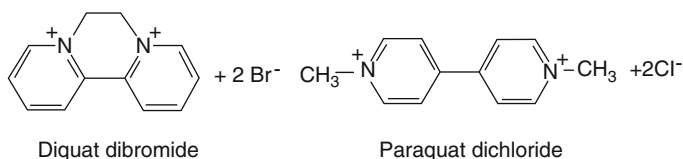
**Fig. 3.8** Chemical structures of diquat dibromide and paraquat dichloride

dependent on the ability of the parent cation to undergo a single electron addition, to form a free radical that reacts with molecular oxygen to reform the cation and concomitantly produce a superoxide anion. This oxygen radical may directly or indirectly cause cell death.

Diquat (1,1′-ethylene-2,2′-dipyridylium dibromide) is a charged quaternary ammonium compound used commercially as a dibromide salt. The structure of diquat dibromide and that of the closely related herbicide paraquat dichloride are shown in Fig. 3.8.

These compounds are nonselective contact herbicides that are used relatively widely and are highly toxic.

## 3.8   Synthetic Halogenated Organic Substances

Halogenated hydrocarbons constitute a widely used family of products. Some of the more common halogenated hydrocarbons are brominated flame retardants and the chlorinated derivatives of methane, ethane, and benzene, which are used mainly as solvents and chemical intermediates. Broad production and use of these compounds began in the early 1900s when chlorinated solvents replaced other flammable substances in a variety of industrial processes. These compounds became popular because the progressive halogenation of a hydrocarbon molecule yields a succession of liquids or solids of increasing density, viscosity, and improved solubility for a large number of inorganic and organic materials. Other physical properties such as flammability, specific heat, dielectric constant, and water solubility decrease with increasing halogen content (Marshall 2003).

In addition to dry cleaning and degreasing solvents, many halogenated organic solvents have also been used in adhesives, pharmaceuticals, and textile processing; as extraction solvents, paint solvents, and coating solvents; and as feedstocks for production of other chemicals. The widespread use and subsequent disposal of chlorinated solvents have led to their being among the most commonly found contaminants at hazardous waste disposal sites. In general, these compounds are considered persistent in the environment, having long half-lives in soil, air, and water in comparison to other, nonhalogenated hydrocarbons. The health effects of these compounds have been studied extensively, as a result of concerns raised about their toxicity and their carcinogenic nature. Due to the large diversity of this group, only few major ubiquitous substances are discussed further here.

### 3.8.1   Chlorinated Hydrocarbons

*Chlorinated derivatives of methane*. This group includes methyl chloride, methylene chloride, chloroform, carbon tetrachloride, and several chlorofluorohydrocarbons (CFC). We discuss carbon tetrachloride (CT) as a representative example of this group. CT was originally prepared in 1839 and was one of the first organic chemicals to be produced on a large scale by the end of the nineteenth century and beginning of the twentieth century. CT is the most toxic of the chloromethanes and the most unstable on thermal oxidation (Holbrook 2000).

In the past, the main uses of CT were for dry cleaning, fabric spotting, and fire extinguisher fluids; as a grain fumigant; and as a solvent in various chemical processes (DeShon 1979). Until recently, CT was used as a solvent for the recovery of tin in tin-plating waste, for metal degreasing, in the manufacture of semiconductors, as a petrol additive and a refrigerant, as a catalyst in the production of polymers, and as a chemical intermediate in the production of fluorocarbons and some pesticides (HSDB 1995).

*Chlorinated ethanes and ethylenes*. This group includes ethyl chloride, ethylene dichloride (1,2 dichloroethane), vinyl chloride, trichloroethylene (TCE), perchloroethylene (PCE), and several CFC. Some of the major uses of these compounds are as degreasing agents, dry cleaning solvents, building blocks for manufacturing of polymers (e.g., PVC and ethyl cellulose), and raw material for the production of tetra-ethyl lead and CFC. We discuss ethylene dichloride, trichloroethylene, and perchloroethylene as examples of this group.

*Ethylene dichloride (EDC)*. This is used primarily in the production of vinyl chloride monomer (HSDB 2000). It also is an intermediate in the manufacture of trichloroethane and fluorocarbons, and is used as a solvent. In the past, EDC was used as a gasoline additive and a soil fumigant.

*Trichloroethylene*. The first documented synthesis of TCE was in 1864, and by the early 1900s, a manufacturing process was initiated, becoming a full industrial process by the 1920s (Mertens 2000). The main use of TCE is metal degreasing (over 90% of production and consumption). TCE was also used extensively for dry cleaning and, in the past, as an extraction solvent for natural fats and oils for food, cosmetic, and drug production (e.g., extraction of palm, coconut, and soybean oils; decaffeination of coffee; and isolation of spice oleoresins) (Doherty 2000a; Linak et al. 1990). Additional applications of TCE are as components in adhesive and paint-stripping formulations, as a low-temperature heat-transfer medium, as a nonflammable solvent carrier in industrial paint systems, and as a solvent base for metal phosphatizing systems. TCE is used in the textile industry as a carrier solvent for spotting fluids and as a solvent in waterless dyeing and finishing operations (Mertens 2000; Doherty 2000a).

TCE is now a common contaminant at hazardous waste sites and many federal facilities in the USA. TCE has been identified in at least 1,500 hazardous waste sites regulated under Superfund or the Resource Conservation and Recovery Act (EPA 2005b). TCE can enter surface waters via direct discharges and groundwater

through leaching from disposal operations and Superfund sites; the maximum contaminant level for TCE in drinking water is 5 ppb. TCE can be released to indoor air from use of consumer products that contain it, vapor intrusion through underground walls and floors, and volatilization from the water supply.

*Tetrachloroethylene (perchloroethylene, PCE)*. PCE was first prepared in 1821, but industrial production of PCE reportedly began in the first decade of the twentieth century (Gerhartz 1986); significant use began only about 100 years after its discovery (Doherty 2000b). The main use of PCE is in the dry cleaning industry. It is also used as a feedstock for chlorofluorocarbon production, for metal cleaning, as a transformer insulating fluid, in chemical maskant formulations, and as a process solvent for desulfurizing coal (Hickman 2000).

*Chlorinated aromatics, including monochlorobenzene (MCB), o-dichlorobenzene (o-DCB), and p-dichlorobenzene (p-DCB)*. These compounds are the major chlorinated aromatic species produced on an industrial scale. MCB is used as both a chemical intermediate and a solvent. As an intermediate, it is used to produce chloronitrobenzene, pesticides, and pharmaceutical products. In solvent applications, MCB is used in the manufacture of isocyanates. Its high solvency allows it to be used with many different types of resins, adhesives, and coatings. o-DCB is used primarily for organic synthesis, especially in the production of 3,4-dichloroaniline herbicides. Like MCB, it can be used as a solvent, especially in the production of isocyanates. It is also used in motor oil and paint formulations. p-dichlorobenzene is used as a moth repellent and for the control of mildew and fungi. It is also used for odor control. It is a chemical intermediate for the manufacture of pharmaceuticals and other organic chemicals.

### 3.8.2    Brominated Flame Retardants

The term *brominated flame retardants* (BFR) incorporates more than 175 different types of substances, which form the largest class of flame retardants; other classes are phosphorus-containing, nitrogen-containing, and inorganic flame retardants (Birnbaum and Sttaskal 2004). The major BFR in use today are tetrabromo-bisphenol A (TBBPA), hexabromocyclododecane (HBCD), and three commercial mixtures of polybrominated diphenyl ethers (PBDEs): decabromodiphenyl ether (DBDE), octabromodiphenyl ether (OBDE), and pentabromodiphenyl ether (pentaBDE); their structures are shown in Fig. 3.9.

BFR have been added to various products (e.g., electrical appliances, building materials, vehicle parts, textiles, and furnishings) since the 1960s, in growing rates (15-fold from the mid-1960s to 2003; DePierre 2003). BFR usually are classified as semi-volatile and hydrophobic, but these properties vary due to the large diversity of this group of compounds. BFR tend to accumulate in organic-rich media such as soils and sediments, and lipid-rich biotic tissues, and are expected to biomagnify in food chains (DePierre 2003).
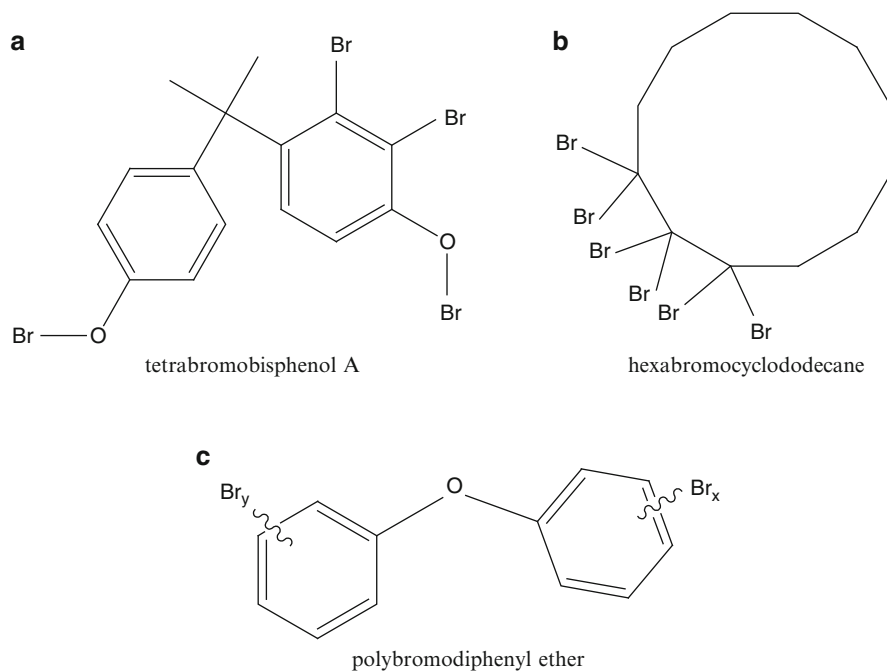
**Fig. 3.9** Chemical structures of (**a**) tetrabromobisphenol A (TBBPA), (**b**) hexabromocyclo-dodecane (HBCD), and (**c**) polybrominated diphenyl ethers (PBDEs)

## 3.9 Petroleum Hydrocarbons and Fuel Additives

Petroleum hydrocarbons (PH) constitute a group of compounds characterized by complex mixtures of hydrocarbons. Overall, hundreds to thousands of individual compounds can be found in the different mixtures, although information about physical and chemical properties is available only for approximately 250 of these compounds, and substantial toxicological data exist just for a small fraction (~10%) of the identified substances (Vorhees et al. 1999). Often these compounds are referred to in the literature as light nonaqueous phase liquids (LNAPL) when they exist as a separate phase. In terms of volumes of contaminants released to the environment, the contamination of land surface, partially saturated zone, and groundwater by PH generally is one of the most serious. This is due to the staggering amounts of PH used mainly as energy sources for electricity, transportation, and heating around the world. Leaking underground and above-ground storage tanks, improper disposal of petroleum wastes, and accidental spills are major routes of soil and groundwater contamination by petroleum products (Nadim et al. 2000).

Upon release to the environment, the bulk phase migrates downward by gravity. As the NAPL phase moves through the partially saturated zone, a fraction of the PH is retained by capillary forces as residual globules in the soil pores, thereby

depleting the contiguous PH mass until movement ceases. If sufficient PH is released, it will migrate until it encounters a physical barrier (e.g., a low permeability stratum) or is affected by buoyancy forces near the water table. Additionally, PH vapors migrate in the porous matrix creating a larger impact zone. Once the capillary fringe is reached, the PH may move laterally as a continuous, free-phase layer along the upper boundary of the water-saturated zone, due to gravity and capillary forces. Upon contact with water in the saturated or partially saturated zone, dissolution of compounds from PH mixture begins. The schematic description of PH distribution patterns in the subsurface is given in Fig. 3.10.

The direct exposure pathways of humans to PHs following a leak are described in Fig. 3.11. Once released to the surface and subsurface environment, PHs can reach humans directly as vapors, solutes, or adsorbed on particles.

Here, we mention several individual compounds which are common constituents of the different PH mixtures, as examples of potential soil–subsurface system contaminants. The main groups are (1) small aromatic compounds, mostly benzene derivatives (e.g., benzene, toluene, ethylbenzene, and xylenes), which are considered slightly soluble in water (150–1,800 mg L$^{-1}$); (2) branched and linear aliphatics (e.g., n-dodecane and n-heptane), which are characterized by relatively low water solubility; and (3) polar hydrocarbons and petroleum additives (e.g., methyl tertiary-butyl ether (MTBE) and alcohols), which are highly soluble. The weight percentage of three selected compounds in various commercial petroleum products is given in Table 3.3.

Benzene is important from an environmental point of view, as it is a major component of various petroleum products. Its weight fraction ranges from practically zero for the heavy distillates to 3.5% for gasoline, as seen in Table 3.3. Its solubility is 1,780 mg L$^{-1}$ and it is very volatile (vapor pressure 100 Torr at 26.1°C); thus, benzene is one of the most common pollutants originating from PH mixtures released into the soil–subsurface zone.
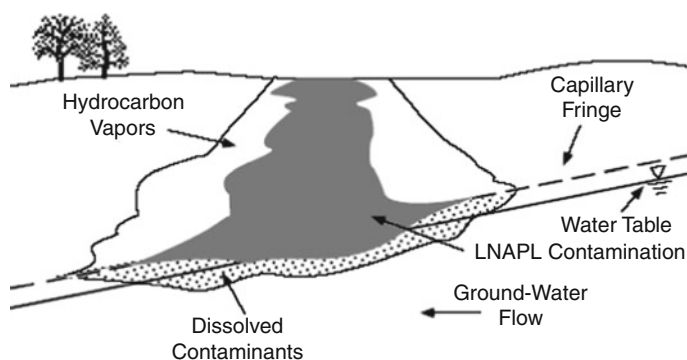


**Fig. 3.10** Simplified conceptual model for light nonaqueous phase liquid (LNAPL) release and migration (after Mercer and Cohen 1990). Reprinted from Mercer JW, Cohen RM, A review of immiscible fluids in the subsurface: Properties, models, characterization and remediation. J Contam Hydrol 6:107–163, Copyright (1990), with permission from Elsevier
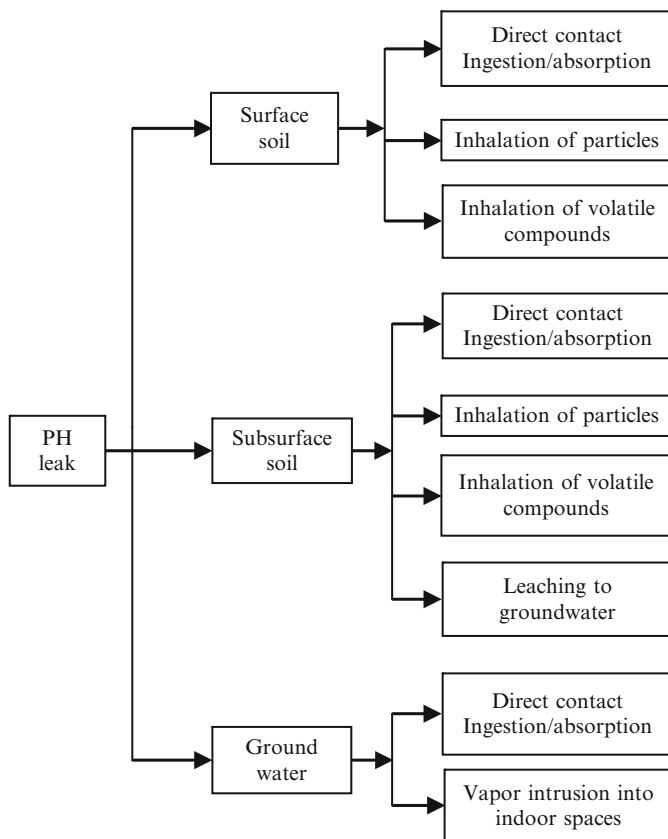
**Fig. 3.11** Example of direct human exposure pathways to petroleum hydrocarbons following release to the surface and subsurface environment (modified after Vorhees et al. 1999). Reprinted with permission

**Table 3.3** Fraction range (in %w) of three hydrocarbons in selected commercial petroleum products, based on data from Gustafson et al. (1997). Reprinted with permission

|          | Crude oil | Diesel      | Fuel oil #2   | Gasoline    | JP-4 |
|----------|-----------|-------------|---------------|-------------|------|
| Benzene  | 0.04–0.4  | 0.003–0.10  | <0.125        | 0.12–3.50   | 0.5  |
| Toluene  | 0.09–2.5  | 0.007–0.70  | 0.025–0.110   | 2.73–21.80  | 1.33 |
| n-Octane | 0.9–1.9   | 0.1         | 0.1           | 0.36–1.43   | 3.8  |

MTBE is an octane enhancer; that is, it promotes more complete burning of gasoline and thereby reduces carbon monoxide and ozone levels. MTBE is very soluble, and once released, it moves through soil and into water more rapidly than other chemical compounds present in gasoline. In groundwater, it is slow to biodegrade and more persistent than other gasoline-related compounds.

## 3.10   Pharmaceuticals and Personal Care Products

A large class of chemicals gaining attention in recent years comprises pharmaceutical, veterinary, and illicit ("recreational") drugs and the ingredients in cosmetics, food supplements, and other personal care products, together with their respective metabolites and transformation products; they are collectively referred to as *pharmaceuticals and personal care products* (PPCP). PPCP are used in large amounts throughout the world, and recent studies have demonstrated their occurrence in aquatic environments around the world (Heberer et al. 2002; Daughton and Ternes 1999; Erickson 2002).

Most PPCP are disposed of or discharged into the environment on a continuous basis, via domestic and industrial sewage systems and wet-weather runoff. In many instances, untreated sewage is discharged into receiving waters (e.g., flood overload events, domestic "straight-piping," or sewage waters lacking municipal treatment). A scheme of possible pathways for the occurrence of PPCP residues in aquatic environments is depicted in Fig. 3.12. The bioactive ingredients are first subjected to metabolism by the dosed user; the excreted metabolites and unaltered parent compounds can then be subjected to further transformations in sewage treatment facilities. The literature shows, however, that many of these compounds survive biodegradation, eventually being discharged into receiving waters. Many of these PPCP and their metabolites are ubiquitous and display persistence in, and bioconcentration from, surface waters. Additionally, by way of continuous infusion into the aquatic
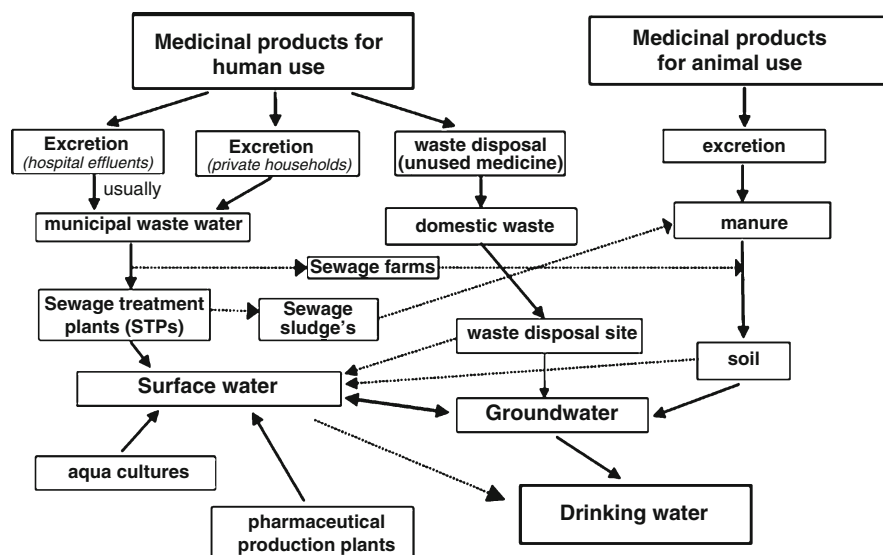


**Fig. 3.12**  Scheme showing possible sources and pathways for the occurrence of pharmaceutical residues in the aquatic environment (Heberer 2002). Reprinted from Heberer T, Occurrence, fate, and removal of pharmaceutical residues in the aquatic environment: a review of recent research data. Toxicology Letters 131:5–17, Copyright (2002), with permission from Elsevier

environment, the PPCP that might have low persistence can display the same exposure potential as truly persistent pollutants, because their transformation and removal rates can be compensated by their replacement rates. While the concentration of individual drugs in the aquatic environment is often low (subparts per billion or subnanomolar, often referred to as *micropollutants*), the presence of numerous drugs sharing a specific mode of action could lead to significant effects through additive exposures.

Many PPCP are used on a daily basis for very long periods, sometimes a good portion of the user's lifetime. Although drugs are usually designed with a specific mode of action in mind, they can also have numerous effects on nontarget or as yet unknown receptors, and possibly cause side effects in the target organism. Furthermore, and of equal importance, nontarget organisms can have receptors, or receptor tissue distributions, that do not exist in the target organisms, and therefore unexpected effects can result from unintentional exposure. Often PPCP are released to the environment in low concentrations for long periods, which in turn may cause genetic selection of the more resistant pathogens that can reduce the effectiveness of current medications.

Traditionally, drugs were rarely viewed as potential environmental pollutants; there was seldom serious consideration as to their fates once they were excreted from the user. On the contrary, until the 1990s, any concerted efforts to search for drugs in the environment would have met with limited success: the requisite chemical analysis tools with sufficiently high separatory efficiencies to resolve drugs from the plethora of other (native and anthropogenic) substances, and with sufficiently low detection limits (i.e., nanograms per liter or parts per trillion), were not commonly available.

## 3.11   Surfactants

Surfactants are defined as surface active agents. These are chemical species that act as wetting agents to lower the surface tension of a liquid. A surfactant molecule is comprised of a water-soluble (hydrophilic) component and a water-insoluble (hydrophobic) component. The hydrophobic part usually contains a hydrocarbon chain of length $C_8$–$C_{18}$, and can be aliphatic, aromatic, or a mixture of both. The sources of hydrophobes are usually natural fats and oils, petroleum fractions, relatively short synthetic polymers, or relatively high molecular weight synthetic alcohols. The hydrophilic groups provide the primary classification to surfactants, and are anionic, cationic, and nonionic in nature. The anionic hydrophiles are the carboxylates (soaps), sulfates, sulfonates, and phosphates. The cationic hydrophiles are some form of an amine product. The nonionic hydrophiles associate with water at the ether oxygens of a polyethylene glycol chain. In each case, the hydrophilic end of the surfactant is attracted strongly to the water molecules, while the force of attraction between the hydrophobe and water is only slight. As a result, surfactant molecules align themselves at the surface and internally so that the hydrophilic ends are oriented toward the water, and the hydrophobic components are aligned away

**Table 3.4** Impact of surfactants on soil. Reprinted from Kuhnt G (1993) Behavior and fate of surfactants in soil. Environ Toxicol Chem 12:1813–1820. Copyright 1993 with permission of John Wiley and Sons

| Soil parameters | Reported impacts | Possible effects |
|---|---|---|
| **Soil physics** | | |
| Soil–water balance | | |
| Surface tension | Reduction | Enhanced water mobility |
| Water/air content | Alteration | Unbalanced water content in different pore fractions |
| Water capacity | Alteration: reduction or enhancement dependent or soil composition and chemical | Changes is soil–water conditions |
| Infiltration and percolation | Reduction by anionic surfactants | Acceleration of soil erosion |
| | Enhancement by cationic surfactants | Washout of nutrients and pollutants |
| | Soil-dependent alteration by nonionic surfactants | |
| Permeability and capillarity | Chemical-dependent alteration | Acceleration of wetting or drying |
| Dispersion | Enhancement by anionic surfactants | Worsening of soil structure Water-logging effects |
| Evaporation | Reduction | |
| Soil structure | | |
| Porosity | Alteration, dependent on type of chemical | Stability or instability of the solid phase |
| Aggregation | | Improvement or worsening of soil–water balance |
| **Soil chemistry** | | |
| pH value | Alteration, dependent on exchange reaction | Altered reactivity and composition of the soil solution |
| Sorption processes | Blocking of exchange surfaces and reduction of exchange capacity | Mobilization of nutrients and/or pollutants |
| Redox potential | Decrease at certain conditions | Alteration of microbial population and/or activity |
| | | Increased persistence of potentially degradable organic chemicals |
| **Soil biology** | | |
| Microorganisms and biological activity | Alteration of population | Higher persistence of organic pollutants |
| | Decrease in activity | |
| | Inhibition of nitrification | Influences on soil fertility and plant nutrition |
| Plants | Influences on growth and cell activity | Enhancement or reduction of growth (direct/indirect) |

from the water. Foaming agents, emulsifiers, and dispersants are surfactants which suspend, respectively, a gas, an immiscible liquid, or a solid in water or some other liquid. Although there is similarity in these functions, in practice the surfactants required to perform these functions differ widely.

The surface tension of soil was found to be reduced even through exposure to low concentrations of surfactants (Law et al. 1966). The change induced to surface tension causes modifications in the capillary pressure, which in turn alter the distribution of water and air in soil–subsurface system pores. Faster drainage and water infiltration are expected when the surface tension is reduced (Kuhnt 1993). Reviewing surfactant behavior in soils, Kuhnt (1993) suggested that reduced surface tension leads to higher wettability of primary soil particles, which consequently decreases aggregate stability and induces dispersion and translocation of soil particles. Surfactants, mostly cationic ones, can also adsorb on the soil and subsurface solid phase, mainly negatively charged clays or organic substances.

Once adsorbed, surfactants can alter hydrophobic interfaces, modifying them to become hydrophilic, which may result in higher runoff rates and accelerated soil erosion. Exchange reactions of anionic surfactants with soil solution can replace hydroxyl groups and consequently change the pH. Alternatively, anionic surfactants can decrease the positive charge of surfaces. Cationic surfactants bind strongly and often irreversibly to soil colloids, especially multilayer clays such as montmorillonite (Kuhnt 1993). Another implication of exposure to surfactants is exchange of sorbed ions (possibly heavy metals), which can alter the soil solution composition. A summary of various soil parameters and the changes induced by exposure to surfactants is given in Table 3.4.

# References

Adriano DC, Bolan NS, Vangronsveld J, Wenzel WW (2005) Heavy metals. In: Hillel D (ed) Encyclopedia of soils in the environment. Elsevier, Amsterdam, pp 175–182

Alan WT (2004) Fertilizers, Kirk-Othmer encyclopedia of chemical technology. Wiley, NY

Allison JD, Brown DS, Novo-Gradac KJ (1990) MINTEQA2/PRODEFA2, A Geochemical Assessment Model for Environmental Systems: Version 3.0. US Environmental Protection Agency, Athens, GA

Antoniadis V, Tsadilas CD (2007) Sorption of cadmium, nickel and zinc in mono- and multimetal systems. Appl Geochem 22:2375–2380

Atanassova I (1999) Competitive effect of copper, zinc, cadmium and nickel on ion adsorption and desorption by soil clays. Water Air Soil Pollut 113:115–125

ATSDR (1999) Toxicological profile for cadmium. U.S. Department of Health and Human Services. Public Health Service. Agency for Toxic Substances and Disease Registry

Avudainayagam S, Megharaj M, Owens G, Kookana RS, Chittleborough D, Naidu R (2003) Chemistry of chromium in soils with emphasis on tannery waste sites. Rev Environ Contam Toxicol 178:53–91

Balbus J, Denison R, Florini K, Walsh S (2005) Getting nanotechnology right the first time. Iss Sci Technol, Summer: 65–71

Barbash JE (2003) Treatise on geochemistry, Vol 9. In: Sherwood Lollar B (ed) Elsevier, 541–577

Birnbaum LS, Sttaskal DF (2004) Brominated flame retardants: cause for concern? Environ Health Perspect 112:9–17

Bradlow HL, Davis DL, Lin G, Sepkovic D, Tiwari R (1995) Effects of pesticides on the ratio of 16 alpha/2-hydroxyestrone: a biologic marker of breast cancer risk. Environ Health Perspect 103:147–50

Brigger I, Dubernet C, Couvreur P (2002) Nanoparticles in cancer therapy and diagnosis. Adv Drug Deliv Rev 54:631–51

Briggs SA (1992) Basic guide to pesticides: their characteristics and hazards. CRC, FL

Brus L (1986) Electronic wave functions in semiconductor clusters: experiment and theory. J Phys Chem 90:2555–2560

Burkholder JM, Mallin MA, Glasgow HB (1999) Fish kills, bottom-water hypoxia, and the toxic Pfiesteria complex in the Neuse River and Estuary. Mar Ecol Prog Ser 179:301–310

C&EN (2002) Call for investigation of Syngenta, Government Concentrates C&EN, 80(23)

Citeau L, Lamy I, van Oort F, Elsass F (2003) Colloidal facilitated transfer of metals in soils under different land use. Colloid Surf A: Physicochem Eng Aspect 217:11–19

Colvin VL (2003) The potential environmental impact of engineered nanomaterials. Nat Biotechnol 21:1166–1170

Cooper R, Chadwick R, Rehnberg G, Goldman J (1989) Effect of lindane on hormonal control of reproductive function in the female rat. Tox Appl Pharm 99:384–394

Danzo BJ (1997) Environmental xenobiotics may disrupt normal endocrine function by interfering with the binding of physiological ligands to steroid receptors and binding proteins. Environ Health Perspect 105:294–301

Daughton CG (2004) Non-regulated water contaminants: emerging research. Environ Impact Asses Rev 24:711–732

Daughton CG, Ternes TA (1999) Pharmaceuticals and personal care products in the environment: agents of subtle change. Environ Health Perspectives 107:907–942

Davis JA (1984) Complexation of trace metals by adsorbed natural organic material. Geochim Cosmochim Acta 48:679–691

Davis JA, Leckie JO (1978) Effect of adsorbed complexing ligands on trace metal uptake by hydrous oxides. Environ Sci Technol 12:1309–1315

Denaix L, Semlali RM, Douay F (2001) Dissolved and colloidal transport of Cd, Pb, and Zn in a silt loam soil affected by atmospheric industrial deposition. Environ Pollut 113:29–38

DePierre JW (2003) Mammalian toxicity of organic compounds of bromine and iodine. Handbook Environ Chem 3:205–251

DeShon ND (1979) Carbon Tetrachloride. Kirk-Othmer Encyclopedia of Chemical Technology, 3rd ed. In: Grayson M, Eckroth D (eds) New York, John Wiley and Sons, Inc. 5:704–714 [as cited by Santodonato J. 1985. Monograph on human exposure to chemicals in the workplace: Carbon tetrachloride; PB86-143377; SRC-TR-84-1123]

Doherty RE (2000a) A history of the production and use of carbon tetrachloride, tetrachloroethylene, trichloroethylene and 1,1,1-trichloroethane in the United States: Part 2 – trichloroethylene and 1,1,1-trichloroethane. J Environ Forensics 1:83–93

Doherty RE (2000b) A history of the production and use of carbon tetrachloride, tetrachloroethylene, trichloroethylene and 1,1,1-trichloroethane in the United States: Part 1-historical background; carbon tetrachloride and tetrachloroethylene. J Environ Forensics 1:69–81

Dorr H, Munnich KO (1991) Lead and cesium transport in European forest soil. Water Air Soil Pollut 57(58):809–818

Dowling A (2004) Development of nanotechnologies. Mater Today 7(suppl 1):30–35

Dror I, Baram D, Berkowitz B (2005) Use of nanosized catalysts for transformation of chloroorganic pollutants. Environ Sci Technol 39:1283–1290

ECB (2005) Risk assessment: Cadmium metal/Cadmium oxide, Final, but not adopted version of Dec 2005. European Chemicals Bureau, Ispra, Italy

ECETOC (1988) Nitrate and drinking water. Brussels, European Chemical Industry Ecology and Toxicology Centre (Technical Report No. 27)

EPA (1987) Estimated national occurrence and exposure to nitrate and nitrite in public drinking water supplies. United States Environmental Protection Agency, Office of Drinking Water, Washington, DC

EPA (1992) Lead poisoning and your children (800-B-92–0002). Office of Pollution Prevention and Toxics, Washington, DC

EPA (1999) Contaminant persistence and mobility factors. The Class V Underground Injection Control Study, Appendices E. United States Environmental Protection Agency, Office of Ground Water and Drinking Water, Washington, DC

EPA (2004) report http://www.epa.gov/opp00001/pestsales/01pestsales/historical_data2001_3.htm

EPA (2005a) http://www.epa.gov/OGWDW/dwh/t-ioc/cadmium.html

EPA (2005b) Environmental Protection Agency. Trichloroethylene (TCE) health risk assessment: Overview. Available at http://oaspub.epa.gov/eims/xmlreport.display?deid=119268&z_chk=31804

EPA (2006) About pesticides http://www.epa.gov/pesticides/

Erickson BE (2002) Analyzing the ignored environmental contaminants. Environ Sci Technol 36:140A–145A

Fendorf SE (1995) Surface reactions of chromium in soils and waters. Geoderma 67:55–71. doi:10.1016/0016-7061(94)00062-F

Gachon L (1969) Les methods d'appréciation de la ferlité phosphorique des sols. Assoc Fr Etude Sol 4:17–31

Gambrell RP (1994) Trace and toxic metals in wetlands - a review. J Environ Qual 23:883–891

Gambrell RP, Khalid RA, Patrick WH Jr (1980) Chemical availability of mercury, lead, and zinc in mobile bay sediment suspensions as affected by pH and oxidation-reduction conditions. Environ Sci Technol 14:431–436

Gerhartz W (ed) (1986) Ullman's encyclopedia of industrial chemistry, 5th edn. Weinheim, New York

Gotoh H, Patrick WH Jr (1974) Transformation of iron in a waterlogged soil as influenced by redox potential and pH. Soil Sci Soc Am Proc 38:66–71

Gustafson JB, Tell JG, Orem D (1997) Selection of representative TPH fractions based on fate and transport considerations total petroleum hydrocarbon criteria, Working Group Series, vol 3. Amherst Scientific Publishers, Amherst, MA

Han FX, Su Y, Monts DL, Plodinec MJ, Banin A, Triplett GE (2003) Assessment of global industrial-age anthropogenic arsenic contamination. Naturwissenschaften 90:395–401

Hayes RB (1997) The carcinogenicity of metals in humans. Cancer Causes Control 8:371–385

Heberer T (2002) Occurrence, fate, and removal of pharmaceutical residues in the aquatic environment: a review of recent research data. Toxicology Letters 131:5–17

Heberer T, Reddersen K, Mechlinski A (2002) From municipal sewage to drinking water: fate and removal of pharmaceutical residues in the aquatic environment in urban areas. Water Sci Technol 46:81–88

Hickman JC (2000) Tetrachloroethylene Kirk-Othmer encyclopedia of chemical technology. http://www.mrw.interscience.wiley.com/emrw/9780471238966/kirk/article/tetrhick.a01/current/pdf

Holbrook MT (2000) Carbon tetrachloride Kirk-Othmer encyclopedia of chemical technology. Wiley. http://www.mrw.interscience.wiley.com/emrw/9780471238966/kirk/article/carbholb.a01/current/pdf

Hook JE (1983) Movement of phosphates and nitrogen in soils following application of municipal wastewater. In: Nielson DW, Elrik DE, Tanji KK (eds) Chemical mobility and reactivity in soil system. Soil Sci Soc Am Spec Pub 11:241–255

Howard CV (2004) Small particles – big problems. Int Lab News 34(2):28–9

HSDB (1995) Hazardous substances data bank. National Library of Medicine, Bethesda, MD (CD-ROM version). Denver, CO: Micromedex, Inc.

HSDB (2000) Hazardous substances data bank. National Library of Medicine, Bethesda, MD. Available online through Toxicology Data Network at http://toxnet.nlm.nih.gov

Hu SP, Chen XC, Shi JY, Chen YX, Lin Q (2008) Particle-facilitated lead and arsenic transport in abandoned mine sites soil influenced by simulated acid rain. Chemosphere 71:2091–2097

ICAIR Life Systems, Inc. (1987) Drinking water criteria document on nitrate/nitrite. United States Environmental Protection Agency, Office of Drinking Water, Washington, DC

Jacks G, Sharma VP (1983) Nitrogen circulation and nitrate in ground water in an agricultural catchment in southern India. Environ Geol 5(2):61–64

Jarup L (2003) Hazards of heavy metal contamination. Br Med Bull 68:167–182

Klaine SJ, Alvarez PJ, Batley GE, Fernandes TF, Handy RD, Lyon DY, Mahendra S, McLaughlin MJ, Lead JR (2008) Nanomaterials in the environment: behavior, fate, bioavailability, and effects. Environ Toxicol Chem 27:1825–1851

Kuhnt G (1993) Behavior and fate of surfactants in soil. Environ Toxicol Chem 12:1813–1820

Kumaresan M, Riyazuddin P (2001) Overview of speciation chemistry of arsenic. Curr Sci 80:837–846

Law JP, Bloodworth ME, Runklers JR (1966) Reactions of surfactants with montmorillonitic soils. Soil Sci Soc Am Proc 30:327–332

Laxen DPH (1985) Trace metal adsorption/coprecipitation on hydrous ferric oxide under realistic conditions. Water Res 19:1229–1236

Letterman RD (ed) (1999) Water quality and treatment: a handbook of community water supplies, 5th Ed. Am Water Works Assoc. McGraw-Hill, Inc., New York

Linak E, Lutz HJ, Nakamura E (1990) $C_2$ chlorinated solvents. In: Linak E, Lutz HJ, Nakamura E (eds) C2 chlorinated solvents, chemical economics handbook. Stanford Research Institute, Menlo Park, CA, pp 632.30000a–632.3001Z

Lindsay WL (1979) Chemical equilibria in soils. Wiley, New York

Marshall KA (2003) Chlorocarbons and chlorohydrocarbons, Survey Kirk-Othmer Encyclopedia of Chemical Technology. Wiley. 6:226–253 http://www.mrw.interscience.wiley.com/emrw/9780471238966/search/firstpage

Maskall JE, Thornton I (1998) Chemical partitioning of heavy metals in soils, clays and rocks at historical lead smelting sites. Water Air Soil Pollut 108:391–409

Matthews GA (2006) Pesticides: health, safety and the environment. Blackwell, Oxford, UK

Mckenzie LC, Hutchison JE (2004) Green nanoscience. Chimica Oggi-Chemistry Today 22:30–33

McLean JE, Bledsoe BE (1992) Behavior of metals in soils. Ground Water Issue US EPA EPA/540/S-92/018 (as cited by U.S. EPA, 1999)

McMurray CT, Tainer J (2003) Cancer, cadmium and genome integrity. Nat Genet 34:239–241

Mengel K (1985) Dynamics and availability of major nutrients in soils. Adv Soil Sci 2:67–134

Mercer JW, Cohen RM (1990) A review of immiscible fluids in the subsurface: properties, models, characterization, and remediation. J Contam Hydrol 6:107–163

Mertens JA (2000) Trichloroethylene Kirk-Othmer encyclopedia of chemical technology http://www.mrw.interscience.wiley.com/emrw/9780471238966/kirk/article/tricmert.a01/current/pdf John Wiley & Sons, Inc.

Milne WGA (1995) Handbook of pesticides. CRC, FL

Mohanty AK, Drzal LT, Misra M (2003) Nano reinforcements of bio-based polymers – the hope and the reality. Polymer Mater Sci Eng 88:60–61

Montgomery JH (1993) Agrochemicals desk reference: environmental data. Lewis, Chelsea, MI

Moore MN (2002) Biocomplexity: the post-genome challenge in ecotoxicology. Aquat Toxicol 59:1–15

Moore MN (2006) Do nanoparticles present toxicological risks for the health of aquatic environment? Environ Int 32:967–976

Murphy EM, Zachara JM (1995) The role of sorbed humic substances on the distribution of organic and inorganic contaminants in groundwater. Geoderma 67:103–124

Nadim F, Hoag GE, Liu SL, Carley RJ, Zack P (2000) Detection and remediation of soil and aquifer systems contaminated with petroleum products: an overview. J Petrol Sci Eng 26:169–178

Nariagu JO (1996) History of global metal pollution. Science 272:223–224

Nel A, Xia T, Madler L, Li N (2006) Toxic potential of materials at the nanolevel. Science 311:622–627

Newman A (1995) Atrazine found to cause chromosomal breaks. Environ Sci Technol 29:450A

Newman ME, Elzerman AW, Looney BB (1993) Facilitated transport of selected metals in aquifer material packed columns. J Contam Hydrol 14:233–246

Nurmi JT, Tratnyek PG, Sarathy V, Baer DR, Amonette JE, Pecher K, Wang CM, Linehan JC, Matson DW, Penn RL, Driessen MD (2005) Characterization and properties of metallic iron nanoparticles: spectroscopy, electrochemistry, and kinetics. Environ Sci Technol 39:1221–1230

Ordish G (2007) History of agriculture beginnings of pest control. Encyclopedia Britannica http://www.britannica.com/eb/article-10711/history-of-agriculture

Owen R, Depledge M (2005) Nanotechnology and the environment: risks and rewards. Marine Pollut Bull 50:609–612

Palmer CD, Wittbrodt PR (1990) Geochemical characterization of the United Chrome Products Site, Final Report. In: Stage 2 deep aquifer drilling technical report, United Chrome Products Site, Corvallis, OR, September 28, 1990. CH2M Hill, Corvallis, OR

Pierzynski GM, Sims JT, Vance GF (2000) Soils and environmental quality, 2nd edn. Lewis Publ, Chelsea

Pratt PF, Jury WA (1984) Pollution of unsaturated zone with nitrate. In: Yaron B, Dagan G, Goldshmid J (eds) Pollutants in porous media. Springer, Berlin, pp 52–67

Reeder AL, Foley GL, Nichols DK, Hansen LG, Wikoff B, Faeh S, Eisold J, Wheeler MB, Warner R, Murphy JE, Beasley VR (1998) Environ Health Perspect 106:261–266

Renner R (2002) Is sludge safe? Environ Sci Technol 36:46A

Royal Society and Royal Academy of Engineering (2004) Nanoscience and nanotechnologies: opportunities and uncertainties. RS policy document 19/04. The Royal Society, London, p 113

Sharpley A, Tunney H (2000) Phosphorus research strategies to meet agricultural and environmental challenges of the 21st century. J Environ Qual 29:176–181

Shaw G (2005) Applying radioecology in a world of multiple contaminant. J Environ Radioactivity 81:117–130

Sims JT, Simard RR, Joern BC (1998) Phosphorus loss in agricultural drainage – historical perspective and current research. J Environ Qual 27:277–293

Sposito G (1984) The surface chemistry of soils. Oxford University Press, New York, NY

Stannard JN (1973) Toxicology of radionuclides. Ann Rev Pharmacol 13:325–357

Tavera-Mendoza L, Ruby S, Brousseau P, Fournier M, Cyr D, Marcogliese D (2002a) Response of the amphibian tadpole (Xenopus laevis) to atrazine during sexual differentiation of the testis. Environ Toxicol Chem 21:527–531

Tavera-Mendoza L, Ruby S, Brousseau P, Fournier M, Cyr D, Marcogliese D (2002b) Response of the amphibian tadpole *Xenopus laevis* to atrazine during sexual differentiation of the ovary. Environ Toxicol Chem 21:1264–1267

Toor GS, Condron LM, Di HJ, Cameron KC, Cade-Menun BJ (2003) Characterization of organic phosphorus in leachate from a grassland soil. Soil Bio Biochem 35:1317–1323

Tsang DCW, Lo IMC (2006) Competitive Cu and Cd and transport in soils: a combined batch kinetics, column, and sequential extraction study. Sci Total Environ 40:6655–6661

Turner DR, Whitfield M, Dickson AG (1981) The equilibrium speciation of dissolved components in freshwater and seawater at 25°C and 1 atm pressure. Geochim Cosmochim Acta 45:855–881

UNSCEAR (2000a) Annex B exposures from natural radiation sources, http://www.unscear.org/pdffiles/annexb.pdf

UNSCEAR (2000b) Annex C exposures to the public from man-made sources of radiation, http://www.unscear.org/pdffiles/annexc.pdf

van Duijvenboden W, Loch JPG (1983) Nitrate in the Netherlands: a serious threat to groundwater. Aqua 2:59–60

van Duijvenboden W, Matthijsen AJCM (1989) Integrated criteria document nitrate. Bilthoven, Rijksintituut voor de Volksgezondheid en Milieuhygiëne (National Institute of Public Health and Environmental Protection) (RIVM Report No. 758473012)

Vorhees DJ, Weisman WH, Gustafson JB (1999) Human health risk-based evaluation of petroleum release sites: implementing the working group approach. In: Total petroleum hydrocarbon criteria working group. Amherst Scientific Publishers, Amherst, MA

Wang Y, Herron N (1991) Nanometer-sized semiconductor clusters: material synthesis, quantum size effects, and photophysical properties. J Phys Chem 95:525–532

Warheit DB (2004) Nanoparticles: health impacts? Mater Today 7:32–35

WHO (1985) Health hazards from nitrates in drinking water. World Health Organization, Geneva

WHO (2001) Arsenic and arsenic compounds. Environmental Health Criteria 224 The International Programme on Chemical Safety (IPCS), http://www.inchem.org/documents/ehc/ehc/ehc224.htm

WHO (2005) The World Health Organization Recommended Classification of Pesticides by Hazard http://www.who.int/ipcs/publications/pesticides_hazard_rev_3.pdf

Wood A (2006) Compendium of Pesticide Common Names – Classified Lists of Pesticides http://www.alanwood.net/pesticides/class_pesticides.html

Yin X, Gao B, Ma LQ, Saha UK, Sun H, Wang G (2010) Colloid-facilitated Pb transport in two shooting range soils in Florida. J Haz Mat 177:620–625

Young CP, Morgan-Jones M (1980) A hydrogeochemical survey of the chalk groundwater of the Banstead area, Surrey, with particular reference to nitrate. J Inst Water Eng Sci 34:213–236

Zhu YG, Shaw G (2000) Soil contamination with radionuclides and potential remediation. Chemosphere 41:121–128

# Chapter 4
# On the Retention and Transformation of Contaminants in Soil and the Subsurface

In the Critical Zone, anthropogenic chemical contaminants come into contact with a soil–subsurface system that exhibits vertical and horizontal heterogeneity, and is subject to seasonal climatic conditions expressed in terms of variations in temperature and water content. As a consequence, the soil–subsurface system displays both aerobic and anaerobic conditions. Active microbial populations that develop under these environmental conditions, as well as plant exudates, also affect contaminant behavior in the soil–subsurface system. Clay minerals and organic geosorbents, characterized by particles of size down to 2 μm, exhibit high surface charge, and selectively control the retention and release of contaminants in the surrounding liquid and gaseous phases of the soil–subsurface system. Specific contaminants may also be retained in the soil–subsurface solid phase as a result of physical or mechanical processes such as precipitation, deposition, or trapping.

Contaminants adsorbed or retained on or within the soil–subsurface solid phase may be transformed by both abiotic and biotic (biologically mediated) processes. As a result, contaminant properties may change and additional metabolites may be formed, which are subject to different interactions in the soil–subsurface system.

This chapter is devoted to a short presentation of contaminant adsorption and release processes on the soil–subsurface solid phase, and of surface-induced and biomediated contaminant transformations in the soil–subsurface environment.

## 4.1 Contaminant Retention by Surface Adsorption

### 4.1.1 Surface Properties of Geosorbents

*Clay minerals* have a permanent negative charge due to isomorphous substitution or vacancies in their structure. This charge ranges from zero to >200 centimoles/kg ($cmol_c$ $kg^{-1}$) and must be balanced by cations (counterions) at or near the mineral

surface that affect the interfacial properties. Chemical composition and charge characteristic of selected layer silicates are shown in Table 4.1.

The stability of clay suspensions in soil water solutions is controlled by low counter-ion charge, low electrolyte concentration, or high dielectric constant of the solvent, which favor a high interparticle electrostatic repulsion force. Interparticle association in negatively charged colloids induces clay flocculation. These behaviors validate the diffuse double-layer model, which treats the layer-silicate surface as a structurally featureless plane with a uniformly distributed negative charge (van Olphen 1967).

*Oxides and hydroxides* of Al, Fe, Mn, and Si are present in the soil–subsurface system, mainly as a mixture rather than as pure mineral phases. This mixture, known as a *solid solution*, is an amphoteric material with no permanent surface charge. Adsorption of potential determining ions as $H^+$ and OH determines cationic or anionic exchange capacity. Different surfaces have a diverse affinity for $H^+$ and $OH^-$ ions, exhibiting different points of zero charge (McBride 1989).

*Humic substances*, including both humic and fulvic acids, are the soil–subsurface system components containing functional groups able to control cation exchange capacity (CEC) and the complexation of metals. The CEC of humic substances was calculated by Oades (1989) to usually be one electric charge per square nanometer, although in some cases it may range from 0.3 to 1.3 (Greenland and Mott 1978). Because of the polydiversity of humic substances and their diverse chemistry, it is difficult to obtain a well-defined quantification of their capacity for ion exchange and metal complexation.

*Organo-mineral association* in the soil–subsurface system is a natural process controlled by a range of bonding mechanisms, and therefore, it is almost impossible to separate one from another. Organo-mineral complexes have surface properties different from their original components. For example, hydrophilic clay surfaces may become hydrophobic as a result of their association with organic compounds.

**Table 4.1** Chemical composition and charge characteristics of selected layer silicate (modified after McBride 1994). Copyright 1989, Soil Science Society of America. Reprinted with permission

| Mineral | Chemical structure | Structure | Charge per half unit cell | | Structural charge, $cmol_c/kg$ |
| --- | --- | --- | --- | --- | --- |
| | | | Tetrahedral | Octahedral | |
| Montmorillonite | $Ca_{0.165}Si_4(Al_{1.67}Mg_{0.33})$ $O_{10}(OH)_2$ | 2:1 Dioctahedral | 0 | −0.33 | 92 |
| Beidelite | $Ca_{0.25}(Si_{3.5}Al_{0.5})$ $Al_2O_{10}(OH)_2$ | 2:1 Dioctahedral | −0.5 | 0 | 135 |
| Talc | $Si_4Mg_3O_{10}(OH)_2$ | 2:1 Trioctahedral | 0 | 0 | 0 |
| Vermiculite | $Mg_{0.31}(Si_{3.15}Al_{0.85})$ $(Mg_{2.69}Fe_{0.23}^{3+}Fe_{0.08}^{2+})$ $O_{10}(OH)_2$ | 2:1 Trioctahedral | −0.85 | +0.23 | 157 |
| Kaolinite | $Si_2Al_2O_5(OH)_4$ | 1:1 Dioctahedral | 0 | 0 | 0 |
| Serpentine | $Si_2Mg_3O_5(OH)_4$ | 1:1 Trioctahedral | 0 | 0 | 0 |

## 4.1.2   Surface Adsorption

Adsorption of contaminants is determined by comparing the excess concentration of chemicals at the soil–subsurface solid interface to the concentration in the environmental bulk solution or gaseous phase, regardless of the nature of the interface region or of the interaction between the adsorbate and the solid phase which causes the excess. Adsorptive removal of a chemical compound from the bulk phase greatly affects the composition of the soil and subsurface environment.

### 4.1.2.1   Adsorption of Ionic Contaminants

Ion exchange is the predominant mechanism for the adsorption of inorganic and organic contaminants on various constituents of the soil and subsurface solid phase. Electrical neutrality on the solid surface requires that an equal amount of positive and negative charge accumulates in the liquid phase near the surface. If the surface is negatively charged, then positively charged cations are electrostatically attracted to the surface. Simultaneously, the cations are drawn back toward the equilibrating solution; as a result, a diffuse layer is formed and the concentration of cations increases toward the surface. On the contrary, ions of the same sign (anions) are repelled by the surface with diffusion forces acting in an opposite direction. The overall pattern is known as a *diffuse double layer* (DDL). The existence of a DDL was developed theoretically by Gouy and Chapman about 100 years ago and is an integral part of *electric double layer theory*. In general, double-layer theory explains the processes occurring in the soil–subsurface system when pollutants have a charge opposite to that of the geosorbent. The double-layer theory is of considerable use in understanding retention of ionic contaminants.

The Gouy–Chapman model assumes that (1) the exchangeable cations exist as point charges, (2) colloid surfaces are planar and infinite in extent, and (3) surface charge is distributed uniformly over the entire colloid surface. Even though this assumption does not correspond to the subsurface environment, it works well for the clay colloid component of the near-surface and subsurface, a fact that may be explained by mutual cancellation of other interferences. Stern (1924) and Grahame (1947) refined the Gouy–Chapman model by recognizing that counterions are unlikely to approach the surface more closely than the ionic radii of the anions and the hydrated radii of the cations.

The Gouy–Chapman model assumes that the charge is spread uniformly over the surface, with the overall charge allocation in solution consisting of a nonuniform distribution of point charges. The solvent is treated as a continuous medium influencing the double layer only through its dielectric constant, which is assumed independent of its position in the double layer. Moreover, it is assumed that ions and surfaces are involved only in electrostatic interactions. The derivation is for a flat surface, infinite in size. The double-layer theory applies equally well to rounded or spherical surfaces (Overbeek 1952). The model of Stern (1924) assumes that the

region near the surface consists of a layer of ions adsorbed at the surface, forming a compact double layer; this is known as the *Stern layer* or the Gouy–Chapman diffuse double layer.

In the Stern model, the surface charge is balanced by the charge in solution, which is distributed between the Stern layer at a distance $d$ from the surface and a diffuse layer having an ionic Boltzman-type distribution. The total charge $\sigma$ is, therefore, due to the charge in the two layers:

$$\sigma = (\sigma_1 + \sigma_2), \tag{4.1}$$

where $\sigma_1$ is the Stern layer and $\sigma_2$ is the diffuse layer charge.

A development of the diffuse double-layer theory (Stern model) also considers the interactions between the two flat layers of the Gouy–Chapman model. The double-layer charge is affected only slightly when the distance between the two plates is large. Grahame (1947) suggests that specifically adsorbable anions may be adsorbed into the Stern layer when they lose their hydration water, whereas the hydrated cations are attracted only electrostatically to the surface. Bolt (1955) added the effects of ion size, dielectric saturation, polarization energy, and Coulombic interactions of the ions, as well as short-range repulsion of ions into the Gouy–Chapman model. Note that the simple Gouy–Chapman model gives fairly reliable results for colloids with a constant charge density not exceeding 0.2–0.3 charges per m$^2$. The Gouy–Chapman model provides an invaluable answer to a number of processes occurring in the soil–subsurface system, by explaining the exchange capacity concept for the range of surface charge densities normally encountered in clays (Bolt et al. 1991).

CEC and selectivity involve the cationic concentration in solution and the cation dimensions, as well as the configuration of exchange sites on the interface. The Gapon relation approaches the process as an exchange of equivalents of electric charges, where the solute concentration is measured in terms of activity and the adsorption on an equivalent basis. Negatively charged surfaces having the same exchange properties do not necessarily interact in the same manner with different cations having the same valence. This is caused by the differential sizes and polarizability of the cations, by the structural properties of the adsorbent surfaces, and by the differences in the surface charge distribution. For example, ammonium ions ($NH_4^+$) are sorbed preferably over anhydrous $H^+$ or $Na^+$ in 1:2 clay minerals, because they may form NH–oxygen links in the hexagonal holes of Si–O sheets, and they may also link to adjacent oxygen planes in the interlayer space by an OH–N–HO bond. Selectivity of the divalent alkaline earth cations is less pronounced. Trivalent cations, such as $Al^{3+}$, coordinated octahedrally to water molecules, link more strongly than hydrated $Ca^{2+}$ ions.

Cation selectivity on organic matter is related mainly to the disposition of the acidic groups in the adsorbent. Multivalent cations adsorb preferentially over monovalent cations, and transition metals adsorb preferably over strong basic metals. Organo-mineral complexes exhibit a CEC smaller than the sum of the CECs of its components. This phenomenon is reflected in the pattern of cation selectivity (Greenland and Hayes 1981).

**Table 4.2** Adsorption of heavy metals on goethite as a function of pH. Data expressed as percent of initial amount of metallic cation solution (modified from Quirk and Posner 1975). Reprinted from Quirk JP, Posner AM, Trace element adsorption by soil minerals. In: Nicholas DJ, Egan AR (eds) Trace elements in soil-plant-animal systems. Academic Press, New York pp 95–107, Copyright (1975), with permission from Elsevier

| Metal | pH | | | | | | | |
|-------|-----|-----|-----|-----|-----|-----|-----|-----|
|       | 4.7 | 5.2 | 5.5 | 5.9 | 6.4 | 7.2 | 7.5 | 8.0 |
| Cu    | 17  | 55  | 75  | 90  |     |     |     |     |
| Pb    |     | 73  | 56  | 75  |     |     |     |     |
| Zn    |     |     |     | 13  | 22  | 68  |     |     |
| Cd    |     |     |     |     | 23  | 44  | 53  |     |
| Co    |     |     |     |     |     | 39  | 54  | 78  |

Heavy metal cations participate in exchange reactions with negatively charged surfaces of clay minerals, with Coulombic and specific adsorption being the processes involved in the exchange. Metal cationic adsorption is affected by pH. At low pH values (<5.5), some heavy metals do not compete with alkali metals (e.g., $Ca^{2+}$) for the mineral adsorption site. At higher pH values, heavy metal adsorption increases greatly; an example of heavy metal adsorption on goethite as a function of pH is given in Table 4.2.

Cationic organic contaminants often compete with mineral ions for the same adsorption site. At low pH, organic cationic molecules are adsorbed more strongly on earth materials than mineral ions of a similar valence. At moderate pH values, however, mineral ions are favored over organic cations. In general, the charge density of the adsorbing surface is a determining factor in adsorption of cationic organic molecules, but their adsorption is also affected by the molecular configuration (Mortland 1970). Organic molecules may be adsorbed by clays via a cationic adsorption mechanism, but this process depends on the acidity of the medium.

Early work by Boyd et al. (1947), performed on zeolites, showed that the ion exchange process is diffusion controlled and that the reaction rate is limited by mass transfer phenomena that are either film-diffusion (FD) or particle-diffusion (PD) dependent. Under natural conditions, the charge compensation cations are held on a representative subsurface solid phase in different ways: within crystals in interlayer positions (mica and smectites), in structural holes (feldspars), or on surfaces in cleavages and faults of the crystals and on external surfaces of clays, clay minerals, and organic matter.

Cations held on external surfaces of the solid phase are immediately accessible to the soil–subsurface water phase. Once removed from the solid phase, cations move to a region of reduced concentration. This movement is controlled by diffusion, and the diffusion coefficient ($D$) can be calculated using the equation used by Nye and Tinker (1977):

$$D = D_e \theta f (dC_{solution}/dC_{ss}), \tag{4.2}$$

where $D_e$ is the diffusion coefficient in water, $\theta$ is the water content in the soil–subsurface solid phase, $f$ is the "impedance" factor related to the subsurface

tortuosity, $C_{ss}$ is the cation concentration in the soil–subsurface (solid and water phases) expressed as mass/volume, and $C_{solution}$ is the cation concentration in solution.

Two aspects should be considered in the cation exchange process: (1) The number of exchange sites occupied by the cation investigated and (2) the selectivity of the cation relative to the concentration of the exchanging cation. Cations held on the external surfaces of clays exhibit a relatively rapid diffusion but are subject to an additional limitation. Because the arrival rate of ingoing cations at the exchange site is much slower than the release rate of the outgoing cations, the rate-determining step is the influx of exchanging cations to negatively charged sites. Sparks (1986) defined the following concurrent processes that take place for $Na^+$ and $K^+$ exchange in vermiculite: (1) Diffusion of $Na^+$ with $Cl^-$ through the solution film that surrounds the particle (FD), (2) diffusion of $Na^+$ ions through a hydrated interlayer space and chemical reaction leading to exchange of $Na^+$ in the particle (PD), (3) chemical reaction leading to exchange of $Na^+$ by $K^+$ ions on the particle surface (CR), (4) diffusion of displaced $K^+$ ions through the hydrated interlayer space of the particle (PD), and (5) diffusion of displaced $K^+$ ions with $Cl^-$ through the solution film away from the particle (FD). Based on a study of the time-dependent sorption of pesticides in soil aggregates, Villaverde et al. (2009) found that diffusion into aggregates may be the major time-limiting process for sorption of organic contaminants in structured soils.

To enable a chemical reaction, the exchange ions must be transported to the active sites of the particles. The film of water adhering to and surrounding the particle, and the hydrated interlayer space within the particle are zones of low contaminant concentration that are depleted constantly by ion adsorption to the sites. The decrease in concentration of contaminant ions in these interfacial zones is then compensated for by ion diffusion from the bulk solution. Ion exchange occurs when a driving force, such as a chemical potential gradient, is maintained between solid and solution or when access to sites is kept free by the use of a hydrated and less preferred cation for exchange.

The properties of the organic and inorganic constituents of the subsurface solid phase, as well as the properties of the contaminants (e.g., ion charge and radius), define the time-span of ion exchange, which may range from a few seconds to days (Yaron et al. 1996). The slowly exchangeable cations are situated on exchange sites in interlayer spaces of the minerals (e.g., smectites) or in cages and channels of organic matter, and exchange and move into solution by diffusive flux.

*Negative adsorption* occurs when a charged solid surface faces an ion of similar charge in an aqueous suspension, and the ion is repelled from the surface by Coulomb forces. The Coulomb repulsion produces a region in the aqueous solution that is relatively depleted of the anion, and an equivalent region far from the surface that is relatively enriched. If, for example, a dilute neutral solution of KCl is added to dry clay, the $Cl^-$ equilibrium concentration in the bulk solution will be greater than the $Cl^-$ concentration in the solution originally added to the clay. Anionic negative adsorption is affected by the anion charge, concentration, pH, the presence of other anions, and the nature and charge of the surface. Negative adsorption may decrease as the subsurface pH decreases and when anions can be adsorbed by

positively charged surfaces. The larger negative charge of the surface results in a greater anion negative adsorption. Acidic organic contaminants in their anionic form are expected to be repelled by negatively charged clay surfaces.

### 4.1.2.2   Adsorption of Nonionic Contaminants

The sorption of a nonpolar organic contaminant on a solid phase is derived by enthalpy- and entropy-related forces. The enthalpy is primarily a function of the changes in the bonding between the adsorbing surface and the sorbate (solute) and between the solvent (water) and the solute. The entropy term is related to the increase or decrease in the order of the system upon sorption. The mechanisms involved in adsorption of nonionic compounds on clay minerals are defined by Hassett and Banwart (1989) as enthalpy-related adsorption forces. The processes involved are as described below.

*Hydrogen bonding* refers to the electrostatic interaction between a hydrogen atom covalently bound to one electronegative atom (e.g., oxygen) and another electronegative atom or group of atoms in a neighboring molecule. The hydrogen atom may be regarded as a bridge between electronegative atoms; this bonding is conceived of as an induced dipole phenomenon. The H bond is generally considered as the asymmetrical distribution of the first electron of the H atom induced by various electronegative atoms.

*Ligand exchange processes* involve replacement of one or more ligands by the adsorbing species. In some instances, the ligand exchange process can be regarded as a condensation reaction (e.g., between a carboxyl group and a hydroxyl aluminum surface).

The *protonation mechanism* includes Coulomb electrostatic forces resulting from charged surfaces. The development of surface acidity by the solid phase of the subsurface offers the possibility that solutes having proton-selective organic functional groups can be adsorbed through a protonation reaction.

The *π bonds* occur as a result of the overlapping of π orbitals when they are perpendicular to aromatic rings. This mechanism can be used to explain the bonding of alkenes, alkylenes, and aromatic compounds to the subsurface organic matter.

*London-van der Waals forces* are generally multipole (dipole–dipole or dipole-induced dipole) interactions produced by a correlation between fluctuating induced multipole (principal dipole) moments in two nearly uncharged polar molecules. Even though the time-averaged, induced multipole in each molecule is zero, the correlation between the two induced moments does not average zero. As a result, an attractive interaction between the two is produced at very small molecular distances. Van der Waals forces also include dispersion forces that arise from correlations between the movement of electrons in one molecule and those of neighboring molecules. Under such conditions, even a molecule with no permanent dipole moment forms an instantaneous dipole as a result of fluctuations in the arrangements of its electron cloud. This instantaneous dipole polarizes the charge of another molecule to give a second induced dipole, resulting in a mutual dipole–dipole attraction. All molecules are subject to

attraction by dispersion forces whether or not more specific interactions between ions or dipoles occur. Although the momentary dipoles and induced dipoles constantly change positions, the net result is a weak attraction. When many groups of atoms in a polymeric structure interact simultaneously, the van der Waals components are additive.

*Chemisorption* denotes the situation in which an actual chemical bond is formed between the molecules and the surface atoms. A molecule undergoing chemisorption may lose its identity as the atoms are rearranged, forming new compounds that better satisfy the valences of the surface atoms. The enthalpy of chemisorption is much greater than that of physical adsorption. The basis of much catalytic activity at surfaces is that chemisorption may organize molecules into forms that can readily undergo reactions. It is often difficult to distinguish between chemisorption and physical sorption, because a chemisorbed layer may have a physically sorbed layer deposited above it.

Entropy-related adsorption force, denoted *hydrophobic sorption* (and/or *solvophobic interaction*), is the partitioning of nonpolar organics out of the polar aqueous phase onto hydrophobic surfaces, which are retained through dispersion forces. Figure 4.1 shows a schematic model of forces contributing to the sorption of hydrophobic organics relevant to the subsurface environment.

A major feature of hydrophobic sorption is the weak interaction between the solute and the solvent. The primary force in hydrophobic sorption appears to be the large entropy change resulting from the removal of the solute from solution. The entropy change is due largely to the destruction of the cavity occupied by the solute in the solvent and the destruction of the structured water shell surrounding the solvated organic. Hydrophobic interfaces may be found mainly on organic matter and on organically coated minerals.
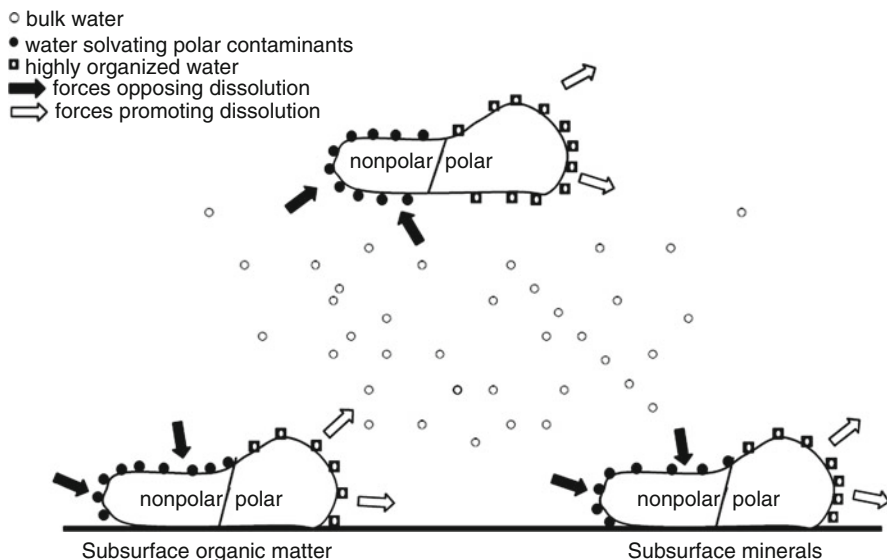


**Fig. 4.1** Forces affecting sorption of nonpolar organic contaminants (after Berkowitz et al. 2008)

Hydrophobic sorption, being an entropy-driven process, provides the major contribution to sorption of hydrophobic contaminants on subsurface solid phases. When a hydrophobic organic compound is adsorbed on a solid phase, the partitioning of the compound and its adsorption by the surface directly from the water phase should be considered. These processes occur in unsaturated and saturated near-surface and subsurface regimes, where water is likely to be the wetting phase. In such cases, the wetting phase completely or partially coats the solid phase surface, thus increasing its sorbing capacity because the wetting phase serves as an additional sink.

Rao et al. (1989) suggested that at least four mechanisms of adsorption should be considered for hydrophobic organic compounds. The first mechanism involves the sorption of neutral molecular species from the aqueous phase, which is similar to hydrophobic sorption. The second mechanism of interest comprises the specific interactions of a dissociated (ionic) species with various functional groups on the sorbent surface. Several models developed for predicting the ion exchange of inorganic ions may be used for predicting this type of sorption. The third sorption mechanism, known as molecular ion pairing, involves transfer of organic ions from the aqueous phase to the organic surface phase. The fourth mechanism covers transfer of organic ions from the aqueous phase to the organic surface while the counterions remain in the electric double layer of the aqueous phase. The relative contribution of each of these mechanisms depends on (1) the extent of compound dissociation as a function of the acid dissociation constant, $pK_a$, and solution pH; (2) the ionic charge status of the solid interface as a function of the pH and of the point of zero charge; and (3) the ionic strength and composition of the water phase.

### 4.1.2.3 Adsorption of Mixtures of Contaminants

Often, contaminants reach the subsurface mainly as complex mixtures, and therefore an understanding of the adsorption process under these more complicated conditions is required. Under a waste disposal site, for example, where organic or organo–metal complexes are involved, sorption may involve multiphase (water and organic) solvent interactions. To deal with complex combinations of organic contaminants and mixtures of solvents containing partially or completely miscible organic solvents, one can use the theoretical approach of Rao et al. (1985) based on the predominance of solvophobic interactions. With increasing volume fractions of a completely miscible organic solvent in a binary mixed solvent, the hydrophobic organic solvent sorption coefficient decreases exponentially as follows:

$$\ln K^m = \ln K^w - \sum \alpha_i \sigma_i f_i, \tag{4.3}$$

where $K$ is the sorption coefficient (moles solvent per kg sorbent), with the superscripts $w$ and $m$ indicating values for sorption from water and mixed solvents, respectively; $\alpha_i$ is a dimensionless term unique to each solvent–sorbate combination

$\sigma_i = \Delta\gamma_i\text{HAS}/(kT)$, where $\Delta\gamma_i$ is the differential interfacial free energy (J nm$^{-2}$) at the solvent–sorbate interface, HAS is the sorbate hydrocarbonaceous surface area (nm$^{-2}$), $k$ is the Boltzmann constant (J/$^\circ$K), $T$ is the thermodynamic temperature; and $f_i$ is the volume fraction of the $i$-th cosolvent.

### 4.1.3 Factors Controlling Adsorption

#### 4.1.3.1 Adsorption Kinetics

Adsorption kinetics involve a time-dependent process that describes the rate of adsorption of chemical contaminants on the solid phase. The "standard" chemical meaning of *kinetics* usually covers the study of the rate of reactions and molecular processes when transport is not a limiting factor; however, this definition is not applicable to soil–subsurface conditions. In the "real" soil–subsurface environment, many kinetic processes are a blend of chemical- and transport-controlled kinetics. Kinetic adsorption may involve concurrent processes that include FD through a solution film surrounding the adsorbant surface, PD through a hydrated interlayer space of a layered adsorbant surface, and CR, a chemical reaction exchange at the adsorbant surface (Sparks 1989; Pignatello 1989).

Understanding the kinetics of contaminant adsorption on the soil–subsurface solid phase requires knowledge of both the *differential rate law*, explaining the reaction system, and the *apparent rate law*, which includes both chemical kinetics and transport-controlled processes. The *differential rates* of chemical processes in the subsurface allow us to predict the time necessary to reach equilibrium or quasi-state equilibrium and understand the reaction mechanism. *Apparent rate laws* consider that diffusion and other microscopic transport phenomena, as well as the structure of the subsurface and/or the flow rate, affect the kinetic behavior. Based on these rate laws, various equations have been developed to describe kinetics of soil chemical processes. As a function of the adsorbent and adsorbate properties, the equations describe mainly first-order, second-order, or zero-order reactions. For example, Sparks and Jardine (1984) studied the kinetics of potassium adsorption on kaolinite, montmorillonite (a smectite mineral), and vermiculite, finding that a single-order reaction describes the data for kaolinite and smectite, while two first-order reactions describe adsorption on vermiculite. Sparks (1989) discussed the application of various kinetic equations to earth materials based on the analysis of a large number of reported studies. Even though different equations describe rate data satisfactorily, Sparks (1989) uses linear regression analysis to show that no single equation best describes every study.

According to the Arrhenius law, the rate of reaction is correlated linearly to the increase in temperature, with the rate constant $k$ given by:

$$k = Ae^{-E/RT}, \tag{4.4}$$

where $A$ is a frequency factor, $E$ is the energy of activation, $R$ is the universal gas constant, and $T$ is the absolute temperature. A low activation energy usually indicates a diffusion-controlled process, while higher activation energy indicates chemical reaction-controlled processes (Sparks and Huang 1985; Sparks 1986). Data on the effect of temperature on the rate of potassium release from potassium-bearing minerals were presented by Huang et al. (1968), and show that a 10 K rise in temperature during the reaction period resulted in a two- to threefold increase in the rate constant.

In the case of soil–subsurface cation exchange, for example, the charge compensation cations are held in the solid phase as follows: within crystals in interlayer positions (mica and smectites), in structural holes (feldspar), or on surfaces in cleavages and faults of the crystals and on external surfaces of clay minerals and organic matter.

The characteristic period of ion exchange in the soil and subsurface ranges from a few seconds to days, as a function of the properties of the solid phase, of the environmental aqueous solution, and of the contaminant charge and radius. The slowly exchangeable cations are situated on exchange sites in interlayer spaces of solid phase minerals or in cages and channels of the soil–subsurface organic matter, and exchange solution by diffusive flux. Ion exchange occurs when a driving force, such as a chemical potential gradient, is maintained between solid and solution phases, or when access to sites is freely maintained by the use of hydrated and less preferred cations for exchange.

### 4.1.3.2   Adsorbant Surface Composition

Independent of the molecular properties of the contaminants, the composition of the solid phase surface constituents is a major factor that controls the adsorption process. Both the mineral and organic components of the solid phases interact differentially with ionic and nonionic pollutants. The structural properties of the subsurface clay fraction are a controlling factor in defining the rate and extent of the ion exchange process. In the case of kaolinite, for example, the tetrahedral layers of adjacent clay sheets are tightly held by H bonds, and only planar external surface sites are available for exchange. Under adequate hydration conditions, the multi-layered smectites are able to swell, allowing a rapid passage of ions into the interlayer space. Vermiculite is characterized by a more structured interlayer space because the region between layers of silicate is selective for certain types of cations such as $K^+$ and $NH_4^+$ (Sparks and Huang 1985). Cation exchange is also affected by the particle size of the mineral fraction. For example, it was reported (Kennedy and Brown 1965) that of the total Ca–Na content of a sand layer, 90% is composed of particles of 0.12–0.20 mm and only 10% contains a 0.20–0.50-mm sand fraction. Similar behavior was observed on silt materials where the exchange rates (Ba–K) on medium and coarse silt diminish with increasing particle size.

The organic fraction composition may influence the exchange capacity process. A key contribution to the exchange capacity of humus in the soil–subsurface system

is given by the carboxyl and phenolic hydroxyl functional groups. Under appropriate pH conditions, uranic acids in polysaccharides or carboxy-terminal structures in peptides can contribute to the negative charge and CEC of the soil organic matter. The basic amino acids lysine, arginine, and histidine are positively charged at pH = 6; the amino terminal groups in peptides and polypeptides can be expected to be the principal contributors to positive charges in soil–subsurface organic materials, in an appropriate pH environment (Talibuden 1981). The CEC of the organo-mineral complexes is less than the sum of each of the separate organic and mineral components. The CEC decrease may be explained by changes occurring in the humus configuration following coating of the mineral surface.

A significant elucidation of the relative contributions of mineral and organic colloids to the adsorption of organic contaminants was made through studies with separated fractions and well-defined model materials (Gaillardon et al. 1977; Kang and Xing 2005; Celis et al. 1996). A different approach was to study and compare adsorption before and after organic matter removal (Saltzman et al. 1972) to assess the relative importance of soil minerals in parathion uptake. Although the removal of organic matter from soil by oxidation with hydrogen peroxide (a commonly used strong oxidation agent) could affect the properties of an adsorbent, the results obtained may provide qualitative information about its role and properties in the contaminant retention process. The reported results showed that parathion has a greater affinity for organic adsorptive surfaces than for mineral ones. The important finding from this approach suggests that adsorption is dependent on the type of association between organic and mineral colloids, which determines the nature and the magnitude of the adsorptive surfaces. Although the importance of organic matter has been well established, the properties of organic colloids relevant to the adsorption of contaminants remain to be characterized thoroughly. The available information suggests that these properties can be related to the presence of humic acids, fulvic acids, and humin, and to their active groups (e.g., carboxyl, hydroxyl, carbonyl, and methoxy) and surface areas with a high CEC.

The main properties affecting the adsorptive capacity of clay are considered to be the available surface area and the CEC, as well as the nature of the saturating cation, the hydration status, and the surface acidity. Although amorphous oxides and hydroxides of iron, aluminum, and silica can adsorb organic molecules, only limited information exists in this direction. It is known, however, that Al and Fe hydroxides can adsorb organic contaminants, and therefore their presence leads to an increase in the adsorption capacity of montmorillonite (Terce and Calvet 1977). For example, after removing Al and Fe oxides from soil particles, the adsorptive capacity of soils for atrazine (an organic herbicide) decreased significantly and the adsorption kinetics were affected (Huang et al. 1984).

### 4.1.3.3  Environmental Climatic Conditions

The adsorption of contaminants on geosorbents is affected also by climatic conditions reflected in near-surface and subsurface temperature and moisture status.

Calvet (1984) showed how the soil moisture content may affect adsorption of contaminants originating from agricultural practices. The moisture content determines the accessibility of the adsorption sites, and water affects the surface properties of the adsorbent. The competition for adsorption sites between the water and, e.g., insecticides may explain this behavior. Preferential adsorption of the more polar water molecules by the soil hinders insecticide adsorption at high moisture content, while reduced competition is found at low moisture content, leading to an increase in adsorption. A negative relationship between pesticide adsorption and soil moisture content has been reported and known for a long time (e.g., Ashton and Sheets 1959; Yaron and Saltzman 1978).

It is important to examine the effect of moisture content on the surface properties of clays and organic matter in relation to the adsorption of organic contaminants. In general, it is accepted that water molecules are attracted to the clay surfaces mainly by the exchangeable cations, forming hydration shells. Adsorbed water provides adsorption sites for organic contaminants. An important feature of water associated with clay surfaces is its increased dissociation, giving the surface a slightly acidic character. A negative relationship usually exists between the surface acidity of clays and their water content.

Strong, sometimes irreversible retention of organic contaminants on hydrated humic substances could be explained by their penetration and trapping into the internal structure of the swollen humic substances. The hydrated exchangeable cations and some dissociated functional groups, as well as water held by various polar groups of the humic substances, may also provide adsorption sites for organic contaminants. At low moisture content, the hydrophobic portions of the organic matter structure may bind hydrophobic nonionic organic contaminants (Burchil et al. 1981).

Adsorption usually increases as the temperature decreases, and desorption is favored by temperature increases. The temperature may indirectly affect adsorption by its effect on organic–water interactions. The complex relationship among adsorbent, adsorbate, and solvent as affected by temperature was described by Mills and Biggar (1969) for the case of an organic insecticide. The adsorption of lindane (1,2,3,4,5,6-hexachlorocyclohexane) and its beta-isomer by a peat (high organic content), a clay soil, a Ca-bentonite, and silica gel decreased as the temperature of the system increased. The authors suggested that this adsorption–temperature relationship reflects not only the influence of energy on the adsorption process, but also the change in solubility of the adsorbate. Mills and Biggar (1969) considered that the change in activity in solution with temperature is related to the change in reduced concentration, which is the ratio between the actual concentration of the solute at a given temperature and its solubility at the same temperature. Adsorption isotherms obtained by using the reduced concentration, in contrast to normal adsorption isotherms, showed an increase in adsorption with increasing temperature. This finding suggests that the heat effect involved in the adsorption process mainly affects solute solubility. Similar results emphasizing the significant influence of temperature on adsorption through its solubility effect were reported by Yamane and Green (1972) for atrazine and by Yaron and Saltzman (1978) for parathion.

## 4.2  Nonadsorptive Retention

Contaminants may be retained in the soil–subsurface solid phase by processes other than surface interactions, such as precipitation, deposition, and trapping. Like adsorptive retention, nonadsorptive retention of contaminants may lead to direct and immediate irreversible changes to the natural soil–subsurface system.

### 4.2.1  Contaminant Precipitation

Precipitation can be defined as the accumulation of a substance to form a new bulk solid phase, and is in contrast to adsorption, which may be defined as a net accumulation at an interface. Precipitation occurs when the solubility limits are reached; it occurs between and within the solid phase aggregates. Both adsorption and precipitation imply a loss of material from an aqueous solution, but adsorption is inherently two dimensional, while precipitation is inherently three dimensional (Sposito 1984). The chemical bonds that develop are similar in the two cases. Mixtures of precipitates can be inhomogeneous solids with one component restricted to a thin outer layer because of poor diffusion. In the presence of lamellar charged particles with impurities, precipitation of cationic contaminants might occur even at concentrations below saturation with respect to the theoretical solubility coefficient of the solvent. Contaminant precipitation is never complete, because precipitates can redissolve, and ions are always present in the supernatant liquid. In the soil–subsurface system, it is more difficult to differentiate between adsorption and precipitation because new solid phases can precipitate homogeneously onto the surfaces of existing solid phases.

Contaminant precipitation is affected by the solution pH. For example, there is a relationship among the solubility of a metal in water, the amount of precipitate formed, and the pH. This relation is expressed according to the equation

$$A_aB_b(\text{solid}) \rightleftharpoons aA^{+b}(\text{aq}) + bB^{-a}(\text{aq}), \qquad (4.5)$$
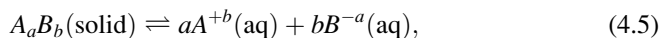
where $A$ is a metal and $B$ is a ligand, which precipitate to form the solid $A_aB_b$, and $a$ and $b$ are stoichiometric coefficients subject to the constraint of electroneutrality.

The ion activity product (IAP) is a measure of the activity of ions present in a solvent. When the IAP is much smaller than equilibrium values, there is no precipitation. When equilibrium is reached, solubility product constants are used to describe saturated solutions of ionic compounds of relatively low solubility. An equilibrium between the solid and dissolved ions is established when the ion concentration in solution reaches saturation. The equilibrium constant is given by

the product of the concentration of ions present in a saturated solution of ionic compounds,

$$K_{sp} = [A^{b+}][B^{a-}]^b, \tag{4.6}$$

where $K_{sp}$ is the solubility product, or the equilibrium constant, between an ionic solid and its saturated solution. When IAP $< K_{sp}$, the solution is supersaturated and precipitation occurs.

### 4.2.2 Particle Deposition and Trapping

Retention of suspended particles in porous media occurs by straining (trapping), physicochemical filtration (deposition), and detachment. Depending on the size of the suspended particle, a number of mechanisms may be responsible for physico-chemical filtration: (1) *gravitational sedimentation*, where the gravitational forces acting on the particle cause it to settle onto a sediment grain (collector), (2) *interception*, where the particle size and trajectory are such that it encounters the collector grain while flowing past, and (3) *Brownian diffusion*, where the particle is brought into contact with a collector due to its Brownian motion (Yao et al. 1971; Elimelech et al. 1995). Geometrical models (Sakthivadivel 1966, 1969) suggest that straining could have a significant influence when the ratio of the particle diameter to the median grain diameter of the porous medium is greater than 0.05. However, recent experimental evidence suggests that straining could be important at much smaller particle to grain size ratios (Bradford et al. 2003). Mobilization (detachment) of deposited particles is also a key process governing colloid transport and fate. Mobilization can take place following drastic changes in pore water chemistry and when the hydrodynamic forces overcome the adhesive forces between particles and the medium grains (Amirtharajah and Raveendran 1993).

Deposition and trapping of contaminants on colloidal materials and other suspended particles may occur during their transport through the vadose zone and thus create an additional route for pollutant distribution in the subsurface. Below hazardous waste sites, for example, an unexpected transport process of cationic radionuclides (e.g., Pu and Am) or various heavy metals has been observed, which can be explained only by colloid-facilitated transport (McCarthy and Zachara 1989; Penrose et al. 1990; Ryan and Elimelech 1996). Laboratory experiments testing colloid-facilitated redistribution in the unsaturated zone confirmed that colloids can accelerate the transport of cationic and anionic metals (e.g., Vilks et al. 1993) or toxic organic chemicals (e.g., Vinten et al. 1983). Colloidal materials involved in the process of enhanced redistribution of contaminants in the subsurface include inorganic matter like clay minerals, oxides, and carbonate particles, with sizes in the range of 10 nm to a few micrometers, as well as organic colloids like humic substances and microbial exudates. Vinten et al. (1983) demonstrated that the

vertical retention of contaminated suspended particles in soils is controlled by the soil porosity and the pore size distribution. Three distinct steps in which contaminant mass transfer may occur can be defined: (1) contaminant adsorption on the porous matrix as the contaminant suspension passes through near-surface and subsurface zones, (2) contaminant desorption from suspended solid phases, and (3) deposition of contaminated particles as the suspension passes through the soil.

Particle deposition from aqueous suspensions onto stationary surfaces is a dynamic phenomenon characterized by a transient or time-dependent rate of deposition. The deposition of contaminated suspended particles is affected by the nature of the surrounding porous medium. A declining deposition rate is observed when particle–particle interactions are repulsive so that the potential deposition zone becomes progressively occluded as particles accumulate; this leads to a blocking phenomenon.

The suspended solid particle size and the volume of effluent also must be considered in defining the solid deposition of contaminants in the soil–subsurface system. For example, under leaching of a waste disposal site or following irrigation with sewage effluent, the coarse fraction of the suspended solid is retained in the upper layer, while the finer colloidal fraction is mobile and its transport is controlled by the porosity of the subsurface solid phase. When the diameter of the suspended solid is greater than the diameter of the pore, the suspended solid is retained and a contaminant deposition zone is formed.

Deposition and trapping of contaminated colloids are a result of their interaction with the subsurface solid phase during transport as flowing suspensions in the incoming water. Ryan and Elimelech (1996) note that conventional filtration theories are applicable only to the initial stage when mineral grains are devoid of retained particles. As particles deposit onto mineral surface sites with charge characteristics favorable for deposition, the particle deposition rate progressively declines due to the blocking phenomenon. The heterogeneity of the subsurface makes application of deposition models very difficult, and therefore they usually are relevant only for well-defined materials. A study of these phenomena by Amitay-Rosen et al. (2005) used magnetic resonance imaging to demonstrate spatial and temporal deposition and trapping patterns of colloids in porous media.

## 4.3   Retention Hysteresis

Reversible and irreversible retention of contaminants on the soil–subsurface solid phase is a major process in defining and controlling contaminant redistribution from the land surface to groundwater. After being retained on or within the soil–subsurface solid phase, contaminants may be released into the subsurface liquid phase, displaced as water-immiscible liquids, or transported into the subsurface gaseous phase or into the atmosphere. The form and the rate of release are governed by the properties of both contaminant and subsurface, as well as by the environmental conditions.

Release can be assessed on the basis of physicochemical and biological processes. In the case of the former, release is caused by a change in the properties of the fluid surrounding the retaining solid phase. Lowering of the pollutant concentration in the liquid phase, for example, may cause a change in the established equilibrium, and as a consequence, enhanced transfer of the adsorbed compound to the liquid phase occurs. Another way to favor a release can be through processes controlled by pollutant bioavailability, where the contaminants enter living organisms by an uptake process.

When not all of the molecules adsorbed or retained in the soil–subsurface solid phase can be transferred back into the gaseous or liquid phase, the process is known as *hysteresis*. In the subsurface, where a multicomponent solid phase is present, and where phenomena other than adsorption–desorption may occur, it is better to use the term *retention hysteresis* rather than *adsorption hysteresis*.

*Retention hysteresis* may vary according to the nature of the contaminant and the solid phase, the site and sample history (e.g., wetting–drying cycles), and the experimental procedure used. True (genuine) and apparent hysteresis may be considered to explain contaminant release from the subsurface solid phase. True hysteresis assumes that observed data are real, and the equilibrium results can be explained on the basis of well-identified phenomena. Apparent hysteresis results from an experimental artifact due, for example, to a failure to reach retention or release equilibrium.

## 4.3.1   True Hysteresis

True hysteresis is considered only when the system is at equilibrium and when released contaminants are those that were adsorbed onto the solid phase surface. Molecules brought back into the solution as result of dissolution, diffusion out of the solid matrix, or biotic/abiotic transformation cannot be considered as desorbed molecules. In the soil–subsurface system, it is almost impossible to distinguish between desorbed molecules and molecules that were not subjected to adsorption and desorption.

Desorption isotherms may differ from adsorption isotherms for systems that are not at equilibrium, because the desorption rate is lower than the adsorption rate. Theoretical treatments by Ponec et al. (1974), for gas adsorption, and Giles et al. (1974), for solute adsorption, indicate that the activation energy for adsorption is zero or near zero. Under these conditions, these authors showed that the activation energy for desorption is greater than that for adsorption; consequently, the rate of desorption is lower than that for adsorption. This behavior pattern is also valid when adsorption is accompanied by dissociation of the adsorbed molecules (Ponec et al. 1974). Adsorbed molecules may be classified according to two categories: molecules retained through physical interactions and able to desorb, and molecules that interact strongly with the solid matrix and therefore are released slowly or not at all (Barriuso et al. 1992a, b). True sorption hysteresis to synthetic and natural

organic solids has been attributed to irreversible alteration of the solid during sorption–desorption cycles. Based on this assumption, Sander et al. (2005) suggested the use of a thermodynamic index of irreversibility (TII) for quantifying hysteresis in soils where natural organic matter dominates the sorption process. This TII is based on the difference in free energy between the real desorption state and the hypothetically fully reversible state. The index is "zero" for the fully reversible state and "one" for the fully irreversible state.

Several other explanations have been advanced to explain retention hysteresis, including (1) surface precipitation of metallic cations whose hydroxides, phosphates, or carbonates are sparingly soluble; (2) chemical reactions with solid surfaces, including organic surfaces, which form complexes with metallic cations; and (3) incorporation in the subsurface organic matter through chemical reactions and biochemical transformation. When dealing with chemical reactions and biochemical transformations (explanation 3), the retention of the toxic chemical may in some situations reach total irreversibility.

### 4.3.2   Apparent Hysteresis

Apparent hysteresis occurs mainly when complete equilibrium is not reached. Diffusion into the solid matrix or into micropores of aggregates is considered a main cause of apparent hysteresis. In a transitory state, sorption will occur concurrently with desorption and the concentration of contaminant in the liquid phase will be erroneously low because some fraction is associated with sorption.

Apparent hysteresis may also be caused by other phenomena. During consecutive extraction and dilution steps that are used as a common technique in desorption studies, *weathering* of the sorbent may occur, resulting in a possible increase in contaminant sorption and decrease in its release. *Degradation* of the contaminant induced by physicochemical or biological factors, or a volatilization process leading to a decreased contaminant concentration in solution, are additional factors affecting a true hysteresis result.

The *moisture status* of the subsurface solid phase also may lead to an apparent hysteresis in the adsorption–desorption process. It is known that clay materials, mainly smectites, and humic substances can hydrate and swell, or dehydrate and shrink. The physicochemical state of many molecules sorbed in wet conditions may be modified on drying, making the substances more difficult to desorb. The retention of sorbate molecules during drying or slow swelling of organic surfaces may be the reason for the decrease in their desorption. Upon rewetting, when molecules are sorbed at polar surface sites, they orient their hydrophobic part toward the solution phase, reducing considerably the access of water, and thus slowing down the swelling and desorption (Mingelgrin and Gerstl 1993).

Drying of the subsurface solid phase can cause an increase in the rate of desorption. If penetration of a sorbate toward inner surfaces does not reach its equilibrium by the time drying commences, a fraction of the sorbate may remain localized at more

accessible outer surfaces in an amount greater than that corresponding to the equilibrium level. Under these conditions, drying of the system may increase the rate of desorption during a successive rewetting.

The *history of the adsorbing surface* is an additional factor affecting the release of contaminants adsorbed on solid phases into the liquid or gaseous phase. For example, the effect of drying on contaminant desorption is influenced by the time allowed for its transport into the aqueous phase. In sorbing systems, like sediments which are permanently wet, the history of the system determines the fate of sorbed molecules (Pignatello 1989).

*Release methodology* may lead to incorrect desorption parameters, which in turn may be (erroneously) interpreted as hysteresis. For example, Hodges and Johnson (1987) used two different experimental techniques (rapidly stirred batch and miscible displacement with slow flow rate) to study sulfate desorption and found that in stirred batch experiments, the desorption readings were less than those obtained by the miscible displacement technique. Even within the miscible displacement technique, the time of leaching was found to have a major effect. For example, leaching during 600 s removed 34% of the adsorbed sulfate and after 14,400 s, 53% was removed. The estimated (by extrapolation) time required for complete desorption was 10–20 times greater than that required for adsorption.

### 4.3.3   Bound Residues

Bound residues are an extreme aspect of contaminant hysteresis and refer mainly to the irreversible retention of organic contaminants (e.g., pesticides). The term *bound residue* was adopted by the International Union of Pure and Applied Chemistry (IUPAC) in 1984. According to this definition and that of the European Commission (adopted in 1991), nonextractable residues in soil are chemical species, originating from pesticides, which are not extracted by methods that do not significantly change the chemical nature of the residue. Fuhr et al. (1998) expanded the meaning of *bound residues* to the "compounds in soil, plant or animals which persist in the matrix form of the parent substance or its metabolites after extraction." Gevao et al. (2000) included the proviso that bound residues do not include metabolites that are indistinguishable from naturally occurring compounds. Expanding this definition for the subsurface environment, we can state that *bound residues may comprise all toxic chemical species of anthropogenic origin (parent and metabolites) associated with the subsurface solid phase that cannot be extracted by current extraction technology*.

Bound residues were first mentioned in the literature by Bailey and White (1964), in relation to pesticide extraction from soils. Over the years, many experiments have shown that the extraction of pesticides from soils is never complete, even when using solvents for which the molecules are highly soluble. Waner et al. (2005) showed by analysis of [14] C-labeled molecules that the fungicide dithianon in soil exhibited bound residues of $\approx$63% of the applied amount after 64 days. Calderbank (1989) showed that for a large number of organic

agrochemicals, up to 90% of the applied radioactively labeled substances become nonextractable. Calderbank (1989) examined a series of experimental data and noticed that different amounts of parent products become irreversibly retained as a function of their molecular structure. Moreover, it was observed that the extractability decreases with aging, probably because the phenomena responsible for hysteresis become more efficient with increasing residence in soil.

The environmental significance of bound residues must be considered in relation to the fate of natural organic matter (Barraclough et al. 2005). Contaminants entering the subsurface contain many functional groups similar to those of natural organic matter and thus become involved in many of the same biological and chemical transformations. If, with aging, the bound residues become indistinguishable from subsurface organic matter, no environmental risk occurs. In contrast, however, if over time the bond residues exhibit properties different than those of natural organic matter, compounds having a toxic character will become a contamination risk for the subsurface.

Bound residues of anthropogenic origin, found in the upper part of the soil–subsurface system, may be compared to those of natural organic molecules released from plant and animal debris and utilized as a source of energy by microbial populations. Parent molecules and their metabolites may interact in the subsurface with the organic matter and then be desorbed and develop further by long-time contact. In this process, known as *aging*, molecules become more tightly bound or entrapped into organic matter or clay fractions of the solid phase. Barraclough et al. (2005) noted that the mass balance of xenobiotics in the subsurface exhibits the same variation as that seen with natural products, in terms of their partitioning between evolved $CO_2$ and their incorporation into the humic and fulvic substances. Note that the data on carbon evolution may show the rate of incorporation of the labeled carbon from xenobiotics into the subsurface solid phase, but such studies alone do not give information on the bonding of parent compounds and their metabolites on molecular levels. The type of interaction, however, is an important factor determining both the likelihood and rate of release and the form in which the molecules are mobilized.

The mechanism of bound residue formation is better understood today due to the use of advanced extraction, analytical and mainly spectroscopic techniques (e.g., electron spin resonance, ESR; nuclear magnetic resonance, NMR; and Fourier transform infrared spectroscopy, FTIR), which are applied without changing the chemical nature of the residues.

Physical entrapment following intraorganic matter diffusion (IOMD) or interparticle diffusion in clay minerals is a potential explanation for the formation of bound residues. Diffusion out of the solid phase may account partly for hysteresis, particularly for molecules that diffused into the organic aggregates. Entrapping in humic polymer aggregates, suggested by Khan (1982) and further examined by Wershaw (1986) and Kan et al. (2000), is a possible explanation for hysteresis of substances compatible with the structure of humic substances. The rapid desorption phase is a result of an entrapped pool of readily desorbed material, and the slow

phase is controlled by an entrapped or irreversible compartment inside the most hydrophobic part of humic aggregates.

To calculate the release through diffusion of an entrapped residue, Barraclough et al. (2005) considered the size of organic matter particles (effective radius $10^{-7}$–$10^{-9}$ cm) and the effective diffusion coefficient of small organic molecules in a sorbing medium ($D \approx 10^{-9}$ cm$^2$ s$^{-1}$). The time for 50% of the material in a sphere to diffuse out is given by

$$t_{1/2} = 0.03 r^2 / D, \tag{4.7}$$

where $r$ is the effective radius (cm) and $t$ is time in seconds (Helfferich 1962).

For these entrapped contaminant "spheres," the diffusion is rapid, of the order of seconds rather than days. Kahn et al. (2000) suggested a diffusion model for xenobiotics with a slow desorption phase, with a half-life of years rather than seconds, assuming that diffusion is hindered by the natural organic matter matrix and occurs when the dimensions of diffusing molecules approach those of the pores. Under these conditions, hindrance from the wall becomes significant (Renkin, 1954) and the drag factor $F$ can be expressed as

$$F = 1 - 2.09(r_{\mathrm{m}}/r_{\mathrm{p}}) + 2.14(r_{\mathrm{m}}/r_{\mathrm{p}})^3 - 0.95(r_{\mathrm{m}}/r_{\mathrm{p}})^5, \tag{4.8}$$

where $r_{\mathrm{m}}$ and $r_{\mathrm{p}}$ are the radii of the molecule and the pore, respectively. To extend the diffusion half-life from seconds to years would require a drag factor of around $10^{-8}$, in the case where no interaction occurs between the diffusing molecules and the entrapping matrix.

Another process leading to formation of bound residues is the chemical binding of contaminant molecules to organic matter (Bollag and Loll 1983). Fulvic and humic acids are the compounds commonly involved in such binding. If binding on the organic matter matrix involves physical entrapment, van der Waals forces, or charge transfer, significant release occurs only as a result of matrix-induced degradation by microorganisms or plant enzymes. The reactions involved appear to be the same as those responsible for humic substance formation. Phenol and aromatic amines may bind to organic matter by oxidative coupling, while substituted urea and triazines may not (Bollag et al. 1992). Binding of toxic organic molecules on an organic matter matrix can take place also during humic substance formation by polymerization processes.

## 4.4   Transformation of Contaminants Retained on Solid Phase

Here, we discuss aspects of contaminant transformation and metabolite formation once contaminants are retained or released within the soil–subsurface geosystem. From an environmental point of view, we do not restrict the transformation of

contaminants only to molecular changes. Rather, we must also consider all deviations from the original properties of a contaminant, which may be relevant to its behavior in the subsurface. For example, in addition to degradation-induced transformation, contaminants may change their physicochemical characteristics as a result of specific reactions with other natural or anthropogenic chemicals found in the soil–subsurface environment.

As a first approximation, we consider the main soil–subsurface transformation processes to comprise (1) reactions leading to chemical transformation or degradation and metabolite formation at the solid–liquid interface, and (2) reactions resulting in complexation of chemicals, which in turn lead to a change in their physicochemical properties.

The soil as the upper part of the soil–subsurface system is characterized by enhanced biological activity. Therefore, contaminant transformation in this zone proceeds mainly by microbial processes, which are often faster than chemical ones. In the deeper subsurface, biological activity is often reduced and, therefore, degradation proceeds, mainly abiotically, at a much slower rate. It should be emphasized, however, that contaminant transformation is related mainly to the formation of metabolites with properties different than those of the parent material (sometimes more polar, more soluble in water, and even more toxic), which may reach the groundwater.

Environmental conditions cause changes in the initial properties of organic and inorganic contaminants and affect their persistence in soil–subsurface system. Relevant external factors include temperature and solar radiation, and principal soil–subsurface properties include water chemistry, the surface properties of the solid phase, and bioactivity. The extent and the rate of transformations due to these conditions are controlled by the molecular properties of each contaminant.

## 4.4.1   Abiotic Transformation

### 4.4.1.1   Catalysis

Catalysis is one of the main transformation mechanisms of contaminants in the soil–subsurface geosystem. The charged surface of a solid may strongly affect polarizable species of contaminants, and therefore, their potential for abiotic transformation is much greater at the solid–liquid interface than in natural bulk waters. Molecules in direct contact with reactive solid constituents are often subject to catalytic properties of the surface or interact with available adsorbing sites, and can therefore undergo many transformations. We refer to a catalyst as an earth material that enables and/or enhances a chemical reaction without undergoing any permanent chemical change. Catalysts provide alternative reactive pathways by which a reaction reaches a local equilibrium, although it does not alter the position of equilibrium (Daintith 1990). A heterogeneous natural domain such as the soil–subsurface system contains a variety of solid surfaces and dissolved

constituents that can catalyze transformation reactions of contaminants. In addition to catalytically induced oxidation of synthetic organic pollutants, which are enhanced mainly by the presence of clay minerals, transformation of metals and metalloids occurs in the presence of catalysts such as Mn-oxides and Fe-containing minerals. These species can alter transformation pathways and rates through phase partitioning and acid–base and metal catalysis.

Catalysis by proton transfer is significant in the subsurface and associated environment, and is common in homogeneous reactions. The strength of the acid or base is determined by the ionization constant, while its efficiency as a catalyst is controlled by the reaction rate. In acid catalysis of organic molecules, the proton located on negatively charged molecules reduces the negative charge so that the transfer of electrons is facilitated. It can be assumed that under such conditions, a metal ion that generally acts as an acid will form a metal–organic complex, which reduces the negative charge and enhances the electron transfer. Unlike a proton, the metal ion can be stabilized by other ligands. Some metal ions, especially of the transition series, have several stable oxidation states that enable them to act as catalysts in redox reactions; these ions can catalyze a wide variety of transformation reactions of organic and inorganic contaminants (Huang 2000).

### 4.4.1.2 Surface-Induced Transformation of Contaminants

Organic Contaminants

*Clay Minerals*

The spatial distribution of ions and their charge are affected strongly by the electric field emanating from clay charged surfaces. As a result, some organic contaminants in direct contact with these surfaces can undergo transformations by catalytic processes. Clay minerals behave like Brönsted acids, donating protons, or as Lewis acids, accepting electron pairs. Catalytic reactions on clay surfaces involve surface Brönsted and Lewis acidity and the hydrolysis of organic molecules, which is affected by the type of clay and the clay-saturating cation involved in the reaction. Dissociation of water molecules coordinated to surfaces of clay-bound cations contributes to the formation active protons, which is expressed as Brönsted acidity. This process is affected by the clay hydration status, the polarizing power of the surface bond, and structural cations on mineral colloids (Mortland 1970, 1986). On the contrary, ions such as Al and Fe, which are exposed at the edge of mineral clay colloids, induce the formation of Lewis acidity (McBride 1994).

Many nonionic organic contaminants require extreme acid conditions to accept $H^+$ ions. In clays, the extent of protonation is related to the electronegativity and polarizing power of structural metal cations, in the following order: $H^+ > Al^{3+} > Fe^{3+} > Mg^{2+} > Ca^{2+} > Na^+ > K^+$ (McBride 1994). Mineral surface acidity also catalyzes hydrolysis of organic contaminants in the subsurface. This transformation pathway depends both on the type of clay mineral forming the

solid phase and on the clay-saturating cation. As clay surfaces become drier, the protons become concentrated in a smaller volume of water, and the surface acidity increases to an extreme value. Under these conditions, even a very weak base can be protonated.

Surface-catalyzed degradation of pesticides has been examined in the context of research on contaminant–clay interactions. Such interactions were observed initially when clay minerals were used as carriers and diluents in the crop protection industry (Fowker et al. 1960). Later, specific studies on the persistence of potential organic contaminants in the subsurface defined the mechanism of clay-induced transformation of organophosphate insecticides (Saltzman et al. 1974; Mingelgrin and Saltzman 1977) and s-triazine herbicides (Brown and White 1969). In both cases, contaminant degradation was attributed to the surface acidity of clay minerals, controlled by the hydration status of the system. Rearrangement reactions catalyzed by the clay surface were observed for parathion (an organophosphate pesticide) when it was adsorbed on montmorillonite or kaolinite in the absence of a liquid phase. The rate of rearrangement reactions increased with the polarization of the hydration water of the exchangeable cation (Mingelgrin and Saltzman 1977). Table 4.3 summarizes a series of reactions catalyzed by clay surfaces, as reported in the literature.

*Dissolved metals* and metal-containing surfaces play an important role in the transformation of organic contaminants in the soil–subsurface environment. Metal ions can catalyze hydrolysis in a way similar to acid catalysis. Organic hydrolyzable compounds susceptible to metal ion catalysis include carboxylic acids, esters, amides, anilides, and phosphate-containing esters. Metal ions and protons coordinate to the organic contaminant so that electron density is shifted away from the site of nucleophilic attack to facilitate the reaction. Metal ion-induced catalysis generally occurs via complexation of the reactant molecule. Stone et al. (1993) and Stone and Torrents (1995) formulated a general pathway of the process as follows: (1) complex formation constants increase as the charge-to-radius ratio of the metal ion increases, (2) polarizable metals and ligands exhibit complex stability through covalent bond formation, and (3) competition for the metal among available ligands becomes greater as complex formation constants increase. The properties of metal ions, in general, and transition metal ions, in particular, make them good catalysts for a broad range of organic and inorganic reactions in the soil–subsurface environment.

*Humic substances* are also able to enhance abiotic transformation of organic substances, such as anthropogenic pollutants, at the solid–liquid interface. The transformation of organic pollutants adsorbed on organic matter surfaces occurs because the natural organic fraction contains many reactive groups that are known to enhance chemical changes in several families of organic substances, and humic substances provide a strong reducing capacity (Stevenson 1994). The presence of relatively stable free radicals in the fulvic and humic acid fractions of subsurface organic matter further supports enhanced abiotic transformations of many organic contaminants. Transformation of toxic organic chemicals by humic substances at the solid–liquid interface may occur mainly through hydrolysis, as discussed in the reviews of Senesi and Chen (1989) and Wolfe et al. (1990). Hydrolysis of triazine herbicides, for example, describes humic-induced transformation of toxic organic

**Table 4.3**  Selected examples of reactions catalyzed by clay surfaces (after Wolfe et al. 1990). Copyright 1990, Soil Science Society of America. Reprinted with permission

| Substrate | Reaction | Type of clay | Remarks |
|---|---|---|---|
| Ethyl acetate | Hydrolysis | Acid clays | – |
| Sucrose | Inversion | Acid clays | – |
| Alcohols, alkene | Ester formation | Al-montmorillonite | – |
| Organophosphate esters | Hydrolysis | Cu- and Mg-montmorillonite, Cu-Beidellite Cu-Nontronite | Cu-montmorillonite better catalyst than other Cu-clays or Mg-montmorillonite |
| Organophosphate esters | Hydrolysis and rearrangement | Na-, Ca-, and Al-kaolinites and bentonites | Room and other temperatures. No liquid phase |
| Phosmet | Hydrolysis | Homoionic montmorillonite | In suspension |
| Ronnel | Hydrolysis and rearrangement | Acidified bentonite; dominant exchangeable cations: H, Ca, Mg, Al, Fe(III) | Al-catalyzed suggested reaction |
| s-Triazines | Hydrolysis | Montmorillonitic clay | Cl analog degrades faster than methoxy or methoxy-thio compounds |
| Atrazine | Hydroxylation | H-montmorillonite | – |
| Atrazine | Hydrolysis | Al- and H-montmorillonite; montmorillonitic soil clay | Ca- and Cu-clays much weaker catalysts |
| 1-(4-methoxy phenyl)–2,3-epoxy propane | Hydrolysis | Homoionic montmorillonites; Na-kaolinite | – |
| DDT | Transformation to DDE | Homoionic clays | Na-bentonite is a better catalyst than H-bentonite |
| Urea | Ammonification | Cu-montmorillonite | Air-dried clay at 20°C |
| Aromatic amines | Redox | Clays (review) | In the presence of metal ions that are good redox agents |
| 3,3′,5,5′-Tetra methyl benzidine | Redox | Hectorite | $O_2$ oxidizing agent |
| Pyridine derivatives, olefines, dienes | Oligomerization | Clays (review) | – |
| Glycine | Oligomerization | Na-kaolinite, Na-bentonite | – |
| Styrene | Polymerization | Palygorskite, kaolinite, and montmorillonite | Weakest catalyst is montmorillonite |
| Fenarimol | Dialdehyde formation | Homoionic montmorillonite | – |

molecules. The formation of H-bonding between humic acids and atrazine was suggested as being responsible for the observed decrease in the activation energy barrier of the reaction. The catalytic effect of humic acids depends not only on the number of effective acid groups, but also on their arrangement in the humic acid

molecule (Li and Felbeck 1972). A general mechanism for the effects of subsurface organic matter on the hydrolysis of hydrophobic organic contaminants was proposed by Purdue and Wolfe (1983). The suggested mechanism is derived from a combination of equations that describe, separately, partitioning equilibrium, acid–base catalysis, and micellar catalysis. The resulting model indicates that the overall reaction rates of toxic organic chemicals can be attributed almost totally to partitioning equilibrium and micellar catalysis.

*Nonspecific* enhanced surface transformation is observed on charged surfaces, which are not specific adsorption sites, found in the vicinity of the surface. Probably the most significant phenomenon in the interfacial region, near the surface of charged solids, is the strong dependence of the concentration of charged solutes on the distance from the surface. The concentration in the interfacial region of charged inductors, catalysts, reactants, and products can therefore be different from their concentration in the bulk solution. Another factor that can affect organic transformations in the interfacial region near charged particles is the aforementioned influence of the electric field on the polarization and dissociation of the solute and solvent.

Inorganic Contaminants

*Metal Ions*

Metal ion complexation to natural organic components in the solid phase is a major example of abiotic interactions of inorganic compounds in the soil–subsurface system. Through these interactions, initial metal ion relationships of the original compounds are changed and contaminant retention, persistence, and transport in the environment exhibit different behaviors. Soil–subsurface organic compounds may form complexes with natural humic substances (about 80%), additional organic substances of biological origin (such as aliphatic and amino acids, polysaccharides, and polyphenols), and xenobiotic organic chemicals released on the land surface accidentally or intentionally.

Potentially toxic compounds in the subsurface, such as $Cd^{2+}$, $Pb^{2+}$, or $Hg^{2+}$, which are generally found in very low concentrations, are considered "soft cations" (Buffle, 1988). These ions have strong affinity to intermediate and soft ligands and therefore bond to them covalently. "Borderline" cations, which embrace transition metals like $Cu^{2+}$ and $Zn^{2+}$, exhibit affinity for the soft cations as well as for alkaline-earth compounds.

## 4.4.2   Biologically Mediated Transformation

### 4.4.2.1   Main Processes

*Aerobic respiration* is one of the major processes mediating chemical transformations, mainly through the activity of heterotrophic microorganisms. Carbon turnover in the subsurface, for example, involves chemicals such as N, S, and P.

The large polymeric molecules, which compose the bulk of biological residues, are often used as a source of energy; they ultimately become humic substances. These substances may further affect the fate of contaminants that originate from anthropogenic activity. Aerobic respiration also causes changes in the molecular structure of organic agrochemicals. Autotrophic and chemoautrophic reactions are among the most important aerobic processes in nitrification. Autotrophic transformation controls, for example, the oxidation of S to $SO_4^{2-}$ or $S_2O_3^{2-}$, conversion of organic Fe compounds to Fe precipitates, and transformation of arsenite (mobile and toxic) to arsenate (nontoxic). Aerobic respiration also has indirect effects on chemical speciation. For example, the release of $CO_2$ affects redox potential and pH, which may lead to the transformation of metal ions by chelation.

*Anaerobic metabolism* occurs under conditions in which the $O_2$ diffusion rate is insufficient to meet the microbial demand, and alternative electron acceptors are needed. The type of anaerobic microbial reaction controls the redox potential (Eh), the denitrification process, reduction of $Mn^{4+}$ and $SO_4^{2-}$, and the transformation of selenium and arsenate. Denitrification may be defined as the process in which N-oxides serve as terminal electron acceptors for respiratory electron transport (Firestone 1982), because nitrification and $NO_3^-$ reduction to $NH_4^+$ produce gaseous N-oxides. In this case, a reduced electron-donating substrate enhances the formation of more N-oxides through numerous electrocarriers. Anaerobic conditions also lead to the transformation of organic toxic compounds (e.g., DDT); in many cases, these transformations are more rapid than under aerobic conditions.

*Microbial methylation* is a reaction that affects mainly properties of toxic, inorganic trace elements. It occurs under aerobic or anaerobic conditions. Mercury methylation, for example, occurs under both conditions and leads to the input of Hg into the atmosphere.

### 4.4.2.2 Biotransformation of Organic Contaminants

The microbial metabolic process is the major mechanism for transformation of toxic organic chemicals in the soil–subsurface environment. The transformation process may be the result of a primary metabolic reaction when the organic molecule is degraded by a direct microbial metabolism. Alternatively, the transformation process may be an indirect, secondary effect of the microbial population on the chemical and physical properties of the subsurface constituents. Bollag and Liu (1990), considering behavior of pesticides, defined the basic processes that are involved in microbially mediated transformation of toxic organic molecules in the soil upper layer environment. These processes are described next.

*Biodegradation* is a process in which toxic organic molecules serve as substrates for microbial growth. In this case, organic molecules are used by one or more interacting microorganisms and metabolized into $CO_2$ and inorganic components. In this way, microorganisms obtain their requirements for growth and toxic organic molecules are completely decomposed, without producing metabolites that in some cases could be more toxic than the parent material. From an environmental point of

view, this process is highly effective and desirable; the presence of a biodegradable compound in a subsurface site may enhance the proliferation of active microbial populations and consequently increase the rate of decomposition of additional contaminants that enter the system.

*Cometabolic transformations* include the degradation of toxic organic molecules by microorganisms that grow at the expense of a substrate other than the toxic organic one. This process, in which enzymes involved in catalyzing the initial reaction lack substrate specificity, may lead to the formation of intermediate products that are in some cases more toxic than the parent material. These products cause adverse environmental impact and may also inhibit microbial growth and metabolism. Environmental factors and the contaminant concentration may affect the nature of the metabolism. Different microorganisms can metabolize a range of toxic organic molecules; microorganisms can transform a molecule by sequential cometabolic attacks, and cometabolic products of one organism can be used as a growth substrate for another organism.

*Polymerization*, or *conjugation*, is the process in which toxic organic molecules undergo microbially mediated transformations by oxidative coupling reactions. In this case, a contaminant or its intermediate product(s) combines with itself or other organic molecules (e.g., xenobiotic residues, naturally occurring compounds) to form larger molecular polymers that can be incorporated in subsurface humic substances.

*Cellular accumulation* is an additional microorganism-mediated transformation pathway of organic contaminants in the subsurface environment. The rate of accumulation differs for various organisms and depends on the type and concentration of toxic organic chemical in the surrounding medium. Microbial uptake is a passive absorption process and not an active metabolism. Early studies (e.g., Johnson and Kennedy 1973) proved that dead, autoclaved cells accumulate toxic organic molecules in amounts similar to those found in living organisms. These results suggest that cell accumulation is not an induced metabolic process but an absorptive one. Once accumulated in microbial cells, toxic organic chemicals may be degraded.

*Nonenzymatic transformation* of toxic organics is an indirect process that may occur in the soil–subsurface system as a result of microbially induced changes in environmental parameters such as pH and redox potential. The activity of microorganisms leads to changes in pH, for example, due to biochemical processes like degradation of proteins or oxidation of organic N to nitrite and nitrate, sulfide to elemental S, or ferrous sulfate to ferric ion. Changes in pH may induce the transformation of exogenous organic contaminants in the aqueous and solid phases. Reductive reactions occurring in a saturated subsurface, due to microbial activity, can lower the redox potential to a range of 0 to $-100\,mV$ (Parr and Smith 1976) and lead to the transformation of organic chemicals.

*Oxidation* of organic contaminants by microorganisms is one of the basic metabolic reactions in the soil–subsurface system and involves the presence of a group of oxidative enzymes such as peroxidases, lactases, and mixed-function oxidases.

*Hydroxylation* can occur on the aromatic ring, on aliphatic groups, and on alkyl side chains. It makes these compounds more polar so that their solubility increases.

*N-dealkylation* results from an alkyl substitution on an aromatic molecule, which is one of the first places where microorganisms initiate catabolic transformation of a xenobiotic molecule. A typical example of N-dealkylation is transformation of pesticides like phenyl ureas, acylanilides, carbamates, s-triazines, and dinitranilines. The enzyme mediating the reaction is a mixed-function oxidase, requiring a reduced nicotinamide nucleotide as an H donor.

*β-oxidation* occurs, for example, when contaminants contain a fatty acid chain. In this case, the reaction proceeds by the stepwise cleavage of two carbon fragments of the fatty acid and ceases when the chain length is two or four carbons.

*Decarboxylation* designates the replacement of a carboxyl group, as a result of enzymatic microbial activity. In a soil–subsurface environment characterized by extensive microbial activity, catalytic decarboxylations for both naturally occurring and exogenous organic compounds may occur.

*Epoxidation* reactions define the insertion of an oxygen atom into a carbon–carbon double bond, leading to the formation of a product with toxicity greater than that of the parent chemical. Highly toxic organochlorinated pesticides are subject to epoxidation in the presence of various microorganisms.

*Oxidative coupling* involves condensation reactions catalyzed by phenol oxidases. In oxidative coupling of phenol, for example, alkoxy or phenolate radicals are formed by removal of an electron and a proton from a hydroxyl group.

*Aromatic* and *heterocyclic cleavage* involves a hydrocarbon being separated from an oxygen atom, which functions to link it to another moiety of the molecule; this process may lead to a decrease in the initial toxicity. The metabolic effects of microorganisms differ with the molecular configuration of the product, which affect aromatic or heterocyclic ring cleavage differently. Aromatic ring cleavage is a microorganism-mediated catabolic process. The type of linkage, the specific substituents, their position, and their number determine the susceptibility of an aromatic ring to fission. Usually, the substituents must be modified or removed and a hydroxyl group inserted in an appropriate position before oxygenase enzymes can cause ring cleavage. Dehydroxylation is usually essential for enzymatic cleavage of the benzene ring under aerobic conditions. The hydroxyl groups must be placed either ortho or para to each other, probably to facilitate the shifts of electrons involved in the ring fission. Dioxygenases are the enzymes responsible for ring cleavage, and they can cause ortho- (intradiol) or meta- (extradiol) fission of a catechol, forming *cis, cis*-muconic acid or 2-hydroxymuconic semialdehyde, respectively.

Heterocyclic ring cleavage also occurs as a metabolic, microorganism-mediated process. For contaminants having a heterocyclic ring, the degradation path is complicated by the heteroatoms, usually N, O, and S, contributing to decomposition reactions through their individual characteristics. These compounds may contain one or more (mostly aromatic) rings having five or six members.

*Sulfoxidation* reactions are characterized by enzymatic conversion of a divalent compound to sulfoxide or, in some cases, to sulfone ($S \rightarrow SO \rightarrow SO_2$). The degradation may also be catalyzed by minerals, converting organic sulfides (thioesters) and sulfites to the corresponding sulfoxides and sulfates. Because it is

difficult to determine if the reaction is chemically or biologically induced, microbially mediated sulfoxidation in the subsurface environment can be established only when a biocatalyst is found.

*Reduction* reactions mediated by microorganisms may include the reduction of nitro bonds and of double or triple bonds, sulfoxide reduction, and reductive dehalogenation. Reduction of the nitro group to amine involves the intermediate formation of nitrase and hydroxyamino groups.

*Hydrolytic* reactions involve organic toxic molecules which have ether, ester, or amide linkages. In the case of hydrolytic dehalogenation, a halogen is exchanged with a hydroxyl group. This reaction is mediated by hydrolytic enzymes, excreted outside the cells by microorganisms. In general, enzymes involved in hydrolytic reactions include esterase, acrylamidase, phosphatase, hydrolase, and lyase. Bollag and Liu (1990) emphasized that it is often difficult to determine the original catalyst of the reaction, because specific environmental conditions or secondary effects of microbial metabolism create opportunities conducive to hydrolysis. Table 4.4 summarizes microbially mediated hydrolytic and reductive reactions of synthetic pesticides that reach the soil–subsurface system via land application.

*Synthetic* reactions lead to contaminant transformation when organic chemicals in the soil–subsurface system merge or are linked to natural organic compounds. Synthetic reactions may be divided into conjugation reactions, which involve the merger of two substances, and condensation reactions, which yield oligomeric or polymeric compounds (Bollag and Liu 1990). Conjugation reactions, such as methylation and acetylation, commonly occur during microbial metabolism of xenobiotics. Microbial phenoloxidases and peroxidases catalyze the transformation of phenolic compounds to polymerized products.

**Table 4.4** Reductive and hydrolytic microbially mediated reactions of synthetic pesticides. R: organic moiety; Ar: aromatic moiety (after Bollag and Liu 1990). Copyright 1990, Soil Science Society of America. Reprinted with permission

Reduction of nitro group
$$RNO_2 \rightarrow ROH$$
$$RNO_2 \rightarrow ROH_2$$
Reduction of double bond or triple bond
$$Ar_2C = CH_2 \rightarrow Ar_2CHCH_3$$
$$RC \equiv CH \rightarrow RCH = CH_2$$
Sulfoxide reduction
$$RS(O)R' \rightarrow RSR'$$
Reductive dehalogention
$$Ar_2CHCCl_3 \rightarrow Ar_2CHCHCl_2$$
Ether hydrolysis
$$ROR' + H_2O \rightarrow ROH + R'OH$$
Ester hydrolysis
$$RC(O)OR' + H_2O \rightarrow RC(O)OH + R'OH$$
Phosphor-ester hydrolysis
$$(RO)_2P(O)OR' + H_2O \rightarrow (RO)_2P(O)OH + R'OH$$
Amide hydrolysis
$$RC(O)NR'R'' + H_2O \rightarrow RC(O)OH + HNR'R''$$
Hydrolytic dehalogenation
$$RCl + H_2O \rightarrow ROH + HCl$$

### 4.4.2.3   Biotransformation of Inorganic Contaminants

The microbially mediated transformation of inorganic contaminants encompasses a broad spectrum of compounds. Here, we survey only a few contaminants that have a major impact on the soil–subsurface system, such as nitrates, phosphates, and toxic metals. In the subsurface, the microbial population distribution generally decreases with depth, and the moisture content and aerobic–anaerobic states fluctuate with time, affected by climatic conditions, depth of groundwater, and human intervention.

*Nitrification–denitrification* involves the conversion of $NH_4^+$ to $NO_2^-$, the oxidation of $NO_2^-$ to $NO_3^-$, and the reduction of $NO_3^-$ to $NO_2^-$. The gases $N_2O$ and $N_2$ are used in the microbially mediated processes involved in the nitrification–denitrification phenomenon. Nitrification is associated with chemoautotropic bacteria, which under aerobic conditions derive their energy from the oxidation of $NH_4^+$ to $NO_2^-$. *Nitrobacter* is the soil bacterium which oxidizes $NO_2^-$ to $NO_3^-$. In most habitats, this bacterium is found together with *Nitrosomonas, Nitrospira*, or *Nitrosovibrio*, which oxidize ammonia ($NH_3$) to the nitrite required for $NO_3^-$ formation. Nitrification is affected by the subsurface pH (with an optimum value varying between 6.6 and 8.0) and the subsurface water–air ratio. Once $NO_3^-$ is formed, it becomes subject to transformation by microorganism-mediated denitrification to gaseous oxides of nitrogen and to $N_2$. The $NO_3^-$ may be taken up by organisms and used in synthesis of amino acids (assimilatory reduction), or in the absence of $O_2$, it may be used by microorganisms as an electron acceptor by reduction to $NH_4^+$ (Paul and Clark 1989). Enzymatic denitrification is the result of assimilatory reduction of $NO_3^-$ by microorganisms and dissimilatory reduction of nitrate to ammonium. This is accomplished by specific organisms in the absence of $O_2$.

Denitrification occurs only in the presence of oxidized nitrogen and in an environment with limited $O_2$ (which prevails in the subsurface). Because denitrification is an enzyme-mediated reaction, the substrate concentration functions as a rate-determining factor. The dominant denitrifying bacteria are heterotrophic. The favored environmental conditions for growth of denitrifying bacteria include a neutral pH (6–8), a favorable water–air (oxygen) ratio, and a subsurface temperature between 20 and 30°C.

*Phosphorus* in the soil–subsurface system originates from a natural parent material or from anthropogenic application on land surface (e.g., fertilizers, pesticides, surfactant products, sludge, and effluents). Phosphorus species concentrations in subsurface aqueous solutions are affected by anthropogenic factors, either directly by the P species disposed of on a particular site or indirectly via pH changes resulting from municipal, agricultural, or industrial composition of the disposed materials. Ambient temperature and the water–air ratio in the subsurface also control rate factors of biologically mediated P species transformation.

Here, we do not discuss P transformation resulting from chemical equilibrium and adsorption–desorption processes; the reader is directed to the comprehensive review of Sims and Pierzynski (2005). Instead, we focus on biologically mediated transformation of organic P in the subsurface. The ultimate and "natural" sources of organic P in the soil–subsurface environment are animal and plant residues. These

are accompanied by additional phosphorus organic chemicals of anthropogenic origin, disposed of on land surface or spilled in surface waters. These residues are decomposed by microorganisms, forming inositol phosphate metabolites that are generally resistant to further, biologically induced, decomposition. The basic inositol group is the six C ring structure, hexahydrobenzene. Inositol phosphates are monoesters with the hexaphosphate ester and phytic acid, which are found commonly in soils (Stevenson 1994). An example of myo-inositol hexaphosphate is shown in Fig. 4.2. Mono-, di-, tri-, tetra-, and pentaphosphates, which are degradation products of the hexaphosphate form of myo-inositol, may also be found.

Phospholipids containing phosphatidyl, inositol, lecithin, serine, and ethanolamine (Stevenson 1994) are the second most abundant identifiable form of organic P in the upper layer of the soil–subsurface system. These groups contain glycerol, fatty acids, and phosphate (Sims and Pierzynski 2005). The P in the structure is a diester, which is more susceptible than monoesters to degradation in soils.

Additional transformable organic P compounds found in the soil–subsurface environment are nucleic acids and phosphonates. Nucleic acids constitute a minor portion of identifiable organic P in the subsurface. They are readily degraded, and their presence in the subsurface environment is due to continuous microorganism production rather than persistence. Phosphonates are organic P compounds with direct C–P bonding, as opposed to the C–O–P bonding typical of most other organo-P molecules commonly found in soils; the main compound reported to date is 2-aminoethyl phosphonic acid (Newman and Tate 1980).

Sims and Pierzynski (2005) noted that the balance between mineralization (due to a biological process where enzymes produced by plants and microorganisms hydrolyze organic compounds, releasing inorganic P into solution) and immobilization (conversion of inorganic P to organic P in biomass) ultimately controls P concentration in the aqueous solution. This concentration, however, is affected by the solution pH and by the properties of the solution surrounding the solid phase. The P products produced in the various stages of microbially mediated transformation have different properties, their transport in the subsurface being affected by the type of speciation involved.
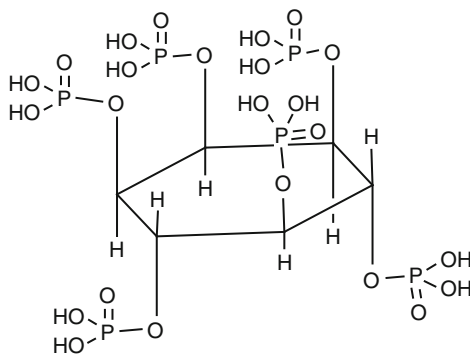


**Fig. 4.2** Myo-inositol hexaphosphate structure (after Sims and Pierzynski 2005). Copyright 2005, Soil Science Society of America. Reprinted with permission

*Metal transformation* includes two main processes: oxidation–reduction of inorganic forms and conversion of metals to organic complex species (and the reverse conversion of organic to inorganic forms). Microbially mediated oxidations and reductions are the most typical pathway for metal transformation. Under acidic conditions, metallic iron ($Fe^0$) readily oxidizes to the ferrous state ($Fe^{2+}$), but at $pH > 5$, it is oxidized to $Fe^{3+}$. Under acidic conditions, $Fe^{3+}$ is readily reduced. *Thiobacillus ferroxidans* mediates this reaction in an acid environment and derives both energy and reducing power from the reaction. Paul and Clark (1989) showed that before $Fe^{3+}$ is microbiologically reduced, it is chelated by organic compounds. During oxidation, electrons are moved through an electron transport chain, with cytochrome c being the point of entry into the transport chain. Oxidation can be caused by direct involvement of enzymes or by microorganisms that raise the redox potential or the pH. Iron reduction occurs when ferric iron ($Fe^{3+}$) serves as a respiratory electron acceptor or by reaction with microbial end products such as formaldehyde or $H_2S$. Microbiologically mediated transformation, as affected by pH, is also observed in the oxidation of $Mn^{2+}$, when both bacteria and fungi can oxidize manganese ions only in neutral and acid environments. Dissimilatory metal reduction bacteria can couple organic matter oxidation to metal contaminant reduction (Lovley 1993). Rates of these reactions depend on the reduction potential of the solid or solution phase metal, the surface area, and the presence of competing terminal electron acceptors.

An additional environmental factor that may affect metal contaminant transformation in the soil–subsurface system is the air–water ratio. A toxic metal like mercury does not remain in a metallic form in an anaerobic environment. Microorganisms transform metallic mercury to methylmercury ($CH_3–Hg^+$) and dimethylmercury ($CH_3–Hg–CH_3$), which are volatile and absorbable by the organic fraction of the subsurface solid phase or by subsurface microorganisms.

# References

Amirtharajah A, Raveendran P (1993) Detachment of colloids from sediments and sand grains. Colloids Surf A 73:211–227

Amitay-Rosen T, Cortis A, Berkowitz B (2005) Magnetic resonance imaging and quantitative analysis of particle deposition in porous media. Environ Sci Tech 39:7208–7216

Ashton FM, Sheets TJ (1959) The relationship of soil adsorption of EPTC to oats injury in various soil types. Weeds 7:88–90

Bailey GW, White JL (1964) Review of adsorption and desorption of organic pesticides by soil colloids with implications concerning pesticide bioavailability. J Agric Food Chem 12:324–382

Barraclough D, Kearney T, Croxford A (2005) Bound residues: environmental solution or future problem? Environ Pollut 133:85–90

Barriuso E, Baer U, Calvet R (1992a) Dissolved organic matter and adsorption-desorption of difemuron, atrazine and carbetamide by soils. J Environ Qual 21:359–367

Barriuso E, Koskinen WC, Sorenson B (1992b) Modification of atrazine desorption during field incubation experiments. Sci Total Environ 123(124):333–344

Berkowitz B, Dror I, Yaron B (2008) Contaminant geochemistry: interactions and transport in the subsurface environment. Springer, Heidelberg, p 412

Bollag JM, Liu SY (1990) Biological transformation processes of pesticides. In: Chen HH (ed) Pesticides in the soil environment: Processes, impacts, and modeling, SSSA Book Series 2. SSSA, Madison, WI

Bollag JM, Loll MJ (1983) Incorporation of xenobiotics in soil humus. Experentia 39:1221–1225

Bollag JM, Myers CJ, Minard RD (1992) Biological and chemical interactions of pesticides with soil organic matter. Sci Total Environ 123(124):205–217

Bolt GH (1955) Ion adsorption by clays. Soil Sci 79:267–278

Bolt GH, De Boodt MF, Hayes MF, McBride MB (eds) (1991) Interactions at the soil colloid-solution interface NATO ASI Series – Applied Science Series F, vol 190. Kluwer, Dordrecht, p 603

Boyd GE, Adamson AW, Mayers LS Jr (1947) The exchange adsorption of anions from aqueous solution by organic zeolites. J Am Chem Soc 69:2836–2848

Bradford SA, Simunek J, Bettahar M, van Genuchten MT, Yates SR (2003) Modelling colloid attachment, straining and exclusion in saturated porous media. Environ Sci Technol 37:2242–2250

Brown CB, White JL (1969) Reactions of 12-triazines with soil clays. Soil Sci Soc Am Proc 33:863–867

Buffle J (1988) Complexation reactions in aquatic systems: an analytical approach. Ellis Horwood, Chichester, England

Burchil SM, Hayes MHB, Greenland DJ (1981) Adsorption. In: Greenland DJ, Hayes MHB (eds) Chemistry of soil processes. Wiley, New York, pp 224–400

Calderbank A (1989) The occurrence and significance of bound pesticides residues in soil. Rev Environ Contam Toxicol 198:69–103

Calvet R (1984) Behavior of pesticides in unsaturated zone. Adsorption and transport phenomena. In: Yaron B, Dagan G, Goldschmid J (eds) Pollutants in porous media. Springer, Heidelberg, pp 143–151

Celis R, Cox L, Hermosin MC, Cornejo J (1996) Retention of metamitron by model and natural particulate matter. Int J Environ Anal Chem 65:245–260

Daintith J (1990) A concise dictionary of chemistry. Oxford University Press, Oxford, UK

Elimelech M, Gregory J, Jia X, Williams RA (1995) Particle deposition and aggregation: measurement, modelling, and simulation. Butterworth-Heinemann, Oxford, England

Firestone MK (1982) Biological denitrification. In: Stevenson FJ (ed) Nitrogen in agricultural soils. Agronomy 22:289–326

Fowker FM, Benesi HA, Ryland RB, Sawyer WM, Detling KD, Folkemer FB, Johnson MR, Sun YP (1960) Clay catalyzed decomposition of insecticides. J Agric Food Chem 8:203–210

Fuhr F, Ophoff H, Burauel P, Wanner U, Haider K (1998) Modification of definition of bound residues. In: Fuhr F, Phoff H (eds) Pesticide bound residues in soils. Wiley, Weinheim, pp 175–176

Gaillardon P, Calvet R, Terce M (1977) Adsorption et desorption de la terbutryne par une montmorillonite – Ca et des acides humiques seules ou en mélanges. Weed Res 17:41–48

Gevao B, Semple KT, Jones KC (2000) Bound pesticide residues in soils: a review. Environ Pollut 108:3–14

Giles CH, Smith D, Huitson A (1974) A general treatment and classification of the solute adsorption isotherms. J Colloid Interface Sci 47:755–765

Grahame DC (1947) The electrical double layer and the theory of electro capillarity. Chem Rev 41:441–449

Greenland DJ, Hayes MHB (eds) (1981) The chemistry of soil processes. Wiley, Chichester

Greenland DJ, Mott CJB (1978) Surfaces of soil particles. In: Greenland DJ, Hayes MHB (eds) The chemistry of soil constituents. Wiley, Chichester, pp 321–355

Hassett IJ, Banwart WL (1989) The sorption of non polar organics by soil and sediments. In: Sawhney BL, Brown K (eds) Reactions and movement of organic chemicals in soils. SSSA Spec. Pub. 22. SSSA, Madison, WI, pp 31–45

Helfferich F (1962) Ion exchange. McGraw-Hill, New York

Hodges SC, Johnson GC (1987) Kinetics of sulfate adsorption and desorption by Cecil soils using miscible displacement. Soil Sci Soc Am J 51:323–327

Huang OM (2000) Abiotic catalysis. In: Sumner ME (ed) Handbook of soil science. CRC, Boca Raton, pp 303–327

Huang PM, Crossan LS, Rennie DA (1968) Chemical dynamics of K release from potassium minerals common in soils. Trans 9th Int Congr Soil Sci 2:705–712

Huang PM, Grover R, McKercher RB (1984) Components and particle size fractions involved in atrazine adsorption by soils. Soil Sci 138:220–224

Johnson BT, Kennedy JQ (1973) Biomagnification of p, p-DDT and methoxychlor by bacteria. Appl Microbiol 26:66–71

Kan AT, Chen W, Tomson MB (2000) Desorption kinetics from neutral hydrophobic organic compounds from field contaminated sediment. Environ Pollut 108:81–89

Kang SH, Xing BS (2005) Phenanthrene sorption to sequentially extracted soil humic acids and humans. Environ Sci Technol 39:134–140

Kennedy VC, Brown TC (1965) Experiments with a sodium ion electrode as a mean to studying cation exchange rate. Clays Clay Miner 13:351–352

Khan SU (1982) Bound pesticides residues in soil and plant. Residue Rev 84:1–25

Li GC, Felbeck GT Jr (1972) A study of the mechanism of atrazine adsorption by humic acid from muck soil. Soil Sci 113:140–148

Lovley DR (1993) Dissimilatory metal reduction. Ann Rev Microbiol 47:263–290

McBride MB (1989) Surface chemistry of soil minerals. In: Dixon JB, Weed SB (eds) Minerals in soil environments. Second ed. SSSA Book Series 1, Madison, WI, pp 35–88

McBride MB (1994) Environmental chemistry of soils. Oxford University Press, Oxford, 286

McCarthy JF, Zachara JM (1989) Subsurface transport of contaminants. Environ Sci Technol 23:496–502

Mills AC, Biggar JW (1969) Solubility-temperature effect on the adsorption of gamma and beta – BHC from aqueous and hexane solutions by soils materials. Soil Sci Am Soc Am Proc 33:210–216

Mingelgrin U, Gerstl Z (1993) A unified approach to the interactions or small molecules with macrospecies. In: Beck AJ, Jones KC, Hayes MHB, Mingelgrin U (eds) Organic substances in soil and water. Royal Society of Chemistry, Cambridge, pp 102–128

Mingelgrin U, Saltzman S (1977) Surface reactions of parathion on clays. Clays Clay Miner 27:72–78

Mortland MM (1970) Clay-organic complexes and interactions. Adv Agron 22:75–117

Mortland MM (1986) Mechanism of adsorption of non humic organic species by clays. In: Huang PM, Schnitzer M (eds) Interaction of soil minerals with natural organics and microbes. SSSA, Madison, WI, pp 59–76

Newman RH, Tate KR (1980) Soil-phosphorus characterization by p-31 nuclear magnetic resonance. Comm Soil Sci Plant Anal 11:835–842

Nye PH, Tinker PB (1977) Solute movement in the soil-root system. Blackwell, Oxford, p 324

Oades JM (1989) An introduction to organic matter in mineral soils. In: Dixon JB, Weed SB (eds) Minerals in soil environment. Soil Sci Soc Am, Madison, WI, pp 89–153

Overbeek JTh (1952) Electrochemistry of the double layer. Colloid Sci 29:119–123

Parr JF, Smith S (1976) Degradation of toxaphene in selected anaerobic soil environments. Soil Sci 121:52–57

Paul EA, Clark FE (1989) Soil microbiology and biochemistry. Academic, New York

Penrose WR, Polzer WL, Essington EH, Nelson DM, Orlandini KA (1990) Mobility of plutonium and americium through a shallow aquifer in a semiarid region. Environ Sci Technol 24:228–234

Pignatello JJ (1989) Sorption dynamics of organic compounds in soils and sediments. In: Sawhney BL, Brown K (eds) Reactions and movement of organic chemicals in soils, SSSA Spec Publ 22. SSSA, Madison, WI, pp 45–81

Ponec V, Knor Z, Cerny S (1974) Adsorption on solids. Butterworth, London, p 234

Purdue EM, Wolfe NL (1983) Prediction of buffer catalysis in field and laboratory studies of pollutant hydrolysis reactions. Environ Sci Technol 17:635–642

Quirk JP, Posner AM (1975) Trace element adsorption by soil minerals. In: Nicholas DJ, Egan AR (eds) Trace elements in soil-plant-animal systems. Academic, New York, pp 95–107

Rao PSC, Horsnby AG, Kilcrease DP, Nkedi-Kizza P (1985) Sorption and transport of hydrophobic organic chemicals in aqueous and mixed solvent system: model development and preliminary evaluation. J Environ Qual 14:376–383

Rao PSC, Lee LS, Nkedi-Kizza P, Yalkowsky SH (1989) Sorption and transport of organic pollutants at waste disposal sites. In: Gerstl Z, Chen Y, Mingelgrin U, Yaron B (eds) Toxic organic chemicals in porous media. Springer, Heidelberg, pp 176–193

Renkin EM (1954) Filtration, diffusion and molecular sieving through porous cellulose membranes. J Gen Physiol 38:224–243

Ryan JN, Elimelech M (1996) Colloid mobilization and transport in ground water. Colloids Surf A 107:1–56

Sakthivadivel R (1966) Theory and mechanism of filtration of non-colloidal fines through a porous medium. Rep. HEL 15–5, 110 pp., Hydraul. Eng. Lab. Univ. of Calif., Berkeley

Sakthivadivel R (1969) Clogging of a granular porous medium by sediment. Rep. HEL 15–7, 106 pp., Hydraulic Engineering Laboratory. University of California, Berkeley

Saltzman S, Kliger L, Yaron B (1972) Adsorption-desorption of parathion as affected by soil organic matter. J Agric Food Chem 20:1224–1227

Saltzman S, Mingelgrin U, Yaron B (1974) The surface catalyzed hydrolysis of parathion on kaolinite. Soil Sci Soc Am Proc 38:231–234

Sander M, Lu y, Pignatello J (2005) A thermodynamically based method to quantify true sorption hysteresis. J Environ Qual 34:1063–1072

Senesi M, Chen Y (1989) Interaction of toxic organic chemicals with humic substances. In: Gerstl Z, Chen Y, Mingelgrin U, Yaron B (eds) Toxic organic chemicals in porous media. Springer, Berlin, pp 37–91

Sims JT, Pierzynski GM (2005) Chemistry of phosphorus in soils. In: Tabatabai MA, Sparks DL (eds) Chemical processes in soils, SSSA Book Series 8, Madison, WI, pp 151–192

Sparks DL (1986) Soil physical chemistry. CRC, Boca Raton, FL, p 324

Sparks DL (1989) Kinetics of soil chemical processes. Academic, New York, p 210

Sparks DL, Huang PM (1985) Physical chemistry of soil potassium. In: Munson RE (ed) Potassium in agriculture. ASA, Madison, pp 201–276

Sparks DL, Jardine PM (1984) Thermodynamics of potassium exchange in soil using a kinetic approach. Soil Sci Soc Am J45:1094–1099

Sposito G (1984) The surface chemistry of soils. Oxford University Press, Oxford, p 234

Stern O (1924) Zur theorie der elecktrolytischen doppelschict. Z Electrochem 30:508–516

Stevenson FJ (1994) Humus chemistry: genesis, composition, reactions, 2nd edn. Wiley, NY

Stone AT, Torrents A (1995) The role of dissolved metals and metal containing surfaces in catalyzing the hydrolysis of organic pollutants. In: Huang PM (ed) Environmental impact of the soil components. Lewis, Boca Raton, FL, pp 275–299

Stone TA, Torrents A, Smolen J, Vasudevan D, Hadley J (1993) Adsorption of organic-compounds processing ligand donor groups at the oxide-water interface. Environ Sci Technol 27:895–909

Talibuden O (1981) Cation exchange in soils. In: Greenland DJ, Hayes MHB (eds) The chemistry of soil processes. Wiley, Chichester, pp 115–178

Terce M, Calvet R (1977) Some observation on the role of Al and Fe and their hydroxides in the adsorption of herbicides by montmorillonite. Sonderdruck Z Planzen – kr Pfanzenschutz Sonderheft VIII

van Olphen H (1967) An introduction to clay colloid chemistry. Wiley, New York, p 220

Vilks P, Cramer JJ, Bachinski DB, Doern DC, Miller AG (1993) Studies of colloids and suspended particles, Cigar Lake uranium deposit, Saskatchewan, Canada. Appl Geochem 8:605–616

Villaverde J, Vanbei um W, Beulke S, Brown CD (2009) The kinetics of sorption by retarded diffusion into soil aggregate pores. Environ Sci Technol 43:8227–8232

Vinten AJ, Yaron B, Nye PH (1983) Vertical transport of pesticides into soil when adsorbed on suspended particles. J Agric Food Chem 31:661–664

Waner U, Fuhr F, deGraaf AA, Burauel P (2005) Characterization of non-extractable residues of the fungicide dithianon in soil using C-13/C-14 labelling. Environ Pollut 133:35–41

Wershaw RL (1986) A new model for humic materials and their interactions with hydrophobic organic chemicals in soil-water or in sediment-water systems. J Contam Hydrol 1:29–45

Wolfe NL, Mingelgrin U, Miller GC (1990) Abiotic transformations in water, sediments, and soil. In: Cheng HH (ed) Pesticides in the soil environment, SSSA Book Series 2. SSSA, Madison WI, pp 103–168

Yamane VK, Green RE (1972) Adsorption of ametryne and atrazine on an oxisol, montmorillonite and charcoal in relation to pH and solubility effects. Soil Sci Soc Am Proc 36:58–64

Yao KM, Habibian MT, O''Melia CR (1971) Water and waste water filtration: concepts and applications. Environ Sci Technol 5:1105–1112

Yaron B, Saltzman S (1978) Soil-parathion surface interactions. Residue Rev 69:1–34

Yaron B, Calvet R, Prost R (1996) Soil pollution processes and dynamics. Springer, Heidelberg, p 310, ISBN 3-540-60927-X

# Chapter 5
# Irreversible Alteration of Soil–Subsurface Matrix Induced by Contaminant Exchange Processes

The natural soil and subsurface solid phase matrix may be changed by irreversible surface adsorption of contaminants. The extent of irreversible adsorption and changes to the solid phase is controlled by the properties of the interacting materials and by the environmental conditions. In this chapter, we describe irreversible adsorption of polar contaminants and induced changes in soil–subsurface mineral and organic phases through ionic exchange pathways. Desorption experiments may lead, in many cases, to an apparent hysteresis; in the examples that follow, we focus on research that reported real, contaminant-induced, irreversible hysteretic effects.

## 5.1 Ionic Exchange on Clay Minerals and Organic Matter: Introductory Considerations

### 5.1.1 Clay Minerals

Clay minerals have a permanent negative charge due to isomorphous substitution or vacancies in their structure. For example, $Mg^{2+}$ may substitute for $Fe^{3+}$ or $Al^{3+}$ in octahedral or tetrahedral coordination. The structural charge must be balanced by cations situated at or in the vicinity of the mineral surface. Cation exchange reactions result primarily from the excess of negative charge which may be permanent, variable, or pH dependent (McBride 1989). A permanent negative charge in clay results from substitution of coordinating cations with a given positive charge by cations with lower positive charge. Isomorphic substitution occurs mostly in tetrahedral or octahedral sheets. In soils and subsurface domains, where the mineral fraction is formed from a mixture of clay materials, a binary cation exchange system prevails. Electrical neutrality on the solid surface requires that an equal amount of positive and negative charge accumulates in the liquid phase near the surface. If the surface is negatively charged, positively charged cations are attracted electrostatically to the surface. Simultaneously, the cations are drawn back toward the equilibrating

solution; as a result, a diffuse layer is formed and the concentration of cations increases toward the surface. On the contrary, ions of the same sign (anions) are repelled by the surface, with diffusion forces acting in an opposite direction.

Sorption of cations by clay minerals is not only a simple ion exchange process. Certain cations are sorbed more selectively than others and are held more firmly against replacement by other cations. Selective sorption and fixation of cations from aqueous solutions on clay minerals, soils, and sediments were one of the main topics of interest in the middle of the last century (Sawhney 1972, and references therein). It was observed that adsorption of contaminant ions with high hydration energy (e.g., $Sr^{2+}$) produces only clay with expanded interlayers; contaminant ions with low hydration energy (e.g., $Cs^+$) cause clay interlayer dehydration and collapse, leading to the their fixation in interlayer positions. Among the large number of theoretical approaches used to derive the binary exchange equation, the most common ones are the mass action equation and double-layer approaches (Evangelou and Phillips 2005, and references therein).

The mass action equation for a calcium–sodium exchange case may be expressed as

$$CaX + 2Na^+ = Ca^{2+} + 2NaX,$$
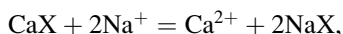
where X refers to an exchangeable anion. The Gapon equation (1933) approached the process as an exchange of mole equivalents of electric charge rather than that of moles. It is an ion exchange equation that has been used widely for soil and subsurface salinity studies. This slightly modified mass action equation is written in the form:

$$Ca_{1/2}X + Na^+ = \frac{1}{2}Ca^{2+} + NaX.$$
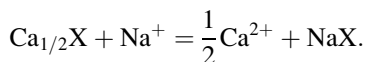
The resulting equilibrium constant is:

$$K_G = [Na^+][Ca_{1/2}X]/[Ca^{2+}]^{1/2}[NaX],$$

where concentrations are used in place of activities for the solution phase and where the ratio of ion activities is assumed to be proportional to the ratio of exchangeable ion concentrations on an equivalent basis. Based on verification of the Gapon equation at low to moderate exchangeable sodium percentage (ESP) values, the U.S. Salinity Laboratory (1954) developed a linear regression between exchangeable sodium ratio (ESR) and sodium adsorption ratio (SAR),

$$ESR = -0.0126 + 0.1465\,SAR,$$

where

$$ESR = [NaX]/[CaX + MgX],$$

and

$$SAR = [Na^+]/[(Ca^{2+} + Mg^{2+})/2]^{1/2}.$$

The *diffuse double layer* (DDL) approach as suggested by Gouy and Chapman was advanced by Stern (1924) and Graham (1947) by recognizing that counterions are unlikely to approach the surface more closely than the ionic radii of the anions and the hydrated radii of the cations. A schematic representation illustrating the fundamental differences between the Gouy–Chapman and Stern models is presented in Fig. 5.1. The DDL, which is of considerable use in understanding the retention of ionic contaminants in the soil–subsurface system, was discussed in Sect. 4.1.2.

*Cation exchange capacity (CEC) and selectivity* are among the most important processes that control the fate of charged (ionic) contaminants in the soil–subsurface system. These processes involve the cationic concentration in solution and the cation
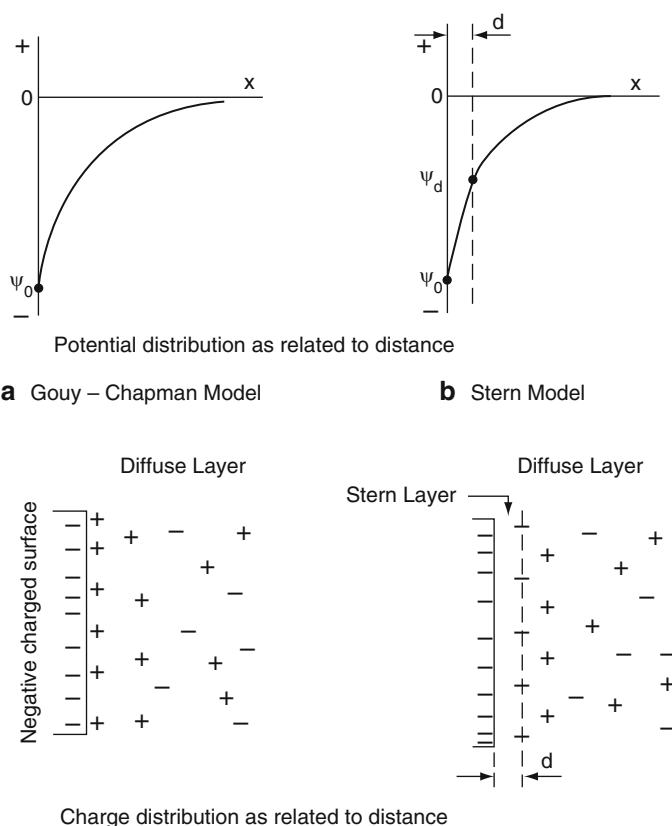


**Fig. 5.1** Distribution of electrical charges and potentials in a double layer according to (**a**) Gouy–Chapman model and (**b**) Stern model, where $\Psi_0$ and $\Psi_d$ are surface and Stern potentials, respectively, and $d$ is the thickness of the Stern layer

dimensions, as well as the configuration of exchange sites on the interface. The Gapon relation approaches the process as an exchange of equivalents of electric charges, where the solute concentration is measured in terms of activity, and the adsorption on an equivalent basis.

Clay–cation adsorbed complexes may be classified as either inner sphere or outer sphere (Sposito 1989; Sposito et al. 1999). The inner sphere does not have water between the surface functional group and the cation or molecule it binds. In contrast, the outer-sphere surface complex comprises solvated adsorbed cations with at least one interposed water molecule. Ions bound in the clay surface complexes are different from the ions adsorbed in the diffuse part of the electrical double layer. In inner-sphere, the ions are immobilized over molecular time scale on the clay interlayer surface which is much longer compared to those of the outer-sphere solvated ions which require only one step to diffuse in the surrounding water solution. A fuller discussion of ion exchange processes was presented previously in Sect. 4.1.2.

*Anionic negative adsorption* or anion exclusion may occur in the near-surface and subsurface when negatively charged clay minerals repel by Coulomb forces anions from the mineral surface (see Sect. 4.1.2). Soils and subsurface – generally characterized by a low pH – which contain relatively large amounts of iron and aluminum hydrous oxides have the ability to retain anions via anion exchange. This process occurs mainly in the case of high salt concentration presence when a progressive collapse of the diffuse double layer takes place. Under such conditions, the positively charged sites on hydrous oxides on the edges of soil and subsurface minerals will no longer be masked by the negative diffuse double layer so that they can begin to attract and exchange anions.

### 5.1.2 Humic Substances

Humic substances may also favor the adsorption of charged contaminants via ion exchange (ionic bonding) processes. Cation exchange properties of humic substances were mentioned in early papers including those of McGeorge (1930), Mitchell (1932), and Lees (1948). Soil organic matter has been shown to have many different types of functional groups contributing to its CEC (Stevenson and Butler 1965). The contribution of various organic groups to the total CEC was estimated as 54% carboxyl groups, 36% phenolic and enolic hydroxyl groups, and about 10% imide nitrogen groups (Broadbent and Bradford 1952). The configuration and dimension of a humic polymer in a specific medium determine the availability of adsorption sites.

#### 5.1.2.1 Metallic Contaminants

Various studies performed between 1950 and 1980 on metal–humic substance interactions confirmed the fact that the uptake of divalent metal ions is a cation

exchange process (Kerndorff and Schnitzer 1980, and references therein). In this study, it was observed that the sorption efficiency tended to increase with the rise in pH, leading to a decrease in metal concentration and an increase in humic acid concentration in the equilibrating solution. There were indications of competition for active sites ($CO_2H$ and phenolic OH groups) on the humic acid among the metals Hg(II), Fe(III), Pb, Cu, Al, Ni, Cr(III), Cd, Co, and Mn used in the experiments. Gamble et al. (1983) consider that the reactive functional groups are the key to the cation exchange reactions, with the equilibria being defined in terms of these reactions. The functional groups found in natural humic materials include carboxyl groups, phenolic groups, and alchohlic-OH, ketonic, and quinone groups (Schnitzer 1978). For the particular case of multiple metals, anion exchange equilibrium with humic acid is only one of several types of interactions.

### 5.1.2.2 Pesticides

Pesticides are a group of toxic organic compounds used widely in agricultural and municipal sectors. We select pesticides for the discussion of adsorption of ionic charged compounds on soil organic matter because cationic, basic, and acid compounds can be found in this group (Saltzman and Yaron 1986).

*Cationic pesticide* interactions with soil organic matter were studied by comparing the adsorption of the pesticides diquat and paraquat and of $Ca^{2+}$ ions by different humic substance components at two pH levels (Best et al. 1972). Both the $Ca^{2+}$ ions and the organic cations appear to compete for the same adsorption sites. The higher charge density at a higher pH level favors the adsorption of the small $Ca^{2+}$ ion on account of the large cation molecule. However, the predominant mechanism for the adsorption of organic cations by humic substances is ion exchange. Unlike clays which have a rigid structure and fixed charge distribution, humic substances have flexible exchange sites, and the charge density is pH dependent.

*Basic (high pH) pesticide* adsorption on soil organic matter was reported in the literature, and several adsorption mechanisms were postulated for the very complex process of interactions between organic colloids and weak bases. Similar to adsorption of cationic pesticides, basic pesticides can also be adsorbed. In the case of basic pesticides, the adsorption mechanism is conditioned by the acidity of the medium. Because basic pesticides include an important group of herbicides that are retained strongly in soils, the mechanism of herbicide adsorption has received special attention. The early infrared (IR) study of Sullivan and Feldbeck (1968) proved that ionic bonding can occur between a protonated secondary amino group of the s-triazine and a carboxylate anion on the humic acid. Successive IR studies (e.g., Senesi et al. 1987) confirmed these results and provided evidence of possible involvement of the acidic phenol-OH of humic acids in the proton exchange of the s-triazine molecule. Weber et al. (1965) demonstrated that maximum adsorption of seven s-triazines by soil organic matter occurred at pH levels close to the $pK_a$ values of the compounds. The molecular structure of the adsorbate and the pH of

the adsorbing medium determined the amount adsorbed. The pH-dependent adsorption and the direct relationship among pH, dissociation constant, and adsorption are strong evidence that protonated basic pesticides can be adsorbed through an ion exchange process. However, later research on the adsorption of s-triazines on humic acids at a molecular level points out that in addition to ionic and hydrogen bonding mechanisms, electron donor–acceptor processes may play an important role in the adsorption of s-triazines by humic acids (Senesi and Testini 1982).

*Acidic pesticides* (such as 2,4-D, 2,4,5-D picloram, and dinoseb) are characterized by their ability to ionize in aqueous solutions to form anion species. At pH values lower than their dissociation constants, these pesticides in aqueous solution are in molecular form. Increasing the aqueous solution pH above their $pK_a$ favors pesticide dissociation. It has been shown that acidic pesticides are adsorbed by soils, their adsorption being correlated to the soil organic matter content (Grover 1971). It is known that soil organic colloids are negatively charged or uncharged, and as a consequence, significant adsorption by anion bonding is excluded. The kinetic studies of 2,4-D and picloram on humic acid performed by Khan (1973b) indicate that adsorption of acidic pesticides on soil organic colloids is a physical, not an exchange, process. Adsorption of acidic pesticides may also be explained by the inverse relationship between their adsorption and the pH of the aqueous solution. This process may be explained by preferential adsorption of undissociated species (Grover 1971). The comprehensive review of Senesi and Chen (1989) on adsorption mechanisms of toxic organic chemicals on humic substances includes additional examples of the exchange-controlled adsorption process in the soil–subsurface system, within the broad spectrum of the Critical Zone environment.

*Hysteresis* of contaminants defines their irreversible adsorption in the soil–subsurface matrix, which in many cases causes modification of the adsorbent matrix. Hysteresis is *genuine* when contaminant release results only from desorption when the system is at equilibrium and released molecules are those adsorbed onto the solid phase surface. Because different mechanisms are involved in the adsorption–desorption process, different types of desorption isotherms can be observed. For example, desorption is sometimes described by a linear isotherm; in other cases, the release is described by an exponential function for equilibrium concentrations in solution (Barriuso et al. 1992a, b). Although the existence of pesticide hysteresis has been attributed by some investigators to experimental artifacts, sufficient evidence exists to suggest that hysteretic behavior is due to a portion of sorbed pesticide that is very strong or irreversibly retained and does not readily desorb from soil and its constituents (Cellis and Koskinen 1999, and references therein). It is known that desorption isotherms which determine the hysteresis dimension depend on the initial contaminant concentration of the adsorbate. It must be considered, however, that the adsorption equilibrium of pesticides in the soil–subsurface system is time dependent, as a function of adsorption sites of the matrix. As a consequence, the initial contaminant concentration used as a basis for calculating the hysteretic behavior may vary with time; this time-dependent effect must be considered in defining the irreversible release of adsorbed contaminants from the soil–subsurface system (Mamy and Barriuso 2007).

*Bounding* depicts the process leading to the formation of nonextractable organic residues in soil that are chemical species, which originate from organic contaminants, and are not extracted by methods that do not significantly change the chemical nature of the residue. Fuhr et al. (1998) extended the meaning of bound residues to include compounds in soil, plant, or animals which persist in the form of the parent substance or its metabolites after subsequent extraction procedures. The extraction methods must not substantially change the compounds themselves or the structure of the adsorbent matrix

Barriuso et al. (2008) depicted the kinetics of bound or nonextractable residue (NER) formation by dividing this process as follows: (1) the first step when the extraction is performed around 24 h after pesticide application; (2) the second step, considered as a "formation step," which is characterized by the kinetic rate. At a high rate, the NER plateau is reached quickly, while at a low rate of NER formation, the plateau is not reached; and (3) the third step, called the "maturation stage," which involves a decrease in NER formation. Barriuso et al. (2008) point out, however, that this general picture of NER formation depends on soil type, environmental conditions, and molecular properties of the pesticides.

## 5.2    Irreversible Adsorption of Contaminants via Exchange Processes and Induced Modification of the Soil–Subsurface Mineral Phase

### 5.2.1    Major Elements

*Sodium*, a cationic inorganic contaminant reaching the land surface through saline irrigation or by disposal of sewage effluents, leads to irreversible soil deterioration by the exchange process between $Na^+$ from water and soil-saturating cations. When $Na^+$ from saline irrigation or waste water disposal first flows through a soil, the relationship between the sodium adsorption ratio (SAR) of the water and the ESP of soil shows no significant correlation. In a column experiment carried out by Thomas and Yaron (1968) on a series of Texas soils of differing mineralogy, the total electrolyte concentration of the saline water was observed to influence the rate of sodium adsorption. At equilibrium, the ESP in the soil was influenced more by the soil mineralogy than by the cationic composition of the water and the total electrolyte concentration (Table 5.1).

Characteristic data for the adsorption of $Na^+$ on Burleson soil at different concentrations and SAR values are shown in Fig. 5.2. Three synthetic aqueous solutions with a total electrolyte concentration of 11 meq $L^{-1}$ and SAR values of 7.5, 14.0, and 28.0 were passed through a Burleson soil column. At equilibrium, the solution with SAR = 7.5 gave an ESP of 8.1, and a solution with SAR = 28 exhibited an ESP of 18.0. It can be seen from Fig. 5.2 that the quantity of aqueous solution that had to be passed through the Burleson soil column to achieve a constant $Na^+$ content in the entire profile increased with SAR in the percolating

**Table 5.1** Effect of SAR and $Na^+$ concentration in water on the ESP of soils with different mineralogy

| Soils | Clay distribution% | | Clay mineralogy | | SAR | $Na^+$ concentration, meq $L^{-1}$ | ESP |
|---|---|---|---|---|---|---|---|
| | <0.2 μm | 2–0.2 μm | <0.2 μm | 2–0.2 μm | | | |
| Burleson | 71 | 29 | $M_1Mi_3K_3$ | $M_2MiK_2Q_2$ | 28 | 11.0 | 18.9 |
| | | | | | | 33.0 | 20.4 |
| Houston Black | 78 | 22 | $M_1$ | $M_2K_2Mi_2Q_2$ | 28 | 11.0 | 16.0 |
| | | | | | | 33.0 | 16.0 |
| Miller | 49 | 51 | $M_1Mi_2K_3$ | $M_2Mi_2K_2Q_2F_3$ | 28 | 11.0 | 25.8 |
| | | | | | | 33.0 | 37.9 |
| Pullman | 41 | 59 | $Mi_2K_2M_2$ | $Mi_2K_2Q_2F_3$ | 28 | 11.0 | 31.7 |
| | | | | | | 33.0 | 32.5 |

*Mi* mica, *K* kaolinite, *M* montmorillonite, *Q* quartz, *F* feldspar

Estimated quantities, subscripts 1: >40%; 2: 10–40%; 3: <10%. Reprinted from Thomas GW, Yaron B (1968) Adsorption of sodium from irrigation water by four Texas soils. Soil Sci 106:213–219. Copyright 1968 with permission of Wolters Kluwer Health
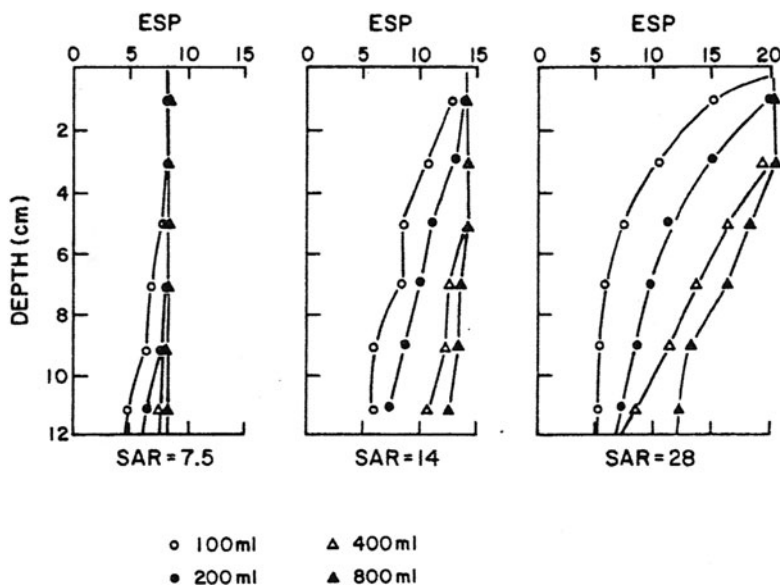


**Fig. 5.2** Exchangeable sodium percentage along a Burleson soil column, as a function of the sodium adsorption ratio of irrigation water. The values were obtained by percolating the soil columns with sodic water (total electrolyte concentration of 11 meq $L^{-1}$). Each curve corresponds to a given applied volume of solution. Reprinted from Thomas GW, Yaron B (1968) Adsorption of sodium from irrigation water by four Texas soils. Soil Sci 106:213–219. Copyright 1968 with permission of Wolters Kluwer Health

solution. In other words, for a given applied volume of solution, greater SAR values led to smaller depths where a constant ESP was achieved.

The structure of a clay material changes with $Na^+$ adsorption. The TEM images in Fig. 5.3 show the morphology of a smectite clay (montmorillonite) with its adsorbing sites saturated with $Na^+$. The lower magnification image of Na-montmorillonite
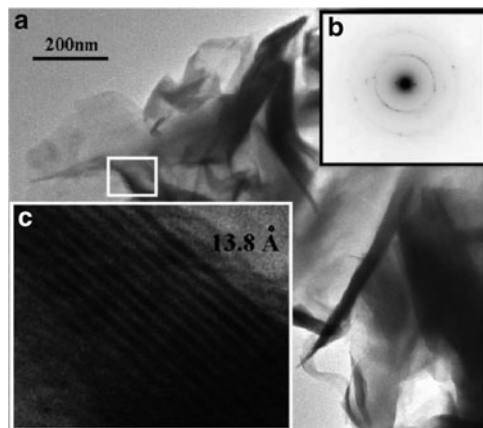
**Fig. 5.3** TEM images of Na-montmorillonite particles (**a**) low-magnification TEM image showing a typical crystalline aggregate; (**b**) the corresponding surface area electron diffraction (SAED) pattern; note the 001 diffraction spots corresponding to the planes parallel to the e-beam; the calculated spacing is 13.83 Å; (**c**) high-resolution TEM image of a particle attached to the edge of the aggregate (white framed in (**a**)) exhibiting the layered structure. The measured lattice spacing (13.8 Å) is in agreement with calculations from the SAED in (**b**) (after Yaron-Marcovich et al. 2005). Reprinted with permission from Yaron-Marcovich D, Chen Y, Nir S, Prost R (2005) High resolution electron microscopy structural studies of organo-clay nanocomposites. Environ Sci Technol 39:1231–1239. Copyright 2005 American Chemical Society

(Fig. 5.3a) reveals the presence of crystalline aggregates composed of relatively small, flakelike nanoscale silicate particles (about 10–50-nm thick and about 50–400 nm long) with no preferred orientation. The microstructure of the thin particles attached to the edges of an aggregate (Fig. 5.3c) discloses a layered structure with layers separated by van der Waals gaps along the axis. The interlayer spacing was 13.8 Å (Yaron-Marcovich et al. 2005).

Atomic force microscopy (AFM) measurements (Schlegel et al. 1999) of individual crystallites of another smectite (hectorite) indicate that Na-exchanged hectorite platelets are well dispersed (Fig. 5.4). The particles are bounded predominantly by $d_{010}$ and $d_{100}$ planes and by another plane oriented at 60° (Fig. 5.4 insert). Based on a model developed following these measurements, Schlegel et al. (1999) found that the number of edge sites per gram of the studied smectite as obtained from the mass of individual particles is about 92.5 μmol g$^{-1}$.

The morphology of a Na-montmorillonite and the pattern of an exchange of $Ca^{2+}$ ions by $Na^+$ ions were discussed above. The change in geometry of the exchanged sites explains and confirms the irreversibility of the phenomenon which was already recognized long ago (e.g., van Bladel and Laudelout 1967). $Na^+$ exchanging $Ca^{2+}$ favors the dispersion of clay platelets and, as a consequence, enhances the redistribution of the clay colloidal fraction within the soil–subsurface cross-section. This irreversible effect induces a change in the soil–subsurface system water transmission and contaminant retention properties. The cation exchange process also has an important effect on the soil solution composition. An increase in salt concentration in the soil and subsurface water causes a decreased preference for divalent ions. Under

**Fig. 5.4** AFM image of hectorite. *Inset*: Close view of particle, showing the respective orientations of the (010) and (110) edges (after Schlegel et al. 1999). Reprinted from Schlegel ML, Charlet L, Manceau A, Sorption of metal ions on clay minerals: II. Mechanism of Co sorption on hectorite at high and low ionic strength and impact on the sorbent stability. J Colloid Interface Sci 220:392–445, Copyright (1999), with permission from Elsevier



~ 60°

0.25 µm
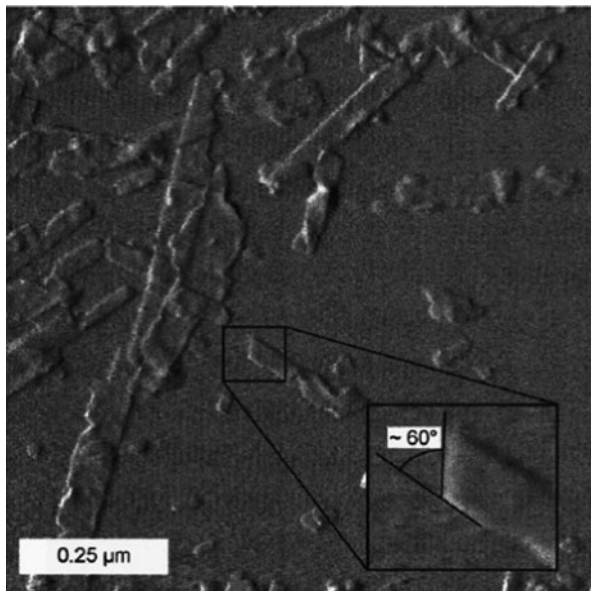
these conditions, $Ca^{2+}$ and $Mg^{2+}$ are released to solution, and $Na^+$ is retained in the solid phase. Irreversible changes in soil–subsurface properties, in terms of water transmission, contaminant retention, and salt precipitation as induced by $Na^+$ ions and elevated alkalinity, are discussed in detailed in Chap. 7.

*Fluoride*, an anionic contaminant originating from diverse industrial processes, reaches the land surface via waste disposal and may be adsorbed by the mineral portion of the soil–subsurface solid phase. Fluoride–clay sorption–desorption isotherms exhibit strong hysteretic behavior, suggesting that fluoride induces irreversible changes in the structural matrix of the adsorbing mineral. A study of fluoride retention by kaolin clay (Kau et al. 1997) supports this statement.

Based on batch experiments, Kau et al. (1997) suggested that fluoride adsorption on kaolin begins with a surface activation process where layers of metal oxides or hydrated layers of clay are displaced to provide easier access to sorption sites. Hydrogen bonding between kaolin sheets may also be disrupted by fluoride that replaces hydroxyl groups. Sorption isotherms for fluoride on kaolin have the appearance of the sum of two associated isotherms. The strong negativity of fluoride also forces the gibbsite and silica sheets apart, further increasing accessibility of fluoride (Fig. 5.5). This induces an exponential increase in fluoride adsorption until the kaolin sheets cannot be separated further, and fluoride ceases to have access to the adsorption sites. X-ray diffraction results show a consistent increase in d-spacing of kaolin sheets during fluoride adsorption.

Desorption studies demonstrate some degree of irreversible fluoride sorption, the rate of desorption being pH dependent. Desorption is much slower at low pH than at high pH. According to the sorption isotherms, it may be assumed that the first component expresses the reversible fraction of fluoride adsorbed, while the second
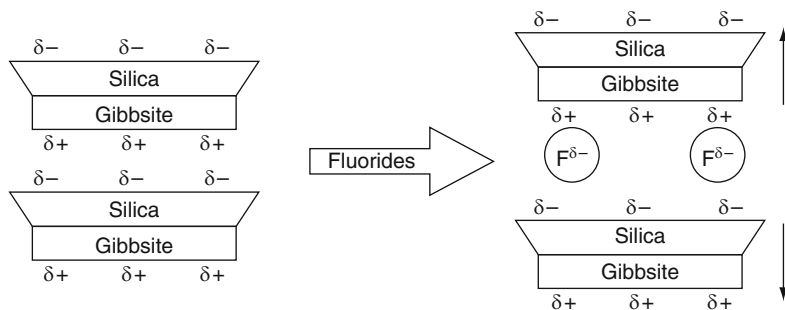
**Fig. 5.5** Proposed layer expansion of kaolin clay with fluoride sorption (after Kau et al. 1997). Reprinted from Kau PMH, Smith DW, Bonning P (1997) Fluoride retention by kaolin clay. J Contam Hydrol 28:267–288, Copyright (1997), with permission from Elsevier
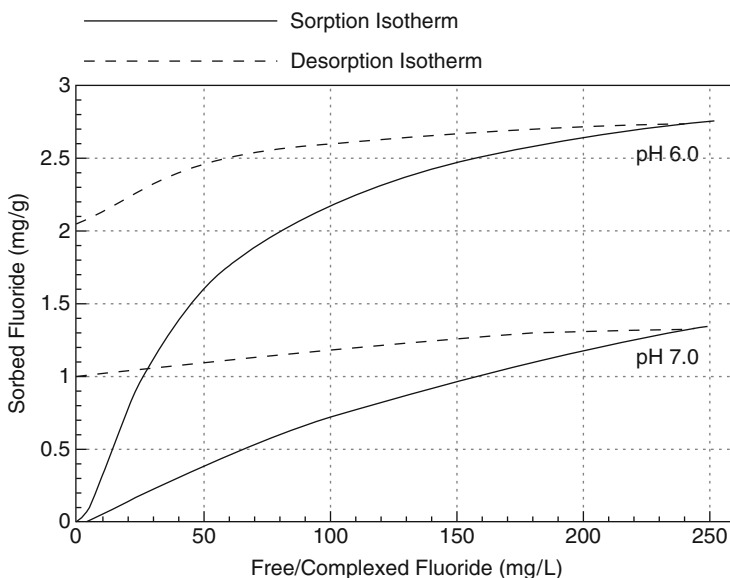


**Fig. 5.6** Fluoride sorption–desorption isotherms at two pH values (Kau et al. 1997). Reprinted from Kau PMH, Smith DW, Bonning P (1997) Fluoride retention by kaolin clay. J Contam Hydrol 28:267–288, Copyright (1997), with permission from Elsevier

one reflects the irreversible fraction. The fraction of irreversibly adsorbed fluoride maintains the d-space difference between natural and fluoride-contaminated kaolin minerals. Comparing sorption–desorption isotherms (Fig. 5.6), Kau et al. (1997) observed that the difference is small at a high, free fluoride concentration and that this difference increases with decreasing contaminant concentration. Modeling the adsorption–desorption process as a function of the breakdown of the kaolin structure caused by extension of kaolin sheet suggests that 75% of sorbed fluoride is bound irreversibly (Kau et al. 1997).

## 5.2.2   Heavy Metals

Heavy metals form a large group of ionic chemicals that exhibit toxic properties even at low concentrations. Heavy metals may reach the soil–subsurface environment as industrial or municipal wastes and following agricultural practices. The results of studies on agriculture-induced contamination of large areas of the European Mediterranean region were described by Peris et al. (2008). Analyzing the heavy metal content in the surface horizon of 77 agricultural soils from Castellon province (Spain), Peris et al. (2008) found that the highest concentrations of anthropogenic heavy metals were recorded for Cd, Cu, Pb, and Zn. Multivariate analysis, including correlation ($r$) and principal component ($p$) analysis, suggests a positive relationship between heavy metals and the soil CEC ($r > 0.200$; $p < 0.05$) and clay content ($r > 0.400$; $p < 0.01$). Douay et al. (2008) surveyed anthropogenic contamination by heavy metals of urban soils, including regions surrounding two smelters in Northern France. Analysis of 18 trace elements from 27 urban top soils indicated that Cd, In, Pb, Sb, and Zn were the major pollutants, followed in lesser quantities by Ag, Bi, Cu, and Hg. Douay et al. (2008) showed that soil reworking in the urban environment can affect the layers even below 1.5 m.

A general illustration of metal ion sorption mechanisms on clay surfaces, shown in Fig. 5.7, includes two simultaneous mechanisms: (1) adsorption of metal ions as surface complexes, in the outer sphere on exchange sites and on the inner sphere on crystallite edges, and (2) coprecipitation of sorbate and sorbent species liberated following the exchange process by dissolution. The properties of the metal ion (charge, ionic radius, and ionic potential), as well as the layer charge characteristics
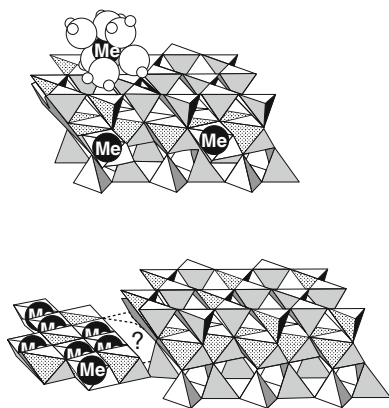


**Fig. 5.7** Illustration of different sorption mechanisms of metal ions on clay minerals. (**a**) Adsorption of metal ions as outer-sphere surface complexes on exchange sites located on basal planes, and as inner-sphere surface complexes on crystallite edges. (**b**) Coprecipitation of the sorbate and sorbent species liberated by dissolution. The *question mark* indicates that the structural relationship between the newly formed and sorbent phases is unknown (after Schlegel et al. 1999). Reprinted from Schlegel ML, Charlet L, Manceau A, Sorption of metal ions on clay minerals: II. Mechanism of Co sorption on hectorite at high and low ionic strength and impact on the sorbent stability. J Colloid Interface Sci 220:392–445, Copyright (1999), with permission from Elsevier

of clays, including surface charge magnitude and point of origin from tetrahedral or octahedral substitution, are factors that influence adsorption selectivity (Quirk and Posner 1975; Sposito 1989) and may control the extent of hysteresis.

A few examples of irreversible retention of heavy metals on clays by exchange with the natural saturating cation, and effects of heavy metals on the clay matrix follow next.

Irreversible uptake of *cobalt* from an aqueous solution onto a clay surface affects the stability of the adsorbing mineral. Schlegel et al. (1999) investigated the mechanism of Co uptake on a Mg-smectite clay (hectorite), as a function of contaminant concentration and ionic strength. Clay stability following irreversible Co sorption was established by measuring Mg dissolution during the exchange process. At low ionic strength (0.01 M $NaNO_3$), high amounts of Co are retained within the first 5 min of reaction, consistent with Co adsorption on exchange sites of hectorite basal plane; the sorption rate subsequently decreases drastically. Schlegel et al. (1999) also found that at high ionic strength (0.3 M $NaNO_3$), Co uptake is much slower during the first 5 min and subsequently higher than at the reaction with the low ionic strength solution. This behavior is consistent with Co adsorption on specific surface sites located on the edges of the mineral.

To define the effect of Co retention on hectorite clay alteration through Mg release, Schlegel et al. (1999) compared Mg to Si release rates in solutions before and after sorption of Co ions from the solution with high ionic strength. A congruent dissolution regime was observed before Co addition. Distinct trends of Mg release were observed after Co addition (Fig. 5.8). Immediately after Co sorption, an excess release of Mg occurred at both high and low ionic strength. At high ionic strength, Mg release nearly equaled the amount of Co sorbed on the clay surface.

Schlegel et al. (1999) considered that part of the excess release of Mg upon Co addition can be correlated to short-term adsorption, which is the first step of the release mechanism. The replacement of Mg, exposed on edges, by adsorbed Co could account for the observed near-equimolarity between Co sorption and Mg release. The second step involves the long-term alteration of smectite. Apparently, the rate of Si release decreased markedly after Co sorption, expressing inhibition of dissolution. This decrease in clay alteration may be explained by the direct consequence of the incorporation of large amounts of Co at layer edges of the clay mineral. Co-clays are more stable than Mg-clays, because adsorbed Co limits the extent of layer edges accessible to dissolution. The results of Schlegel et al. (1999) provide clear proof of irreversible changes to a clay mineral (e.g., smectite-hectorite) matrix following contamination by cobalt.

*Lead*, a heavy metal used extensively in industrial processes, may reach the land surface either directly in high concentrations, as a solute in industrial effluents, or in low concentrations in municipal wastewater. Using batch equilibrium studies, Strawn and Sparks (1999) found that Pb could be adsorbed on a clay surface (montmorillonite) via two mechanisms, depending on the ionic strength.

The effects of ionic strength and pH on the adsorption of Pb on montmorillonite are shown in Fig. 5.9. At low ionic strength, Pb adsorption is pH independent and is consistent with an outer-sphere complexation mechanism, where the majority of Pb is

**Fig. 5.8** Kinetics of Mg and
Si release before and after Co
uptake at high ionic strength.
Hectorite 1.95 g L$^{-1}$, pH 6.5.
Dissolution trends for Mg
(*square*) and Si (*diamond*)
before and after Co addition
to the suspension (after
Schlegel et al. 1999).
Reprinted from Schlegel ML,
Charlet L, Manceau A,
Sorption of metal ions on clay
minerals: II. Mechanism of
Co sorption on hectorite at
high and low ionic strength
and impact on the sorbent
stability. J Colloid Interface
Sci 220:392–445, Copyright
(1999), with permission from
Elsevier
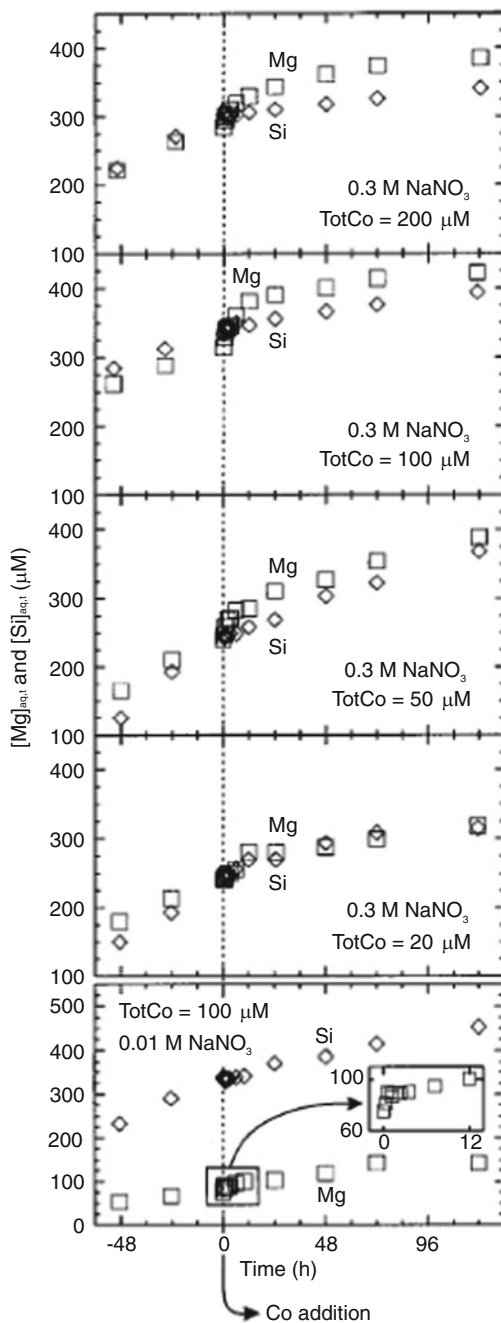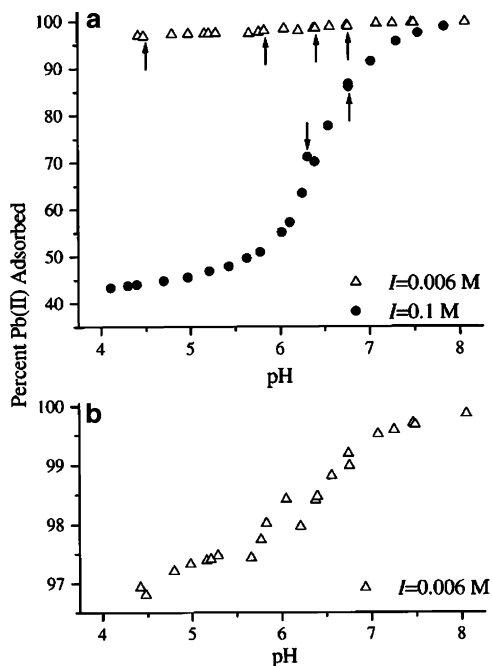
**Fig. 5.9** Lead adsorption on montmorillonite as function of pH. (**a**) *Arrows* indicate the equilibrium conditions of the montmorillonite samples used for the EXAFS analysis. (**b**) Range of the *y*-axis is decreased to illustrate the pH-dependent adsorption behavior of Pb-montmorillonite samples equilibrated at an ionic strength of $I = 0.006$ M (after Strawn and Sparks 1999). Reprinted from Strawn DG, Sparks DL, The use of XAFS to distinguish between inner- and outer-sphere lead adsorption complexes on montmorillonite J Colloid Interface Sci 216:257–269, Copyright (1999), with permission from Elsevier

adsorbed on planar sites. At high ionic strength, adsorption is pH dependent, suggesting inner-sphere complexation as the adsorption mechanism, with the functional groups existing on montmorillonite edges. However, based on X-ray adsorption fine structure spectroscopy (EXAFS) and X-ray adsorption near-edge structures (XANES), Strawn and Sparks (1999) found that at a specific pH, the lead adsorbed on montmorillonite may form both inner- and outer-sphere complexes.

Adsorbed lead may be retained irreversibly on clay mineral surfaces, causing changes in the matrix of the soil and subsurface clay fraction (e.g., Brigatti et al. 1995; Auboiroux et al. 1996). Several examples serve to support this statement. In a study to evaluate potential Pb mobility in groundwater in calcareous urban soils of Ancona (Italy), measurements of Pb sorption–desorption isotherms for 21 urban soils were performed (Bussinelli et al. 2009). It was found that high pH values in soil cause a completely irreversible adsorption of Pb. The approach of Vega et al. (2009), based on a hysteresis index (HI), may quantify the sorption irreversibility of heavy metals, in general, and the irreversibility of Pb retention in the soil–subsurface system, in particular. Based on the statistics of hysteresis of heavy metals (including Pb) in

a large number of soils, Vega et al. (2009) developed the conception of hysteresis index, defined as the ratio between retention ($K_r$) and sorption ($K_s$) where HI $= K_r/K_s$ is measured in μmol/g soil. Using the HI, Vega et al. (2009) showed that the sorption of heavy metals is completely irreversible in more basic soils with large CEC, caused by a high clay mineral content.

The above studies, performed on a very large number of samples, point to the irreversibility of Pb retention on earth materials. The findings of Vega et al. (2009) contradict previous experimental results of Pb desorption from aluminum oxide reported by Strawn et al. (1998), who found that 98% of adsorbed Pb was released. Experiments reported by Jozja et al. (2006) on Pb-induced irreversible changes in two smectite clays – a Wyoming Na-montmorillonite transformed into Mg-montmorillonite, and a Prrenjas Mg-bentonite – help to clarify this contradiction. In both clays, when Pb is sorbed by exchanging the clay cations, a good agreement between sorbed Pb and the sum of released cations was found (Fig. 5.10). The exchange of clay cations by Pb affects the pH of the surrounding water solution. As a function of Pb initial concentration, the pH of the water solution may range from 4.6 to 7.3.

TEM observations show that Pb-exchanged samples of natural Prrenjas Mg-bentonite display microaggregates or microstructural units consisting largely of an association of small particles packed together without interparticle pore space (Fig. 5.11c, d). Pb-exchanged samples of natural Wyoming Mg-montmorillonite, however, illustrate a decrease in particle dimensions without modifying the typical structure of smectite (Fig. 5.11a, b). XRD analysis of the two lead-contaminated clays shows that Pb exchange results in a shift of the peak to higher angles. For both materials, the $d_{001}$ values decrease when the concentration of Pb is higher than 1 mmol L$^{-1}$. This effect is greater in Pb-Wyoming clay than in Pb-Prrenjas clay.

X-ray photoelectron spectroscopy (XPS) analysis shows the variation of Pb/Si atomic ratio for the two studied Pb-contaminated clays. Figure 5.12 shows the variation in Pb/Si atomic ratio as a function of Pb concentration (in mmol L$^{-1}$) in solution. Prrenjas bentonite exhibits a lower binding energy than Wyoming montmorillonite, a property due to its lower $d_{001}$ spacing.
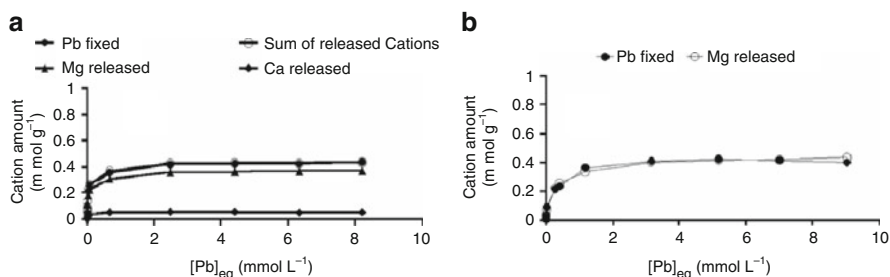


**Fig. 5.10** Amounts of sorbed Pb and released cations as a function of Pb concentration in equilibrium solution (**a**) Prrenjas bentonite; (**b**) Wyoming Mg-montmorillonite (after Jozja et al. 2006). Reprinted with permission: www.schweizerbart.de
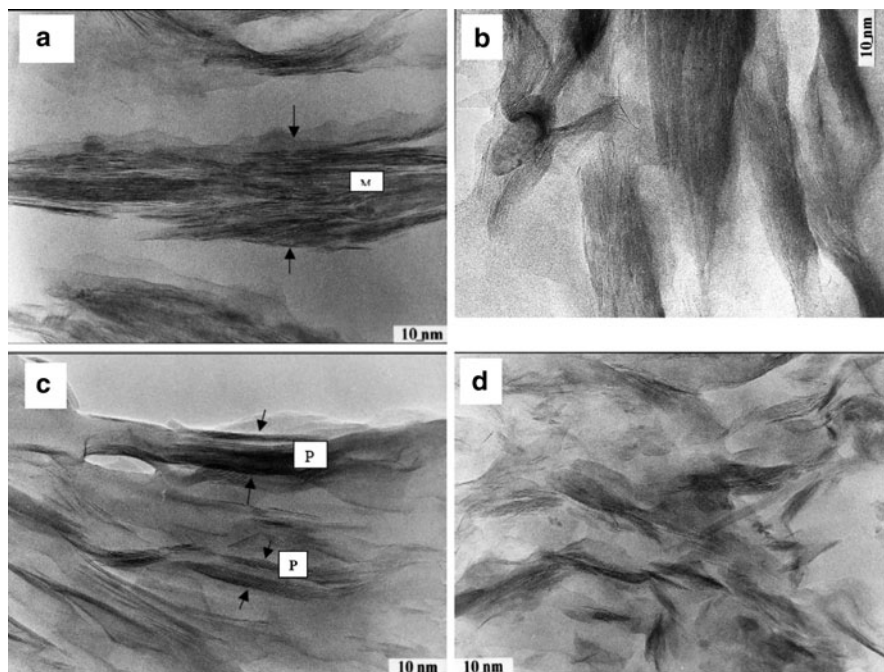
**Fig. 5.11** TEM image of Prrenjas bentonite and Wyoming montmorillonite at natural and Pb (NO$_3$)$_2$-treated conditions. (**a**) natural bentonite showing a microaggregate (M) between two *arrows*; (**b**) bentonite treated with 0.01 M Pb(NO3)2 solution with numerous small particles; (**c**) natural Mg-montmorillonite showing two particles (P); (**d**) Mg-montmorillonite treated with 0.01 M Pb(NO$_3$)$_2$ solution (modified after Jozja et al. 2006). Reprinted with permission: www.schweizerbart.de

*Zinc* is chosen here to describe the retention of heavy metals on hydroxy-interlayered mineral (HIM) complexes, with implications for irreversible pollution of the soil–subsurface system. HIM complexes are phyllosilicates containing hydroxy polymers in their interlayers. Specifically, the retention of Zn on the surface of hydroxyaluminum (HyA) and hydroxyaluminum-smectite (HAS) complexes is considered. Based on EXAFS analysis, Jacquat et al. (2009) concluded that in Zn–HAS, the heavy metal is octahedrally coordinated to oxygen at 2.06–2.08 Å, and surrounded by Al atoms at 3.03–3.06 Å in the second shell. With increasing molar Zn/HyA ratio, the coordination number of the second shell Al decreases from 6.6 to 2.1. These results were interpreted as a progressive shift from Zn trapping in vacancies of the mineral Al polymers to Zn adsorption on incomplete Al polymers, and finally uptake by cation exchange in the polymer-free interlayer space of HAS with increasing Zn loading.

The irreversible adsorption of Zn on silicate complexes causes a significant reduction in permanent negative charge, a substantial increase in pH-dependent negative charge, a drastic reduction of internal surface, and a slight increase in external surface area (Barnhishel and Bertsch 1989). A comparison between Zn adsorption on montmorillonite (Mt) and Zn adsorption occurring on HyA-Mt and
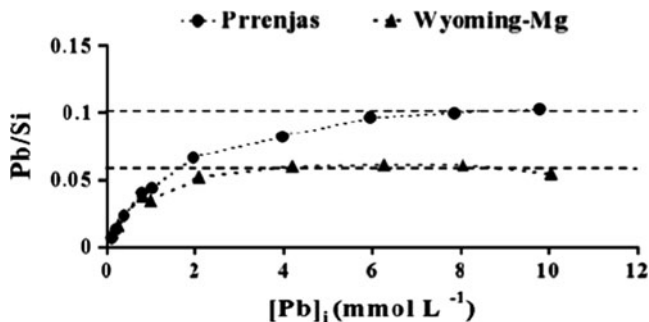
**Fig. 5.12** Variation of Pb/Si atomic ratio, determined by XPS, as function of lead concentration in the initial solution for Wyoming Mg-montmorillonite and Prrenjas bentonite (after Jozja et al. 2006). Reprinted with permission: www.schweizerbart.de
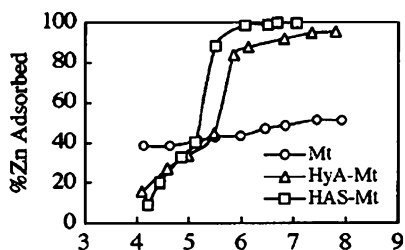


**Fig. 5.13** Fractional adsorption of zinc as a function of pH, for *HAS* hydroxyaluminosilicate, *HyA* hydroxyaluminum, *Mt* montmorillonite (after Saha et al. 2001). Copyright 2001, Soil Science Society of America. Reprinted with permission

HAS-Mt complexes (Fig. 5.13), as reported by Saha et al. (2001), showed an abruptly altered behavior with respect to adsorption of Zn on the treated clay. Adsorption of Zn on the clay complexes showed a stronger pH-dependent effect in comparison to that on Mt. From the partitioning of the adsorbed metal into strongly and weakly held fractions, as defined from sequential desorption of contaminant, Saha et al. (2001) concluded that specific adsorption of Zn may occur on the interlayered HyA-Mt and HAS-Mt. Figure 5.14 shows the total strongly and weakly adsorbed Zn on montmorillonite and hydroxy-interlayered clay, which supports the above consideration. These results suggest that retention of strongly adsorbed Zn on hydroxy-interlayered clay is potentially irreversible.

Zinc incorporation into the hydroxy-Al interlayers of clay soils by specific adsorption may have a substantial impact on irreversible sequestration of zinc in the soil solid phase. The abundance of Zn contaminant, in a series of HIM-containing soils with various physical and chemical properties, and determination of Zn reactivity were described by Jacquat et al. (2009). For this purpose, they used EXAFS analysis and batch and sequential extraction by determining Zn fate in eight top soils from Switzerland formed on different parent materials already contaminated by Zn due to their location close to the foundation of galvanized power line towers. Physicochemical properties and Zn contents of the studied soils are shown in Table 5.2.
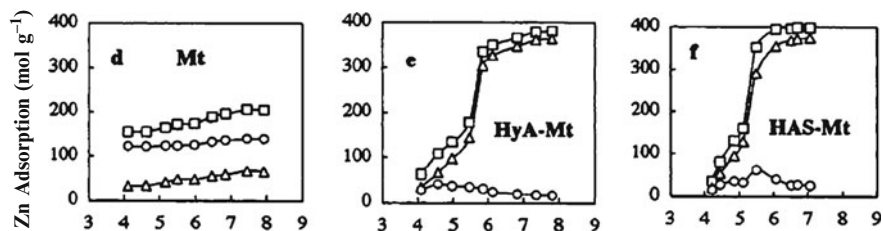
**Fig. 5.14** The amounts of total, adsorbed zinc on the clays as a function of pH for *HAS* hydroxyaluminosilicate, *HyA* hydroxyaluminum, *Mt* montmorillonite (modified after Saha et al. 2001). Copyright 2001, Soil Science Society of America. Reprinted with permission

**Table 5.2** Physicochemical properties and Zn contents of soil samples (after Jacquat et al. 2009). Reprinted from Rytwo G, Tropp D, Serban C, Adsorption of diquat, paraquat and methyl green on sepiolite: experimental results and model calculations. Applied Clay Sci 20:273–282, Copyright (2002), with permission from Elsevier

| Soil | Geology | pH (CaCl$_2$) | TOC (g/kg) | TIC (g/kg) | Texture (g/kg) Clay | Silt | Sand | ECEC[a] | Total Zn (mg/kg) | Exch. Zn[b] (mg/kg (%)) |
|------|---------|------|-----|-----|------|-----|------|------|------|------|
| GER | Alluvium | 4.1 | 27 | – | 48 | 348 | 604 | 40 | 403 | 104 (26) |
| MOM | Paragneiss | 4.6 | 37 | – | 77 | 302 | 621 | 25 | 1039 | 286 (28) |
| SAR | Schist | 4.6 | 52 | – | 105 | 700 | 195 | 78 | 251 | 35 (14) |
| CHI1 | Orthogneiss | 4.9 | 14 | – | 42 | 149 | 809 | 4 | 971 | 118 (12) |
| BUN | Conglomerate | 535 | 44 | – | 215 | 455 | 330 | 149 | 852 | 139 (16) |
| GRU | Glacial till | 6.0 | 36 | 0.3 | 253 | 363 | 384 | 146 | 852 | 99 (12) |
| BIB2 | Conglomerate | 6.1 | 36 | 1.1 | 324 | 344 | 32 | 232 | 861 | 21 (2) |
| HAU | Limestone | 6.9 | 42 | 0.2 | 227 | 320 | 453 | 102 | 276 | <1 (<0.3) |

[a]Effective cation exchange capacity
[b]Exchangeable Zn in 0.1 M BaCl$_2$ (SSR 30 mL/g; in parentheses, percentage of total Zn)

Overall, EXAFS spectra of soils analyzed by linear combination fitting (LCF) indicate that Zn-HIM, Zn-containing phyllosilicates, and adsorbed Zn are the major adsorbed Zn species in the studied soils. All of the soils contained hydroxy-Al interlayered vermiculite clay. Analysis of EXAFS spectra by LCF generally indicated that Zn in the soils was to a substantial extent sequestrated into Zn-HIM; a fraction of total Zn was contained in HIM with high Zn loading. Uptake of Zn into HIM tends to result in a relatively similar local Zn coordination in HIM in all soils. For most soils, LCF results also indicate the presence of Zn in phyllosilicates with intermediate to high Zn/Mg ratio. Jacquat et al. (2009) noted that Zn-HIM was identified in a range of soils from acidic to near-neutral pH, indicating high stability of Zn-HIM even in environments where other Zn phases could form. The limited adsorption capacity of HIM does not allow a continuous input of high levels of Zn into soils.

Based on a seven-step sequential procedure for contaminant extraction developed by Zeien and Brummer (1989), Jacquat et al. (2009) also examined irreversible adsorption of Zn on soils. According to their hypothetical interpretation, each extraction step reveals the bonding of Zn on various soil constituents as follows: the first

extraction step (F1) may extract the readily soluble and exchangeable Zn; the second step (F2) extracts Zn bound on $CaCO_3$; the third step (F3) extracts Zn bound on Mn oxides; the fourth step (F4) extracts Zn bound to organic substances; the fifth step (F5) extracts Zn bound to amorphous and poorly crystalline Fe oxides; the sixth step (F6) extracts Zn bound to crystalline Fe oxides; and the seventh step (F7) comprises citrate-extractable and citrate-nonextractable residual Zn fractions. Details of the composition of extraction solutions are given in Fig. 5.15.

Sequential extraction results of Jacquat et al. (2009) show a systematic decrease in exchangeable Zn with increase in soil pH (Fig. 5.15). Apart from the soil pH, 49–66% of the total Zn remained in fractions F6 and F7, indicating that most Zn was present in a stable form. The residual material after step F6 was submitted to an additional extraction with Na-citrate (F7) to dissolve the hydroxy-Al interlayers of phyllosilicate minerals. Despite this additional extraction, where 40–80% of the residual Zn after the extraction step F6 was mobilized, a substantial amount of Zn still remained sequestrated in the matrix of the studied soil. The retention of Zn adsorbed on minerals



**Fig. 5.15** Sequential extraction of contaminated soil materials and of quartz powder spiked with Zn-HIS-6.9-pH5, Zn-gibbsite-4.0, low Zn-birnessite, and lithiophorite (modified after Jacquat et al. 2009). Reprinted from Jacquat O, Voegelin A, Kretzschmar R, Local coordination of Zn in hydroxy-interlayered minerals and implications for Zn retention in soils. Geochim Cosmochim Acta 73:348–363, Copyright (2009), with permission from Elsevier

was also tested by Jacquat et al. (2009) on hydroxy-interlayered smectite (HIS), gibbsite, and birnessite, and the sequential extraction procedure was the same used for soils. It may be observed (Fig. 5.15) that the amount of citrate-extractable and nonextractable Zn decreases in the order HIS < gibbsite. Zinc bound on birnessite is released completely by the first four steps of the sequential extraction.

Given that in a natural environment we are not dealing with sequential extraction of Zn but rather with its release in soil and subsurface water, within a pH range of 5–8, we can state firmly that under natural conditions, there is irreversible retention of a fraction of initially Zn adsorbed on soil and soil minerals.

### 5.2.3   Radionuclides

Radionuclide ions generally reach soil–sediment clay surfaces as a mixture of radio-active compounds with various hydration energies. The adsorption of radionuclides on layered clay surfaces influences the clay interlayer geometry and, as a consequence, ion interaction with the clay surface. Cations with low hydration energy induce interlayer collapse, because of their dehydration and thus their fixation into the clay matrix. On the contrary, cations with high hydration energy favor expansion of the clay interlayer and facilitate the release of adsorbed cations from the clay matrix.

$^{137}Cesium$ is one of the major radioactive contaminants in waste emanating from the nuclear power industry. Because of its high solubility in water, it may be transported from the land surface to aquifers if it does not encounter clay fractions in the soil–surface system, where it can be adsorbed. Cesium, with a low hydration energy, is an example of just one of the radionuclides that may be retained irreversibly, on a human time scale. Cesium is adsorbed on clay minerals by balancing the negative charge of the alumino-silicate structure. In the case of a radioactive spill, the clay charge, which under natural conditions is compensated in its outer and inner multilayered mineral surfaces by counter ions such as $Na^+$, $K^+$, $Ca^{2+}$, and $Mg^{2+}$, can be exchanged by cesium. Broken bonds at the edges of the clay crystals, and hydroxyl groups on the surfaces of oxide minerals, may also serve as adsorption sites.

Cesium adsorption is controlled by the type of clay and by the solution ionic strength, as well as pH, temperature, competitive ion concentration, and the time of contact between the clay mineral and the Cs-contaminated solution. These properties enable Cs to harm its hydration shell upon entering the clay interlayers, causing interlayer dehydration and collapse (Cornell 1993, and references therein). The retention and release of Cs by sediments and phyllosilicates have been investigated intensely since anthropogenic cesium became a concern as an environmental contaminant (e.g., Francis and Brinkley 1976; Evans et al. 1983). These early studies observed that adsorption–desorption of Cs to and from clay or soil surfaces proceeds in two steps: a rapid initial reaction followed by a slower continued reaction. This behavior was attributed to interaction with three different chemical surface sites: (a) nonselective exchange sites on phyllosilicates, (b) selective frayed edge sited (FES)

formed by removal of K, and (c) interlayer sites enriched by $^{137}$Cs. Nonselective exchange sites weakly retained $^{137}$Cs, which is rapidly desorbed.

The fact that the radius of the dehydrated Cs ion is similar to that of the ditrigonal siloxane cavity of the layer silicates favors adsorption of Cs to siloxane sites and leads to inner-sphere complexation. Isomorphic substitution of $Al^{3+}$ for $Si^{4+}$ in the tetrahedral sheet comprising the siloxane site enhances the stability of Cs–siloxane surface complex by promoting dehydration of Cs cation (Kim et al. 1996; Chorover et al. 1999). This may explain the fact that in the most desorption studies, $^{137}$Cs was not completely recovered and consequently its adsorption on layer silicates may be considered irreversible (McKinley et al. 2001).

Cesium adsorption on clay minerals as a function of surface coverage was determined by Bostick et al. (2002), using extended EXAFS. They examined Cs adsorption on three layered clay minerals: vermiculite, illite, and montmorillonite. Cesium adsorption capacity was largest for montmorillonite ($783 \pm 0.6$ mmol kg$^{-1}$) and significantly lower for vermiculite ($271 \pm 6.8$ mmol kg$^{-1}$) and illite ($150 \pm 2.9$ mmol kg$^{-1}$). Bostick et al. (2002) considered that Cs exhibits a variable coordination environment with a Cs–O distance between 3.2 and 4.3 Å, and with a disorder that prevents the resolution of all oxygen shells. Based on Cs loading and exchangeability, Bostick et al. (2002) identified both inner-sphere and outer-sphere adsorption complexes. The shorter Cs–O bond distance is associated with outer-sphere complexes typical of hydrated ions. In the inner-sphere complexes, partially or fully dehydrated Cs coordinates directly to siloxane groups of the clay minerals by forming longer Cs–O bonds. Bostick et al. (2002) suggested a model structure for Cs sorbed on clay showing the formation of an inner-sphere complex for the Cs atom within the trigonal layer of the phyllosilicate interlayer (Fig. 5.16).

The results of Bostick et al. (2002) showed that Cs complex adsorption that occurs in the mineral inner sphere is more strongly adsorbed than in the outer-sphere Cs complex. It may be concluded that Cs bound to external planar surface sites can generally be exchanged by other cations, whereas Cs bound in collapsed, dehydrated interlayer sites or at frayed edges of collapsed interlayers is strongly sorbed and difficult to remove via ion exchange, thus forming an "irreversible" Cs fraction retained within the clay matrix.

The higher sorption capacity of montmorillonite reflects the increased availability of interlayer sorption sites. Inner-sphere complexes may also form in the interlayer adjacent to locations where isomorphous substitution occurs in the tetrahedral sheet. This induces Cs coordination to the ditrigonal cavity within the tetrahedral sheet of vermiculite and illite, causing partial collapse of the interlayer. In such an environment, the interlayer Cs is less exchangeable than Cs adsorbed to planar sites (Comans et al. 1991).

Irreversible retention of Cs adsorbed on clay mineral surfaces may be observed from desorption studies. Initial studies of Cs desorption from clays usually measured Cs exchange with various competing cations, but suspensions in a Cs-free aqueous phase were also examined. In both types of experiments, Cs was held strongly on the frayed edge sites of the mineral surfaces. This strong retention led to the hypothesis that Cs may be trapped irreversibly at these sites (Sawhney 1964;
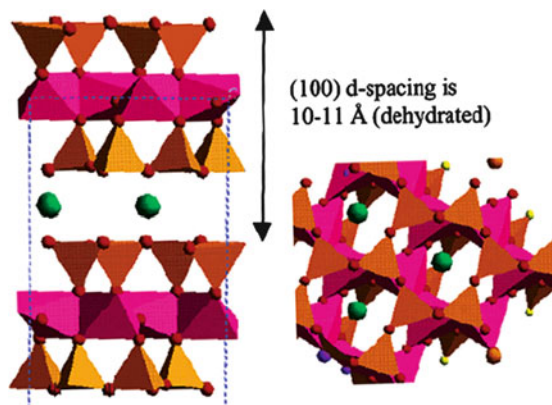
**Fig. 5.16** Model structure for Cs-sorbed clays, showing the formation of an inner-sphere complex for the Cs atoms (*spheres*) within the trigonal layer of the phyllosilicate interlayer. The $d_{001}$ spacing is about 12–14 Å for partially hydrated, Cs-exchanged, 2:1 clay minerals; the $d_{001}$ spacing decreases to 10 Å when fully dehydrated (after Bostick et al. 2002). Reprinted with permission from Bostick BC, Vairavamurthy MA, Karthikeyan KG, Chorover J (2002) Cesium adsorption on clay minerals: an EXAFS spectroscopic investigation. Environ Sci Technol 36:2670–2676. Copyright 2002 American Chemical Society

Coleman and Le Roux 1965). Later studies indicated the effect of clay-saturating cations on reversibility of adsorbed Cs. Based on an experiment on Cs desorption from illite, by replacing the starting solution with a fresh Cs-free aqueous phase, Comans et al. (1991) found that Cs sorption was reversible for potassium-illite and partially irreversible for calcium-illite. Comans et al. (1991) suggested that in the latter case, a proportion of high-affinity sites was located in the interior of the frayed edges, causing partial irreversible adsorption of Cs on illite.

Irreversibility of Cs adsorption on clays increases with time due to the aging process, because Cs fixation may be affected by environmental factors. As mentioned above, the interaction of Cs with the solid phase comprises two steps. The first step after Cs release is characterized by a fast reversible sorption. The second step involves slow Cs retention when the fraction of Cs sorbed by the solid phase increases with time, and the retention process may be affected by environmental factors such as temperature and drying–wetting cycles. This second step is known as "aging," and is attributed to solid-state migration into specific sites in the wedge area, closer to the collapsed core where Cs is less exchangeable and retained irreversibly (Hird et al. 1996).

Cs aging is a significant process due to interlayer collapse by dehydration and strong adsorption of Cs complexes. For the discussion here, we consider an investigation on two soils with low organic matter content, for which Cs retention is due mainly to the soil clay content. Roig et al. (2007) studied the factors accelerating Cs aging in soils caused by enhancement of Cs trapping from clay interlayer collapse, in laboratory experiments. The selected soils were an Entisol (Belville, France) with a CEC of 6.5 cmol$_c$ kg$^{-1}$ and an Alfisol (Barcelona, Spain) with a CEC of 16.4 cmol$_c$ kg$^{-1}$.

Figure 5.17a shows Cs extraction from these soils contaminated with soluble ^{137}Cs and submitted to aging over 1 year at a constant hydration and at temperatures ranging between −20 and +70°C. It may be observed that at the beginning of the experiment, the extractable Cs from the two soils was in the range of 50% from the amount applied (Entisol 44.3%; Alfisol 53.3%). An increase in temperature led to a significant aging process of the Entisol; the effect is less pronounced in the case of Alfisol. It may be seen that application of drying–wetting cycles (Fig. 5.17b) accelerates the aging process of both Entisol and Alfisol with respect to the effect of time and temperature only. The effect of drying–wetting on Cs aging may be explained by dehydration of clay interlayers and subsequent interlayer collapse, causing Cs trapping and a decrease in desorption. The experiments of Roig et al. (2007) clearly show that time and temperature may induce irreversible retention of Cs in the clay fractions of the soils, an effect that increases under a regime of drying–wetting cycles.

*Radium* ([226]Ra) contaminants may be found in the soil environment in areas adjacent to uranium processing facilities. Zhang et al. (2001) used $Ba^{2+}$ as a [226]Ra
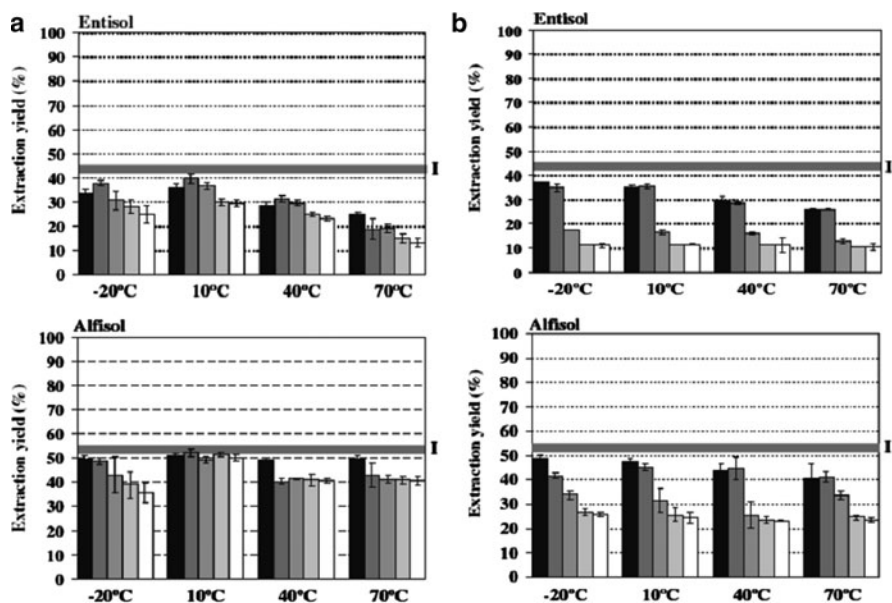


**Fig. 5.17** Radiocesium aging in Entisol and Alfisol soils. I denotes initial extraction yields. (**a**) Effect of temperature (−20, 10, 40, and 70°C) and time (black: 5 days; dark gray: 1 month; medium gray: 4 months; light gray: 8 months; white: 12 months) on Cs extraction yields in examined soils. (**b**) Cs extraction yields obtained from the same soils contaminated with ^{137}Cs and kept under similar temperature and time conditions as those described above, but submitted to additional drying–wetting cycles (modified after Roig et al. 2007). Copyright 2007, American Society of Agronomy, Crop Science Society of America, and Soil Science Society of America. Reprinted with permission

analog to simulate radium interaction with montmorillonite, obtaining mechanistic insights into $^{226}$Ra behavior in soil matrices. Based on results obtained using EXAFS, Zhang et al. (2001) found that a small fraction of $Ba^{2+}$ – as a $^{226}$Ra proxy – is adsorbed on the montmorillonite edges, forming an inner-sphere surface complex through sharing oxygen atoms from deprotonated –OH groups in an Al octahedral layer. Results from bulk experiments and spectroscopic analysis suggested the coexistence of outer- and inner-sphere surface complexes for $Ba^{2+}$ sorbed on a Na-montmorillonite surface. The distances between Ba and O in the first shell, and Ba and Al in the second shell are 2.7–2.8 and 3.7–3.9 Å, respectively, consistent with the geometry of an inner-sphere complex at the edge site. The results of Zhang et al. (2001) for Ba-montmorillonite interactions are in accord with other metal-montmorillonite adsorption studies which show the formation of an inner-sphere complex associated with the predominant outer-sphere complex (e.g., Zachara and Smith 1994; Kim et al. 1996). The formation of the inner-sphere complex suggests the possibility of irreversible retention of $^{226}$Ra in the inner-sphere domain of the layered clay.

## *5.2.4   Polar Organic Contaminants*

Adsorption and release of polar organic contaminants, on and from clay surfaces, are controlled by clay exchangeable cations which affect the hydration status of the clay interlayers, the interlayer distance, the size of the sorptive domain, and the abilities of sorbate functional groups to interact with interlayer cations. As a consequence, the magnitude of polar organic contaminant adsorption is proportional to the fraction of clay interlayers saturated with a specific cation (Li et al. 2004).

Below, we have selected a few examples from two major groups of polar organic contaminants, pesticides and charged liquids (e.g., ionic liquids and surfactants), to illustrate the irreversible retention and induced modification of/on soil subsurface mineral phases by polar organic contaminants.

### 5.2.4.1   Pesticides

Pesticides comprise a large number of organic compounds that may reach the land surface following agricultural practices or industrial accidents. According to their specific molecular properties, pesticides partition between solid and aqueous phases of the soil–subsurface geosystem, and under the influence of environmental conditions, pesticides may be redistributed among the land surface, vadose zone, and groundwater. Irreversible adsorption of pesticides on the soil and subsurface mineral phase may be described by two interrelated processes: desorption hysteresis and binding. The behavior of polar pesticides is illustrated by the following examples.

*Diquat* (1,1′-ethylene-2,2′-dipyridylium dibromide) and *Paraquat* (1,1′-dimethyl-4,4′-bipyridinium dichloride) are cationic herbicides used broadly for

crop protection. They may contaminate the land surface and subsequently pollute the subsurface zone and groundwater after being leached by rain or irrigation water. Retention and release of these herbicides – charged organic molecules – on and from clay minerals have been the subject of many investigations during the second half of the last century.

The complete adsorption of diquat and paraquat by bentonite and kaolinite, as measured by the absence of detectable bipyridyl in solutions equilibrated with these minerals, was observed by Weber et al. (1965). The extent of adsorption reaches the limit of the mineral CEC (Knight and Tomlinson 1967). Weber and Weed (1968) confirmed that diquat and paraquat are adsorbed by montmorillonitic and kaolinitic clay minerals to approximately their CEC. After desorption caused by leaching with 1 MBaCl$_2$, about 20 and 95% of each of the herbicides was retained on kaolinite and montmorillonite, respectively. Knight and Denny (1970) explained the high retention of paraquat by montmorillonite through interlamellar absorption.

Rytwo et al. (2002) show FTIR spectra deformation after methylene blue and diquat adsorption on sepiolite clay (Fig. 5.18). It may be seen that pure sepiolite exhibits two clear peaks at 789 and 764 cm$^{-1}$. Adsorption of a monovalent organic cation, such as methylene blue at 1/3 of the CEC (MB 0.05), shows almost no influence on the peaks; but at higher loads, for example, at the full CEC (MB 0.15), a considerable deformation of the peaks is observed. Divalent organic cations, such as diquat, do not affect the O–H doublet at any adsorbed load. When both diquat and MB are co-adsorbed up to the CEC, the deformation appears but is attributed to the binding of the monovalent organic cation to the neutral sites.

Hysteresis in the sorption and desorption of diquat and paraquat may occur also when they are in competition with an additional ion for the adsorbing sites of the
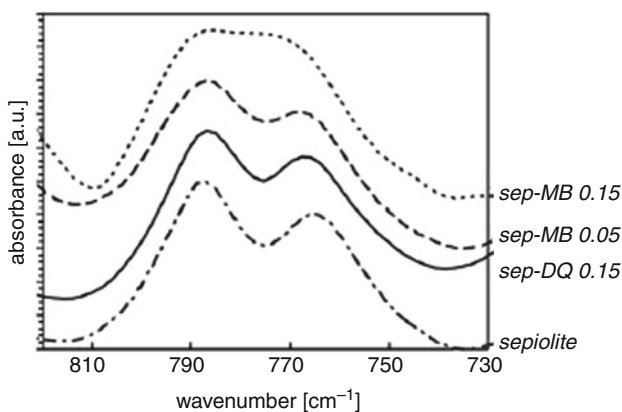


**Fig. 5.18** IR spectra of the O–H vibration in pure sepiolite, sepiolite with 0.05 and 0.15 mol$_c$ methylene blue/kg clay (sep-MB 0.05 and sep-MB 0.15), and sepiolite with 0.15 mol$_c$ diquat/kg clay (sep-DQ 0.15) (after Rytwo et al. 2002). Reprinted from Rytwo G, Tropp D, Serban C, Adsorption of diquat, paraquat and methyl green on sepiolite: experimental results and model calculations. Applied Clay Sci 20:273–282, Copyright (2002), with permission from Elsevier

clay fraction of soil. In vineyard soils, cationic herbicides may interact with inorganic cations such as copper, which is used as a fungicide, or from application of animal manure. Effects of aged copper on the adsorption–desorption of paraquat and diquat in polluted vineyard soils in Spain were studied by Pateiro-Moure et al. (2007). The two studied soils were acidic (pH 5.2–5.8) and characterized by a surface area of 66–78 m$^2$ g$^{-1}$; the total Cu contents of the two soils were 42 and 583 mg kg$^{-1}$. Both diquat and paraquat were adsorbed strongly by the soils (Fig. 5.19). However, the removal of Cu from soils by EDTA extraction led to a small increase in the paraquat and diquat concentrations. The increase in herbicide retention was equivalent to the replacement of 6.4 and 1.6% of the charges theoretically released by Cu$^{2+}$ from the two studied soils.

Desorption tests showed that both diquat and paraquat are retained irreversibly on soil even after six sequential extractions with an EDTA aqueous solution (Table 5.3). One soil exhibited less than 1% desorption of the two herbicides, while the second soil exhibited a somewhat higher percentage. Paraquat was desorbed in proportions from 1% in the first extraction step to 0.2% in the sixth step. Diquat desorption never exceeded 4% and tended to decrease as the desorption sequence progressed. The presence of paraquat and diquat in soil solution favors copper desorption (Table 5.4), showing that these polar herbicides in soil solution replace the copper.

*Glyphosate* (*N*-phosphonomethylglycine) – a broad-spectrum herbicide – is a small molecule comprising three polar functional groups (phosphonic acid, carboxylic acid, and secondary amines), which is sorbed strongly by soil minerals.
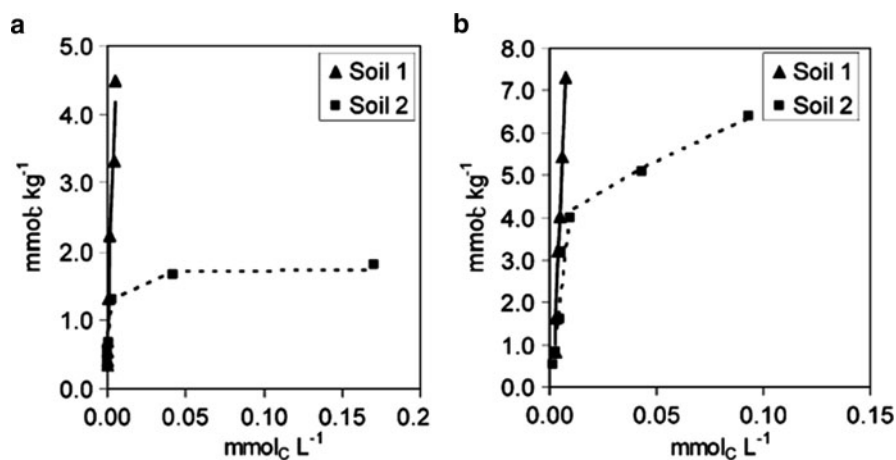


**Fig. 5.19** Adsorption isotherms of (**a**) paraquat and (**b**) diquat in two acidic vineyard soils (1 and 2) (modified after Pateiro-Moure et al. 2007). Reprinted with permission from Pateiro-Moure M, Pérez-Novo C, Arias-Estévez M, López-Periago E, Martínez-Carballo E, Simal-Gándara J (2007) Influence of copper on the adsorption and desorption of paraquat, diquat and difenzoquat in vineyard acid soils. J Agri Food Chem 55:6219–6226. Copyright 2007 American Chemical Society

**Table 5.3** Percent desorption of paraquat (PQ) and diquat (DQ) (modified after Pateiro-Moure et al. 2007)[a].Reprinted with permission from Pateiro-Moure M, Pérez-Novo C, Arias-Estévez M, López-Periago E, Martínez-Carballo E, Simal-Gándara J (2007) Influence of copper on the adsorption and desorption of paraquat, diquat and difenzoquat in vineyard acid soils. J Agri Food Chem 55:6219–6226. Copyright 2007 American Chemical Society

| Soil sample | Desorption (%) | | | | | | |
|---|---|---|---|---|---|---|---|
| | | Step 1 | Step 2 | Step 3 | Step 4 | Step 5 | Step 6 |
| 1 | PQ | 1.0 | 0.4 | 0.3 | 0.2 | <0.08 | <0.08 |
| | DQ | 0.5 | 0.5 | 0.3 | 0.3 | 0.2 | <0.01 |
| EDTA-1 | PQ | <0.08 | <0.08 | <0.08 | <0.08 | <0.08 | <0.08 |
| | DQ | <0.01 | <0.01 | <0.01 | <0.01 | <0.01 | <0.01 |
| 2 | PQ | 1.5 | 0.9 | 0.7 | 0.7 | 0.5 | 0.2 |
| | DQ | 3.2 | 3.2 | 3.6 | 3.3 | 3.2 | 2.1 |
| EDTA-2 | PQ | 0.3 | 0.2 | 0.4 | 0.4 | 0.3 | 0.2 |
| | DQ | 1.9 | 1.5 | 0.5 | 1.4 | 1.1 | 0.5 |

[a]Standard deviations: lower than 3%

**Table 5.4** Influence of paraquat (PQ) and diquat (DQ) on copper desorption from vineyard soils, expressed by the metal concentration in equilibrium solution (modified after Pateiro-Moure et al. 2007). Reprinted with permission from Pateiro-Moure M, Pérez-Novo C, Arias-Estévez M, López-Periago E, Martínez-Carballo E, Simal-Gándara J (2007) Influence of copper on the adsorption and desorption of paraquat, diquat and difenzoquat in vineyard acid soils. J Agri Food Chem 55:6219–6226. Copyright 2007 American Chemical Society

| Soil | Equilibrium [Cu] (mM) | | | |
|---|---|---|---|---|
| | Initial [Cu] (mM) | Cu | Cu + PQ | Cu + DQ |
| 1 | 0.16 | 0.056 (35) | 0.091 (57) | 0.084 (53) |
| | 0.80 | 0.310 (39) | 0.425 (53) | 0.412 (52) |
| | 1.6 | 0.785 (49) | 0.932 (58) | 0.944 (59) |
| | 3.2 | 1.782 (57) | 1.755 (56) | 2.077 (66) |
| 2 | 0.16 | 0.006 (4) | 0.015 (9) | 0.014 (9) |
| | 0.80 | 0.122 (15) | 0.290 (36) | ND |
| | 1.6 | 0.441 (28) | 0.763 (48) | 0.783 (49) |
| | 3.2 | 1.759 (56) | ND | 1.668 (53) |

Glyphosate (GP) can only be sorbed onto variable-charge surfaces and not onto permanent negative sites of layer silicates, because it is has anionic properties in the relevant pH range (Borggaard and Gimsing 2008, and references therein). The most important soil and subsurface sorption sites for GP retention may be found on aluminum and iron oxides, defectively ordered aluminum silicates, and edges of layer silicates.

Table 5.5 provides a view of ensemble GP sorption values on various synthetic earth minerals, as a function of their surface area. It can be seen that silicate clay (saturated with $K^+$) has a limited capacity to sorb GP; the amount appears to depend on the cationic composition of the solution cation. Sorption of GP on montmorillonite, illite, and kaolinite decreases according to the following order of cation

**Table 5.5** Glyphosate sorption at pH 7 by synthetic aluminum and iron oxides, and pure $K^+$-saturated layer silicates. Reprinted from Borggaard OK, Gimsing AL (2008) Fate of glyphosate in soil and the possibility of leaching to ground and surface waters: a review. Pest Manage Sci 64:441–456. Copyright 2008 with permission of John Wiley and Sons

| Earth minerals | Specific surface area ($m^2\ g^{-1}$) | Glyphosate sorption ($mmol\ kg^{-1}$) |
|---|---|---|
| Aluminum and iron oxides | | |
| Gibbsite | 45 | 72 |
| Ferrihydrite | 343 | 635 |
| Goethite | 85 | 125 |
| Hematite | 33 | 86 |
| Clay silicates | | |
| $K^+$-Kaolinite 1 | 12 | 3.9 |
| $K^+$-Kaolinite 2 | 22 | 6.9 |
| $K^+$-Illite | 43 | 5.2 |
| $K^+$-Montmorillonite | 32 | 6.5 |

presence: $Al^{3+} > Fe^{3+} > Cu^{2+} > Mg^{2+} > Zn^{2+} > Mn^{2+} > Ca^{2+} > Na^+$ (Glass 1987). The increased sorption of divalent and trivalent cations in multilayered clays may be explained by the formation of complexes between interlayer cations and glyphosate. In comparison, Table 5.5 also shows that the aluminum and iron oxides sorb considerably more GP. The discrepancy between the oxides and silicates can be attributed to the number and distribution of sorption sites. Clay silicates offer adsorption sites only on octahedral layers exposed to mineral edges.

Studies of GP–soil interaction showed that the clay type and content, and clay CEC control the herbicide adsorption (Glass 1987; Dion et al. 2001). Additional studies led to the conclusion that herbicide complexation by the exchangeable cation through water bridges or by cation exchange is the dominant adsorption pathway of GP adsorption on montmorillonite (e.g., Shoval and Yariv 1979; McConnell and Hossner 1985, 1989). The pH dependence of GP adsorption on montmorillonite, demonstrated by Damonte et al. (2007), is shown in Fig. 5.20a. Damonte et al. (2007) suggested that the first part of the adsorption isotherm should be ascribed to adsorption on the external surface. The low GP surface coverage increasing with ionic strength (Fig. 5.20b) is indicative of inner-sphere surface complex formation. The second part of the adsorption isotherm can be assigned to external surface and interlayer adsorption, which is reached at GP concentrations higher than $10^{-3}$ M. Adsorption increases more strongly with the ionic strength. In this case, the electrical double layer is compressed and GP reaction with the edge site of the mineral becomes more favorable. GP adsorption increases with decreasing pH. At very low pH ($<3$), both montmorillonite and GP become positively charged and electrostatic repulsion decreases the amount adsorbed.

Additional immobilization of GP in soils is due to the formation of surface complexes with metal ions (Damonte et al. 2007, and references therein). The stability of such complexes reveals the tridentate character of glyphosate. A 1:1 stable GP chelate complex with copper ions may be formed, involving carboxylate, amino, and phosphonate groups. However, the coordination of Fe(III) with
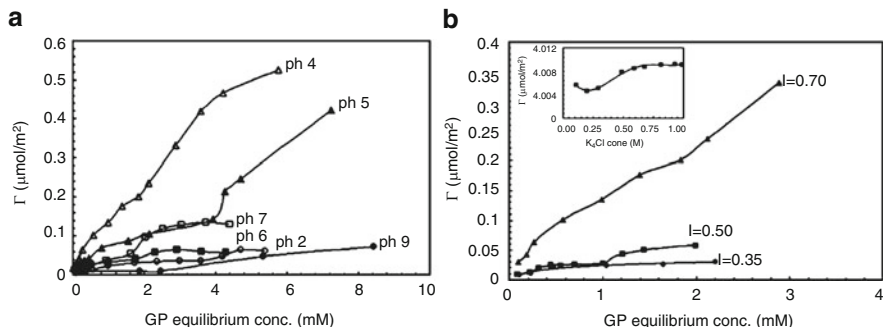
**Fig. 5.20** Influence of pH and ionic strength on montmorillonite particles in the presence or absence of glyphosate (GP). (**a**) GP absorption isotherms at various pH values; (**b**) GP isotherms at various ionic strength solutions (modified after Damonte et al. 2007). Reprinted from Damonte M, Torres Sánchez RM, dos Santos Afonso M, Some aspects of the glyphosate adsorption on montmorillonite and its calcined form. Applied Clay Sci 36:86–94, Copyright (2007), with permission from Elsevier

GP, for example, differs between aqueous and solid states. In the soil–subsurface system, Fe(III) forms a 1:1 Fe(III)/PG complex in aqueous phase; in the solid phase, the same Fe(III) is chelated by the phosphonate and carboxylic acid, whereas the amino group remains protonated. Ligand adsorption occurs on edge surface hydroxyl groups which are exchanged by ligands. Lower pH favors adsorption of anions coupled with release of OH ions and formation of bidentate surface chelate, as in the case of GP adsorption on goethite (Barja and dos Santos Afonso 2005). In this particular case, monodentate and bidentate phosphonate complexes are predominant, while carboxylate and amino groups are not coordinated to the surface.

The presence of a strongly complexing metal such as Cu(II), either in soil solution or adsorbed on soil minerals, leads to a decrease in glyphosate adsorption as result of the formation of Cu–GP complexes. Such a decrease was noted by Morillo et al. (1997) in the case of GP–montmorillonite interaction in the presence of Cu, when the formed GP–Cu complexes have a lower tendency to be adsorbed on the mineral than the free GP.

Overall, it may be concluded that GP is sorbed in the soil–subsurface system onto variable-charge mineral surfaces, mainly on aluminum and iron oxides, and on disordered aluminum silicate. Sorption increases with increasing specific sorbent surface area, and is related inversely to an increase in pH. GP is strongly bonded to singly coordinated Al–OH and Fe–OH surface sites, by Al–O–P and Fe–O–P bonds that form mononuclear, monodentate and/or binuclear, bidentate surface complexes.

The sorption of GP through phosphonate groups is similar to phosphate sorption and, as a consequence, there is a potential for competition between them for the surface sites. Gimsing and Borggaard (2002) showed that the degree of competition between glyphosate and phosphate depends on the type of adsorbing clay mineral. They found that the competition favors phosphate on goethite, and less so on
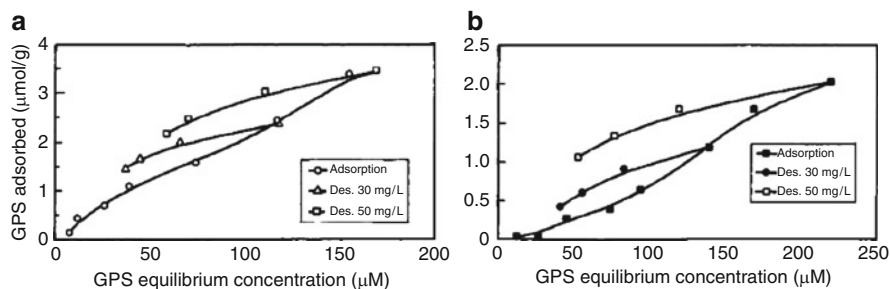
**Fig. 5.21** Adsorption–desorption isotherms of GP on montmorillonite, (**a**) in the absence and (**b**) in the presence of Cu (after Morillo et al. 1997). Reprinted with permission from Morillo E, Undabeytia T, Maqueda C (1997) Adsorption of glyphosate on the clay mineral montmorillonite: Effect of Cu(II) in solution and adsorbed on the mineral. Environ Sci Technol 31:3588–3592. Copyright 1997 American Chemical Society

gibbsite, and that on illite, montmorillonite, and kaolinite, the competition is almost equal. As a consequence, the addition of phosphate to GP-contaminated land may lead, under specific conditions, to a partial release of the contaminant.

The adsorption–release pattern, however, exhibits a hysteretic pathway. Hysteretic effects were observed during adsorption–desorption studies of glyphosate on soils and clay minerals, suggesting a potentially irreversible retention of GP in the soil–subsurface medium. As an example, we consider the study of Morillo et al. (1997) on GP retention and release on/from montmorillonite, in the presence and absence of Cu ions in the desorbing aqueous electrolyte solution. The desorption curves (Fig. 5.21a) showed that about 60% of GP initially adsorbed on montmorillonite was retained on the clay surface after three successive desorption procedures. In this case, some GP initially adsorbed on broken borders of montmorillonite is replaced by hydroxyl groups or by water during the desorption process. When Cu ions are present in the electrolyte equilibrium solution (containing Na ions), a reduction is observed in the amount of GP that is retained (Fig. 5.21b). Here, some Cu desorbs by cation exchange with Na ions from the electrolyte solution, favoring formation of GP–Cu complexes.

When dealing with irreversible retention of a chemical contaminant, we must consider also potential contaminant degradation in the soil–subsurface environment, as well as the fate of metabolites formed as a result of the degradation pathway. Soils in general favor degradation of GP, the degradation rate being different from one soil to another and affected by the ambient temperature. Glyphosate degradation in the soil–subsurface system is due to both microbiological (Rueppel et al. 1977) and abiotic (Barrett and McBride 2005) factors, and is relatively rapid. The degradation pathway of GP induced by microorganisms involves either the formation of sarcosine and glycine, or the formation of aminomethylphosphonic acid (AMPA). Of these metabolites, AMPA is the most persistent because it is strongly sorbed and resistant to further microbial degradation (Borggaard and Gimsing 2008). In a recent field study, Mamy et al. (2008) compared GP and its AMPA metabolite distribution with depth, during 200 days
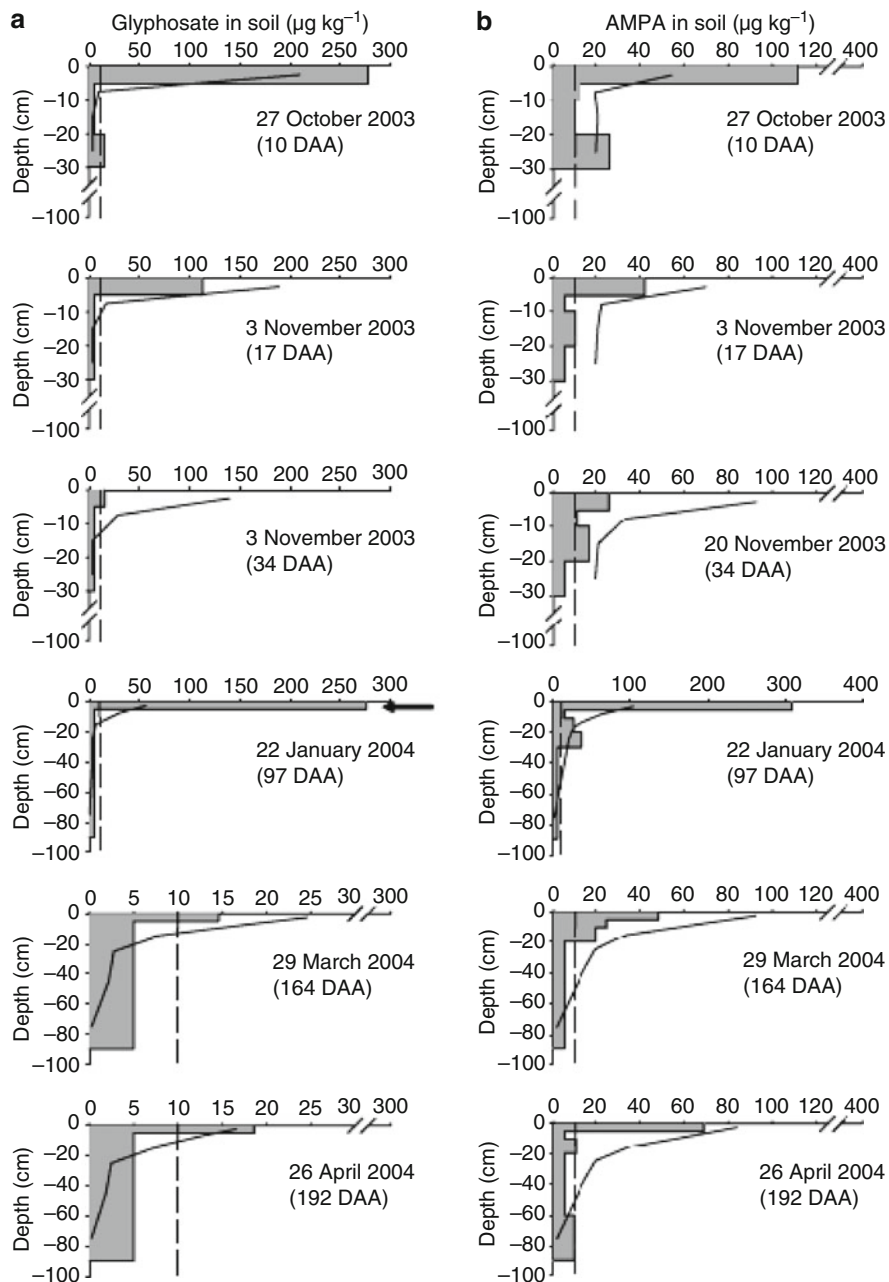
**Fig. 5.22** Observed (*bars*) and simulated (*line*) vertical distribution of (**a**) glyphosate and (**b**) its degradation product aminomethylphosphonic acid (AMPA) as a function of time in a field soil (Dijon, France) (modified after Mamy et al. 2008). Reprinted from Mamy L, Gabrielle B, Barriuso E (2008) Measurement and modelling of glyphosate fate compared with that of herbicides replaced as a result of the introduction of glyphosate-resistant oilseed rape. Pest Manag Sci 64:262–275. Copyright 2008 with permission of John Wiley and Sons

following contaminant application (Fig. 5.22). Due to its high adsorption and rapid degradation, applied GP was concentrated initially in the soil upper layer; over time, the GP concentration decreases due to degradation (Fig. 5.22a). The AMPA concentration in the upper layer also decreased with time as a result of its mobility and redistribution with depth (Fig. 5.22b). However, because of its persistence, the cumulative concentration of AMPA in the field soil on a 100-cm depth remained almost the same.

The study of Mamy et al. (2008) provides a case where the concentration of a contaminant retained in the soil upper layer decreases with time, because of its redistribution with depth, but exhibits an irreversible presence along a vertical cross-section within the unsaturated zone. Nonextractable $^{14}C$ from $^{14}C$-glyphosate was detected by Barriuso et al. (2008) at the onset of herbicide application on three French soils. In soils from Chalon and Dijon, the bound fraction decreased during incubation; in the loamy sand Toulouse soil, with a low pH, the bound fraction remained constant at a value of 7% from the initial amount applied (Fig. 5.23).

Barriuso et al. (2008) mentioned that their results are in accord with previous findings (e.g., Smith and Aubin 1993; von Wiren-Lehr et al. 1997), but did not find an explanation for the difference in GP behavior between the soils studied in terms of their main characteristic constituents. It should be noted that the use of a $^{14}C$ marker to determine the nonextractable toxic chemical yields both the original compound and its metabolites formed during degradation in the soil–subsurface environment. Glyphosate is characterized by a rapid degradation and its degradation compound the AMPA is highly persistent. It is likely that the measured nonextractable $^{14}C$ is a combination of both GP and AMPA; Mamy et al. (2008) demonstrated the formation over time of an irreversible, nonextractable bound fraction of glyphosate in soils.
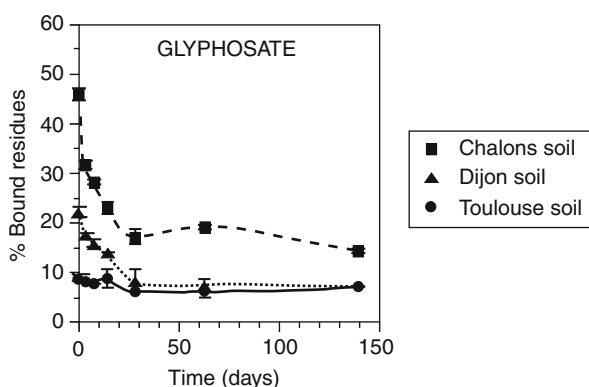


**Fig. 5.23** Nonextractable (bound) residues kinetics of glyphosate in three different French soils (Barriuso et al. 2008). Reprinted with permission from Barriuso E, Benoit P, Dubus IG (2008) Formation of nonextractable (bound) residues in soil: magnitude, controlling factors and reversibility. Environ Sci Technol 42:1845–1854. Copyright 2008 American Chemical Society

### 5.2.4.2   Charged Liquids

Charged liquids are an additional group of organic chemicals in aqueous solution which may affect the natural properties of clays in the soil–subsurface environment. For didactic purposes, we group ionic alternative solvents and surfactants separately.

*Ionic alternative solvents* by definition contain ions positively or negatively charged because they have too few or too many electrons, or some other charge imbalance. Ionic liquids, which are ionic salt-like materials that are liquid below 100°C, usually comprise quaternary nitrogen-containing organic cations, such as alkyl imidazolium, alkyl pyridinium, or alkyl pyrrolidinium coupled to a diverse range of organic or inorganic anions often containing fluorine. Ionic liquids are a fast-growing class of novel substances used mainly as substitutes for conventional solvents. The novel properties of these substances make them ideal, nonvolatile media for a large number of industrial processes involving organic synthesis, alternative electrolytes, and lubricants. Currently, there is no evidence of environmental pollution caused by ionic liquids, but given the likelihood for their increased use, we discuss here the potential for this group of substances to exhibit irreversible retention in the soil–subsurface environment.

To the best of our knowledge, the first study of this subject, by Gorman-Lewis and Fein (2004), investigated adsorption of 1-butyl-3-methylimidazolium chloride (BMIM) on gibbsite, quartz, and Na-montmorillonite (Na-SWy). BMIM, a commercially available dialkylimidazolium, is stable in the pH range 6–10; the adsorption experiments were done with an aqueous solution having an ionic liquid concentration of $9.3 \times 10^{-4}$ M. The general structure of imidazolium is given in Fig. 5.24. BMIM was not adsorbed on gibbsite and quartz; BMIM adsorption on Na-montmorillonite was independent of pH, and increased with increasing ionic strength and with increasing concentration of clay mineral in the BMIM aqueous solution (Fig. 5.25). On the basis of these experiments, Gorman-Lewis and Fein (2004) suggested that the retention of this class of ionic liquid on earth materials may be significant when a large fraction of interlayer clays is present.

Adsorption–desorption of BMIM and 1-hexyl-3-methylimidazolium chloride (HMIM) on two clay soils from Poland (57.9 and 60.50% clay content) was reported by Stepnowsky et al. (2007). Adsorption isotherms (Fig. 5.26a, b) reveal that sorption is essentially complete with the longest alkyl chain entity (HMIM) in
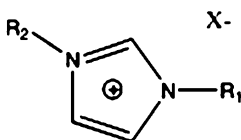


**Fig. 5.24** General structure of an imidazolium salt where R1 and R2 can be alkyl chains of varying lengths and X- is an inorganic anion. In solution, the imidazolium ion and the anion dissociate completely (after Gorman-Lewis and Fein 2004). Reprinted with permission from Gorman-Lewis DJ, Fein JB (2004) Experimental study of the adsorption of an ionic liquid onto bacterial and mineral surfaces. Environ Sci Technol 38:2491–2495. Copyright 2004 American Chemical Society
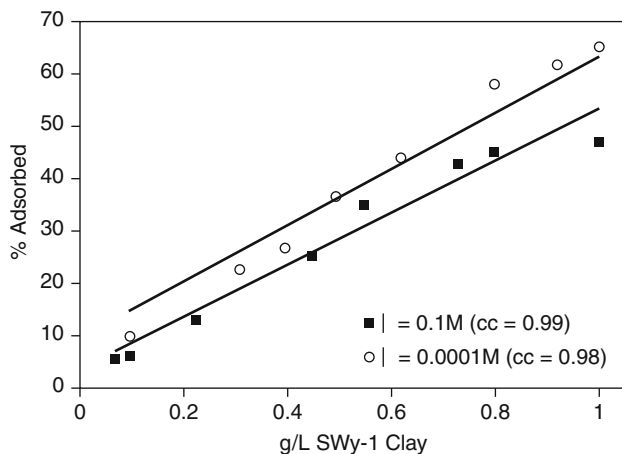
**Fig. 5.25** Percent of BMIM (initial aqueous concentration $9.3 \times 10^{-4}$ M) adsorbed onto varying concentrations of Na-montmorillonite clay (Na-SWy), at an ionic strength of $10^{-1}$ and $10^{-4}$ M, agitated for 3 h ($2\sigma$ *error bars* shown are within data points). The *lines* represent adsorption modeled with a $K_d$ value of 1,735 L kg$^{-1}$ and 1,133 L kg for the $10^{-4}$ and $10^{-1}$ M ionic strengths, respectively (after Gorman-Lewis and Fein 2004). Reprinted with permission from Gorman-Lewis DJ, Fein JB (2004) Experimental study of the adsorption of an ionic liquid onto bacterial and mineral surfaces. Environ Sci Technol 38:2491–2495. Copyright 2004 American Chemical Society
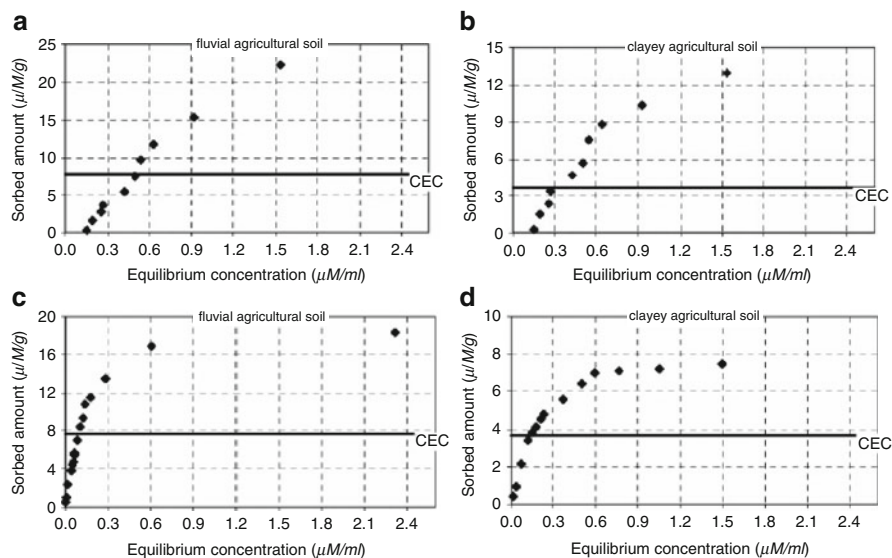


**Fig. 5.26** Sorption isotherms of (**a**) 1-butyl-3-methylimidazolium chloride and (**b**) *N*-butyl-4-methylpyridinium chloride on clay soils with 58 and 61% clay content (modified after Stepnowsky et al. 2007). Reprinted with permission from Stepnowski P, Mrozik W, Nichthauser J (2007) Adsorption of alkylimidazolium and alkylpyridinium ionic liquids onto natural soils. Environ Sci Technol 41:511–516. Copyright 2007 American Chemical Society

the highest concentration range, and incomplete in the case of the shorter alkyl chain (BMIM) liquid. However, the maximum achievable surface concentrations of adsorbed ionic liquids are in most cases above the CEC of the tested clay soils. This may be explained by the fact that initially sorbed solute may modify the sorbent matrix, favoring further sorption of ionic liquid. Desorption measurements of ionic liquids from both clay soils indicated a decrease in desorption with an increase in alkyl chain length. Of the initially sorbed HMIM, 2% was desorbed, compared to about a 10% desorption of the BMIM. These results suggest that both ionic liquids are bound irreversibly to the clay soil component, and that the molecular composition of the ionic liquid defines the amount that is irreversibly retained.

Three additional compounds were selected by Matzke et al. (2009) to investigate the adsorption–desorption of ionic liquids on soils and mineral constituents of the soil–subsurface system. The tested compounds were 1-butyl-3-methyl-imidazolium tetrafluoroborate (IM14 BF$_4$), 1-methyl-3-octyl tetrafluoroborate (IM18 BF$_4$), and 1-butyl-3-methyl-imidazolium bis(trifluoromethylsulfonyl) imide (IM14 (CF$_3$SO$_2$)$_2$N); their structures are presented in Fig. 5.27. The adsorbents used in the experiments were a reference standard soil from Germany (Lufa2.2) and a reference soil enriched with 10 and 15% smectite or kaolinite.

The amounts of ionic liquid adsorbed on the reference standard soil varied for the compounds tested; the maximum amount of ionic liquid adsorbed was 73%, for a nominal concentration of 1,000 μmol L$^{-1}$ of IM18 BF$_4$, whereas only 25% of IM14 (CF$_3$SO$_2$)$_2$ N was sorbed from a nominal concentration of 1,000 μmol L$^{-1}$. In general, the addition of smectite to the soil drastically increased the amount of adsorption, for all three compounds. This behavior may be explained by the high surface area and CEC of the smectite mineral. In comparison, the addition of kaolinite, with a lower surface area and CEC, has in general a minor and ambiguous effect on ionic liquid adsorption. Figure 5.28 summarizes the adsorption and desorption of ionic liquids to/from soils examined by Matzke et al. (2009).

Desorption experiments provide information regarding the retention capacity of ionic liquids of soil and clay–soil treatments, and insight on potentially irreversible
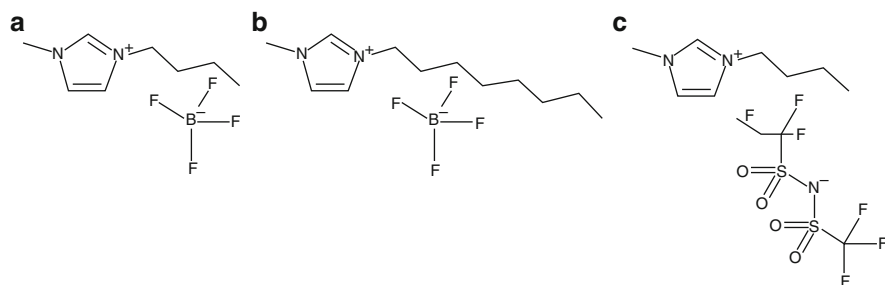


**Fig. 5.27** The structure of ionic liquids tested by Matzke et al. (2009): (**a**) 1-butyl-3-methyl-imidazolium tetrafluoroborate (IM14 BF$_4$), (**b**) 1-methyl-3-octyl tetrafluoroborate (IM18 BF$_4$), and (**c**) 1-butyl-3-methyl-imidazolium bis(trifluoromethylsulfonyl) imide (IM14 (CF$_3$SO$_2$)$_2$N). Reprinted from Matzke M, Thiele K, Müller A, Filser J, Sorption and desorption of imidazolium based ionic liquids in different soil types. Chemosphere 74:568–574, Copyright (2009), with permission from Elsevier
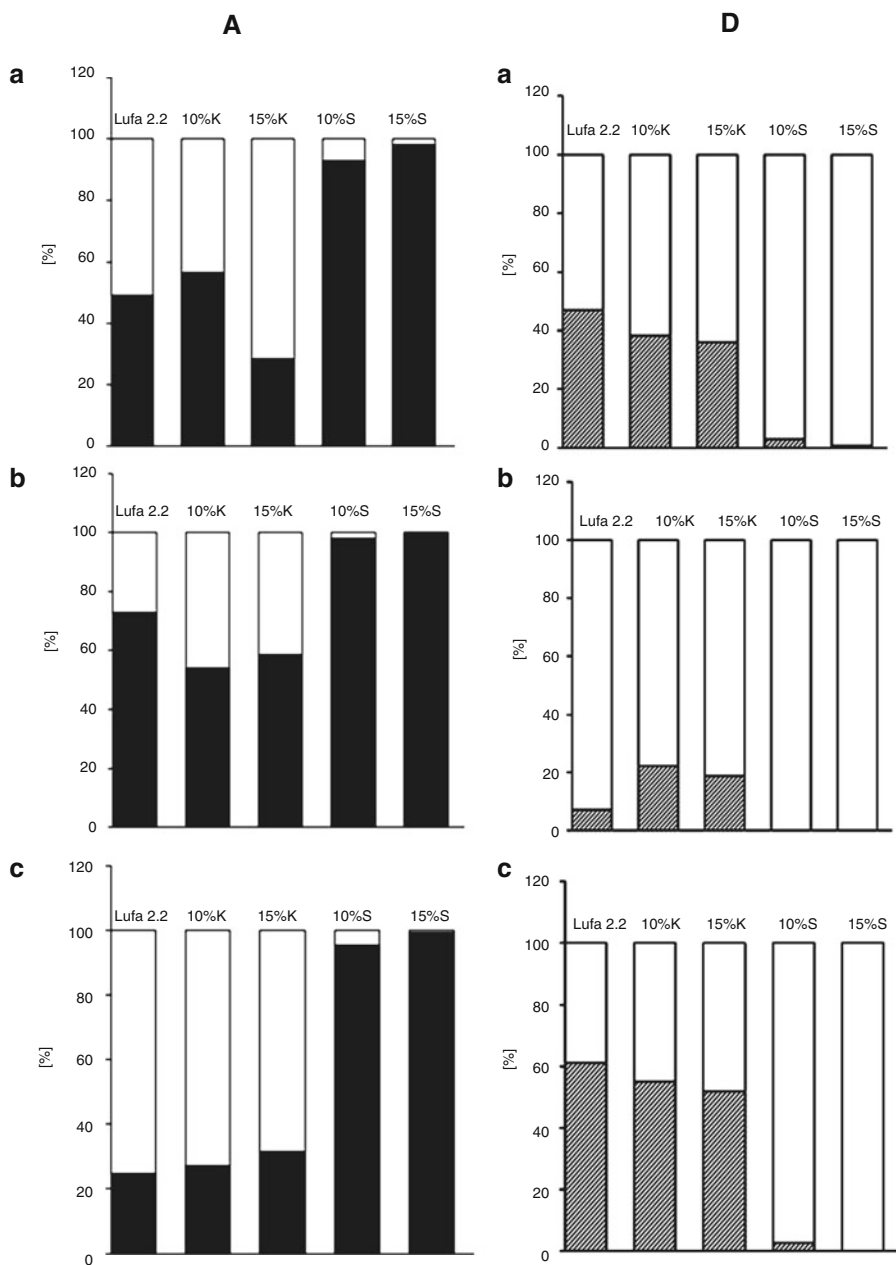
**Fig. 5.28** Sorption (A) and desorption (D) of ionic liquid measured at a nominal test concentration of 1,000 μmol L$^{-1}$: (**a**) IM14 BF$_4$, (**b**) IM18 BF$_4$, and (**c**) IM14 (CF$_3$SO$_2$)$_2$N; Lufa 2.2 = reference soil, K = Lufa 2.2 + kaolinite for a total clay concentration of 10 and 15 wt.%, respectively; S = Lufa 2.2 + smectite for a total clay concentration of 10 or 15 wt.%, respectively (modified after Matzke et al. 2009). Reprinted from Matzke M, Thiele K, Müller A, Filser J, Sorption and desorption of imidazolium based ionic liquids in different soil types. Chemosphere 74:568–574, Copyright (2009), with permission from Elsevier

processes. Retention of the ionic liquids in the reference soil is also influenced by the structure of the compound. About 95% of the adsorbed IM18 $BF_4$ was retained in the reference soil, while 40% of the IM14 $(CF_3SO_2)_2$ N was retained. Addition of 15% smectite to the reference soil led to complete retention of all three ionic liquids. On the contrary, enrichment of soil by kaolinite did not affect significantly the amount of compound remaining in soil after desorption.

The study of Mrozik et al. (2009), testing the mobility in soils of a large number of ionic liquids, shows that short-chain compounds desorb more easily from soils than long-chain compounds. Desorption of ionic liquids is correlated inversely to the sorption intensity, which is controlled by the CEC of the adsorbing soils. Mrozik et al. (2009) concluded that the retention of the ionic liquid – which may become irreversible – is favored by the presence of clay minerals, like smectite, that have an expanding nature and a negative charge.

*Surfactants* may reach the land surface as pollutants that originate from disposal of pharmaceutical and municipal wastes, effluent irrigation, and agricultural dispersing agents, or as co-solvents in soil and water restoration technologies. Although surfactants are generally biodegradable, their adsorption on the soil solid phase may produce irreversible microstructural changes in the clay matrix.

Cationic surfactants may be adsorbed on soil mineral surfaces, forming aggregate structures called hemimicelles and admicelles. When the surfactant cation concentration in aqueous solution is below the CEC of the soil–subsurface matrix, adsorption occurs according to electrostatic forces between charged surfaces and solutes with opposite charge. Surfactants with large organic cations displace smaller inorganic cations until the surface charge is balanced, forming a kind of hemimicelle. Holsen et al. (1991) showed that the surfactant monomers in the hemimicelle are oriented with the cationic heads close to the mineral surface and the long hydrophobic tails in contact with the solution. When the concentration of monomers from solution is near or exceeds the CEC, organic cations may be adsorbed through hydrophobic tail–tail interaction by the hemimicelle layer. Cationic surfactant adsorption beyond the CEC of the solid may occur also via admicelles.

However, this type of adsorption is susceptible to rapid desorption (Brown and Burris 1996). The mechanism of adsorption of cationic surfactants on clay minerals may vary as a function of clay characteristics. Xu and Boyd (1995) revealed such differences by studying cationic surfactant adsorption on swelling (e.g., smectite) and non-swelling (e.g., kaolinite) silicates, defining a relation between surfactant layer and the stability of surfactant–clay complexes. In their experiments, hexadecyltromethylammonium (HDTMA) was adsorbed on Na–Wyoming montmorillonite (Na–SWy), Na–Arizona montmorillonite (Na–SAz), and Na–kaolinite; the resulting adsorption isotherms are shown in Fig. 5.29.

Based on adsorption isotherms (Fig. 5.29), X-ray diffraction, and electromobility analysis, Xu and Boyd (1995) consider that cationic surfactant adsorption by swelling layer silicates is much more complex than that of nonswelling clays. This complexity is caused by the structure of the adsorption layer of cationic surfactants in the interlayers of the swelling clays. A highly dispersed swelling clay induces a random HDTMA/inorganic cation distribution in the interlayers and a loose structure of the
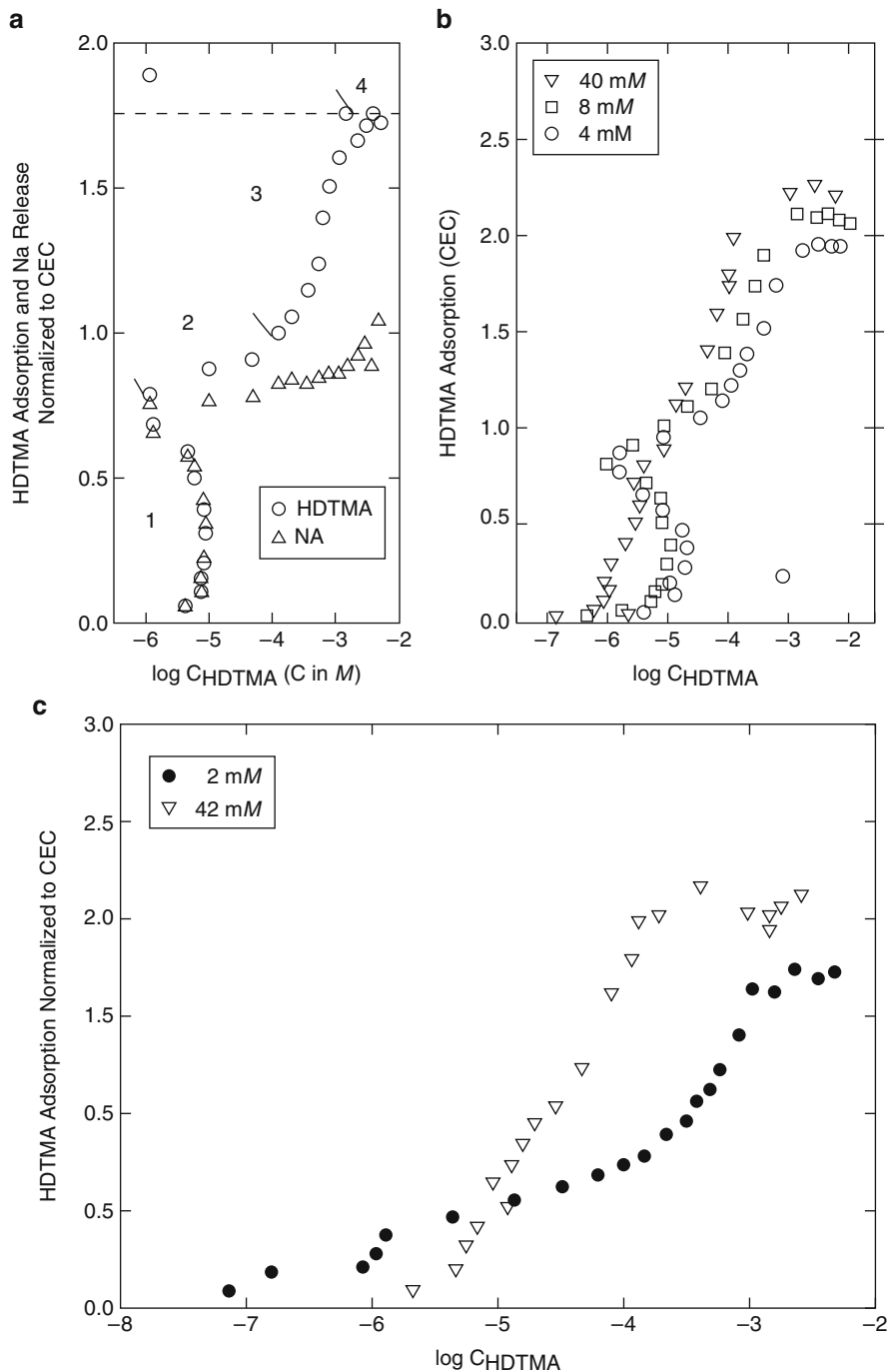
**Fig. 5.29** Adsorption of HDTMA on (**a**) Na-SWy (smectite), (**b**) Na-SAz (smectite), and (**c**) sodium kaolinite, in NaCl solutions (modified after Xu and Boyd 1995). Reprinted with permission from Xu S, Boyd SA (1995) Cationic surfactant adsorption by swelling and nonswelling layer silicates. Langmuir 11:2508–2514. Copyright 1995 American Chemical Society

adsorption layer at low HDTMA loadings. This behavior causes lateral interactions between alkyl C-16 groups of HDTMA to increase minimally with surfactant loading as the contact among adsorbed molecules increases. Flocculation of swelling montmorillonite as a consequence of Ca or Cs saturation, or a high ionic strength before HDTMA application, causes a segregated cation distribution and formation of a compact surfactant layer. This causes restricted access of HDTMA to the edges of clay flocks and an important lateral interaction among the alkyl groups even at a low surfactant loading. Under these conditions, HDTMA adsorption isotherms differ from adsorption isotherms of nonswelling clays.

The negative surface charges of the clay minerals are essentially independent of the surrounding solution conditions. Exchanges of inorganic molecules from the swelling clay surface with organic molecules cause displacement of the original interlayer cations, and lead to microstructural changes in the adsorbing clay. The intercalated molecules are known to align themselves in an ordered structure within the interlayer space (Legally 1982, 1994) and can accommodate guest molecules by increasing interlayer distance (Ogawa and Kuroda 1997). As an example, we consider microstructural changes occurring in montmorillonite induced by a cationic surfactant, as discussed by Lee et al. (2005). HDTMA-modified montmorillonites were prepared by adding HDTMA-bromide up to three times the CEC of the tested montmorillonites (SWy and SAz). Basal spacing increased stepwise when HDTMA was added in increasing amounts (Fig. 5.30). The increase in basal spacing is correlated to the CEC of the clay and surfactant loading. Adsorption of HDTMA on SWy (CEC = $0.9$ mol$_c$ kg$^{-1}$) and on SAz (CEC = $1.25$ mol$_c$ kg$^{-1}$) led to increases in basal spacing from 14.8 to 21.0 Å, and from 15.2 to 37.7 Å, respectively.

Although the amount of loaded HDTMA decreases over time due to natural attenuation, we can assume that changes in the basal spacing of the HDTMA-montmorillonite may decrease but never return to the initial value. The change will remain irreversible, although the degree of change will vary among samples. Microscopic measurements reported by Lee et al. (2005) and reproduced in Figs. 5.31 and 5.32 reinforce the above. SEM micrographs show the morphology of montmorillonites (SWy and SAz) modified by adding increasing HDTMA cation loadings (Fig. 5.31). SWy morphology progressively changed from an adhesive, interwound pattern to a "corn flake" pattern (Fig. 5.31a, b), while SAz morphology changed from a grain-like structure to a special aggregated form (Fig. 5.31c, d).

TEM images (Fig. 5.32) of SWy show an increase in lattice fringe space of up to 20 Å, by adding an amount of HDTMA surfactant equivalent to the montmorillonite CEC. HDTMA-SAz images show an increase in lattice fringes (up to 27 Å) with an increase in interlayer adsorption of HDTMA. The lack of coherent interlayer spacing of HDTMA-SAz may indicate local variation in the density of interlayer charge. Legally (1994) explains this behavior by the variation in the extent of isomorphous substitution on the 2:1 layer silicates.

Modification of Na-montmorillonite by other cationic surfactants, such as benzyltrimethylammonium (BTMA) and benzyltriethylammonium (BTEA), was observed through TEM studies reported by Yaron-Marcovich et al. (2005). The TEM images of BTMA-montmorillonite and BTEA-montmorillonite when
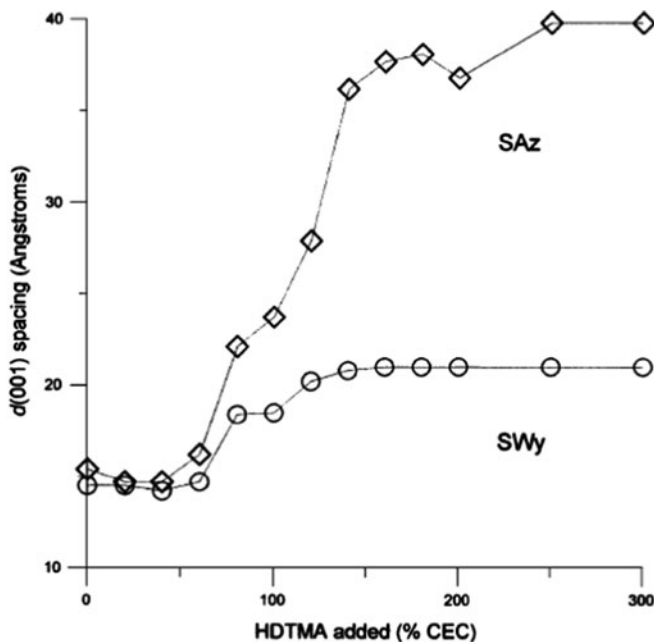
**Fig. 5.30** Basal spacing changes of HDTMA–Wyoming (SWy) and Arizona (SAz) montmorillonites as a function of amount of HDTMA added (after Lee et al. 2005). Reprinted from Lee SY, Cho WJ, Hahn PS, Lee M, Lee YB, Kim KJ, Microstructural changes of reference montmorillonites by cationic surfactants. Appl Clay Sci 30:174–180, Copyright (2005), with permission from Elsevier

surfactant loading was at 100% of clay CEC are shown in Figs. 5.33 and 5.34. At lower magnification, BTMA- and BTEA-montmorillonite morphologies differ from those of the untreated montmorillonite, exhibiting aggregates composed of small, thin crystalline particles showing no preferred orientation. High-resolution TEM (HRTEM) images (inserts c and d) reveal changes in interlayer configuration evidenced by local variation in the $d_{001}$ layers. Analysis of the respective lattice images yields $d_{001}$ values of 14–15 Å for BTMA-montmorillonite and 13.8–14.5 Å for BTEA-montmorillonite, compared to 13 Å for untreated Na-montmorillonite.

## 5.3   Irreversible Adsorption via Exchange Processes and Induced Modification of the Soil Organic Phase

In comparison to the existing information involving contaminant exchange processes in the soil–subsurface mineral phase, knowledge of such processes in soil–subsurface organic phases is relatively limited. As a consequence, our discussion of this aspect is less extensive and includes only several examples.
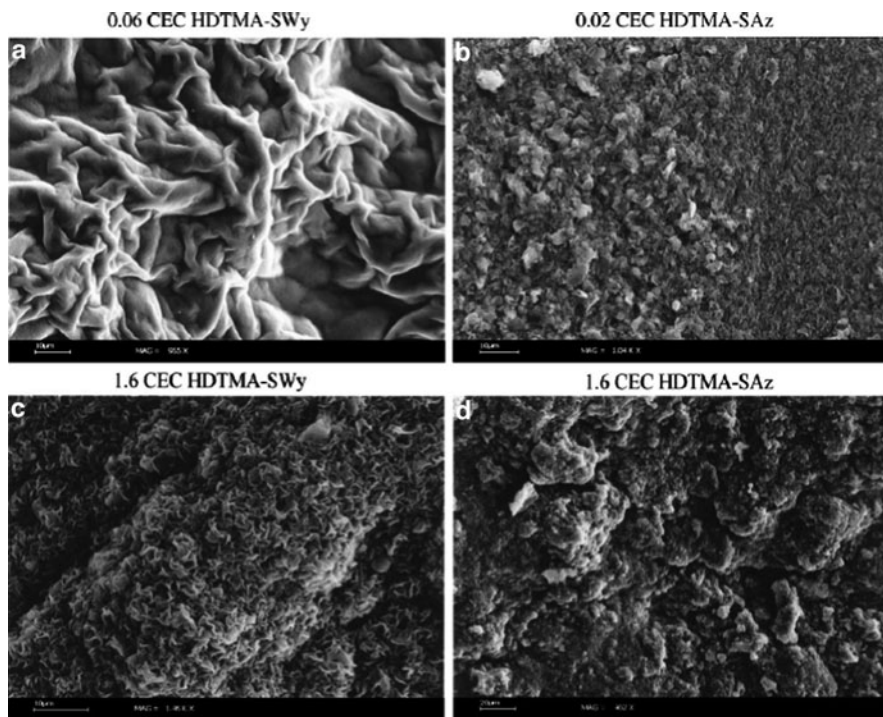
**Fig. 5.31** SEM micrographs of Wyoming (SWy) and Arizona (SAz) montmorillonite particles with increasing HDTMA loading (Lee et al. 2005). Reprinted from Lee SY, Cho WJ, Hahn PS, Lee M, Lee YB, Kim KJ, Microstructural changes of reference montmorillonites by cationic surfactants. Appl Clay Sci 30:174–180, Copyright (2005), with permission from Elsevier

In general, the special role of cation exchange properties of undissolved humic materials was recognized by Schnitzer and Khan (1972) and Jackson et al. (1978), who showed that adsorption of organic contaminants on humic substances occurs via cation exchange between the adsorbate and the ionized carboxylic and phenolic hydroxyl functional groups of the adsorbent. A divalent cationic contaminant (e.g., diquat) may react with a number of negatively charged sites on the humic substances. The amount of charged organic contaminant adsorbed is in some cases considerably lower than the CEC of the humic adsorbent. This may be explained by the presence of large organic cations within humic substances, which cause steric hindrance effects.

Ionic exchange of less basic organic contaminants (e.g., s-triazines), which become cationic through protonation, is controlled by the pH of the water-adsorbent system (Senesi and Chen 1989, and references therein). The potential irreversibility of ionic contaminant bonding, and changes in the structure of humic substances are indicated by hysteresis phenomena in the micro- and macro-molecular configurations of this natural constituent. Differences in the molecular structure and composition of humic acids in soil solutions and in solid phases affect contaminant-induced transformation of humic materials.
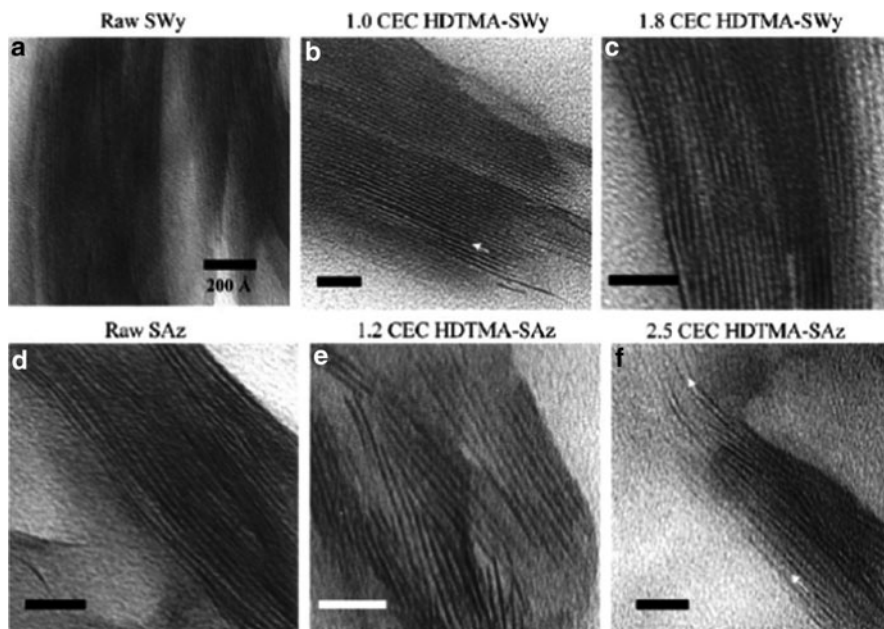
**Fig. 5.32** TEM lattice fringe images of HDTMA montmorillonites. (**a**) Raw Wyoming (SWy) montmorillonite (layer spacing ~14 Å). (**b**) HDTMA loading equivalent to the CEC (~20 Å), except in some layers (*arrow*). (**c**) No significant increase in the layer spacing (~21 Å) at higher loading. (**d**) Raw Arizona (SAz) montmorillonite (~15 Å). (**e**) Layer spacings of 24–27 Å with increasing HDTMA loading. (**f**) Some highly expanded layers (>40 Å, *arrows*) at high HDTMA loading (after Lee et al. 2005). Reprinted from Lee SY, Cho WJ, Hahn PS, Lee M, Lee YB, Kim KJ, Microstructural changes of reference montmorillonites by cationic surfactants. Appl Clay Sci 30:174–180, Copyright (2005), with permission from Elsevier

Humic acids in soil–subsurface solutions are less aromatic and more highly oxidized than those in the solid phase. Moreover, humic acids in soil–subsurface solutions have fewer sugars and amino acids than those in the soil–subsurface solid phase. Clapp et al. (2005) suggested that sugar and amino acids are less exposed to enzymatic attacks, and may induce hydrophobic constituents such as long-chain hydrocarbons and fatty acids to become physically protected by association with mineral colloids. Conformational changes in the humic substances may lead to breaks in sugar and peptide association, and their release into the soil–subsurface solution (Schnitzer 1994).

## 5.3.1   Metal Ions

Metal ion exchange in soil organic matter was studied and reported in a series of papers (e.g., Bunzl 1974a,b: Bunzl et al. 1976; Kerndorff and Schnitzer 1980; Crist et al. 1996), which examined adsorption–desorption of various metals, including
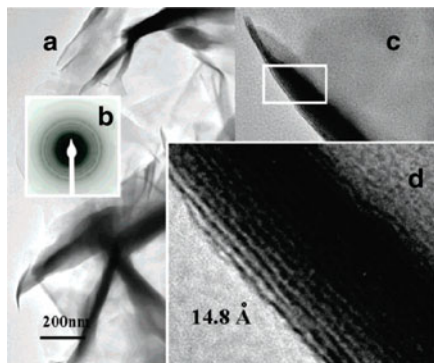
**Fig. 5.33** TEM images of a sample of benzyltrimethylammonium (BTMA)-montmorillonite at 100% loading: (**a**) low-magnification TEM image; (**b**) the corresponding selected area electron diffraction pattern; (**c**) high-resolution TEM image of a particle from the aggregate in panel **a**; (**d**) enlarged image of the white framed area in panel **c** showing an interlayer spacing of 14.8 Å (after Yaron-Marcovich et al. 2005). Reprinted with permission from Yaron-Marcovich D, Chen Y, Nir S, Prost R (2005) High resolution electron microscopy structural studies of organo-clay nanocomposites. Environ Sci Technol 39:1231–1239. Copyright 2005 American Chemical Society
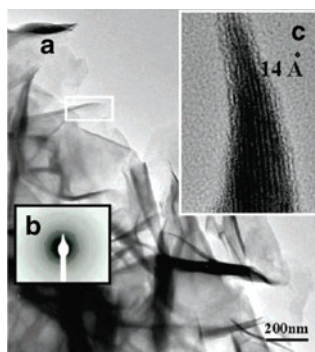


**Fig. 5.34** Typical TEM images of benzyltriethylammonium (BTEA)-montmorillonite at 100% loading: (**a**) low-magnification TEM image; (**b**) the corresponding selected area electron diffraction pattern; (**c**) high-resolution TEM image of the particle attached to aggregate in panel **a** (*white framed*) exhibiting an interlayer spacing of 14 Å (after Yaron-Marcovich et al. 2005). Reprinted with permission from Yaron-Marcovich D, Chen Y, Nir S, Prost R (2005) High resolution electron microscopy structural studies of organo-clay nanocomposites. Environ Sci Technol 39:1231–1239. Copyright 2005 American Chemical Society

$Pb^{2+}$, $Cu^{2+}$, $Cd^{2+}$, and $Zn^{2+}$ on and from H- and Ca-saturated peat. Metal uptake on peat is actually a process of ion exchange at acidic sites that resulted from the humification process. Metals can react with carboxylic and phenolic acid groups of fulvic and humic acids to release protons or, at sufficiently high pH, metals can react with humic acid anion sites to displace an existing metal.

The order for the selective uptake of metal ions by H-saturated peat is $Pb^{2+} > Cu^{2+} > Cd^{2+} > Zn^{2+}$. All heavy metal ion adsorption–desorption isotherms on and from peat show a hysteretic process, which points to their irreversible retention on the

organic solid phase. Figure 5.35 presents the adsorption–desorption isotherms of $Pb^{2+}$, $Cd^{2+}$, and $Zn^{2+}$ on and from peat 4 days after exposure to metal. It may be observed that $Pb^{2+}$ hysteresis is greater than that of $Cd^{2+}$ and $Zn^{2+}$, which is due to the differences in the amount of metal adsorbed. Hysteresis increases with an increase in the amount adsorbed.

Kerndorff and Schnitzer (1980) reported on multiple metal ion exchange experiments. Measuring the equilibration of eleven heavy metal ions between a humic acid and soil solutions, Kerndorff and Schnitzer (1980) found that the metal ions compete among each other for humic acid ion exchange sites. Based on these findings, and on various other experimental results, a theoretical description of multiple metal ion–humic acid cation exchange was developed. Adapting a law of mass action formalism and mole fraction relationships, simultaneous ion exchange equilibria of metal cations with humic acid were described (Gamble et al. 1983).

Based on adsorption–desorption experiments, Bunzl et al. (1976) suggested that the relative rates of desorption show longer times for lead and copper, and shorter times for cadmium and zinc. Thus, over limited time frames, such as the period of a human life, lead and copper may be considered to be retained irreversibly on humic substances, thus favoring an irreversible change in the conformational structures of humic substances.
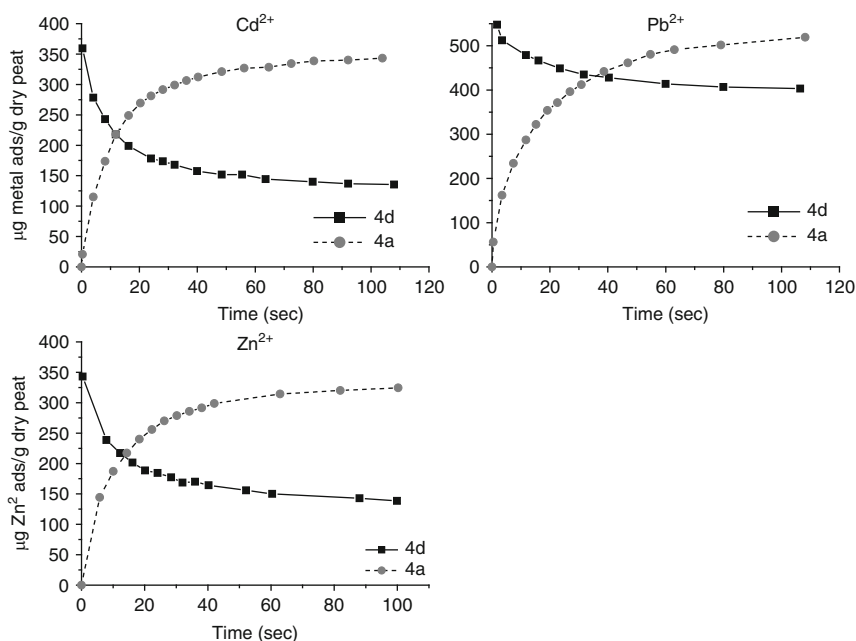


**Fig. 5.35** Amount of metal ions adsorbed and subsequently desorbed by peat, 4 days after exposure to metal. Reprinted from Bunzl K, Schmidt W, Sansoni B (1976) Kinetics of ion exchange in soil organic matter V. Adsorption-desorption of $Pb^{2+}$, $Cu^{2+}$, $Cd^{2+}$, $Zn^{2+}$ and $Ca^{2+}$ by peat. Eur J Soil Sci 27:32–41. Copyright 1976 with permission of John Wiley and Sons

An ion exchange process was observed in uptake of metals on a Ca-saturated organic compound (Canadian sphagnum peat moss) having a total organic matter content of 98% (Crist et al. 1996). Metals bind to anionic sites at high pH by displacing protons from acid groups or existing metals from anionic sites. Acidification of the native peat moss caused release of metals, as shown in Fig. 5.36. The most abundant metal was Ca, at 140 $\mu$eq g$^{-1}$, while Mg, K, Na, and Zn total 103 $\mu$eq g$^{-1}$. Crist et al. (1996) suggest that protons are displaced relatively easily from the peat moss by Ca and Mg. This may be due to the presence of relatively strong acids or result from a chelation effect which releases protons from carboxylic acid groups when a divalent metal ion also binds to an adjacent phenolic OH or carboxyl acid.

Although metal bonding on organic matter can be viewed as an ion exchange process between H$^+$ and metal ions on acidic functional groups, the high degree of selectivity shown by organic matter for certain metals suggests that some metals coordinate directly by forming inner-sphere complexes with the functional groups (McBride 1989). Following this approach, the hysteresis of heavy metals on humic substances (which may indicate irreversible retention over a limited time frame) is due not only to cationic exchange, but also to an associated ligand exchange process.
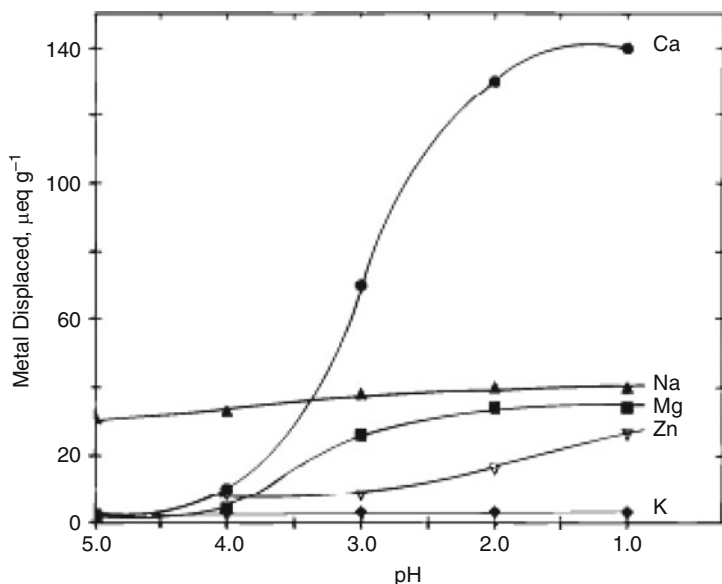


**Fig. 5.36** Effect of pH on protons displacing metals from native peat moss (PM-N) (after Crist et al. 1996). Reprinted with permission from Crist RH, Martin JR, Chonko J, Crist DR (1996) Uptake of metals on peat moss: an ion-exchange process. Environ Sci Technol 30:2456–2461. Copyright 1996 American Chemical Society

### 5.3.2 Chemical Fertilizer

Chemical fertilizer disposed on lands during agricultural practices may irreversibly change the conformational arrangement of natural soil and subsurface humic substances. Zhou et al. (2010) applied a combination of solid state cross-polarization magic angle spinning (CPMS), solid state $^{13}$C nuclear magnetic resonance (CPMS-$^{13}$C-NMR), and thermochemoanalysis-GC/MS to investigate the molecular composition of particulate organic matter after long-term application of a mixture of chemical fertilizers. This investigation aimed to compare the chemical compositions of organic matter in natural paddy soils in soils altered by long-term fertilizer application. The annual amount of chemical fertilizer applied in a cultivated field over 20 years included 427.5 kg ha$^{-1}$ urea, 45 kg ha$^{-1}$ superphosphate-P, and 54 kg ha$^{-1}$ KCl-K. Because the applied fertilizers are charged chemicals, it is assumed that their retention on humic substances is due to an exchange process.

Solid-state spectra of organic matter samples extracted from the natural paddy soil, and from the paddy soil after long-term application of fertilizer, are shown in Fig. 5.37; the relative amounts of carbon species obtained by integration of CPMS-$^{13}$C-NMR spectra are reported in Table 5.6. The two samples displayed similar spectral patterns. However, a difference between the conformational structure of untreated and fertilizer-treated samples, revealed by NMR spectra, was related to the relative content of O-alkyl-C carbohydrates and polysaccharides. The amount of O-alkyl-C carbohydrates in the 60–110-ppm interval increased in fertilized treatment from 42.2 to 48.7. Also, slight increases under fertilized treatment are observed in the relative content of aromatic-C and methoxy-C. In contrast, the relative content of alkyl-C decreases from 21.5 to 14.7 in the particulate organic
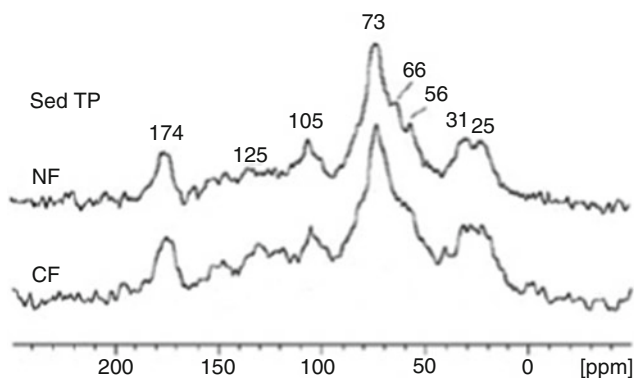


**Fig. 5.37** CPMS-$^{13}$C-NMR spectra of particulate organic matter extracted from a paddy soil without fertilizer treatment (NF) and after fertilizer application (CF). Reprinted from Zhou P, Pan GX, Spaccini R, Piccolo A (2010) Molecular changes in particulate organic matter (POM) in a typical Chinese paddy soil under different long term fertilizer treatments. Eur J Soil Sci 61:231–242. Copyright 2010 with permission of John Wiley and Sons

**Table 5.6** Distribution of carbon species (%) in CPMS-$^{13}$C-NMR particulate organic matter spectra of natural (NF) and fertilized (CF) paddy soil. Reprinted from Zhou P, Pan GX, Spaccini R, Piccolo A (2010) Molecular changes in particulate organic matter (POM) in a typical Chinese paddy soil under different long term fertilizer treatments. Eur J Soil Sci 61:231–242. Copyright 2010 with permission of John Wiley and Sons

| Treatments | Relative abundance of total area (%) | | | | | |
|---|---|---|---|---|---|---|
|  | Carbonyl-C | Phenolic-C | Aromatic-C | O-alkyl-C | Methoxy-C | Alkyl-C |
| NF | 7.5 ± 0.2 | 6.3 ± 0.3 | 12.4 ± 0.7 | 42.2 ± 1 | 10.1 ± 0.2 | 21.5 ± 0.6 |
| CF | 4.9 ± 0.3 | 3 4.2 ± 0.6 | 14.3 ± 0.8 | 49.7 ± 1 | 12.2 ± 0.3 | 14.7 ± 0.7 |
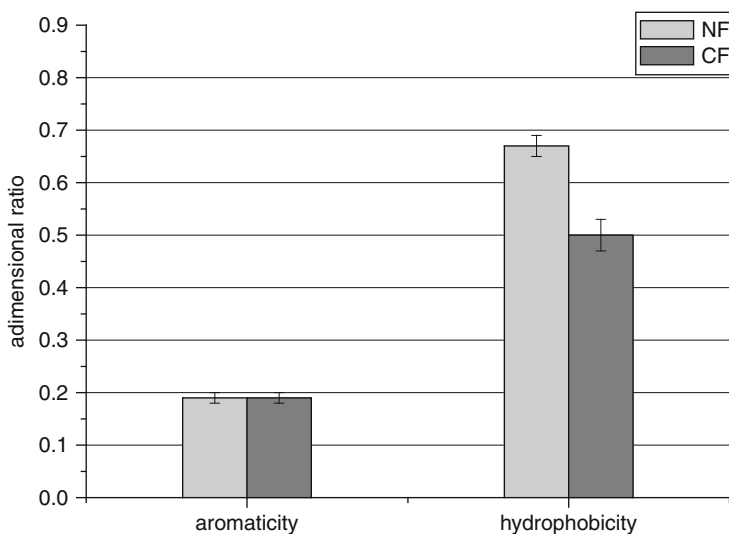


**Fig. 5.38** Variations in aromaticity and hydrophobicity of particulate organic matter in soil: (1) no fertilizer application (NF), (2) chemical fertilizers (CF). Reprinted from Zhou P, Pan GX, Spaccini R, Piccolo A (2010) Molecular changes in particulate organic matter (POM) in a typical Chinese paddy soil under different long term fertilizer treatments. Eur J Soil Sci 61:231–242. Copyright 2010 with permission of John Wiley and Sons

matter composition of the fertilized field. The changes in the configuration of paddy soils particulate organic matter were reflected in their aromaticity and hydrophobicity.

Zhou et al. (2010) found that soil fertilization did not affect the aromaticity of the particulate organic matter but influenced its hydrophobicity index (Fig. 5.38). The low hydrophobicity as revealed by NMR may partially explain the significant increase in organic carbon mineralization rate previously found for this system (Zheng et al. 2007). This case demonstrates a fertilizer-induced, irreversible change in the conformational structure of the humic substances. The structural change leads also to a change in humic substance hydrophobicity, which may further affect interactions with organic contaminants.

### 5.3.3 Organic Amendments

Organic amendments are used in agricultural practices to improve soil water transmission properties and to replace or complement industrial fertilizers. Analyses of molecular changes in soil organic matter and humic acids found in sewage sludge-amended soil and in compost were reported by Adani and Tambone (2005) and Spaccini et al. (2009), respectively. These studies support the argument that organic soil amendments induce irreversible changes in the original conformational structure of natural humic substances.

#### 5.3.3.1 Sludge

The aim of the experiment reported by Adani and Tambone (2005) was to determine molecular-level changes induced by long-term application of sludge-containing humic acid on soil humic acid. The impact of sludge humic acid on untreated soil humic acid may be deduced from comparison of elemental analysis of humic acid extracted from soil, sludge, and sludge-treated soil (Table 5.7). The fact that humic acids from sludge-treated soil showed higher C and H contents and lower N, S, and O contents indicates a sludge effect on soil humic acid, confirming the early work of Boyd et al. (1980).

Diffuse reflection infrared Fourier transformation (DRIFT) spectra of humic acid extracted from sludge, soil, and sludge-treated soil provide evidence of the effect of sludge humic acid on soil humic acid composition. The spectra in Fig. 5.39 show a difference in the band intensity between humic acid from treated and untreated soil. The contents of both aliphatic (bands at 2,991, 2,852, 1,455, and 1,374 $cm^{-1}$) and proteinaceous or amide moieties (bands at 3,281, 1,665, and

**Table 5.7** Elemental analysis of humic acid extracted from sludge and soils (after Adani and Tambone 2005). Reprinted from Adani F, Tambone F (2005) Long-term effect of sewage sludge application on soil humic acids. Chemosphere 60:1214–1221, Copyright (2005), with permission from Elsevier

| | SS-HAa (g $kg^{-1}$) | SU-HAb (g $kg^{-1}$) | ST-HAc (g $kg^{-1}$) |
|---|---|---|---|
| C | 557.5 ± 6.1[c] | 522.7 ± 4.2[a] | 537.5 ± 0.9[b] |
| H | 70.0 ± 1.0[c] | 53.6 ± 0.0[a] | 54.5 ± 0.3[b] |
| N | 77.6 ± 1.1[c] | 57.3 ± 0.2[b] | 55.8 ± 0.3[a] |
| S | 21.9 ± 0.1[c] | 9.5 ± 1.7[b] | 8.8 ± 0.4[a] |
| O | 272.2 ± 6.2[a] | 356.9 ± 4.5[c] | 343.4 ± 1.1[b] |
| Ash | 9 | 19.4 | 25.4 |
| H/C | 0.12 | 0.10 | 0.10 |
| C/N | 7.18 | 9.12 | 9.63 |
| C/O | 2.05 | 1.46 | 1.57 |

[a]Sewage sludge humic acid
[b]Humic acid from untreated soil
[c]Humic acid from soil treated with sewage sludge

**Fig. 5.39**  Diffuse reflection infrared Fourier transformation (DRIFT) spectra of humic acid extracted from sludge (SS), untreated soil (SU), and treated soil (ST) (after Adani and Tambone 2005). Reprinted from Adani F, Tambone F (2005) Long-term effect of sewage sludge application on soil humic acids. Chemosphere 60:1214–1221, Copyright (2005), with permission from Elsevier
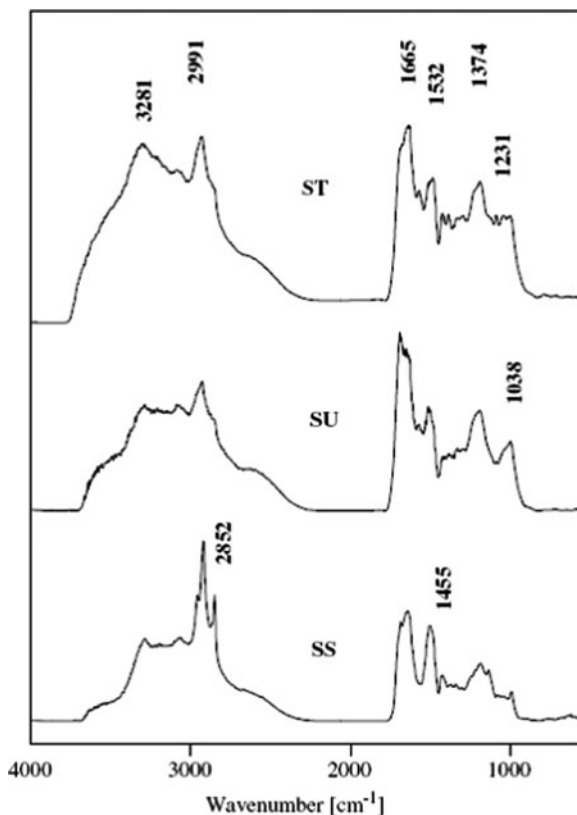


$1,532 \text{ cm}^{-1}$) were more pronounced for soil-treated humic acid than for the untreated soil humic acid. On the contrary, bands at 1,038 and $1,931 \text{ cm}^{-1}$ representing lignin-like material, and bands at $1,700$–$1,715 \text{ cm}^{-1}$ due to carboxylic acid were less evident in the spectra of humic acid in sludge-treated soils than in untreated soils.

### 5.3.3.2   Compost

Molecular changes in soil organic matter following compost application were reported by Spaccini et al. (2009). These changes were determined by pyrolysis in the presence of tetramethylammonium hydroxide, followed by gas chromatography-mass spectroscopy (Pyr-TMAH-GC-MS). No significant differences in the molecular composition of soil organic matter were observed in the control (non-amended) soil after 1 year of cultivation. Adding compost led to significant qualitative and quantitative changes in soil organic matter, including increasing amounts and diversified components of fatty acids, n-alkanes, and various biopolyester derivates such as hydroxyl-alkanoic and alkanoic acids (Fig. 5.40).
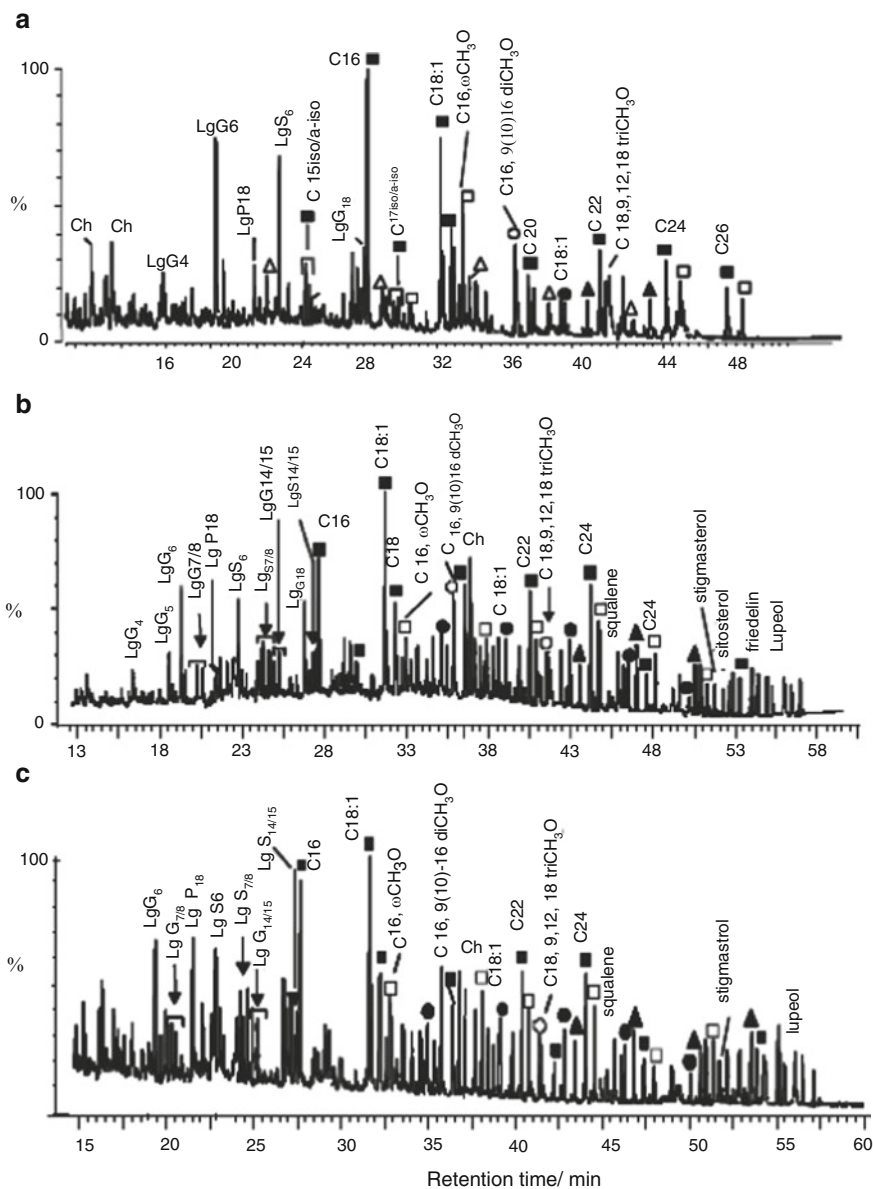
**Fig. 5.40** Total ion chromatogram of thermochemoanalysis products released from (**a**) final control soil, (**b**) soil 30 ton ha$^{-1}$ compost, (**c**) soil 60 ton ha$^{-1}$ compost. *Ch* carbohydrates, *Lg* lignin; *Filled square*, FAME; *Filled triangle*, *n*-alkanes; *triangle*, branched alkanes; $\omega$, hydroxyalkanoic acid; *Filled circle*, alkyldioic acids; *open circle*, mid-chain hydroxyalkanoic acids. Reprinted from Spaccini R, Sannino D, Piccolo A, Fagnano M (2009) Molecular changes in organic matter of a compost-amended soil. Eur J Soil Sci 60:287–296. Copyright 2009 with permission of John Wiley and Sons

For example, two different groups of cyclic lipid compounds which were not previously detected in the control soil were revealed by thermochemoanalysis of compost as methyl esters and esters of diterpenoid and triterpenoid structures. Also, large amounts of guiacyl and siringyl lignin units were found in the compost-treated soil. While the absolute of amount of 3-(4-methoxyphenyl) 2-propenoic acid was increased significantly by addition of compost, no other derivates of p-hydroxy phenyl structure were found among lignin products, suggesting that $P_{18}$ monomer was mainly associated with suberin biopolyesters. The largest relative increase with respect to the control soil was found for straight-chain n-alkanes, showing an overall distribution and composition induced by addition of compost.

Spaccini et al. (2009) also showed that in addition to the most abundant 9–16- and 10–16-dimethoxy hexadecanoic and 9,10,18-trimethoxy octadecanoic acids, additional $C_{16}$ and $C_{18}$ cutin components such as 10-methoxy and 9,10,16-trimethoxy hexadecanoic acid and 9,10,12,18-tetramethoxy octadecanoic acid, characteristic of compost, were released from the compost-treated soil. In addition, the exogeneous origin of the lipids is indicated by the rising content of different sterols, triterpenols, and diterpenes detected as thermochemoanalysis products in the compost-amended soil. With the variance in their basic composition, the humic substances irreversibly affected by compost or sludge disposal may be considered as a different anthropogenically induced soil material created from the existing natural soil organic matter. The study of Khiry et al. (1996) on the adsorption of aqueous nucleobases, nucleosides, and nucleotides on a specific "compost-derived humic acid" is another example of this phenomenon.

### 5.3.4 Pesticide Adsorption

Pesticide adsorption on humic substances may affect the toxic properties of the pesticide. However, pesticides can also be incorporated into the molecular composition of humic substances, inducing a change in their natural conformational arrangement. In many cases, pesticide association with humic compounds is partially or completely irreversible (e.g., bound residues), inducing an irreversible change in the conformational arrangement of humic substances. Pesticides in cationic form, in aqueous solution, may be adsorbed on humic substances via ionic bonding or cation exchange. The most reactive groups of the humic substances, i.e., carboxylic, phenolic, and hydroxylic, may be ionized (Senesi 1992). A few examples of pesticide-induced changes by exchange processes follow below.

*Chlorodimeform* is a pesticide that completely ionizes in water, giving the cation $CfH^+$ and a chloride anion; the molecular structure of chlorodimeform hydrochloride (CfHCl) is shown in Fig. 5.41. The changes in the conformational arrangements of fulvic (FA) and humic (HA) acids following chlorodimeform adsorption, as reported by Maqueda et al. (1990), are discussed below.
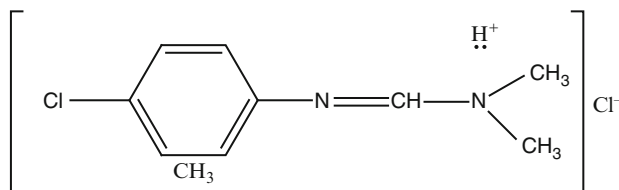
**Fig. 5.41** Molecular structure of chlorodimeform hydrochloride
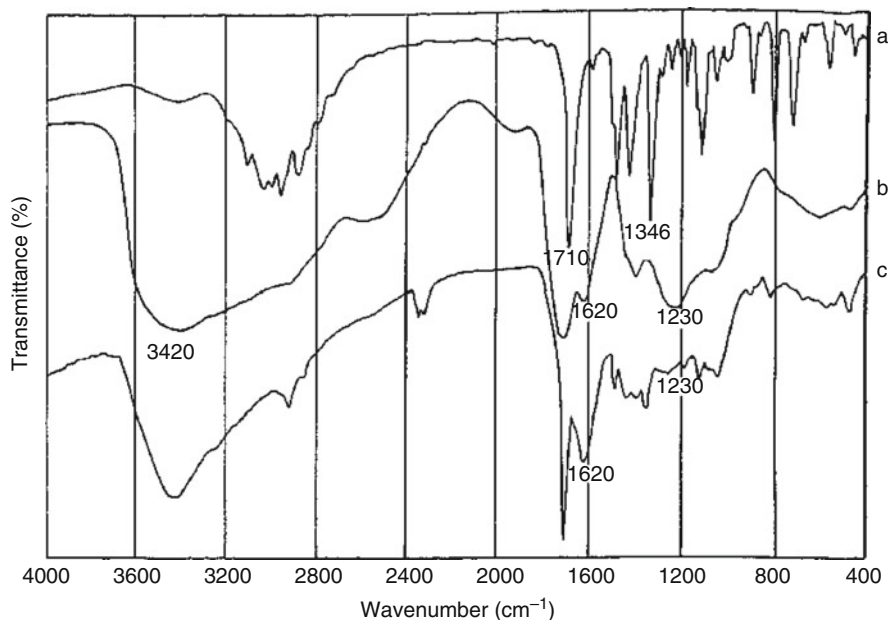


**Fig. 5.42** IR spectra of (**a**) chlorodimeform, (**b**) fulvic acids, and (**c**) fulvic acid–chlorodimeform complexes. Reprinted from Maqueda C, Morillo S, Pérez Rodríguez JL, Justo A (1990) Adsorption of chlordimeform by humic substances from different soils. Soil Sci 150:431–437. Copyright 1990 with permission of Wolters Kluwer Health

The humic substances on which chlorodimeform was adsorbed were fulvic acids extracted from Podosol and Andosol acid soils and humic acids from Chromoxerert neutral or basic soils. The differences between the two humic substances lie in their structural and functional groups, which are mainly responsible for the adsorption of chlorodimeform. A comparison among IR structural spectra of chlorodimeform (CfH$^+$), FA, HA, and FA-, HA-CfH$^+$ complexes determined and interpreted by Maqueda et al. (1990) is presented in Figs. 5.42 and 5.43.

The IR adsorption spectrum of the fulvic acid–chlorodimeform complexes (Fig. 5.42c) shows many bands attributed to chlorodimeform, as well as bands of the fulvic acids (expressed by the carboxyl bands at 1,725–1,690 cm$^{-1}$); the increase in carboxylate intensity (bands 1,630–1,590 and 1,425–1,380 cm$^{-1}$)
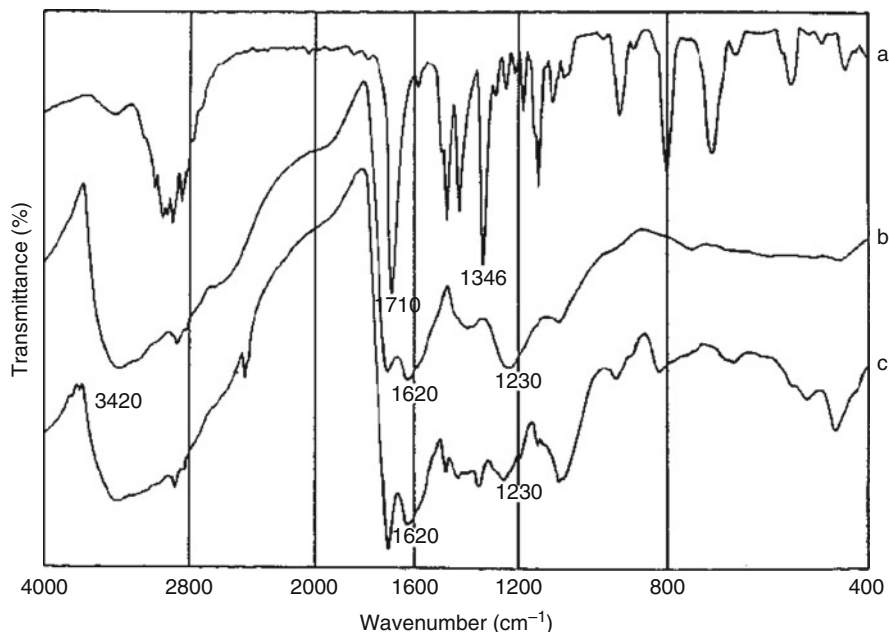
**Fig. 5.43** IR spectra of (**a**) chlorodimeform, (**b**) humic acids, and (**c**) humic acid–chlorodimeform complexes. Reprinted from Maqueda C, Morillo S, Pérez Rodríguez JL, Justo A (1990) Adsorption of chlordimeform by humic substances from different soils. Soil Sci 150:431–437. Copyright 1990 with permission of Wolters Kluwer Health

supports the conclusion that cation exchange is the mechanism of chlorodimeform adsorption on fulvic acid. The increase in intensity of the carboxyl band $(1,620 \text{ cm}^{-1})$ proves the formation of ionic bonding of the cationic chlorodimeform with the carboxyl group. Shifting of 1,346 and 1,719 $\text{cm}^{-1}$ bands to higher values is attributed by Maqueda et al. (1990) to the existence of fulvic acid–chlorodimeform complexes. The fact that the OH bond in the FA appears at a lower frequency in the FA complex and exhibits a different shape indicates that hydroxyl, carboxyl, and phenolic groups are also involved in the adsorption of chlorodimeform by fulvic acids. The strong reduction of the OH band $(1,230 \text{ cm}^{-1})$ indicates the presence of hydrogen bonds in the pesticide. IR spectra of the humic acid with chlorodimeform (Fig. 5.43c) indicate in general a similarity to the FA–chlorodimeform complexes with minor modification. As a consequence, the adsorption of chlorodimeform by soil-extracted HA is also a cation exchange process associated with charge-transfer and hydrogen bridge mechanisms. In both cases, the pesticide induces changes in the structural configuration of humic and fulvic acids.

*Diquat and paraquat* are two bipyridylium compounds used as nonselective contact herbicides normally applied as dibromide salts to weeds on the land surface. Burns et al. (1973) showed that the rate of adsorption of paraquat on soil organic matter appears to be controlled by the rate of diffusion within the adsorbent matrix. This may explain the potential hysteresis in desorption of paraquat adsorbed on

humic substances. The time to reach adsorption equilibrium is affected by the molecular complexities of the organic matter and by interactions between paraquat and the adsorbent matrices. Burns et al. (1973) did not detect any paraquat decomposition during paraquat adsorption by humic materials.

The inhibitory effect of salts on the strength of interaction between humic acid and paraquat or diquat depends also on the salt composition and herbicide concentration in the soil solution (Cserhati 1993). It was found that the lipophilicity values



**Fig. 5.44** Adsorption isotherms for paraquat and humic acid in the presence of KNO$_3$. All isotherms were determined at pH 6 and the point size reflects the experimental uncertainty. *Filled circle* 0 M KNO$_3$; *open circle* 0.01 M KNO$_3$; *filled square* 0.05 M KNO$_3$; *open square* 0.10 M KNO$_3$ (after Guy et al. 1980). Copyright 1980 Canadian Science Publishing or its licensors. Reproduced with permission
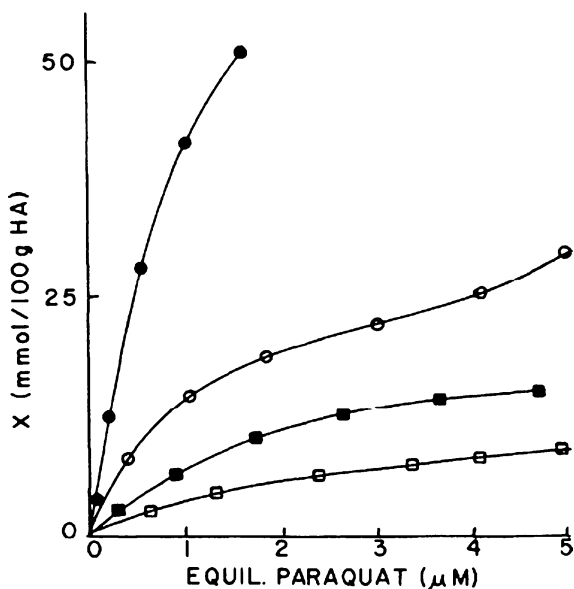


**Fig. 5.45** Adsorption isotherms for paraquat and humic acid at different values of solution pH. All isotherms were determined in solutions of 0.005 M KNO$_3$. *Filled circle* pH 8.2; *filled triangle* pH 6.2; *filled square* pH 2.5 (after Guy et al. 1980). Copyright 1980 Canadian Science Publishing or its licensors. Reproduced with permission
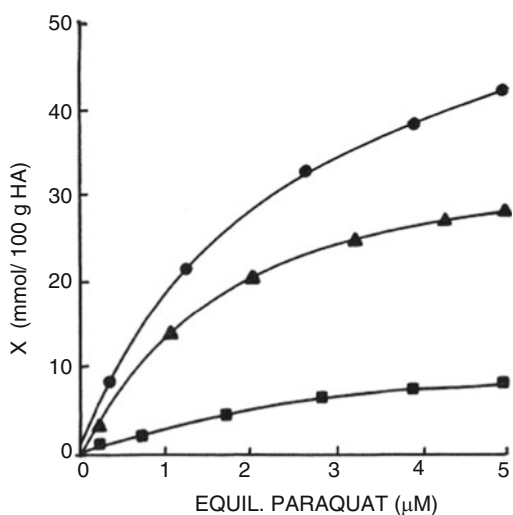
depend significantly on the concentration of humic acid and on the salt concentration and composition. The influence of divalent cations is considerably higher than that of monovalent cations, indicating a hydrophilic character of the interaction process. As may be seen from the results of Guy et al. (1980), the adsorption of paraquat on humic acid is affected by both solution ionic strength and pH (Figs. 5.44 and 5.45).

Results of desorption experiments reported by Guy et al. (1980) indicate that paraquat may be completely released from humic acids at very high ionic strength (0.10 M KNO$_3$) and acidity (pH 1). In nature, however, the soil–subsurface regime never reaches such a high acidity. Thus, paraquat residues adsorbed on humic substances will be retained, incorporated in the humic substances, thus changing their natural structural molecular configuration. Moreover, the HA–paraquat complexes are more susceptible to variation in pH and ionic strength than clay–paraquat complexes.

IR spectroscopy and potentiometric studies (e.g., Khan 1973a; Narine and Guy 1982) show that ion exchange is the dominant mechanism for adsorption of diquat
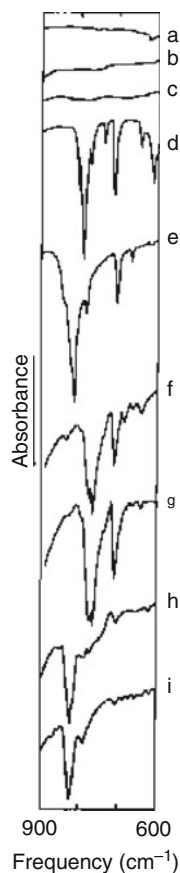


**Fig. 5.46** The infrared spectra in the region 600–900 cm$^{-1}$. (**a**) KBr; (**b**) HA; (**c**) FA; (**d**) diquat; (**e**) paraquat; (**f**) HA–diquat; (**g**) FA–diquat; (**h**) HA–paraquat; (**i**) FA–paraquat (after Khan 1973a)

HUMIC SUBSTANCE                    DIQUAT
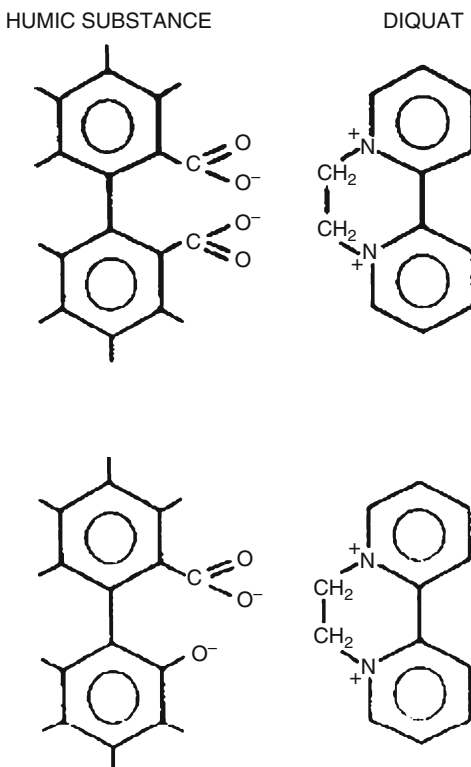


and paraquat by humic substances. In general, it may be shown that divalent cationic bipyridylium pesticides can react with two negatively charged sites on humic substances, such as COO⁻ groups or one COO⁻ together with a phenolate ion.

In the discussion that follows, we describe changes in the molecular configuration of humic substances resulting from the ionic exchange with diquat and paraquat. The mechanism of interaction between these herbicides with humic and fulvic acids is revealed by Khan (1973a), using IR. Evidence for the formation of charge-transfer $\pi$ region at 600–900 cm$^{-1}$ for the interacting materials is presented in Fig. 5.46. The strong bands at 792 cm$^{-1}$ in diquat and 815 cm$^{-1}$ in paraquat characterize the herbicides before interaction with humic substances. The interaction of paraquat with humic and fulvic acids leads to a shift of the umbrella band to 825 cm$^{-1}$, whereas the corresponding band in diquat shows a shift to 765 cm$^{-1}$. This supports the possibility of charge-transfer complexes between humic substances and diquat and paraquat. Khan (1973a) suggested that on charge-transfer complex formation with paraquat, the electrophilic nature of HA or FA molecules reduced the $\pi$-electron density of the aromatic nucleus, thus decreasing the ability of the carbon binding orbitals to follow the attached hydrogen atoms during a bending vibration. It should be pointed out that in the case of HA– and FA–paraquat interactions, the effective force constant for the vibration is not reduced significantly, and relatively higher out-of-plane C–H banding results. In contrast,

**Fig. 5.48** FTIR spectra
(900–700 cm$^{-1}$) of (**a**) HA,
(**b**) diquat, (**c**) HA–diquat,
(**d**) paraquat, and (**e**)
HA–paraquat (after Senesi
et al. 1995). Reprinted from
Senesi N, D'Orazio V, Miano
TM, Adsorption mechanism
of s-triazine and bipyridylium
herbicides on humic acids
from hop field soils.
Geoderma 66:273–283,
Copyright (1995), with
permission from Elsevier
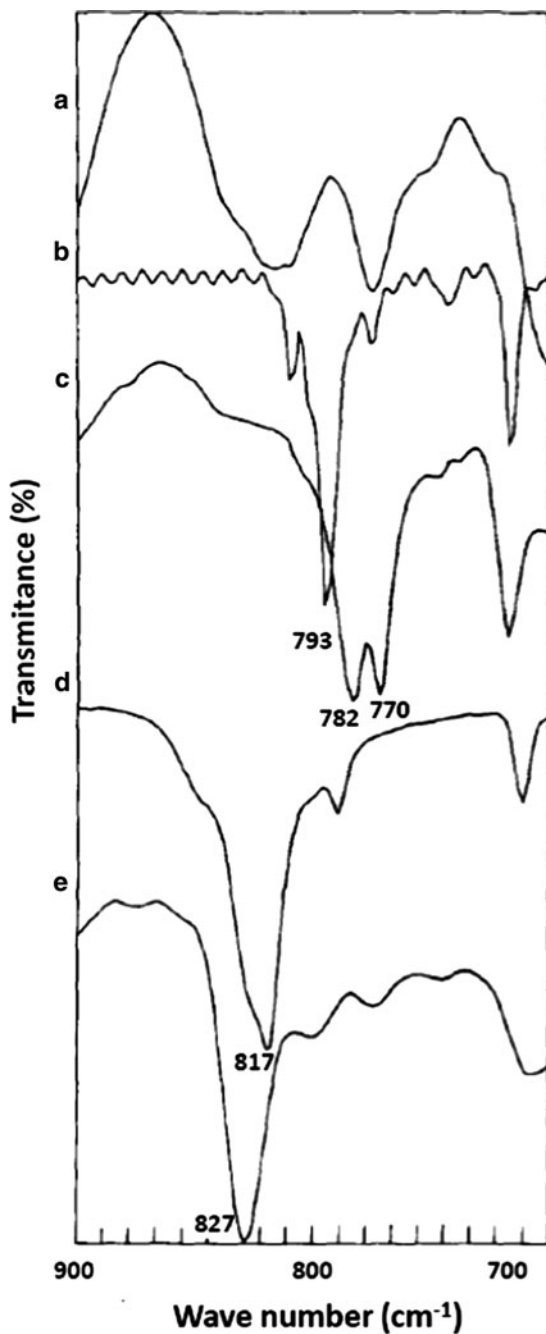
the HA– and HF–diquat molecules seem to be coplanar with the aromatic ring, leading to a full effect of resonance. The steric influence effect leads to a decrease of π-electrons in the ring, causing a lower out-of-plane C–H vibration frequency.

Figure 5.47 shows the pathway proposed by Senesi (1992) for the ionic bond between humic substances and bipyridylium compounds (e.g., diquat). In a subsequent study of molecular and mechanistic aspects of the diquat or paraquat adsorbed on humic acid in soils, compared to a native humic acid, Senesi et al. (1995) found that multiple binding mechanisms occur in the adsorption processes of those compounds. The humic acid functional group responsible for exchange properties is a carboxylic acid. The pH and ionic strength variation of paraquat indicate that the ion exchange reaction is the predominant interaction with the humic acids.

One mechanism considers that ionic bonds between carboxylate groups of humic acid and positively charged diquat and paraquat may occur through charge-transfer bonds between the electron acceptor of deactivated diquat and paraquat rings and complementary electron-donor structural moieties of the humic acid. Interpreting FTIR spectra (Fig. 5.48) of the pure humic acid in comparison to the spectra of humic acid after its interaction with diquat and paraquat, Senesi et al. (1995) showed that the herbicide induced modification in the molecular structure of the humic acids based on the following consideration "(a) a weak band appears at $3,088–3,068$ cm$^{-1}$ (aromatic C–H stretching of bipyridilium rings); (b) the relative intensity of the bands at about $1,720$ and $1,225$ cm$^{-1}$ (mainly carboxyl groups) decreases and that of the bands at $1,653–1,641$ and $1,385$ cm$^{-1}$ (carboxylate groups) increases; (c) two weak bands appear at about $1,570–1,500$ cm$^{-1}$ (aromatic C = N and C = C of the bipyridilium ring); (d) a new band appears at $782$ cm$^{-1}$ for HA–diquat and at $827$ cm$^{-1}$ for HA–paraquat, ascribed to the shift of diagnostic out-of-plane C–H vibration modes that are positioned in pure diquat at $793$ cm$^{-1}$, and in pure paraquat at $817$ cm$^{-1}$."

All of the above results showed a change in the humic acid configuration as a result of interactions with the charged pesticides.

# References

Adani F, Tambone F (2005) Long-term effect of sewage sludge application on soil humic acids. Chemosphere 60:1214–1221

Auboiroux M, Baillif P, Tourray JC, Bergaya F (1996) Fixation of Zn$^{2+}$ and Pb$^{2+}$ on Ca-montmorillonite in brine and dilute solutions: preliminary results. Appl Clay Sci 11:117–126

Barja BC, dos Santos Afonso (2005) Aminomethylphosphonic acid and glyphosate adsorption onto goethite: a comparative study. Environ Sci Technol 39:585–593

Barnhishel RI, Bertsch PM (1989) Chlorite and hydroxy-interlayered vermiculite and smectite. In: Dixon JB, Weed SB (eds) Minerals in the soil environment, SSSA Book Series 1, Madison, WI pp 730–789

Barrett KA, McBride MB (2005) Oxidative degradation of glyphosate and aminomethylphosphonate by manganese oxide. Environ Sci Technol 39:9223–9228

Barriuso E, Baer U, Calvet R (1992a) Dissolved organic matter and adsorption-desorption of difemuron, atrazine and carbetamide by soils. J Environ Qual 21:359–367

Barriuso E, Koskinen WC, Sorenson B (1992b) Modification of atrazine desorption during field incubation experiments. Sci Total Environ 123(124):333–344

Barriuso E, Benoit P, Dubus IG (2008) Formation of nonextractable (bound) residues in soil: magnitude, controlling factors and reversibility. Environ Sci Technol 42:1845–1854

Best JA, Weber JB, Weed SB (1972) Competitive adsorption of diquat, paraquat and $Ca^{2+}$ on organic matter and exchange resins. Soil Sci 144:444–450

Borggaard OK, Gimsing AL (2008) Fate of glyphosate in soil and the possibility of leaching to ground and surface waters: a review. Pest Manag Sci 64:441–456

Bostick BC, Vairavamurthy MA, Karthikeyan KG, Chorover J (2002) Cesium adsorption on clay minerals: an EXAFS spectroscopic investigation. Environ Sci Technol 36:2670–2676

Boyd SA, Sommers LE, Nelson W (1980) Change in the humic acid fraction of soil resulting from sludge application. Soil Sci Soc Am J 44:1179–1186

Brigatti MF, Corradini F, Franchini GC, Mazzoni S, Medici L, Poppi L (1995) Interaction between montmorillonite and pollutants from industrial waste-waters: exchange of $Zn^{2+}$ and $Pb^{2+}$ from aqueous solutions. Appl Clay Sci 9:383–395

Broadbent FE, Bradford GR (1952) Cation exchange groupings in the soil organic fracture. Soil Sci 74:447–457

Brown MJ, Burris DR (1996) Enhanced organic contaminant sorption on soil treated with cationic surfactants. Ground Water 34:734–744

Bunzl K (1974a) Kinetics of ion exchange in soil organic matter II. Ion exchange during continuous addition of $Pb^{2+}$ ions to humic acid and peat. J Soil Sci 23:43–56

Bunzl K (1974b) Kinetics of ion exchange in soil organic matter III. Differential ion exchange reactions of $Pb^{2+}$ ions in humic acids and peat. J Soil Sci 25:17–34

Bunzl K, Schmidt W, Sansoni B (1976) Kinetics of ion exchange in soil organic matter V. Adsorption-desorption of $Pb^{2+}$, $Cu^{2+}$, $Cd^{2+}$, $Zn^{2+}$ and $Ca^{2+}$ by peat. Eur J Soil Sci 27:32–41

Burns IG, Hayes MHB, Stacey M (1973) Effects of temperatures, time and adsorbate degradation on paraquat adsorption. Weed Res 13:67–78

Bussinelli D, Massaccesi L, Onofri A (2009) Evaluation of Pb and Ni mobility to groundwater in calcareous Urban soils of Ancona, Italy. Water Air Soil Pollut 201:185–193

Cellis R, Koskinen WC (1999) Characterization of pesticides desorption from soils by isotopic exchange. Soil Sci Soc Am J 63:1659–1666

Chorover J, DiChiaro MJ, Chadwick OA (1999) Structural charge and cesium retention in a chronosequence of tephritic soils. Soil Sci Soc Am J 63:169–177

Clapp CE, Hayes MHB, Simpson AJ, Kingery WI (2005) Chemistry of soil organic matter, Chap 2. In: Sparks DL, Tabatabai MA (eds) Chemical processes in soils, 2005. Soil Science Society of America, Madison, WI, pp 1–150

Coleman NT, Le Roux FH (1965) Ion exchange displacement of cesium from soil vermiculite. Soil Sci 99:243–248

Comans RNJ, Haller M, Depreter P (1991) Sorption of cesium on illite: non-equilibrium behavior and reversibility. Geochim Cosmochim Acta 55:433–440

Cornell RM (1993) Adsorption of cesium on minerals: a review. J Radioanal Nucl Chem 171:483–500

Crist RH, Martin JR, Chonko J, Crist DR (1996) Uptake of metals on peat moss: an ion exchange process. Environ Sci Technol 30:2456–2461

Cserhati T (1993) Interaction of diquat and paraquat with humic acid and the influence of salt concentration and pH on the strength of interaction. Fresnius J Anal Chem 345:541–544

Damonte M, Torres Sánchez RM, dos Santos Afonso M (2007) Some aspects of the glyphosate adsorption on montmorillonite and its calcined form. Appl Clay Sci 36:86–94

Dion HM, Harsh JB, Hill HH (2001) Competitive sorption between glyphosate and inorganic phosphate on clay minerals and low organic matter soils. J Radioanal Nucl Chem 249:385–390

Douay F, Pruvot C, Roussel H, Ciesielski FH, Proix N, Waterlot C (2008) Contamination of urban soils in an area of Northern France polluted by dust emissions of two smelters. Water Air Soil Pollut 188:247–260

Evangelou VP, Phillips RE (2005) Cation exchange in soils. In: Tabatabai MA, Sparks DL (eds) Chemical processes in soils. SSSA, Madison, WI, pp 343–410

Evans DW, Alberts JJ, Clark RA (1983) Reversible ion-exchange fixation of cesium-137 leading to mobilization from reservoir sediments. Geochem Cosmochim Acta 47:1041–1048

Francis CW, Brinkley FS (1976) Preferential adsorption of Cs-137 to micaceous minerals in contaminated freshwater sediment. Nature 260:511–513

Fuhr F, Ophoff H, Burauel P, Wanner U, Haider K (1998) Modification of definition of bound residues. In: Fuhr F, Phoff H (eds) Pesticide bound residues in soils. Wiley, Weinheim, pp 175–176

Gamble DS, Schnitzer H, Kerndorff H, Lanforf CH (1983) Multiple metal ion exchange equilibria with humic acid. Geochim Cosmochim Acta 47:1311–1323

Gimsing AL, Borggaard OK (2002) Competitive adsorption and desorption of glyphosate and phosphate on clay silicates and oxides. Clay Miner 37:509–515

Glass RL (1987) Adsorption of glyphosate by soils and clay minerals. J Agric Food Chem 35:497–500

Gorman-Lewis DJ, Fein JB (2004) Experimental study of the adsorption of an ionic liquid onto bacterial and mineral surfaces. Environ Sci Technol 38:2491–2495

Graham DC (1947) The electrical double layer and the theory of electro capillarity. Chem Rev 41:441–449

Grover R (1971) Adsorption of picloram on soil colloids and various other adsorbents. Weed Sci 19:417–418

Guy RD, Narine DR, de Silva S (1980) Organocation speciation I. A comparison of the interactions of methylene blue and paraquat with bentonite and humic acid. Can J Chem 58:547–554

Hird AB, Rimmer DL, Livens FR (1996) Factors affecting the sorption and fixation of cesium ion on organic soils. Eur J Soil Sci 47:97–104

Holsen TM, Taylor ER, Seo YC, Anderson PR (1991) Removal of sparingly soluble organic chemicals from aqueous solutions with surfactant-coated ferrihydrite. Environ Sci Technol 25:1585–1589

Jackson KS, Jonasson IR, Skippen GB (1978) The nature of metals-sediment-water interactions in freshwater bodies, with emphasis on role of organic matter. Earth Sci Rev 14:97–146

Jacquat O, Voegelin A, Kretzschmar R (2009) Local coordination of Zn in hydroxy-interlayered minerals and implications for Zn retention in soils. Geochim Cosmochim Acta 73:348–363

Jozja N, Baillif P, Touray JC, Muller F, Clinard C (2006) Incidence of lead uptake on the microstructure of a (Mg, Ca)-bearing bentonite (Prrenjas, Albania). Eur J Miner 18:361–368

Kau PMH, Smith DW, Bonning P (1997) Fluoride retention by kaolin clay. J Contam Hydrol 28:267–288

Kerndorff H, Schnitzer H (1980) Sorption of metals on humic acid. Geochim Cosmochim Acta 28:1701–1708

Khan SU (1973a) Interaction of humic substances with bipyridylium herbicides. Can J Soil Sci 53:199–204

Khan SU (1973b) Equilibrium and kinetic studies of the adsorption of 2,4-D and pichloram on humic acid. Can J Soil Sci 53:429–434

Khiry AH, Davies G, Ibrahim HZ, Ghabbour EA (1996) Adsorption of aqueous nucleobases, nucleosides and nucleotides on compost-derived humic acid. J Phys Chem 100:2410–2416

Kim Y, Kirkpatrick RJ, Cygan RT (1996) Cs-133 NMR study of cesium on the surfaces of kaolinite and illite. Geochim Cosmochim Acta 60:4059–4074

Knight BAG, Denny PJ (1970) The interaction of paraquat with soil: adsorption by expanding lattice clay mineral. Weed Res 10:40–48

Knight BAG, Tomlinson TE (1967) The interaction of paraquat with mineral soils. J Soil Sci 18:233–243

Lee SY, Cho WJ, Hahn PS, Lee M, Lee YB, Kim KJ (2005) Microstructural changes of reference montmorillonites by cationic surfactants. Appl Clay Sci 30:174–180

Lees H (1948) The copper-retaining powers of different cacao soils (1048). Biochem J 43:181–213

Legally G (1982) Layer charge heterogeneity in vermiculites. Clays Clay Miner 30:215–222

Legally G (1994) Layer charge determination by alkylammonium ions. In: Memut AR (ed) Layer charge characteristics of 2:1 silicate clay minerals. The Clay Mineral Society, Boulder, pp 2–46

Li H, Teppen BJ, Laird DA, Johnstone CT, Boyd AS (2004) Geochemical modulation of pesticide sorption on smectite clay. Environ Sci Technol 38:5393–5399

Mamy L, Barriuso E (2007) Desorption and time-dependent sorption of herbicides in soils. Eur J Soil Sci 58:174–187

Mamy L, Gabrielle B, Barriuso E (2008) Measurement and modelling of glyphosate fate compared with that of herbicides replaced as a result of the introduction of glyphosate-resistant oilseed rape. Pest Manag Sci 64:262–275

Maqueda C, Morillo S, Pérez Rodríguez JL, Justo A (1990) Adsorption of chlordimeform by humic substances from different soils. Soil Sci 150:431–437

Matzke M, Thiele K, Müller A, Filser J (2009) Sorption and desorption of imidazolium based ionic liquids in different soil types. Chemosphere 74:568–574

McBride MB (1989) Reactions controlling heavy metals solubility in soils. Adv Soil Sci 10:1–47

McConnell JS, Hossner LR (1985) pH-dependent adsorption isotherms of glyphosate. J Agric Food Chem 33:1075–1078

McConnell JS, Hossner LR (1989) X-ray diffraction and infrared spectroscopic studies of adsorbed glyphosate. J Agric Food Chem 37:555–560

McGeorge WT (1930) The base exchange properties of organic matter in soils. Ariz Agr Exp Sta Tech Bull 30:181–213

McKinley JP, Zeissler JC, Zaxhara JM, Lindstrom RM, Serne RJ, Schaef HT, Orr DR (2001) Distribution and retention of $^{137}$Cs in sediments at Hanford Site Washington. Environ Sci Technol 35:3433–3441

Mitchell J (1932) The origin nature and importance of soil organic constituents having base exchange properties. J Am Soc Agron 24:256–273

Morillo E, Undabeytia T, Maqueda C (1997) Adsorption of glyphosate on the clay mineral montmorillonite: effect of Cu(II) in solution and adsorbed on the mineral. Environ Sci Technol 31:3588–3592

Mrozik W, Jungnickel C, Ciborowski T, Pitner WR, Kumirska J, Kackzinski Z, Stepnowski P (2009) Predicting mobility of alkylmidazolium ionic liquids in soils. J Soil Sediment 9:237–245

Narine DR, Guy RD (1982) Binding of diquat and paraquat to humic acids in aquatic environments. Soil Sci 133:356–363

Ogawa M, Kuroda K (1997) Preparation of inorganic-organic nanocomposites through intercalation of organoammonium ions into layer silicates. Bull Chem Soc Jpn 70:2593–2618

Pateiro-Moure M, Pérez-Novo C, Arias-Estévez M, López-Periago E, Martínez-Carballo E, Simal-Gándara J (2007) Influence of copper on the adsorption and desorption of paraquat, diquat and difenzoquat in vineyard acid soils. J Agric Food Chem 55:6219–6226

Peris M, Recatala L, Mico C, Sanchez R, Sanchez J (2008) Increasing the knowledge of heavy metal contents and sources in agricultural soils of the European Mediterranean region. Water Air Soil Pollut 192:25–37

Quirk JP, Posner AM (1975) Trace element adsorption by soil minerals. In: Nicholas DJ, Egan AR (eds) Trace elements in soil plant animal system. Academic, New York, pp 95–107

Roig M, Vidal M, Rauret G, Rigol A (2007) Prediction of radionuclide aging in soils from the Chernobyl and Mediterranean areas. J Environ Qual 36:943–952

Rueppel ML, Brightwell BB, Schaefer J, Marvel J (1977) Metabolism and degradation of glyphosate in soil and water. J Agric Food Chem 25:517–528

Rytwo G, Tropp D, Serban C (2002) Adsorption of diquat, paraquat and methyl green on sepiolite: experimental results and model calculations. Appl Clay Sci 20:273–282

Saha UK, Taniguchi S, Sakarai K (2001) Adsorption behavior of cadmium, zinc and lead on hydroxyaluminum and hydroxyaluminosilicate-montmorillonite complexes. Soil Sci Soc Am J 65:694–703

US Salinity Lab Staff (1954) Diagnosis and improvement of saline and sodic soils. Agri Hand 60 USDA Gov Print Office, Washington, DC

Saltzman S, Yaron B (eds) (1986) Pesticides in soils. Van Nostrand Reinhold Co, New York, p 374

Sawhney BL (1964) Sorption of cesium from diluted solutions. Soil Sci Soc Am Proc 29:25–28

Sawhney BL (1972) Selective sorption and fixation of cations by clay minerals: a review. Clays Clay Miner 20:93–100

Schlegel ML, Charlet L, Manceau A (1999) Sorption of metal ions on clay minerals: II. Mechanism of Co sorption on hectorite at high and low ionic strength and impact on the sorbent stability. J Colloid Interface Sci 220:392–445

Schnitzer M (1978) Humic substances chemistry and reactions. In: Schnitzer M, Khan SU (eds) Soil organic matter. Elsevier, Amsterdam, pp 1–64

Schnitzer M (1994) A chemical structure for humic acid. In: Senesi N, Miano TMI (eds) Humic substances in the global environment and implications on human health. Elsevier, Amsterdam, pp 57–69

Schnitzer M, Khan SU (1972) Humic substances in the environment. Marcel Dekker, New York

Senesi N (1992) Metal-humic substances complexes in the environment. Molecular and mechanistic aspects by multiple spectroscopic approach, (Chapter 16). In: Adriano Domy DC (ed) Biogeochemistry of trace metals. CRC, Boca Raton, FL, pp 425–491

Senesi N, Chen Y (1989) Interactions of toxic organic chemicals with humic substances. In: Gerstl Z, Chen Y, Mingelgrin U, Yaron B (eds) Toxic organic chemicals in porous media. Springer, Heidelberg, pp 37–90

Senesi N, Testini C (1982) Physico-chemical investigations of interaction mechanisms between s-triazine herbicides and soil humic acid. Geoderma 28:129–146

Senesi N, Testini C, Miano TM (1987) Interaction mechanisms between humic acids of different origin and nature and electron donor herbicides: a comparative IR and ESR study. Org Geochem 11:25–30

Senesi N, D'Orazio V, Miano TM (1995) Adsorption mechanism of s-triazine and bipyridylium herbicides on humic acids from hop field soils. Geoderma 66:273–283

Shoval S, Yariv S (1979) The interaction between roundup (Glyphosate) and montmorillonite I. Infrared studies of the sorption of glyphosate by montmorillonite. Clays Clay Miner 26:19–28

Smith AE, Aubin AJ (1993) Degradation of $^{14}$C-glyphosate in Saskatchewan soils. Bull Environ Contam Toxicol 50:499–505

Spaccini R, Sannino D, Piccolo A, Fagnano M (2009) Molecular changes in organic matter of a compost-amended soil. Eur J Soil Sci 60:287–296

Sposito D (1989) The chemistry of soils. Oxford University Press, New York

Sposito G, Skipper NT, Dutton R, Park SH, Soper AK (1999) Surface chemistry of clay minerals. Proc Nat Acad Sci USA 96:3358–3364

Stepnowski P, Mrozik W, Nichthauser J (2007) Adsorption of alkylimidazolium and alkylpyridinium ionic liquids onto natural soils. Environ Sci Technol 41:511–516

Stern O (1924) Zur theorie der electrolitischen doppelschiest. Z Electrochem 30:508–516

Stevenson FJ, Butler JHA (1965) Chemistry of humic acids and related pigments. In: Eglinton G, Murphy MTG (eds) Organic geochemistry. Springer, Heidelberg, pp 534–557

Strawn DG, Sparks DL (1999) The use of XAFS to distinguish between inner- and outer-sphere lead adsorption complexes on montmorillonite. J Colloid Interface Sci 216:257–269

Strawn DG, Scheidegger AM, Sparks DL (1998) Kinetics and mechanisms of Pb(II) sorption and desorption at the aluminum oxide-water interface. Environ Sci Technol 32:2596–2601

Sullivan JD, Feldbeck GT (1968) A study of the interaction of s-triazines herbicides with humic acids from three different soils. Soil Sci 206:42–50

Thomas GW, Yaron B (1968) Adsorption of sodium from irrigation water by four Texas soils. Soil Sci 106:213–220

van Bladel R, Laudelout H (1967) Apparent irreversibility of ion exchange reactions in clay suspensions. Soil Sci 140:134–137

Vega FA, Covelo EF, Andrade ML (2009) Hysteresis in the individual and competitive sorption of cadmium, copper and lead by various soil horizons. J Colloid Interface Sci 331:312–317

Von Wiren-Lehr S, Komossa D, Glassgen WE, Sanderman H, Scheunert I (1997) Mineralization of $^{14}$C glyphosate and its plants – associated residues in arable soils originating from different farming systems. Pest Sci 51:436–442

Weber JB, Weed SB (1968) Adsorption and desorption of diquat and paraquat by montmorillonitic and kaolinitic clay minerals. Proc Soil Sci Soc Am 32:485–487

Weber JB, Perry PW, Upchurch RP (1965) The influence of temperature and time on the adsorption of paraquat, diquat, 1,4D and prometone by clays, charcoal and an anion exchange resin. Proc Soil Sci Soc Am 29:678–688

Xu S, Boyd SA (1995) Cationic surfactant adsorption by swelling and nonswelling layer silicates. Langmuir 11:2508–2514

Yaron-Marcovich D, Chen Y, Nir S, Prost R (2005) High resolution electron microscopy structural studies of organo-clay nanocomposites. Environ Sci Technol 39:1231–1239

Zachara JM, Smith SC (1994) Edge complexation reactions of cadmium on specimen and soil-derived smectite. Soil Sci Soc Am J 58:762–769

Zeien H, Brummer GW (1989) Chemische Extraktionen zur bestimmung von scwermetalbin-dungsformen in boden Mitt Dtsch Bodenkundl. Ges 59:505–510

Zhang PC, Brady PV, Arthur SE, Zhou WQ, Sawyer D, Hesterberg DA (2001) Adsorption of barium(ii) on montmorillonite: an EXAFS study. Colloids Surf A-Physicochem Eng Aspects 190:239–249

Zheng JF, Zhang XH, Lq L, Pan CX (2007) Effect of different long-termnfertilization on C mineralization and production of $CH_4$ and $CO_2$ under anaerobic incubation from bulk samoles and particle size fraction. Agric Ecosyst Environ 120:129–138

Zhou P, Pan GX, Spaccini R, Piccolo A (2010) Molecular changes in particulate organic matter (POM) in a typical Chinese paddy soil under different long term fertilizer treatments. Eur J Soil Sci 61:231–242

# Chapter 6
# Irreversible Alteration of Soil–Subsurface Matrix Induced by Contaminant Binding

In the previous chapter, we discussed irreversible adsorption of polar contaminants, and induced changes in clay mineral phases through ionic exchange pathways. However, as a function of the properties of the adsorbent and the environmental aqueous solution, some contaminants may be adsorbed either by cation exchange or by chemical or physical binding. Pollutants in the bound state behave differently from freely dissolved molecules, and as a consequence, they act differently on the adsorbing matrix. We therefore separate the discussion as contaminant adsorption via ion exchange (Chap. 5) and as a result of binding processes.

This chapter describes changes occurring in the soil mineral and organic phases of the Critical Zone as a result of contaminant binding. While in Chap. 5 we surveyed contaminant retention by exchange, mainly on clay and humic substances, we discuss in this chapter the role of iron oxides as potential contaminant adsorbents.

## 6.1 Binding of Contaminants on Mineral and Organic Solid Phases: An Introductory Consideration

In Chap. 4, we discussed at length the chemisorption of nonionic contaminants on clay minerals and humic substances. Enthalpy- and entropy-related forces lead to the retention of these contaminants on the soil–subsurface solid phase. Enthalpy-related forces induce binding between the adsorbing surface and solutes via various pathways, including hydrogen bonding, ligand exchange, protonation, $\pi$ bonds, and London-van der Waals interactions. Entropy-related adsorption forces lead to hydrophobic sorption interactions following partitioning between nonpolar organics and the polar aqueous phase. In this case, retention onto hydrophobic surfaces occurs through dispersion forces. The major feature of hydrophobic sorption is the weak interaction between the solute and the solvent.

Usually, contaminants are disposed on the land surface as complex mixtures, and under these conditions, their retention on the soil–subsurface solid phase is

controlled by a number of different processes acting simultaneously. As an example, we may assume the simultaneous presence of organo-metal complexes, organic solvents, and an aqueous solution involving a multiphase interaction with the solid phase. In such a case, Rao et al. (1989) suggested that an approach based on the predominance of solvophobic interactions may be considered for predicting sorption of hydrophobic organic chemicals from mixed solvents.

In addition to clay minerals and humic substances, contaminants with non-exchangeable functional groups may be adsorbed on other inorganic constituents of the soil–subsurface solid phase, such as Al, Fe, Mn, and Si oxide and hydroxides. McBride (1989, and references therein) show that the chemisorption of these contaminants may lead to (1) indirect release of as many as two $H^+$ for each $M^{2+}$ ion adsorbed; (2) a high degree of specificity shown by oxides for particular metals; (3) changes in surface properties of the oxides; and (4) increased surface positive charge of oxides. Additional evidence of oxide interaction is due to the replacement of $H_2O$ coordinated to the metal by another ligand, thus altering the crystal field-splitting energy of the d-orbitals as demonstrated by $Cu^{2+}$ bound on Al hydroxide (Fig. 6.1).

Various oxides have the ability to chemisorb metals; for example, $Mn^{2+}$ oxide is characterized by its unusually high selectivity for metals such as $Pb^{2+}$, $Co^{2+}$, $Cu^{2+}$, and $Ni^{2+}$ (Golden et al. 1986). Direct evidence of the nature of chemisorbed metal ions on oxides has been obtained by electron spin resonance (ESR) of $Cu^{2+}$ on titanium dioxide (Bleam and McBride 1986). The sorption curves (Fig. 6.2) reveal
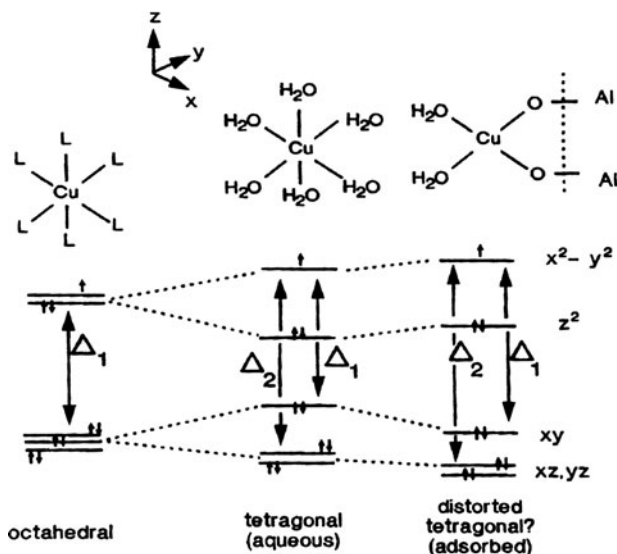


**Fig. 6.1** Diagram of d-orbital energy levels for octahedral $Cu(H_2O)_6^{2+}$, tetragonal $Cu(H_2O)_6^{2+}$, and oxide-bound $Cu^{2+}$ on Al-hydroxide (after McBride 1989)

**Fig. 6.2** $Cu^{2+}$ sorption on $TiO_2$ suspension as a function of pH and at three levels of $Cu^{2+}$ addition (equivalent to 0.5, 1.0, and 4.0 monolayers at the surface) (after McBride 1989)
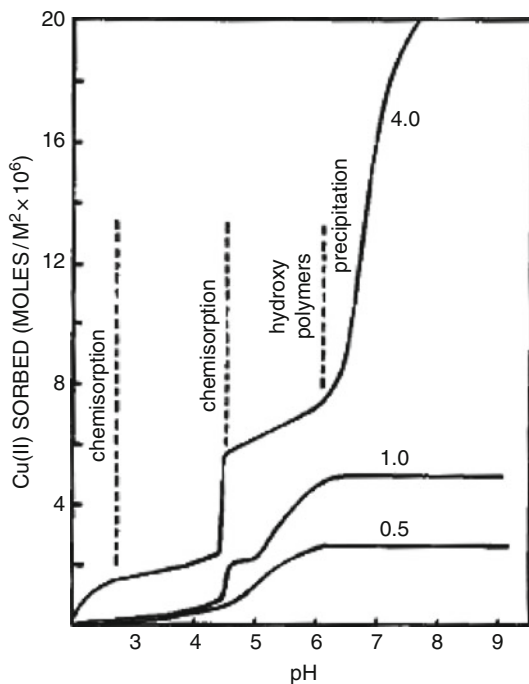


two distinct adsorption events as a function of pH, showing that $Cu^{2+}$ chemisorbs strongly at a low pH to sites that retain it by a bidentate mechanism, and that $Cu^{2+}$ forms a weaker complex with single Ti–OH groups at a higher pH.

According to chemisorption theory, desorption of a contaminant always requires an activation energy ($E_d*$) greater than the activation energy necessary for its adsorption ($E_a*$) on a mineral or organic solid phase, according to $E_d* = E_a* + \Delta H$, where $\Delta H$ is higher at low chemisorption levels. An energy diagram (Fig. 6.3) for the adsorption of a metal M at anion surface site $A^-$ illustrates this process.

Overall, the forces involved in adsorption can range from weak, physical, van der Waals (e.g., partitioning), and electrostatic (e.g., ion exchange) to chemical complexation. When adsorption occurs in an inner-sphere site, we are dealing with an inner-sphere complexation that may involve a ligand exchange mechanism, covalent bonding, hydrogen bridges, and steric or orientation effects. In this case, the applicability of the reversible mass action relationship becomes questionable and the contaminant adsorption may be potentially irreversible.

Further in-depth discussions of pollutant chemisorption on subsurface components can be found in the classical review of Mortland (1970); in the reviews of Calvet (1989), Hasset and Banwart (1989), McBride (1989), Hayes and Mingelgrin (1991), and Delle Site (2001); and in a number of books (e.g., Theng 1974; Greenland and Hayes 1981; Saltzman and Yaron 1986; Yaron et al. 1996; Schwarzenbach and Gshwend 2003; Berkowitz et al. 2008).

**Fig. 6.3** Energy diagram for
the adsorption of metal, M, at
anion surface sites,
$A^-$ (after McBride 1989)
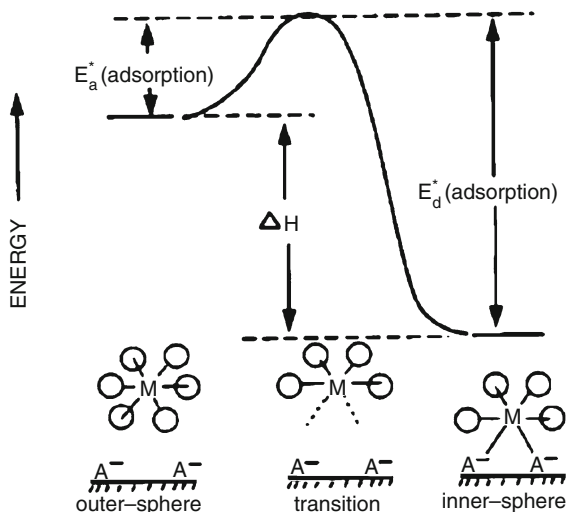


## 6.2   Induced Changes in Mineral and Organic Soil–Subsurface Constituents Following Contaminant Binding

Inorganic adsorbents that favor binding of inorganic and organic contaminants in the solid phase of the Critical Zone may comprise metal oxides, hydroxides, amorphous aluminum silicates, and broken edges of clay minerals. Humic substances comprised of humic and fulvic acids form the main organic adsorbent of contaminants in the soil and subsurface system, which may be changed as result of chemical contamination. Below, we illustrate the diverse effects of contaminants on these main soil and subsurface constituents as affected by environmental conditions.

### 6.2.1   Iron Oxide and Hydrous Oxide Sorbents

Nanoparticulate iron oxides comprising minerals such as goethite, hematite, and ferrihydrite are important constituents of the soil–subsurface system (Waychunas et al. 2005, and references therein). Iron is one of the important earth transition metals, which may be leached from minerals by weathering or by biologically induced processes; it forms iron oxide phases through oxidation (White and Brantley 1995). Here, we discuss several cases of iron oxidation and potential formation of nanoparticulate iron oxide minerals in the soil–subsurface environment. Throughout the presentation below, we use the abbreviation "FeOX" for iron oxide (Waychunas et al., 2005).

Oxidation of dissolved iron is one of the main reactions that produces iron oxide phases in the soil–subsurface environment. The high solubility of leached Fe(II) in an anaerobic medium drops from 0.5 M in hexa-aqua species to $10^{-12}$ M when Fe(II) is oxidized to hexa-aqua Fe(III) or to a polymerized form (Baes and Mesmer 1976). Nitrate may also induce iron oxidation under anaerobic conditions when this process is coupled to nitrate reduction and the FeOX formed is an oxyhyroxide (Straub et al. 1996). Because nitrate reduction takes place in the Critical Zone where iron oxidation in the microaerophilic environment may be catalyzed by microorganisms, we focus more on this pathway.

Chan et al. (2004) used spectromicroscopy to show that microbially generated iron oxyhydroxide (FeOOH) filaments contain polysaccharides. Mineralization occurs when extracellular polysaccharides come into contact with oxidized iron. This provides an explanation for the formation of akaganeite pseudo-single crystals – an iron(III) oxide-hydroxide/chloride mineral with the formula $Fe^{3+}O(OH,Cl)$ – with an aspect ratio of about 1,000:1. Akaganeite pseudo-single crystals are about 2–3 nm in diameter and thousands of nanometers in length. Akaganeite crystals of biological origin display microstructure and morphology similar to that of nonbiological akaganeite crystals. Chan et al. (2004) inferred that cells extrude the polysaccharide strand to localize FeOOH precipitation in proximity to the cell membrane, to harness the proton gradient for energy generation. Oxidation of iron outside the cell surface is coupled to reduction of oxygen and consumption of a proton at an oxidase on the inside of the cytoplasmic membrane. The oxidation of each $Fe^{2+}$ in solution generates two protons, acidifying the microenvironment adjacent to the membrane. Proton generation localized near the cell wall enhances the proton motive force, increasing the energy-generating potential of the cell.

A more specific case of FeOX generation is the oxidation of pyrite ($FeS_2$), which originates from pyrite-rich rocks associated with ore deposits. Oxidation of sulfide produces solutions with low pH (~2) and high concentrations of aqueous Fe(II) and Fe(III) solutions. The Fe(II) is oxidized by mixing with oxygenated surface water or by catalytic microbial activity (Edwards et al. 2000), which may produce large quantities of FeOX nanoparticles. Fe(III) phases which form from solution start as small clusters of octahedral Fe and evolve to large polymeric sizes when a decrease in surface energy provides the driving force for aggregate or crystal formation (Combes et al. 1989). In general, nano- to micro-size particles or aggregates of small particles are metastable in comparison to particles larger than a few microns.

In the Critical Zone, reduction of minerals such as ferrihydrite, goethite, and other FeOX phases can couple microorganisms to the oxidation of organic carbon. Fe(II) can be sequestered in FeS phases or be free to be oxidized. Waychunas et al. (2005) considered that such nanoparticulates exhibit properties very different than that of larger crystallites, given their relatively large surface area (e.g., $50\text{–}200 \, \mathrm{m^2 \, g^{-1}}$ for ferrihydrite), and thus their large reactivity potential. Also, FeOX may exhibit contracted or expanded surface layers (e.g., oxide nanocrystals) compared to bulk phases. The sorption properties of FeOX are also different from those of natural crystallites in terms of their irregular surface morphology

(e.g., curvature), quantum confinement effects, surface energy, and phase stability or surface complexation geometry.

We extend the discussion here on FeOx natural nanoparticles by noting the structure of ferrihydrite established by Michel et al. (2007). Ferrihydrite, an iron oxide with a composition commonly given as $Fe_5HO_8 \cdot 4H_2O$, is a natural nanomaterial that may be considered a typical precursor of more stable iron oxide minerals such as goethite or hematite. It can act as a strong sorbent for chemical contaminants like heavy metals or arsenate. Michel et al. (2007) elucidated the structure of this nanocrystalline material, uncovering the atomic arrangement by real-space modeling of the pair distribution function (PDF) derived from Fourier transformation of the total X-ray scattering. The PDF for "ideal" ferrihydrites is consistent with a single phase structure containing 20% tetrahedrally and 80% octahedrally coordinated iron, and having a basic structural motif (Fig. 6.4).

Adsorption–desorption of contaminants on FeOX may exhibit strong hysteresis due to effects caused by various surface processes, such as precipitation, catalysis, or internal sequestration where post-sorption oriented aggregation leads to the trapping of sorbed contaminant species within bound crystallites (Banfield et al. 2000). The reactivity properties of a nanoparticulate FeOX may be altered by incorporation of impurity atoms that originate from chemical contamination. For example, a low concentration of Zn (e.g., 0.2 mol %) incorporated in pyrite drastically changed the mineral photochemical behavior of pyrite without inducing a change in its structure (Buker et al. 1999).

In general, the ability of a mineral to host impurities depends on the structural characteristics of the solid, the size and the charge discrepancy between the impurity and the intrinsic ion, and the response of the structure to the perturbation associated with ion incorporation (Cornell and Schwertmann 2003; Gilbert and Banfield 2005). Under natural environmental conditions, a contaminant may be retained irreversibly within nanoparticulate iron oxide minerals during a "lifetime period," and be released only after nanoparticulate dissolution. Contaminants retained within the FeOX natural structure and/or properties are considered as mineral "impurities" that can be detected by transmission electron microscopy (TEM) as layers or clusters. These layers or clusters preserve the contaminant structure but have a local composition exceeding the bulk solubility of the adsorbed species. Natural growth of FeOX nanoparticulates during aging, which occurs through the oriented attachment of individual nanoparticles (Waychunas et al. 2005, and references therein), may control the incorporation of contaminants such as heavy metals, with consequences on irreversible retention.

Before discussing contaminant-induced modification of FeOX, we summarize the results of Waychunas et al. (2005) concerning changes occurring in iron oxide nanoparticulate features during aging. FeOX nanoparticulates with an initial size of 3–5 nm and oblong shape were found to aggregate after approximately 30 days of aging, exhibiting an abundance of particles with rod-like morphology (Fig. 6.5).

Aging can be a result of a phase transition process when a progressive and continuous increasing degree of structural order may be observed over time. Figure 6.6 shows K-edge extended X-ray absorption fine structure spectroscopy

**Fig. 6.4**  Polyhedral representation of the ideal ferrihydrite structure. The central $FeO_4$ tetrahedra are surrounded by 12 $FeO_6$ octahedra (after Michel et al. 2007). From Michel FM, Ehm L, Antao SM, Lee PL, Chupas PJ, Liu G, Strongin DR, Schonen MAA, Phillips BL, Parise JB (2007) The structure of ferrihydrite, a nanocrystalline material. Science 316:1726–1729. Reprinted with permission from AAAS
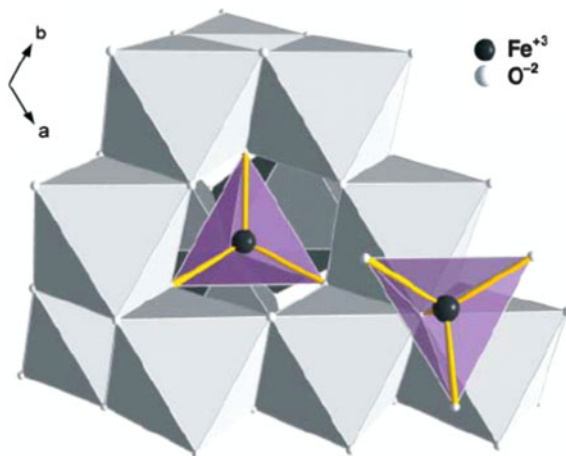


**Fig. 6.5**  High-resolution (×500,000) transmission electron microscopy (TEM) images of synthetic goethite nanoparticles that aggregated from more oblong shapes. (**a**) Two such particles connected through oriented attachment as viewed by their lattice fringes, (**b**) 3–4 nanoparticles have aggregated to create a different, more elongated morphology compared to the initial particles. (**c**) After 33 days of aging, many rods have formed, although many of the initial oblong nanoparticles remain (after Waychunas et al. 2005)
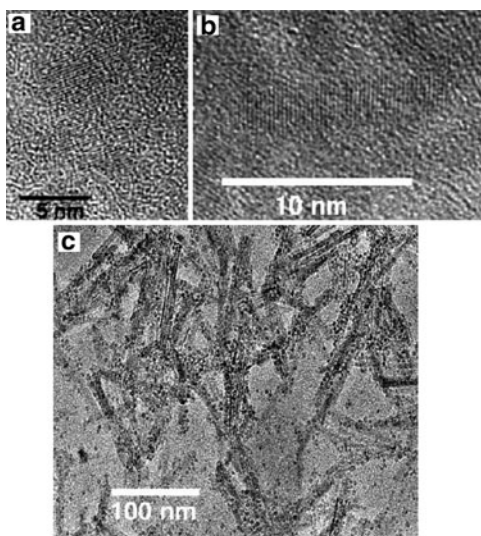


(EXAFS) spectra and Fourier transformation spectra showing an increasing intensity of the second-neighbor peaks consistent with an increase in Fe–Fe atom distance. Waychunas et al. (1993) considered that Fe–O–Fe polymerization occurred during the aging process. The "youngest" ferrihydrite exhibited a small degree of polymerization, with a structure characterized by very short single octahedral or dioctahedral chains having minimal cross-linking; with aging, the dioctahedral chains were abundant and cross-linking occurred. After seven weeks, the Fe–Fe distances were closer to those of goethite. Waychunas et al. (2005) interpreted this trend to be a result of the increase in the proportion of Fe atoms and a decline in the proportion of surface-terminated Fe atoms, with aging, which led from poorly ordered ferrihydrite to goethite.
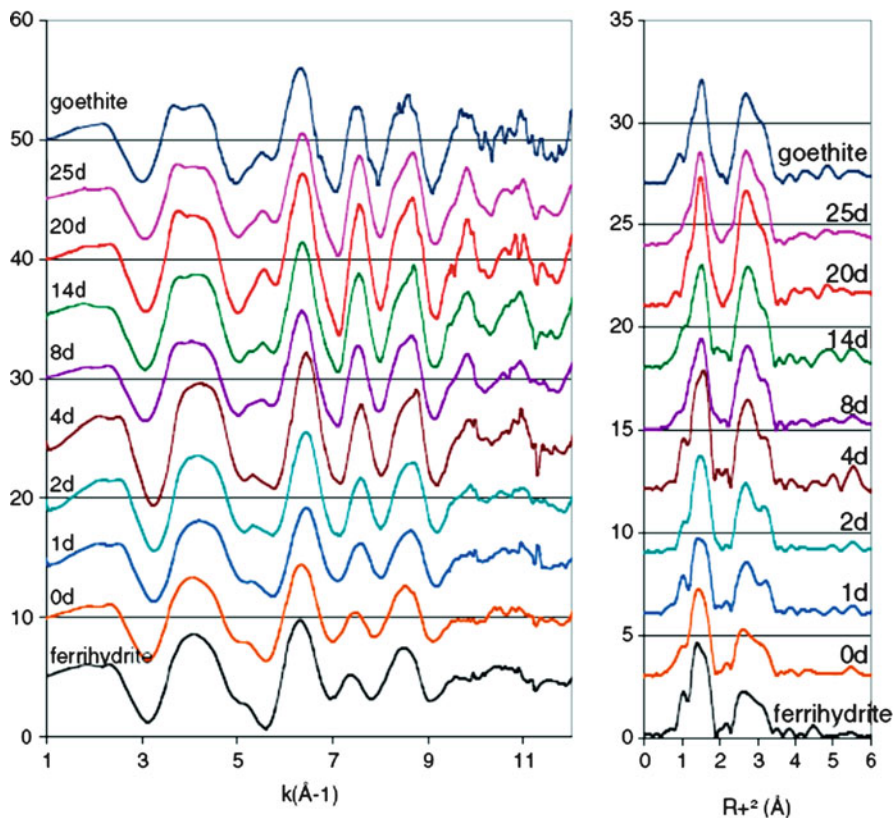
**Fig. 6.6** Fe K-edge EXAFS spectra and Fourier transformation spectra showing an increasing degree of structural order over time, indicating the transformation of ferrihydrite to goethite (after Waychunas et al. 2005)

Heavy metals and metalloids of anthropogenic origin may, after reaching the soil–subsurface environment, complex by organic or inorganic ligands. Precipitated metal–ligand compounds or metal–ligand complexes are adsorbed on iron oxide and hydrous oxide surfaces from the surrounding water solution. Several examples of metal and metalloid contaminant effects on iron oxides and hydrous oxides on earth materials follow next.

Arsenic contaminants may be found in the soil–subsurface environment in two forms (As(III), As(V)) as arsenite, $AsO_3^{3-}$, and arsenate, $AsO_4^{3-}$. Arsenate acts as an analog of phosphate uncoupling phosphorylation in the glycolytic conduit, while arsenite has a high affinity for the sulfhydryl groups of amino acids. Iron oxides have been shown by many researchers to have a high affinity for both arsenate and arsenite, goethite being the most abundant iron oxide found in the soil–subsurface environment; therefore, almost all of the studies carried out on As–FeOX interactions involved goethite.

Early information at a molecular level on arsenate adsorption on ferrihydrite using EXAFS showed the presence of a dominant bidentate-binuclear surface complex (Waychunas et al. 2005) of a type similar to that observed for phosphate. Later studies using EXAFS (Fendorf et al. 1997) defined the local coordination environment of arsenate on goethite surfaces. Based on the oxyanion–Fe distance, it was concluded that three different surface complexes exist on goethite: a monodentate complex, a bidentate-binuclear complex, and a bidentate-mononuclear complex.

The parameters defining the local coordination environment of arsenate sorbed on goethite are given in Table 6.1. It may be observed that surface complexes of organic compounds with As(V) changed with surface coverage, and that the monodentate complex was more important at a lower surface coverage. An increase in surface coverage led to a greater contribution of the bidentate complexes to the characteristics of the spectra (Fendorf et al. 1997).

The adsorption mechanism of arsenite and arsenate adsorption on α-FeOOH was interpreted by Sun and Doner (1996) as a replacement of two singly coordinated surface OH groups to form binuclear bridging complexes. Grossl et al. (1997) proposed that the adsorption of arsenate on α-FeOOH involves a two-step ligand exchange reaction by which an inner-sphere bidentate surface complex is formed. Additional information on the adsorption and stability of As(III) on goethite based on spectroscopic evidence for inner-sphere complexes is given in Manning et al. (1998). EXAFS measurements yielded an average As(III)–Fe interatomic distance of $3.378 \pm 0.014$ Å, indicating a bidentate-binuclear bridging. As(III) complexes exhibit a similarity to other oxyanions that adsorb on α-FeOOH through an inner-sphere mechanism. Using a known crystallographic Fe(III)–O interatomic distance of 2.02 Å for goethite (Manceau and Charlet 1994) as well as As(III)–O and As(III)–Fe distance from EXAFS analysis, Manning et al. (1998) developed a

**Table 6.1** Parameters defining local coordination environment of arsenate sorbed on goethite as determined by EXAFS spectroscopy (after Fendorf et al. 1997). Reprinted with permission from Fendorf SE, Eick MJ, Grossl PR, Sparks DL (1997) Arsenate and chromate retention mechanisms on goethite 1. Surface structure. Environ Sci Technol 31:315–320. Copyright 1997 American Chemical Society

| Surface excess, log $\Gamma$ | Shell | Distance (Å) | CN | $\sigma^2(\text{Å}^2)$ |
|---|---|---|---|---|
| –2.05 | As–O | 1.66 | 3.8 | 0.0018 |
| | As–Fe | 2.85 | 1.3 | 0.0022 |
| | | 3.24 | 1.6 | 0.0031 |
| | | 3.59 | 0.41 | 0.0055 |
| –2.15 | As–O | 1.66 | 3.7 | 0.0019 |
| | As–Fe | 2.84 | 0.92 | 0.0026 |
| | | 3.23 | 1.3 | 0.0029 |
| | | 3.59 | 0.67 | 0.0062 |
| –2.27 | As–O | 1.67 | 3.9 | 0.0019 |
| | As–Fe | 2.85 | 0.61 | 0.0017 |
| | | 3.24 | 0.96 | 0.0038 |
| | | 3.60 | 1.05 | 0.0050 |

structural diagram of the As(III)–α-FeOOH surface complex, showing H-bonding at low pH and deprotonation at increased pH (Fig. 6.7).

Availability of arsenic forms in the soil–subsurface environment depends on soil-solution chemistry, including factors such as redox potential or pH, and on the presence of additional inorganic or organic compounds that can compete for adsorption sites of mineral phases. As a consequence, naturally occurring competitive inorganic and organic ligands are of major importance in defining both the adsorption of As forms on mineral and organic solid phases and its potential transformation in the environmental liquid phase.

The presence of various naturally occurring compounds may induce a decrease in the adsorption of As(III) and As(V) on goethite and ferrihydrite, which is dependent on the pH of the system, the type of FEOX surface, the properties of the naturally occurring compounds, and the type of iron oxide adsorbents (Grafe et al. 2001). Here, we present studies on arsenic chemisorption as affected by the presence of two naturally occurring compounds that may compete with arsenic for the adsorption sites of iron oxide surfaces: silicic acid (Waltham and Eick 2002), and humic and fulvic acids (Grafe et al. 2001, 2002).

Silicic acid is a natural inorganic ligand found in the soil–subsurface environment at concentrations that favor strong chemisorption of both arsenate and arsenite on iron oxides surfaces (Elgawhary and Lindsay 1972). The influence of the silicic acid (0.10 and 1.0 mM) over a range of pH (4, 6, and 8) on the adsorption kinetics of arsenic on goethite was reported by Waltham and Eick (2002). The rate of As(III) and As(V) adsorption in the presence of silicic acid was greatest at pH values near the pK values (9.29 for arsenious and 2.24 for arsenic acids). Silicic acid has a



**Fig. 6.7** Structural diagram of bidentate-binuclear and monodentate-mononuclear As(III) surface complexes on the $d_{110}$ plane of goethite (α-FeOOH) showing (**a**) the protonated bidentate surface species at 3.38 Å $S_2HAsO_3$ and (**b**) the deprotonated bidentate surface species ($S_2AsO_3^-$) (after Manning et al. 1998). Reprinted with permission from Manning BA, Fendorf SE, Goldberg S (1998) Surface structures and stability of arsenic(III) on goethite: spectroscopic evidence for inner-sphere complexes. Environ Sci Technol 32:2383–2388. Copyright 1998 American Chemical Society
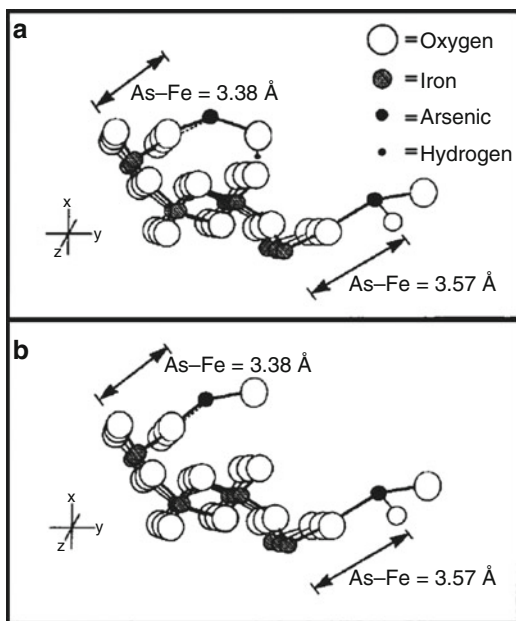
similar pK value (9.49) which decreases with a decrease in pH. Adsorption of As(III) and As(V) and silicic acid (Fig. 6.8) exhibited biphasic kinetics comprising a rapid adsorption reaction followed by a much slower reaction. Waltham and Eick (2002) considered that the slow rate within the biphasic kinetic adsorption is due to surface precipitation, interparticle diffusion, and/or changes in the type of surface complex.

The adsorption of silicic acid at all pH values and concentrations decreased the rate and amount of arsenite adsorbed; about 40% less arsenite was adsorbed in the presence of 1.0 mM silicic acid at all pH values (Fig. 6.8). The quantity of arsenite adsorbed decreased as the surface concentration of silicic acid increased. In contrast, only the adsorption rate of arsenate was reduced by the presence of silicic acid, while the total amount of As(V) adsorbed was not affected. Summarizing their findings, Waltham and Eick (2002) showed that adsorbed silicic acid can modify the surface potential of the iron oxide by blocking reactive functional groups and preventing As adsorption. Both arsenite and arsenate were strongly chemisorbed to iron oxide surfaces. However, in the natural environment, arsenite is more mobile than arsenate. This fact may be related to the presence of adsorbed silicic acid, which reduces both the quantity and the rate of arsenite adsorption (Fig. 6.9a, b).

Competition of natural organic ligands (humic acid from peat (HAp) and fulvic acids (FA)), and a synthetic dissolved organic compound (citric acid (CA)) with As (III) and As(V), for sorption on surface sites of iron oxides and hydrous oxides was studied by Grafe et al. (2001, 2002). For ease of discussion here, we consider these ligands as "dissolved organic carbon," denoted as DOC. Adsorption of DOC on soil–subsurface constituents occurs via multiple mechanisms, including ligand exchange reactions of COOH and phenol/catechol OH functional groups (Gu et al. 1994). In the As-DOC-mineral system (Grafe et al. 2001, 2002), competition for the available sites of the mineral surface may develop between the arsenic forms and dissolved organic carbon compounds. The adsorption of As(III), As(V), HAp, FA, and CA on goethite and ferrihydrite is presented in Fig. 6.10. As(III) and As(V) adsorption on goethite is typical of oxy-acids with maximum adsorption near their respective $pK_1$ values. Adsorption of As(III), As(V), and DOC on ferrihydrite is two to three times greater than that on goethite.

Grafe et al. (2001, 2002) assumed that HAp and FA adsorption on iron oxide minerals involves a dynamic interaction among several mechanisms between the organic functional groups and surface hydroxyls, including ligand exchange reactions, hydrogen bonding, and electrostatic interaction. HAp and FA adsorption reached a maximum at a pH around 9, while CA showed adsorption maxima on goethite at pH 5.

The type of iron oxide mineral surface controls the adsorption of As(III) and As(V) in the presence of natural organic ligands and synthetic citric acid. The experimental results of Grafe et al. (2001, 2002) illustrate this behavior (Fig. 6.11). Adsorption of As(V) on goethite in the presence of humic acid is reduced by 27% at pH 6–9, while fulvic acid presence induces a decrease in adsorption of 17% at a pH ranging from 3 to 8. The presence of citric acid did not affect the amount of As(V) adsorbed. In contrast, As(III) adsorption on ferrihydrite was inhibited in the

**Fig. 6.8** Kinetics of As(III), As(V) adsorption on goethite as a function of pH and concentration of silicic acid (after Waltham and Eick 2002). Copyright 2002, Soil Science Society of America. Reprinted with permission
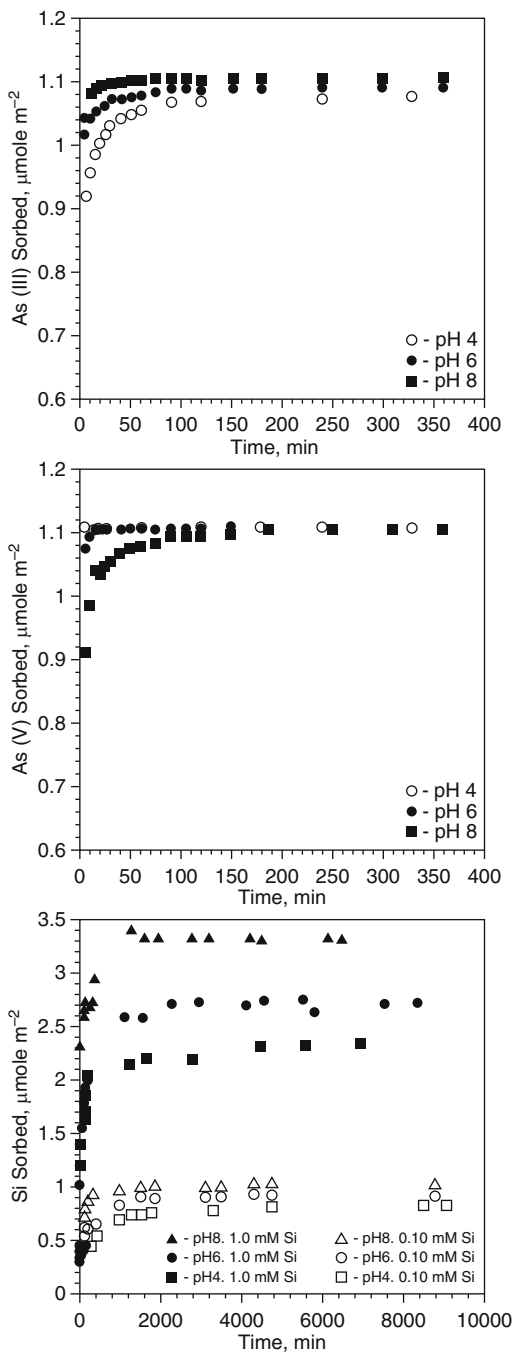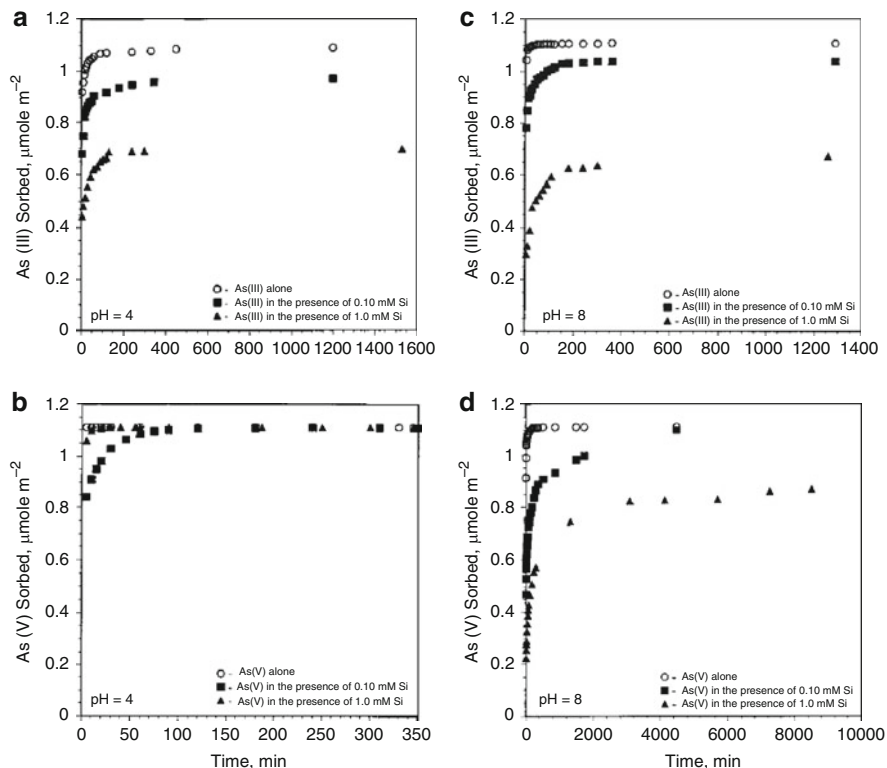
**Fig. 6.9** Kinetics of As(III) and As(V) adsorption on goethite at pH 4 (**a**, **b**) and 8 (**c**, **d**) in the presence and absence of silicic acid (after Waltham and Eick 2002). Copyright 2002, Soil Science Society of America. Reprinted with permission
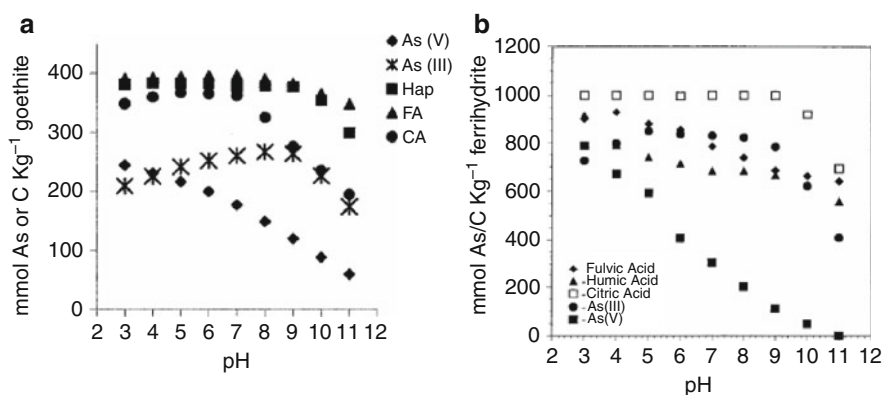


**Fig. 6.10** Adsorption of As(III), As(V), humic acid peat (Hap), fulvic acid (FA), and citric acid (CA) on (**a**) goethite (after Grafe et al. 2001); and (**b**) ferrihydrite (after Grafe et al. 2002). Copyright 2002, American Society of Agronomy, Crop Science Society of America, and Soil Science Society of America. Reprinted with permission
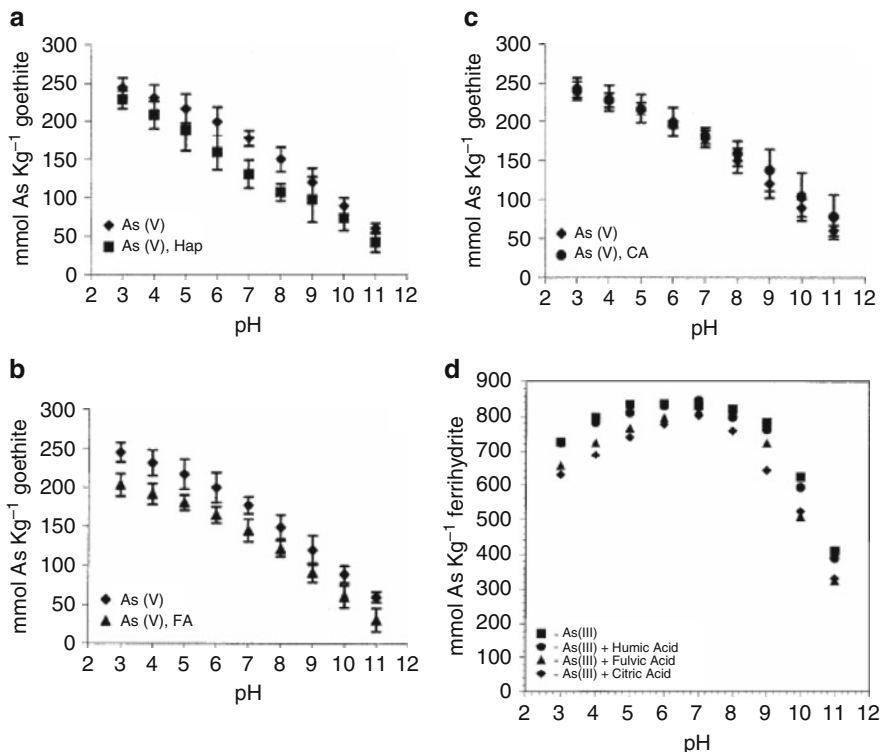
**Fig. 6.11** Adsorption of As(V) on goethite in the presence and absence of (**a**) humic, (**b**) fulvic, and (**c**) citric acids (after Grafe et al. 2001); and (**d**) adsorption of As(III), on ferrihydrite in the presence and absence of humic, fulvic, and citric acids (after Grafe et al. 2002). Copyright 2002, American Society of Agronomy, Crop Science Society of America, and Soil Science Society of America. Reprinted with permission

presence of citric acid, decreasing by 17–20% at pH 3–5, but not affected at all by humic and fulvic acids. These results demonstrate the significance of the solid phase configuration in adsorption and competitive adsorption processes between As and DOC species; ferrihydrite has a greater surface site density than goethite (Dzombak and Morel (1990) report 16.8 versus 5.75 $\mu$mol sites m$^{-2}$).

Summarizing their results, Grafe et al. (2001, 2002) showed the following:

1. As(V) adsorption on goethite in the presence of DOC decreases according to the order HAp > FA > CA, while As(V) adsorption on ferrihydrite decreases only in the presence of CA.
2. In the presence of DOC, As(III) adsorption on goethite decreases similarly to that of ferrihydrite, CA > FA = HAp. However, As(III) adsorption on ferrihydrite is greater than that on goethite.

Under natural conditions, the sorption of arsenate on ferrihydrite leads to the formation of poorly crystalline products, considered as an amorphous ferric

arsenate (Krause and Ettel 1989). This mineral resembles scorodite, a common hydrated iron arsenate mineral, with the chemical formula $FeAsO_4 \cdot 2H_2O$. The transformation of ferric arsenate adsorption materials, initially synthesized at pH 3 and 8 and at different Fe/As molar ratios, was determined by Jia et al. (2006), using X-ray diffraction (XRD) measurements. Arsenate ferrihydrite formed minerals at pH 3 (Fig. 6.12a) exhibit XRD bands that lie between the characteristic bands of ferrihydrite and poorly crystalline ferric arsenate.

With increasing initial Fe/As molar ratio, the shapes of both bands change appreciably, the first peak shifting to higher degrees. For the Fe/As = 2 samples, the location and the intensity of the peaks are clear XRD features of poorly crystalline ferric arsenate, because the shoulders are characteristic XRD bands of ferrihydrite. This demonstrates that in the case of Fe/As = 2, arsenate ferrihydrite sorption materials comprise both poorly crystalline ferric arsenate and ferrihydrite. At pH 8, arsenate ferrihydrite formed minerals (Fig. 6.12b) show different XRD patterns compared to those formed in acidic conditions (e.g., pH = 3). For Fe/As = 8, the XRD bands of the arsenate ferrihydrite materials are located in the same position as those of ferrihydrite, indicating that in this "new" arsenate
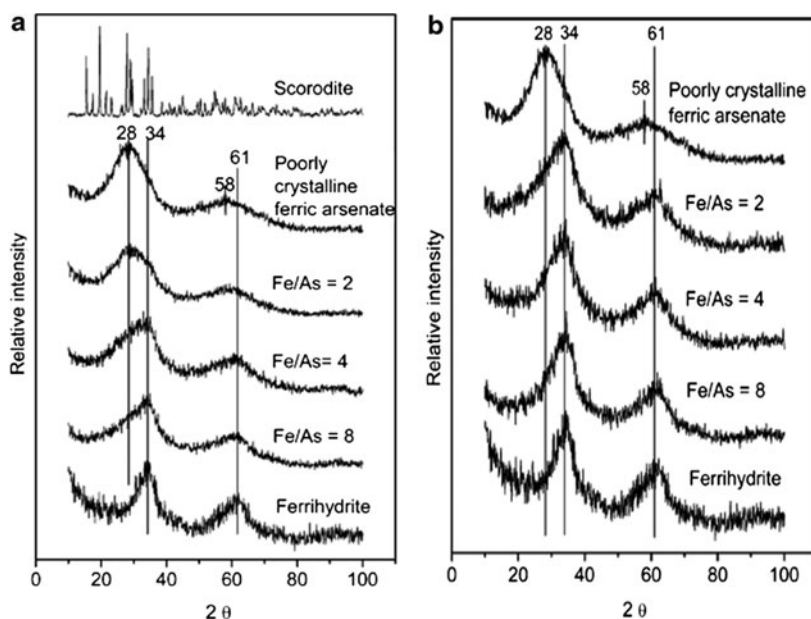


**Fig. 6.12** Comparison of XRD patterns of (**a**) pH 3 arsenate ferrihydrite, and (**b**) pH 8 arsenate ferrihydrite, sorption materials with reference materials (ferrihydrite, poorly crystalline ferric arsenate, and scorodite). The sorption materials were synthesized at pH 3 and 8, respectively, with different initial Fe/As molar ratios and equilibration time of 2 weeks (modified after Jia et al. 2006). Reprinted with permission from Jia Y, Xu L, Fang Z, Demopoulos GF (2006) Observation of surface precipitation of arsenate on ferrihydrite. Environ Sci Technol 40:3248–3253. Copyright 2006 American Chemical Society

material, ferrihydrite remains the major mineral. Because the presence of a ferric arsenate phase cannot be ignored, Jia et al. (2006) considered that arsenate is adsorbed on the surface of ferrihydrite by inner-sphere complexation. Based on XRD measurements, it was suggested that ferric arsenate surface precipitate forms when arsenate is sorbed on ferrihydrite at acidic pH, whereas surface complexation dominates the process at mildly alkaline pH.

Changes induced in the ferrihydrite matrix by arsenate sorption were confirmed also by Raman spectroscopy (Fig. 6.13). Ferrihydrite exhibits band characteristics of iron oxyhydroxide as follows: three strong bands at 222, 289, and 407 $cm^{-1}$, and a weaker band at 606 cm. Scorodite shows two strong bands at 803 and 890 $cm^{-1}$, while poorly crystalline ferric arsenate shows a strong band at 825 $cm^{-1}$ and a shoulder at 910 $cm^{-1}$. The band at 825 $cm^{-1}$ that appears in Fe/As = 4, pH 3 sample occurs at the same position as the As-stretching vibration of poorly crystalline ferric arsenate, confirming the precipitation of ferric arsenate in an acidic environment. The Raman spectrum of the pH 8 arsenate ferrihydrite sorption product at 845 $cm^{-1}$ confirms arsenate adsorption on the surface ferrihydrite via bidentate complexation.

The XRD and Raman spectroscopy studies of Jia et al. (2006) also suggest that As(V) precipitation occurs in the bulk soil–subsurface solution. This process probably involves an initial uptake of arsenate by surface complexation, followed by a transition to ferric arsenate formation. From this evidence, it may be concluded that surface precipitation of arsenate on the FeOX surface, as well as
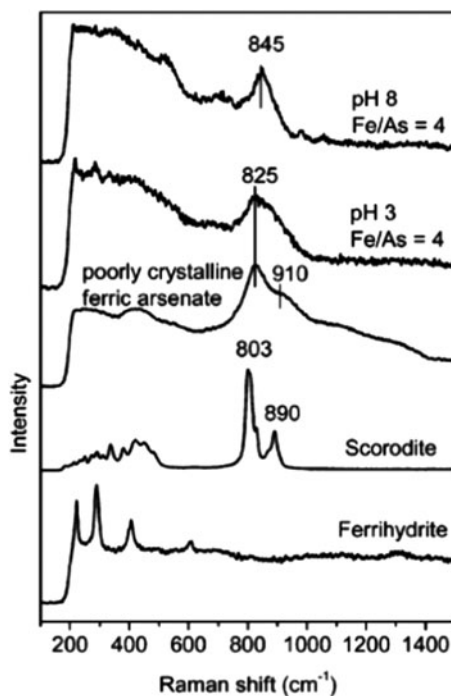


**Fig. 6.13** Raman spectra of arsenate–ferrihydrite sorption materials and reference materials (scorodite, poorly crystalline ferric arsenate, and ferrihydrite). The sorption materials were synthesized at pH 3 and 8 with initial molar ratio Fe/As 4 and equilibration time of 2 weeks (after Jia et al. 2006). Reprinted with permission from Jia Y, Xu L, Fang Z, Demopoulos GF (2006) Observation of surface precipitation of arsenate on ferrihydrite. Environ Sci Technol 40:3248–3253. Copyright 2006 American Chemical Society

contaminant complexation, leads to an irreversible change in the matrix of the adsorbent mineral phase.

The effect of residence time on arsenate sorption on FeOX and its impact on the adsorbent matrix were studied by O'Reilly et al. (2001) and Pigna et al. (2006). In general, adsorption/desorption of metals and metalloids on soil minerals depends on the residence time, different sites of reactivity, surface nucleation, and diffusion into matrix micropores (Sparks 2002). As mentioned above, arsenate is adsorbed on iron oxides through an inner-sphere complex via a ligand mechanism, and the major bonding mechanism is a bidentate-binuclear complexation (Waychunas et al. 1993; Manceau and Charlet 1994).

Sorption studies of arsenate on goethite over a period of one year proved that 93% of the total arsenate adsorbed was sorbed during the first 24 h of contact (O'Reilly et al. 2001). Transformation following arsenate sorption led to the formation of a FeOX similar to natural scorodite ($FeAsO_4$). The transformation pathway over time is shown in Fig. 6.14, using extended EXAFS and Fourier transform IR (FTIR) spectroscopy (O'Reilly et al. 2001).

The EXAFS spectra revealed the presence of two distinct atomic shells around the adsorbed As(V). The closed atomic shell is an O atom and the next one is a Fe atom. It may be observed in Fig. 6.14a that a sinusoidal beat pattern characteristic of an O-shell is present in all of the samples. The As–Fe bond distance of 3.30 Å indicates the formation of a bidentate bond between the arsenate atoms and the goethite surface. However, the numerous frequencies characteristic of the second shell decrease with time of contact between As(V) and goethite, reflecting the As(V)-induced transformation of goethite to scorodite. The radial structure functions generated by FTIR spectroscopy (Fig. 6.14b) support the EXAFS results confirming this transformation.

Batch studies of macroscopic kinetics coupled to the previously described microscopic results showed a two-phase adsorption/desorption pattern of As(V) on FeOX surfaces. For example, at pH 6, 35% of the total adsorbed As(V) was desorbed within 24 h, but a significant amount of arsenate remained bound to goethite even 5 months later. Another study of the kinetics of arsenate sorption on metal oxides (Pigna et al. 2006) confirmed these residence time effects on contaminant retention on goethite and ferrihydrite.

### 6.2.1.1    More on Ferrihydrite Transformations

From early in the last century, it was observed that an "amorphous" Fe(III) hydroxide – known later as the ferrihydrite mineral – may transform into goethite and hematite under the influence of temperature and environmental acidity (Bohm 1925). Transformation rates are affected by pH (Schwertmann and Murad 1983), ionic strength (Torrent and Guzman 1983), sorption/coprecipitation of ions (Baltpurvins et al. 1997), temperature (Lewis and Schwertmann 1979), and rate of initial precipitation (Martnes and McBride 1998). Only more recently was ferrihydrite transformation connected to the presence of contaminants. Laboratory
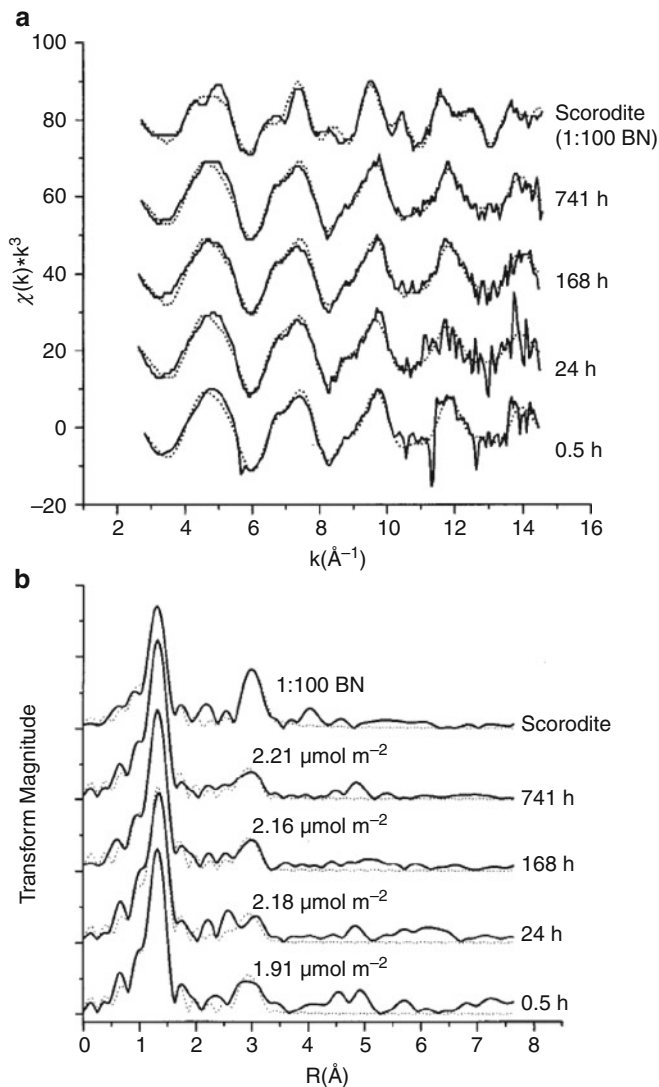
**Fig. 6.14** Transformations of goethite–arsenite during aging as reflected in EXAFS and FTIR spectra $\chi$ functions for samples incubated with arsenate for different lengths of time and the scorodite sample diluted 1% by weight in boron nitride. The *solid line* represents the experimental data, and the *dotted line* represents the multi-shell fit to the data. (**a**) EXAFS analysis, with background-subtracted $k^3$-weighted $\chi$ functions. (**b**) FTIR of the $\chi$ functions (modified after O'Reilly et al. 2001). Copyright 2001, Soil Science Society of America. Reprinted with permission

studies indicate that Cd, Co, Cr, Cu, Ni, Np, Pb, Sr, and Zn are sorbed irreversibly, to some extent, during the aging and transformation of synthetic ferrihydrite (Table 6.2).

**Table 6.2** Irreversible retention of heavy metals on ferrihydrites during aging (after Arthur et al. 1999, and references therein)

| Metal | Sorption conditions | Sorption mechanisms |
|---|---|---|
| Cd | pH 9.5 to pH 4.5 cycles | Adsorption/desorption |
|  | Alkaline coprecipitation | Isomorphic substitution |
|  | Aged 86 weeks, pH 7 | Partially occluded |
|  | coprecipitation, aged 14 d at pH 8, 50 or 70°C | Isomorphic substitution for Fe in hematite |
|  | Coprecipitation, 100 mg Cd kg$^{-1}$, pH 6, aged 250 d | |
| Co | Coprecipitation, aged 20 d pH 12, 70°C | 28–59% Sorbed at 25°C more after 60 d at 70°C |
|  | Added to ferrihydrite, aged <100 h, pH 10.5–12, 70°C | Isomorphic substitution for Fe in goethite or magnetite |
|  | Alkaline coprecipitation | |
|  | Aged 86 weeks, pH 7 | |
| Cr | pH 9.5 to pH 4.5 cycles | Partially occluded |
|  | Alkaline coprecipitation | 94–97% Bound 21.5 h |
|  |  | Isomorphic substitution for Fe in goethite |
| Cu | pH 9.5 to pH 4.5 cycles | 10–15% Slowly reversible Isomorphic substitution for |
|  | Coprecipitation, aged 20 d pH 12, 70°C | Fe in goethite, hematite, or spinel. Isomorphic substitution |
|  | Alkaline coprecipitation | 94% sorbed, constant to more after 60 d at 70°C |
|  | Coprecipitation, 1,500 mg Cu kg$^{-1}$, pH 6, aged 250 d | |
| Ni | pH 9.5 to pH 4.5 cycles | ~20% Slowly reversible |
|  | Coprecipitation, pH 7.5 to 13 | Ni-goethite pH > 11.5 Ni-hematite pH 8–pH 11.5 |
|  | Coprecipitation, pH 6, aged 400 h at 70°C | Incorporation in goethite and hematite |
| Np | Coprecipitation, pH 6.0 or 7.7, 90°C, 198 h | 100% sorbed at pH 7.7 11% sorbed at pH 6.0 |
| Pb | pH 9.5 to pH 4.5 cycles | 40–60% Slowly reversible Isomorphic substitution |
|  | Alkaline coprecipitation | Adsorbed on oxides but only 10% occluded |
|  | Coprecipitation, pH 6, aged 400 h at 70°C | 100% sorbed, some desorption after 60 d at 70°C |
|  | Coprecipitation, 1,500 or 500 mg Pb kg$^{-1}$, pH 6, aged 250 d | |
| Sr | Ferrihydrite aged at pH 12, 40°C for 150 h | 100% Sorbed initially, 60% sorbed on goethite |
| U | Ferrihydrite aged | Partial desorption during transformation |
| Zn | pH 9.5 to pH 4.5 cycles plus aging up to 44 h | 4–43% Remained adsorbed. Isomorphic substitution for Fe in goethite, hematite, or spinel, up to 5 mol % |
|  | Coprecipitation, aged 20 d pH 12, 70°C | 58% Sorbed, more after 60 d at 70°C |
|  | Coprecipitation, 3,000 mg Zn kg$^{-1}$, pH 6, aged 250 d | |

Soil–subsurface system pH may change as a result of pollutant disposal in the Critical Zone. The transformation of ferrihydrites into goethite and hematite under various pH conditions and over a long residence time (about 3 years) was reported by Schwertmann and Murad (1983). The rate of transformation and the time

required for half conversion of ferrihydrite as a function of pH are shown in Fig. 6.15. The residual ferrihydrite decreased with increasing pH; at pH $\geq$ 7, about 98% of the initial amount of ferrihydrite was transformed into goethite and hematite.

The hematite–goethite ratio in the transformed product varied strongly with pH. Schwertmann and Murad (1983) showed that whereas at pH 12 only goethite was formed, mixtures of goethite and hematite were formed at all other tested pH values. Maximum hematite formation occurred at pH 7–8. The crystallinity of the two formed minerals is affected also by the pH (Fig. 6.16). These results show that goethite and hematite formed by transformation of ferrihydrite via two different, competitive mechanisms: goethite crystals formed in solution from dissolved Fe(III) ions, whereas hematite formed through internal dehydration and rearrangement within the ferrihydrite aggregates.

The presence of heavy metal contaminants may retard the transformation of ferrihydrites into crystalline products. Sun et al. (1996) showed that addition of Cd led to an increase in the amount of hematite in the mixture of ferrihydrite transformation products, until goethite formation was suppressed entirely and replaced by Cd–hematite (Fig. 6.17). Adding Cd to ferrihydrites led to the precipitation of iron initially present in the system. However, when the amount of Cd added to ferrihydrite was greater than the binding capacity of the FeOX, cadmium also coprecipitated or was incorporated into the crystalline transformation products. The chemical analysis and XRD measurements showed that Cd was incorporated into the lattice of the iron oxide, forming Cd–hematite and Cd–goethite minerals. In the absence of Cd, the transformation product obtained was a mixture of about 70% goethite and 30% hematite.

The shape and the size of hematite in the ferrihydrite transformation products are changed following addition of cadmium. These changes are presented in Fig. 6.18,
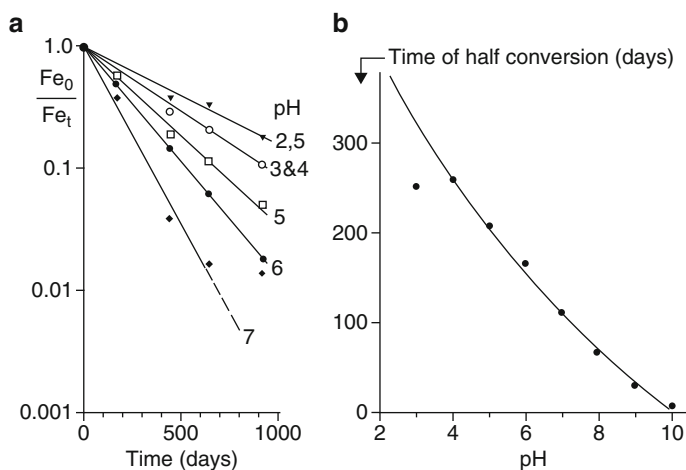


**Fig. 6.15** Transformations of ferrihydrite to goethite and hematite during aging: (**a**) first-order reaction plot for the transformation of ferrihydrite at various pH values, (**b**) length of time for half conversion of ferrihydrite to goethite and hematite versus pH (modified after Schwertmann and Murad 1983). Reprinted with permission
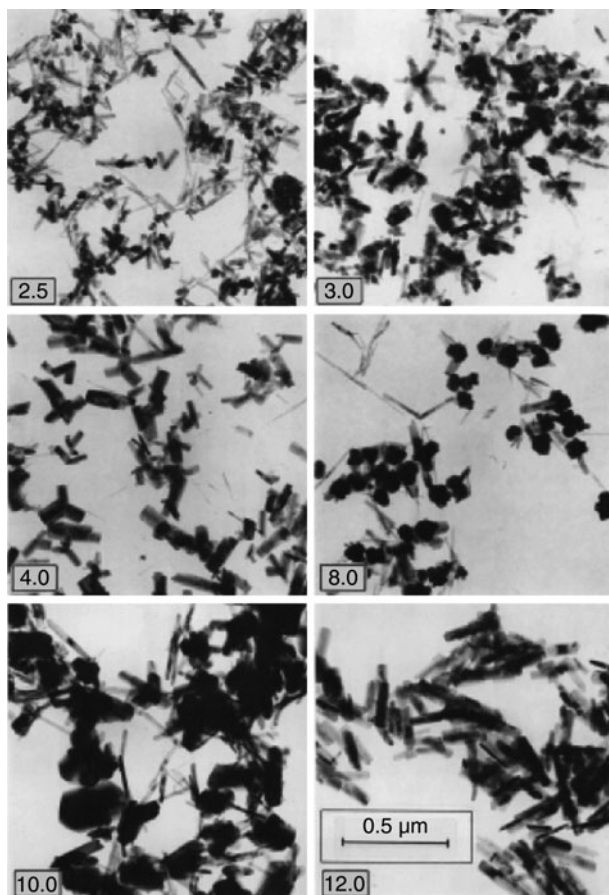
**Fig. 6.16** Electron micrographs of goethites and goethite–hematite mixtures produced from ferrihydrite at various pH values (after Schwertmann and Murad 1983). Reprinted with permission



**Fig. 6.17** The ratio of H/(H + G) in the crystalline products, as a function of the mole % of Cd initially present in the system. The experiment was performed at pH 8 and 70°C. The transformation period was 14 days (after Sun et al. 1996)
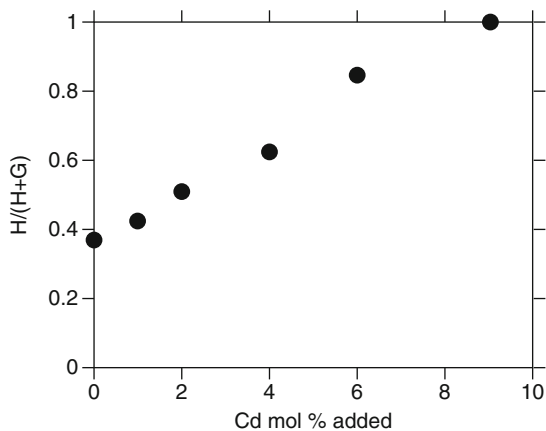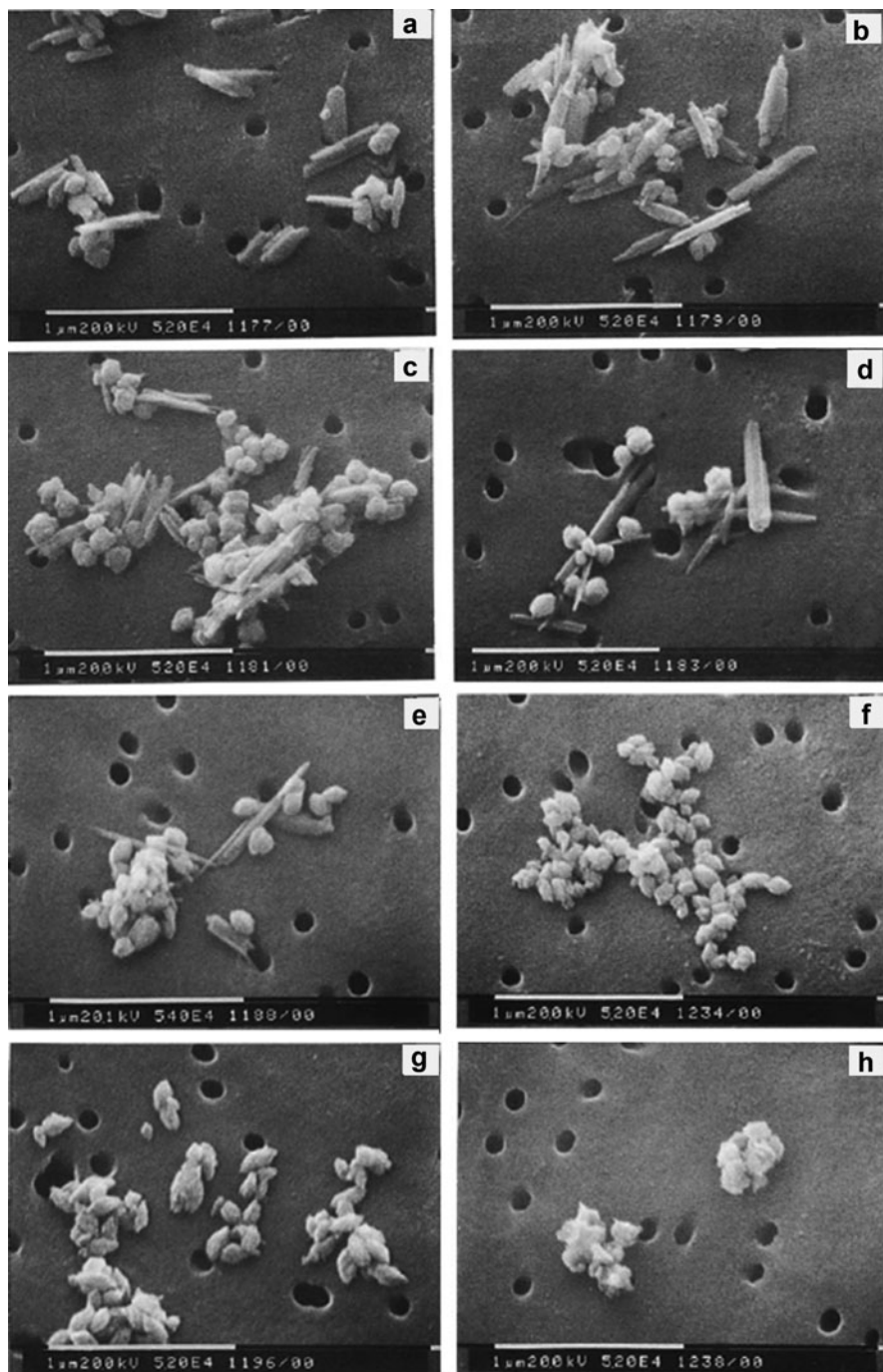
**Fig. 6.18** Scanning electron micrographs of the ferrihydrite crystalline transformation products with different mole % of Cd initially present in the system after 14 days of aging. (**a**) Cd absent, product was goethite 65%; hematite 35%. (**b**) 1 mole % Cd product was goethite 55%; hematite 45%. (**c**) 2 mole % Cd product was goethite 47%; hematite 53%. (**d**) 4 mole % Cd product was

where scanning electron micrographs of the crystalline transformation products, for different concentration of Cd initially present in the system, are reproduced. Based on chemical analysis and Scanning electron microscopy (SEM) observations, Sun et al. (1996) suggested that the morphological changes in a Cd–ferrihydrite system have little relationship to the incorporation of Cd in the lattice of hematite, and depend on the sorption of Cd on the surface of growing crystals. Cd prevents the formation of goethite by hindering the dissolution of ferrihydrites and/or by interfering with its nucleation and growth in solution. It was also observed that the presence of Cd has only a slight effect on the morphology of goethite.

Conversion of ferrihydrites into more crystalline products such as goethite becomes faster with increases in pH and temperature. Therefore, for experimental convenience, laboratory studies on ferrihydrite transformation in aqueous suspensions are performed under a relatively high environmental pH and temperature. Arthur et al. (1999) investigated sorption of Ba (as an analog for Ra) contaminants during ferrihydrite transformation occurring in the alkaline pore water of a nuclear waste repository. Changes in Ba adsorption/desorption during aging of ferrihydrite and its transformation into goethite in an aqueous FeOx suspension at pH 12 and at a temperature of 50°C are shown in Fig. 6.19.

Analysis of the suspension filtrate indicates that 100% of the Ba added was initially adsorbed on ferrihydrite. After 70 h of aging, only 7% of the amount desorbed was found in the aqueous phase. However, during aging, the ferrihydrite was transformed to goethite, Ba being desorbed from the poor crystalline ferrihydrite and occluded in the goethite. Maximum desorption of Ba coincided with 95–99% transformation of ferrihydrite into goethite. It is clear that the majority of the Ba added is retained irreversibly. About 50% of the added Ba was occluded during ferrihydrite transformation. Arthur et al. (1999) considered that the desorption of Ba – as little as there is – is caused by the decrease in FeOX surface area and adsorption sites due to transformation of ferrihydrite into goethite.

Arthur et al. (1999) also showed that Sr adsorption/desorption patterns in the ferrihydrite aqueous suspension during aging are different than those of Ba. These differences can be attributed to the lower acidity of the suspension of the Sr–ferrihydrite solution (pH 8). Maximum Sr desorption occurred when transformation of ferrihydrite was 99% complete. At least 25% of the added Sr was sorbed irreversibly during the initial stage of ferrihydrite transformation to hematite and goethite. As in the Ba–ferrihydrite case, the transformation caused a large decrease in sorbing surface area, leading to a further decrease in Sr adsorption. The results of Arthur et al. (1999) demonstrate that contaminants may be retained irreversibly on iron oxide surfaces during their transformation from a poor crystalline to a crystalline form.

**Fig. 6.18** (continued) goethite 37%; hematite 63%. (**e**) 6 mole % Cd product was goethite 17%; hematite 83%. (**f**) 9 mole % Cd, product was hematite. (**g**) 9 mole % Cd, product was hematite. (**h**) 9 mole % Cd, product was hematite (Sun et al. 1996)

## 6.2.2 Clay Mineral Sorbents

Clay materials constitute the major component of the soil–subsurface system that reacts with anthropogenic contaminants. A short characterization of soil–subsurface clay minerals was presented in Chap. 1. Here, we consider induced changes to the natural clay matrix as a result of chemical contaminant binding. Based on existing macroscopic studies and molecular scale methodology, Boyd et al. (2009) developed a comprehensive approach to describe sorption of nonionic organic contaminants (NOC) on layered clays. The ideas of Boyd et al. (2009) can be summarized as follows:

1. NOC sorption by a layered clay – as smectite – is controlled by the relationship among the contaminant functional groups, the mineral layer charge, and the hydration of the clay interlayer cations.
2. The strongest NOC clay sorbents exhibit a low layer charge obtained by tetrahedral substitution. Such a property optimizes the size and hydrophobicity of the sorption domain parallel to the clay surface, and favors adsorption domains perpendicular to the clay surface. Such a pattern promotes solute dehydration and interaction with opposing siloxane sheets.

### 6.2.2.1 Nonionic Surfactants

Nonionic surfactants reach the soil–subsurface environment in agrochemical formulations such as detergents and additives. Interactions between nonionic surfactants and soil–subsurface components such as clays and organic matter cause reciprocal changes during their "coexistence" in the Critical Zone.

Irreversible modification of clay materials by grafting surfactants has been used in the last decades for prevention or remediation of soil and water contamination. Initially, such engineered organo-clay materials were used mainly with cationic surfactants. More recent studies have shown the use of nonionic surfactants to synthesize a new family of organo-clay composites. This technology can be used to
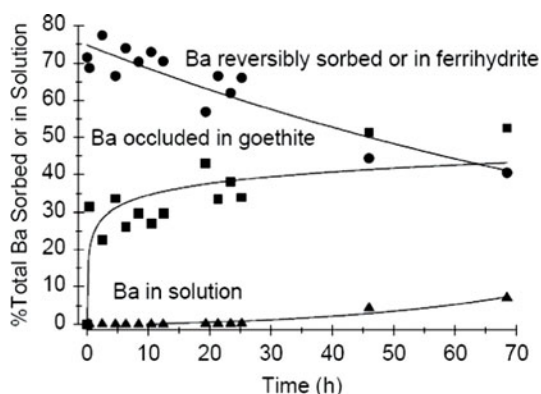


Fig. 6.19 Changes in Ba sorption during aging of ferrihydrite suspensions at 50°C and pH 12 in 0.01 M $KNO_3$ (after Arthur et al. 1999)

elucidate potential modifications to soil–subsurface clay minerals following contamination with nonionic chemicals.

Nonionic surfactants are generally composed of hydrophilic polymeric segments and hydrophobic aliphatic hydrocarbon or alkylphenol groups. Binding aliphatic tails to clay minerals increases the hydrophobicity of the mineral surfaces (Michot and Pinnavaia 1991). Below we present some specific cases of clay modification resulting from nonionic surfactant contamination.

*Poly(ethylene oxide) hydrophilic polymers (PEOs)* used as nonionic surfactants were bound and intercalated in smectite by Deng et al. (2003, 2006a) to test clay–surfactant interactions. Deng et al. (2003) reported that intercalation of two nonionic surfactants – Brij56 (polyoxyethylene(10) cethyl ether) and Igepal CO 720 (polyoxyethylene (12) nonylphenyl ether) – led to expansion of the smectite interlayer. Ca-smectite and modified surfactant–Ca-smectite $d_{001}$ basal spacings, as determined by XRD, are shown in Fig. 6.20. The initial 1.56-nm $d$-spacing of Ca-smectite increased to 1.73 nm by Brij56 binding and to 1.65 nm by Igepal CO 720 binding.

In addition to the higher diffraction orders of $d_{003}$ and $d_{005}$ that are found in Ca-smectite and in surfactant–smectites, the modified clays exhibit additional $d_{002}$ and $d_{006}$ diffraction peaks. The surfactant-induced higher order diffraction peaks suggest regularity of the nonionic surfactants in the smectite interlayer. Deng et al. (2003) found that $d$-spacings measured by XRD are in accord with those obtained from adsorption isotherms. The binding of the nonionic surfactants on smectite and the $d_{001}$ basal spacing of surfactant–smectite did not increase with excess
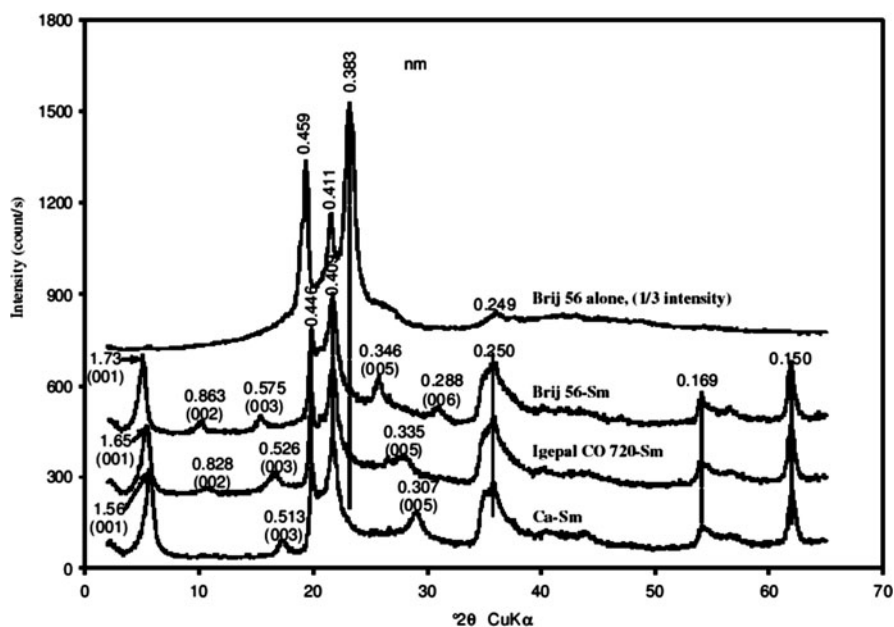


**Fig. 6.20**   XRD patterns of surfactant *Brij56*, powder-mounted smectite and two surfactant–smectite composites *Brij56* and Igepal CO 720 (after Deng et al. 2003) Reprinted with permission

**Table 6.3** $d_{001}$ spacing of surfactant–smectite composites after washing with water (after Deng et al. 2003). Reprinted with permission

| No. of washings | $d_{001}$ spacing after washing (nm) | |
|---|---|---|
| | Brij 56-Sm | Igepal CO 720-Sm |
| 0 | 1.738 | 1.651 |
| 1 | 1.757 | 1.603 |
| 2 | 1.738 | 1.619 |
| 3 | 1.775 | 1.603 |
| 4 | 1.738 | 1.588 |
| 5 | 1.757 | 1.573 |
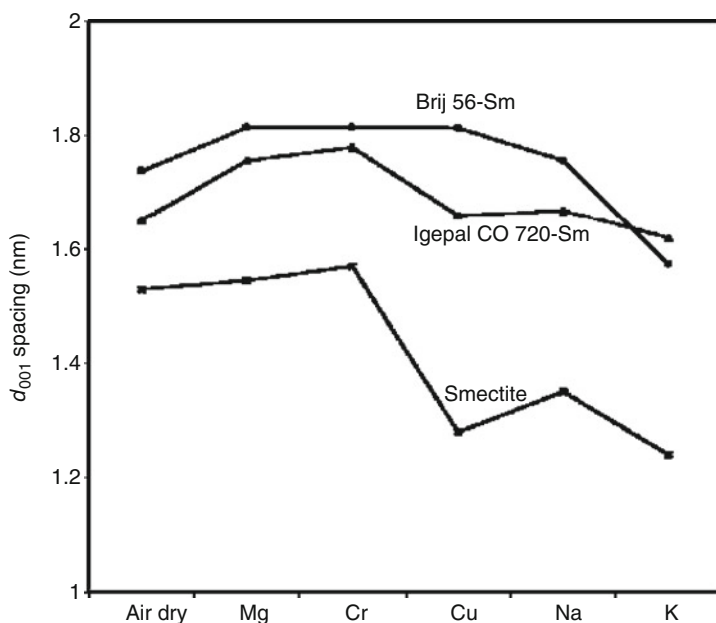


**Fig. 6.21** Effect of washing of smectite and smectite-surfactant composites by chloride electrolyte solutions (containing 1 M $Cl^{-1}$) on $d_{001}$ spacing (after Deng et al. 2003). Reprinted with permission

surfactant. As a consequence, Deng et al. (2003) considered that surfactant intercalation into smectite interlayer galleries was limited to two molecular layers, and that the surfactant remained mostly in the marginal area of the interlayer galleries.

The layer spacing of the experimented nonionic surfactant–smectites was well preserved during water and electrolyte solution washing; the increase in $d_{001}$ spacing remained almost the same after repeated washing with water (Table 6.3) and demonstrated a slight change when washed with $Mg^{2+}$, $Cu^{2+}$, $Cr^{3+}$, and Na chloride electrolyte solution (Fig. 6.21). A different effect was produced by washing with KCl water solution. In this case, there was a significant decrease in $d_{001}$ spacing, which may be related to the low hydration energy of the $K^+$ ion. However, surfactant–smectites always have higher $d_{001}$ spacing than the corresponding

smectite washed with the same electrolyte solution, showing that nonionic surfactants may induce an irreversible modification of the natural smectite matrix. Even washing by KCl solution induces only a partial desorption of surfactants, suggesting an irreversible intercalation of only a fraction of the surfactant molecules in the interlayer galleries of Ca-smectite.

Additional studies by Deng et al. (2006a) extended knowledge on the PEO bonding mechanism, molecular conformation of surfactants in smectite layers, and surfactant–smectite configurations in comparison to the original smectite matrix. The PEO-based nonionic surfactants considered in this study were: Brij 56, Brij 700 (polyoxyethylene (100) stearyl ether), and PE-PEG (polyethylene-block-poly(ethylene glycol). Various cations saturated the Brij 56-smectite organo-clay compound. XRD patterns of the surfactants were almost identical to the pure PEG (poly(ethylene glycol)) polymer, showing the two strongest diffraction peaks near 0.46 and 0.38 nm.

FTIR spectra of the pure surfactants and PEG in the crystalline state showed the occurrence of 1,358, 1,280, and 1,061 cm$^{-1}$ bands arising from the helical PEO chain and the 1,344, 1,241, and 962 cm$^{-1}$ bands that can be assigned to a planar zigzag chain. Based on these results, Deng et al. (2006a) considered that the crystalline surfactant molecules had both helical/extended diblock (Fig. 6.22a) and planar zigzag conformation (Fig. 6.22b). Moreover, the FTIR spectra showed that the adsorbed surfactants had the same molecular conformation as the amorphous polymers. Smectite saturating cations did not affect the conformation of the surfactant adsorbed in the interlayers.

As a conclusion, Deng et al. (2006a) postulated that as a function of surfactant loading, smectite adsorbs in its interlayer one or two layers of surfactant, and suggested schematic models for a modified smectite following PEO-based surfactant adsorption (Fig. 6.23).

Intercalation of triethylene glycol monodecyl ether ($C_{10}E_3$) into a smectite clay is another example demonstrating surfactant-induced modification of clay material
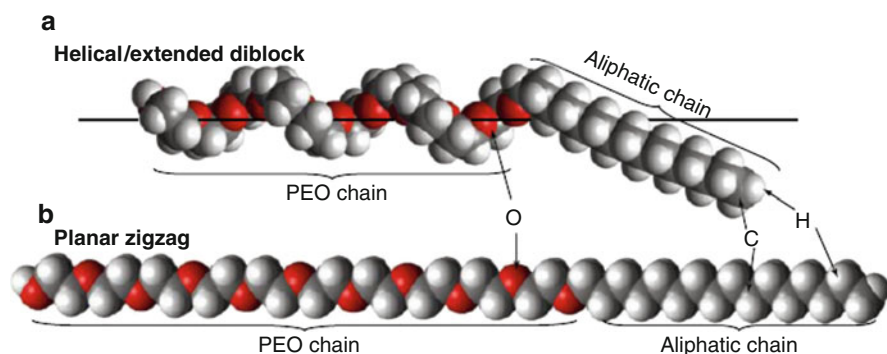


**Fig. 6.22** Two possible molecular conformations of PEO-based surfactants in a crystalline state: (**a**) a favored helical/extended diblock conformation and (**b**) a fully extended planar zigzag conformation. Intermediate forms between these two conformations exist in an amorphous state (after Deng et al. 2006a)
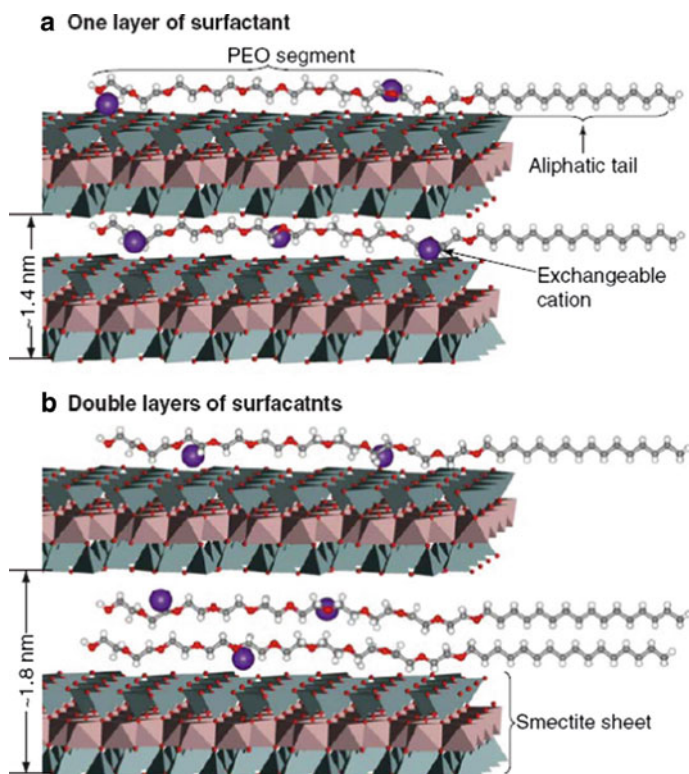
**Fig. 6.23** Schematic models of PEO-based surfactant–smectite composites: (**a**) one layer, and (**b**) double layers of surfactants in the interlayer of smectite. The PEO segment of a surfactant molecule lost its favored helical conformation and became disordered and more extended. The exchangeable cations can be hydrolyzed. Water molecules are not shown in the models (after Deng et al. 2006a)

(Guegan et al. 2009). $C_{10}E_3$ is a nonionic surfactant comprised of, at room temperature and in the presence of water, several membrane lamellar and sponge phases. The lamellar phase consists of a stack of surfactant molecules aggregated into a two-dimensional membrane, with a layer of water displaying a structure having long range order (Le et al. 2001). $C_{10}E_3$ has a molecular weight of 290, a critical micellar concentration (CMC) of $6 \times 10^{-4}$ mol $L^{-1}$, length 23 Å, and height 5 Å.

The $C_{10}E_3$ adsorption isotherm on clay shows a gradual increase in the amount adsorbed, with the equilibrium concentration reaching a final steady state. It should be emphasized that Ca-smectite exhibits a strong affinity for $C_{10}E_3$, and its adsorption could result from several interaction processes with the surface and between the confined molecules including the hydrophobic interaction. Guegan et al. (2009) found no $Ca^{2+}$ in the resulting solution, which confirmed that no cation exchange occurred. In the sorption model of Deng et al. (2003, 2006a), nonionic surfactants formed H-bonds with water; these bonds form in the hydration shells of

**Fig. 6.24** FTIR spectra of pure BDTAC, BDTAC-clay (*washed once*), and BDTAC-clay (*washed twice*) at the concentration of $1.31 \times 10^{-2}$ mol $L^{-1}$ (i.e., 4 $\times$ CEC) and Ca-smectite, over wavenumber range 2,700–3,700 $cm^{-1}$ (after Guegan et al. 2009). Reprinted with permission
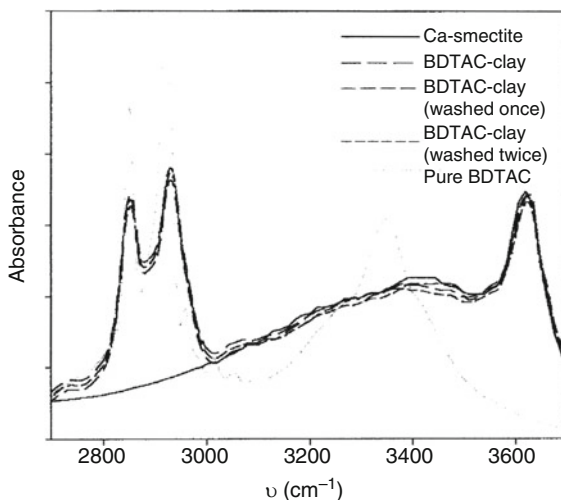


exchangeable cations of smectite, and/or directly through ion–dipole H-bonding to the inorganic cations. Guegan et al. (2009) considered that $C_{10}E_3$ sorption on Ca-smectite depends on several possible mechanisms, such as ion–dipole H-bonding, van der Waals forces, and hydrophobic interactions.

Ca-smectite modification by $C_{10}E_3$ sorption and the stability of $C_{10}E_3$-smectite were observed in FTIR spectra of pure surfactant and clay, and of surfactant-modified clay, immediately after adsorption and after two washing cycles (Fig. 6.24). The spectra of Ca-smectite and the modified organo-smectite exhibited a broad band in the range 3,000–3,600 $cm^{-1}$ of adsorbed $H_2O$ and OH groups of the $C_{10}E_3$. The presence of the band corresponding to OH stretching indicates that nonionic surfactant adsorption involved ion–dipole H-bonding and hydrophobic interactions. $CH_2$ symmetric and antisymmetric stretching modes are reflected in the 2,850 and 2,920 $cm^{-1}$ adsorption bands. A weak hydrophobic interaction favors a decrease in the integrated intensity of the $CH_2$ stretching band during washing (about 5% each time). We consider, however, that a portion of $C_{10}E_3$ from the amount initially adsorbed on Ca-smectite remains, over a "lifetime scale," irreversibly bonded on the clay surface; as a consequence, the smectite configuration remains irreversibly altered.

The XRD patterns determined by Guegan et al. (2009) revealed that $d_{001}$ spacing of $C_{10}E_3$-smectite increases with increasing amounts of adsorbed surfactant. For small concentrations, the basal spacing increased from 11.7 to 14 Å, corresponding to the adsorption of the surfactant monolayer. Large concentrations led to an increase in $d_{001}$ spacing to 17.2 Å, which then remained constant. These results demonstrated that the strong affinity of the $C_{10}E_3$ to the smectite surface and the narrow opening of the basal spacing led to a complete reorganization of the lamellar phase into isolated molecules which are adsorbed parallel to the surface.

The hydrophobic interaction allows $C_{10}E_3$ molecules to be intercalated into the smectite layer, to increase the basal *d*-spacing of the smectite, and to achieve modification of natural clay mineral.

### 6.2.2.2  Nonionic Polymers

Polymers may reach the soil–subsurface system as agrochemical additives applied to agricultural lands, and as municipal and industrial wastes disposed on soils and in surface waters. In addition, some polymers are used in soil and water restoration practices and in the modification of soil constituent properties, to increase their contaminant retention properties. Nonionic polymers are used also to stabilize soil structure, to increase water infiltration, and to prevent soil erosion.

Uncharged polymers tend to have random coil conformations in aqueous solutions. As a consequence, in terms of their sorption on clay particle surfaces, surface accessibility and entropy effects play an important role. There are two pathways for the modification of clay minerals by polymers (Liu 2007). The first one is physical adsorption controlled by thermodynamic criteria, which change the surface properties of clay. The second pathway involves the grafting of functional polymers to the surface of clay minerals. This conduit comprises two different pathways. The first one, a one-step grafting method, consists of condensation of functional polymers with reactive groups of the clay substrate. In this step, chemisorption of the first fraction of polymer chains hinders the diffusion of the following chains. The second mechanism, two-step grafting, involves an initial covalent attachment of a monolayer from a polymerizable molecule to the clay solid phase. After this activation starts, the chains continue to grow in the polymer–clay interface, with the limit to propagation being the diffusion of monomers to the active species (Liu 2007).

From the microstructural point of view, a polymer-layered silicate may have two morphological types (1) *intercalated* structure, where the polymer is inserted between the well-ordinated silicate layer, and (2) *exfoliated* structure, where the adsorbed polymer induces a wide distance between the silicate layers while avoiding interaction of adjacent layers.

Entry of a polymer molecule into a clay interlayer space may change the clay swelling ability, due to its capability to reduce the natural interlayer space. Inyang and Bae (2005) defined two modal types of sites for binding of polymer molecules on expanding clays: sorption on internal pore surfaces and penetration into interlayer sites (Fig. 6.25). The interlayer hydration water is depicted in Fig. 6.25a; polymer sorption on clay particles forming the pore walls and polymer penetration between the clay interlayers are given in Fig. 6.25b.

The dimension of the interlayer space variation in each type of clay and the specific molecular size and radius of the contaminant polymer are factors that control the chemical penetration into the clay. At a high polymer concentration, coil overlap can limit opportunities for movement of free molecules into the layer
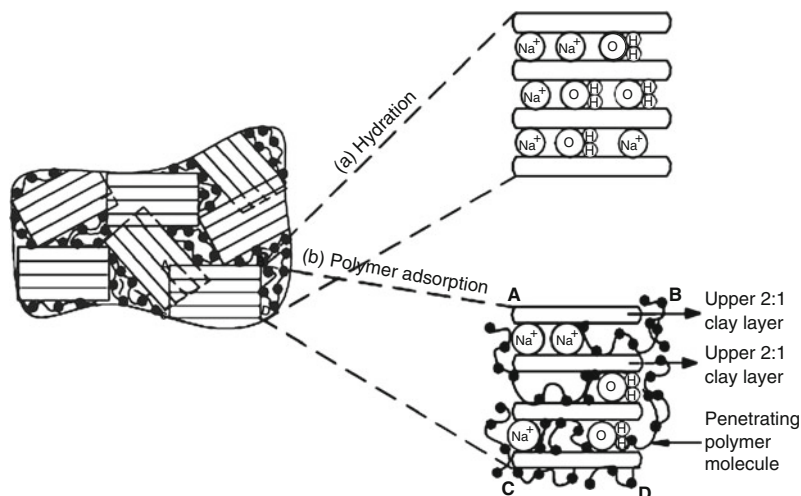
**Fig. 6.25** Schematic diagram of clay unit arrangement for (**a**) hydration and (**b**) polymer adsorption (after Inyang and Bae 2005). Reprinted from Inyang HI, Bae S, Polyacrylamide sorption opportunity on interlayer and external pore surfaces of contaminant barrier clays. Chemosphere 58:19–31, Copyright (2005), with permission from Elsevier

space of the clay. Based on relative size ratio and molecular availability, Inyang and Bae (2005) evaluated the potential for polyacrylamides (PAM) to enter the inter-layer space of Na-montmorillonite and kaolinite (Fig. 6.26).

PAM are water-soluble polymers formed by the polymerization of acrylamide. Pure PAM is a homopolymer of identical acrylamide units. Formulated with copolymers, PAM can exhibit specific charges and/or various molecular weights (Barvenik 1994). Increasing molecular weight leads to an increase in the polymer chain length and viscosity of PAM solutions. The charge density of PAM compounds is determined by the percent of acrylamide group.

PAM are applied to soils to control soil hydraulic conductivity and soil erosion. It has been shown that PAM can be adsorbed irreversibly on soils (Ben-Hur et al. 1992) and clays (Breen 1999). High molecular weight PAM proved to be more effective than low molecular weight compounds. Michaels (1954) suggested that nonionic polymers are too tightly coiled to induce beneficial clayey soil interactions, and that only charged PAM should be used. As a consequence, only cationic and anionic PAM were used for soil reclamation purposes until about two to three decades ago (Green and Stott 2001).

Bonding of nonionic PAM on clay surfaces has been examined in a number of publications. It was suggested, for example, that hydrophobic bonding occurs when the hydrophobic backbone of nonionic PAM are adsorbed to the hydrophobic basal siloxane surface of kaolinite (Laird 1997), or are bound to montmorillonite by hydrophobic segments (Volpert et al. 1998). Copolymerization of nonionic PAM
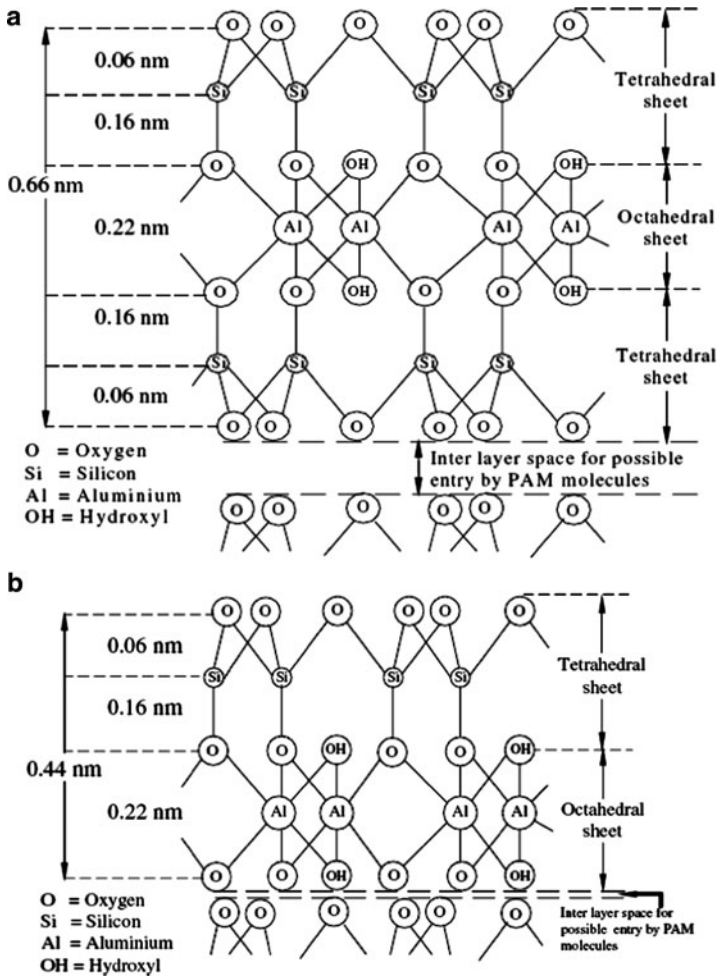
**Fig. 6.26** Schematic diagram of atomic arrangement in the unit of (**a**) montmorillonite showing expandable interlayer (internal) space for possible entry by PAM molecules. (**b**) kaolinite showing constricted interlayer space that may not be sufficiently large for significant entry by PAM molecules (after Inyang and Bae 2005). Reprinted from Inyang HI, Bae S, Polyacrylamide sorption opportunity on interlayer and external pore surfaces of contaminant barrier clays. Chemosphere 58:19–31, Copyright (2005), with permission from Elsevier

often occurs in commercial products, and favors these types of bonding. Water bridging is an additional way of indirectly linking nonionic PAM to the exchangeable cations of the clay surface (Theng 1979).

Deng et al. (2006b,c) investigated PAM interactions with clay materials, and specifically, effects of PAM on layered clay surfaces. To understand the different effects of uncharged and charged PAM on smectite clays, nonionic PAM were studied in comparison to cationic and anionic PAM–smectite complexes.

Fig. 6.27 Structure of the studied nonionic polyacrylamide (PAM) (modified after Deng et al. 2006b). Copyright 2006, Soil Science Society of America. Reprinted with permission
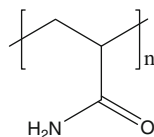
Nonionic PAM 903N
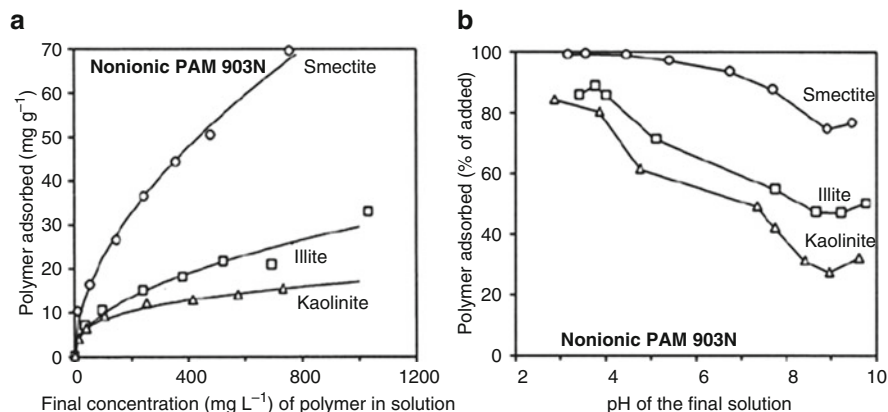


Fig. 6.28 Adsorption of nonionic PAM on smectite, illite, and kaolinite: (**a**) adsorption isotherm, (**b**) pH effect (modified after Deng et al. 2006c). Reprinted from Deng Y, Dixon JB, White GN, Loeppert RH, Juo ASR, Bonding between polyacrylamide and smectite. Colloids and Surfaces A 281:82–91, Copyright (2006), with permission from Elsevier

The structure of the nonionic acrylamide polymer (M.W. $\sim 10 \times 10^6$ Da) is presented in Fig. 6.27. The surface areas of the adsorbent clay minerals are smectite 787 $m^2\ g^{-1}$, illite-predominant mixture 256 $m^2\ g^{-1}$, and kaolinite 73 $m^2\ g^{-1}$.

### 6.2.2.3 Adsorption of Nonionic PAM on Clays

The adsorption isotherms of nonionic PAM on clays are of L-type (Fig. 6.28a), and are correlated to the clay surface area in the order smectite > illite > kaolinite (Deng et al. 2006c). Nonionic PAM adsorption on clays increases steadily with an increase in polymer concentration, the rate of increase being greatest in the case of smectite–nonionic PAM interactions. In the reported experiments, the amounts of nonionic PAM adsorbed on clays were greater than those of anionic and cationic PAM.

The adsorption of nonionic PAM decreases with an increase in pH, for all of the clays studied (Fig. 6.28c). The most sensitive clay was kaolinite, which exhibited the greatest decrease in adsorption. The response of nonionic PAM adsorption to solution pH may be explained as an hydrolysis effect, with PAM becoming a carboxylate group ($-CONH \rightarrow -COOH \rightarrow -COO^-$).

**Table 6.4** Assignments of IR bands ($cm^{-1}$) of PAM, smectite, and $Ca^{2+}$-saturated nonionic PAM 903N–smectite complex

| PAM | | Smectite | $Ca^{2+}$–PAM–smectite | Vibration[b] |
|---|---|---|---|---|
| Observed | Calculated[a] | | | |
| | | 3,622 | 3,622 | $v$, OH |
| | | 3,422 | | $v$, $H_2O$ |
| 3,342 | 3,338 | | 3,483 | $v_a$, $NH_2$ |
| 3,199 | 3,171 | | 3,385 | $v_s$, $CH_2$ |
| 2,955 | 2,965 | | 2,953 | $v_a$, $CH_2$ |
| 2,935 | 2,912 | | | $v_s$, $CH_2$ |
| | 2,856 | | | $v$, CH |
| 1,660 | 1,651 | | 1,663 | $v$, C=O |
| 1,618 | 1,614 | | 1,603 | $\delta$, $NH_2$ |
| 1,450 | 1,452 | | 1,456 | $\delta$, $CH_2$ |
| 1,413 | 1,422 | | 1,419 | $v$, C–N |
| 1,347 | 1,340 | | | $\omega$, CH2 |
| 1,319 | 1,321 | | | $\delta$, CH |
| 1,193 | 1,208 | | | $\omega$, $NH_2$ |
| | | | 1,000–1,200 | $v$, Si–O |
| 1,123 | 1,120 | | | $v_a$, C–C |
| | | 918 | 917 | $\delta$, OH(AlAl–OH) |
| | | 844 | 845 | $\delta$, OH (AlMg–OH) |
| | | 794 | 795 | ? |
| 759 | 780 | | | $\omega$, CH |
| | | 628 | 628 | $\delta$, Si–O–Si |
| 620 | 614 | | | $\gamma$, C–C |
| 559 | | | | |
| | | 522 | 522 | $\delta$, Si–O–Al |
| | | 470 | 470 | $\delta$, Si–O–Mg |

Symbols: $v_a$ asymmetric stretching, $v_s$ symmetric stretching, $\delta$ deformation (bending), $\omega$ wagging, $\gamma$ rocking

[a,b]References included in the original paper (after Deng et al. 2006b). Copyright 2006, Soil Science Society of America. Reprinted with permission

### 6.2.2.4   Formation of Nonionic PAM–Clay Complexes

FTIR spectroscopy provides information on the structural changes occurring in the clay matrix following PAM contamination. The results of FTIR studies performed by Deng et al. (2006b) are summarized in Table 6.4, which shows FTIR bands ($cm^{-1}$) of PAM, smectite, and a $Ca^{2+}$-saturated nonionic PAM–smectite complex.

The relevant functional groups (amino ($NH_2$), carbonyl (C = O), and C–N bond of the amide ($CONH_2$)) provide insight into the mechanism of bonding between the polymer and the mineral. Deng et al. (2006c) interpreted FTIR measurements only in terms of the behavior of these groups. Figure 6.29 shows the FTIR spectra of Ca-smectite and the respective functional groups of the nonionic PAM (PAM 903N) and of the PAM 903N–smectite complex (PAM 903N–Sm).
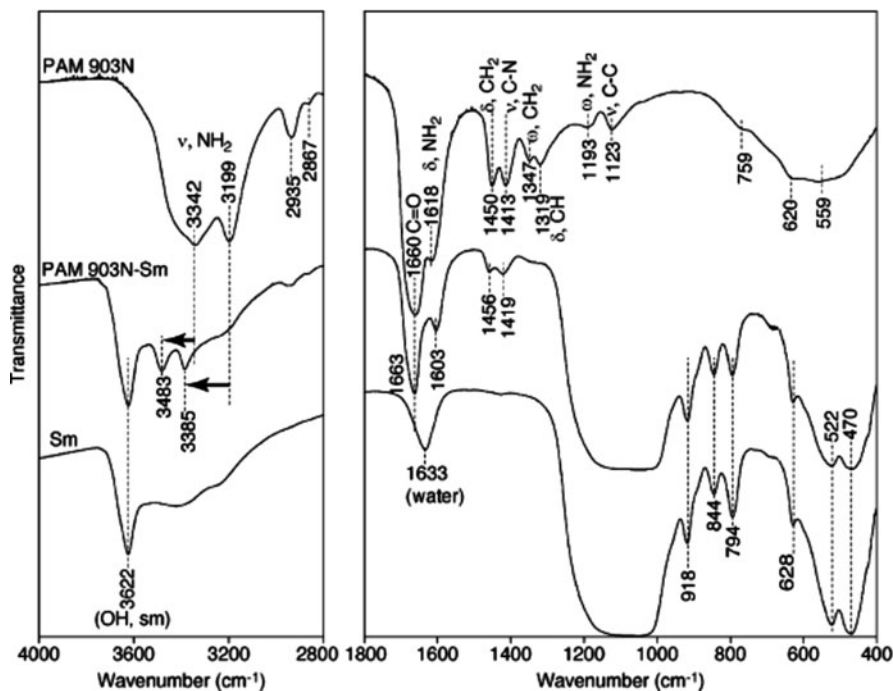
**Fig. 6.29** FTIR spectra of nonionic PAM 903N, $Ca^{2+}$-PAM 903N–smectite complex, and $Ca^{2+}$-smectite (after Deng et al. 2006b). Copyright 2006, Soil Science Society of America. Reprinted with permission

Adsorption on Ca-smectite led to formation of distinct shifts in the FTIR bands of PAM 903N: the asymmetric-stretching band of $NH_2$ groups shifted by 141 $cm^{-1}$; the symmetric stretching band blue-shifted by 186 $cm^{-1}$; the C = O stretching vibration shifted by 3 $cm^{-1}$; and the $NH_2$ banding vibration red-shifted by 15 $cm^{-1}$. Based on these "band shifts," Deng et al. (2006b) considered that PAM 903N adsorption on smectite led to the N–H bond strength of the amide group without appreciably affecting the carbonyl C = O bond strength. Deng et al. (2006b) attributed the FTIR band shifts of the adsorbed nonionic PAM units to the following three pathways (1) break of H-bonds between the amide groups due to separation of polymer chains; (2) direct ion–dipole interactions or coordination between amide groups and exchangeable cations; and (3) formation of H-bonds between amide groups and water molecules in the hydration shells of exchangeable cations.

Induced effects of PAM 903N bonding on Ca-smectite – with various band frequency differences – were observed when the mineral was saturated with cations other than Ca (Fig. 6.30). Small differences in the band position were detected between the PAM 903N–smectite complexes when the mineral was initially saturated with alkali cations or with transition metal cations. The corresponding bands of complexes saturated with alkaline earth cations were located between
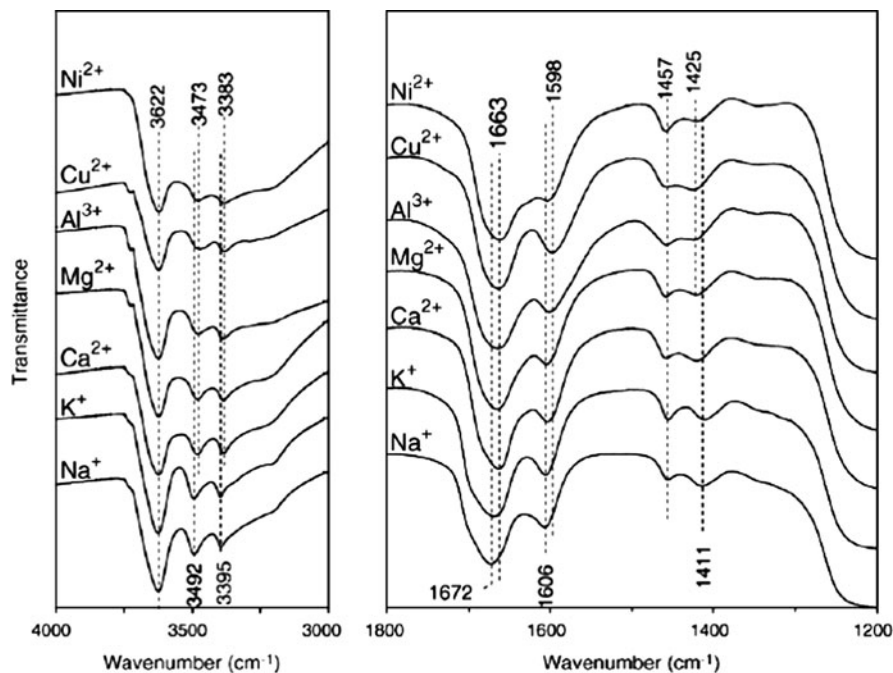
**Fig. 6.30** FTIR spectra of PAM 903N–smectite complexes saturated or exchanged with different cations (after Deng et al. 2006b). Copyright 2006, Soil Science Society of America. Reprinted with permission

those of complexes containing the alkali cations and those containing transition metal cations. The FTIR band shifts related to saturating smectite cations suggest that the amide group of nonionic PAM was bonded more strongly by transition metal cations than by alkali cations. The FTIR analysis showed that smectite was intercalated by the nonionic PAM 903N and that the bonding between the nonionic PAM units and the clay mineral occurred through an ion–dipole interaction/coordination and H-bonding. The differences in FTIR band positions among the PAM–smectite complexes saturated or exchanged with different cations suggest that the exchangeable cation of the adsorbing mineral directly influences the bonding strength between the polymer and the smectite.

Based on the above findings, Deng et al. (2006b) proposed a conceptual model (Fig. 6.31) for bonding and conformation of the nonionic PAM–smectite complex; the *d*-spacing allows only one layer of PAM to intercalate in the smectite interlayer. In the proposed model, exchangeable cations saturating the mineral, water molecules and nonionic PAM chain interact within the smectite interlayer via water bridging and/or ion dipole interaction/coordination.

Intercalation/exfoliation ratios in a PVP–montmorillonite depend on the hydration status of the system. Based on XRD analysis, Koo et al. (2003) showed that the diffraction pattern of PVP–montmorillonite changes with the concentration of
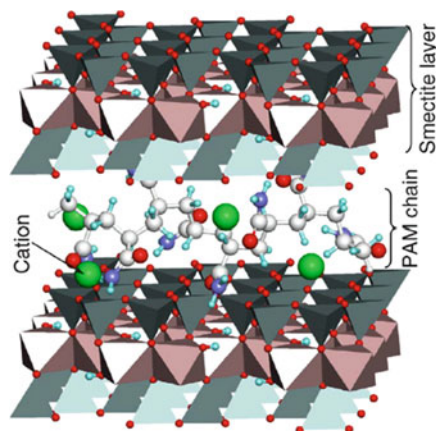
silicate (Fig. 6.32). The $d_{001}$ reflection peak does not appear up to a silicate concentration of 15% wt. and is clearly visible above 20% wt. This indicates that clay exfoliation occurs up to 15% wt. silicate content and that intercalated morphology appears above 20% wt. The $d$-spacing between adjacent layers gradually decreases with the concentration of silicates in the intercalation region.

The stability of nonionic PAM–smectite complexes was tested by determining their resistance to water, electrolyte washing, and heating (Deng et al. 2006a,b). Three and four consecutive washings with distilled water and aqueous electrolyte solution did not desorb more than 3% from the amount of initial nonionic PAM intercalated into Ca-smectite layers, proving the irreversibility of nonionic PAM sorption by smectite minerals. Heating of Ca-smectite to a temperature of 250°C led to a complete collapse of the layered mineral. Once nonionic PAM adsorbed, the
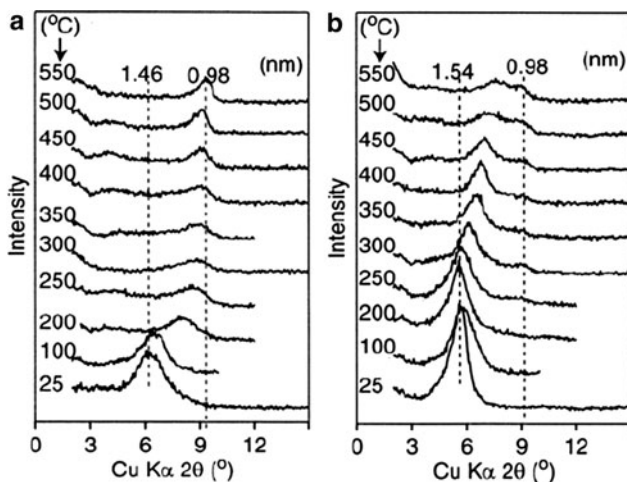
**Fig. 6.33** X-ray diffraction patterns of (**a**) Ca-smectite, (**b**) nonionic PAM 90 (Deng et al. 2006c). Reprinted from Deng Y, Dixon JB, White GN, Loeppert RH, Juo ASR, Bonding between polyacrylamide and smectite. Colloids and Surfaces A 281:82–91, Copyright (2006), with permission from Elsevier

PAM–smectite complex was stable up to a temperature of 300°C and exhibited a total collapse only at 350°C. The resistance to heating was reflected in the different diffraction patterns of smectite and nonionic PAM–smectite complex, as shown in Fig. 6.33.

Ca-smectite $d$-spacing was found to collapse to 1.0 nm at 250°C and higher temperatures. Nonionic PAM–smectite complex maintained its $d_{001}$ spacing >1.4 nm at a temperature lower than 300°C and gradually collapsed to 1.1 nm until the temperature rose to 550°C. In a complementary experiment, samples of PAM 903N–smectite complex and smectite saturated with different cations were kept for 1 h at a temperature of 300°C. XRD analysis indicated that PAM 903N–smectite complexes with exchangeable $Na^+$, $K^+$, $Mg^{2+}$, $Al^{3+}$, $Cu^{2+}$, and $Ni^{2+}$ had nearly the same $d_{001}$ spacing of 1.5 nm at room temperature, and after 1 h at 300°C, the $d_{001}$ decreased only to 1.4 nm. Both washing and heating treatments proved the irreversibility of the PAM-induced smectite modification.

*Polyvinylpyrrolidine* $(C_6H_9NO)_n$, known also under the name of PVP, is a nonionic water-soluble polymer with amphiphilic character made from the monomer *N*-vinylpyrrolidone. PVP may reach soil clay minerals (e.g., smectites and kaolinite) as an agrochemical additive or within engineering organo-clays to be used as contaminant adsorbents within the soil–subsurface environment.

The interfacial conformation of PVP adsorbed on smectite clays depends on the chain length and type of the clay exchangeable cation. When the polymer binds to the smectite surface, the higher molar mass PVP forms longer tails and loops (Sequaris et al. 2000, 2002). Coverage of a smectite surface by the polymer remained nearly constant, suggesting that the PVP chains lay parallel to the surface.

Additional PVP adsorption was not affected by the charge density of the smectite layer or by the location of the charge (Blum and Eberl 2004).

### 6.2.2.5   PVP-Induced Effects on Smectite Exfoliation

Interlayer adsorption of PVP on $K^+$, $Na^+$, $Ca^{2+}$, and $Mg^{2+}$ monoionic montmorillonites, as reflected in the $d_{001}$ spacing, was determined by Levy and Francis (1975). PVP-induced changes in the $d_{001}$ spacing of the PVP–montmorillonite complexes are shown in Table 6.5. Saturating cations of montmorillonite control the PVP-induced change of the clay $d_{001}$ spacing. The $K^+$-montmorillonite–PVP complex was characterized by a $d_{001}$ spacing of $13.2 \pm 0.4$ Å; this decreased to 10 Å after heating, indicating that dehydrated $K^+$-montmorillonite did not adsorb PVP in the interlayers. $Ca^{2+}$- and $Mg^{2+}$-montmorillonite $d_{001}$ spacing decreased from $19.9 \pm 05$ to 16.0 Å after heating, and remained constant even when heating temperatures rose to $300°C$. The interlayer adsorption of PVP is confirmed by this behavior.

The $d_{001}$ spacing of the $Na^+$-montmorillonite–PVP complex is controlled by the hydration status. The amount of PVP adsorbed is affected by the interlayer distance prior to adsorption. The presence of water affects the swelling of $Na^+$-montmorillonite, so that more layers are able to adsorb PVP.

The stability of PVP-induced changes in the $d_{001}$ spacing of $K^+$-, $Na^+$-, $Ca^{2+}$-, and $Mg^{2+}$-montmorillonite may be observed by subjecting PVP–montmorillonite complexes to an elevated heating up to $300°C$. First-order basal spacings of $K^+$-, $Na^+$-, and $Ca^{2+}$-$Mg^{2+}$-montmorillonite–PVP complexes, as a function of rising temperature from ambient conditions up to $300°C$ in hydrated and dehydrated systems, are shown in Fig. 6.34. It may be noted that the PVP-induced $d_{001}$ spacing remained constant even at high temperatures when the polymer was adsorbed within the interlayers of the PVP–montmorillonite complexes.

Szczerba et al. (2010) showed that in a PVP–smectite system, PVP formed a layer of about 5–6 Å thickness on the $d_{001}$ spacing of smectite surface. As a consequence, the concentration of atoms at close distance to the smectite layer was enhanced; the higher concentration of atoms occurred in the first 3 Å of the layer. PVP chains bound directly to the clay surface appeared to be more rigid, while the outer parts were more flexible. Based on experimental results, Szczerba et al. (2010) suggested a new representation (Fig. 6.35) of a PVP–smectite composite which differs completely from the Na-smectite mineral structure.

### 6.2.2.6   Zeta Potential

Under some specific conditions (e.g., sodium effect), clay may be dispersed and transported into the vadose zone as suspended particles. The zeta potential expresses a particular environmental state which may control the vertical redistribution of clay colloids in the soil–subsurface system. The PVP-induced

**Table 6.5** First-order basal spacing (reported in Å) of four monoionic PVP–montmorillonite complexes in equilibrium with 1% PVP ethanol solutions containing different amounts of water (after Levy and Francis 1975). Reprinted from Levy R, Francis CW, Interlayer adsorption of polyvinylpyrrolidone on montmorillonite. J Colloid Interface Sci 50:442–450, Copyright (1975), with permission from Elsevier

| Water (%) | K-montmorillonite[a] | | Ca-montmorillonite[a] | | Mg-montmorillonite[a] | | Na-montmorillonite[a] | | Na-montmorillonite[b] | |
|---|---|---|---|---|---|---|---|---|---|---|
| | Immediately | After 24 h | Immediately | After 24 h | Immediately | After 24 h | Immediately | After 24 h | Immediately | After 24 h |
| 0 | 13.4 | 12.6 | 19.6 | 19.2 | 19.6 | 18.8 | Diffused | 25.2 | 17.7 | 17.7 |
| 5 | 13.0 | 12.8 | 19.6 | 19.2 | 19.6 | 19.6 | Diffused | 25.2 | 17.7 / Diffused | 23.2 / 17.0 |
| 10 | 13.0 | 12.6 | 19.6 | 19.2 | 19.6 | 19.2 | Diffused | 25.2 | Diffused / Diffused | 26.6 / 17.3 |
| 20 | 13.0 | 12.8 | 19.2 | 19.2 | 19.6 | 17.0 | Diffused | 25.2 | Diffused / Diffused | 27.6 / 17.6 |
| 30 | 13.0 | 12.8 | 19.2 | 18.8 | 19.2 | 17.0 | Diffused | 26.8 | Diffused / Diffused | 27.6 / 17.6 |
| 40 | 13.0 | 13.2 | 19.2 | 18.8 | 19.2 | 17.0 | Diffused | 24.5 | Diffused / Diffused | 26.0 / 17.6 |
| 50 | 13.0 | 12.6 | 18.8 | 17.7 | 19.2 | | Diffused | 24.5 | Diffused / Diffused | 26.0 / 17.3 |
| 60 | 13.6 | 13.0 | 18.8 | 17.0 | 20.5 | 17.3 | Diffused | 24.5 | Diffused / Diffused | 32.7 / 17.3 |
| 70 | 13.4 | 13.0 | 19.6 | 19.2 | 21.0 | 17.7 | Diffused | 28.5 | Diffused / Diffused | 33.9 / 17.3 |
| 80 | 13.0 | 12.6 | 19.6 | 19.2 | 21.5 | 17.0 | Diffused | 28.5 | Diffused / Diffused | 31.5 / 17.0 |

[a]Dehydrated by three successive washes with ethanol
[b]Dehydrated by five successive washes with ethanol
[c]Two first-order basal spacings

**a**

SPACING (Å)

○ ETHANOL WASHED
● PVP-COMPLEX IN EQUILIBRIUM WITH 1 % PVP ETHANOL SOLUTION
■ PVP-COMPLEX IN EQUILIBRIUM WITH 1 % PVP - WATER SOLUTION

TEMPERATURE (˚C)

**b**

○ ETHANOL WASHED
● ᵃPVP-COMPLEX IN EQUILIBRIUM WITH 1 % PVP-ETHANOL SOLUTION
▲ ᵇPVP-COMPLEX IN EQUILIBRIUM WITH 1 % PVP-ETHANOL SOLUTION
■ PVP-COMPLEX IN EQUILIBRIUM WITH 1 % PVP-WATER SOLUTION

SPACING (Å)

a MONTMORILLONITE DEHYDRATED BY 3 ETHANOL WASHES
b MONTMORILLONITE DEHYDRATED BY 5 ETHANOL WASHES

TEMPERATURE (˚C)

**c**

SPACING (Å)

○ ETHANOL WASHED
● PVP-COMPLEX IN EQUILIBRIUM WITH 1 % PVP ETHANOL SOLUTIONS
■ PVP-COMPLEX IN EQUILIBRIUM WITH 1 % PVP - WATER SOLUTIONS

TEMPERATURE (˚C)

**Fig. 6.34** First-order basal spacing of (**a**) potassium-, (**b**) sodium-, and (**c**) calcium–magnesium–PVP–montmorillonite complexes as a function of temperature (modified after Levy and Francis 1975). Reprinted from Levy R, Francis CW, Interlayer adsorption of polyvinylpyrrolidone on montmorillonite. J Colloid Interface Sci 50:442–450, Copyright (1975), with permission from Elsevier

modification of raw clays may affect their zeta potential and, as a consequence, their transport as suspended particles within soil and subsurface water. The zeta potential is the potential difference between the dispersion medium and the stationary layer of fluid attached to the dispersed particles. The zeta potential indicates the degree of repulsion between adjacent, similarly charged particles in dispersion. Under low zeta potential, attraction exceeds repulsion and the dispersed clay colloids break and flocculate. Thus, colloids with high zeta potential (negative or positive) are electrically stabilized, while colloids with low zeta potentials tend to coagulate or flocculate.

Al Juhaiman et al. (2010) found that raw and Na-bentonite modified by PVP adsorption exhibit different zeta potential values as a function of amount of PVP added to the system. The variation in the zeta potential of raw bentonite and

**Fig. 6.35** A representation of the possible distribution of PVP between adjacent smectite layers (after Szczerba et al. 2010). Reprinted from Szczerba M, Środoń J, Skiba M, Derkowski A (2010) One-dimensional structure of exfoliated polymer-layered silicate nanocomposites: A polyvinylpyrrolidone (PVP) case study. Appl Clay Sci 47:235–241, Copyright (2010), with permission from Elsevier
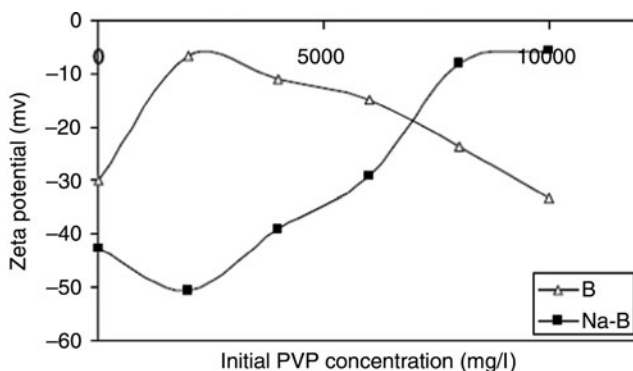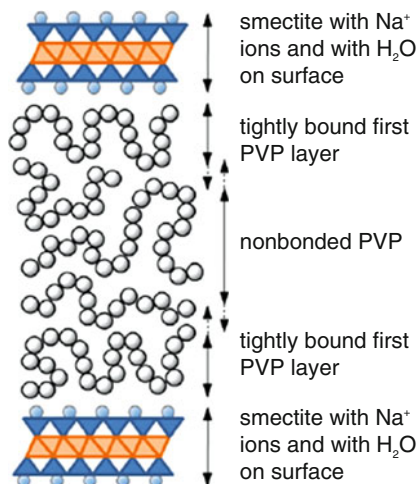


**Fig. 6.36** The variation in zeta potential of bentonite (B) and sodium bentonite (Na-B) suspensions at different PVP concentrations. Reprinted from Al Juhaiman LA, Mekhamer WK, Al-Boajan AM (2010) Effect of poly(vinyl)pyrrolidone on the zeta potential and water loss of raw and Na-rich Saudi bentonite. Surf Interface Anal 42:1723–1727. Copyright 2010 with permission of John Wiley and Sons

Na-bentonite as a function of PVP concentration is shown in Fig. 6.36. Before addition of PVP, the zeta potentials of bentonite and Na-bentonite were −30 and −41 mV, respectively. The negative zeta potential of the bentonite suspension decreased to a minimum value (−6.65 mV) in the presence of 1,000 mg $L^{-1}$ PVP, and then increased with increasing PVP concentration.

This behavior is explained by the competition between the adsorption of water and PVP molecules on bentonite surfaces, which favor bridging of individual PVP molecules. This led to the formation of loose aggregates and a subsequent decrease in zeta potential. With increase in PVP concentration, flocculation decreased and the zeta potential increased. A reverse trend was observed in the

case of Na-bentonite suspensions, due to sodium induced swelling of bentonite, which caused a reduction in PVP molecule bridging and a decrease in clay flocculation.

### 6.2.2.7   Nonionic Pesticides

Hundreds of pesticides are nonionic organic compounds, belonging to chemical groups such as chlorinated hydrocarbons, organophosphates, carbamates, ureas, anilines, anilides, uracils, and benzonitriles. The significant differences among the properties of these groups, and even among compounds from the same group, are reflected in the variability of their adsorption behavior and of their potential to complex with clay minerals. Nonionic organic pesticides are not expected to be strongly attracted by charged clay surfaces, and compete with hydration water for the adsorption sites of the minerals. Despite the fact that nonionic pesticides are only slightly soluble in water, mechanisms are postulated for formation of various bonds: cation dipole, coordination, hydrogen, $\pi$, and van der Waals. Because of their low solubility, these organic pesticides are adsorbed by clays, even when the clay surface exhibits a low hydration status. Advanced instrumental techniques (e.g., DTA, XRD, FTIR, NMR, and EXAFS) and molecular modeling provide the possibility of defining the mechanism of nonionic pesticide–clay complex formation and stability within the soil–subsurface environment.

Parathion (0,0-diethyl 0-p-nitrophenyl phosphorothioate) is an organophosphorus insecticide which was used widely as a crop protection chemical. Due to its highly toxic properties, it is considered a very dangerous contaminant. A number of studies examined parathion adsorption and degradation, as well as related compounds such as phenol and p-nitrophenol, on clays (Yaron and Saltzman 1972; Saltzman and Yariv 1975, 1976; Yaron 1975; Prost et al. 1977; Mingelgrin and Saltzman 1979; Gerstl and Yaron 1981). These studies are discussed here to illustrate contaminant-induced changes in the host adsorbent matrix. Compared to p-nitrophenol, the parathion molecule has a less polar character so that a weaker interaction with the clay surface may occur. Both functional groups of parathion, $NO_2$ and $P = S$, interact with clay.

In comparing the adsorption isotherms of parathion from hexane solution on oven-dried clays kaolinite (1:1 type), montmorillonite (2:1 type), and attapulgite (fibrous), Prost et al. (1977) found that montmorillonite and attapulgite have similar adsorption capacities, while the adsorption capacity of kaolinite is significantly lower (Fig. 6.37a). The hydration state of the clay affects its capacity of adsorption. Figure 6.37b, for example, shows the decrease in adsorption capacity of attapulgite for parathion when dried at 105°C, and at 8.5 and 15.0% relative humidity. This phenomenon can be explained by competition between water and parathion molecules (Yaron and Saltzman 1972; Kyle 1981), and by changes in the coordination between hydrated and nonhydrated clay–parathion complexes (Saltzman and Yariv 1976).
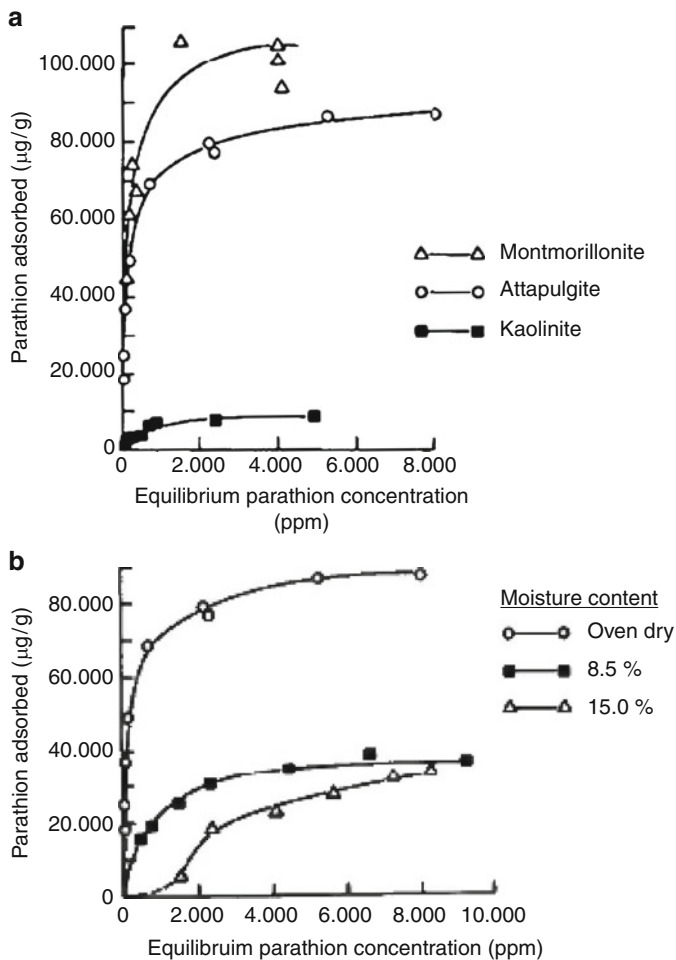
**Fig. 6.37** Adsorption of parathion (**a**) on oven-dried clays from hexane solution, and (**b**) on attapulgite as affected by moisture content (after Prost et al. 1977)

Parathion adsorption on montmorillonite leads to a change in the basal spacing of the clay mineral (Table 6.6). It was observed by X-ray studies that the type of clay saturating cation affects the extent of the parathion-induced change in basal spacing. For example, the basal spacing was observed to increase in the case of Li and Na-clays, to remain unchanged in K- and Mg-clays, and to decrease in Ca- and Al-clays. The hydration of parathion–montmorillonite complex at 40% relative humidity resulted in a decrease in $d$-spacing of the clays saturated with monovalent cations.

Cation–water–parathion assemblages formed in the clay interlayer spaces reveal, on the one hand, contaminant-induced changes on the original clay matrix, and on the other hand, clay-induced modification of the contaminant molecule.

**Table 6.6**  Basal spacing of parathion–montmorillonite complexes

| Saturating cation | Parathion–clay complex | | | Untreated clay | |
|---|---|---|---|---|---|
| | a $\overset{\circ}{\text{A}}$ | b $\overset{\circ}{\text{A}}$ | c $\overset{\circ}{\text{A}}$ | a $\overset{\circ}{\text{A}}$ | c $\overset{\circ}{\text{A}}$ |
| Li | 15.2 | 14.2 | 12.3 | 14.5 | 12.8 |
| Na | 13.6 | 12.4 | 11.9 | 12.8 | 9.8 |
| K | 12.3 | 12.1 | 11.9 | 12.3 | 10.4 |
| Mg | 15.2[a] | 15.2[b] | 14.7 | 15.2 | 10.0 |
| Ca | 15.2[a] | 15.2[b] | 14.7 | 15.5 | 9.7 |
| Al | 15.3[a] | 15.8[b] | 15.2 | 15.8 | 10.3 |

a: before heating; b: hydrated at 40% relative humidity; c: after heating at 200°C under vacuum (after Saltzman and Yariv 1976). Copyright 1976, Soil Science Society of America. Reprinted with permission

[a]Almost integral order of reflection
[b]Integral order of reflection

Infrared adsorption bands of Na-montmorillonite, parathion in hexane solution, and dry and hydrated parathion–montmorillonite complexes in the 600–1,600 cm$^{-1}$ wave number region are shown in Fig. 6.38. It can be observed, for example, that Na-montmorillonite was enriched following parathion adsorption by additional $NO_2$ antisymmetric and symmetric rings, with characteristic vibrations in the range 1,359–1,550 cm$^{-1}$. In all air-dried complexes, on the contrary, adsorbed parathion $NO_2$ antisymmetric stretching frequencies were shifted to lower values, indicating that only one of the O-atoms of the nitro groups is involved in coordination. Additional data on changes in parathion vibrational frequency as a result of adsorption on clays (montmorillonite and attapulgite) are given in Table 6.7.

The stability of parathion-induced changes was tested by studying the resistance of the contaminant–clay complex to heat and to desorption in water. Saltzman and Yariv (1976) observed that in the process of dehydration by heating under vacuum, clear differences appeared between mono- and polyvalent cation vibrations. Antisymmetric and symmetric $NO_2$ vibrations were shifted by 2–6 cm$^{-1}$ when the mineral fraction from the montmorillonite–parathion complex was saturated with monovalent cations. In contrast, the stretching frequencies of both antisymmetric and symmetric nitro groups were not changed compared to those of parathion in solution, in the case of polyvalent cations. Attapulgite–parathion complexes exhibit different configurations in hydrated and dehydrated systems. Infrared spectroscopy studies by Prost et al. (1977) showed that parathion is bound on attapulgite via H-bonds between the $NO_3$ group of the pesticide and the hydrogen in water molecules of the hydration shell of the adsorbed cation. Upon dehydration, these bonds were not observed, whereas a change in P-S moiety of the parathion molecule appeared as a result of direct linkage to the adsorbed cation itself (Table 6.8).

Infrared spectra of pure parathion heated at 100°C did not differ from those of unheated parathion, except for a decrease in intensity. The behavior of parathion–clay complexes is different. Gerstl and Yaron (1981) noted that in parathion–attapulgite complexes, pesticide hydrolysis was minimal and that heating at 100°C led to the isomerization of parathion on hydrated, partially

**Fig. 6.38** IR spectra of
(**a**) parathion, (**b**) Mg-
montmorillonite–parathion
air dried, (**c**) Mg–Mg-
montmorillonite–parathion at
180°C under vacuum, (**d**) Al-
montmorillonite–parathion
air dried, (**e**) Al-
montmorillonite–parathion
at 180°C under vacuum,
(**f**) Ca-montmorillonite
(modified after Saltzman and
Yariv 1976; Dellisanti and
Valdré 2005). Copyright
1976, Soil Science Society
of America. Reprinted with
permission
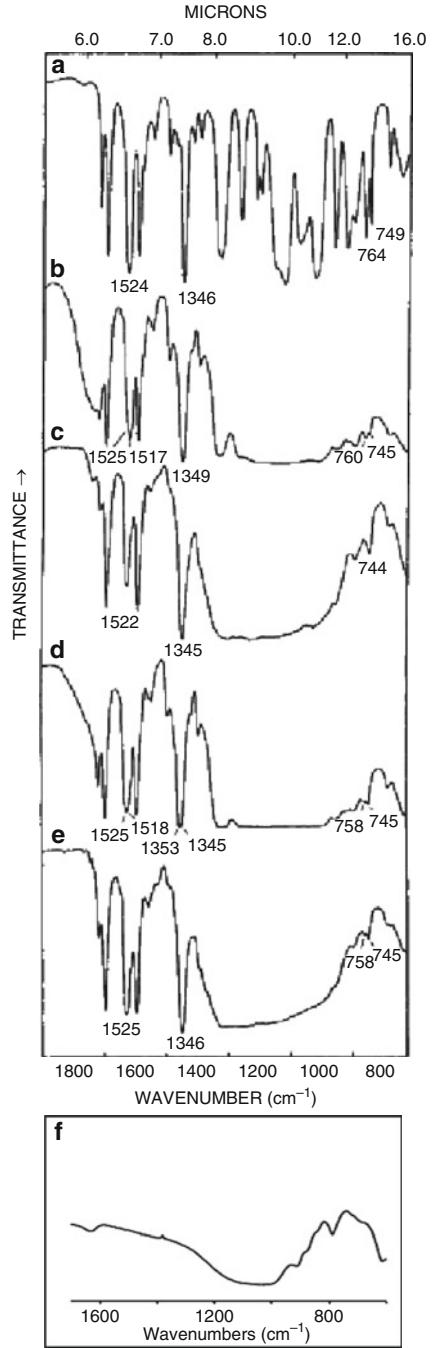
**Table 6.7** Vibrational frequencies (cm$^{-1}$) of parathion in hexane solution and adsorbed on attapulgite and montmorillonite (after Prost et al. 1977)

| Vibration type | Parathion in hexane solution | Parathion on attapulgite | | Parathion on Ca-montmorillonite film |
| --- | --- | --- | --- | --- |
| | | In KBr disks | Deposited on AgBr windows | |
| NO$_2$ antisymmetric stretching | 1,529 | 1,527 | 1,516 | 1,518 |
| No$_2$ symmetric stretching | 1,344 | 1,348 | 1,348 | 1,350 |
| Ring vibrations | 1,614 | 1,616 | 1,614 | 1,614 |
| | 1,595 | 1,593 | 1,591 | 1,590 |
| | 1,491 | 1,493 | 1,491 | 1,492 |
| P = S stretching | 762 | 764 | 763 | 764 |

**Table 6.8** Effect of heating on vibrational frequencies of parathion–attapulgite complexes (after Prost et al. 1977)

| Vibration type | Parathion in hexane solution | Temperature (°C) | Free parathion on AgBr | Adsorbed on attapulgite |
| --- | --- | --- | --- | --- |
| NO$_2$ anti symmetric stretching | 1,529 | 20 | 1,521 | 1,516 |
| | | 65 | 1,518 | 1,522 |
| | | 110 | * | * |
| NO$_2$ symmetric stretching | 1,344 | 20 | 1,347 | 1,344 |
| | | 65 | 1,344 | 1,345 |
| | | 110 | * | 1,345 |
| | 1,614 | 20 | 1,616 | 1,614 |
| | | 65 | 1,614 | 1,621 |
| | | 110 | * | 1,628 |
| Ring vibrations | 1,595 | 20 | 1,592 | 1,591 |
| | | 65 | 1,591 | 1,591 |
| | | 110 | * | 1,591 |
| | 1,491 | 20 | 1,492 | 1,490 |
| | | 65 | 1,492 | 1,491 |
| | | 110 | * | * |
| P = S stretching | 762 | 20 | 763 | 763 |
| | | 65 | 763 | 749 |
| | | 110 | * | * |

*Not present

dehydrated, and dehydrated clay. Distortion of the phosphate moiety by the oxygen of the ligand toward a trigonal bipyramid structure puts the three P–O bonds of parathion into one plane, enabling the S–C bond of the isomer to form more easily. Based on the fact that almost no hydrolysis products were found in the attapulgite–parathion complex (0.4% at 110°C), Gerstl and Yaron (1981) concluded that isomerization is the main reaction occurring on Ca–attapulgite and that the formed isomer is stable at 110°C.

   While heating experiments provide insight into the transformation of organic contaminants within a contaminant–clay complex, desorption studies provide

**Fig. 6.39** Parathion
desorption isotherm from
attapulgite: (*open circle*)
hydrated, (*closed circle*)
partially dehydrated, and
(*triangle*) modified
dehydrated (modified after
Gerstl and Yaron 1978).
Reprinted with permission
from Gerstl Z, Yaron B
(1978) Adsorption and
desorption of parathion from
attapulgite as affected by the
mineral structure. J Agric
Food Chem 26:569–573.
Copyright 1978 American
Chemical Society
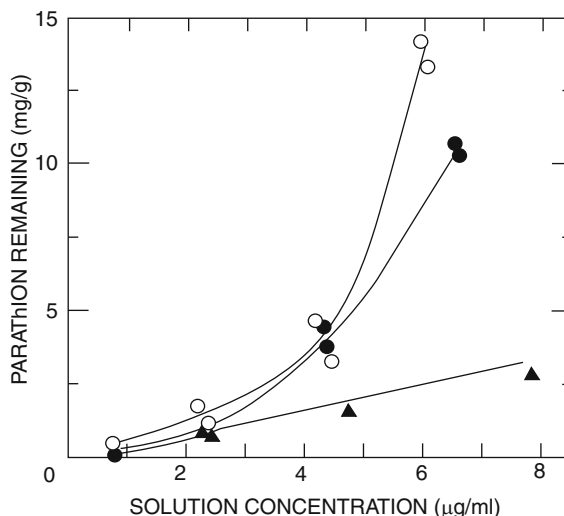


information on the reversibility of contaminant-induced alteration of clay minerals. Gerstl and Yaron (1981) showed that under equilibrium conditions, the hydration status of adsorbing clay controls the release of parathion from a parathion–-attapulgite complex in water solution. Two characteristic groupings for the release of parathion from parathion–attapulgite complex were defined (1) linear desorption for the dehydrated attapulgite, with a nearly complete release, and (2) nonlinear release from hydrated and partially hydrated attapulgite, with significant retention of contaminant within the parathion–attapulgite complex. This nonlinear release exhibited a hysteretic process that suggests irreversible adsorption of parathion on the attapulgite surface (Fig. 6.39).

It was shown that parathion may induce changes in the matrix of clay minerals. Once adsorbed on clay surfaces, parathion may degrade through hydrolysis of the phosphate ester bond into nitrophenol and phosphate. The rate of degradation is affected by clay type and hydration status.

Alachlor, 2-chloro-N-(2,6-diethylphenyl)-N-(methoxymethyl)acetamide, is a non-ionic herbicide used widely for pre-emergence weed control. Study of interactions between alachlor and montmorillonite saturated with different cations (Bosetto et al. 1993) found a correlation between adsorption and the polarizing power of exchangeable cation. XRD measurements showed that alachlor penetrates the interlayer space of the clay, and FTIR analysis confirmed that the alachlor molecule is adsorbed on monoionic montmorillonite by a coordination bond, through a water bridge, between C = O groups and the clay exchangeable cation. Extended instrumental research, including DTA, XRD, SEM, and thermo-FTIR spectroscopy, by Nasser et al. (1997) enabled delineation of the changes occurring on montmorillonite as induced by alachlor adsorption; these results are discussed below.

Differential thermal analysis (DTA) of Na-montmorillonite, alachlor, and Na-montmorillonite treated with alachlor is shown in Fig. 6.40. The Na-montmorillonite
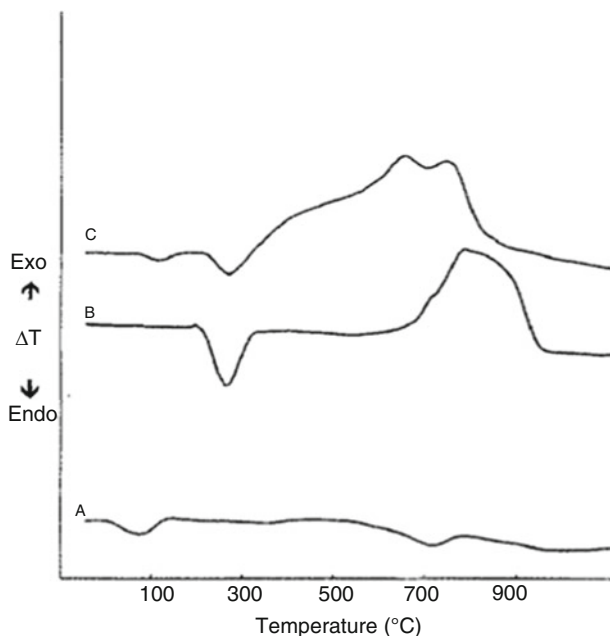
**Fig. 6.40** DTA curves of (**A**) Na-montmorillonite, (**B**) alachlor, and (**C**) Na-montmorillonite treated with alachlor (modified after Nasser et al. 1997)

curve shows small dehydration and dehydroxylation endothermic peaks at 90 and 690°C. The DTA curve of alachlor shows an endothermic peak at 220°C and an exothermic peak at 770°C. The DTA curve of alachlor–Na montmorillonite complexes is characterized as follows: a dehydration peak at 90°C characteristic of Na-montmorillonite almost disappeared due to alachlor replacing water in the clay interlayers; the peak at 220°C is explained by the presence of free alachlor in the sample; oxidation of adsorbed alachlor began at 390°C and continued by exhibiting two exothermic peaks at 600 and 700°C.

XRD analysis showed an increase at room temperature (25°C) of the interlayer spacing of Na-montmorillonite, from 1.09 nm to 1.60 nm, as a result of alachlor adsorption. Heating the samples to 300°C led to a decrease in the Na-montmorillonite d-spacing, from 1.09 to 0.97 nm, in contrast to the alachlor–Na montmorillonite complex d-spacing which was not affected by temperature increases.

SEM showed clear differences in clay morphology before and after contamination by alachlor (Fig. 6.41). While Na-montmorillonite shows a plate-like structure, the alachlor–Na-montmorillonite complex forms flocks with significant edge-to-edge associations of the blocks. Nasser et al. (1997) explained the formation of flocks by the fact that the alachlor molecule is to some extent amphipathic. The polar head N–(CO–CH$_2$–Cl)(CH$_2$–O–CH$_3$) is bound to the broken layer edge, while the aromatic ring is hydrophobic and is directed to the opposite side when adsorbed
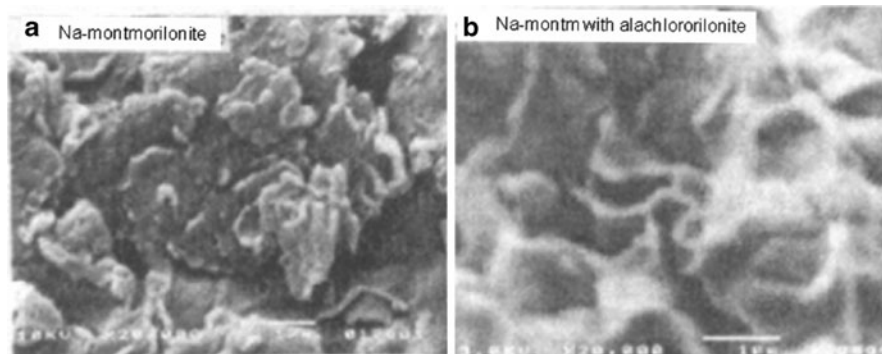
**Fig. 6.41** Representative scanning electron micrographs of (**a**) Na-montmorillonite and (**b**) Na-montmorillonite treated with alachlor (modified after Nasser et al. 1997)

**Table 6.9** Assignment and wave number ($cm^{-1}$) of characteristic absorption bands in IR spectra of neat alachlor, alachlor–Na-montmorillonite complex in fresh sample, and alachlor–Na-montmorillonite complex in aged samples (modified after Nasser et al. 1997)

|                | Band assignment | Neat | Na-mont. |
|----------------|-----------------|------|----------|
| Fresh samples  | CH(aromatic)    | 3,067, 3,026 | 3,070br, 3,026sh |
|                | $CH_3$          | 2,972, 2,880 | 2,972, 2,880 |
|                | $CH_2$          | 2,940, 2,834 | 2,940, 2,835sh |
|                | $C = O$         | 1,688 | 1,677, 1,671 |
|                |                 |       | 1,656, 1,647 |
|                | Ring            | 1,590vw, 1,438 | 1,590vw, 1,431 |
|                |                 | 1,413, 1,410 | 1,419, 1,407 |
|                | $C–CH_3$        | 1,458, 1,373 | 1,458, 1,375 |
|                | C(aromatic)-N   | 1,319, 1,311sh | 1,323, 1,310 |
|                | C(aliphatic)-N  | 1,245 | 1,251, 1,241 |
|                |                 | 1,193 | 1,193 |
| Aged samples   | NH              |       | 3,385, 3,261 |
|                | $C = O$ stretching (amide I) |  |  |
|                | Primary         |       | 1,684 |
|                | Secondary       |       | 1,653 |
|                | Tertiary        |       | 1,678sh |
|                | NH deformation (amide II) |  |  |
|                | Secondary       |       | 1,526 |

*br* broad, *sh* shoulder, *vw* very weak

to the clay edge. The edge-to-edge association is obtained by van der Waals interactions between the edges.

From thermo-FTIR spectroscopy results, Nasser et al. (1997) suggested that adsorption of alachlor occurs through hydrogen bonds between interlayer water molecules and the N or O atoms of the amide groups. Assignments and wave numbers ($cm^{-1}$) of characteristic adsorption bands in the IR spectra of neat alachlor and adsorbed by Na-montmorillonite immediately after alachlor application are given in Table 6.9.

Thermo-FTIR spectroscopy performed 6 months after alachlor was added to Na-montmorillonite exhibited weaker bands in comparison to those detected immediately after alachlor incorporation. However, due to molecule hydrolysis, for example, new bands appeared in the range 3,200–3,400 cm$^{-1}$; these are attributed to primary or secondary amides. Details on new bands appearing in IR spectra (cm$^{-1}$) of alachlor–Na-montmorillonite composites with aging are given in Table 6.9. One can observe that once a chemical contaminant adsorbed on a clay surface is degraded, its degradation products continue to maintain a modified clay, relative to the uncontaminated mineral.

Dinitrophenol herbicides, such as 4,6-dinitro-o-cresol (DNOC) and 4,6-dinitro-o-sec-butyl phenol (DINOSEB), interact with swelling clays. The mechanisms of interaction have been an important research topic over the last two decades. Early study showed that swelling clay minerals may have either high or low affinity for certain compounds, as a function of the number and substitution pattern of NO$_2$ groups and by the presence of non-NO$_2$ substituents on the aromatic rings (Haderlein and Schwarzenbach 1993; Weissmahr et al. 1997). For example, contrasting $K_d$ (L g$^{-1}$) values of 37 and 0.064 were obtained for DNOC and DINOSEB sorption from aqueous suspensions on a high charge K-montmorillonite (Haderlein et al. 1996), despite the minor structural differences between the two compounds. Subsequent investigations shed additional light on the adsorption of nitroaromatic compounds such as DNOC and DINOSEB on clay surfaces, and on herbicide-induced changes in clay configuration as a result of adsorption (Sheng et al. 2001, 2002; Johnston et al. 2001, 2002; Li et al. 2004; Pereira et al. 2008). These various studies yielded contradictory interpretations on the possible adsorption mechanisms of nitroaromatic compounds on clay surfaces. Here, we review these studies in the context of our focus on how contaminants induce changes in the clay matrix, without discussing the specific mechanisms of dinitrophenol herbicide adsorption on clay surfaces.

Because of the presence of strongly electron-withdrawing nitro ($-$NO$_2$) groups, DNOC was the herbicide most strongly adsorbed on a K-smectite (50 mg per g of clay; Sheng et al. (2001)). For this reason, we select this dinitrophenol herbicide as an example of a nonionic pesticide that has the potential to form a clay complex with a matrix structure different than that of the initial adsorbent. Sheng et al. (2002) report on adsorption of DNOC from an aqueous solution on montmorillonite surface, which is affected by both solution pH and the clay saturating cation. From Fig. 6.42a, it may be seen that DNOC adsorption increases with decreasing pH in the water solution. Decreasing the pH from 7 to 2.5 led to nearly complete conversion of the dissociated anionic species of DNOC to a molecular-neutral species, indicating that the herbicide is adsorbed primarily as a neutral species. Adsorption was affected also by the type of exchangeable cation of the clay (Fig. 6.42b). Among the cations tested, K$^+$- and Cs$^+$-clays were found to be the most effective for DNOC adsorption. This phenomenon is explained by the lower hydration energy of K$^+$ and Cs$^+$, and consequently by a greater free, nonhydrated adsorption domain on the siloxane surfaces between exchangeable cations available for DNOC adsorption.

It may be concluded that the high affinity for dinitrophenol herbicide sorption on clay smectites is due to site-specific interactions with exchangeable cations

**Fig. 6.42** Effect of (**a**) pH,
and (**b**) exchangeable cations
on DNOC adsorption on
Wyoming-montmorillonite
(after Sheng et al. 2002).
Reprinted with permission
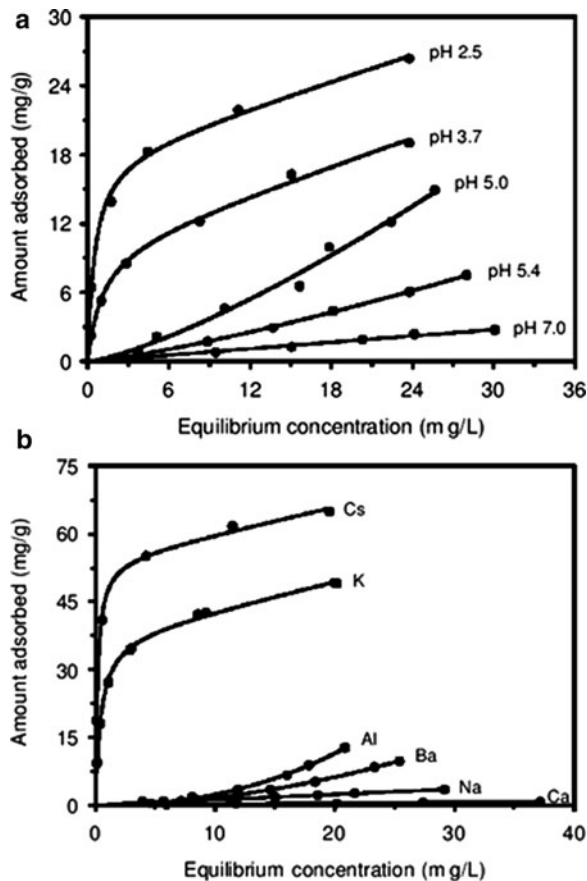


and nonspecific van der Waals interactions with the siloxane surface. FTIR analysis allows observation of molecular level changes occurring in the clay matrix following dinitrophenol adsorption; the data of Johnston et al. (2002) support this conclusion. FTIR spectra of DNOC and DINOSEB sorbed on a Wyoming-montmorillonite in the 4,000–600 cm$^{-1}$ are given in Fig. 6.43, which shows the spectral region with bands of smectite, water, and DNOC/DINOSEB. The region from 1,600–1,200 cm$^{-1}$ is dominated by the spectral contribution of the two dinitrophenol herbicide–montmorillonite complexes. Figure 6.44 shows FTIR spectra in the specific range 1,575–1,225 cm$^{-1}$, which shows the asymmetric and symmetric bands of dinitrophenol.

FTIR spectra of DNOC (Fig. 6.45) determined along several points of the sorption isotherm (Fig. 6.45) provided information on the effect of contaminant loading on the molecular changes of the adsorbing montmorillonite. The most intense DNOC bands in the FTIR spectra were the two symmetric NO$_2$ stretching bands at 1,351 and 1,334 cm$^{-1}$.
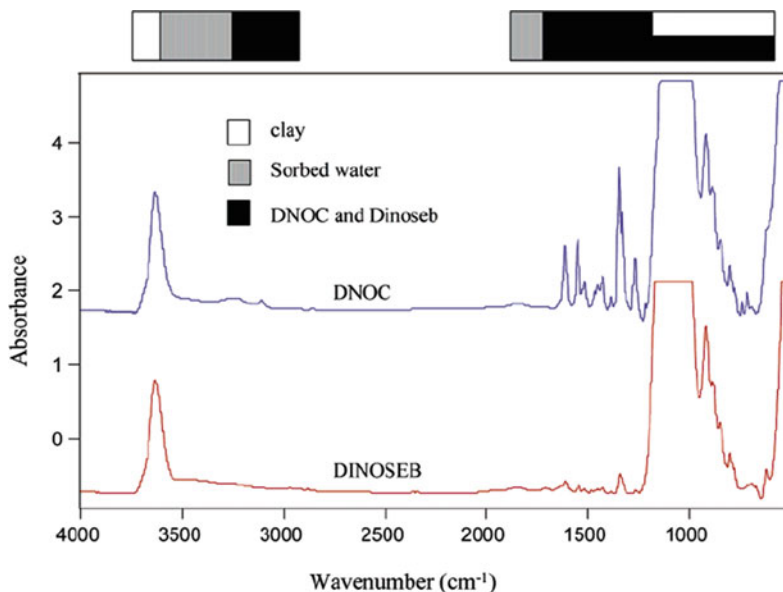
**Fig. 6.43** Survey FTIR spectra of DNOC and DINOSEB sorbed to K-Wyoming bentonite in the 4,000–600 $cm^{-1}$ region. The approximate regions where the vibrational modes associated with DNOC and DINOSEB, smectite, and sorbed water are shown at the top of the diagram (after Johnston et al. 2002). Reprinted with permission from Johnston CT, Sheng G, Teppen BJ, Boyd SA, de Oliveira MF (2002) Spectroscopic study of dinitrophenol herbicide sorption on smectite. Environ Sci Technol 36:5067–5074. Copyright 2006 American Chemical Society

Based on these spectroscopic studies, Johnston et al. (2002) suggested that interaction sites of dinitrophenol herbicides with smectite clay may include exchangeable cations, water molecules surrounding the exchangeable cations, and the siloxane surface. The $NO_2$ groups are expected to interact with the interlayer cations or with polarized water clusters surrounding these cations in the inter-lamelar region of the clay. Figure 6.46 presents an illustration of sorbed DNOC molecules lying flat on the siloxane surface, with siloxane surface and water molecules surrounding the exchangeable cations (Johnston et al. 2002).

Intercalation of nitroaromatic contaminants such as dinitrophenol herbicides into swelling clay interlayers, as emphasized by the above FTIR studies, results in major changes in the clay mineral. These changes should be considered irrevers-ible over scales of at least a "lifetime."

## 6.2.3   Humic Substances as Contaminant Sorbents

Humic substances in the soil–subsurface system result from the weathering of a complex, heterogeneous mixture of decomposed and chemically altered materials of biovegetative origin that include lignin, protein, carbohydrates, and cuticular
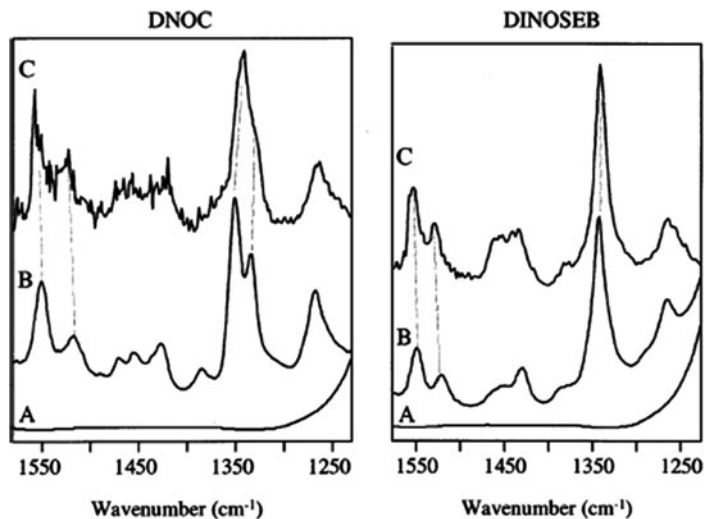
**Fig. 6.44** FTIR spectra in the 1,575–1,225 cm$^{-1}$ region of (**A**) K-Wyoming-montmorillonite, (**B**) herbicide sorbed to K-Wyoming-montmorillonite, and (**C**) ATR-FTIR spectra of the herbicide in aqueous solution (100 ppm at pH 2.5 in 0.1 M KCl) (after Johnston et al. 2002). Reprinted with permission from Johnston CT, Sheng G, Teppen BJ, Boyd SA, de Oliveira MF (2002) Spectroscopic study of dinitrophenol herbicide sorption on smectite. Environ Sci Technol 36:5067–5074. Copyright 2006 American Chemical Society
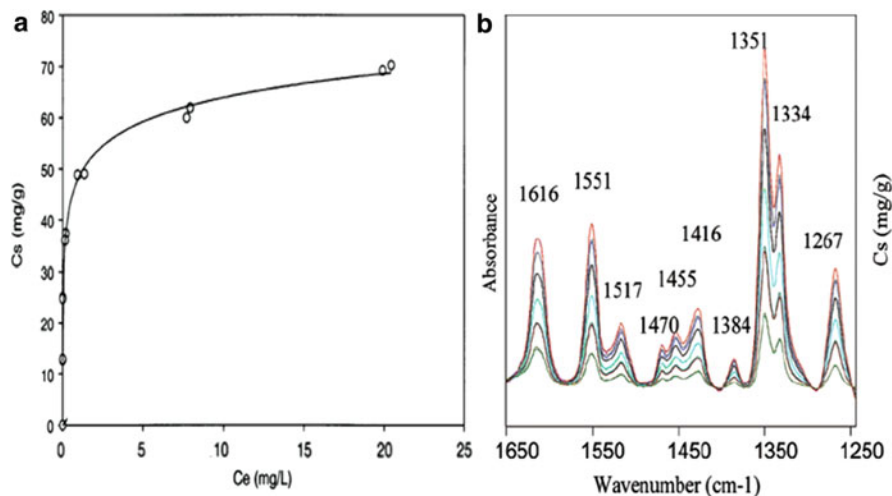


**Fig. 6.45** FTIR spectra of DNOC sorbed to K-montmorillonite in the 1650–1250 cm$^{-1}$ region. (**a**) Sorption isotherm, (**b**) spectra collected at points along the sorption isotherm such that the surface loading of DNOC was known for each IR measurement (modified after Johnston et al. 2002). Reprinted with permission from Johnston CT, Sheng G, Teppen BJ, Boyd SA, de Oliveira MF (2002) Spectroscopic study of dinitrophenol herbicide sorption on smectite. Environ Sci Technol 36:5067–5074. Copyright 2006 American Chemical Society
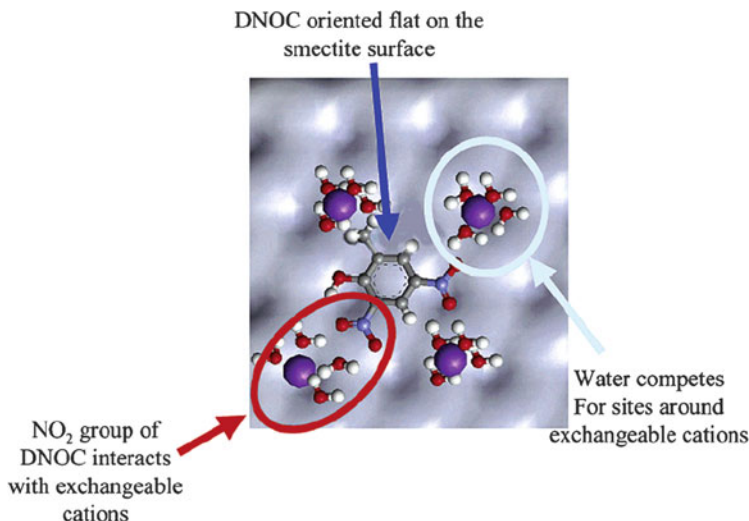
**Fig. 6.46** Illustration of a sorbed DNOC molecule lying flat on the siloxane surface, showing the siloxane surface and water molecules surrounding the exchangeable cations. The dimensions of the DNOC molecule and the distance between the exchangeable cations are drawn to scale (after Johnston et al. 2002). Reprinted with permission from Johnston CT, Sheng G, Teppen BJ, Boyd SA, de Oliveira MF (2002) Spectroscopic study of dinitrophenol herbicide sorption on smectite. Environ Sci Technol 36:5067–5074. Copyright 2006 American Chemical Society

material. Humic substances may be found in the soil–subsurface solid phase adsorbed on minerals, dissolved in the soil–subsurface water solution, and transported as dissolved materials or suspended particles in natural water.

Due to the complexity of humic molecules, expressed in terms of their variability in shape and composition, contaminant retention on humic material may occur on several types of binding sites. In the soil–subsurface environment and under natural conditions, humic substances are found mainly in the solid phase, bound on the mineral fraction, or dissolved in the water phase. In the soil–subsurface solution, however, conformation and polarity of dissolved humic substances are controlled to a large extent by the environmental liquid-phase chemistry.

Interactions between humic molecules and functional groups of anthropogenic chemicals, as well as the chemistry of the soil–subsurface solution (such as pH, ionic strength, and type of ions present), control the chemical and physical properties of the humic material (Ghosh and Schnitzer 1980; Cornel et al. 1986). For experimental purposes, extreme conditions are often applied, to investigate structural changes of the initial soil organic matter. It should be noted, however, that the ecological accident in the Danube plain of Hungary (September 2010), wherein highly toxic residues from the alumina industry "bleached" large land surfaces, showed that such extreme contamination may occur also in large-scale natural conditions.

The effect of pH in the flowing water phase on the conformational arrangement of dissolved humic substances was confirmed by X-ray studies (Myneni et al. 1999). The dependence of pH on the amount of humic substances dissolved in the mobile

water phase should also be considered. For example, humic substances form globular and thread- or net-like structures at low humic substance concentration, and both coiled and sheet-like structures in concentrated solution. Dilute alkaline humic solutions always exhibit small aggregates (<100 nm) without discernible structure. Solution pH significantly affects the humic substance macromolecular structure but plays a minor role in the case of concentrated humic substance solutions. A "traditional" assumption considered that dissolved humic substances are large polymers that exhibit linear or coiled conformation according to the environmental water chemistry. Later developments indicated that dissolved humic materials are composed of small units held together by weak hydrophobic forces or a structure of randomly self-associated small heterogeneous molecules (Conte and Piccolo 1999).

Spectra of humic and fulvic acids as determined by cross-polarization magic angle spinning carbon-13 nuclear magnetic resonance (CPMAS-$^{13}$C NMR) are shown in Fig. 6.47. In general, humic acids show sharper resonance for aliphatic carbons than for fulvic acids, which expose more signals for peptides and carbohydrates. These spectra indicate contaminant-induced changes as a result of chemical binding.

During sedimentation and diagenesis, organic materials in the soil and subsurface domain are degraded, which over time and under metamorphic conditions may be altered to form humic substances with composition and properties different than the original material. Luthy et al. (1997) considered that diagenesis and weathering of soil and subsurface organic matter lead to changes in the relative amounts of functional groups containing oxygen, and H/O or O/C atomic ratios that affect their sorption affinity toward hydrophobic organic contaminants. Luthy et al. (1997) discussed sequestration of nonpolar hydrophobic organic contaminants on humic substances, emphasizing the diversity of organic geosorbent composition due to diverse origins and geologic history.

Polar and nonpolar contaminants exhibit a substantially higher degree of sorption on terrestrial humic acids than on aquatic humic and fulvic acids (Niederer et al. 2007). The number of available sorption sites per mass of sorbent, rather than the type of intermolecular sorbent–sorbate interaction, defines the differences between terrestrial and aquatic humic materials. Dissolved humic substances can



Fig. 6.47 CPMAS-$^{13}$C NMR spectra of humic acid (HA$_1$) and fulvic acid (FA$_1$) (modified after Conte and Piccolo 1999). Reprinted with permission from Conte P, Piccolo A (1999) Conformational arrangement of dissolved humic substances: influence of solution composition on association of humic molecules. Environ Sci Technol 33:1682–1690. Copyright 2006 American Chemical Society
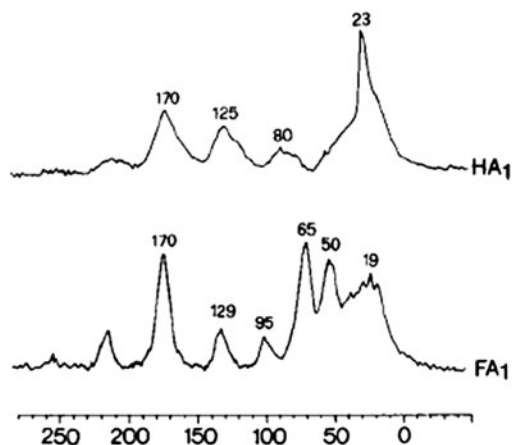
form stable complexes with trace organic contaminants (e.g., Wershaw et al. 1969; Boehm and Quinn. 1973), as measured quantitatively for various polycyclic aromatic hydrocarbons (PAH), insecticides, and herbicides (e.g., Carter and Suffet 1982; Wijayaratne and Means 1984; Landrum et al. 1984). Here, we discuss a number of examples where dissolved humic substance configuration was altered following contact with different organic contaminants.

Methanol ($CH_3OH$) is a polar, nonionic solvent used broadly for industrial purposes, and used also as a fuel additive. Due to its high solubility in water, methanol may be found as a major organic pollutant in both surface and ground water. Changes in conformational arrangement of dissolved humic substances as a result of interaction with a solution of methanol are reported by Conte and Piccolo (1999), who used high-pressure size exclusion chromatography. Samples were modified in a control solution of 0.05 M $NaNO_3$ at pH 7.1, with addition of methanol ($4.6 \times 10^{-7}$ M) when the pH remains in the same range (pH 6.97). UV chromatograms showed the distribution of molecular absorptivity of humic chromophore groups, whereas retention index (RI) chromatograms provided the overall mass distribution of humic matter.

Methanol-induced changes in humic acid molecular sizes were observed by comparing size exclusion chromatograms of the control phase without and with the addition of methanol, without changing the solution pH (Fig. 6.48). From the UV chromatogram, it may be observed that adding methanol led to complete disappearance of the first peak and a major decrease in the second peak, in terms of both intensity and elution time (Fig. 6.48-1). The RI chromatogram confirms these changes, even showing the appearance of low molecular size fractions in the elution volume (Fig. 6.48-2).

A numerical representation of average molecular weight (MW) and polydispersity (P) differences between the control mobile phase and methanol-altered mobile phase of humic and fulvic acids is presented in Table 6.10. Both UV and RI MW values show that molecular sizes of humic acids are greater than those of fulvic acids. Methanol presence in the mobile phase induced a decrease in humic acid molecular size and polydispersity, by more than 50% compared to the unaltered mobile phase. The MW and P values of fulvic acids decreased only by 10 and 6.7%, respectively, when the mobile phase was contaminated with methanol.

Based on these results, Conte and Piccolo (1999) emphasized that the molecular size distribution of humic substances may be affected largely by the presence of methanol even when the ionic strength of the eluting solution remains constant. Conte and Piccolo (1999) explained the changes in size distributions of humic substances by the capacity of methanol to form van der Waals bonds with the hydrophobic humic components, and hydrogen bonds with the oxygen-containing functional groups present in the humic substance. The shifting of peaks in the UV chromatograms is explained by these weak interactions. The RI chromatograms show a shift in humic mass toward elution volumes specific to material with lower molecular weight. The very small amount of methanol in the eluting solution disrupted the weak forces that temporarily stabilized the humic substance in apparently large aggregates.
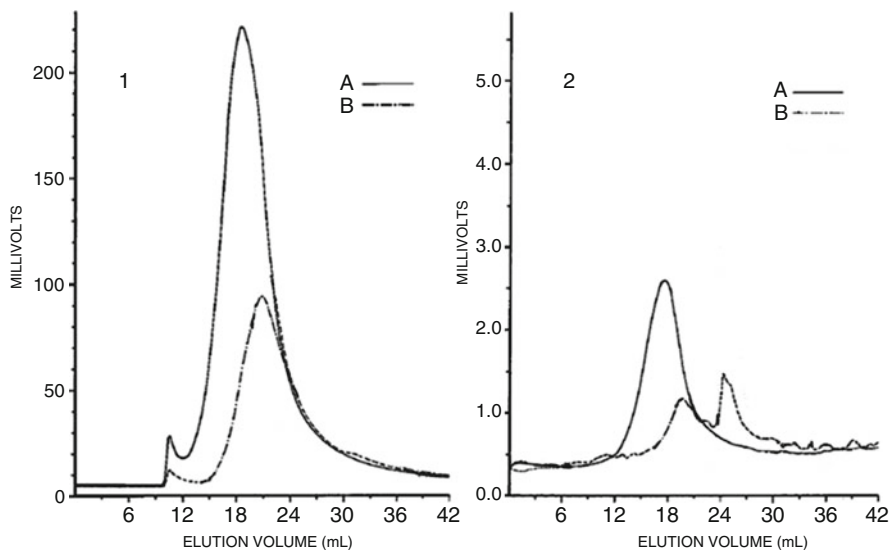
**Fig. 6.48** Size exclusion chromatograms of humic acid recorded with (1) UV–vis detector and (2) RI detector. In both (1) and (2): (**A**) control mobile phase, (**B**) control with $4.6 \times 10^{-7}$ M methanol (modified after Conte and Piccolo 1999). Reprinted with permission from Conte P, Piccolo A (1999) Conformational arrangement of dissolved humic substances: influence of solution composition on association of humic molecules. Environ Sci Technol 33:1682–1690. Copyright 2006 American Chemical Society

**Table 6.10** Weight-average, molecular weight (MW), and polydispersity (P) of humic acid (HA) and fulvic acid (FA) samples as determined by UV and RI detectors, showing % change in MW as a result of methanol presence in the mobile phase (modified after Conte and Piccolo 1999). Reprinted with permission from Conte P, Piccolo A (1999) Conformational arrangement of dissolved humic substances: influence of solution composition on association of humic molecules. Environ Sci Technol 33:1682–1690. Copyright 2006 American Chemical Society

|     | Sample | A | | B | | % Change in MW |
| --- | --- | --- | --- | --- | --- | --- |
|     |     | MW | P | MW | P | |
| HA | UV | 17,000 | 2.0 | 7,900 | 1.5 | 53.5 |
|     | RI | 16,650 | 3.5 | 7,790 | 1.7 | 53.2 |
| FA | UV | 10,000 | 1.6 | 9,000 | 1.6 | 10.0 |
|     | RI | 5,470 | 2.0 | 5,100 | 1.9 | 6.7 |

Intermolecular interactions between humic molecules and intramolecular interactions among molecular functional groups change the chemical and physical properties of humic materials. These interactions govern the self-association and ultimately the size, shape, and polarity of humic substances (Schlautman and Morgan 1993). Self-association of dissolved humic materials, and thus their configuration, in a natural environment is affected by specific parameters of the water solvent, such as pH, ionic strength, and type of ion.

In situ investigations by Schlautman and Morgan (1993) on the effect of pH, ionic strength, and the presence of bivalent cations on the binding of PAH by well-characterized aquatic humic substances clarified this process. In particular, Schlautman and Morgan (1993) studied binding of nonpolar, nonionogenic PAH compounds such as anthracene ($C_{14}H_{10}$), pyrene ($C_{16}H_{10}$), and perylene ($C_{20}H_{12}$) on dissolved humic and fulvic acids. The effects of aqueous chemistry on the binding of pyrene and anthracene on humic acid (Figs. 6.49 and 6.50), and of perylene on humic and fulvic acids (Fig. 6.51) are clearly observed.

In NaCl solutions, the binding of PAH on dissolved humic materials was found to generally decrease with increases in pH (constant ionic strength) and in ionic strength (fixed pH). Schlautman and Morgan (1993) considered that the binding of PAH on humic substances depends on the hydrophobicity of the contaminant, on the size of the solute molecule, and on its ability to fit into hydrophobic cavities of humic and fulvic materials that can change their molecular configuration. In addition, Schlautman and Morgan (1993) showed that the presence of $Ca^{2+}$ in water at a concentration of 1 mM and a pH 4 had little effect on PAH binding, while the binding increased when pH was between 7 and 10.

PAH binding and the chemistry of the soil solution have implications for the mechanism of association between PAH and humic substances at the molecular level. For example, Schlautman and Morgan (1993) showed that an increase in water salinity led to a decrease in PAH concentrations due to the "salting-out" effect, and consequently, to a decrease in PAH binding on humic substances. A decrease in pH led to a coagulation of dissolved humic molecules which also affects interactions between PAH and dissolved humic materials.

It is generally accepted that dissolved humic materials do not behave as a homogeneous body during the sorption process. Various approaches have been developed to establish the affinities of the dissimilar components of dissolved humic materials for different types of organic contaminants (e.g., Khalaf et al. 2003; Golding et al. 2005; Smejkalova et al. 2009). Using reverse heteronuclear saturation transfer difference NMR spectroscopy ($^1H(^{19}F)$RHSTD), Longstaffe et al. (2010) defined molecular level changes occurring in specific adsorption sites of a dissolve peat humic acid following contamination by perfluoro-2-naphthol molecules. $^1H(^{19}F)$RHSTD is based on magnetic dipole–dipole interactions between the $^{19}F$ nuclei of the organo fluoride and the $^1H$ nuclei of the humic acid. Dipole–dipole interactions act independently of atomic bonding, probing noncovalent interactions between organic compounds in solution. By this method, the molecular components in a mixture that bind a contaminant species are identified directly. Longstaffe et al. (2010) compared the $^1H$ NMR spectrum of peat humic acid (Fig. 6.52) to the $^1H(^{19}F)$RHSTD spectra of a humic acid–perfluoro-2-naphthol mixture solution (Fig. 6.53) at various loading ratios.

In the case of humic acid–perfluoro-2-naphthol mixtures, signals of humic acid are enhanced by perfluoro-2-naphthol signals, suggesting a change in the initial molecular structure of the humic acid. It may be observed also that a deviation from this behavior suggests that certain domains in the humic acid were preferentially selected for interaction with the perfluoro-2-naphthol contaminant. In contrast to the binding of contaminants from solid organic matter, where the nonideality of binding is due to
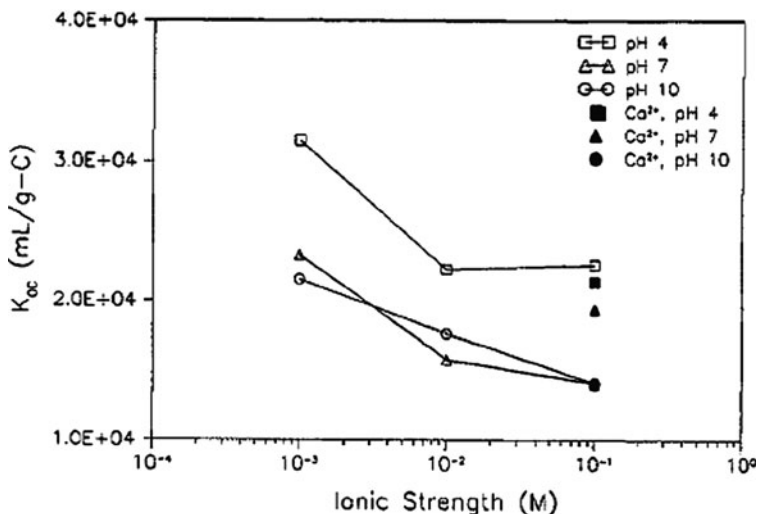
**Fig. 6.49** Binding of pyrene by humic acid. Data for 1 mM Ca$^{2+}$ at a total ionic strength of 0.1 M. Open symbols connected by lines refer to NaCl solutions. Single (solid) points refer to experiments with 1 mM Ca$^{2+}$ at the appropriate pH values (after Schlautman and Morgan 1993). Reprinted with permission from Schlautman MA, Morgan JJ (1993) Effects of aqueous chemistry on the binding of polycyclic aromatic hydrocarbons by dissolved humic materials. Environ Sci Technol 27:961–969. Copyright 1993 American Chemical Society
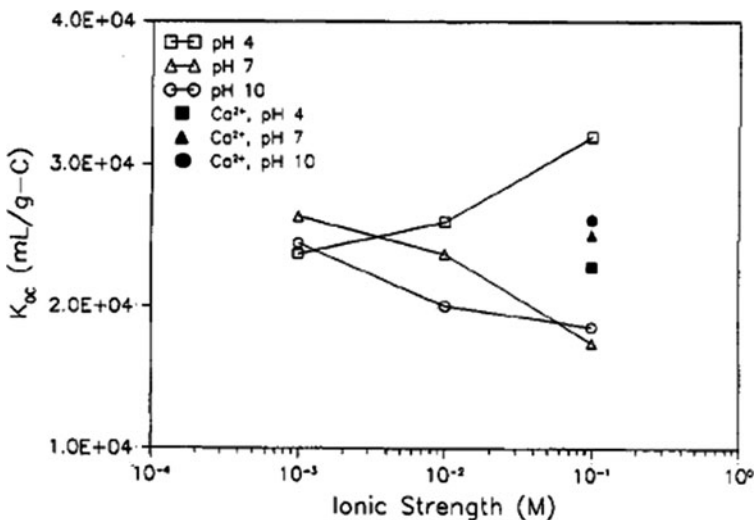


**Fig. 6.50** Binding of anthracene by humic acid. Data for 1 mM Ca$^{2+}$ at a total ionic strength of 0.1 M. Open symbols connected by lines refer to NaCl solutions. Single (*solid*) points refer to experiments with 1 mM Ca$^{2+}$ at the appropriate pH values (after Schlautman and Morgan 1993). Reprinted with permission from Schlautman MA, Morgan JJ (1993) Effects of aqueous chemistry on the binding of polycyclic aromatic hydrocarbons by dissolved humic materials. Environ Sci Technol 27:961–969. Copyright 1993 American Chemical Society
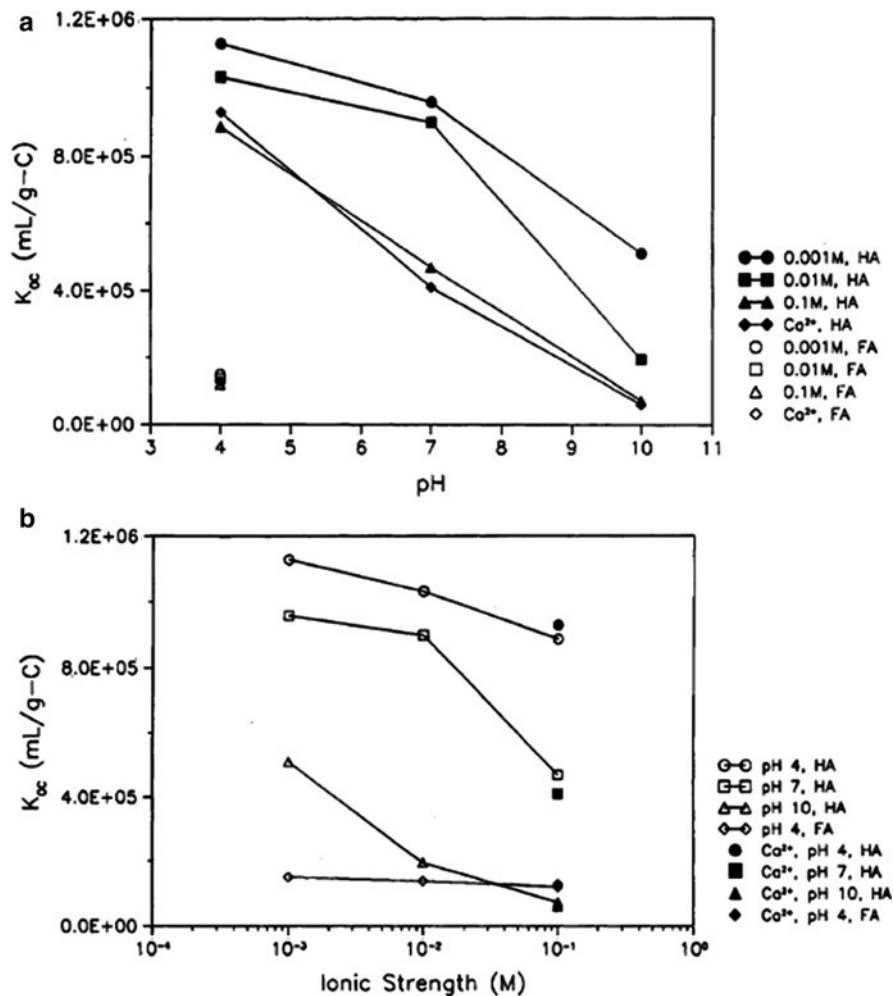
**Fig. 6.51** Binding of pyrene by humic acid. Data for 1 mM $Ca^{2+}$ at a total ionic strength of 0.1 M. (**a**) $K_{oc}$ versus pH. Solid symbols connected by lines refer to experiments with humic acid. Single (*open*) points at pH 4 refer to experiments with fulvic acid. (**b**) $K_{oc}$ versus ionic strength. *Open symbols* connected by *lines* refer to experiments in NaCl solutions. Single (*solid*) points at 0.1 M ionic strength refer to experiments with 1 mM $Ca^{2+}$ (after Schlautman and Morgan 1993). Reprinted with permission from Schlautman MA, Morgan JJ (1993) Effects of aqueous chemistry on the binding of polycyclic aromatic hydrocarbons by dissolved humic materials. Environ Sci Technol 27:961–969. Copyright 1993 American Chemical Society

differences in the physical homogeneity of the sorbent, nonideality of binding in the case of dissolved organic matter (DOM) results from chemical heterogeneity of the sorbent. For example, from Fig. 6.53, a limit in binding capacity of perfluoro-2-naphthol on the aromatic site (e.g., lignin material) and a continued increase in binding interaction with the aliphatic material can be observed. Longstaffe et al. (2010)
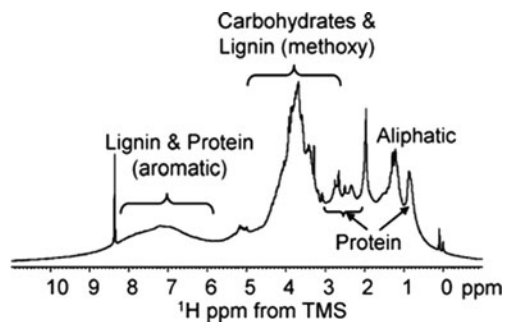
**Fig. 6.52** The $^1$H NMR spectrum of the International Humic Substance Society peat humic acid in D$_2$O. Major spectral features corresponding to the key humic acid biopolymers are highlighted: lignin, carbohydrates, aliphatics, and proteins. Note: Humic acid is a very complex mixture; the assignments are based on extensive multidimensional NMR assignments for this sample. Only the major components pertinent to this study are labeled (after Longstaffe et al. 2010). Reprinted with permission from Longstaffe JG, Simpson MJ, Maas W, Simpson AJ (2010) Identifying components in dissolved humic acid that bind organofluorine contaminants using $^1$H ($^{19}$F) reverse heteronuclear saturation transfer difference NMR spectroscopy. Environ Sci Technol 44:5476–5482. Copyright 2010 American Chemical Society

suggested that potential contaminant-induced changes in the molecular configuration of a dissolved humic acid (DHA) are controlled by both the properties of the contaminant and the chemical characteristics of the humic acid.

Contaminants present in the soil–subsurface solution may affect the conformational arrangement of dissolved humic substances. Engelbretson and van Wandruszka (1994) showed that dissolved humic acids exhibit different organizational rearrangements when exposed to metal ions in solution. High ionic concentrations lead to the well-known salting-out effect, and the formation of hydrophobic colloids. A lower salt concentration may lead to the formation of intramolecular humic pseudo micelles and intramolecular interactions.

Using high pressure size exclusion chromatography, Conte and Piccolo (1999) reported on the conformational changes of humic and fulvic acids with a neutral mobile phase (0.05 M NaNO$_3$, pH 7) by addition of methanol (pH 6.97), hydrochloric acid (pH 5.54), and acetic acid (pH 5.69). In this case, the initial solution composition was changed but the ionic strength was constant. A decrease in molecular size of the dissolved humic substances was caused by an increase in the acidity of the mobile phase. The most significant conformational changes occurred in the disruption of the apparent high molecular size of humic substances into several smaller molecule associations. In contrast to the binding of contaminants to solid organic matter, where the nonideality of binding is due to differences in the physical homogeneity of the sorbent, nonideality of binding in the case of DOM results from chemical heterogeneity of the organic matter. Conte and Piccolo (1999) found also that significant conformational changes of dissolved humic substances occurred in acidic mobile phases, where hydrogen bonding formation was induced.
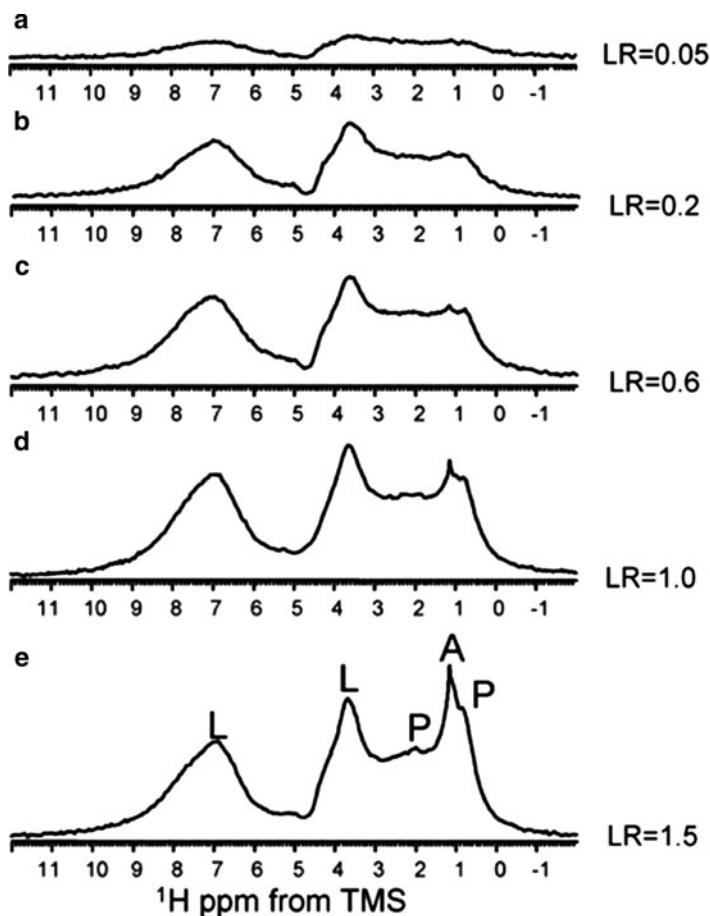
**Fig. 6.53** $^{1}$H($^{19}$F)RHSTD spectra of International Humic Substance Society peat humic acid mixed with different loading ratios of (**a–e**) perfluoro-2-naphthol. Loading ratios, LR, are reported as the mass ratio of organofluoride to humic acid in solution. Major spectral features corresponding to the key humic acid biopolymers are highlighted: *L* lignin, *A* aliphatics, *P* protein (modified after Longstaffe et al. 2010). Reprinted with permission from Longstaffe JG, Simpson MJ, Maas W, Simpson AJ (2010) Identifying components in dissolved humic acid that bind organofluorine contaminants using $^{1}$H ($^{19}$F) reverse heteronuclear saturation transfer difference NMR spectroscopy. Environ Sci Technol 44:5476–5482. Copyright 2010 American Chemical Society

Conte and Piccolo (1999) considered that humic substances in solution are loosely bound self-association of relatively small molecules and that intermolecular hydrophobic interactions are the predominant binding forces. The stability of such a conformation in solution is attributed to the entropy-driven tendency to exclude water molecules from humic association, thus decreasing total molecular energy. Conte and Piccolo (1999) and Cozzolino et al. (2001) suggested a model in which small and heterogeneous humic molecules self-assemble in supramolecular conformations, stabilized only by weak forces (van der Waals, π–π, and CH–π

bonds) and hydrogen bonding. New formation of intermolecular hydrogen bonding and alteration of preexisting hydrophobic interactions accounted for the disruption of original supramolecular association.

By the end of the last century, it was possible to observe molecular level transformations of solid state organic matter (SOM) in studies on SOM–chemical contaminant interactions, using nuclear magnetic resonance (NMR) spectroscopy. NMR can monitor noncovalent interactions among organic molecules by measuring the spin–lattice ($T_1$) and spin–spin ($T_2$) relaxation times, which are a function of the overall molecular translational and rotational motion. This technique allows direct observations of interactions between humic and contaminant molecules, specifically on interactions among atoms within molecules (Simpson 2006, and references therein).

Cross-polarization magic angle spinning (CPMAS) $^{13}$C NMR spectroscopy has been employed to establish the relationship between contaminant adsorption on humic substances and the relative percentage of aromatic carbon (e.g., Xing 1997; Chefetz et al. 2000; Ahmad et al. 2001). The structure of humic acids, extracted from peat and soil by oximation, hydrolysis, and bleaching, was reported by Simpson et al. (2003). Solid state $^{13}$C CP/MAS NMR spectra and integrated parameters, aromaticity, and aliphaticity of natural and chemically modified humic acids are shown in Fig. 6.54 and Table 6.11. It can be seen that all three extraction procedures induced chemical modification of the humic acids, leading to an increase or decrease in their aromaticity and in removal of specific structures. *Hydrolysis* caused the removal of carbohydrates and amines from humic materials, expressed by a decline of signals in the 50–112 ppm region of the NMR spectra. Removal of polysaccharides led to a relative increase in the aromaticity of the humic acids. *Oximation* of humic substances occurs by a reaction of hydroxylamine with carbonyl groups, producing oxime (C = N) groups and a decline in the carbonyl group. A relative increase in aromaticity of both peat- and soil-extracted humic acid was observed. Alteration or removal of protonated constituents of the humic acids was confirmed by $^{13}$C CP/MAS NMR data. *Bleaching* resulted in almost total removal of the aromatic carbon signal (128–150 ppm) from the $^{13}$C CP/MAS NMR spectra of the peat humic acid, and in substantial removal from the soil humic acid. The C/N ratio of the bleached humic acids decreased only slightly compared to the untreated samples, because the C- and N-containing groups were removed nonselectively.

*Halogen-substituted phenols* are polar hydroxylic compounds of serious environmental concern; this class of compounds includes the biotoxic chemicals 2,4-dichlorophenol, 2,4,6-trichlorophenol, and 2,4,6-trifluorophenol. Chlorophenols are highly toxic compounds reaching the environment as waste incineration products, wood preservatives, and agricultural pesticides. Their interaction with humic materials, as studied by NMR spectroscopy, is discussed here with regard to induced changes in the natural soil–subsurface organic constituents.

Šmejkalová and Piccolo (2008) report on 2,4-dichlorophenol behavior in association with humic (HA) and fulvic (FA) acids. Upon association of humic materials with 2,4-dichlorophenol complexes, H3, H5, and H6 proton signals of
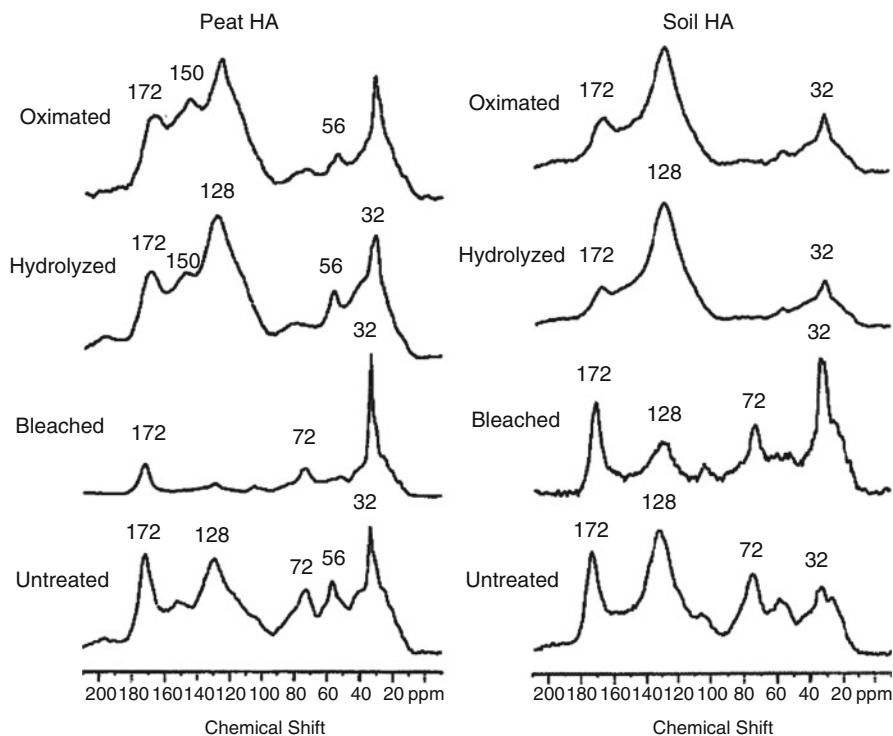
**Fig. 6.54** Cross-polarization magic angle spinning $^{13}C$ nuclear magnetic resonance (CPMAS $^{13}C$ NMR) spectra for structurally modified humic acids (modified after Simpson et al. 2003). Copyright 2003, Crop Science Society of America, and Soil Science Society of America. Reprinted with permission

the associated contaminant are shifted upfield. The shifting of proton signals and their broadening were greater for HA–contaminant than for FA–contaminant complexes, and increased when the amount of humic substances increased in the contaminant–humic complex that formed. The changes in 2,4-dichlorophenol $^1H$ relaxation time of spin–lattice ($T_1$) and spin–spin ($T_2$) may be considered as an index of a newly formed structural conformation of a humic–contaminant complex. The results of Šmejkalová and Piccolo (2008) showed that without humic materials, the $T_1$ relaxation times for the contaminant proton signals are much greater for H3 than for H5 and H6. For both $T_1$ and $T_2$ relaxation times, a decreasing trend with increasing humic concentration is observed. As an indication, Fig. 6.55 presents the percentage of humic-associated 2,4-dichlorophenol as a function of FA and HA initial concentration.

The presence of enzymes in natural humic soils may lead to a different pathway of induced changes in the molecular configuration of chlorophenol–humic complexes. Covalent binding of phenolic compounds to soil humic materials, obtained via enzyme-catalyzed redox reactions, was described by Bollag et al. (1980, 1992).

**Table 6.11** Cross-polarization magic angle spinning $^{13}$C nuclear magnetic resonance (CPMAS $^{13}$C NMR) integration parameters, aromaticity, and aliphaticity values for humic acids (modified after Simpson et al. 2003, Copyright 2003, American Society of Agronomy, Crop Science Society of America, and Soil Science Society of America. Reprinted with permission

| Sample | Alkyl C (0–50 ppm) | O-alkyl C (50–112 ppm) | Aromatic C (112–145 ppm) | Aromatic C–O (145–163 ppm) | Carboxyl + carbonyl C (163–215 ppm) | Aromaticity | Aliphaticity |
|---|---|---|---|---|---|---|---|
| Peat humic acid | | | | | | | |
| Untreated | 24 | 28 | 24 | 9 | 15 | 39 | 61 |
| Bleached | 50 | 27 | 8 | 3 | 12 | 12 | 88 |
| Hydrolyzed | 22 | 21 | 31 | 12 | 15 | 50 | 50 |
| Oximated | 20 | 18 | 34 | 15 | 13 | 56 | 44 |
|  | 25 | 16 | 42 | 12 | 6 | 57 | 43 |
| Soil humic acid | | | | | | | |
| Untreated | 17 | 29 | 29 | 9 | 16 | 45 | 55 |
| Bleached | 35 | 30 | 17 | 5 | 13 | 25 | 75 |
| Hydrolyzed | 16 | 14 | 46 | 12 | 12 | 66 | 34 |
| Oximated | 17 | 13 | 42 | 13 | 15 | 65 | 35 |
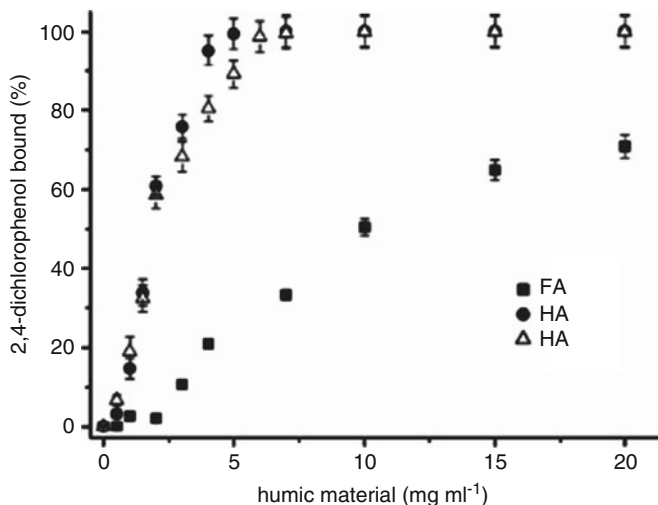
**Fig. 6.55** Percentage of humic-associated 2,4-dichlorophenol (1 mg mL$^{-1}$) as a function of fulvic (FA) and humic acid (HA) concentration (after Šmejkalová and Piccolo 2008). Reprinted with permission from Šmejkalová D, Piccolo A (2008) Host-guest interactions between 2,4, dichlorophenol and humic substances as evaluated by $^1$H NMR relaxation and diffusion ordered spectroscopy. Environ Sci Technol 42:8440–8445. Copyright 2008 American Chemical Society

Using high-resolution $^{13}$C NMR spectroscopy, Hatcher et al. (1993) further clarified the mechanism of enzymatic covalent binding of $^{13}$C-labeled 2,4-dichlorophenol to peat humic acid. It was found that in the absence of enzymes, only carbons of the free 2,4-dichlorophenol were detected (Fig. 6.56a). The $^{13}$C NMR spectrum contained only two signals at 119.95 and 123.10 ppm, assigned to be C6 and C2 carbons of $^{13}$C-labeled 2,4-dichlorophenol. In contrast, the spectrum of the 2,4-dichlorophenol–humic acid complex obtained via enzymatic covalent binding displayed a large dispersion of $^{13}$C chemical shifts (Fig. 6.56b).

Adsorption–desorption studies on 2,4-dichlorophenol on various components of soil organic matter such as straw, lignin, composted straw, and humic acid reported by Benoit et al. (1996) showed that from 25 to 36% of the adsorbed compound is retained irreversible. These results, as well as those discussed above, suggest that transformation of humic materials as a result of their contamination by halogenated phenols is at least partially irreversible.

*Monoaromatic hydrocarbons* comprise a large group of organic contaminants which in contact with soil–subsurface humic substances exhibit predominantly noncovalent interactions such as hydrogen bonding, π–π bonds, electrostatic attraction, and van der Waals and dipole–dipole interactions.

Nanny (1999) and Nanny and Maza (2001) used deuterium NMR spectroscopy ($^2$H NMR) spin–lattice relaxation ($T_1$) measurements to study interaction between monoaromatic compounds with humic and fulvic acids. The $T_1$ relaxation time of the deuterium nuclei decreases as the overall molecular motion of the
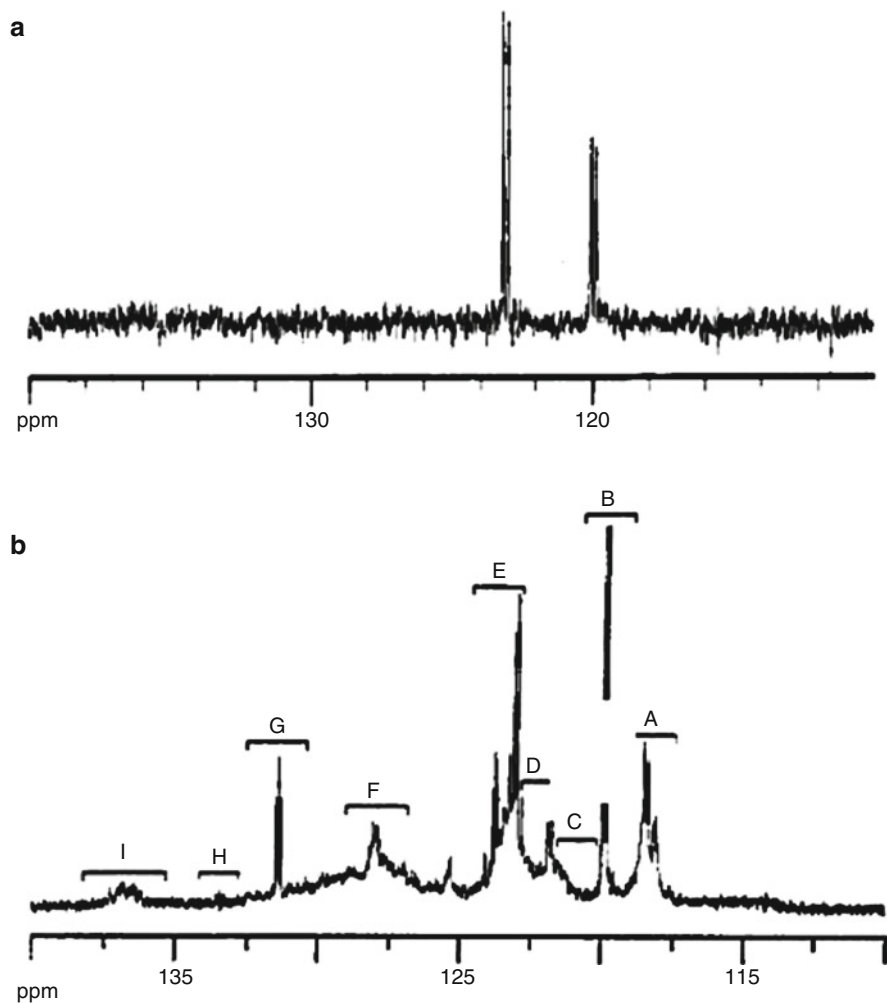
**Fig. 6.56** $^{13}$C NMR spectrum of $^{13}$C-labeled 2,4-dichlorophenol expanded region 110–140 ppm (**a**) added to Minnesota peat humic acid at basic pH in the absence of horseradish peroxidase, (**b**) bound to Minnesota peat humic acid after enzymatic treatment with horseradish peroxidase (modified after Hatcher et al. 1993). Reprinted with permission from Hatcher PG, Bortiatynski JM, Minard RD, Dec J, Bollag JM (1993) Use of high-resolution carbon-13 NMR to examine the enzymatic covalent binding of carbon-13-labeled 2,4-dichlorophenol to humic substances. Environ Sci Technol 27: 2098–2103. Copyright 1993 American Chemical Society

monoaromatic compound is reduced, due to noncovalent interactions with dissolved fulvic or humic acid or with the aqueous solvent.

Below, we review some experimental results for estimating potential changes in the configuration of humic materials following their contamination by mono-aromatic hydrocarbons. Three monoaromatic contaminants, phenol-d$_5$, pyridine-d$_5$,

and benzene-$d_6$, all of which have similar structure but different polarity and proton donating or accepting capability, were used to examine noncovalent interactions between the deuterated compounds and Suwannee River fulvic and humic acids, as a function of solution pH.

### 6.2.3.1  Changes in Fulvic Acid

Nanny (1999) observed that a chemical shift of phenol-$d_5$ and pyridine-$d_5$ is explained by a process of protonation/deprotonation over a pH ranging from 2.1 to 10.9. This behavior suggests, at first consideration, that phenol or pyridine induces changes in the conformation of the fulvic acid host molecule. However, a decrease in relaxation time ($T_1$) at a high pH (9.8) indicates a decrease in phenol motion upon deprotonation. As a consequence, the deprotonated phenol in an anionic state forms a stronger hydrogen bond with the water molecule, which is much more prevalent and stronger than that with fulvic acid. In contrast, relaxation times $T_1$ of deuterium nuclei demonstrate that pyridine interacts noncovalently with fulvic acid even at pH values ranging 3–8 when protonated phenols of fulvic acid are the sites of interaction with pyridine (Fig. 6.57).

The relaxation time value for benzene is affected by the presence in the water solution of fulvic acid, independent of its concentration. The fulvic acid modifying solvent matrix led to an increase in benzene solubility, indicating that in water
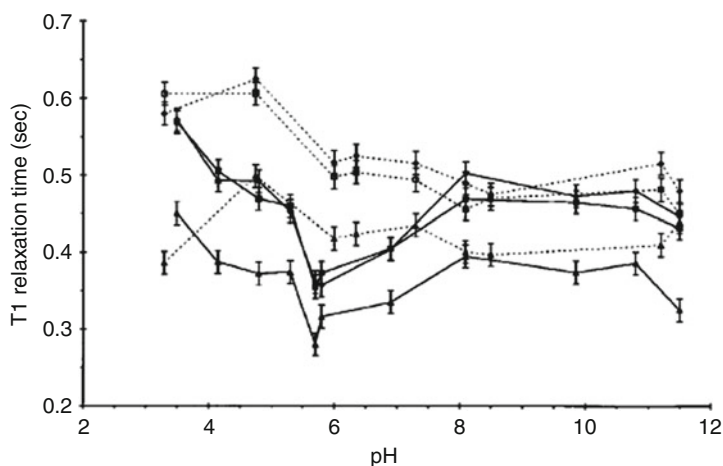


**Fig. 6.57**  $T_1$ relaxation time, as a function of pH, for pyridine-$d_5$ (0.1% v/v) in the presence and absence of 1.0 mg Suwannee River fulvic acid/ml. The data for pyridine-$d_5$ in pure water are shown for comparison purposes. Fulvic acid absent (*dotted lines*): α deuterium (*open diamonds*), β deuterium (*open squares*), γ deuterium (*open triangles*); Suwannee River fulvic acid present: α deuterium (*closed diamonds*), β deuterium (*closed squares*), γ deuterium (*closed triangles*) (after Nanny 1999). Reprinted from Nanny MA, Deuterium NMR characterization of noncovalent interactions between monoaromatic compounds and fulvic acids. Organic Geochem 30:901–999, Copyright (1999), with permission from Elsevier

solution, fulvic acid solubilizes benzene rather than forming benzene–fulvic acid discrete bonds. In conclusion, Nanny (1999) showed that as a function of their properties and of the environmental pH, monoaromatic contaminants may form complexes with fulvic acids. Pyridine, for example, which is a proton acceptor at pH value above 5.4, interacts with fulvic acid; the extent of this interaction depends upon the aromatic and polar character of the host molecule.

### 6.2.3.2   Changes in Humic Acid

Nanny and Maza (2001) performed deuterium NMR $T_1$ relaxation studies to investigate interactions in aqueous solvents of benzene and pyridine with humic acids extracted from soil, peat, and Suwannee River. Noncovalent interactions in the solutions were examined as a function of solution pH, monoaromatic functional groups, and humic acid origin.

Benzene interactions with dissolved humic acids were studied over a range of pH values. These interactions increased with a decrease in pH and were generally proportional to the percent of aromaticity in the humic acid. Evidence that benzene interacts with humic acids is given by the $T_1$ values for benzene in the presence of humic acids, which are smaller than those of benzene in pure water (Fig. 6.58). Additional evidence is the increase in the signal of benzene in the presence of peat humic acid, to 7.34 Hz, from 2.48 Hz in pure water. The composition of humic acid controls its pH-dependent interaction with benzene. If the benzene–soil humic acid
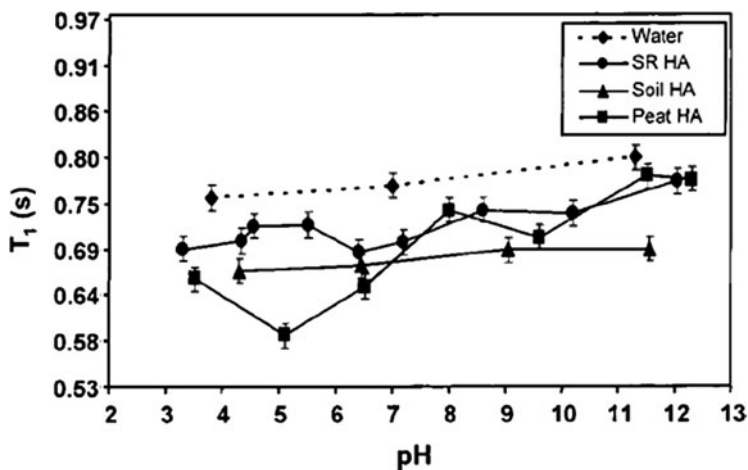


**Fig. 6.58** $T_1$ relaxation time, as a function of pH, for benzene-d$_6$ in the presence of water, soil humic acid, Suwannee River (SR) humic acid, and peat humic acid (after Nanny and Maza 2001). Reprinted with permission from Nanny MA, Maza JP (2001) Noncovalent interactions between monoaromatic compounds and dissolved humic acids: A deuterium NMR $T_1$ relaxation study. Environ Sci Technol 35:379–384. Copyright 2001 American Chemical Society

interaction is not affected by a change in the solvent $pH_s$ (3–11), then the benzene–peat humic acid interaction is pH dependent. At pH < 8, for example, the hydrophobic character of the peat humus acid is strongly pH dependent (Fig. 6.58). Nanny and Maza (2001) assumed that the hydrophobic character of the peat humic acid increased upon protonation of the carboxylic acid functional group, as well as from the formation of humic acids even though the solution remained visible. This case demonstrates the potential for induced modification – at a molecular scale – of the humic acid extracted from peat materials by mono-aromatic contaminants.

Pyridine interacts with all three humic acids studied (Nanny and Maza 2001). Figure 6.59 shows the change in $T_1$ for the three deuterium nuclei of pyridine in pure water as a function of pH. At pH 3.4, pyridine displays anisotropic motion; below pH 5.4, a protonated cation readily forms hydrogen bonds with the negative charges of oxygen atoms of water; above this value, the pair of electrons of nitrogen forms a weak hydrogen bond with water.

Based on the above results, Nanny and Maza (2001) considered that two types of interactions between humic acid and pyridine may occur as a function of pH and humic acid identity: (1) bonding with the lone pair of electrons on the nitrogen of pyridine, and (2) π–π interactions between the aromatic ring of pyridine and aromatic components of humic acids.

### 6.2.3.3   Main Factors Affecting $^2$H NMR Spin–Lattice Relaxation $T_1$

Changes in $T_1$ of organic contaminants in water solutions containing natural humic substances may be an indicator of potential alteration of the natural host materials. As noted above, Nanny and Maza (2001) determined the effect of pH and the percentage of aromaticity in dissolved humic substances on $T_1$ of monoaromatic compounds. Based on these data, they illustrated an alteration effect on the $T_1$ for benzene and pyridine in aqueous solutions containing humic and fulvic acids (Fig. 6.60). It can be observed that the solution pH has a significant impact on the $T_1$ relaxation time of benzene (Fig. 6.60a), and thus on noncovalent interactions between benzene and the humic and fulvic acids when their percent aromaticity is between 25 and 50%. A percent aromaticity greater than 50% favors benzene sorption on humic and fulvic acids, while an aromaticity lower than 25% leads to the enhancement of the overall molecular motion of benzene. This behavior is in accord with the findings of Chiou et al. (1987), which showed that sorption of hydrophobic compounds on natural organic matter (NOM) is related directly to the percent aromaticity and related inversely to NOM polarity.

Pyridine exhibits a similar response to pH and humic and fulvic aromaticity percentage on the contaminant relaxation time ($T_1$), but it is less pronounced than for benzene. Nanny and Maza (2001) concluded that the interaction of pyridine with humic and fulvic acids may be modified further by additional molecular interactions, such as hydrogen bonding on the monoaromatic polar functional
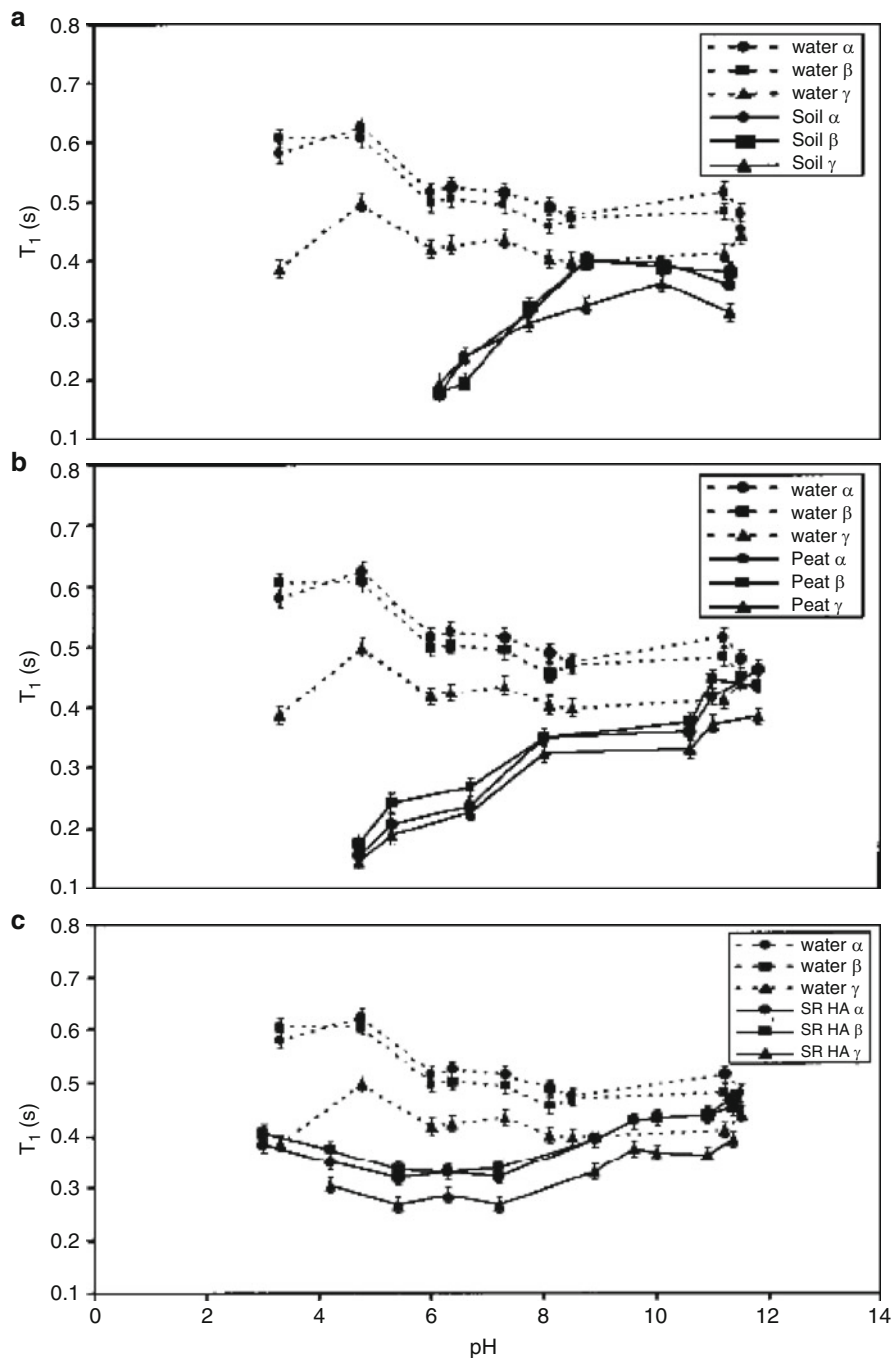
**Fig. 6.59** $T_1$ relaxation time, as a function of pH, for pyridine-$d_5$ in the presence of water, soil humic acid (**a**), peat humic acid (**b**), and Suwannee River humic acid (**c**) (after Nanny and Maza 2001). Reprinted with permission from Nanny MA, Maza JP (2001) Noncovalent interactions between monoaromatic compounds and dissolved humic acids: A deuterium NMR $T_1$ relaxation study. Environ Sci Technol 35:379–384. Copyright 2001 American Chemical Society
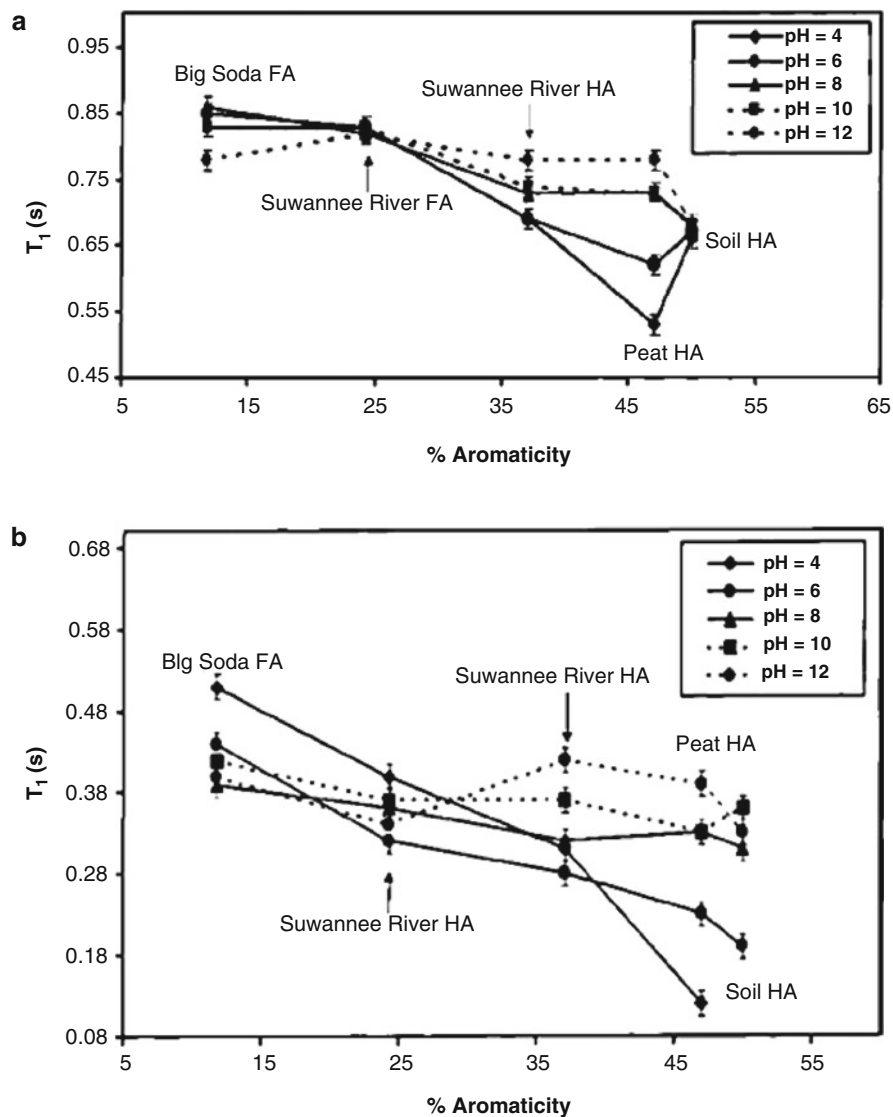
**Fig. 6.60** $T_1$ relaxation time as a function of humic and fulvic acid percent aromaticity and pH, for (**a**) benzene-$d_6$ and (**b**) pyridine-$d_5$ (after Nanny and Maza 2001). Reprinted with permission from Nanny MA, Maza JP (2001) Noncovalent interactions between monoaromatic compounds and dissolved humic acids: A deuterium NMR $T_1$ relaxation study. Environ Sci Technol 35:379–384. Copyright 2001 American Chemical Society

groups, and/or on phenol groups present in humic substances (Kang and Xing 2005).

It can be concluded that both monoaromatic compounds described above may favor – under specific pH conditions – a change in the molecular configuration of dissolved natural humic and fulvic acids. These changes are controlled by the pH of the water solution and by the natural identity of the contaminated humic materials.

PAH comprise one of the most hazardous groups of hydrophobic organic contaminants reaching the soil–subsurface environment. Phenanthrene ($C_{14}H_{10}$) is a PAH composed of three fused benzene rings. Over the years, it was studied extensively and used as a representative model for nonpolar hydrophobic organic chemicals binding on soil–subsurface constituents. Published data on the adsorption of phenanthrene to aromatic and aliphatic sorption domains of soil organic matter (SOM) were reviewed and interpreted by Chefetz and Xing (2009); see Fig. 6.61.

In contrast to the existing concept that higher sorption of aromatic pollutants occurs on aromatic components rather than on aliphatic components of NOM (e.g., Ahmad et al. 2001; Kulikova and Permkinova 2002), Chefetz and Xing (2009) did not find any specific correlation between adsorption and aromaticity in the large data set that was considered. Moreover, phenanthrene, like other hydrophobic organic contaminants, also has a strong affinity for SOM aliphatic domains; in some cases, this affinity is higher than that for aromatic domains (Fig. 6.61b). As a consequence, neither of the individual molecular descriptors – aromaticity or aliphaticity – explains the retention of phenanthrene to SOM surfaces or the formation of phenanthrene–humic complexes. However, knowledge of the molecular descriptor configuration of SOM may provide information on further changes that occur at a molecular level following PAH contamination.

It is interesting to note how sequential changes in humic substances may affect phenanthrene sorption. Kang and Xing (2005) performed sequential extraction from humic acids and humins with solutions of 0.1 M $Na_4P_2O_7$ and 0.1 M NaOH. They determined chronological changes in humic material structural configurations, and the capacity of each extract for phenanthrene sorption. From diffuse reflectance infrared Fourier transform spectroscopy (DRIFTS) measurements (Fig. 6.62), Kang and Xing (2005) deduced that earlier extracted HA had higher polarity compared to later extracted samples. The band between 1,610 and 1,620 $cm^{-1}$ is assigned to aromatic C = C stretching and/or asymmetric stretching of ionized carboxyl groups, with the peak at ~1,530 $cm^{-1}$ corresponding to the ortho-substituted aromatic compounds. The ratios of the sum of aliphatic carbon peak heights (2,930, 2,850, 1,450, 1,150, 1,074 $cm^{-1}$) to the sum of aromatic carbon peak heights (3,050, 1,610, 1,530 $cm^{-1}$), shown in Fig. 6.63, enable the estimation of the relative structural change in the HA and humins with increasing extraction.

Phenanthrene binding to the modified humic substances was greatly affected by structural and chemical changes occurring during progressive extractions of HA and humins (Kang and Xing, 2005). In general, there were significant chemical and structural differences among the HA fractions and humins. All phenanthrene sorption isotherms were nonlinear, and the nonlinearity decreased with the increase
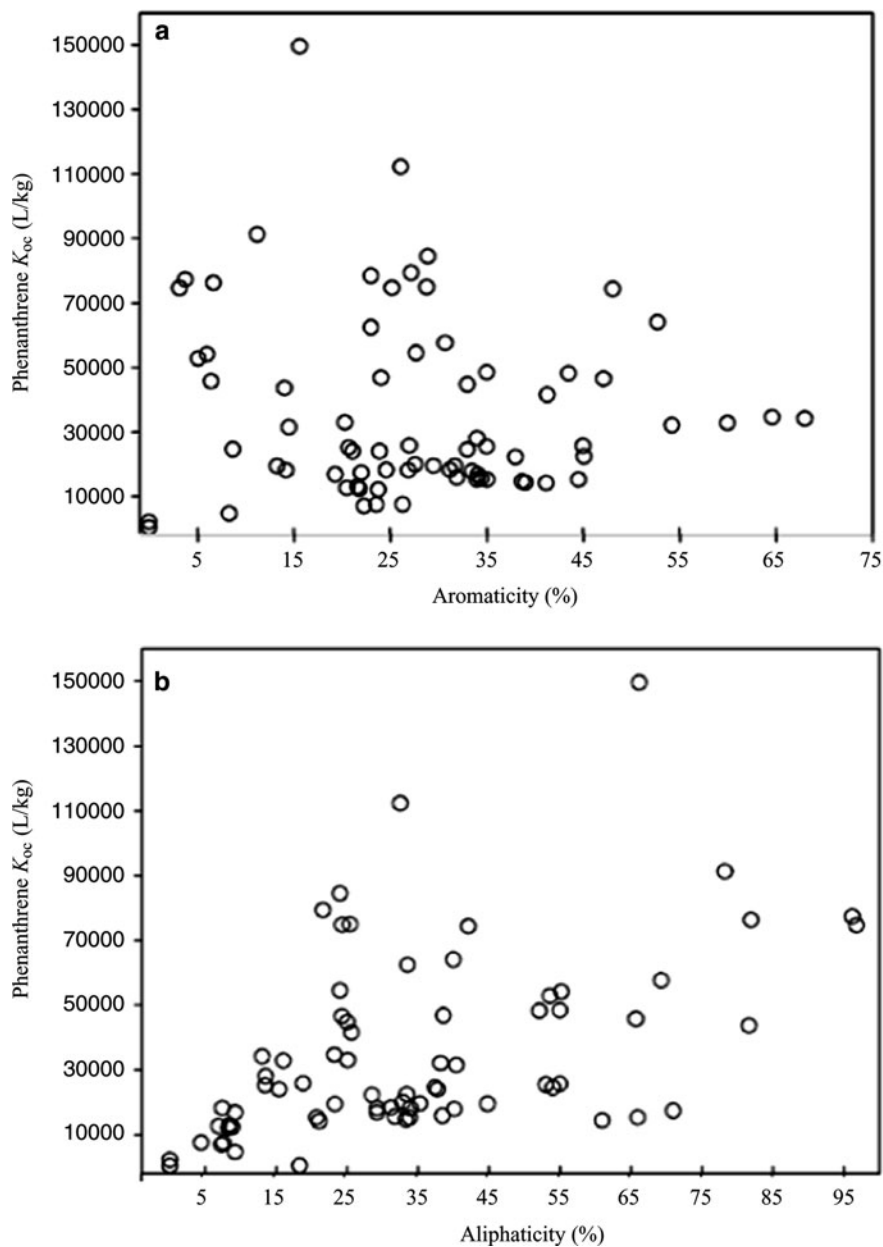
**Fig. 6.61** Relationship between phenanthrene $K_{OC}$ values (at an equilibrium concentration of 10 μg/L) and the (**a**) aromaticity or (**b**) aliphaticity level of natural sorbents (modified after Chefetz and Xing (2009) and references within). Reprinted with permission from Chefetz B, Xing B, 2009, Relative role of aliphatic and aromatic moieties as sorption domains for organic compounds: A review. Environ Sci Technol 43:1680–1688. Copyright 2009 American Chemical Society

**Fig. 6.62** Diffused
reflectance infrared Fourier
transform spectroscopy
(DRIFTS) spectra of the
humic acids (F 1–10) and
humins (HuH, HuL) (after
Kang and Xing 2005).
Reprinted with permission
from Kang S, Xing B (2005)
Phenanthrene sorption to
sequentially extracted soil
humic acids and humins.
Environ Sci Technol
39:134–140. Copyright 2005
American Chemical Society
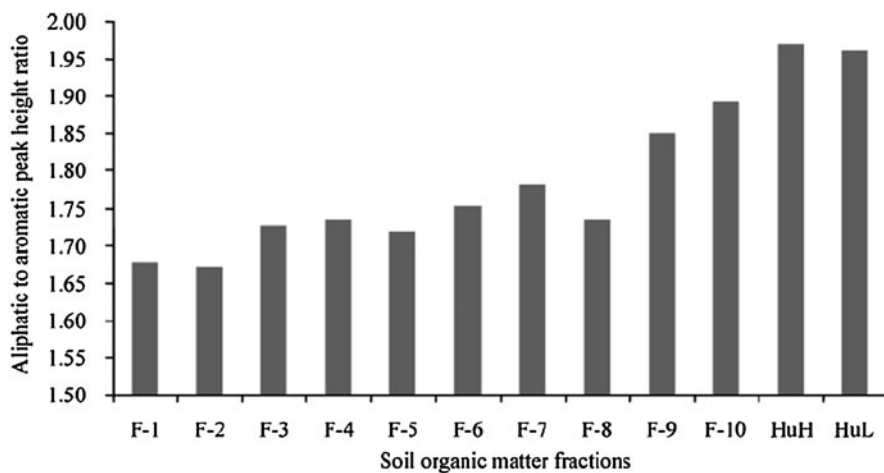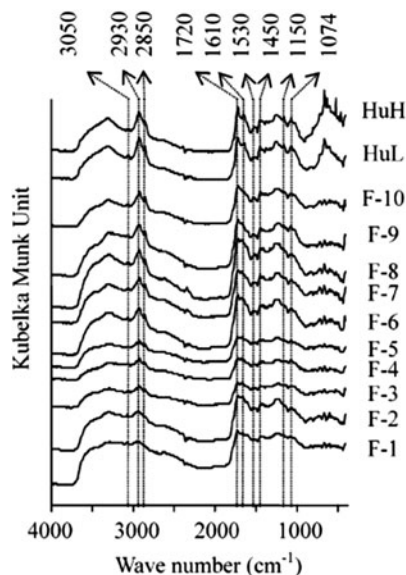




**Fig. 6.63** Ratio of the sum of peak heights for aliphatic carbons to that of aromatic carbons, as observed from diffused reflectance infrared Fourier transform spectroscopy (DRIFTS) spectra (after Kang and Xing 2005). Reprinted with permission from Kang S, Xing B (2005) Phenanthrene sorption to sequentially extracted soil humic acids and humins. Environ Sci Technol 39:134–140. Copyright 2005 American Chemical Society

in extraction number. A positive trend was observed between the sorption coefficient and the aliphaticity of the sorbent; in contrast, a negative relation was found between the nonlinearity and the aliphaticity, and between sorption capacity and polarity of HA.

Sorption hysteresis of phenanthrene provides information on potential, irreversible changes occurring in humic substance configurations following contaminant binding. Oren and Chefetz (2005) measured adsorption–desorption of phenanthrene to/from humic acids extracted from downstream and upstream sediments of the Kishon River (Israel), and found that all adsorption–desorption isotherms showed hysteresis (Fig. 6.64).

An increase in adsorption–desorption hysteresis on humic acids was observed at higher phenanthrene loading levels. Sorption hysteresis of hydrophobic organic compounds by solid organic matter was confirmed by the formation of metastable states of adsorbate in fixed mesopores, and irreversible deformation of the sorbent by the sorbate (Sander et al. 2005; Ge et al. 2006). For the particular case of phenanthrane–HA mentioned above, the decrease in desorption at high phenanthrene concentration level was hypothesized to be due to the formation of a concentration gradient forcing the sorbed molecule to penetrate deeply into HA
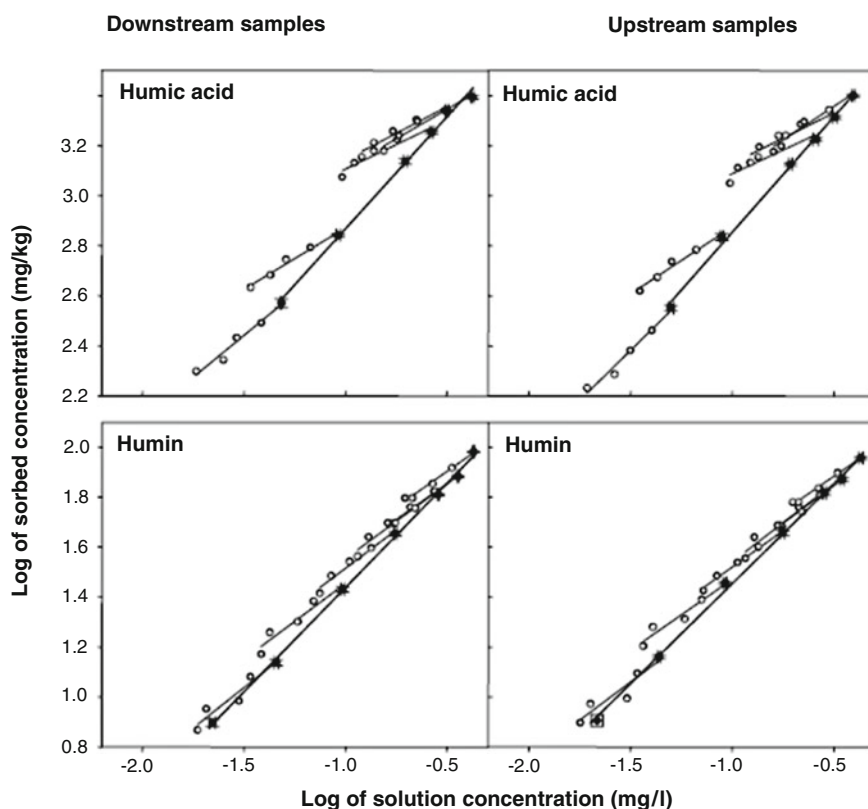


**Fig. 6.64** Adsorption (*filled symbols*) and desorption (*open symbols*) isotherms of phenanthrene by downstream and upstream humic acid and humin samples (modified after Oren and Chefetz 2003). Reprinted from Oren A, Chefetz B, Sorption-desorption of polycyclic aromatic hydrocarbons in upstream and downstream river sediments. Chemosphere 61:19–29, Copyright (2003), with permission from Elsevier

micropores, thus leading to micropore deformation. Because phenanthrene penetration into HA micropores occurs in an open system, the resulting contaminant-induced change in the humic acid micropore matrix can be considered to be irreversible.

Adsorption/desorption characteristics of the phenanthrene–DHA system, as affected by solution pH, were studied by Pan et al. (2007). Interpreting their results to evaluate adsorption/desorption hysteresis, Pan et al. (2007) used the thermodynamic index of irreversibility (TII) proposed by Sander et al. (2005). The desorption isotherm of phenanthrene from dissolved humic acid at pH 4 displayed hysteresis, showing that the solute molecules tend to bind more with DHA during desorption. Calculated TII values indicated significant hysteresis for all phenanthrene concentrations studied, which generally increased as the pH decreased. Pan et al. (2007) noted a possible change in conformation of DOM after binding with phenanthrene.
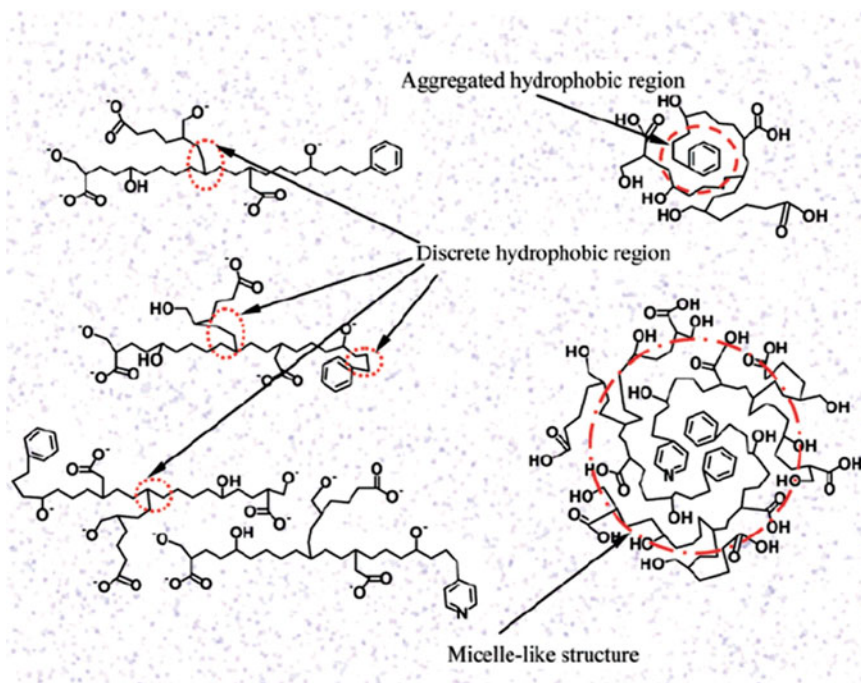


**Fig. 6.65** Schematic diagram of possible conformation changes of DOM at different pH values. Discrete hydrophobic region (*circle with dots*), aggregated hydrophobic region (*circle with dashes*), and micelle-like structure (*circle with dots and dashes*) are the possible sorption region for hydrophobic organic compounds. The area in color represents the water molecules (after Pan et al. 2007). Reprinted with permission from Pan B, Ghosh S, Xing B (2007) Nonideal binding between dissolved humic acids and polyaromatic hydrocarbons. Environ Sci Technol 41:6472–6478. Copyright 2005 American Chemical Society

Considering that composition of DOM did not change at different pHs, only changes in DOM molecular conformation are responsible for sorption deviation and irreversible hysteresis. A schematic diagram (Fig. 6.65) of possible conformation changes of DOM at different pH values was suggested by Pan et al. (2007).

In suggesting this diagram, Pan et al. (2007) considered that for apolar organic compounds such as PAH, hydrophobic interaction is mainly responsible for binding with DOM. At alkaline and neutral conditions (pH 7 and 11), carboxyl and hydroxyl functional groups of DOM are deprotonated, and the molecules are overall negatively charged. The molecules are stretched and opened because of the inter- or intra-molecular repulsion. However, part of the hydrophobic microenvironment may be too narrow to allow PAH access to binding sites, and other regions may have higher energy for sorption. As a consequence, the overall sorption displays a nonlinear isotherm behavior. Pan et al. (2007) assumed the presence of discrete hydrophobic sites for pH 7 and 11, and the formation of protonated carboxyl and hydroxyl groups under acidic pH. The surface charge of the DOM molecules being neutralized, the self-coiling and aggregation of DOM molecules were facilitated. The discrete hydrophobic microenvironment could be aggregated to form large hydrophobic regions, and the loosely coiled structure could form a more compact structure (Fig. 6.65). At low pH, several molecules form larger aggregates, a micelle-like conformation forms, and the binding with PAH is enhanced leading, to a more favorable π–π interaction environment.

# References

Ahmad R, Kookana RS, Am A, Skjemstad JQ (2001) The nature of soil organic matter affects sorption of pesticides 1. Relationship with carbon chemistry as determined by $^{13}$C CP/MAS spectroscopy. Environ Sci Technol 35:878–884

Arthur SE, Brady PV, Cygan RT, Anderson HL, Westrich HR (1999) Irreversible sorption of contaminants during ferrihydrite transformation. In: Proc. WM 1999 Conference, Boulder-Colorado, pp 13

Baes CF, Mesmer RE (1976) The hydrolysis of cations. FL Krieger Publishing, Malebar, FL

Baltpurvins KA, Burns RC, Lawrance GA, Stuart AD (1997) Effect of $Ca^{2+}$, $Mg^{2+}$ and anion type on the aging of iron(III) hydroxide precipitates. Environ Sci Technol 31:1024–1032

Banfield JF, Welch SA, Zhang HS, Ebert TT, Penn RL (2000) Aggregation-based crystal growth and microstructure development in natural iron oxide biomineralization. Science 280:741–744

Barvenik FW (1994) Polyacrylamide characteristics related to soil application. Soil Sci 58:235

Ben-Hur M, Clark P, Letey J (1992) Exchangeable Na, polymer and water quality effects on water infiltration and soil loss. Arid Soil Res Rehab 4:311–317

Benoit P, Barriusso E, Houot S, Calvet R (1996) Influence of the nature of soil organic matter on the sorption-desorption of 4-chlorophenol, 2,4-dichlorophenol and the herbicide 2,4 dichloro-phenoxyacetic acid (2,4-D). Eur J Soil Sci 47:567–578

Berkowitz B, Dror I, Yaron B (2008) Contaminant geochemistry. Springer, Heidelberg

Bleam PR, McBride MB (1986) The chemistry of adsorbed Cu(II) and Mn(II) in aqueous titanium dioxide suspensions. J Colloid Inter Sci 110:335–346

Blum AE, Eberl DD (2004) Measurement of clay surface areas by polyvinylpyrrolidone (PVP) sorption and its use for quantifying illite and smectite abundance. Clays Clay Minerals 52:589–602

Boehm PD, Quinn JG (1973) Solubilization of hydrocarbons by the dissolved organic matter in seawater. Geochim Cosmochim Acta 37:2459–2477

Bohm J (1925) Uber aluminium und eisenoxide. Z Anorg Chem 149:203–218

Bollag JM, Liu SY, Minard RD (1980) Cross-coupling of phenolic humus constituents and 2,4-dichlorophenol. Soil Sci Soc Am J 44:52–56

Bollag JM, Myers CL, Minard RD (1992) Biological and chemical interactions of pesticides with soil organic matter. Sci Total Environ 123:205–217

Bosetto M, Arfaioli P, Fusi P (1993) Interactions of alachlor with homoionic montmorillonites. Soil Sci 155:105–113

Boyd SA, Johnston CT, Laird DA, Teppen BJ, Li H (2009) A comprehensive analysis of organic contaminant adsorption by clays. In: Programs and Abstracts, Clay Mineral Society, 46th Annual Meeting, Billings MT, p 73

Breen C (1999) The characterisation and use of polycation-exchanged bentonites. Appl Clay Sci 15:187–219

Buker K, Flechter S, Tribush H (1999) Photochemistry of highly Zn-doped pyrite as compared with isostructural $FeS_2$. J Electrochem Soc 146:261–265

Calvet R (1989) Adsorption of organic chemicals in soils. Environ Health Perspect 83:145–177

Carter CW, Suffet IH (1982) Binding of DDT to dissolved humic materials. Environ Sci Technol 16:735–740

Chan IX, De Stasio G, Welch SA, Girasole M, Frazer BH, Nesterova MV, Fakra S, Banfield JF (2004) Microbial polysaccharides template assembly of nanocrystal fibers. Science 303: 1656–1658

Chefetz B, Xing B (2009) Relative role of aliphatic and aromatic moieties as sorption domains for organic compounds: a review. Environ Sci Technol 43:1680–1688

Chefetz B, Deshmukh AP, Hatcher PG, Guthrie EA (2000) Pyrene sorption by natural organic matter. Environ Sci Technol 34:2925–2930

Chiou CT, Kile DE, Brinton TI, Malcom RL, Leenheer JA, MacCarthy P (1987) A comparison of water solubility enhancements of organic solutes by aquatic humic materials and commercial humic acids. Environ Sci Technol 21:1231–1234

Combes JM, Manceau A, Calas G, Bottero JY (1989) Formation of ferric oxides from aqueous solutions: a polyhedral approach by X-ray absorption spectroscopy 1. Hydrolysis and formation of ferric gels. Geochim Cosmochim Acta 53:583–594

Conte P, Piccolo A (1999) Conformational arrangement of dissolved humic substances: influence of solution composition on association of humic molecules. Environ Sci Technol 33: 1682–1690

Cornel PK, Summers RS, Roberts PV (1986) Diffusion of humic-acid in dilute aqueous-solution. J Colloid Interface Sci 110:149–164

Cornell RM, Schwertmann U (2003) The iron oxides: structure: properties, reactions, occurrences and uses. Wiley, Weinheim

Cozzolino A, Conte P, Piccolo A (2001) Conformational changes of humic substances induced by hydroxyl-, keteo-, and sulfonic acids. Soil Biol Biochem 33:563–571

Delle Site A (2001) Factors affecting sorption of organic compounds in natural sorbent-water systems and sorption coefficients for selected pesticides: a review. J Phys Chem Ref Data 30:187–439

Dellisanti F, Valdré G (2005) Study of structural properties of ion treated and mechanically deformed commercial bentonite. Appl Clay Sci 28:233–244

Deng Y, Dixon JB, White GN (2003) Intercalation and surface modification of smectite by two non-ionic surfactants. Clays Clay Miner 51:150–161

Deng Y, Dixon JB, White GN (2006a) Bonding mechanisms and conformation of poly(ethylene oxide)-based surfactants in interlayer of smectite. Colloid Polymer Sci 284:347–356

Deng Y, Dixon JB, White GN (2006b) Adsorption of polyacrylamide on smectite, illite, and kaolinite. Soil Sci Soc Am J 70:297–304

Deng Y, Dixon JB, White GN, Loeppert RH, Juo ASR (2006c) Bonding between polyacrylamide and smectite. Colloids Surf A Physicochem Eng 281:82–91

Dzombak DA, Morel F (1990) Surface complexation modeling: hydrous ferric oxide. Wiley, New York, p 393

Edwards KJ, Bond PI, Druschel GK, McGuire MM, Hamers RJ, Banfiels JF (2000) Geochemical and biological aspects of sulfide mineral dissolution: lesson from Iron Mountain, California. Chem Geol 169:383–397

Elgawhary SM, Lindsay WL (1972) Solubility of silica in soils. Soil Sci Soc Am Proc 36:439–442

Engelberetson RR, van Wandruszka R (1994) Microorganization in dissolved humic acids. Environ Sci Technol 28:1934–1041

Fendorf SE, Eick MJ, Grossl PR, Sparks DL (1997) Arsenate and chromate retention mechanisms on goethite 1. Surface structure. Environ Sci Technol 31:315–320

Ge XP, Zhou YM, Lu CH, Tang HX (2006) AFM study on the adsorption and aggregation behavior of dissolved humic substances on mica. Sci China Ser B Chem 49:256–265

Gerstl Z, Yaron B (1978) Adsorption and desorption of parathion from attapulgite as affected by the mineral structure. J Agric Food Chem 26:569–573

Gerstl Z, Yaron B (1981) Stability of parathion on attapulgite as affected by structural and hydration changes. Clays Clay Mineral 29:53–59

Ghosh K, Schnitzer M (1980) Macromolecular structures of humic substances. Soil Sci 129: 266–276

Gilbert B, Banfield JF (2005) Molecular-scale processes involving nanoparticulate minerals in biogeochemical systems. Rev Mineral Geochem 59:99–155

Golden DC, Dixon JB, Chen CC (1986) Ion-exchange, thermal transformations, and oxidizing properties of birnessite. Clays Clay Miner 34:511–520

Golding CJ, Smernic RJ, Birch GF (2005) Investigation of the role of structural domains identified in sedimentary organic matter in sorption of hydrophobic organic compounds Investigation of the role of structural domains identified in sedimentary organic matter in sorption of hydrophobic organic compounds. Environ Sci Technol 39:3925–3932

Grafe M, Eick MJ, Grossl PR (2001) Adsorption of As(V) and As(III) on goethite in the presence and absence of dissolved organic carbon. Soil Sci Soc Am J 65:1680–1687

Grafe M, Eick MJ, Grossl PR, Saunders AM (2002) Adsorption of As(V) and As(III) on ferrihydrite in the presence and absence of dissolved organic carbon. J Environ Qual 31: 1115–1123

Green SV, Stott DE (2001) Polyacrylamide: a review of the use, effectiveness and cost of a soil erosion control amendment. In: Stott DE, Mohtar RH, Steindhardt GC (eds) Sustaining the global farm. pp 384–389

Greenland DJ, Hayes MHB (eds) (1981) The chemistry of soil processes. Wiley, Chichester

Grossl PR, Eick MJ, Sparks DL, Goldberg S, Ainsworth CC (1997) Arsenate and chromate retention mechanisms on goethite 2. Kinetic evaluation using a pressure jump relaxation technique. Environ Sci Technol 31:321–326

Gu B, Schmitt J, Chen Z, Liang L, McCarthy JF (1994) Adsorption and desorption of natural organic matter on iron oxide: mechanisms and models. Environ Sci Technol 28:38–46

Guegan R, Gautier M, Beny JM, Muller F (2009) Adsorption of a $C_{10}E_3$ non-ionic surfactant on a Ca-smectite. Clay Clay Miner 57:502–509

Haderlein SB, Schwarzenbach RP (1993) Adsorption of substituted nitrobenzenes and nitrophenols in mineral surfaces. Environ Sci Technol 27:316–327

Haderlein SB, Weissmar KW, Schwarzenbach RP (1996) Specific adsorption of nitroaromatic explosives and pesticides to clay minerals. Environ Sci Technol 30:612–622

Hasset U, Banwart WL (1989) The sorption of nonpolar organics by soils and sediments. In: Sawhney BL, Brown K (eds) Reactions and movement of organic chemicals in soils, Soil Sci Soc Am Spec Pub 22. SSSA, Madison, WI, pp 31–45

Hatcher PG, Bortiatynski JM, Minard RD, Dec J, Bollag JM (1993) Use of high-resolution carbon-13 NMR to examine the enzymatic covalent binding of carbon-13-labeled 2,4-dichlorophenol to humic substances. Environ Sci Technol 27:2098–2103

Hayes MHB, Mingelgrin U (1991) Interactions at the soil colloid solution interface. In: Bolt GH, De Boodt MF, Hayes MF, McBride MB (eds) NATO ASI Series-Applied Science Series F 190. Kluwer, Dordrecht, pp 324–401

Inyang HI, Bae S (2005) Polyacrylamide sorption opportunity on interlayer and external pore surfaces of contaminant barrier clays. Chemosphere 58:19–31

Jia Y, Xu L, Fang Z, Demopoulos GF (2006) Observation of surface precipitation of arsenate on ferrihydrite. Environ Sci Technol 40:3248–3253

Johnston CT, Oliveira MFD, Teppen BJ, Sheng G, Boyd SA (2001) Spectrocopic study of nitroaromatic-smectite sorption mechanism. Environ Sci Technol 35:4767–4772

Johnston CT, Sheng G, Teppen BJ, Boyd SA, de Oliveira MF (2002) Spectroscopic study of dinitrophenol herbicide sorption on smectite. Environ Sci Technol 36:5067–5074

Al Juhaiman LA, Mekhamer WK, Al-Boajan AM (2010) Effect of poly(vinyl)pyrrolidone on the zeta potential and water loss of raw and Na-rich Saudi bentonite. Surf Interface Anal 42:1723–1727

Kang S, Xing B (2005) Phenanthrene sorption to sequentially extracted soil humic acids and humins. Environ Sci Technol 39:134–140

Khalaf M, Kohl SD, Klumpp E, Rice JA, Tombacz F (2003) Comparison of sorption domains in molecular weight fractions of a soil humic acid using solid state $^{19}$F NMR. Environ Sci Technol 37:2855–2860

Koo CM, Ham HT, Choi MH, Kim SO, Chung IJ (2003) Characteristics of polyvinylpyrrolidone-layered silicate nanocomposites prepared by attrition ball milling. Polymer 44:681–689

Krause E, Ettel VA (1989) Solubilities and stabilities of ferric arsenate. Hydrometallurgy 22:311–337

Kulikova NA, Permkinova IV (2002) Binding of atrazine to humic substances from soil, peat and coal related to their structure. Environ Sci Technol 36:3720–3724

Kyle BG (1981) Soil-water equilibria for nonionic organic compounds. Science 213:683

Laird DA (1997) Bonding between polyacrylamide and clay mineral surfaces. Soil Sci 162:826–832

Landrum PF, Nihart SR, Eadie BJ, Gardner WS (1984) Reverse-phase separation method for determining pollutant binding to Aldrich humic-acid and dissolved organic-carbon of natural-waters. Environ Sci Technol 18:187–192

Le TD, Olsson U, Mortensen K, Zipfel J, Richtering W (2001) Nonionic amphiphilic bilayer structures under shear. Langmuir 17:999–1008

Levy R, Francis CW (1975) Interlayer adsorption of polyvinylpyrrolidone on montmorillonite. J Colloid Interface Sci 50:442–450

Lewis DG, Schwertmann U (1979) Influence of aluminum on the formation of iron- oxides 4. Influence of [Al], [OH], and temperature. Clays Clay Miner 27:195–200

Li H, Teppen BJ, Johnston CT, Boyd SA (2004) Thermodynamics of nitroaromatic compound adsorption from water by smectite. Environ Sci Technol 38:5433–5442

Liu P (2007) Polymer modified clay minerals: a review. Clay Sci 38:64–76

Longstaffe JG, Simpson MJ, Maas W, Simpson AJ (2010) Identifying components in dissolved humic acid that bind organofluorine contaminants using $^1$H ($^{19}$F) reverse heteronuclear saturation transfer difference NMR spectroscopy. Environ Sci Technol 44:5476–5482

Luthy RG, Aiken GR, Brusseau ML, Cunningham SD, Gschwend PM, Pignatello JJ, Reinhard M, Traina SJ, Weber WJ Jr, Westall JC (1997) Sequestration of hydrophobic organic contaminants by geosorbents. Environ Sci Technol 31:3341–3347

Manceau A, Charlet L (1994) The mechanism of selenite adsorption on goethite and hydrous ferric oxide. J Colloid Interface Sci 168:87–93

Manning BA, Fendorf SE, Goldberg S (1998) Surface structures and stability of arsenic(III) on goethite: spectroscopic evidence for inner-sphere complexes. Environ Sci Technol 32:2383–2388

Martnes CE, McBride MB (1998) Coprecipitates of Cu, Pb, Zn in iron treatment. Clays Clay Miner 46:537–545

McBride MB (1989) Reactions controlling heavy metal solubility in soils. Adv Soil Sci 10:1–47

Michaels AS (1954) Aggregation of suspensions by polyelectrolytes. Ind Eng Chem 46: 1485–1490

Michel FM, Ehm L, Antao SM, Lee PL, Chupas PJ, Liu G, Strongin DR, Schonen AAM, Phillips BL, Parise JB (2007) The structure of ferrihydrite, a nanocrystalline material. Science 316:1726–1729

Michot LJ, Pinnavaia TJ (1991) Adsorption of chlorinated phenols from aqueous solution by surfactant-modified pillared clays. Clays Clay Miner 39:634–641

Mingelgrin U, Saltzman S (1979) Surface reactions of parathion on clays. Clays Clay Miner 27:72–76

Mortland MM (1970) Clay-organic complexes and interactions. Adv Agron 22:75–117

Myneni SCB, Brown JT, Martinez GA, Meyer-Ilse W (1999) Macromolecular structures of humic substances in water and soils under varying solution conditions. Abstracts of the American Chemical Society 217:U738–U738

Nanny MA (1999) Deuterium NMR characterization of noncovalent interactions between monoaromatic compounds and fulvic acids. Organic Geochem 30:901–999

Nanny MA, Maza JP (2001) Noncovalent interactions between monoaromatic compounds and dissolved humic acids: a deuterium NMR $T_1$ relaxation study. Environ Sci Technol 35: 379–384

Nasser A, Gal M, Gerstl Z, Mingelgrin U, Yariv S (1997) Adsorption of alachlor on montmorillonites. J Thermal Anal 50:257–268

Niederer C, Schwarzenbach RP, Goss KU (2007) Elucidating differences in the sorption properties of 10 humic and fulvic acids for polar and nonpolar organic chemicals. Environ Sci Technol 41:6711–6717

O'Reilly SE, Strawn DG, Sparks DL (2001) Residence time effects on arsenate adsorption/ desorption mechanisms on goethite. Soil Sci Soc Am J 65:67–77

Oren A, Chefetz B (2005) Sorption-desorption of polycyclic aromatic hydrocarbons in upstream and downstream river sediments. Chemosphere 61:19–29

Pan B, Ghosh S, Xing B (2007) Nonideal binding between dissolved humic acids and polyaromatic hydrocarbons. Environ Sci Technol 41:6472–6478

Pereira TR, Laird DA, Thompson ML, Johnston CT, Teppen BJ, Li H, Boyd SA (2008) Role of smectite quasicrystal dynamics in adsorption of dinitrophenol. Soil Sci Soc Am J 72:347–354

Pigna M, Krishnamurty GSR, Violante A (2006) Kinetics of arsenate sorption-desorption from metal oxides: effect of residence time. Soil Sci Soc Am J 70:2017–2017

Prost R, Gerstl Z, Yaron B, Chaussidon J (1977) Infrared studies of parathion-attapulgite interactions. In: Horowitz M (ed) Israel-France symposium on behavior of pesticides in soils. The Volcani Center, Bet Dagan, Israel, pp 27–32

Rao PSC, Lee LS, Nekedi-Kiza P, Yalkowsky SH (1989) Sorption and transport of organic pollutants at waste disposal sites. In: Gerstl Z, Chen Y, Mingelgrin U, Yaron B (eds) Toxic organic chemicals in porous media. Springer, Heidelberg, pp 176–193

Saltzman S, Yariv S (1975) Infrared study of the sorption of phenol and p-nitrophernol by montmorillonite. Soil Sci Soc Am Proc 39:474–479

Saltzman S, Yariv S (1976) Infrared and X-ray study of parathion-montmorillonite complexes. Soil Sci Soc Am J 40:34–38

Saltzman S, Yaron B (1986) Pesticides in soils. Van Nostrand Reinhold Comp, New York, p 374

Sander M, Lu YF, Pignatello JJ (2005) A thermodynamically based method to quantify true sorption hysteresis. J Environ Qual 34:1063–1072

Schlautman MA, Morgan JJ (1993) Effects of aqueous chemistry on the binding of polycyclic aromatic hydrocarbons by dissolved humic materials. Environ Sci Technol 27:961–969

Schwarzenbach RP, Gshwend PM (2003) Environmental organic chemistry, 2nd edn. Wiley, New York

Schwertmann U, Murad E (1983) Effect of pH on the formation of goethite and hematite from ferrihydrite. Clay Clay Miner 31:277–284

Sequaris JM, Camara Decimavilla S, Corrales Ortega JA (2002) Polyvinylpyrrolidone sorption and structural studies on homoionic Li, Na, K, and Cs-montmorillonite – montmorillonite colloidal suspensions. J Colloid Interface Sci 252:93–101

Sequaris JM, Hind A, Narres HD, Schwuger MJ (2000) Polyvinylpyrrolidone sorption on Na-montmorillonite: Effect of polymer interfacial conformation on the behavior and binding of chemicals. J Colloid Interface Sci 230:73–83

Sheng GY, Johnston CF, Teppen JB, Boyd SA (2001) Potential contributions of smectite clays and organic matter in pesticide retention in soils. J Agric Food Chem 49:2899–2907

Sheng GY, Johnston CT, Teppen BJ, Boyd SA (2002) Adsorption of dinitrophenol herbicides from water by montmorillonites. Clay Clay Miner 50:25–34

Simpson MJ (2006) Nuclear magnetic resonance based investigations of contaminants interactions with soil organic matter. Soil Sci Soc Am J 70:995–1004

Simpson MJ, Chefetz B, Hatcher PG (2003) Phenanthrene sorption to structurally modified humic acids. J Environ Qual 32:1750–1758

Šmejkalová D, Spaccini R, Fontaine B, Piccolo A (2009) Binding of phenol and differently halogenated phenols to dissolved humic acid as measured by NMR spectroscopy. Environ Sci Technol 43:5377–5382

Šmejkalová D, Piccolo A (2008) Host-guest interactions between 2,4, dichlorophenol and humic substances as evaluated by 1H NMR relaxation and diffusion ordered spectroscopy. Environ Sci Technol 42:8440–8445

Sparks DL (2002) Environmental soil chemistry. Academic, New York

Straub KL, Bentz M, Schink B, Widdel F (1996) Anaerobic nitrate dependent microbial oxidation of ferrous iron. Appl Environ Microbiol 62:1458–1460

Sun T, Paige CR, Snodgrass WJ (1996) The effect of cadmium on the transformation of ferrihydrite into crystalline products at pH 8. Water Air Soil Pollut 91:307–325

Sun X, Doner HE (1996) An investigation of arsenite and arsenic bonding structures on goethite by FTIR. Soil Sci 161:865–872

Szczerba M, Środoń J, Skiba M, Derkowski A (2010) One-dimensional structure of exfoliated polymer-layered silicate nanocomposites: a polyvinylpyrrolidone (PVP) case study. Appl Clay Sci 47:235–241

Theng BKC (1974) The chemistry of clay organic reactions. Adam Hilger, London

Theng BKC (1979) Formation and properties of clay–polymer complexes. Elsevier, Amsterdam

Torrent J, Guzman R (1983) Crystallization of Fe(III)-oxides from ferrhydrite in salt solutions: osmotic and specific ion effects. Clay Miner 17:463–469

Volpert E, Selb J, Candau F, Green N, Argillier JF, Audibert A (1998) Adsorption of hydrophobically associating polyacrylamides on clays. Langmuir 14:1870–1879

Waltham AC, Eick MJ (2002) Kinetics of arsenic adsorption on goethite in the presence of sorbed silicic acid. Soil Sci Soc Am J 66:818–825

Waychunas GA, Rea BA, Fuller CC, Davis JA (1993) Surface chemistry of ferrihydrite: part 1 EXAFS studies of the geometry of coprecipitated and adsorbed arsenate. Geochim Cosmochim Acta 57:2251–2269

Waychunas GA, Kim SC, Banfield JF (2005) Nanoparticulate iron oxide minerals in soils and sediments: unique properties and contaminant scavenging mechanisms. J Nanopart Res 7:409–433

Weissmahr KW, Haderlein SB, Schwazenbach RP (1997) In situ spectroscopic investigations of adsorption mechanisms of nitroaromatic compounds at clay mineral. Environ Sci Technol 31:240–247

Wershaw RL, Burcar PJ, Goldberg MC (1969) Interaction of pesticides with natural organic material. Environ Sci Technol 3:271–273

White AF, Brantley SI (1995) Chemical weathering rates of silicate minerals. Rev Mineral 31:1–583

Wijayaratne R, Means JC (1984) Sorption of polycyclic aromatic hydrocarbons by natural estuarine colloids. Mar Environ Res 11:77–89

Xing B (1997) The effect of the quality of soil organic matter on sorption of naphthalene. Chemosphere 35:633–642

Yaron B (1975) Chemical conversion of parathion on soil surfaces. Soil Sci Soc Am Proc 39:639–643

Yaron B, Calvet R, Prost R (1996) Soil pollution-processes and dynamics. Springer, Heidelberg

Yaron B, Saltzman S (1972) Influence of water and temperature on adsorption of parathion by soils. Soil Sci Soc Am Proc 36:583–586

# Chapter 7
# Contaminant-Induced Irreversible Changes in Properties of the Soil–Subsurface Regime

The literature contains a large spectrum of research results that show alteration of soil–subsurface properties as a result of their contact with anthropogenic chemical compounds in the Critical Zone environment. In such an open thermodynamic system, contaminants induce changes in the soil subsurface that will never return to their initial state, thus becoming irreversible. By "irreversible," we consider long-term, stable, and persistent transformations in soil–subsurface solid phase properties that are also resistant to remediation procedures and/or natural attenuation. The extent of the transformation process is controlled by environmental parameters in the Critical Zone.

Irreversible changes to the soil–subsurface solid phase are reflected in terms of both physical and chemical properties. Here, we present a series of examples from the literature of anthropogenically induced chemical contamination of natural soil–subsurface solid phase properties, leading to the formation of a "new" soil–subsurface porous medium with properties different than those of the natural one. We examine irreversible changes in the soil–subsurface system caused by contaminants originating from sodic and saline waters, effluents and treated wastewaters, agrochemicals, and soil reclamation products of industrial or urban origin.

## 7.1   Sodic and Saline Water Effects

Saline waters may reach the soil–subsurface regime via irrigation with saline water and wastewater, by intrusion from sea water, and/or by dissolution of clustered salt crystals. Within the components of saline water, sodium may strongly affect soil and subsurface water transmission properties. Changes in hydraulic conductivity and infiltration rate are controlled by the porosity of the medium and by the clay content and clay mineralogy of the solid phase. Soil clays – with expanding layer mineralogy – may swell and disperse upon contact with sodic water, changing the architecture of the natural host porous medium and affecting its water transmission

properties. Swelling and dispersion of clays have been proposed to explain the decrease in hydraulic conductivity of soils.

Swelling-induced partial blocking of conducting pores in clay, by sodic water, was addressed in the early studies of Quirk and Schofield (1955), McNeal and Coleman (1966), and Russo and Bresler (1977). This process was considered a principal cause of decreases in hydraulic conductivity. Moreover, soil clay mineralogy was determined to be a main factor in the extent of hydraulic conductivity decrease in soils leached with sodic water (Yaron and Thomas 1968). Deflocculation and movement of clay in conducting pores were subsequently considered to be another major factor causing decreases in hydraulic conductivity (Frenkel et al. 1978; Shainberg and Letey 1984, and references therein). Whereas a change in soil hydraulic conductivity due to sodic water induced swelling is a partially irreversible process, changes due to dispersion and particle redistribution in the conducting pores of the soil–subsurface regime are absolutely irreversible. Examples of changes occurring to various physical properties of soil and subsurface under irrigation with saline and sodic water are discussed below.

## 7.1.1 Swelling

Swelling of soil clays occurs over a range of sodium concentrations in saline or waste waters; it is dependent on the properties of the clay, the extent of the layer charge, and the type of interlayer cations. Swelling of soil clays, expressed by interlayer expansion, is attributed to the repulsive force between electrical double layers on adjacent platelets (McBride 1989), and based on the fact that layer silicate clays approach a maximum hydration state beyond which they do not extend. Farmer and Russell (1971) explained swelling qualitatively, as a simple model of H-bonding when interlayer expansion is driven initially by the energy of hydration of the exchangeable cations. Swelling was explained later by noting that the zeta potential of $Na^+$-clay is much lower than that anticipated from $Na^+$ ions fully dissociated from the surface in a suspension of layered silicates in water (Low 1981).

Interlayer expansion of a layered clay is shown in Fig. 7.1, where the arrangements of $H_2O$ chains linking a divalent cation to the surface of a 2.0-nm hydrate of smectite clay are characterized by 2:1 layers. The force inducing clay expansion arises from ion–dipole interactions, while the force opposing clay swelling emanates from electrostatic interactions. In general, the swelling of 2:1 silicates is considered to be induced by hydration of charge-compensating counterions in the interlayer space of clay.

Laird (2006) defined six separate processes driving the swelling of smectite clays saturated with alkali and alkaline earth cations in an aqueous system, as follows: crystalline swelling, double-layer swelling, quasi-crystal formation, cation demixing, co-volume swelling, and Brownian swelling. In an aqueous system, some of these processes may act concurrently, affecting swelling dimension. An increase
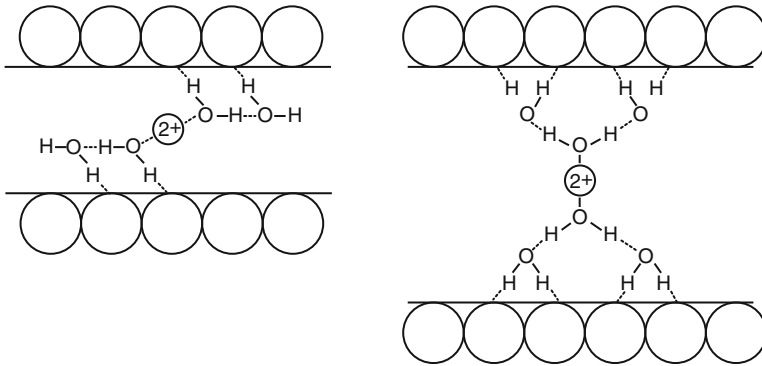
**Fig. 7.1** Arrangement of H$_2$O chains linking a divalent exchange cation to the surfaces of a 2.0-nm hydrate of smectite (modified after Farmer 1978, in McBride 1989). Copyright 1989, Soil Science Society of America. Reprinted with permission

in layer charge leads to a decrease in crystalline swelling, but increases the size and stability of smectite clay quasi-crystals. When two smectite quasi-crystals approach each other in an aqueous suspension, a portion of their double layer may fuse expelling anions, cations, and water from the contact surfaces. In dilute aqueous suspensions, Na-smectite can be almost completely delaminated, a diffuse double layer is formed between the individual layers, and each layer behaves as a stable individual colloid (Sposito 1992; Laird 2006). A schematic diagram depicting the breakup and formation of quasi-crystals is given in Fig. 7.2, leading to an increase in soil clay swelling.

Swelling of soil clay induced by dissolution of incorporated salt crystals was examined by Mokni et al. (2010). Salt crystals clustered in soils and rocks – usually formed by evaporation of saline waters – attract fresh water and form brine as a consequence of an osmotic flux phenomenon; the brine is associated with a low water activity. It can be observed that this total volume is composed of volumes occupied by salt crystals, fluids (water and air), and the soil solid phase (Fig. 7.3). The fluid volume is controlled by the initial porosity. As a result of dissolution of the crystals, the pore volume available for fluids increases, inducing a deformation in the initial porosity. In a soil–subsurface environment, chemical osmosis may be explained by the theory of irreversible thermodynamics employed by Katchalsky and Curran (1965) for describing the transport of matter through biological membranes.

In situ laser microscopy combined with digital image analysis was used by Suzuki et al. (2005) to investigate the swelling of bentonite aggregates in a NaCl solution of variable concentration. Changes in quasi-crystal shape after contact with NaCl solutions are shown in Fig. 7.4. The change in basal spacing of bentonite was expressed by the expansion ratio, and defined by the difference in the basal spacing values in the dry and wet states. Figure 7.5 shows the expansion ratio of a smectite aggregate as a function of time, and NaCl concentration: the expansion ratio value decreased with increase of NaCl concentration, from about 800% in the case of pure
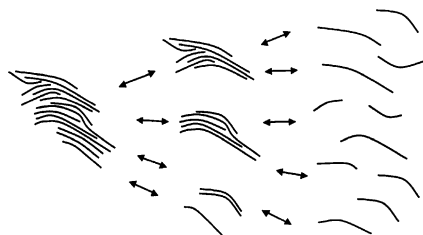
**Fig. 7.2** Schematic diagram depicting the breakup and formation of quasi-crystals. On the *left*, the layers are grouped together in a single quasi-crystal; in the middle, the same layers are split into four quasi-crystals; on the right, the layers are completely delaminated (after Laird 2006). Reprinted from Laird AD, Influence of layer charge on swelling of smectites. Applied Clay Sci 34:74–87, Copyright (2006), with permission from Elsevier
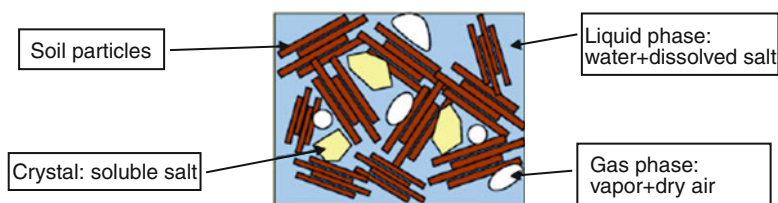


**Fig. 7.3** Schematic representation of the total volume of a porous unit occupied by fluid (gas and liquid) and the soil skeleton (after Mokni et al. 2010). Reprinted from Mokni N, Olivella S, Alonso EE, Swelling in clayey soils induced by the presence of salt crystals. Appl Clay Sci 47:105–112, Copyright (2010), with permission from Elsevier

deionized water to less than 10% when the water solution had a NaCl concentration of 1.0 mol dm$^{-3}$.

The results of Suzuki et al. (2005) refer only to a simple NaCl water solution. However, in natural soil–subsurface conditions, saline irrigation water and groundwater contain also divalent cations which can exchange with Na$^+$ ions in bentonite. As a consequence, the results of Suzuki et al. (2005) are significant only for understanding the mechanism of Na$^+$-controlled swelling of expandable soil clays.

Hysteresis was noted in investigations of clay swelling, beginning with the early pioneering studies of Mooney et al. (1952) and Norrish (1954). Swelling hysteresis was attributed to changes in the energy levels of expansion and attraction (e.g., Wada et al. 1990) and to the rigidity of the unit layer (e.g., Norrish 1954) or to the clay–water system (e.g., Fu et al. 1990). Evidence of swelling hysteresis was observed in various experiments using gravimetric measurements and basal spacing determination, as well as various relative humidity and salt concentrations (Laird et al. 1995, and references therein). In general, swelling was explained in terms of restructured arrangements of the clay and changes in interactions between layers upon expansion or contraction. It was also considered that swelling and shrinking of clay minerals are causes of hysteresis.
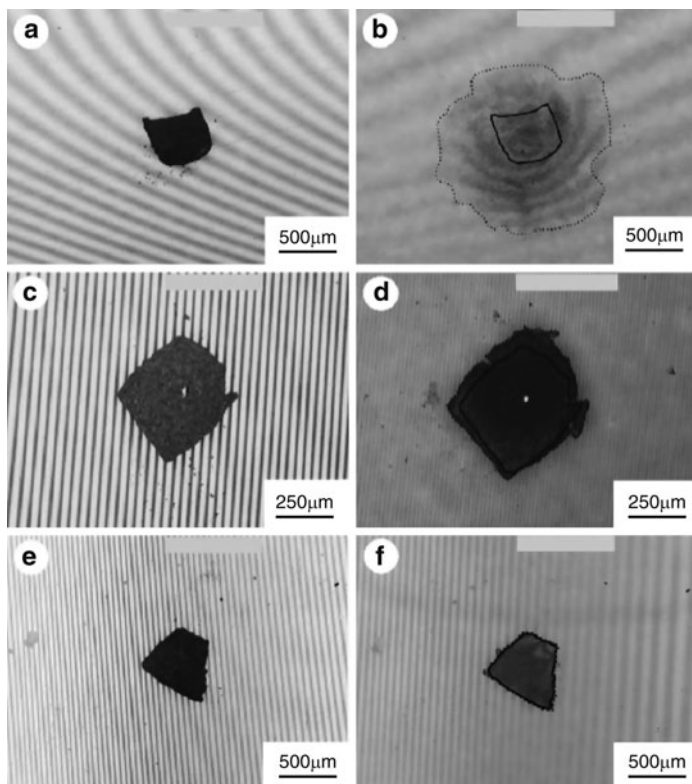
**Fig. 7.4** Changes in a quasi-crystal shape before (**a**, **c**, **e**) and after (**b**, **d**, **f**) coming into contact with NaCl solutions with concentrations of (**a**, **b**) 0.01, (**c**, **d**) 0.30, and (**e**, **f**) 1.00 mol/dm$^3$ NaCl. The *solid line* indicates the outline of a quasi-crystal before coming into contact with the solution, and the *dashed line* indicates the outline of the quasi-crystal 15 min after exposure to the solution (after Suzuki et al. 2005). Reprinted from Suzuki S, Prayongphan S, Ichikawa Y, Chae BG, In situ observations of the swelling of bentonite aggregates in NaCl solution. Appl Clay Sci 29:89–98, Copyright (2005), with permission from Elsevier

Smectites are major clay components of the soil–subsurface regime. Laird et al. (1995) reported an experiment designed to quantify the relationship between hysteresis due to swelling and surface properties of the smectites. Smectites were equilibrated to reach a basal spacing of 15.5–19 Å for adsorption and 19–15.5 Å for desorption. Direct and continuous equilibration procedures were used for preparing WB (Wyoming) and IMV (Florida) bentonites. The relationship between basal spacing and H$_2$O activity of equilibrating NaCl solutions is shown in Fig. 7.6. Differences between the adsorption and desorption curves define distinct hysteresis loops for the WB and IMV smectites. Tests performed on three additional smectites collected from different locations displayed similar hysteresis magnitude.

Correlation coefficients relating hysteresis magnitude to surface charge density, percentage of tetrahedral charge, and surface area are not significant, indicating that

**Fig. 7.5** Expansion ratios for one aggregate as a function of time for various NaCl concentrations (in mol dm$^{-3}$) (after Suzuki et al. 2005). Reprinted from Suzuki S, Prayongphan S, Ichikawa Y, Chae BG, In situ observations of the swelling of bentonite aggregates in NaCl solution. Appl Clay Sci 29:89–98, Copyright (2005), with permission from Elsevier
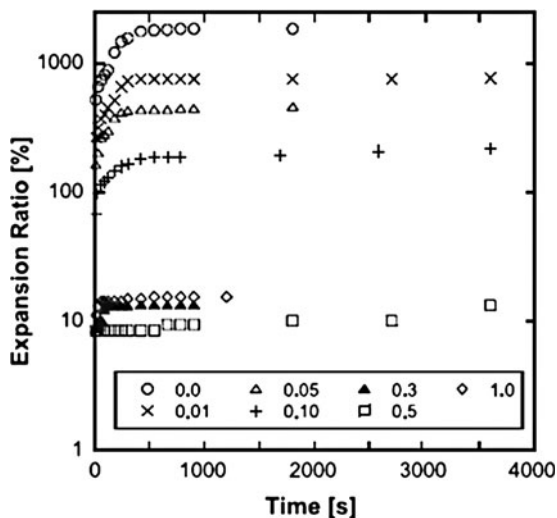


the magnitude of hysteresis is independent of the surface charge properties of the smectites. Based on these results, Laird et al. (1995) considered that crystalline swelling is an "irreversible thermodynamic process." In support of irreversibility, free-energy changes occurring during swelling and collapse can be classified as free energy of expansion, free energy of attraction, and free energy of transition. Free energy of expansion is due to changes in the hydration states of the interlayer cations and negative charge sites, free energy of attraction is due to changes in the net electrostatic attraction between layers, and free energy of transition is due to the irreversible work needed to affect transfer of heat and mass during swelling and collapse. As a consequence, the cause of hysteresis in crystalline swelling is attributed to both intrinsic and extrinsic processes. Intrinsic hysteresis is a consequence of changes in expansion and attraction energy levels during swelling caused by the rigidity of the clay–water system. Extrinsic hysteresis is caused by factors that contribute to additional rigidity of smectite quasi-crystals.

Based on grand-canonical molecular simulation of a Na-clay, Tambach et al. (2006) concluded that the thermodynamic origin of swelling hysteresis is a free-energy barrier separating the layered hydrates. The free-energy barrier is a result of breaking and formation of hydrogen bonds between and within water layers. The free energies of a simulated Arizona Na-montmorillonite at relative humidities of 8.9 and 67% are shown in Fig. 7.7. At a low relative humidity, one-layer hydrates formed at a basal spacing of 12 Å, and at the relative humidity of 67%, two-layer hydrates formed at 14.75 Å. These two stable states were separated by a free-energy barrier with a maximum at 13.5 Å.

As soon as this point is reached, the one-layer hydrate can swell to the two-layer hydrate. From this state, the reverse process of shrinking the clay mineral is in practice not possible because the system cannot overcome the free-energy barrier to be dehydrated. The fact that the free-energy barrier and metastable state are the

**Fig. 7.6** Relationship
between basal spacing and
$H_2O$ activity of equilibrating
NaCl solutions for Wyoming
(WB) and Florida (IMV)
bentonites. Samples for the
desorption curves were
equilibrated using the direct
equilibration (DE),
continuous equilibration
(CE), and direct equilibration
from 18 Å (DE-18)
techniques (after Laird et al.
1995). Reprinted from Laird
DA, Shang C, Thompson ML,
Hysteresis in crystalline
swelling of smectites.
J Colloid Interface Sci
171:240–245, Copyright
(1995), with permission
from Elsevier
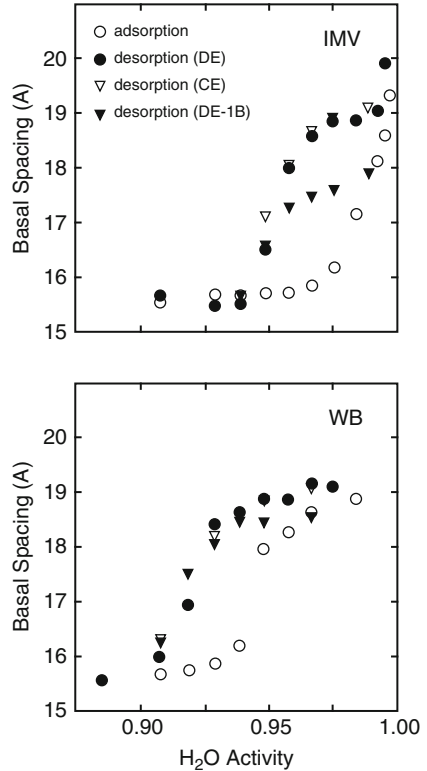


origin of simulated clay swelling hysteresis may be seen in Fig. 7.8. Tambach et al.
(2006) considered that this free-energy barrier disappears with an increase in clay
interlayer humidity. At a critical point equivalent to the free energy specific to the
humidity of single layer clay, the process can become reversible, forming a
"hysteresis loop." We consider, however, that in the soil–subsurface environment
where clay minerals are complexed with organic matter, the conditions required for
a completely reversible process are difficult to establish.

## 7.1.2   Dispersion: Flocculation

Dispersion and flocculation of colloidal earth material are other processes induced
by sodium contamination, comprising both inorganic and organic compounds,
which may affect water transfer properties of the soil–subsurface system. Principal
factors related to clay dispersion–flocculation processes following contact of sodic
water with a soil surface include the water electrolyte concentration, pH, and
sodium adsorption ratio (SAR) expressed by the ratio between $Na^+$ and $Ca^{2+}$ +
$Mg^{2+}$ concentrations (SAR = $[Na^+]/[(Ca^{2+} + Mg^{2+})/2]^{1/2}$).
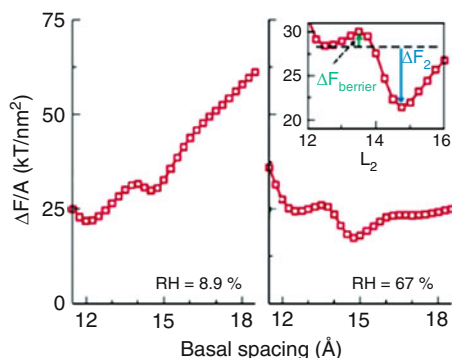
**Fig. 7.7** Simulated free energy per clay platelet area ($\Delta F/A$), at an external pressure ($P_{ext}$) of 1 atm, as a function of the basal spacing for Arizona Na-montmorillonite at low (*left*) and intermediate (*right*) relative humidities of 8.9% and 67%, respectively. The inset shows a zoom on a particular area of the free-energy curve of Na-montmorillonite at 67% relative humidity, which expresses the free-energy barrier ($\Delta F$ barrier) and the free energy of the two-layer hydrates ($\Delta F_2$) relative to the free energy of the one-layer hydrate (modified after Tambach et al. 2006). Reprinted with permission from Tambach T, Bolhuis PG, Hensen EJM, Smit B (2006) Hysteresis in clay swelling induced by hydrogen bonding: accurate predicting of swelling states. Langmuir 22:1223–1234. Copyright 2006 American Chemical Society
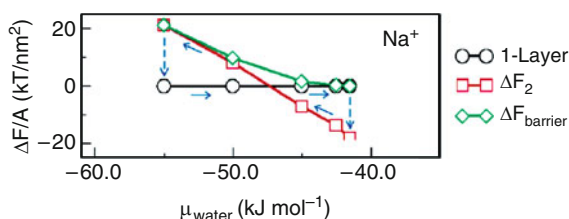


**Fig. 7.8** Simulated hysteresis loops as a function of the water chemical potential or, equivalently, the relative humidity for Arizona Na-montmorillonite. The *arrows* indicate the direction of the loop. The free energy of the two-layer hydrate ($\Delta F_2$) and the free energy of the barrier ($\Delta F_{barrier}$) are expressed per clay platelet area ($A$) and relative to the free energy of the one-layer hydrate (modified after Tambach et al. 2006). Reprinted with permission from Tambach T, Bolhuis PG, Hensen EJM, Smit B (2006) Hysteresis in clay swelling induced by hydrogen bonding: accurate predicting of swelling states. Langmuir 22:1223–1234. Copyright 2006 American Chemical Society

*Dispersion* and release of clay particles from the soil solid matrix are considered to be the major source of mobile colloidal particles in the subsurface (Ryan and Elimelech 1996). Release of colloidal particles is controlled by their surface interaction with the solid matrix and by hydrodynamics of the kinetics of water flow as described by the Derjaguin, Landau, Vervey, and Overbeek (DLVO) theory (discussed by Lagaly and Ziesmer 2003; Grolimund and Borkovec 2006, and references therein). Particle release is also considered as the result of an escape

process (Dahneke 1975) where, under fixed boundary conditions, the release rate coefficient increases with the increase of ionic strength.

Clay dispersion is governed by the attractive and repulsive forces in the electrical double layer at the surface of charged colloids; the balance between the forces is determined by factors such as exchangeable cation concentration and ionic strength (Rengasamy and Olsson 1991). The critical ion concentration for clay dispersion from soil aggregates is lower than the flocculation values (see below) observed in the separated clay soils. Chorum et al. (1994) attributed this behavior to the high negative charge of separated soil clays, due to exposure of surfaces that were originally bound in aggregates.

Chorum et al. (1994) investigated the dispersion of clay from sodic soil in relation to changes in net charge on clay particles. A positive relationship was obtained between pH and the percentage of dispersible clay from different soils. The percentage increase in negative charge was correlated also to the pH. Based on their experimental results, Chorum et al. (1994) considered that the negative charge was the primary factor in clay dispersion, with the pH affecting clay dispersion by changing the net charge on the soil clay. Summarizing the existing information in this field, Grolimund and Borkovec (2006) showed that (1) particle release is usually enhanced by lowering the ionic strength, (2) release process depends on the solution composition whereby monovalent counterions promote this process most effectively, (3) release is influenced by the pH, (4) release kinetics are exponential, and (5) aging effects should be considered.

*Flocculation*, or coagulation, of Na-clay dispersion systems occurs in most cases between the negative edges and the negative faces of the clay particle. The flocculation value of a clay suspension in a sodic water is defined as the minimum concentration of $Na^+$ in the aqueous electrolyte solution necessary to flocculate a suspension of clay in a given time, under specific conditions of exchangeable cation concentration, pH, and suspension concentration.

Based on a number of experiments on coagulation of Na-montmorillonite dispersions, Lagaly and Ziesmer (2003) found that the anisometric shape and charge distribution on montmorillonite particles caused very low critical coagulation concentration of inorganic salts. Adsorption of multivalent anions increased the density of the negative edge charges. As a consequence, the edge/face coagulation became a face/face coagulation with a high critical salt concentration. Lagaly and Ziesmer (2003) pointed out that in dispersion of high montmorillonite contents, the flocculation may be initiated by edge/edge aggregation.

Flocculation between the positive edge and the negative face occurs only at pH <6. The critical flocculation concentrations of the clay fraction extracted from three strongly structured soils from Natal (two dominated by smectite and one by kaolinite) were compared to those of smectite from Wyoming and kaolinite from Georgia in Na-saturated forms (Frenkel et al. 1992a, b). They found that the soil clays had much higher critical flocculation concentration than their Na-saturated clay reference counterparts. This difference was attributed to the existence of humic acid coating on soil clay surfaces.

### 7.1.3   Water Transmission Properties

Hydraulic conductivity (HC) is one of the main factors to be considered within the physical properties of the soil–subsurface system. HC is expressed as $K = \rho g k/\mu$, where $\rho$ is the fluid density, $g$ is gravity, $\mu$ is fluid dynamic viscosity, and $k$ is intrinsic permeability which depends on the size and shape of the soil–subsurface pores.

Swelling and dispersion are the two processes affecting the soil–subsurface hydraulic conductivity. The $Na^+$ cations from incoming contaminated water are adsorbed on clay minerals, inducing their swelling and/or dispersion. The extent of this process is governed by the concentration of the $Na^+$ cations in the incoming water. In their review on sodium and electrolyte concentration effects on soil HC, Yaron and Shainberg (1973) noted that swelling is not the main cause for the decrease in HC of clayey soils. In contrast, dispersion of clay due to $Na^+$ is the main cause of irreversible reduction in HC of clays, because it results in rearrangements and blocking of the pores through which flow takes place.

It is clear that clay dispersion is a major factor that irreversibly affects the HC of soils irrigated with sodic water (Shainberg and Letey 1984, and references therein). Oster et al. (1980) found that clay dispersion is highly sensitive to low levels of exchangeable Na, and increases sharply with very small increases in exchangeable sodium percentage (ESP). Yaron and Shainberg (1973) report on the movement of water through clay systems when HC was affected only by swelling (Fig. 7.9a) and when the water movement was affected by both swelling and dispersion of particles (Fig. 7.9b).

Soil HC at equilibrium with salt-contaminated water is determined by the concentration of electrolytes, the ionic composition of the water, and the exchangeable cations in the soil complex. Quirk and Schofield (1955) examined the ionic effect on soil HC, by saturating soil samples with Na, K, Ca, and Mg, and percolating through them a solution characterized by a single ion system. It can be seen from Fig. 7.10 that after 3-h percolation, the HC decreased by 88% for the Na-saturated soil and by 40% for the K-saturated soil. When the exchange capacity was saturated with the divalent cations, there was practically no change in HC. Because homoionic systems seldom exist in nature, the influence of a single ion on hydraulic conductivity is mainly of theoretical interest.

In a mixed system, ESP is the most important characteristic influencing HC. This was noted by Quirk (1957), who showed that soil permeability decreases with increasing percentage of exchangeable sodium (Fig. 7.11). A quantitative relationship between solution concentration and ESP was expressed as a "threshold concentration." The threshold concept was proposed initially by Quirk and Schofield (1955) and is defined as the salt concentration needed to maintain the hydraulic conductivity in a Na-saturated system 20% below that existing in a Ca-saturated system.

The relationship between soil hydraulic conductivity and electrolyte type, and concentration of the infiltrating water is affected by the soil–subsurface mineralogy.
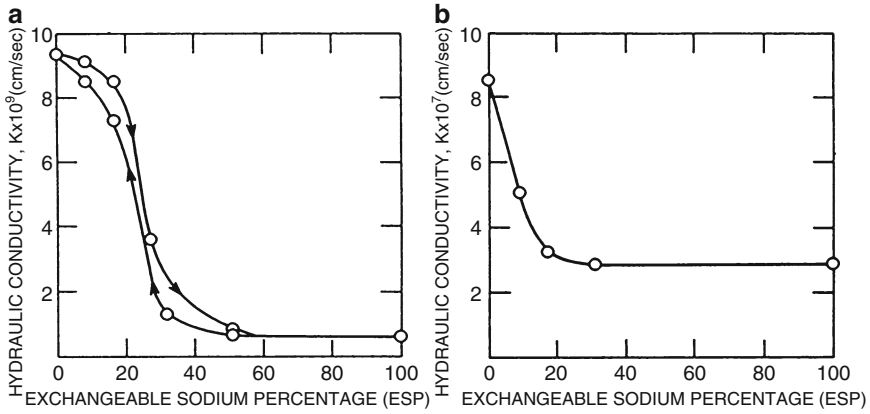
**Fig. 7.9** The hydraulic conductivity of (**a**) the clay membrane, and (**b**) clay pastes, as a function of exchangeable sodium percentage, ESP (modified after Yaron and Shainberg 1973)



**Fig. 7.10** Hydraulic conductivity as affected by soil cation saturation. Reprinted from Quirk JP, Schofield RK (1955) The effect of electrolyte concentration on soil permeability. Eur J Soil Sci 6:251–259. Copyright 1955 with permission of John Wiley and Sons
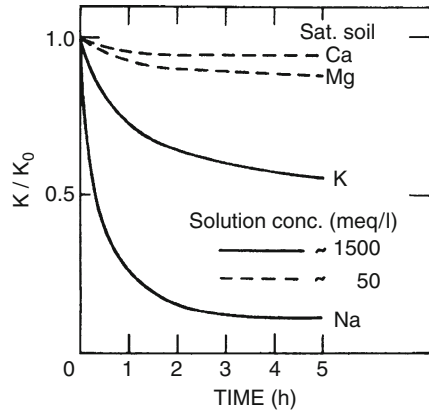
McNeal and Coleman (1966) indicated that in soils where the clay minerals are dominated by the extent of 2:1 layer silicates, and where there are moderate amounts of montmorillonite, ESP values in excess of 15 can often be maintained without causing a serious reduction in HC, provided that the concentration of the permeating solution is about 3 meq L$^{-1}$. Yaron and Thomas (1968) studied the effect of ESP on the hydraulic conductivity of various Texas soils, finding that a 20% HC decrease was produced by an ESP of 10 in montmorillonite soils, by an ESP of 16 in a soil with mixed mineralogy, and by an ESP of 23 in a kaolinitic soil (Fig. 7.12).

The composition of the permeating water – in terms of the ratio between sodium and other cations – has a significant effect on the exchange process and on the hydraulic conductivity of soils. In dealing with the effect of saline or waste water on HC, one must consider the SAR. Under dynamic conditions, when an initially non-

**Fig. 7.11** Effect of the degree of sodium saturation on the permeability of Sawyers soils (after Quirk 1957)
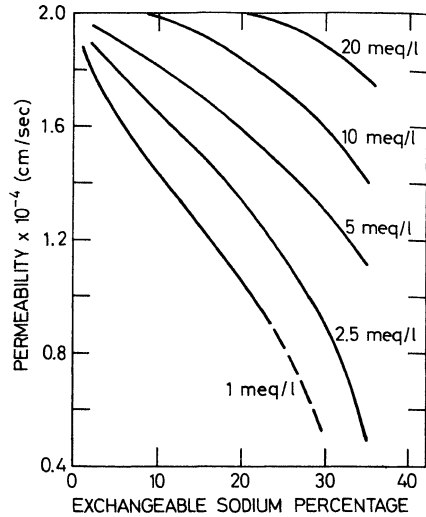


**Fig. 7.12** The relation between the exchangeable sodium percentage and the relative hydraulic conductivity for soils with different mineralogy: Burleson and Houston montmorillonite; Miller mixed; Pullman illite and kaolinite. Reprinted from Yaron B, Thomas GW (1968) Soil hydraulic conductivity as affected by sodic water. Water Resour Res 4:545–552. Copyright 1968 American Geophysical Union. Reproduced/modified by permission of American Geophysical Union
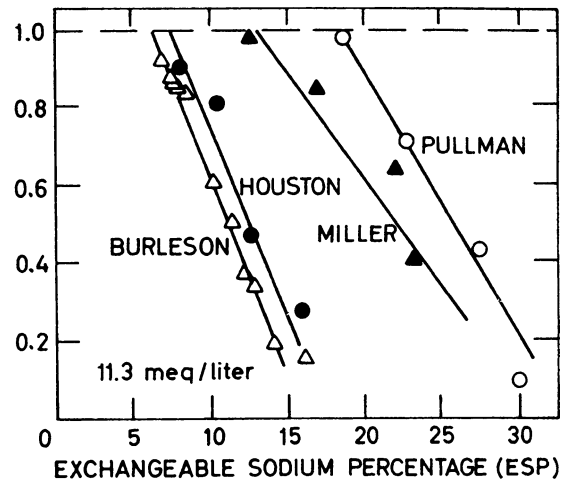


sodic soil is irrigated with sodic water, the HC decreases continuously until the exchangeable sodium in the entire soil profile equilibrates with the permeating solution.

Yaron and Thomas (1968) showed that this decrease in HC is characterized by a curve whose shape depends on the nature of the soil, the cationic composition, and the total salt concentration of the permeating solution. The hydraulic conductivity depends on the mean ESP of the soil profile and is independent of the volume of the effluent. Moreover, an increase in SAR results in a decrease in hydraulic conductivity. Figure 7.13 shows the reduction in HC when three electrolyte water solutions with one value of total concentration (11 meq $L^{-1}$) and three SAR values

**Fig. 7.13** Effect of sodium
adsorption ratio (SAR) on soil
hydraulic conductivity (soil
Burleson; total electrolyte
concentration of irrigation
water = 11 meq $L^{-1}$.
Reprinted from Yaron B,
Thomas GW (1968) Soil
hydraulic conductivity as
affected by sodic water.
Water Resour Res 4:545–552.
Copyright 1968 American
Geophysical Union.
Reproduced/modified by
permission of American
Geophysical Union
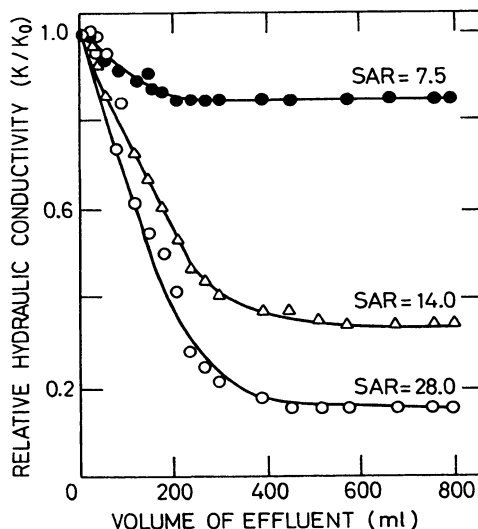


(7.5, 14.0, and 28.0) were passed through columns of a Burleson loamy clay
vertisol. At equilibrium, a SAR value of 7.5 resulted in a 15% decrease in HC,
whereas a SAR of 28 reduced initial HC by 84%. These results are in agreement
with those of other parallel studies (e.g., Reeve and Tamaddoni 1965; McNeal and
Coleman 1966; McNeal 1968; Lagerwerff et al. 1969), showing that total electro-
lyte concentration and SAR can be used to predict the decrease in saturated HC of a
soil following percolation with sodic water.

The decrease in soil hydraulic conductivity can be attributed to changes occur-
ring in the soil matrix. Chen and Banin (1975) performed scanning electron
microscopy measurements in a sandy soil (6% clay) and a clayey soil (55% clay),
the clay fraction in both cases having similar mineralogy. With an increase in SAR,
fine particles were detached from coarse sandy soil, creating a new matrix arrange-
ment containing a continuous network in the voids. Although clay movement was
more limited in the clayey soil, Chen and Banin (1975) considered that the same
mechanism caused the changes in the solid matrix, indicating possible clay particle
migration along the soil profile.

The irreversibility of the salt effect on soil hydraulic conductivity was
emphasized by Dane and Klute (1977), who determined the effect of percolating
solution composition on both HC (Fig. 7.14) and soil bulk density (Fig. 7.15). The
tested soil was a clayey Weld soil with a composition of 24% sand, 33% silt, and
43% clay. The clay mineralogy consisted of 60% smectite, 20% mica, and 20%
kaolin. When soil samples were subjected to percolation by NaCl solutions with
decreasing concentration and a constant SAR of 40, it was observed that the
decrease in total electrolyte concentration led to a decrease in HC (Fig. 7.14). No
changes were observed for a reference solution ($CaCl_2$) with a concentration of
1,000 meq $L^{-1}$ and a SAR value of 0.

**Fig. 7.14** Hydraulic
conductivity volumetric soil
content relations for a soil
sample (load 13.3 g cm$^{-2}$)
subjected to a series of
solutions of decreasing
concentration at SAR = 40
(after Dane and Klute 1977).
Copyright 1977, Soil Science
Society of America.
Reprinted with permission
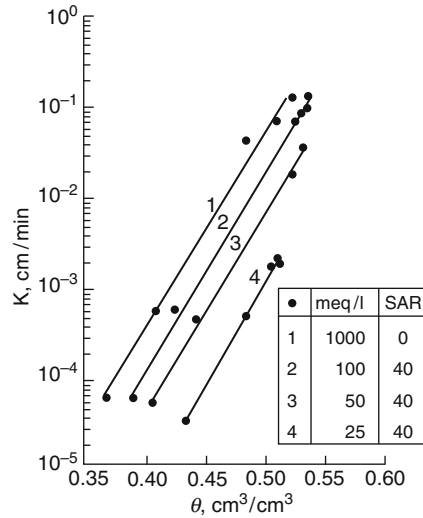


The composition of the percolating solution affected also the soil bulk density. The data presented in Fig. 7.15a, b correspond to soil samples leached with solutions at constant SAR values of 25 and 40, respectively. When the SAR of the solutions was 40, the bulk density decreased with a decrease in the concentration of percolating solution. In the experiment with SAR = 25, it was found that increasing the solution concentration in a second sequence caused the bulk density to increase steadily, although it did not attain the same value as during the first sequence.

Dane and Klute (1977) considered that a decrease in the electrolyte concentration of the surrounding solution caused clay platelets to increase their distance of separation. Under these conditions, the repulsive forces begin to dominate over the attractive forces, with the clay particles forming an unstable arrangement. A partial collapse of the clay particle configuration causes the bulk volume of the soil to decrease, explaining the increase in bulk density when solution concentration decreases. Re-percolating the soil samples with an electrolyte solution of an increasing concentration never enables a return to the initial state.

Rearrangement of silt and sand particles in soil occurs after partial dispersion and translocation. This is associated with the swelling of clay aggregates, caused by soil percolation with sodic water at a low electrolyte concentration. As a consequence, this is an irreversible process.

In the surface of sodic soils from arid and semi-arid regions, characterized by the presence of dissolved carbonate and bicarbonate, pH may exhibit high values ranging from 8 to ~10. The effect of pH on clay dispersion in Na-saturated soils was reported by Schofield and Samson (1954), who showed that kaolinite edge faces become negatively charged at high pH and positively charged at low pH. The pH-induced soil clay dispersion effect was subsequently reported in many publications, including those of van Olphen (1977), Arora and Coleman (1979),
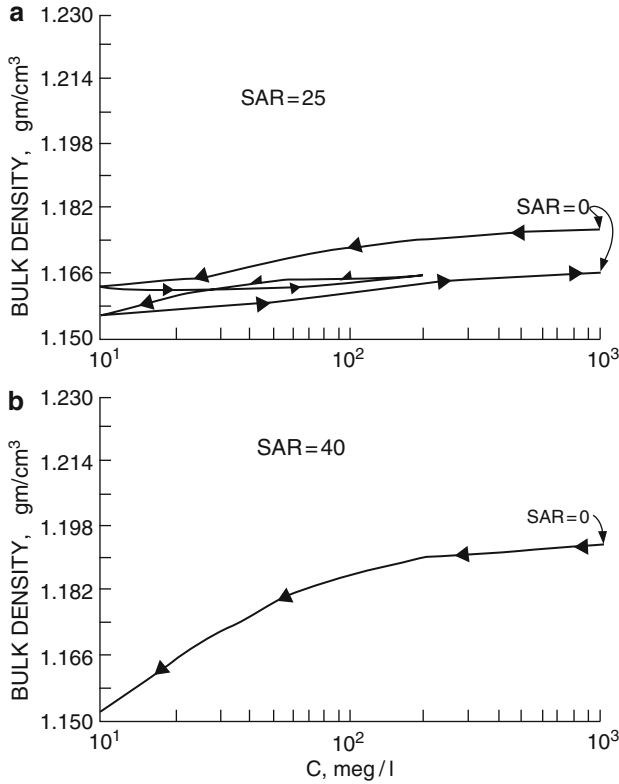
**Fig. 7.15** Bulk density during conditions of ponded solution for a soil sample (load 13.3 g cm$^{-2}$) subjected to series of solutions of varying concentration at (**a**) SAR = 25, and (**b**) SAR = 40. *Arrows* indicate the sequence of solution application (modified after Dane and Klute 1977). Copyright 1977, Soil Science Society of America. Reprinted with permission

Oster et al. (1980), and Suarez and Frenkel (1981). An example of the effect of pH on kaolinitic Shortlands soil clay in Na solution is found in Frenkel et al. (1992a, b), where the critical flocculation value, defined as the NaCl concentration required to sediment 8% of the clay after standing for 24 h, was measured. The critical flocculation values determined at pH values of 6.6, 7.3, and 8.5 are shown in Fig. 7.16.

A specific study on pH–electrolyte associated effects on soil HC and dispersion was reported by Suarez et al. (1984). Soils with different properties (see Table 7.1) were tested in laboratory column experiments. The effects of pH on HC (transmission) properties of the soils, studied by percolating aqueous solutions with different electrolyte concentrations and SAR of 20, are presented in Fig. 7.17. It can be observed that pH–electrolyte associated effects on HC are controlled by the soil clay mineralogy: Arlington soil with vermiculite predominance is not affected by the solution pH. The HC of montmorillonitic and kaolinitic soils decreased with a
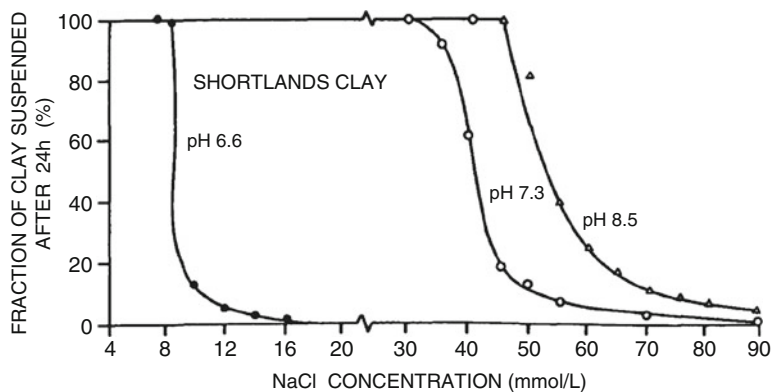
**Fig. 7.16** Effect of pH on flocculation of Shortlands clay in NaCl solution (after Frenkel et al. 1992b). Copyright 1992, Soil Science Society of America. Reprinted with permission

**Table 7.1** Selected physical and chemical properties of soil used in Suarez et al. (1984) experiments (after Suarez et al. 1984). Copyright 1984, Attributed to the Soil Science Society of America

| Soil | Particle size | | | | Surface area ($m^3 g^{-1}$) | Organic carbon (%) | Dominant clay |
|---|---|---|---|---|---|---|---|
| | Sand % | Salt % | Clay % | $CaCO_3$ % | | | |
| Bonsail (fine, montmorillonite, thermic Natric Palexeralfs) | 58 | 23 | 19 | 0 | 69 | 0.45 | Montmorillonite-vermiculite, mica, kaolinite |
| Fallbrook (fine-loamy, mixed, thermic Typic Haploxeralfs) | 51 | 22 | 27 | 0 | 130 | 0.28 | Kaolinite, vermiculite, mica, montmorillonite |
| Arlington (coarse-loamy, mixed, thermic Haptic Durixeralfs) | 25 | 52 | 23 | trace | 111 | 0.21 | Vermiculite, mica, kaolituite |

pH increase from 7 to 9, and with a decrease in electrolyte concentration. The results from HC experiments were generally consistent with optical transmission measurements of dispersion. Reversibility of HC decrease was evaluated for the Bonsall montmorillonitic soil by leaching with 250 $mmol_c$ $L^{-1}$. It was found that the changes in HC were not reversible upon application of water with different electrolyte levels.

A laboratory study by Mace and Amrhein (2001) investigated irreversible changes in HC following reclamation procedures. Columns packed with Milham clay loam soil, having a clay fraction dominated by smectite, were leached with electrolyte solutions of various concentrations and with a SAR ranging from 1 to 8. After leaching, the soil columns were amended with top dressings equivalent to 5 t $ha^{-1}$ gypsum or to 3 t $ha^{-1}$ sulfuric acid; these concentrations are greater than
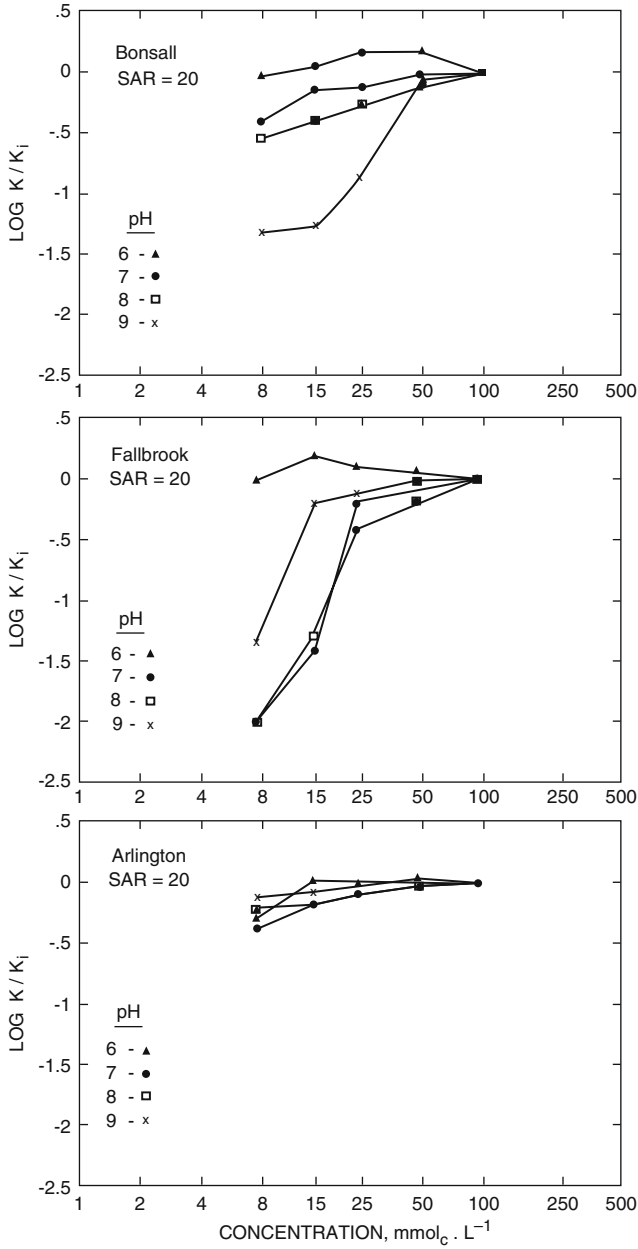
**Fig. 7.17** Relative hydraulic conductivity vs. electrolyte concentration for Bonsall, Fallbrook, and Arlington soils at SAR = 20 and pH 6, 7, 8, and 9 (after Suarez et al. 1984). Copyright 1984, Attributed to the Soil Science Society of America

the amount required to remove exchangeable Na from the altered soil. The amended soil columns were then leached with deionized water; HC and swelling were estimated by determining the clay concentration in the leachate. These data were used to quantify the clay dispersion and internal soil swelling.

The changes in HC following percolation with aqueous solutions of different qualities are shown in Fig. 7.18. HC decreased as a function of increasing SAR and decreasing electrolyte concentration. As the electrolyte concentration in the leaching solution was reduced, the cumulative quantity of dispersed clay in the effluent increased. A significant increase in dispersed clay occurred when the salt concentration in the applied water was below 5 $mmol_c$ $L^{-1}$, and tended to rise in the order SAR 8 > 5 > 3 > 1. The relative increase in swelling followed a similar trend to the dispersed clay.

After addition of gypsum to the undisturbed soil surface, a fast, dramatic increase in HC was observed initially, followed by a quick HC decrease with subsequent leaching (Fig. 7.19). Mace and Amrhein (2001) explain this "apparent reversibility" in HC decrease by the correlation between the HC and internal swelling pathways of the soil, which can be attributed to an ionic strength effect (Fig. 7.20). With each subsequent leaching, there was less gypsum, the electrolyte concentration of the infiltrating water gradually decreased, and swelling increased.
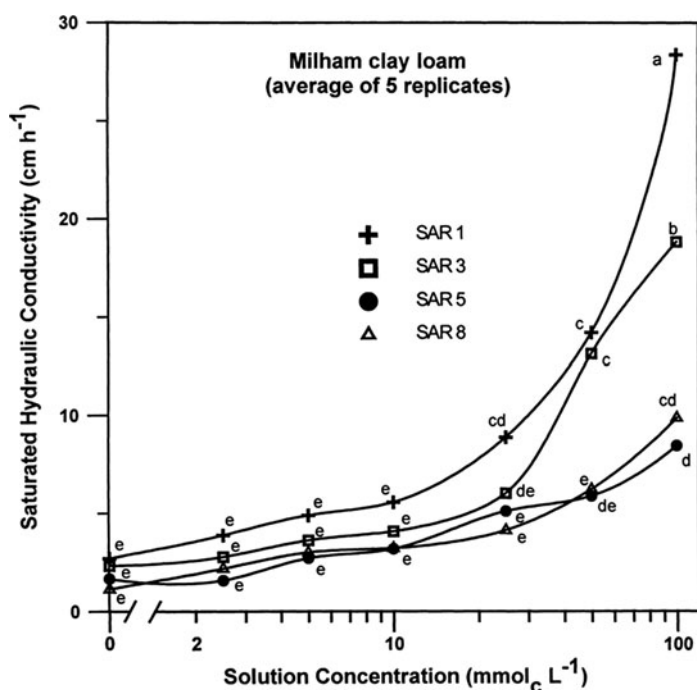


**Fig. 7.18** Hydraulic conductivity as a function of SAR and electrolyte concentration. Statistically significant differences are indicated by different letters (after Mace and Amrhein 2001). Copyright 2001, Soil Science Society of America. Reprinted with permission
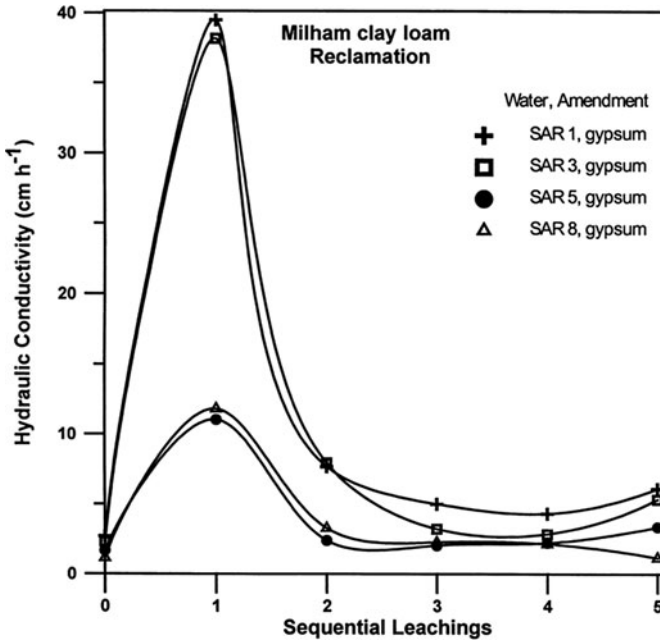
**Fig. 7.19** Hydraulic conductivity of the soil following a surface application of gypsum (5 Mg ha$^{-1}$ equivalent) and leached with deionized water (after Mace and Amrhein 2001). Copyright 2001, Soil Science Society of America. Reprinted with permission

The soil originally leached with high SAR waters had the lowest HC values, and the most internal swelling even after reclamation. Internal soil swelling at low electrolyte concentrations reduces the number of large pores and increases the water holding capacity of the soil at low tension. This leads, at the soil surface after gypsum application, to the partial reversibility of HC. At relatively high SAR (from 5 to 8), which is relevant to soils in arid and semi-arid regions, there was an irreversible plugging of soil pores due to both dispersed clays and internal swelling. These laboratory findings of Mace and Amrhein (2001) may be extrapolated to field conditions, where sodium-induced changes in water transmission properties will not return to the initial state following reclamation techniques.

## 7.1.4 Crust Formation and Infiltration Rate

Surface "sealing" of the soil surface by crust formation, which is caused mechanically by rain and is affected by the presence of sodium in irrigation water (which favors clay dispersion), may change significantly the infiltration rate of the natural soil–subsurface water transmission properties (Hillel 1971; Shainberg 1985; Painuli and Abrol 1986). Infiltration rate (IR) is defined as the volume flux of water flowing
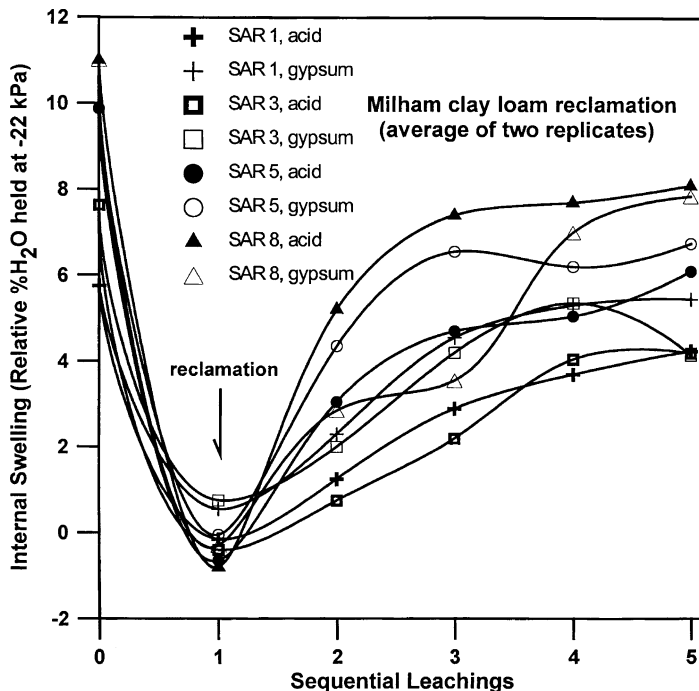
**Fig. 7.20** Internal swelling of the soil following surface application of gypsum or $H_2SO_4$ and leached with deionized water. Internal swelling was measured by the amount of water held by the soil at $-22$ kPa relative to the amount of 100 mmol$_c$ L$^{-1}$ solution held at the same tension (after Mace and Amrhein 2001). Copyright 2001, Soil Science Society of America. Reprinted with permission

into the soil–subsurface cross-section per unit of surface area. IR is defined by the relationship $i = i_c + (i_0 - i_c) e^{-kt}$, where $i$ is the infiltration rate, $i_c$ is the asymptotic final infiltration rate reached at time $t$, $i_0$ is the initial infiltration capacity of the soil, and $k$ is a constant that determines how quickly $i_0$ decreases to $i_c$.

Using a rain simulator to ensure a constant mechanical breakdown of soil aggregates by the beating action of raindrops, Kazman et al. (1983) determined the effect of soil ESP on the water infiltration rate in sandy loam (Hamra) and silty loam (loess) soils (Fig. 7.21). Because the raindrop impact energy was constant, differences in soil IR were due only to soil sodicity. In soils exposed to rain, 3–5% exchangeable Na was sufficient to cause clay dispersion, forming a crust on the surface and inducing a decrease in the infiltration rate. Crust formation is favored by the mechanical input of raindrops, by low electrolyte concentration of the rainwater, and by the relative ease of particle redistribution on the soil surface. The "classical ESP" of 15, established by US Salinity Laboratory Staff (1954) and associated studies (e.g., McNeal and Coleman 1966; McNeal 1968), is generally accepted as a critical level for soil deterioration.
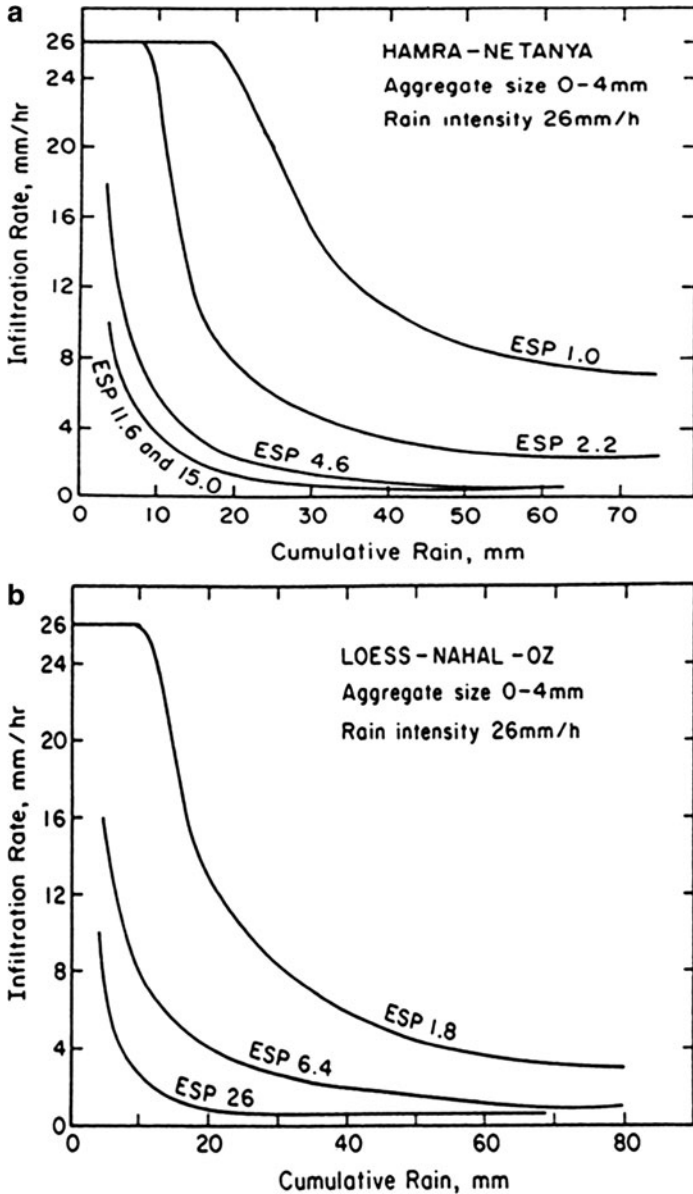
**Fig. 7.21** The effect of soil exchangeable sodium percentage (ESP) on infiltration rates in two soils, (**a**) sandy loam (Hamra) and (**b**) silty loam (loess). Reprinted from Kazman Z, Shainberg I, Gal M (1983) Effect of low levels of exchangeable sodium and applied phosphogypsum on the infiltration rate of various soils. Soil Sci 135:184–192. Copyright 1983 with permission of Wolters Kluwer Health

Clay dispersion during crust formation may lead also to irreversible transport of mineral colloids and to their redistribution with depth. Because this process depends on the frequency of natural drying and wetting cycles, the rate of transport and redeposition of clays into the soil–subsurface cross-section, and thus changes in soil–subsurface matrix and properties, may be very low. Dispersion of the soil clay surface can be prevented by increasing the electrolyte concentration of the raindrops artificially; this is achieved by adding gypsum – a slow release salt – at the soil surface. This was verified by Kazman et al. (1983) in additional experiments.

## 7.2 Effluents and Treated Wastewater Effects

Application of suspended organic solid to soils occurs during irrigation and land disposal of (treated and untreated) wastewater and sludge. The effects of solid organic wastes on the properties of the soil and subsurface regime depend on the persistence and distribution with depth of the wastes, and on their chemical and physical interactions with the soil–subsurface solid phase. As a consequence, physical properties such as water retention capacity, bulk density, porosity, and structure of the soil–subsurface solid phase may be changed irreversibly. Both effluents and sludge are characterized by a high organic matter content which may vary from 1% to 70%. As a function of their origin, effluents, treated wastewaters, and the resulting sludge may contain chemical contaminants such as salts, heavy metals, surfactants, and other organic compounds that may cause irreversible changes to the soil–subsurface solid phase (Yaron et al. 1984; Feigin et al. 1991; Levy et al. 2010).

Treated wastewater (TWW) for irrigation is used as a major method to dispose of effluents from municipal sources, and to sustain agricultural production in arid and semi-arid regions characterized by shortages of fresh water. As a function of the quality of the raw sewage water and the degree of treatment, TWW and associated sludges exhibit a range of concentrations of electrolytes, organic and inorganic contaminants, dissolved organic matter (DOM), and suspended solids. Various studies have shown that coupling TWW to a high sodium content induces an increase in soil clay dispersivity and higher flocculation values compared to the net sodic water (e.g., Frenkel et al. 1992a, b; Tarchitzky et al. 1999). This finding is reflected in the blockage of pores and a decrease in soil HC (e.g., Vinten et al. 1983; Metzger and Yaron 1987; Magesan et al. 1999).

## 7.2.1 Surfactants

Surfactants, or "surface active agents," are organic compounds of natural or anthropogenic origin that reduce the surface tension of water. Surfactants may interact with the porous medium solid phase, and as a consequence, they may affect

the soil–subsurface water transmission properties. Surfactants are organic compounds comprising hydrophobic and hydrophilic components. Surfactants may be hydrophilic when the surfactant is ionic or highly polar. Surfactants may be anionic, cationic, amphoteric, or nonionic. Due to an amphipathic structure, surfactant molecules exhibit a specific orientation at interfaces within multiphase systems where they concentrate. In these cases, the interfacial tension is reduced. Surfactants form micelles at critical solution concentrations. The types of surfactants that may be found in soils following irrigation with sewage water, or land disposal of effluents and sludges, are summarized by Cirelli et al. (2009) and reproduced in Table 7.2.

When sewage water contaminated by surfactants reaches the land surface, e.g., in an irrigated field or in a disposal site, several physical interactions between the surfactant and the soil–subsurface solid phase occur (Tumeo 1997, and references therein). The surfactant induces changes in hydraulic conductivity, due to the alteration of the liquid phase properties and to a direct effect on the physical properties of the solid phase. While changes occurring in the liquid phase are reversible, surfactant-induced alteration of the solid phase becomes irreversible under specific conditions; this leads to an irreversible change in the soil–subsurface water transmission properties. Here, we present some examples from the literature that show the irreversibility of changes induced by anthropogenic surfactants on soil–subsurface water transmission properties.
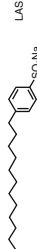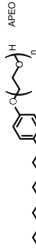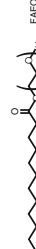
The types of surfactant and soil control surfactant-induced effects on soil–subsurface water transmission properties. Allred and Brown (1994) performed laboratory tests on hydraulic conductivity of sandy and loam soils leached with nonionic, anionic, cationic, and amphoteric surfactants. It is apparent that the ionic surfactants caused a greater HC decrease than the nonionic surfactants. Maximum HC decreases were 47% for the sandy soil and more than two orders of magnitude for the loamy soil (Fig. 7.22). Based on additional experimental results, Allred and Brown (1994) showed that in the case of ionic surfactants, in the studied soils, either solution pH or viscosity was the cause of HC decrease. In the loamy soil, anionic surfactant-induced precipitation of calcium salts is an additional factor causing irreversible HC decrease.
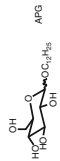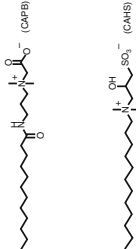
Similar analyses (Liu and Roy 1995) in a Ca-saturated subsurface soil (from Louisiana, USA) found that maximum adsorption and precipitation of the anionic surfactant sodium dodecylsulfate occurred when the surfactant concentration was similar to the critical micelle concentration. Cation exchange between soil and this sodium surfactant led to the release of $Ca^{2+}$, subsequent precipitation of calcium, and irreversible decrease in HC.

Surfactant-induced deflocculation and dispersion of clay particles into the soil–subsurface matrix are other factors leading to irreversible changes in the soil HC. The application of nonionic surfactants either before or during irrigation was found to increase the dispersion of hydrophobic sandy soils (Mustafa and Letey 1969), leading to a decreased flow rate (Miller et al. 1975).

Sodium dodecylbenzenesulfonate (SDBS) is a major constituent of synthetic detergents used in household products and industrial processes; it has been found in

Table 7.2 Selected surfactants in sludge-amended agricultural soils (after Cirelli et al. 2009)

| Surfactants | Alkyl tail | Polar head | Example |
|---|---|---|---|
| Anionic | $C_8$–$C_{20}$ straight or branched chain | –COOH |  soap |
| | $C_8$–$C_{15}$ alkylbenzene residues | –$SO_3Na$ |  LAS |
| | $C_8$–$C_{20}$ straight-chain ethoxylated | –$OSO_3Na$ |  LES |
| Cationic | $C_8$–$C_{18}$ straight chain | –$N(CH_3)_3Cl$ |  CTAC |
| | $C_8$–$C_{18}$ straight chain | –$N(CH_3)_2Cl$ |  DODAC |
| Nonionic | $C_8$–$C_9$ alkylphenol residues | –$(CH_2CH_2O)_n$–OH n = 4–22 |  APEO |
| | $C_8$–$C_{20}$ straight or branched chain | –$COO(CH_2CH_2O)_n$–OH n = 4–22 |  FAEO |

| | | |
|---|---|---|
| C$_8$–C$_{20}$ straight or branched chain | –(CH$_2$CH$_2$O)$_n$-OH n = 2–22 | (AEO) |
| C$_8$–C$_{20}$ straight or branched chain | Glucose | (APG) |
| C$_{10}$–C$_{16}$ amidopropylamine residue | –N$^+$(CH$_2$)$_2$CH$_2$COO$^-$ | (CAPB) |
| C$_8$–C$_{18}$ straight chain | –N$^+$(CH$_2$)$_2$CH$_2$CH(OH) CH(OH)CH$_2$SO$_3$$^-$ | (CAHS) |
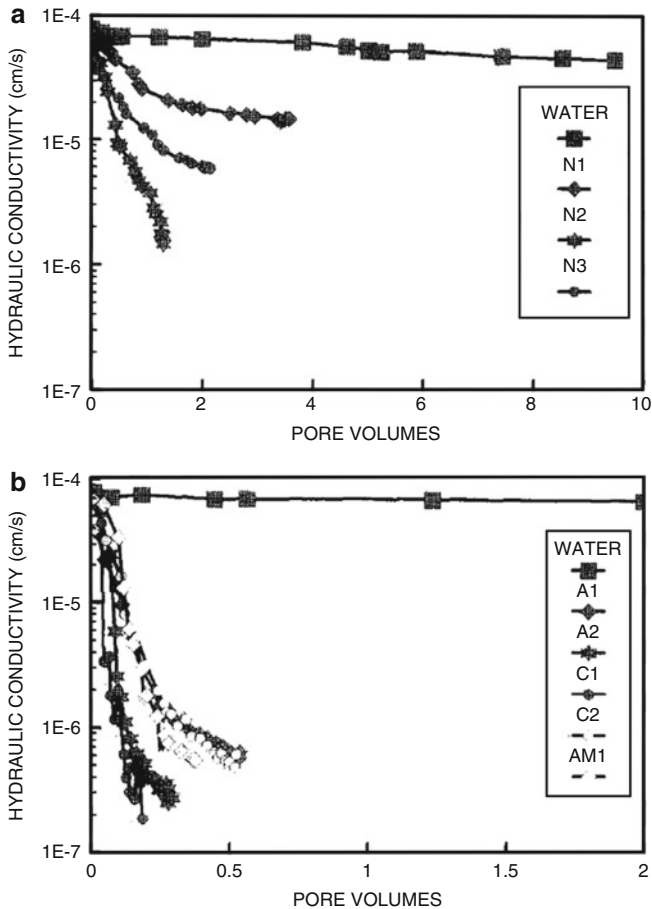
Amphoteric

**Fig. 7.22** Hydraulic conductivity versus pore volume (1 mol kg$^{-1}$ solution concentration) for (**a**) nonionic surfactants and (**b**) ionic surfactants. N$_{1-3}$ nonionic; A$_{1,2}$ anionic; C$_{1,2}$ cationic; AM1-amphoteric surfactants. Reprinted from Allred B, Brown GO (1994) Surfactant-induced reductions in soil hydraulic conductivity. Ground Water Monitoring Review 14:174–184. Copyright 1994 with permission of John Wiley and Sons

municipal sewage waters. Rao et al. (2006) used SDBS in a laboratory experiment to test the effect of anionic surfactants on dispersivity and hydraulic conductivity of sodium and calcium saturated silty loam paddy soil. Dispersion of Na- and Ca-soil with SDBS in NaCl solutions was determined by measuring the relative absorbance ($A_R$) of the suspensions. Relative absorbance is defined as $A_R = A_x/A_0$, where $A_x$ and $A_0$ are the absorbance of soil suspensions at increasing SDBS and NaCl concentrations, respectively.

The $A_R$ of the suspension in the SDBS solution increased with SDBS concentration, indicating an increase in the stability of the suspensions (Fig. 7.23). To explain this behavior, Rao et al. (2006) suggested the following mechanism: 1. Adsorption
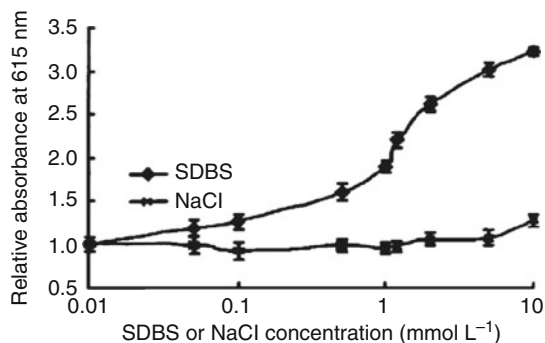
**Fig. 7.23** Effect of sodium dodecylbenzenesulfonate (SDBS) and NaCl on the stability of soils saturated with calcium at $25 \pm 1°C$ measured by relative absorbance (modified after Rao et al. 2006). Reprinted from Rao PH, He M, Yang X, Zhang YC, Sun SQ, Wang JS, Effect of an anionic surfactant on hydraulic conductivities of sodium- and calcium-saturated soils. Pedosphere 16:673–680, Copyright (2006), with permission from Elsevier
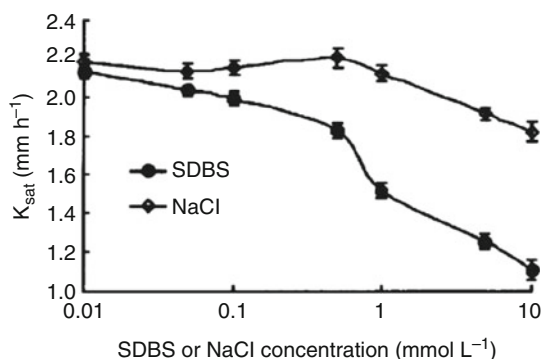


**Fig. 7.24** Variations of saturated hydraulic conductivity, $K_{sat}$, with concentration of sodium dodecylbenzenesulfonate (SDBS) and NaCl injected into soils saturated with calcium at $25 \pm 1°C$ (modified after Rao et al. 2006). Reprinted from Rao PH, He M, Yang X, Zhang YC, Sun SQ, Wang JS, Effect of an anionic surfactant on hydraulic conductivities of sodium- and calcium-saturated soils. Pedosphere 16:673–680, Copyright (2006), with permission from Elsevier

of SDBS on the clay particles, which increases the repulsive forces and causes dispersion of particles; 2. adsorbed SDBS tends to decrease interface tension, supporting particle dispersion; and 3. increase of $Na^+$ in the Ca-soil suspension, promoting the particle dispersion. Combination of these three processes results in an increase in the stability of the Ca-soil suspension. In contrast, the $A_R$ of the suspension in NaCl solution varied little below 1.0 mmol $L^{-1}$ NaCl. Above this value, the $A_R$ increased slowly.

The dispersion of clay particles in Ca-soil columns leached by SDBS and NaCl-aqueous solution led to an irreversible decrease in soil hydraulic conductivity (Fig. 7.24). The higher the SDBS or NaCl concentration in the flushing solution,

the greater the extent of the HC decrease. However, as in the dispersion experiments, the effect of SDBS was much greater than that of NaCl.

## 7.2.2  Anionic Compounds

Anionic compounds may also reach the soil surface as chemical contaminants during irrigation with wastewater, or following land disposal of municipal effluents or sludges. When organic or inorganic anions reach the soil as contaminants in wastewater, dispersion and redistribution of clay particles are favored and irreversible changes in natural water transmission properties may occur. For example, Shanmuganathan and Oades (1983) demonstrated that organic and inorganic anions increased clay dispersion in a kaolinitic soil. Three groups of anions were distinguished with respect to effects of dispersion and flocculation, and in the order of the amount of anion adsorbed by soil treated with Fe(III) polycations as follows: phosphate and fulvate > citrate, oxalate, silicate, tartrate > salicylate, catachol, aspartate, lactate, acetate. The different groups of anions caused different amounts of clay to disperse when added to samples previously flocculated by addition of 0.07% Fe (Fig. 7.25).

Moreover, the addition of anions to soil influenced aggregate stability and porosity, because phosphate, fulvate, and citrate significantly reduced the number of particles of 50–250 μm diameter and increased the <2 μm fraction, confirming the dispersion of clay. TEM images of clay fractions of 0.07% Fe-treated soils before and after addition of anions are shown in Fig. 7.26.

Clay-induced dispersion by addition of anions to soil has an irreversible effect on clay redistribution with depth, and on water transmission. Examples of irreversible effects of anions on hydraulic conductivity of clay–sand mixtures are given by Frenkel et al. (1992a, b). In laboratory column experiments, Ca-saturated kaolinite, smectite, and illite were mixed with quartz sand and leached by an aqueous solution containing Na salts of various inorganic and organic anions. Examples of hydraulic conductivity and clay dispersion as a function of the various added anions are shown in Figs. 7.27 and 7.28.

These results show that the HC of smectite clay–sand mixtures decreased following addition of various anions. Dispersed clay, however, appeared in the effluent only upon addition of citrate or hexametaphosphate. In the latter case, the HC began to increase once maximum clay concentration reached the effluent. Dispersion of smectite was one order of magnitude lower than that of kaolinite; illite exhibits an intermediate value. Frenkel et al. (1992a, b) attributed this behavior to kaolinite having the highest ratio of positively charged edge surfaces to negatively charged planar surfaces, which leads to a high adsorption capacity. In the case of smectite, HC decreases through partial blocking of pores by short-distance migration of dispersed particles.
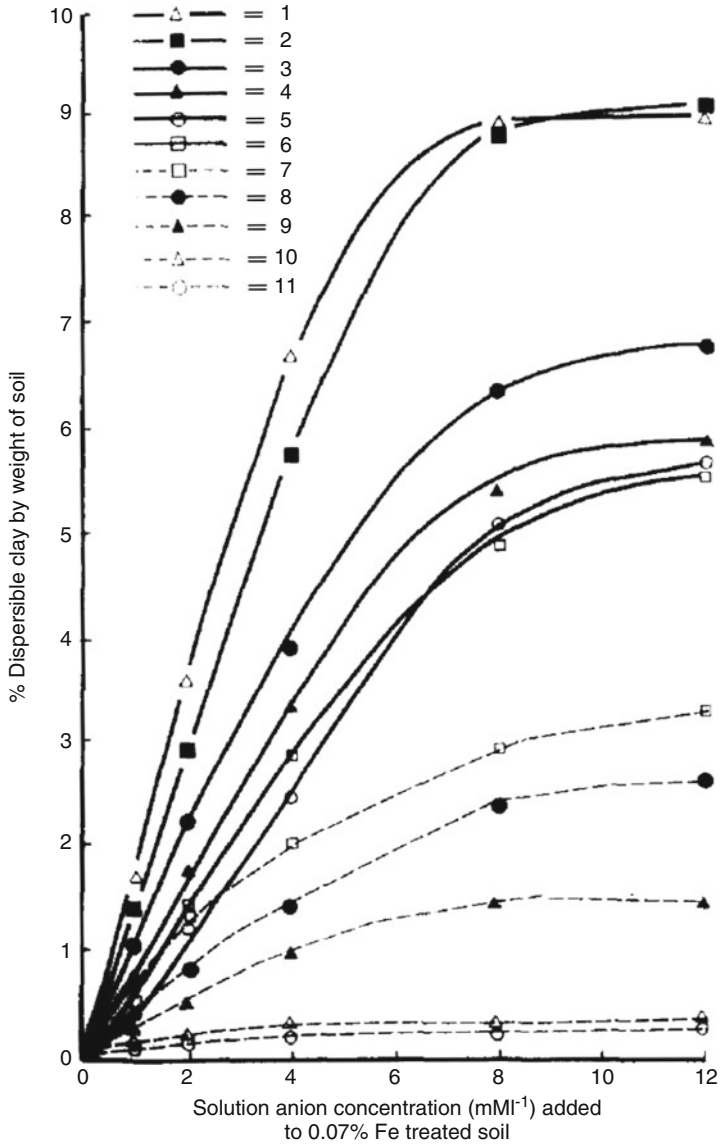
**Fig. 7.25** Changes in dispersible clay of 0.07% Fe-treated soil after addition of anions. 1 = phosphate; 2 = fulvate; 3 = citrate; 4 = oxalate; 5 = silicate; 6 = tartrate; 7 = salicylate; 8 = catechol; 9 = aspartate; 10 = lactate; 11 = acetate (after Shanmuganathan and Oades 1983). Reprinted from Shanmuganathan RT, Oades JM, Influence of anions on dispersion and physical properties of the A horizon of a red-brown earth. Geoderma 29:257–277, Copyright (1983), with permission from Elsevier
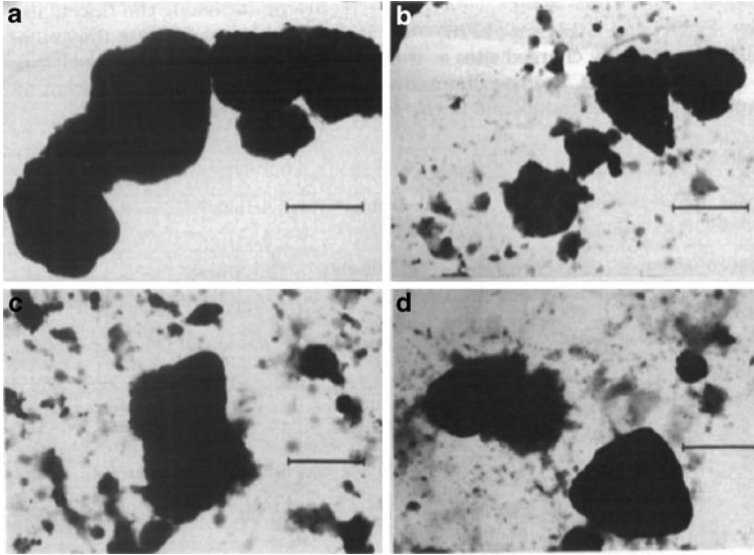
**Fig. 7.26** Transmission electron micrograph of clay fraction of 0.07% Fe-treated soils before and after addition of anions. *Horizontal bar* = 1 pm. (**a**) control (0.07% Fe); (**b**) phosphate; (**c**) fulvate; (**d**) citrate (after Shanmuganathan and Oades 1983). Reprinted from Shanmuganathan RT, Oades JM, Influence of anions on dispersion and physical properties of the A horizon of a red-brown earth. Geoderma 29:257–277, Copyright (1983), with permission from Elsevier

## 7.2.3   Sludge and Compost

Application of sludge and compost (SC) was considered, in the last half of the past century, to be a generally advantageous and environmentally sound method for increasing soil fertility and improving soil physical properties. Sludges are obtained from wastewater purification treatments; compost is mainly a mixture of solid agricultural residues, municipal residues, and sewage sludge.

Because some of the organic carbon found in SC is resistant to degradation, the organic matter content of the soil increases under repeated application; in this case, irreversible alteration of the physical properties is possible. With few exceptions, such as temporary plugging of the uppermost soil layer as a result of liquid sludge application, the organic components of sludge affect the water transmission properties, influencing the bulk soil density, aggregation, and porosity.

Many studies have shown an increase in the HC after sludge application, which is usually explained by a parallel decrease in the bulk density and an increase in the total porosity. For soils with a wide range of textures, HC in sludge-amended plots and sludge soil mixtures is usually higher than that in control plots, although a large
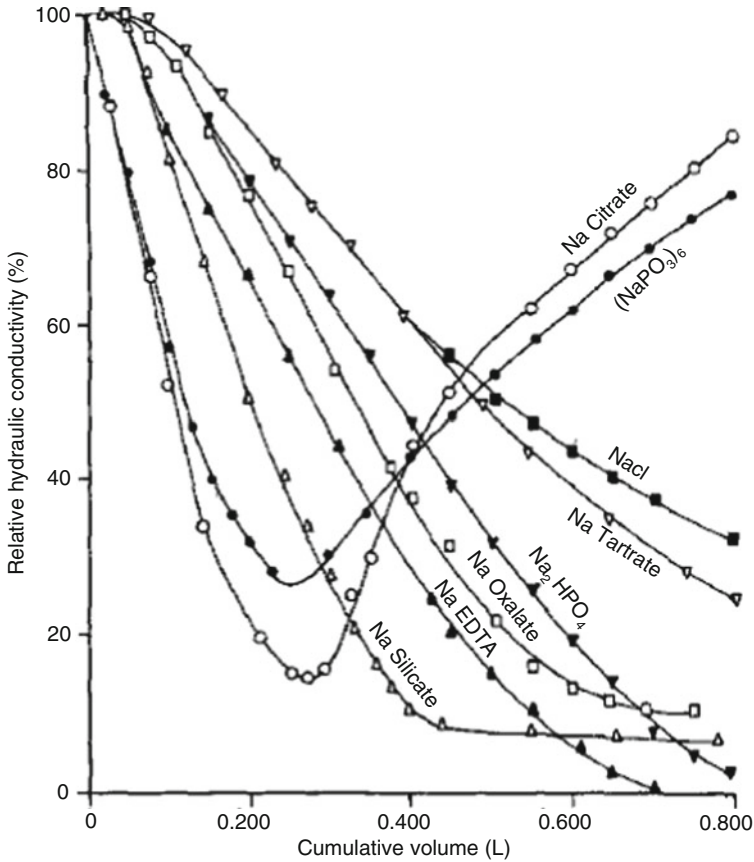
**Fig. 7.27** Relative hydraulic conductivity of Wyoming smectitie–sand mixtures (3 g 100 g$^{-1}$ clay) as a function of cumulative leaching with 1 mol m$^{-3}$ anionic solutions (after Frenkel et al. 1992a). Reprinted with permission

quantity per unit area of sludge or compost additions is necessary to induce statistically significant changes in HC (Metzger and Yaron 1987, and references therein).

Some examples related to SC effects, discussed below, include the relationship between bulk density and porosity, aggregation, and clogging.

### 7.2.3.1   Relationship Between Bulk Density and Porosity

Bulk density of soil is reduced after SC application on land surface. Several studies have reported that the bulk density of a sludge amended sandy soil is negatively correlated to the organic carbon content of the applied sludge, and to the application rate, and positively correlated to the soil porosity (Lindsay and Logan 1998;
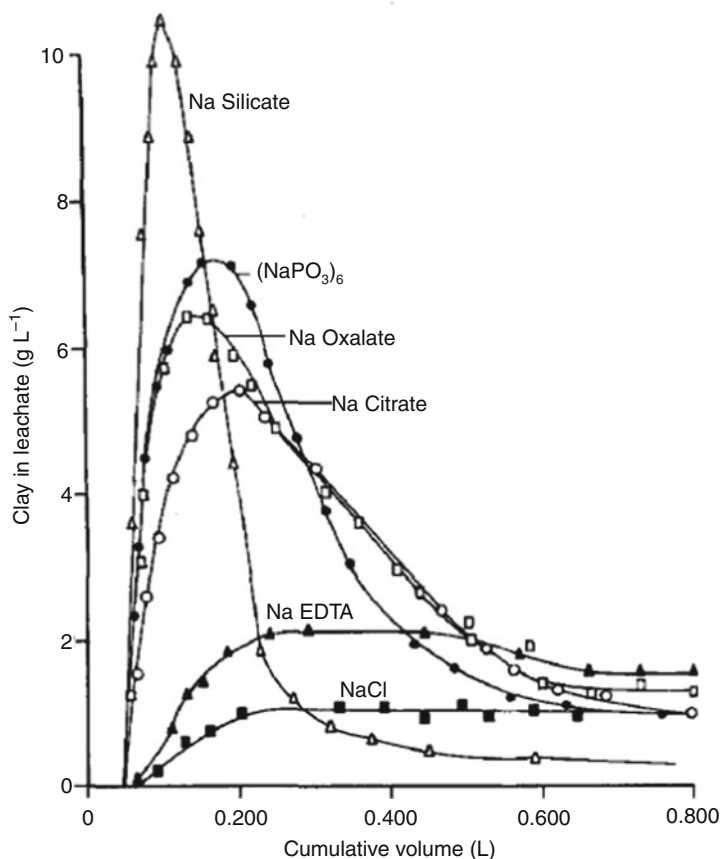
**Fig. 7.28** Clay concentration in the leachate as a function of cumulative volume of leaching solution from 3 g 100 g$^{-1}$ illite–sand mixtures leached with 1 mol m$^{-3}$ sodium silicate, hexametaphosphate, citrate, EDTA, and chloride solutions (after Frenkel et al. 1992a). Reprinted with permission

Bahremand et al. 2003). Based on analysis of 12 studies dealing with short- and long-term application of SC on bulk density, Khaleel et al. (1981) proposed an empirical relationship between the soil organic carbon content and the reduction in bulk density.

The effect of sludge application rate on the bulk density and porosity of a silt loam from Columbus, Ohio, USA, is shown in Fig. 7.29. The soil porosity increased approximately linearly ($r^2 = 0.728$; $P < 0.01$), while the bulk density decreased approximately linearly ($r^2 = 0.815$; $P < 0.01$) as a function of sludge application rate. Lindsay and Logan (1998) considered the effect of sludge on soil physical properties to depend largely on the rate of sludge decomposition and on the contribution to soil organic carbon. In the reported cases, these effects could still be seen 4 years after sludge application. This finding is in accord with the results of
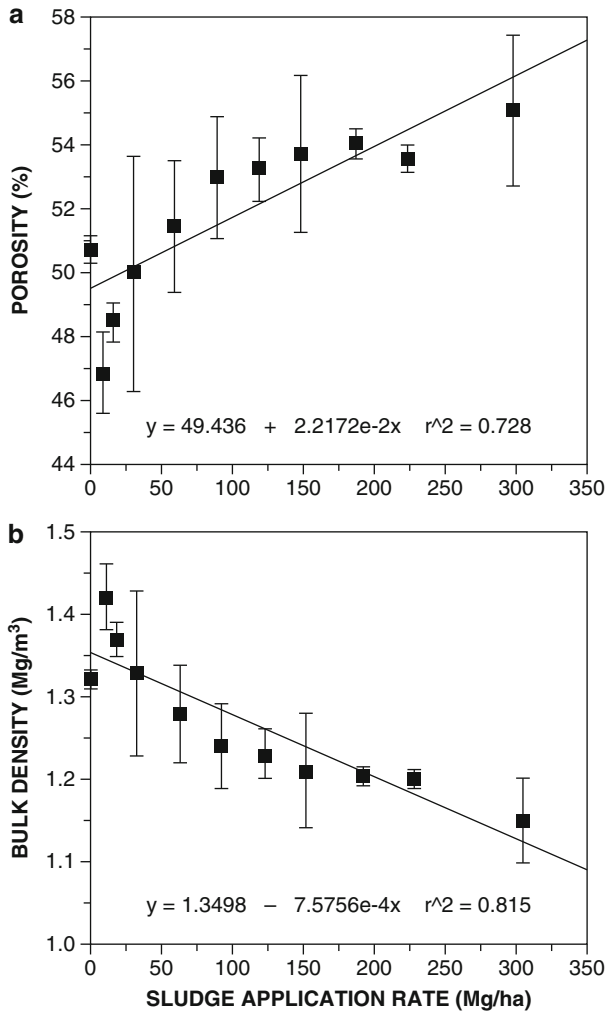
**Fig. 7.29** Effect of sludge application rate on (**a**) total porosity and (**b**) bulk density (modified after Lindsay and Logan 1998). Copyright 1998, American Society of Agronomy, Crop Science Society of America, and Soil Science Society of America. Reprinted with permission

Pagliai et al. (1981), who found that 6 months after sludge application on a sandy loam soil, the total porosity reached values ranging between 24 and 31%, compared to 17.5% for the control. Wei et al. (1985), too, showed that 6 years after application of a dewatered sludge to a clay soil, the "large pore" space increased on account of capillary pore space.

The total porosity of soils is changed also by the application of compost. Aggelides and Londra (2000) reported that application of a compost containing 17% sawdust, 21% sewage sludge, and 62% municipal wastes to loamy and clay

soils succeeded in significantly changing their total porosity. The increases – compared to the control soil – were 11.0, 27.0, and 32.8% in the loamy soil, and 5.4, 8.3, and 9.9% in the clay soil for 75, 159, and 300 m$^3$ ha$^{-1}$ compost rates, respectively. These results suggest that despite the decomposition of organic matter, sludge-induced changes in soil porosity on a lifetime scale are partially irreversible.

### 7.2.3.2   Aggregation

An aggregate is a group of primary particles that adhere more strongly to each other than to other surrounding soil particles. The stability of aggregates is a function of how the cohesive forces between particles withstand the applied disruptive forces (Kemper and Rosenau 1986). Soil aggregation status is generally controlled by the organic carbon (OC) content, which may change following application of OC-rich sludge or compost. Indeed laboratory and field studies show that sludge application to soil induces an increase in the number and size of water-stable aggregates (WSA).

Figure 7.30 illustrates the typical morphology of WSA (200–2,000 µm in diameter) in a loamy soil following sludge application. Compared to control aggregates (Fig. 7.30a), WSA obtained in sludge-amended soil (Fig. 7.30b) are characterized by a large size and a loose and porous internal structure. From the aggregation patterns observed in Fig. 7.31, for three soils amended with sludge, three distinct phases can be identified: a short 10-day period characterized by a rapid rate of WSA formation, a period of similar duration displaying a moderate decrease in WSA content, and finally a longer period characterized by a slow secondary increase in WSA content over a scale of months (Metzger et al. 1986).

Experiments performed on various soils and under different climatic conditions confirm that aggregate sizes in a sludge-amended soil decrease with time, over a scale of months (Metzger and Yaron 1987, and references therein). Moreover, long-lasting effects of sludge on the structural stability of modified aggregates are reported by Wei et al. (1985), who found aggregates in a modified silty clay loam soil, 6 years after 112 t ha$^{-1}$ of sludge was added to a field soil in a single application.

Both biological and chemical agents affect the aggregation processes that occur in soil–sludge mixtures. Scanning electron microscope observations (Metzger and Yaron 1987) of WSA, formed in a loamy soil following sludge application (Fig. 7.32), showed the presence of three types of microorganisms: bacteria (Fig. 7.32c, f), actinomycetes (Fig. 7.32d), and fungi (Fig. 7.32e), as well as of cements of organic origin (Fig. 7.32b). The interpretation of the results indicated that fungi represent the dominant contribution to the increase in WSA content following sludge application.

Metzger et al. (1986) concluded that the two main binding mechanisms responsible for aggregate formation are the cementation of primary particles by fungal polysaccharides, and the physical entanglement of primary particles in the fungal
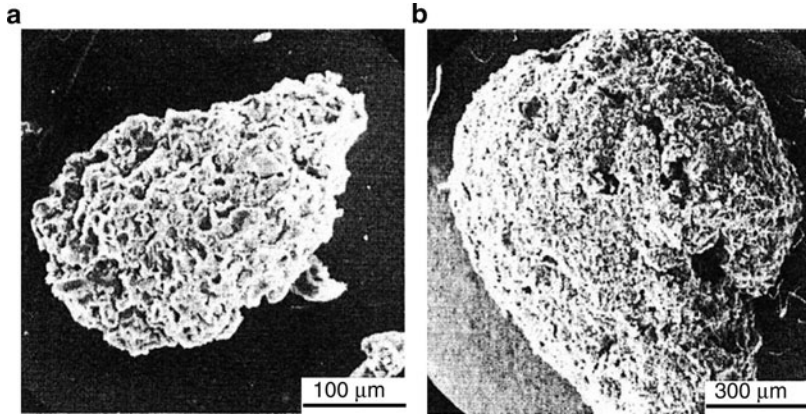
**Fig. 7.30** SEM images showing general features of water-stable aggregates isolated from (**a**) a silt loam soil and (**b**) a silt-loam sludge (5%) mixture after 16 days of incubation at 25°C (after Metzger and Yaron 1987)
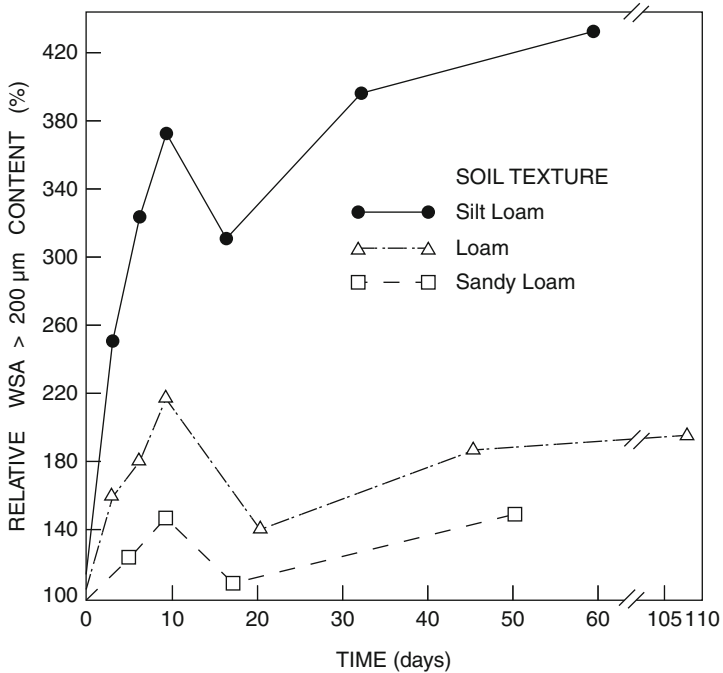


**Fig. 7.31** Dynamics of the aggregation status (expressed as the content of water-stable aggregates, WSA >200 µm) in three types of soil after addition of 5% sludge (incubation temperature 25°C) (after Metzger and Yaron 1987)
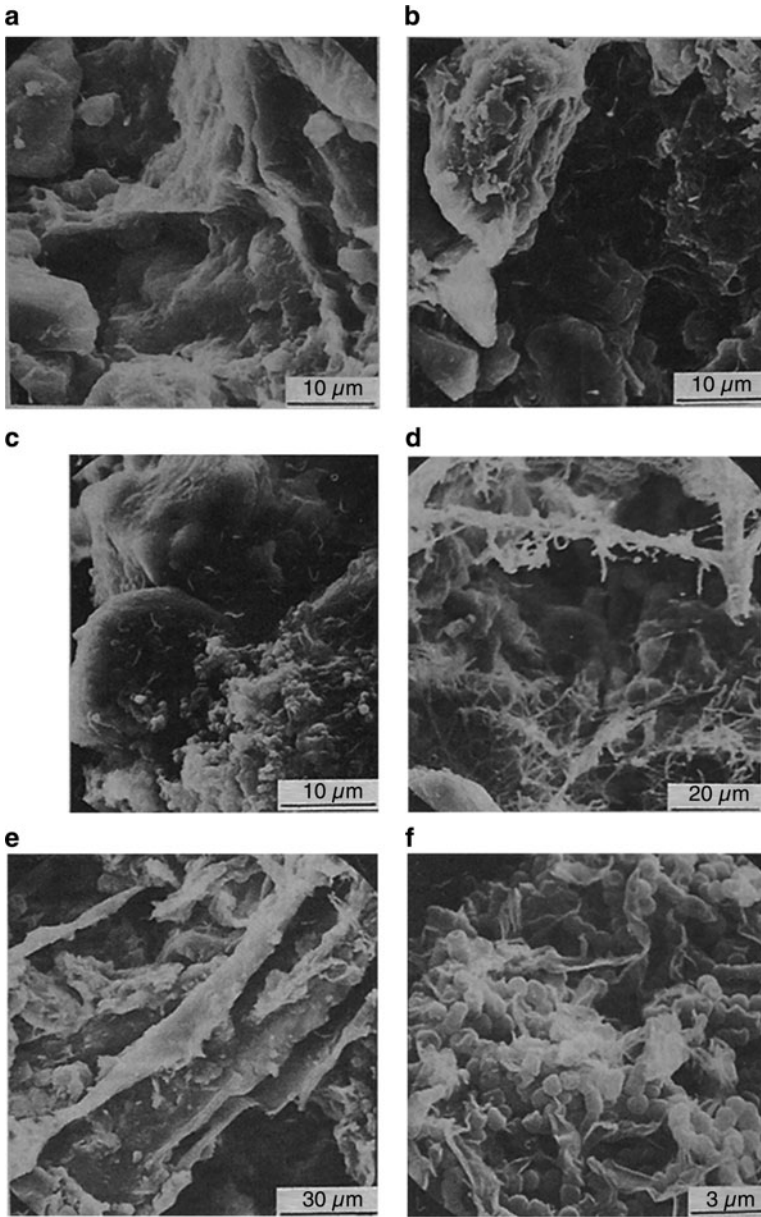
**Fig. 7.32** SEM micrographs representative of internal structure of water-stable aggregates, in (**a**) a silt loam soil (control); and showing presence of bacteria, actinomycetes, and fungi in (**b–f**) a silt-loamy sludge (5%) mixture after 16 days of incubation at 25°C (after Metzger and Yaron 1987)

**Fig. 7.33** Scleroglucan – an extracellular polysaccharide – adsorbed on kaolinite particles (after Chenu and Tessier 1995)



<div style="text-align:right">1 µm</div>
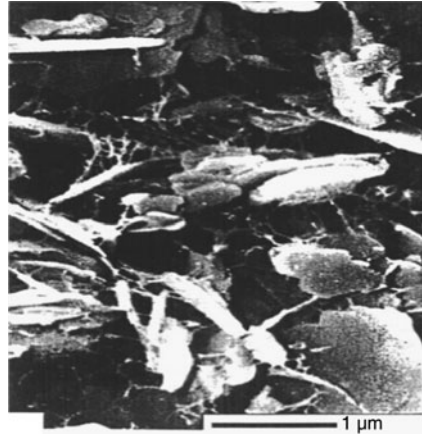
hyphae. It was also observed that polysaccharides, as a byproduct of soil microbial activity, exhibit a positive correlation to WSA stability over time (e.g., Cheshire et al. 1984). It was also found that the role of sludge water-soluble components contribute to binding of well-defined soil constituents such as kaolinite or montmorillonite (Metzger and Robert 1985).

The effect of microbial colonies growing on soil solid surfaces and forming polymer bridges that bind mineral particles was confirmed in a series of studies (Chenu and Guerif 1991; Chenu 1993; Chenu and Tessier 1995). A clear illustration of clay with an extracellular polysaccharide coating is shown in Fig. 7.33, where scleroglucan is adsorbed on kaolinite particles. It can be observed that the presence of the extracellular polysaccharide coating creates a sustainable open structure among clay particles, favoring water transport in soils. More information on physical processes affecting microbial habitats in porous media appears in the review of Or et al. (2007).

The organic hydrophobic fraction of sludge has also been proposed as being responsible for aggregate stabilization. Based on an experiment on paper sludge amendments applied on a clay loam and silty clay loam, Hafida et al. (2007) considered that pore occlusion by biologically mediated formation of neutral and uronic sugars and lipids contributes to aggregate stability. As a consequence, it can be concluded that addition of organic amendments to soils causes increases in pore surface roughness and pore occlusion, which contribute more to the formation of stable aggregates than to growth of surface wetting angles. In agricultural practice, sludges are repeatedly applied to the land surface, and organic residues continue to accumulate, providing a quasi-continuous source of energy for microbial populations. As a result, we can expect that sludge-induced changes in the microstructure of WSA are an irreversible process on the scale of human lifetimes.

### 7.2.3.3 Clogging

Clogging of pores by suspended particles, following disposal of wastewater or sludges on the land surface and their vertical transport during rainfall or irrigation, is an additional process that causes changes in the microstructure of the soil–subsurface domain and on its water transmission properties. The dominant mechanism of clogging depends on the physical and chemical properties of the soil–subsurface domain, the composition of the wastewater or sludge, the method of application on land surface, and the time scale involved. In the short term, physical clogging of pores by suspended solids in the upper part of the soil layer forms a surface mat; this is a major feature that reduces the hydraulic conductivity. The process of filtration at depth leads to a reduction in soil hydraulic conductivity, but at a slower rate than that of clogging of surface pores. The stability of clogging, and thus its irreversible impact, should also be considered in terms of microbial habitats and activity during drying–wetting cycles in the unsaturated zone.

Soil column laboratory experiments by Vinten et al. (1983) showed the relative amounts of deposition of suspended solids in the top 50 mm, following leaching of three different soils with about 100 cm of wastewater (characterized by 98 mg $L^{-1}$ suspended solids) (Fig. 7.34). In silt loam soil, the water was filtered before use, giving a concentration of 38 mg $L^{-1}$. The soil type strongly influences the rate of clogging. In the sandy soil, the hydraulic conductivity decreases much slower than that of silt loam, despite the filtering of the effluent before application. SEM photographs of the top sections of the soils are presented in Fig. 7.35. A coarse matrix of deposited solids occurred at the surface of the sandy loam soil (Fig. 7.35a). In the silt loam, the uniform surface exhibited much smaller pores than the sandy loam (Fig. 7.35b); Fig. 7.35c shows a longitudinal view of silt loam, with a well-defined layer of deposited solids of 60-μm thickness overlying the soil matrix.

Amitay-Rosen et al. (2005) used MRI as a noninvasive measurement technique to examine the kinetics of suspended particle deposition in a porous medium, showing significant clogging of pores (Fig. 7.36). Both the mechanism of porous medium clogging and its effect on water transmission properties during clogging were discussed in depth.

Onsite wastewater systems are used widely around the world as an alternative to centralized treatment facilities. Septic tanks connected to subsurface trenches, used in onsite water systems, form point sources for accumulation of organic matter components in the soil–subsurface domain. These components clog pores and cause a decrease in water transmission properties. Some studies have revealed biochemical processes under onsite wastewater disposal systems, with associated clogging and decrease of infiltration.

McKinley and Siegrist (2010) analyzed the clogging layer (1.5 cm thickness) in an onsite wastewater disposal system in a sandy loam soil (Golden, Colorado), finding that most organic materials accumulated in the upper 0.7-cm segment. The concentrations of total organic carbon (TOC), humic acid (HA), and fulvic acid
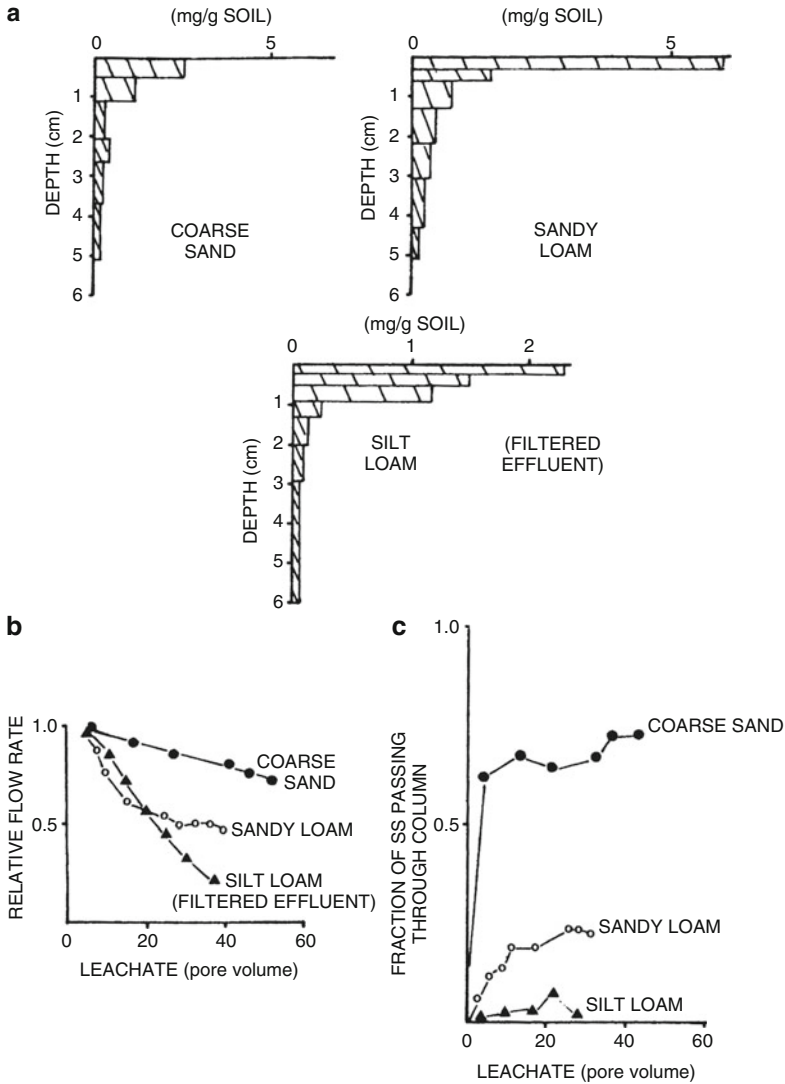
**Fig. 7.34** (**a**) Deposited solids distribution in three soils leached with wastewater, showing (**b**) the effect on soil hydraulic conductivity, and (**c**) transport of suspended solids through the soils (after Vinten et al. 1983). Reprinted with permission from Vinten AJA, Yaron B, Nye PH (1983) Vertical transport of pesticides into soil when adsorbed on suspended particles. J Agri Food Chem 31:662–664. Copyright 1983 American Chemical Society

(FA), as well as of polysaccharides, found in the clogging layer are shown in Fig. 7.37. In this particular site, the less humified carbonaceous materials (polysaccharide and fulvic acids) were in low concentration compared to the more humified carbonaceous materials; the latter are less degradable because they contain a more

**Fig. 7.35** Scanning electron micrographs of soil after leaching with effluent: (**a**) surface of sandy loam after 1,000 mm of unfiltered effluent, (**b**) surface of silt loam soil after 700 mm of filtered effluent, (**c**) vertical section of sample in (**b**) (after Yaron et al. 1984)
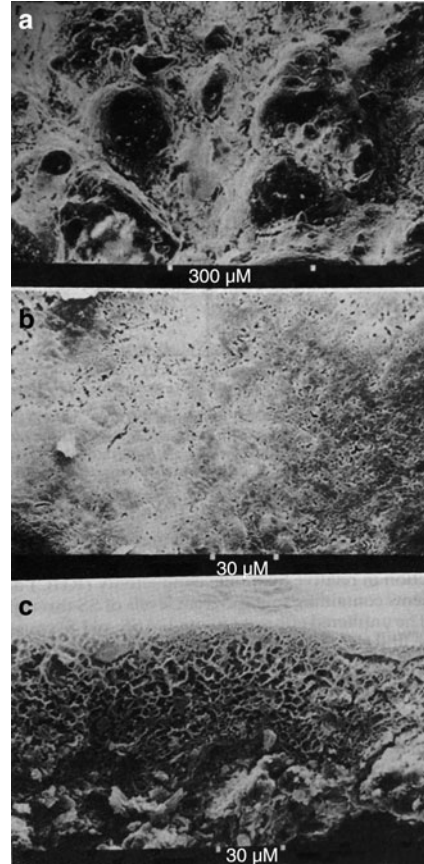


complex molecular structure. As a result, the less degradable materials can accumulate in soil pores and become a key agent responsible for long-term, irreversible clogging.

The microstructure of clogged soils in soil wastewater treatments under prolonged exposure was detected using fluorescence microscopy (Jiang and Matsumoto 1995). Detailed information on soil clogging by entrapment of suspended particles, microbial cells, and their metabolized products is shown in Fig. 7.38. For the investigated experimental conditions, Jiang and Matsumoto (1995) identified (1) physical clogging which occurs horizontally in the surface zone, due to trapping in pores of suspended and colloidal materials, and (2) biological clogging that occurs vertically along the soil profile, resulting from accumulation of microbial products in soil pores under anaerobic conditions. Physical and biological clogging are interrelated, and enhance each other. Under anaerobic conditions, decomposition of metabolic products is low, even tending to be negligible, when they are adsorbed on suspend solids and colloidal materials. This suggests the irreversibility of the process.
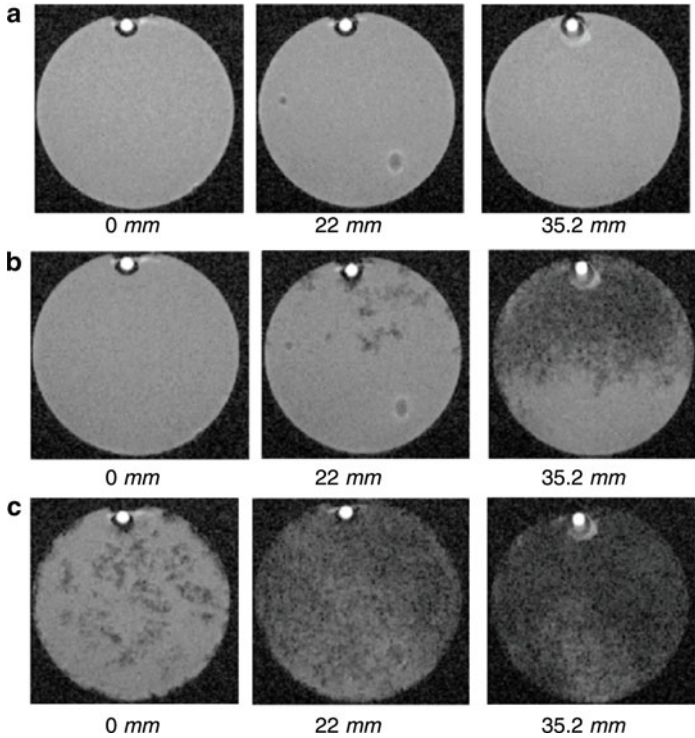
**Fig. 7.36** Selected axial images of the porous medium at several distances from the *inlet*, for an experiment with 12-μm particles: (**a**) 0, (**b**) 120, (**c**) 180 min. The column was oriented horizontally, with the reference tube (*white spot*) positioned at the top (after Amitay-Rosen et al. 2005). Reprinted with permission from Amitay-Rosen T, Cortis A, Berkowitz B (2005) Magnetic resonance imaging and quantitative analysis of particle deposition in porous media. Environ Sci Technol 39:7208–7216. Copyright 2005 American Chemical Society

## 7.2.4   *Hydrophobic Organics and Soil Water Repellency*

Effluents and wastes disposed on the land surface may affect the natural repellency properties of the soil and subsurface matrix. Soil-subsurface water repellency is defined as a change in the rate of wetting, retention, and transport of water in the soil–subsurface domain, caused by the presence of hydrophobic coatings on solid phase particles. Solid phase repellency should be considered as a specific property of a particular soil–subsurface system, with a negative aspect reflected in water transmission properties. The main impacts of soil–subsurface water repellency are reduced infiltration capacity, increased overland runoff, creation of preferential water flow, and general formation of a variably distributed pattern of water.

In a repellent soil, the contact angle between a drop of water and the soil solid phase is $>90°$; in "common" soils, the contact angle can be less than $30°$. The level
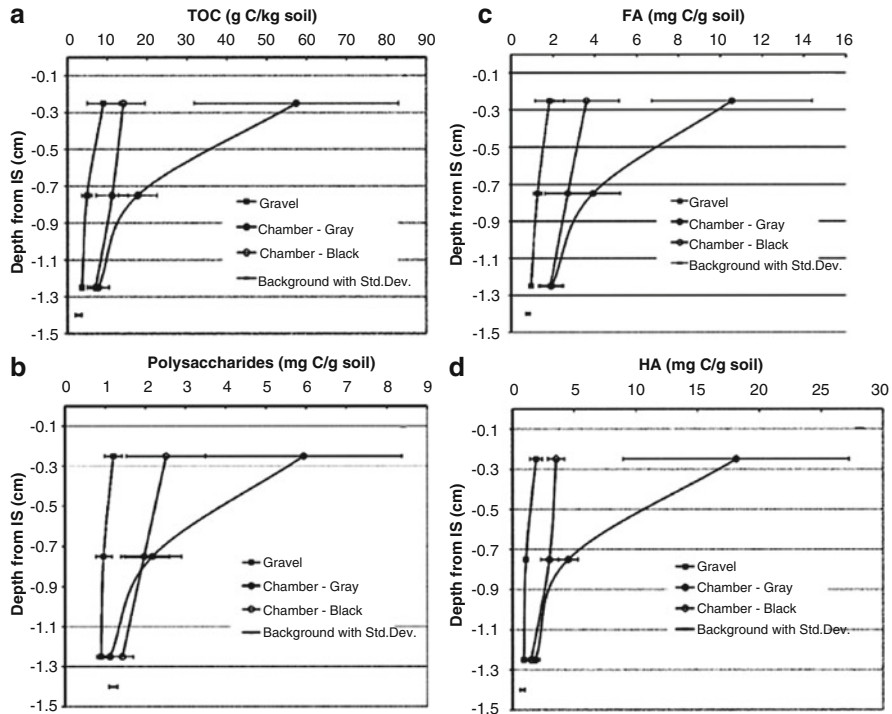
**Fig. 7.37** Effect of sewage effluent organic matter on infiltration in a sandy loam soil. (**a**) Total organic carbon (TOC) versus penetration depth, (**b**) polysaccharides versus penetration depth, (**c**) fulvic acid (FA) versus penetration depth, and (**d**) humic acid (HA) versus penetration depth (modified after McKinley and Siegrist 2010). Copyright 2010, Soil Science Society of America. Reprinted with permission

of repellency depends on the proportion of soil–subsurface particles with a hydrophobic surface coating, and on the surface area of the solid phase (DeBano 2000; Hallett 2007, and references therein). The relationship between soil–subsurface repellency and the water–solid phase contact angle is given in Fig. 7.39.

Soil moisture content is a key parameter affecting water repellency. Dry soils exhibit the highest level of repellency, whereas above a critical moisture content, soils appear not to be water repellent (Dekker and Ritsema 1994). Based on a broad survey on soil repellency properties of major soil and land-use types, in a humid temperate climate, Doerr et al. (2006) concluded that water repellency persistence generally decreased with depth (Fig. 7.40); soil repellency was evaluated using the water drop penetration time (WDPT) test (Doerr 1998).

The hydrophobic coating of repellent soil–subsurface materials may originate, for example, from root exudates, specific fungal species, leaf waxes, and organic matter decomposition products, as well as from hydrophobic contaminants reaching the land surface. It has been noted that organic matter components such as aliphatic hydrocarbons and amphiphilic substances may induce soil water repellency by
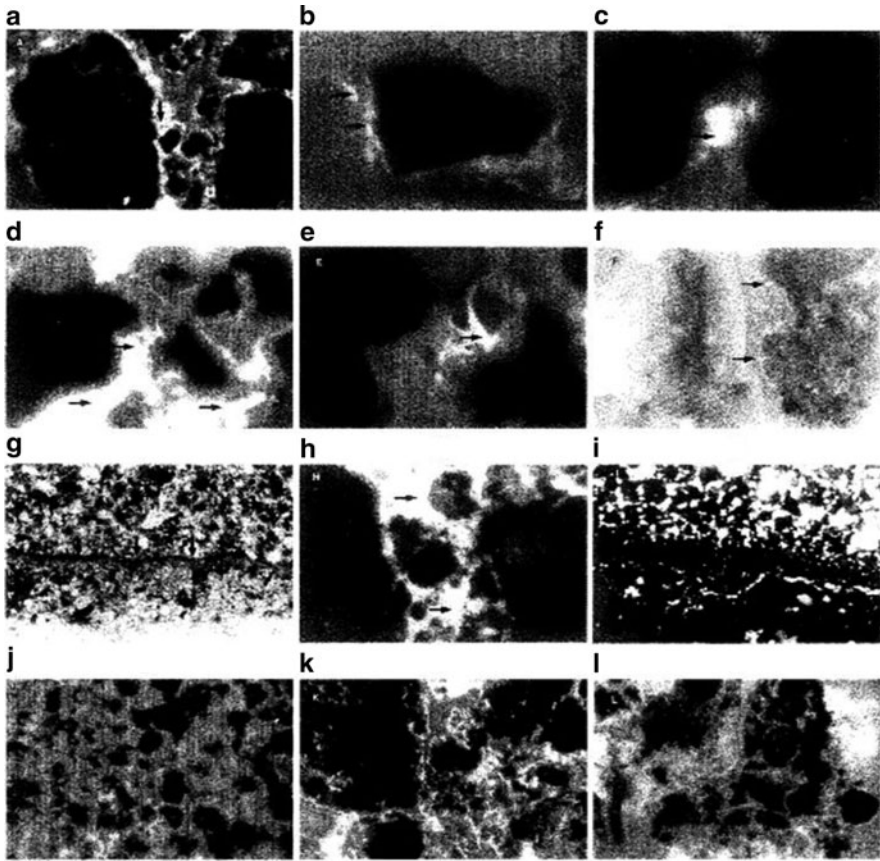
**Fig. 7.38** Microstructure of clogged soil under anaerobic conditions. (**a**) Andosol after submergence for 4 months. Soil pores were filled with fine particles, suspended solid materials, bacteria cells, and bacterial synthesized products (frame length 750 μm). (**b**) Arenosol after submergence for 4 months. A bridge structure. Organic materials (*arrows*) clogged only a narrow portion between two sand particles (frame length 750 μm). (**c**) Andosol after submergence for 2 months. *Arrow* indicates the initial state of clogging in the portion connecting two grains. (**d** and **e**) Andosol after submergence for 4 months. Soil pores were fully sealed by polysaccharides. (**f**) Andosol after submergence for 4 months. Bacterial cells (*arrows*) in soil pores. (**g**) Fluvisol after submergence for 4 months. Compact grain structure. Dark girdle (*arrows*) consists of the layer accumulated materials. (**h**) Andosol after submergence for 4 months. Soil pores were sealed by suspended solid material, fine particles, and polysaccharides. (**i**) Andosol after submergence for 4 months. Structure of layer of accumulated materials. (**j**) Andosol after submergence for 4 months. Structure of layer of accumulated materials. Soil pores were completely filled with organic materials. Aggregates were destroyed to form fine particles. (**k**) Andosol after submergence for 4 months. An aggregate (*left*) and a destroyed aggregate (*right*). (**l**) As in (**k**), destroyed aggregate (after Jiang and Matsumoto 1995). Reprinted with permission

hydrophobic coating (e.g., Roy and McGill 2000). Specific compounds responsible for soil water repellency of sandy soils from the Netherlands and United Kingdom were determined by Mainwaring et al. (2004). They found a great abundance of
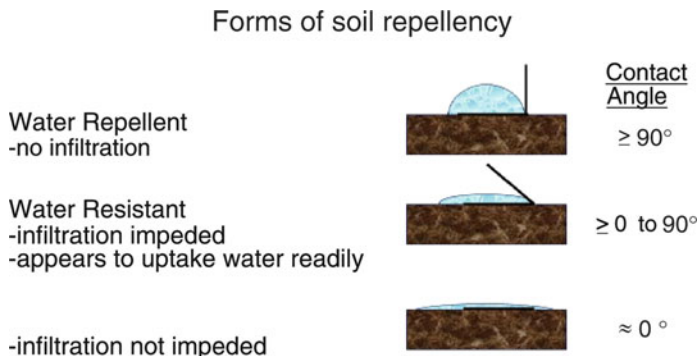
**Fig. 7.39** Forms of water repellency in soil, based on the contact angle between water and soil (after Hallett 2007)
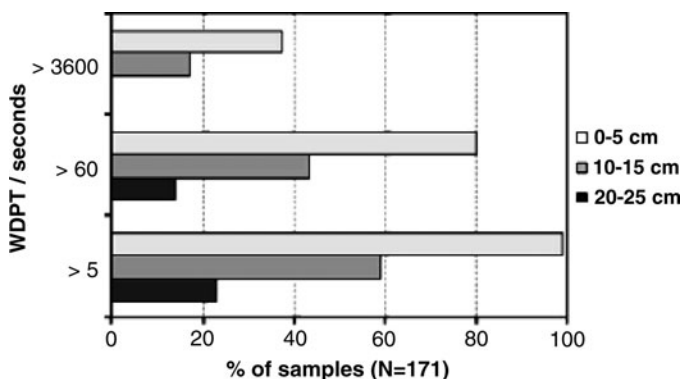


**Fig. 7.40** Frequency distribution of water drop penetration time (WDPT) of air-dried soil samples at depths of 0–5, 10–15, and 20–25 cm (after Doerr et al. 2006). Water repellency is related directly to values of WDPT. Reprinted from Doerr S, Shakesby RA, Dekker LW, Ritsema CJ (2006) Occurrence, prediction and hydrological effects of water repellency amongst major soil and land-use types in a humid temperate climate. Eur J Soil Sci 57:741–754. Copyright 2006 with permission of John Wiley and Sons

high molecular mass polar compounds in the water repellent samples. In general, fatty acids ($C_{16}$–$C_{24}$), amides ($C_{14}$–$C_{24}$), aldehydes/ketones ($C_{23}$–$C_{31}$), alkanes ($C_{25}$–$C_{33}$), and complex ring-containing structures were detected in all samples.

Treated sewage effluents reaching the land surface in the form of irrigation water, or discharged from disposal sites containing organic matter with a hydrophobic character, may under specific conditions cause soil water repellency. Such behavior was reported to occur in a commercial citrus growth from the Coastal Plain of Israel, under irrigation with treated sewage effluents (Wallach et al. 2005; Wallach and Graber 2007). The study comprised two irrigation–rain cycles, wherein the annual amount of contaminated water, ~700 mm, was applied in the dry season, followed in the rainy season by leaching with ~500 mm rain (fresh)
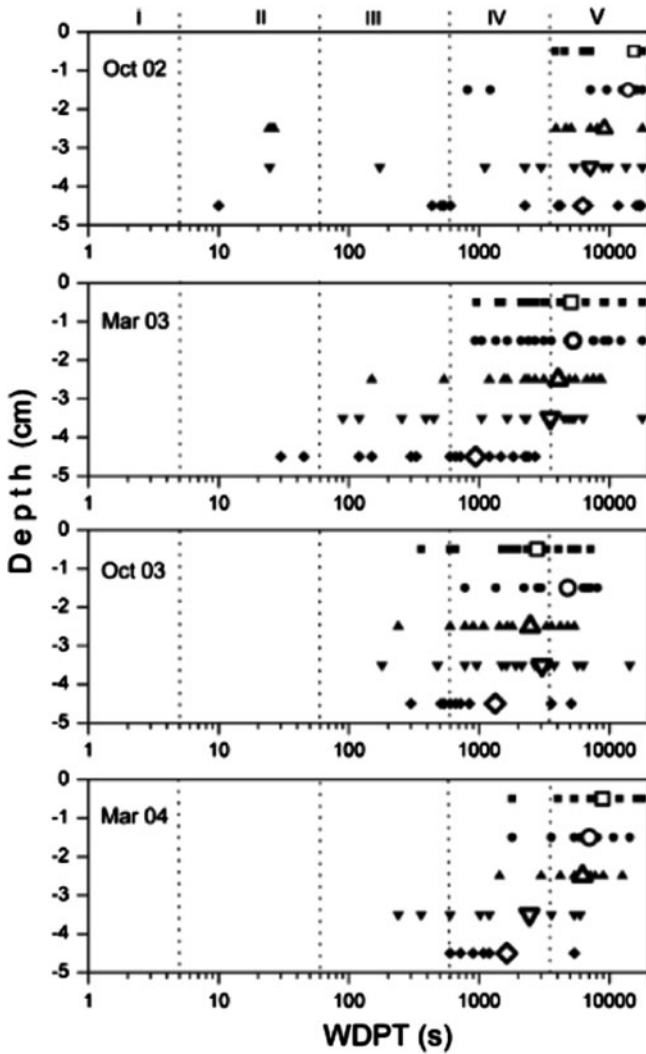
**Fig. 7.41** Water drop penetration time in different seasons from orchard irrigated for more than 20 years by sewage effluents. The abscissa represents water drop penetration time (WDPT) in log scale, and the ordinate represents the average depth of each 1-cm slice below ground surface. Individual results are denoted by small solid markers, while the average WDPT of the layer is denoted by a large, open similar marker. The *squares* represent 0–1 cm, *circles* 1–2 cm, *triangles* 2–3 cm, *inverted triangles* 3–4 cm, and *diamonds* 4–5 cm. The vertical *dotted lines* indicate the boundaries between the different repellency classes (after Wallach et al. 2005). Copyright 2005, American Society of Agronomy, Crop Science Society of America, and Soil Science Society of America. Reprinted with permission

water. The soil repellency values, determined by WDPT, were grouped into five classes, from non-repellent (1) to extremely water repellent (5). The WDPT results for the 0–5-cm soil surface layer transects, in a field irrigated with treated sewage

effluents in October 2002 and March 2004, are shown in Fig. 7.41. A degree of water repellency can be observed, occurring and persisting during the 2 years of sampling in the entire surface layer. Horizontal and vertical variability of WDPT values is also apparent. However, notwithstanding the considerable variability in individual results, the average WDPT in each of five sampled layers shows a clearly decreasing trend with depth.

The persistence of water repellency in soil induced by sewage effluents, indicated by large WPDT times, can be seen in Fig. 7.42. Here, WDPT results show persistence of water repellent soil during 2 years of alternation of drying (summer) and wetting (winter) cycles.

The extent of soil repellency properties in soils under cover of citrus orchards should also take into account the possible contribution of citrus-derived organic residues in inducing soil water repellency (Jamison 1947). The results presented in Figs. 7.41 and 7.42 should thus be reconsidered, recognizing the contribution of the citrus-derived organic matter to changes in natural soil repellency.

Arye et al. (2011) reported only moderate changes in soil repellency as a result of wastewater disposal in a recharge basin site. The site is located in an area of rolling sand dunes, underlain by a calcareous sandstone aquifer. WDPT tests clearly indicated that hydrophobicity prevailed in the upper soil of the disposal site. The WDPT values decreased from 232 s and 87 s in the upper layers, to 18 s and 12 s at depths of 4.5 cm and 100 cm, respectively.

The hydrophobicity effect of soils irrigated with treated wastewater, in commercial fields situated in the western Galilee of Israel, was studied by Tarchitzky et al. (2007). A representative picture of water repellency in irrigated soil is presented in Fig 7.43, where two flow cells filled with red brown soil were subjected to drip irrigation with fresh and treated wastewater. During the fourth irrigation interval, a lenticular structure characteristic of hydrophobic conditions was observed on the soil surface below the dripper, in contrast to the onion-like wet profile under fresh water irrigation. Tarchitzky et al. (2007) considered that hydrophobicity in soils irrigated with treated wastewater was found to be related to changes in organic matter content and characteristics of the upper soil profile.

## 7.2.5  Long-Term Irrigation Effects

Long-term irrigation with effluents includes alternate disposal on soil of waste and rain (fresh) water. In such a situation, the major pollutants (e.g., salts and organics) from wastewater disposed in the irrigated root zone of the soil may be retained or leached into the subsurface zone by rain (fresh) water. The composition of soil irrigated with wastewater is generally characterized by a higher load of DOM, suspended solids, higher SAR, and higher salinity compared to soil irrigated with fresh water (Feigin et al. 1991; Hamilton et al. 2007). It is important to determine if these changes in soil properties are irreversible over time. To the best of our knowledge, however, very few experimental investigations have studied the long-
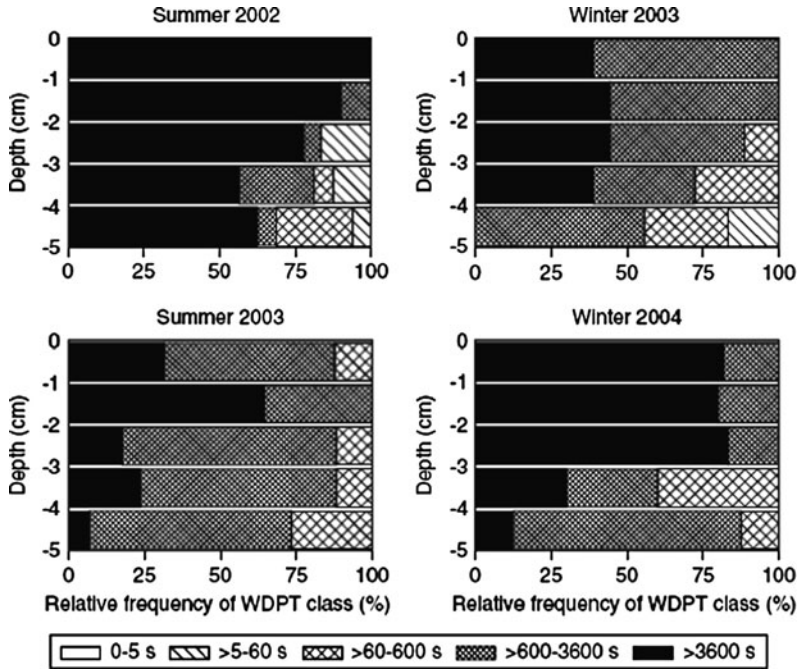
**Fig. 7.42** Relative frequency of water drop penetration time (WDPT) class in transects between adjacent trees, obtained in different seasons from an orchard irrigated for more than 20 years by treated sewage effluent. The number of samples in each transect ranges from 12 to 20. The WDPT test was performed on undisturbed samples obtained from the orchard and maintained at the initial field moisture content. Reprinted from Wallach R, Graber ER (2007) Infiltration into effluent irrigation-induced repellent soils and the dependence of repellency on ambient relative humidity. Hydrol Proc 21:2346–2355. Copyright 2007 with permission of John Wiley and Sons
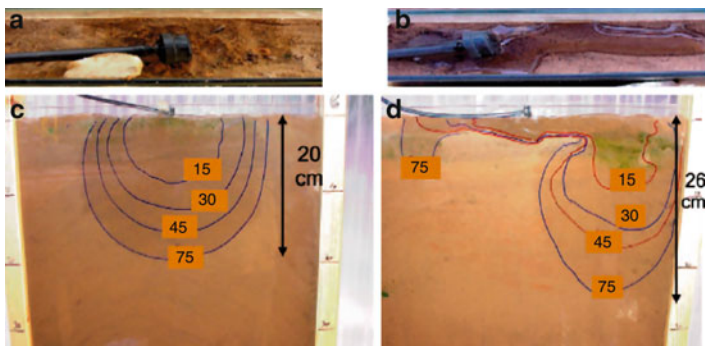


**Fig. 7.43** Flow cells filled with red–brown soil and dripper-irrigated: (**a**) fresh water (FW)-soil surface; (**b**) treated wastewater-soil surface; (**c**) fresh water (FW)-soil profile. The *lines* indicate the wetting front's position at the time indicated by the numbers near the borders; (**d**) treated wastewater-soil profile. Reprinted from Tarchitzky J, Lerner O, Shani U, Arye G, Loewengart-Aycicegi A, Brener A, Chen Y (2007) Water distribution pattern in treated wastewater irrigated soils: hydrophobicity effect. Euro J Soil Sci 58:573–588. Copyright 2007 with permission of John Wiley and Sons

term effect of wastewater irrigation; Assouline and Narkis (2011) provide one analysis of the effect of long-term irrigation with treated wastewater on the hydraulic properties of a clayey soil.

Assouline and Narkis (2011) compared the water transmission properties of soils under an avocado plantation (Western Galilee, Israel) irrigated over 15 years with treated wastewater (WW) and fresh water (FW). The avocado fields were irrigated with an annual seasonal amount of 650 mm WW or FR; the yearly amount of rain water during the winter season was around 550–600 mm. The soils were analyzed up to a depth of 60 cm. The clay (montmorillonite) fraction of the WW and FW irrigated soils was about 60%. WW-irrigated soils exhibit higher ESP and higher DOM than the FW-irrigated soils. Moreover, it was found that after 15 years of irrigation, the saturated hydraulic conductivity, sorptivity, and infiltration rate are consistently lower in WW-irrigated soil than in FW-irrigated soil. Water retention and soil hydraulic conductivity function were altered by the long-term use of WW due to ESP, contact angle, and pore size distribution changes. These data suggest that changes in soil transmission properties induced by long-term WW irrigation are irreversible even under cycling of WW irrigation and FW (rain water) infiltration.

## 7.3 Agrochemical Effects

Agrochemicals applied periodically to the land surface, such as fertilizers, plant protection chemicals, and reclamation amendments, may be retained irreversibly within the soil–subsurface solid phase. For example, nitrogen and ammonia containing fertilizers can induce soil acidity. Long-term application of phosphorus from fertilizers results in increased P concentrations along the soil profile. Micronutrients (trace elements) are affected by the soil pH, and as a consequence, by the long-term addition of N and P compounds (Schwab et al. 1990, and references therein). Alkaline and acid properties of the soil–subsurface domain may be changed also by chemical amendments such as gypsum and lime. These amendments also affect the fate of other agrochemicals fate; together, these compounds lead, directly or indirectly, to changes in soil–subsurface physical properties. A number of examples are discussed below to demonstrate these phenomena.

### 7.3.1 Major Elements

*Nitrogen* forms detected in soils include $NO_3^-$, $NO_2^-$, exchangeable and mineral-fixed $NH_4^+$, and nitrous oxide ($N_2O$). Mineral-fixed $NH_4^+$ content is a function of soil type and environmental conditions, constituting from 10 to 50% of the total N. When large amounts of $NH_4^+$ are applied, it can, theoretically, become a dominant

exchangeable cation and like $Na^+$, it may stimulate dispersion of soil colloids. However, in most situations, $NH_4^+$ is rapidly nitrified into $NO_3^-$, and thus favors soil colloid dispersion only under unusual conditions of low pH and low moisture content (Haynes 1984).

In agricultural management practices of decades ago, when this process was ignored, $NH_4^+$-induced dispersion of soil colloids caused crust formation and reduction in infiltration rate. For example, Pilsbury (1947) reported a significant decrease in the soil infiltration capacity of an irrigated Californian soil after application of $(NH_4)_2SO_4$. This resulted in a pronounced decrease in soil pH, a drastic reduction in nitrification, and a large accumulation of $NH_4$ in the soil. A decreased nitrification process under low temperature conditions caused soil colloid dispersion, crust formation, and erosion following broad application of $NH_4NO_3$ on soil from Nebraska (Fox et al. 1952). Soil dispersion and crusting after continual application of $(NH_4)_2SO_4$ on an irrigated soil were also reported by Aldrich et al. (1945). They concluded that under irrigation, dispersed soil colloids were transported at depth, clogging the subsurface pores and irreversibly changing the infiltration rate of the soil. Moreover, soil dispersion and crust formation following $NH_4$ accumulation can stimulate soil erosion, which also is an irreversible process.

*Phosphorus* forms include organic and inorganic fractions, consisting of compounds characterized by different solubility and availability. Ca-phosphates, which are predominant stable compounds in soils, are characterized by various solubilities as follows: $H_2PO_4 > H_2PO_4^{2-} > PO_4^{3-}$. Stable phosphate compounds such as tricalcium phosphate and apatite are favored by high pH, while Al- and Fe-phosphate are formed at low pH. In a field experiment testing phosphate application on a red–yellow podzolic soil from North Carolina, Lutz et al. (1966) observed that P-treated plots were moist, loose, and easy to plough, or had a lower bulk density and a higher moisture content compared to untreated control plots. Later studies by this group (Lutz and Pinto 1965; Lutz et al. 1966) on the effect of phosphorus on soil water retention and soil hardness provide more specific information on this phenomenon.

The effect of phosphorus on soil hardness was determined in laboratory experiments by measuring the modulus of rupture (Lutz and Pinto 1965). The effects of phosphoric acid, $H_3PO_4$, and monocalcium phosphate, $Ca(H_3PO_4)_2$, on

**Table 7.3** Properties of soil used in the experiments of Lutz and Pinto (1965). Copyright 1965, Soil Science Society of America. Reprinted with permission

| Soil | Mineral species | Amounts (relative) | % Free iron |
|---|---|---|---|
| Georgeville | Kaolin | High | 4.93 |
| | 2:1–2:2 | Medium | |
| | Gibbsite | Low | |
| | Goethite | Low | |
| White Store | Montmorillonite | High | 2.19 |
| | Illite (clay mica) | Medium to low | |
| | Kaolin | Medium to low | |
| Iredell | Montmorillonite | High | 3.72 |
| | Kaolin | Medium | |

**a**



**b**
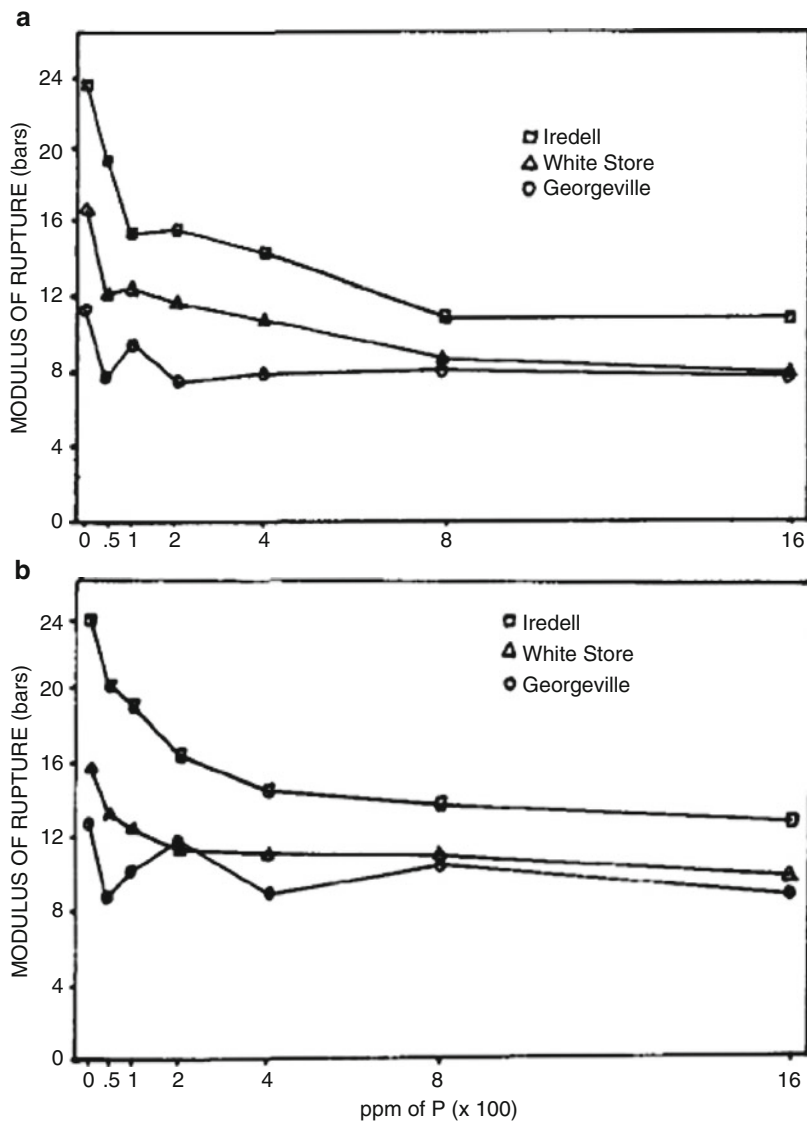


**Fig. 7.44** Effect of P on the modulus of rupture of three soils using (**a**) $H_3PO_4$ and (**b**) $Ca(H_2PO_4)_2$ as sources of P (modified after Lutz and Pinto 1965). Copyright 1965, Soil Science Society of America. Reprinted with permission

the modulus of rupture of three soils with different mixed mineralogy (Table 7.3) are shown in Fig. 7.44. For all of the studied soils, the modulus of rupture decreased with increasing amounts of P; phosphoric acid had a greater effect than

**Table 7.4** Phosphorus associated with Fe and Ca in Georgeville soil (after Lutz et al. 1966). Copyright 1966, Soil Science Society of America. Reprinted with permission

| Source of P added | P added, ppm | ppm P present as | | | Al-phosphate |
|---|---|---|---|---|---|
| | | Al-phos | Fe-phos | Ca-phos | Fe-phosphate |
| 85% HaPO₄ | 0 | 21 | 87 | 3 | 0.24 |
| | 153 | 98 | 163 | 4 | 0.60 |
| | 306 | 114 | 268 | 12 | 0.43 |
| | 612 | 254 | 291 | 14 | 0.87 |
| | 1224 | 428 | 580 | 17 | 0.73 |
| Ca(H₂PO₄)₂ | 0 | 23 | 81 | 2 | 0.28 |
| | 153 | 145 | 139 | * | 1.04 |
| | 306 | 147 | 230 | * | 0.64 |
| | 612 | 316 | 297 | 8 | 1.06 |
| | 1224 | 254 | 603 | 13 | 0.38 |

monocalcium phosphate. Exposure of both phosphoric acid and monocalcium phosphate yielded greater reductions in the modulus of rupture in soils containing higher amounts of montmorillonite (swelling) clay.

Lutz et al. (1966) studied the effect of phosphorus on water retention properties of soils, using experiments similar to those described above, with the same soils and types of phosphate fertilizers. Water retention was measured by determining the percent water held at increasing pressure, from 1/10 to 15 bars. In all soils studied, P appreciably increased the soil water retention properties. Associated particle charge determination established that P increased the negative charge of the particles, and that surface charge is the dominant factor in water retention. Data from Table 7.4 show that charge is correlated to the Al-phosphate/Fe-phosphate ratio and that both vary as an irregular series with increasing rate of phosphorus. Lutz et al. (1966) also showed that the increase in water retention capacity is related directly to the increase in negative charge of the soil particles, and that the charge is related closely to the Al-phosphate/Fe-phosphate ratio.

Haynes (1984) showed that P addition to acid soils results in the precipitation of Al as insoluble Al-phosphates, which act as flocculating and cementing agents in a similar way to hydroxy-Al compounds. Haynes (1984) argued that the findings of Lutz et al. (1966) may occur only in acid soils containing high levels of soluble and exchangeable Al, where relatively high content P fertilizers are applied (Haynes and Naidu 1998). Because dispersion and flocculation are, in the case of acid soils, part of the pathway of phosphate-induced changes in soil hardness and water holding capacity, we consider that such changes are irreversible.

## 7.3.2   Trace Elements

Cu and Zn are two trace elements that may sorb strongly on the surfaces of soil–subsurface layer silicates. Sorption studies in pure systems have shown that the clay fractions of soil bind Cu and Zn by ion exchange, fixation, and hydrolysis

reactions, with the binding being pH dependent. In a study performed on acidic clay, Cavallaro and McBride (1984) found that the oxide fraction of the soil solid phase most strongly controls Zn and Cu fixation. In the studied pH range (4–7), up to 95% of the sorbed metal was retained irreversibly, exhibiting a hysteretic process. The results of Lopez-Periago et al. (2008) on copper retention kinetics showed that independent of metal loading, the release rate coefficients were more than ten times lower than those of retention, confirming the irreversibility of the process. In the examples that follow, a direct change in soil rheological properties after Zn disposal is noted, while in the case of Cu application, the soil bacterial community is initially affected, leading to a change in the soil aggregation status.

*Zinc* $(Zn^{2+})$ effects on soil rheological properties, under different pH and zinc concentrations, were studied by Ouhadi et al. (2006). More specifically, Ouhadi et al. (2006) examined the influence of zinc on the osmotic compressibility and consolidation of bentonite, under variable pH regimes. Changes in the creep behavior or volume strain of earth material, upon exposure to a high concentration of inorganic electrolytes, are explained in terms of the osmotic compressibility (consolidation) phenomenon and the formation of macropores among aggregates (Suzuki et al. 2005). Ouhadi et al. (2006) also showed that the addition to pore water of a trace element such as $Zn^{2+}$, in increasing amounts, decreases both the soil–clay Atterberg liquid limits and the plasticity index of soil bentonite (Table 7.5). The Atterberg liquid limits are a basic measure of the nature of a fine-grained soil clay at various solid–liquid ratios. The liquid limit is the water content at which a soil clay changes from plastic to liquid behavior; the plasticity index is a measure of soil clay plasticity.

The consolidation performance (measured in terms of pore ratio) of soil bentonite, with different $Zn^{2+}$ concentrations in pore water, is presented in Fig. 7.45. It can be observed that the consolidation performance increases with the increase in $Zn^{2+}$ concentration in pore water. Based on this series of rheological tests, Ouhadi et al. (2006) showed that the presence of $Zn^{2+}$ in pore water causes the formation of a kind of osmotic pressure. This pressure in turn changes the osmotic equilibrium of the natural system, and thus affects the natural rheological properties of the soil–subsurface system.

*Copper* $(Cu^{2+})$ addition as a micronutrient to agricultural lands, in quantities greatly in excess of those required by crops, occurs with sewage sludge application on orchards and vineyard growths where $Cu^{2+}$ salts are used as pesticides. For

**Table 7.5** Atterberg liquid limits (LL) and plasticity index (PI) as affected by increasing $Zn^{2+}$ concentrations in bentonite–heavy metal (nitrate forms) mixtures (after Ouhadi et al. 2006). Reprinted from Ouhadi VR, Yong RN, Sedighi M, Influence of heavy metal contaminants at variable pH regimes on rheological behaviour of bentonite. Appl Clay Sci 32:217–231, Copyright (2006), with permission from Elsevier

| Cation type | Atterberg limits | Contaminant concentration (mol $L^{-1}$) | | | | |
|---|---|---|---|---|---|---|
| | | 0.005 | 0.01 | 0.1 | 0.5 | 1.0 |
| $Zn^{2+}$ | LL | 310.9 | 247.4 | 121.3 | 101.9 | 93.2 |
| | PI | 274.6 | 209.9 | 82.1 | 57.8 | 47.4 |
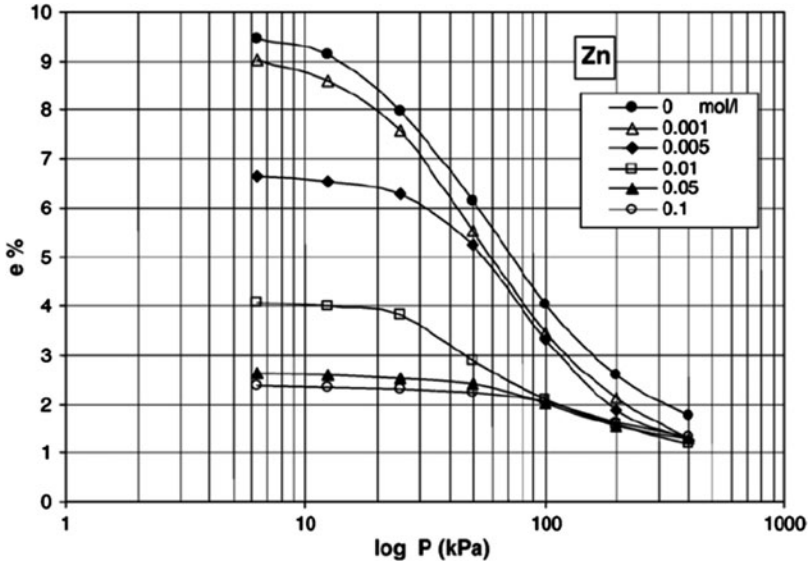
**Fig. 7.45** Consolidation performance of bentonite samples, at different concentrations of $Zn^{2+}$ in pore fluid; e denotes void ratio and P denotes osmotic pressure (after Ouhadi et al. 2006). Reprinted from Ouhadi VR, Yong RN, Sedighi M, Influence of heavy metal contaminants at variable pH regimes on rheological behaviour of bentonite. Appl Clay Sci 32:217–231, Copyright (2006), with permission from Elsevier

example, according to Epstein and Bassein (2001), ca. $3.8 \times 10^3$ ton of $Cu^{2+}$ was used as pesticides in 1997 in California. Copper-induced phytotoxicity has been reported in vineyards and orchards after long-term application, and copper presence was even considered as a potential crop toxicity indicator (McBride 2001).

Copper salts accumulated in soils after long-term application also have a toxic effect on soil–subsurface bacterial communities, affecting their enzymatic activities. In an experiment on tolerance of bacterial communities to long-term copper application in vineyards soils in Spain, Diaz-Ravina et al. (2007) found that increased soil bacterial toxicity to $Cu^{2+}$ was observed at concentrations greater than 100 mg $Cu^{2+}$ $kg^{-1}$ soil. Wyszkowska et al. (2005) experimented on heavy loamy and sandy silty loam soils, finding that soil contamination with $CuSO_4 \cdot 5H_2O$ at doses ranging from 150 to 600 mg $Cu^{2+}$ $kg^{-1}$ inhibited the activity of dehydrogenase, ureases, acid phosphatases, and alkali phosphatases. Dehydrogenase and urease, which are indicators of the activity of soil microorganisms (Kiss 1999), are found to be good sensors for $Cu^{2+}$ contamination of soils. It can be seen from Fig. 7.46 that the inhibition of the activity of these two enzymes, reflecting the decrease in the activity of soil microbial communities, is closely associated with the amount of copper added to the soil; the degree of inhibition varies among soils.
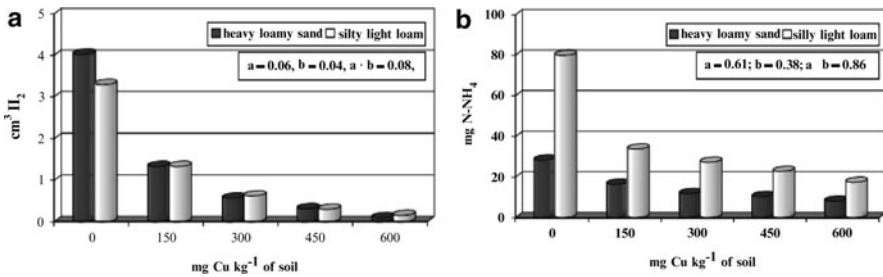
**Fig. 7.46** The activity of (**a**) dehydrogenases (cm$^3$ H$_2$ d$^{-1}$ kg$^{-1}$ soil) and (**b**) urease (mg N-NH$_4$ h$^{-1}$ kg$^{-1}$ soil), in copper-contaminated soils (modified after Wyszkowska et al. 2005)

The soil microbial population contributes to the formation and stabilization of soil aggregates. Potential binding agents among soil mineral particles include filamentous microbes (fungal hyphae), metabolites produced by the decomposer, and organic substances anthropogenically introduced into the soil–subsurface medium (Guidi 1981; Morel and Guckert 1983). Experimental results confirmed that for soil–sludge mixtures in which microbial activity was suppressed, no aggregative processes were recorded (Metzger et al. 1986; Metzger and Yaron 1987). As a consequence, copper contaminants which impact negatively on soil microbial communities may indirectly alter the process of aggregate formation and aggregate stability in soils. A high copper content in contaminated soil defines the irreversibility of this process.

## 7.4    Compounds of Industrial and Urban Origin

There are numerous types of compounds of industrial and urban origin that can reach the soil–subsurface system and irreversibly affect its original properties. We present here a number of examples that illustrate irreversible effects of acid rain and of oil and other hydrocarbon products on soil properties.

Acid rain is any form of atmospherically deposited acidic substance containing strong mineral acids mainly of industrial and urban origin. Acid rain represents an acidic deposition, which occurs in both wet and dry forms. The most common acidic substances are compounds containing hydrogen (H$^+$), sulfates (SO$_4^{2-}$), and nitrates (NO$_3^-$). Source of these compounds are from the combustion of fossil fuels such as coal, petroleum, and petroleum byproducts, primarily gasoline. Power plants that burn coal contribute over 50% of atmospheric sulfates and 25% of nitrates. While agriculture is also a major source of nitrates, we refer to acid rain as an inorganic contaminant of industrial and urban origin.

Oil and hydrocarbon contamination of the soil–subsurface domain may be caused by accidental spillage or leakage, or by intentional application, during urban or agricultural management. Long-term leakage of hydrocarbons can stimulate

the formation of oxidation–reduction zones in the soil–subsurface domain (Schumacher, 1996).

## 7.4.1   Acid Rain Effects

Rain and snow in equilibrium with carbon dioxide exhibit a pH of about 5.6. However, as result of a strong acid atmospheric pollution, the pH can decrease to 4. Records from a 30-year period (1963–1993) show, for example, that rain and snow in the northeastern USA had an average annual pH of 4.05–4.3, and that sulfuric acid contributed 55–75% of this measurable acidity (Likens and Bormann 1995). Another case is the rapid industrialization in China, which has led to a significant increase in acid rains caused mainly by the extensive use of coal and larger emission of pollutants. Wet and dry deposition of acidifying compounds, including $H_2SO_4$ and $HNO_3$, occurs in most populated parts of China; the only exception is the desert areas, where alkaline dust largely neutralizes the acids in the deposition materials (Larssen et al. 2006).

Acidification of soils due to acid enrichment of the atmosphere from industrial pollution complements natural acidification processes. The effect of acid deposition on soil depends on the effects of both intensity and capacity (Reuss et al. 1987). Intensity effects include changes occurring in the soil solution as a response to strong acid anion concentration in the acid deposition, which is buffered by the properties of the natural soil. The main capacity effect occurs as a result of sulfate adsorption and the increased leaching of base cations associated with strong acid anion mobility. A schematic view of the key processes governing soil acidification is given in Fig. 7.47.

As a "mobile" anion from acidic deposition, $SO_4^{2-}$ can be retained by soils from solution, regardless of whether or not this retention results in the stoichiometric displacement of another anion. In general, this retention is considered as "$SO_4$ adsorption." In many forest soils from the northeastern USA and some regions in Canada, it has been found that as a result of acid rain, the amount of $SO_4^{2-}$ loading is presently higher compared to pre-industrial levels. Harrison et al. (1989) reviewed the degree of $SO_4^{2-}$ adsorption reversibility following a decrease in anthropological inputs, and suggested the pathway of soil solution sulfate concentration with and without adsorption (Fig. 7.48). It can be observed that an important portion of retained sulfate remains completely irreversible in the polluted soil.

Based on this observation, Harrison et al. (1989) examined, in a laboratory study, the relative $SO_4^{2-}$ adsorption capacities and reversibility of a large number of soil samples. The samples were collected from a wide variety of forest sites in the USA, Canada, and Norway, and were subject to different environmental conditions and past atmospheric deposition levels. The measure of reversibility of $SO_4^{2-}$ adsorption was calculated by making two estimates of irreversibility of adsorbed sulfate, by comparing the difference in phosphate extractable fractions, and by comparing $SO_4^{2-}$ desorption from treated and untreated soils. The results showed that ~80% of
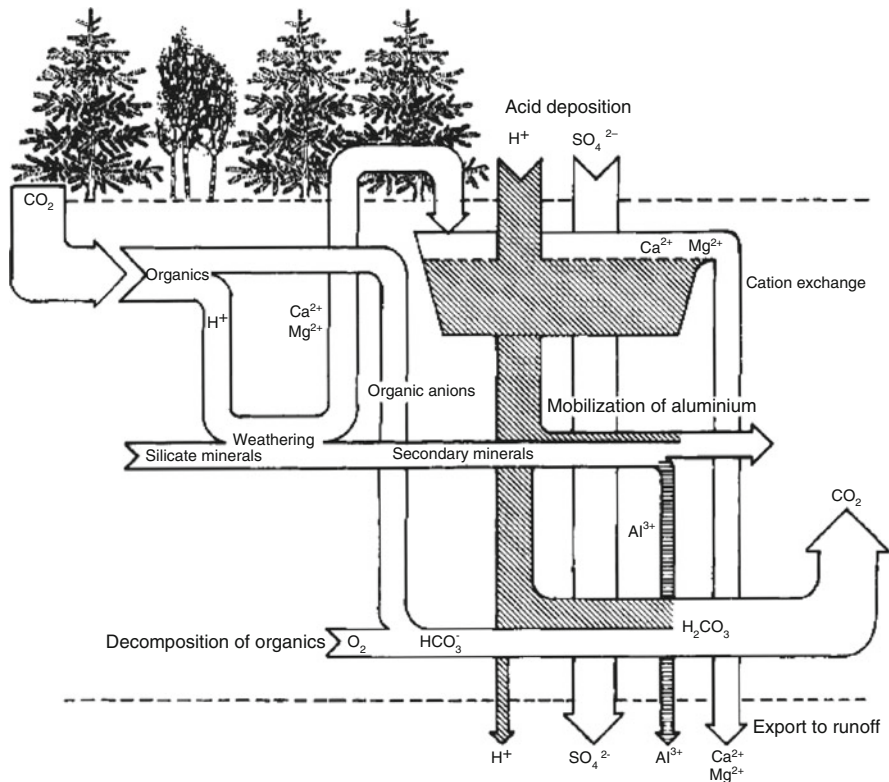
**Fig. 7.47** Schematic view of key processes governing acidification of soil and water (after Reuss et al. 1987). Reprinted by permission from Macmillan Publishers Ltd: Reuss JO, Cosby BJ, Wright RF, Chemical processes governing soil and water acidification. Nature 329:27–32, Copyright 1987

the tested soils irreversibly retained some of the adsorbed $SO_4^{2-}$. In general, soils that adsorbed higher amounts of $SO_4^{2-}$ also showed higher amounts of irreversibly adsorbed sulfate (Fig 7.49). On average, ~36% of the adsorbed $SO_4^{2-}$ was adsorbed irreversibly, for all soils studied.

Another laboratory study by Selim et al. (2004), on mobility of sulfate in Swedish forest soils, showed that sulfate retention during transport in different soil layers is controlled by kinetic reactivity of $SO_4^{2-}$ and by hysteretic mechanisms. Moreover, model parameter estimates indicated that the reactivity of $SO_4^{2-}$ during transport is concentration dependent.

Dissolution of aluminum in acidic soils has an important irreversible effect of acid deposition. The depletion and redistribution of aluminum with depth have been studied in Dutch field conditions (van Bremen et al. 1984; Mulder et al. 1987, 1989). In these cases, it was observed that aluminum fractions are leached from acidic sandy soils, inducing depletion of certain aluminum fractions within several decades (Table 7.6). The organic aluminum is removed annually from the surface layer at a rate of 1–2%.
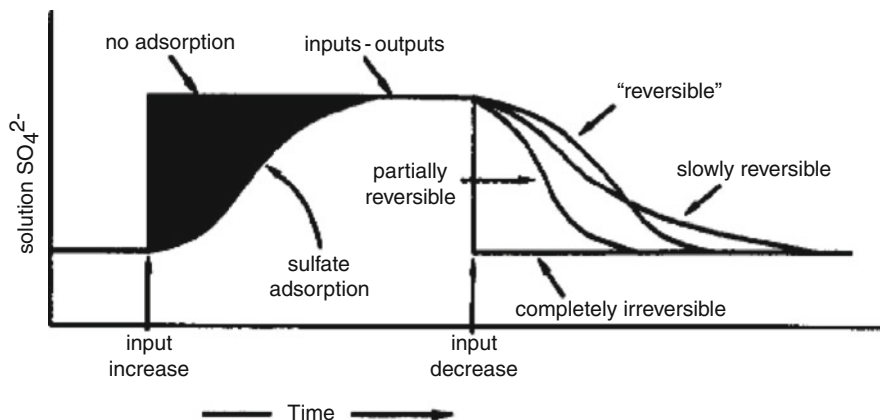
**Fig. 7.48** Pathways of soil solution sulfate concentration with and without adsorption following deposition increase, and showing a variety of sulfate reversibility responses following deposition decreases (after Harrison et al. 1989). Copyright 1989, American Society of Agronomy, Crop Sciences Society of America, and Soil Science Society of America. Reprinted with permission
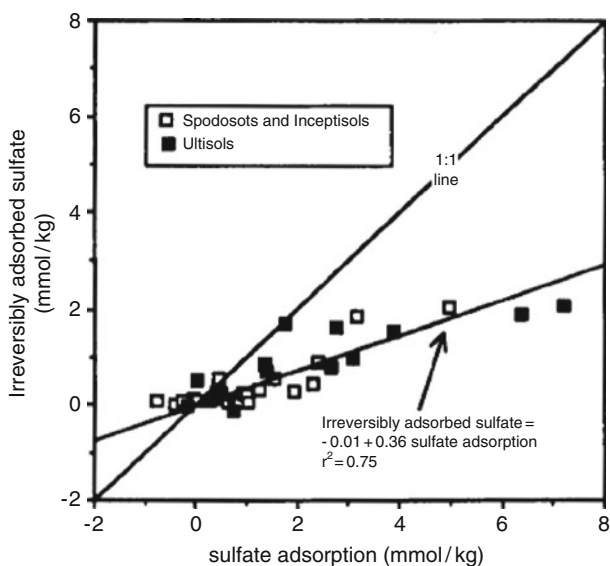


**Fig. 7.49** Irreversibly adsorbed $SO_4^{2-}$ versus total $SO_4^{2-}$ adsorption from 0.25 mM $CaSO_4$ solution for soils (after Harrison et al. 1989). Copyright 1989, American Society of Agronomy, Crop Sciences Society of America, and Soil Science Society of America. Reprinted with permission

Aluminum mobilization rates relative to those in the field were obtained in a laboratory experiment performed by Mulder et al. (1989), applying HCl at a rate of 20 mmol $H^+$ per kg of soil per 24 h; this rate was considerably higher than the existing acid load in the field (4 mmol $H^+$ $kg^{-1}$ $yr^{-1}$). The cumulative amount of

**Table 7.6** Amounts of soil-phase aluminum in three acidic, sandy soils from the Netherlands, before laboratory leaching treatments, and annual aluminum mobilization rates from the respective soil layers in the field (modified after Mulder et al. 1989). Reprinted by permission from Macmillan Publishers Ltd: Mulder J, van Breemen N, Eijck HC, Depletion of soil aluminum by acid deposition and implication for acid neutralization. Nature 337:247–249, Copyright 1989

| Site | Soil | Depth horizon (cm) | Extractable aluminum (mmol kg$^{-1}$) | | | Total aluminum (mmol kg$^{-1}$) | Annual removal of aluminum (mmol kg$^{-1}$) |
|------|------|------|------|------|------|------|------|
| | | | KCl | Na$_4$P$_2$O$_7$ | (NH$_4$)$_2$C$_2$O$_4$ | | |
| Gerritsfies | Driftsand | 0–10°C | 2.2 | 33.3 | 3.7 | 450 | 0.5 |
| | | 10–40°C | 0.7 | 35.7 | 6.3 | 427 | 0.3 |
| Tongbersven | Podzol | 0–12 E | 1.3 | 5.0 | 1.5 | 101 | 0.1 |
| | | 12–35 B | 13.7 | 196 | 3.3 | 446 | 0.4 |
| Hasselsven | Podzol | 0.7 E | 11.1 | 21.2 | 7.7 | 221 | 0.5 |
| | | 7–22 B | 16.3 | 55.8 | 13.5 | 273 | 0.1 |
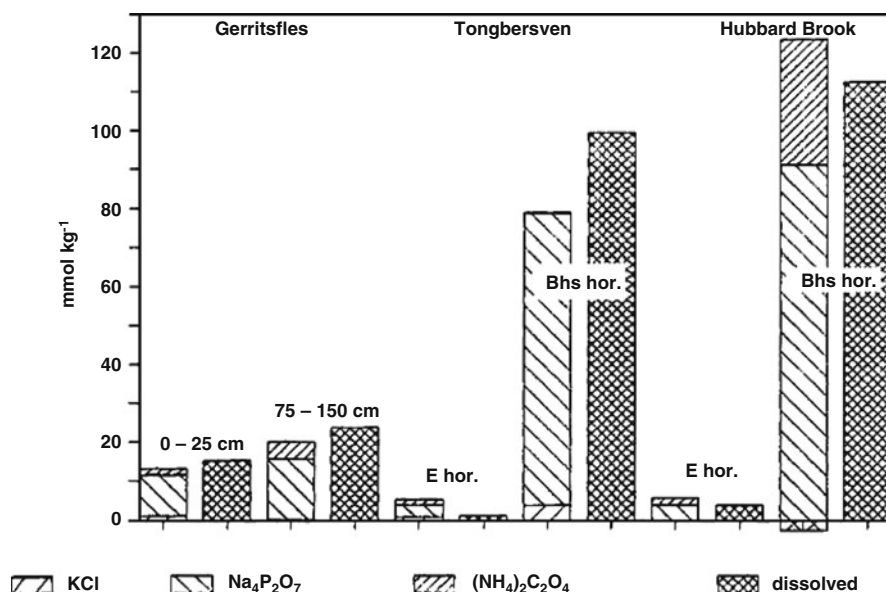


**Fig. 7.50** The decrease in solid phase aluminum, after leaching with HCl (dissolved), and amount of aluminum removed in the leachates for six soil samples (after Mulder et al. 1989). Reprinted by permission from Macmillan Publishers Ltd: Mulder J, van Breemen N, Eijck HC, Depletion of soil aluminum by acid deposition and implication for acid neutralization. Nature 337:247–249, Copyright 1989

aluminum dissolved by HCl was found to be close to the amount of free (extractable) aluminum removed (Fig. 7.50).

Aluminum is transferred to solution mainly from the organically complexed solid phase. Mulder et al. (1989) showed that the current depletion of alumino-

organics in the podzols was most pronounced in the upper layer of the soil profile, and that as a consequence, acid rain input produced a drastic change in the naturally occurring podzolization process. Mulder et al. (1989) concluded that "...the current rapid depletion of organic aluminum in the rooting zone of many acid sandy soils is irreversible on a time scale of decades or centuries."

Acid rains may affect also the molecular configuration and the properties of soil humic compounds. Calace et al. (2001) reported a laboratory experiment in which humic and fulvic acids extracted from a natural soil were subjected to simulated acid rains, until a soil pH of 4 was obtained. The effect of soil acidification on the humic and fulvic substances was determined in terms of humic/fulvic substance molecular weight and composition of the soil, before and after soil treatment. Neither molecular weight nor the FTIR spectrum of humic acid was influenced by the acidification process. In contrast, both the molecular weight and the FTIR spectrum of the fulvic acid were affected. The differences between FTIR spectra of pristine and acidified fulvic acids with molecular weights of 50 kDa and 3 kDa, respectively, are shown in Fig. 7.51.
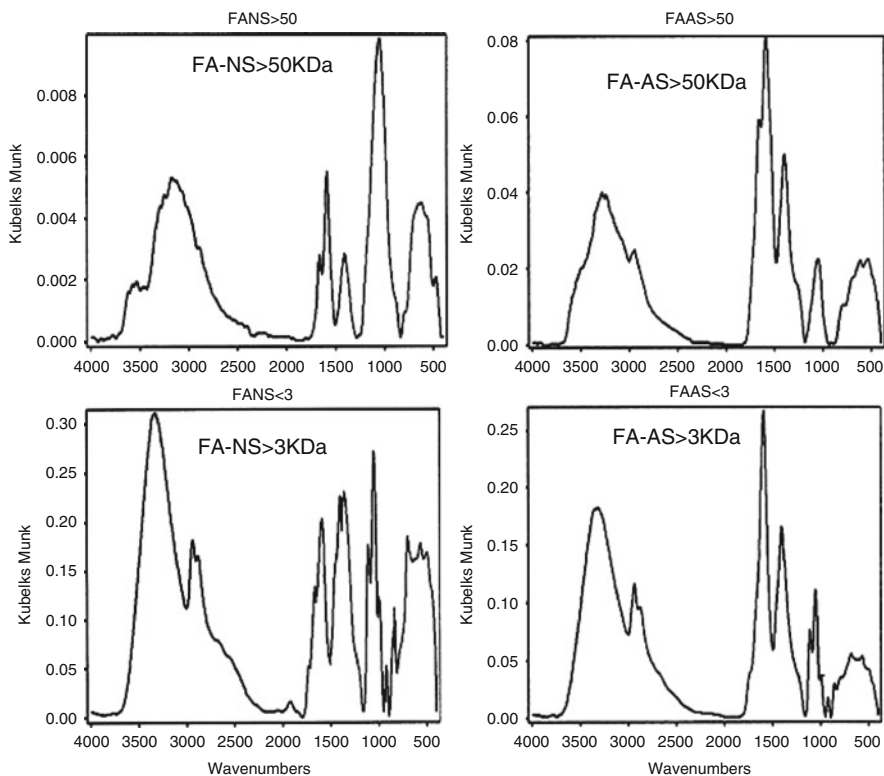


**Fig. 7.51** FTIR spectra of fulvic acid (FA) indicating the structural differences induced by soil acidification. *NS* natural soil, *AS* acidified soil (modified after Calace et al. 2001). Reprinted from Calace N, Fiorentini F, Petronio BM, Pietroletti M, Effects of acid rain on soil humic compounds. Talanta 54:837–846, Copyright (2001), with permission from Elsevier

The fulvic acids extracted from the pristine soil (FA–NS) reveal a greater alcohol and carbohydrate content (1,050–1,250 cm$^{-1}$) and higher adsorption than the acidified samples (FA–AS). This is due to antisymmetrical vibration of –COO$^-$ groups (1,550–1,650 cm$^{-1}$); to –CO stretching vibrations of esters, ketones, and aldehydes; and to –CO absorption and –NH$_2$ deformation of amide I and II bands (1,650–1,750 cm$^{-1}$). In the acidified fulvic acid, the carboxyl group content (1,700 cm$^{-1}$) dominated the –CO stretching of esters (shoulder at 1730 cm$^{-1}$). The differences between the two absorption peaks are more evident in the fraction smaller than 3 kDa, which shows only the peak due to –COO$^-$ groups. Fulvic acid acidification caused the peak corresponding to –OH deformation and –CO stretching of alcohols and phenols to decrease (1,050–1,350 cm$^{-1}$). These data show that the main effect of soil acidification is reflected in the structural composition of fulvic acids and in the breakup of the original molecules, due probably to a hydrolysis process. This suggests an irreversible increase in fulvic acid solubility.

Acid rain leaching leads also to changes in the composition of DOC. Release of different components of DOC obtained from a red clay soil (China), under leaching with simulated acid rain at pH of 2.5–5.6, was studied by Liu et al. (2009) using three-dimensional excitation–emission matrix spectroscopy (EEMS). Figure 7.52 shows the EEMS contour map of the eluate after leaching with simulated acid rain at pH 3.5. Five main peaks were identified, defining (A) humic acid, (B) fulvic acid, (C&D) microbial byproducts, and (E) aromatic proteins. Humic and fulvic acids, as
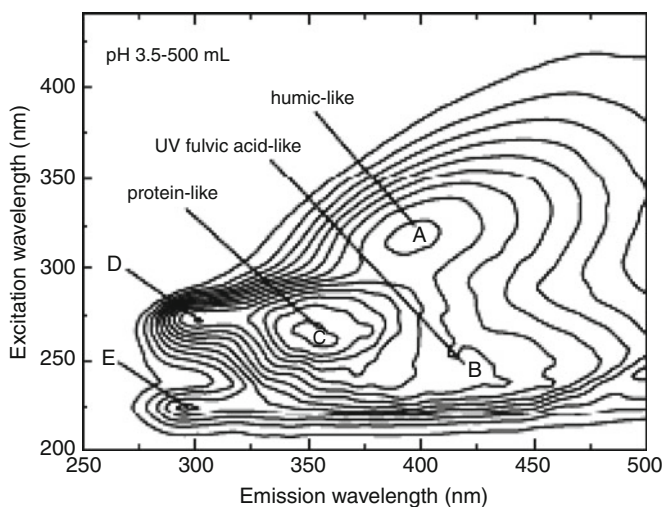


**Fig. 7.52** Excitation–emission matrix spectroscopy (EEMS) contour map of the eluate leached from red soil with 500 mL acid rain of pH 3.5. Peak-A: humic acid-like material; peak-B: fulvic acid-like material; peak-C and peak-D: microbial byproduct-like material; peak-E: simple aromatic proteins (after Liu et al. 2009). Reprinted from Liu L, Song C, Yan Z, Li F, Characterizing the release of different composition of dissolved organic matter in soil under acid rain leaching using three-dimensional excitation-emission matrix spectroscopy. Chemosphere 77:15–21, Copyright (2009), with permission from Elsevier
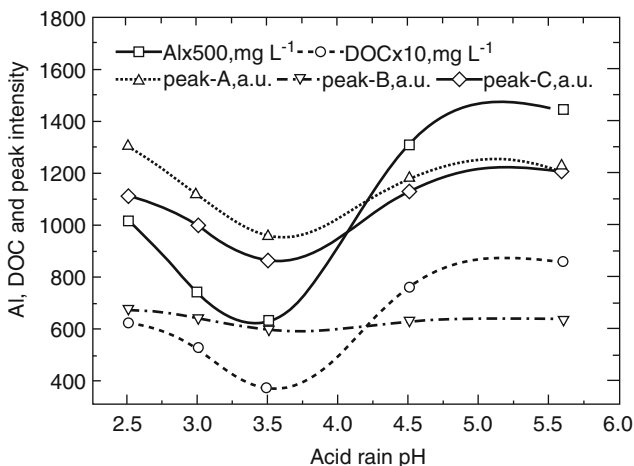
**Fig. 7.53** Effect of pH on aluminum and DOC content, and reflected peak intensity. Comparison of the effects of acidity of five simulated acid rains on the fluorescence intensities of humic acid-like (peak-A), fulvic acid-like (peak-B), and microbial byproduct-like (peak C) compounds in red soil (after Liu et al. 2009). Reprinted from Liu L, Song C, Yan Z, Li F, Characterizing the release of different composition of dissolved organic matter in soil under acid rain leaching using three-dimensional excitation-emission matrix spectroscopy. Chemosphere 77:15–21, Copyright (2009), with permission from Elsevier

well as microbial byproduct materials, were released at the beginning of leaching with low pH solution; in contrast, aromatic proteins were released with a greater time of leaching and a high pH.

Figure 7.53 shows the effects of pH of the simulated acid rain on the fluorescence intensity of humic and fulvic acids, and microbial byproducts from the eluate. Humic acid (A) and microbial byproduct (C) peaks decreased, from pH 2.5, to lowest intensity at pH 3.5; the peaks then increased with increasing pH, indicating that both the lower and higher pH values cause loss of DOC fractions. The pH effect on the fulvic acid peak (B) is smaller, suggesting that the loss of fulvic acid from the studied soil was only weakly dependent on pH. Eluate EEMS analysis clearly showed that the composition of DOM in the studied soil changed irreversibly with changes in acidity and leaching volume of acid rain. Most DOC was lost from the red soil in the early phases of leaching.

Atmospheric deposition can affect DOC in soil by changing either the soil acidity or the ionic strength of the soil solution. An increase in soil acidity as a result of acid rain deposition may lead to a decrease in DOC. Potential anthropogenically induced changes in the DOC status in the soil–subsurface domain can be deduced by extrapolating the findings of large, multinational monitoring programs on atmospherically deposited sulfur and sea salts on continental surface waters.

Monteith et al. (2007) used the results of 25 years of monitoring studies in Europe and North America, on DOC content in surface waters located on glaciated, acid-sensitive terrain, to define DOC trends resulting from changes in atmospheric
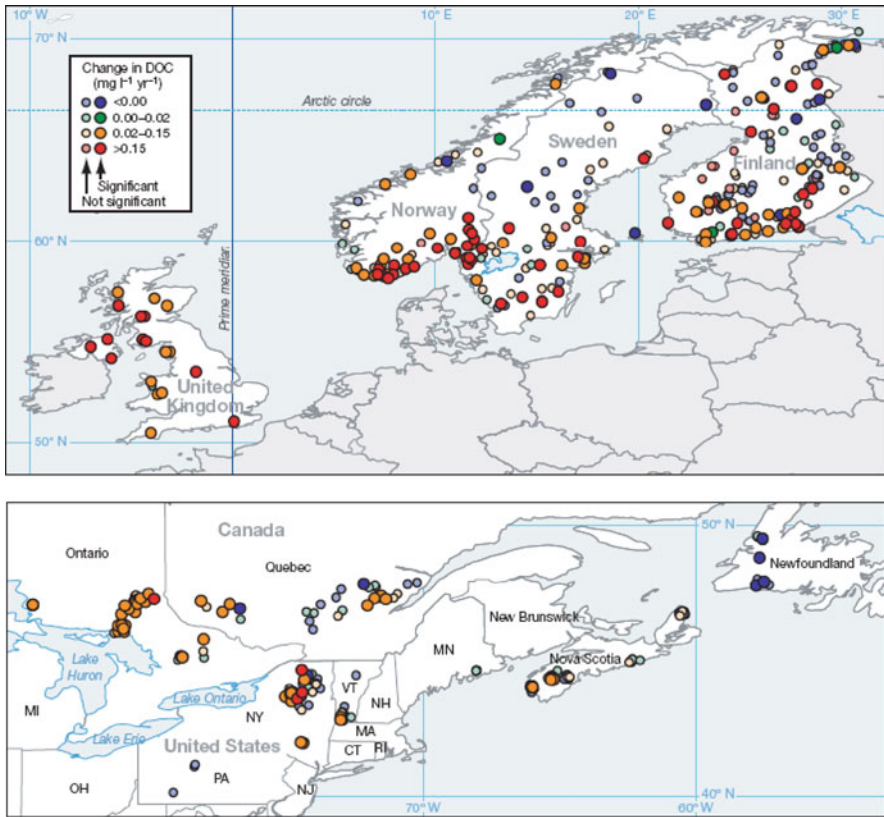
**Fig. 7.54** Trends in dissolved organic carbon (mg L$^{-1}$ yr$^{-1}$). Data are shown for monitoring sites on acid-sensitive terrain in Europe (*upper panel*) and North America (*lower panel*) for the period 1990–2004 (after Monteith et al. 2007). Reprinted by permission from Macmillan Publishers Ltd: Monteith DT, Stoddard JL, Evans CD, de Wit HA, Forsius M, Høgåsen T, Wilander A, Skjelkvåle BL, Jeffries DS, Vuorenmaa J, Keller B, Kopácek J, Vesely J, Dissolved organic carbon trends resulting from changes in atmospheric deposition chemistry. Nature 450:537–540, Copyright 2007

deposition chemistry. Monitoring data (Fig. 7.54) showed that between 1990 and 2004, some of the sites measured a DOC increase; this finding was attributed to a gradual decline in the sulfate content of atmospheric deposition. Using a simple model that included changes in deposition chemistry and catchment acid sensitivity, Monteith et al. (2007) demonstrated that DOC concentrations increased in proportion to the rates at which atmospherically deposited anthropogenic sulfur and sea water declined.

The ecosystem has been partially buffered by changes in organic acidity, and the rise in DOC is related to recovery from acidification. The effect on the ecosystem of a decrease in DOC due to acid deposition is irreversible. We suggest that even with global efforts to reduce sulfur emissions into the atmosphere, and a decrease in soil acidity, the soil DOC will never return to its initial concentration.

## 7.4.2  *Hydrocarbon-Induced Irreversible Changes*

### 7.4.2.1  Diagenesis in Hydrocarbon Microseepages

Diagenesis is a term used to describe any geological alterations occurring in the soil–subsurface domain. Diagenesis can be applied also to alterations occurring in hydrocarbon microseepages surrounding major oil fields. Microseepages are formed in networks of fractures and bedding planes that provide permeable routes for hydrocarbons and other fluids within the overlying parent formations. The presence of microseepages is expressed in an array of chemical or mineralogical alterations and anomalies.

An example of the extent of this phenomenon is shown in Fig. 7.55, where the locations of hydrocarbon-related alterations in the continental USA are depicted. The knowledge on hydrocarbon-induced diagenetic changes to soil parent materials as clay–minerals, sandstones, carbonates, and sulfides provides a perspective on potential, irreversible hydrocarbon-induced alteration of the soil–subsurface domain.
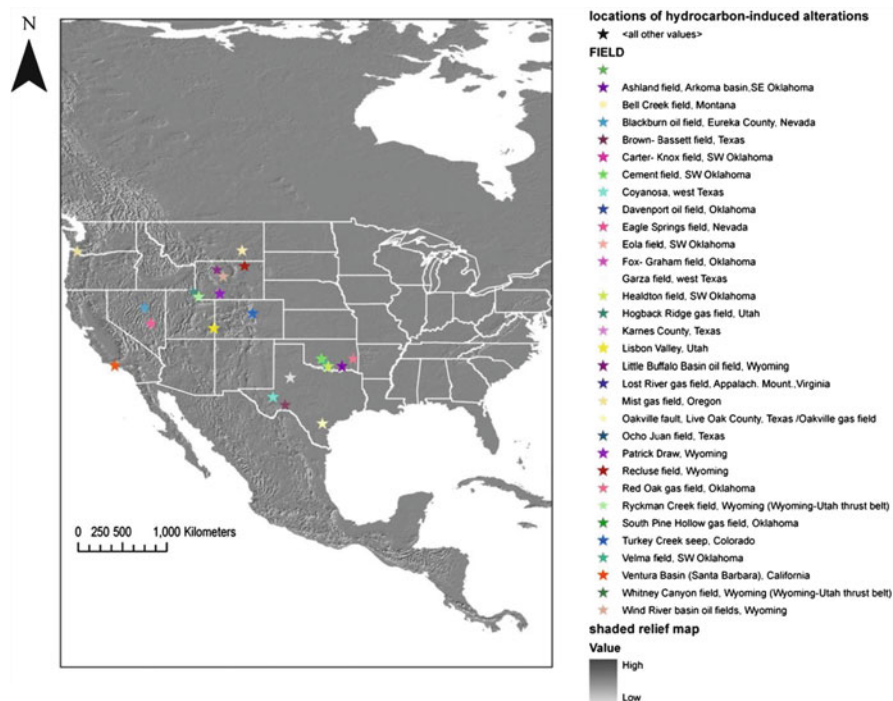


**Fig. 7.55** Shaded relief map of the continental USA showing locations of hydrocarbon-related alterations reported in the literature represented by stars (after Petrovic et al. 2008, and references within). Reprinted from Petrovic A, Khan SD, Chafetz HS, Remote detection and geochemical studies for finding hydrocarbon-induced alterations in Lisbon Valley, Utah. Marine Pet Geol 25:696–705, Copyright (2008), with permission from Elsevier
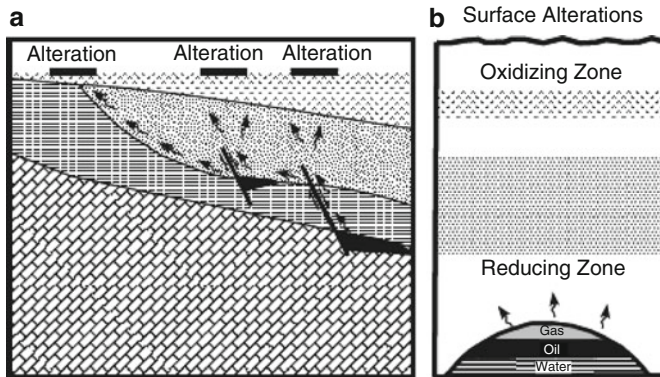
**Fig. 7.56** (**a**) Processes by which microseeping hydrocarbons migrate from a reservoir to the surface through faults, fractures, and stratigraphic boundaries. (**b**) Generalized model of hydrocarbon-induced geochemical alterations of soils and sediments (modified by Khan and Jacobson 2008). Reprinted with permission

Microseepages that result from the vertical movement of hydrocarbons from their respective reservoirs to the surface are depicted in Fig 7.56a. Schumacher (1996) suggested a simplified blueprint to describe hydrocarbon-induced alteration of the soil–subsurface matrix and properties. These alterations occur due to leaking hydrocarbons in near-surface oxidation and/or reduction zones that favor the development of a diverse array of chemical and mineralogical changes (Fig. 7.56b).

*Mineral alteration* in the vicinity of microseepages may result from microbial oxidation of hydrocarbons, which creates a reducing, slightly acidic environment. Initially, aerobic bacteria oxidize hydrocarbons to form carbon dioxide or bicarbonate, which may precipitate as carbonate. Once oxygen is depleted, other bacteria reduce sulfate to produce hydrogen sulfide. As a result, the environmental oxidation–reduction potential and the pH of the system are changed, affecting stability of minerals within the surrounding geosystem. An example of the effect of hydrocarbons on mineral stability in a microseepage diagenetic zone in the Southwest Wyoming, USA, is given in Fig. 7.57, which shows the mineralogical composition in samples in altered and unaltered zones.

The presence of bleached and discolored red sandstones in zones of petroleum accumulation occurs when acidic or reducing fluids are present to remove hematite, favoring pyrite and siderite formation. Hydrocarbons act as one such reducing agent. In the Lisbon Valley (Utah, USA) field, bleached portions of Wingate Sandstone approximate the geographic limits of the oil and gas reservoir at depth. The red color of the unbleached Wingate was found to result from a pervasive hematite–clay mixture, whereas the bleached Wingate exhibited a gray color due to the absence of hematite (Segal et al. 1984, 1986). The bleached Wingate contained three to five times more kaolinite than the unaltered rock (Conel and Alley, 1985), which may explain the hydrocarbon-induced change in the original rock.
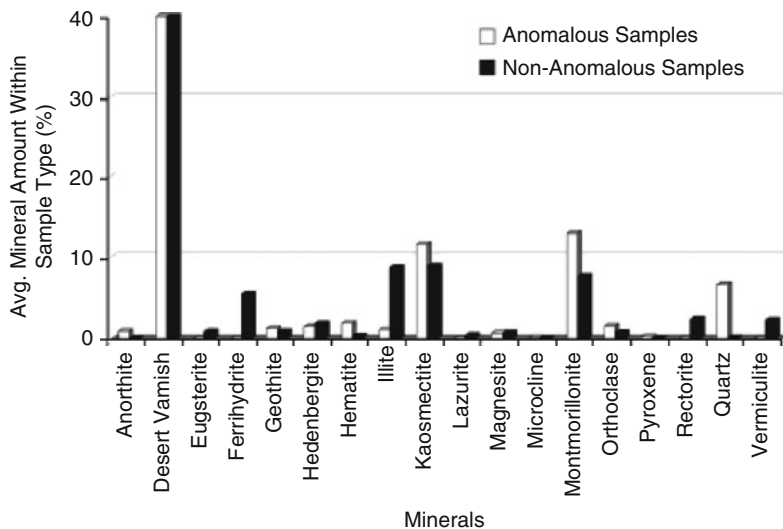
**Fig. 7.57** Average mineral composition of anomalous and non-anomalous mineral samples (after Khan and Jacobson 2008). Reprinted with permission

*Carbonates* and carbonate cements are among the most common hydrocarbon-induced alterations associated with petroleum seepage (Schumacher, 1996). Diagenetic carbonates are formed as a byproduct of petroleum oxidation, particularly methane, via fluctuating aerobic and/or anaerobic reaction pathways. When such reactions occur, carbon dioxide evolves and produces bicarbonates that react with water. The bicarbonate bonds with calcium and magnesium, and precipitates as carbonate or carbonate cement having an isotopic signature matching that of the parent hydrocarbon(s).

For example, in the Cement-Chickasha oil field in Oklahoma (USA), sandstones at the surface are highly cemented by secondary calcite and dolomite, but they contain little or no carbonate cement away from the field. Hydrocarbons induced formation of diagenetic carbonates in this oil field, including calcite, ferron calcite, high Mg- and Mn-calcite, dolomite, ankerite, aragonite, siderite, and rhodochrosite. The carbon isotopic compositions of these diagenetic carbonates range from $-2$ to $-35\%$, with the most negative values occurring along the structural axis of the field (Donovan et al. 1974; Al-Shaieb et al. 1994). However, variation in the carbon isotopic composition of subsurface carbonate cement may be found along the hydrocarbon seepages; an example is presented in Fig. 7.58.

*Sulfide* formation in hydrocarbon seep environments is another important diagenetic process. A typical example is hydrocarbon-induced formation of secondary pyrite. In a reducing environment, pyrite can precipitate in the presence of a source of sulfur and iron. Schumacher (1996) noted that the major source of sulfur in a petroleum region is hydrogen sulfide gas, which originates from petroleum transformation. The main source of iron is iron oxide grain coatings in sandstone, pore-
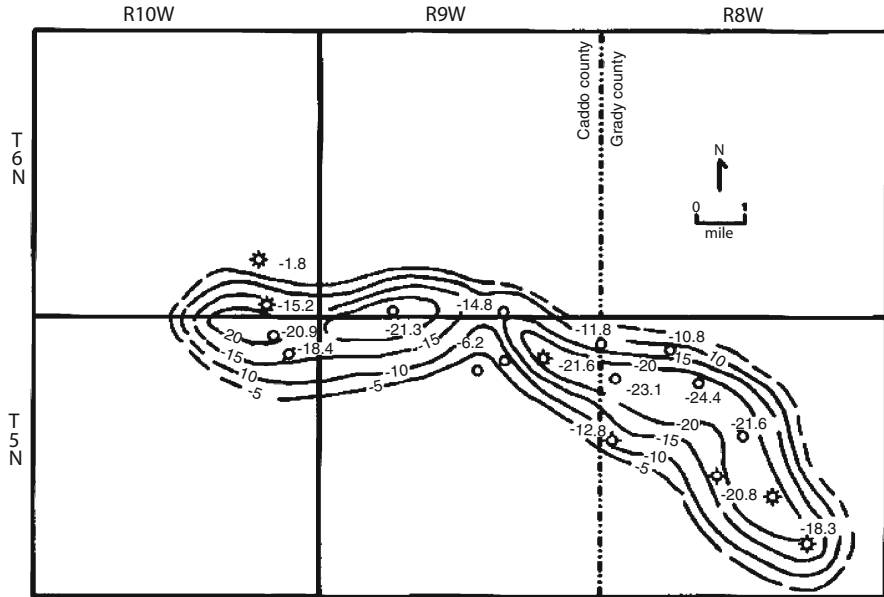
**Fig. 7.58** Variation in the carbon isotopic composition of subsurface carbonate cements from Cement-Chickasha field, Caddo County, Oklahoma (after Al-Shaieb et al. 1994)

filling clays such as chlorite, and rock fragment inclusions. The reaction between hydrogen sulfide and iron induces precipitation of pyrite. The development of a pyrite alteration zone depends on the sulfur content of the hydrocarbons, the geology and groundwater chemistry, and the nature of the bacterial degradation.

As an example, a hydrocarbon-induced pyrite zone developed in the Cement-Chickasha oil field in Oklahoma (USA), as shown in Fig. 7.59. In this case, pyrite is abundant in cuttings from on-field wells and generally absent in cuttings from off-field wells. The average value of the sulfur isotopic composition of the pyrite ($-3.6\%$) compares favorably to that of the sulfur in the associated oil ($-4.7\%$), strongly suggesting that $H_2S$ associated with the oil was the major source of sulfur in the pyrite (Al-Shaieb et al. 1994).

### 7.4.2.2  Petroleum Hydrocarbons

The soil–subsurface domain, around the world, is threatened by spilled petroleum products which generally consist of complex hydrocarbon mixtures. These mixtures contain components with a large range of carbons (e.g., $C_6$ to $C_{30}$) and different vapor pressures and solubilities.

The retention capacity of kerosene – a petroleum product containing about 100 hydrocarbon components – and its physical attenuation in soil–subsurface systems were studied by Fine et al. (1997), Yaron et al. (1998), and Dror et al. (2002). It was
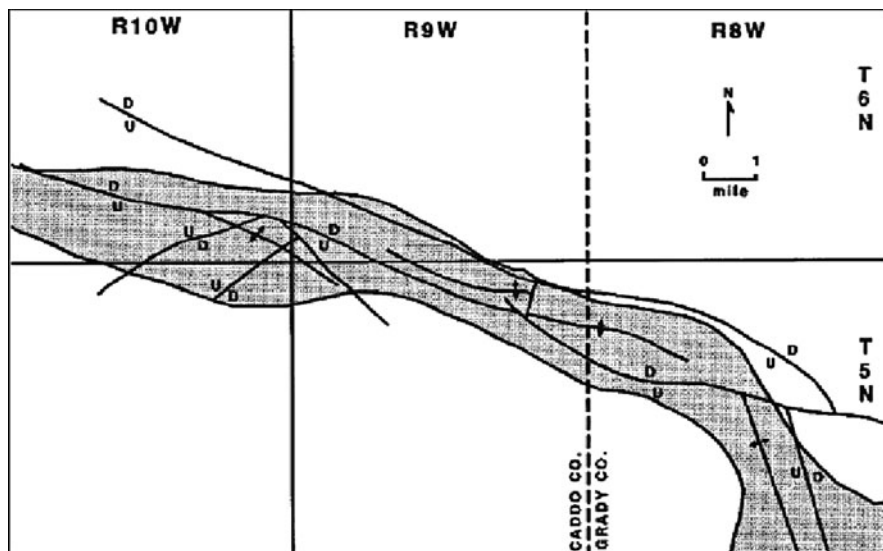
**Fig. 7.59** Subsurface limits of pyrite mineralization in Cement-Chickasha field, Caddo County, Oklahoma. The limits of the pyritized zone coincide with the pre-Permian structure (after Al-Shaieb et al. 1994)

found that during disposal in the soil–subsurface domain, the light petroleum fractions volatilize or dissolve in the surrounding air and aqueous phases, leaving behind a nonaqueous liquid phase (NAPL) that contains a heavy hydrocarbon fraction. In the soil–subsurface domain, the petroleum hydrocarbon NAPL forms entrapped ganglia that resemble discontinuous blobs within large pores (Schwille 1984; Powers et al. 1994). These ganglia functionally alter the original porous media architecture. In the case of kerosene contamination, for example, it was found that the kerosene residual content (KRC) in soil varies from soil to soil, and is inversely linearly related to the moisture and linearly related to the soil texture as expressed by clay content (Fig. 7.60).

Under equilibrium conditions, multicomponent dissolution can be described in terms of a constant partition coefficient among all of the organic mixture components and the aqueous solution. An example of kerosene–water partitioning at equilibrium is presented in Fig. 7.61, where kerosene was in contact with an aqueous electrolyte solution (0.01 N NaCl) at a temperature of 22°C for 100 h. From gas chromatogram analysis, it can be seen that aliphatic and branched aliphatic hydrocarbons in the range $C_9$–$C_{16}$ comprise the major group of components in neat kerosene, with only a minor group of aromatic compounds. In the aqueous electrolyte solution, aromatic compounds, especially branched benzenes and naphthalene, make up the majority of the compounds in the aqueous phase. The $C_9$–$C_{10}$ aliphatic and branched aliphatic components do not appear in the chromatogram of the aqueous kerosene, because aromatic components are several orders of magnitude more soluble than aliphatic components.
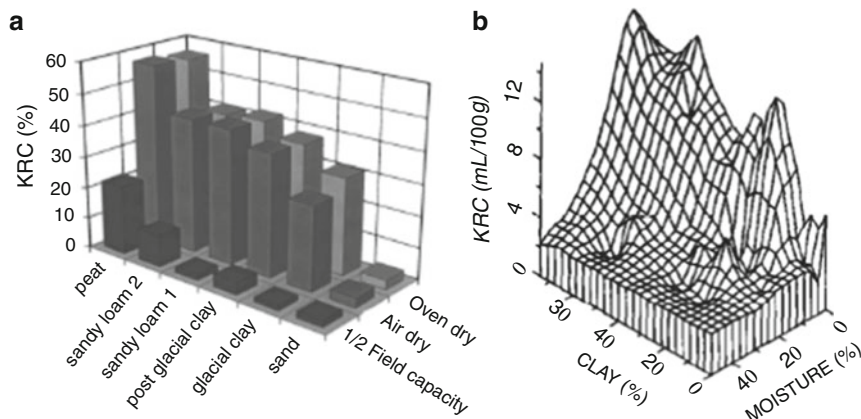
**Fig. 7.60** Kerosene residual content (KRC) in soils, (**a**) as affected by type of soil and moisture content (after Jarsjö et al. 1994) and (**b**) as a function of clay and moisture content (after Fine and Yaron 1993). Reprinted from Jarsjö J, Destouni G, Yaron B, Retention and volatilization of kerosene: Laboratory experiments on glacial and post-glacial soils J Contam Hydrol 17:167–185, Copyright (1994), with permission from Elsevier, and from Fine P, Yaron B, Outdoor experiments on enhanced volatilization by venting of kerosene component from soil. J Contam Hydrol 12:355–374, Copyright (1993), with permission from Elsevier

Losses of kerosene deposited on soil, through volatilization, is controlled by the vapor pressure of each of the kerosene components, concentration gradients in the subsurface, pore geometry, moisture content, temperature, and type of soil. The effect of volatilization on residual kerosene remaining in three different soils, over 7 days, is shown in Fig 7.62. It can be observed that kerosene losses are greatest in sand and lowest in peat.

The physical properties of the residual liquid also change as the composition of the initial mixture changes. Loss of the light fraction of kerosene by volatilization led to an increase in the liquid viscosity. The relationship between the viscosity of kerosene after volatilization and the relative concentration of the kerosene major components is shown in Fig. 7.63. An increase in kerosene viscosity was accompanied by a relative increase in the heavy fraction ($C_{13}$–$C_{15}$) and a decrease in the light fraction ($C_9$–$C_{11}$). The increase in viscosity causes a change in soil–subsurface porosity, through the formation of ganglia and discontinuous blobs within large pores. Because these heavy kerosene residues are not easily biodegraded on a human lifetime scale, we can expect such porosity changes to be essentially irreversible.

*Water transport properties* of soils may be changed irreversibly following hydrocarbon contamination. The extent of changes is controlled by the type of soil and pollutant properties. Irreversible effects on water transmission properties are related to the retention of petroleum products in the soil–subsurface matrix. Hydrocarbon products can be retained in the porous matrix by entrapment in the pore network and/or by sorption at particle surfaces. Physical and chemical properties of the soil–subsurface solid phase, including hydration status, mineral content, and organic matter content, control the degree of hydrocarbon entrapment and sorption.
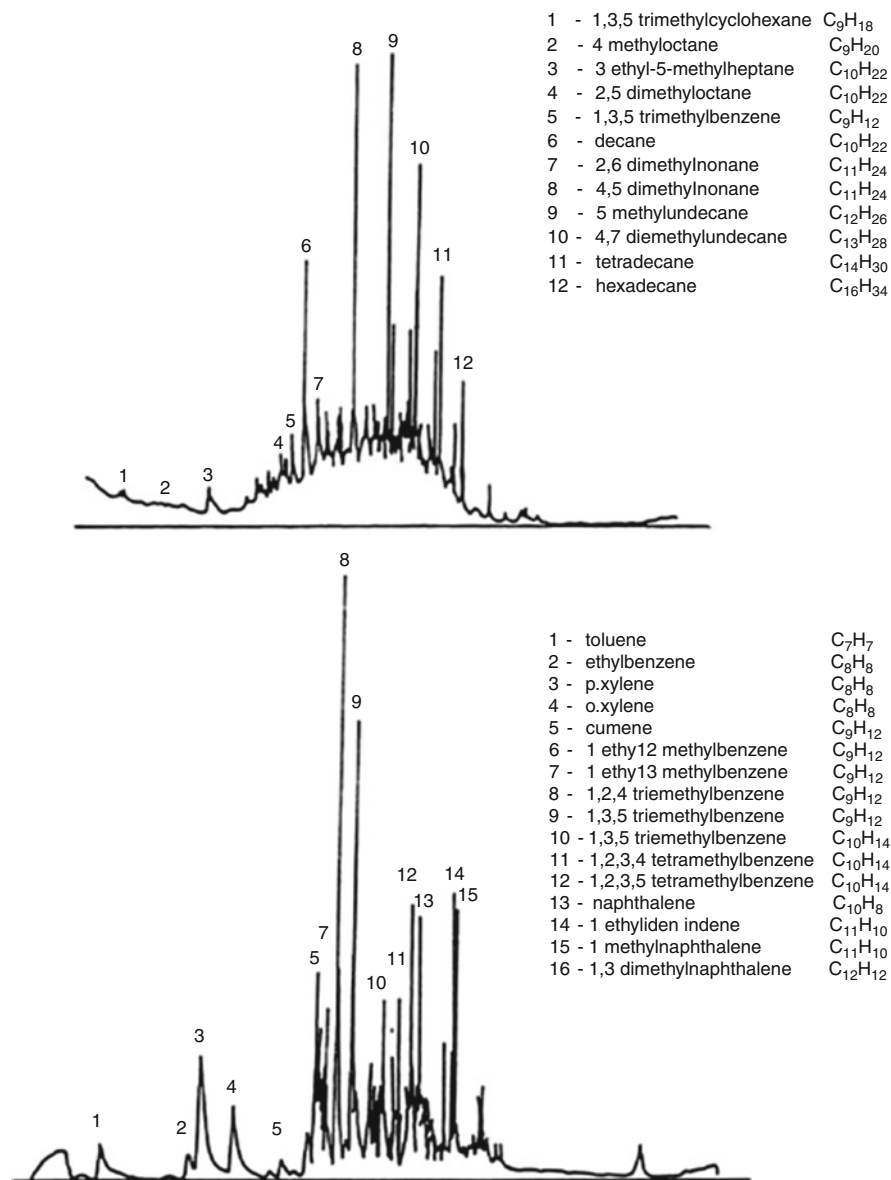
**Fig. 7.61** Gas chromatography of (**a**) neat kerosene and (**b**) kerosene dissolved in 0.01 N NaCl aqueous solution (after Dror et al. 2002). Reprinted from Dror I, Gerstl Z, Prost R, Yaron B, Abiotic behavior of entrapped petroleum products in the subsurface during leaching. Chemosphere 49:1375–1388, Copyright (2002), with permission from Elsevier

Caravaca and Roldán (2003) examined changes occurring to soil texture and porosity following contamination with petroleum hydrocarbons. These authors considered an extreme case of soil pollution near an oil refinery in the province

**Fig. 7.62** Gas
chromatograms of kerosene
recovered from sand, sandy
loam, and peat after 7 days of
volatilization at 27°C,
showing the disappearance of
kerosene components (after
Jarsjö et al. 1994). Reprinted
from Jarsjö J, Destouni G,
Yaron B, Retention and
volatilization of kerosene:
Laboratory experiments on
glacial and post-glacial soils.
J Contam Hydrol
17:167–185, Copyright
(1994), with permission from
Elsevier
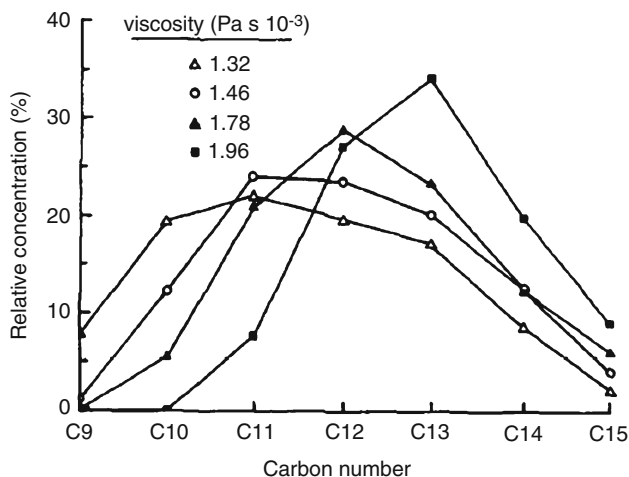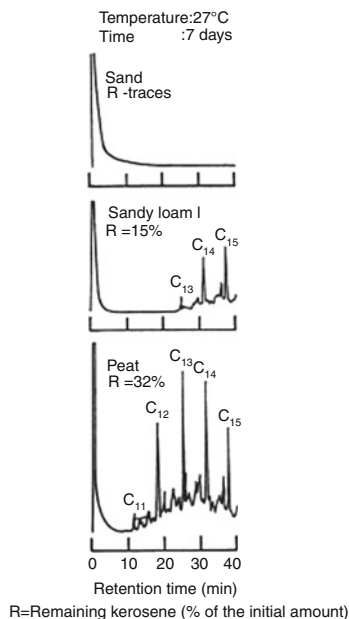


**Fig. 7.63** Composition of kerosene as a function of viscosity (after Gerstl et al. 1994). Copyright 1994, American Society of Agronomy, Crop Science Society of America, and Soil Science Society of America. Reprinted with permission

of Murcia (Spain), which released uncontrolled amounts of hydrocarbon over nearly 10 years. The total soil organic carbon (TOC) increased during this period from 7.2 to 73.8 g kg$^{-1}$. In the contaminated soil samples, Caravaca and Roldán

**Table 7.7**  Effect of contamination by hydrocarbons on soil pores larger than 50 μm and pore size class distributions (after Caravaca and Roldán 2003). Reprinted from Caravaca F, Roldán A, Assessing changes in physical and biological properties in a soil contaminated by oil sludges under semiarid Mediterranean conditions. Geoderma 117:53–61, Copyright (2003), with permission from Elsevier

| Soil | [a]Porosity (%) | [b]Size classes of pores (%) | | | | | | |
|---|---|---|---|---|---|---|---|---|
| | | 50–100 (μm) | 100–200 (μm) | 200–300 (μm) | 300–400 (μm) | 400–500 (μm) | 500–1,000 (μm) | 1,000–2,000 (μm) |
| Control | 0.8 (0.1) | 5.1 (1.4) | 11.5(3.0) | 20.5(5.8) | 9.0 (2.1) | 7.7 (2.9) | 21.8 (3.2) | 24.4 (10.8) |
| Contaminated | 11.9 (0.1) | 2.2 (0.1) | 11.1(0.7) | 21.4(3.6) | 9.7 (1.7) | 17.1(7.3) | 28.8 (3.7) | 9.7 (1.5) |

Standard error for each measure is given in parentheses
[a]Soil is expressed as a percentage of area occupied by pores >50 μm per thin section
[b]Pore size class distributions are expressed as a percentage of total porosity

(2003) found a decrease in the clay faction from 33 to 21%, relative to the natural soil, and an increase in sand fraction from 45 to 58%. Soil macroporosity (defined as pores >50 μm) in the hydrocarbon-contaminated soil increased about 15-fold compared to that in the control soil, affecting water transport in the soil–subsurface system. This modification is reflected also in the pore size classes (Table 7.7).

Shrinkage of the soil surface was determined by Caravaca and Roldán (2003) to be higher in the control soil than in the soil contaminated by hydrocarbons. Moreover, the size distribution of cracks in the control soil differed from the contaminated soil (Fig. 7.64).

Soil water holding capacity and water repellency are additional factors that should be considered in relation to soil water transmission properties. The effect of varying petroleum hydrocarbon contamination on the hydraulic properties of Ottawa sand was tested by Burckhard et al. (2000). In general, it was observed that soil–water retention curves for hydrocarbon-contaminated sand were different from the retention curves of pristine Ottawa sand. Figure 7.65 shows volumetric water content versus pressure for various total petroleum hydrocarbon levels. At higher suction (i.e., lower pressure) values, the contaminated samples had a higher holding capacity, leading to a reduction in the soil hydraulic conductivity.

Soil water repellency caused by petroleum hydrocarbon contamination was reported by Roy et al. (2003), based on a large study of 12 hydrocarbon-contaminated soils from Alberta, Canada. Water repellency, defined by the molarity of ethanol droplet (MED) method, dichloromethane-extractable organics (DEO), and TOC , were examined; results are presented in Fig. 7.66 for the three soil horizons. All three parameter values were significantly higher in hydrocarbon-contaminated repellent soils than in the adjacent pristine soils. The results indicated that in the studied sites, petroleum hydrocarbon-induced repellency is predominantly a surface phenomenon. The fact that most crude oil naturally contains a small fraction of dichloromethane-insoluble material and that this fraction tends to substantially increase once reaching the soil (e.g., Connaughton et al. 1993; Reid et al. 2000) suggests that hydrocarbon-induced repellency of soils is an irreversible change at least over human lifetime scales.
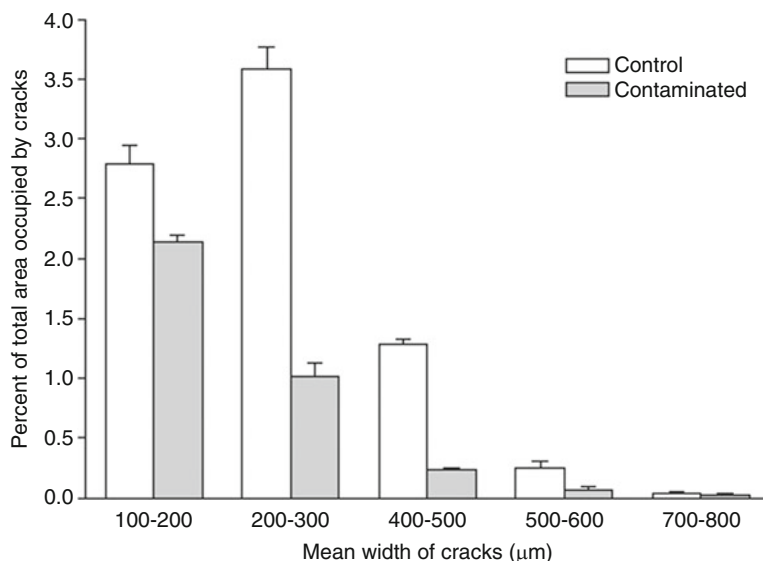
**Fig. 7.64** Size distribution of cracks of a soil in response to contamination by hydrocarbons. *Bars* represent standard error for each measure ($n = 4$) (after Caravaca and Roldán 2003). Reprinted from Caravaca F, Roldán A, Assessing changes in physical and biological properties in a soil contaminated by oil sludges under semiarid Mediterranean conditions. Geoderma 117:53–61, Copyright (2003), with permission from Elsevier

Similar relationships between water repellency and total petroleum hydrocarbon concentrations were observed in oil-contaminated sandy and clayey soils from a humid tropical environment (Adams et al. 2008). Hydrocarbon contamination clearly induced soil repellency and reduced soil water retention, as expressed by field capacity value. In both soils, Adams et al. (2008) found a positive linear relationship between total petroleum hydrocarbon content and water repellency. However, the persistence of water repellency was much greater in sandy soils than in the clayey soils. Such changes in soil water transmission properties can be considered irreversible, although they may be partially mitigated following remediation treatments.

*Geotechnical and geoelectrical properties* of the soil–subsurface system also may be affected irreversibly by oil contamination. A study of geotechnical properties of sandy loam and silty loam soils of basaltic origin (Rahman et al. 2010) showed changes in the soil Atterberg plastic and liquid limits following contamination with petroleum hydrocarbons (Fig. 7.67). It is clearly seen that both liquid and plastic limits decreased with increases in the amount of petroleum hydrocarbon in the soils. The decrease in liquid limit was greater in the silty loam soil (38%) than in the sandy soil (16%); these values are significantly lower than the liquid limit values (66% and 62%) in the pristine soils. Plastic limits also increased with increases in amounts of petroleum hydrocarbons. Testing other geotechnical

**Fig. 7.65** Volumetric water content versus pressure for various total petroleum hydrocarbon (TPH) levels (after Burckhard et al. 2000)
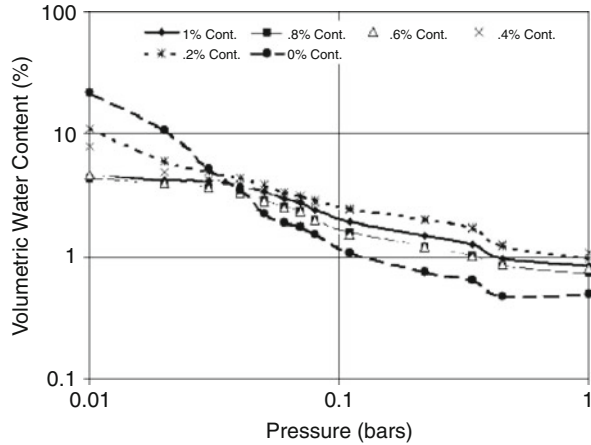


parameters, Rahman et al. (2010) found that the soil maximum dry density and optimum moisture content dropped due to increases in petroleum hydrocarbon content in the contaminated soils. Similar behaviors were observed on measurements of permeability and shear strength of the soils.

Geoelectrical properties of the soil–subsurface system, such as dielectric constant, conductivity, and resistivity, may also be altered following contamination by petroleum hydrocarbons. Based on the fact that electromagnetic properties of geomaterials are related directly to the liquid retained in the pore space, Darayan et al. (1998) determined the dielectric constant and the conductivity of a soil contaminated by a spill of diesel oil. Figure 7.68 shows the conductivity values and the relative dielectric constants of the clayey horizon of a soil from the Texas Sugar Land area (USA), before and after addition of diesel oil. It can be seen that the dielectric constant increases with the addition of diesel oil. Darayan et al. (1998) attributed these results to the replacement of water by diesel oil in the pore space.

Are changes to geotechnical and geoelectrical properties induced by petroleum hydrocarbon contamination of the soil–subsurface system irreversible? Given that a heavy fraction of the hydrocarbon remains in the soil–subsurface pore matrix, after volatilization of the light fraction, changes to these properties can be considered irreversible over human lifetime scales.

## 7.5    Soil Amendment Effects

Management of soil often involves application of various reclamation compounds. Here, we discuss irreversible changes occurring to original soils as result of such reclamation procedures.

**Fig. 7.66** Median molarity
of ethanol droplet (MED)
index, dichloromethane-
extractable organics (DEO)
content, and total organic
carbon (TOC) content for
profile soil samples from the
soil horizons A, B, C in
altered soils (*solid*) and
control soil pits (*hatched*)
(after Roy et al. 2003).
Copyright 2003, American
Society of Agronomy, Crop
Science Society of America,
and Soil Science Society of
America. Reprinted with
permission
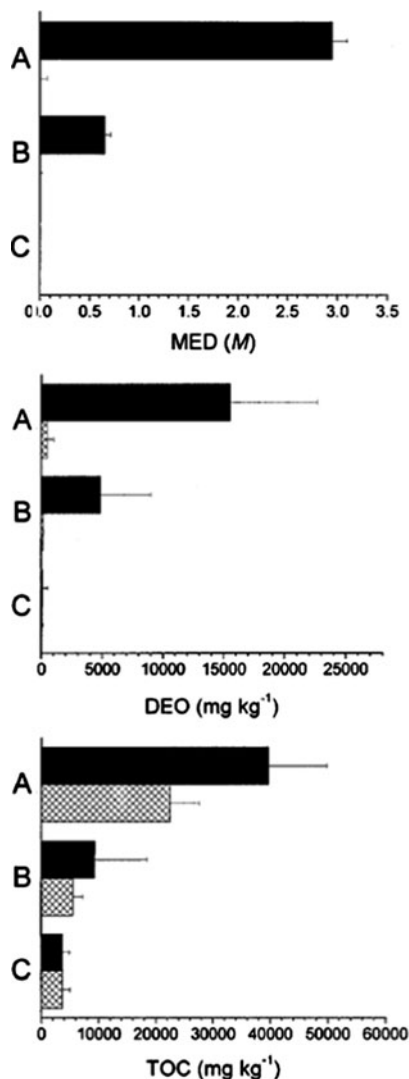
## 7.5.1   Reclamation of Soils with Extreme pH Values

Properties of agricultural soils exhibiting extreme pH values are improved by
adding various forms of lime and gypsum. Successive application of these
compounds over many years has led to changes in soil properties which, on a
lifetime scale, become irreversible.
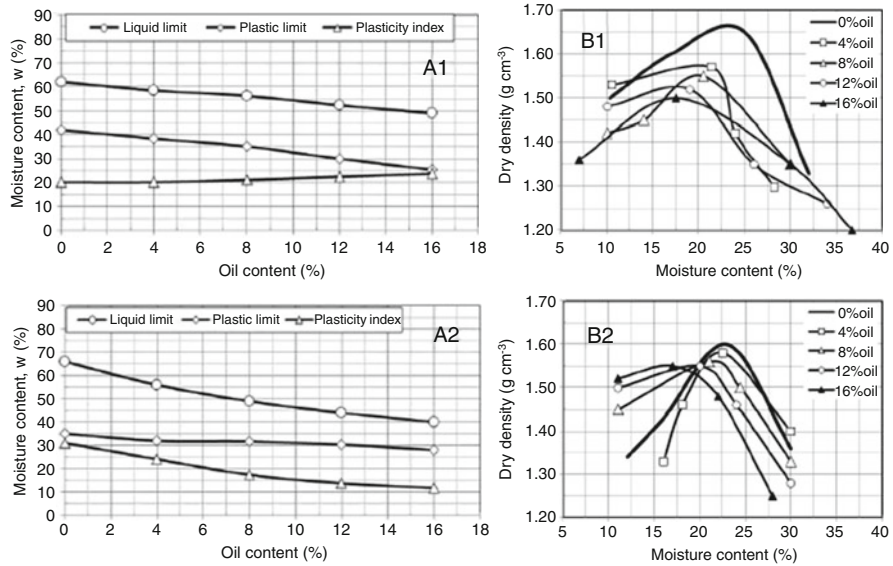
**Fig. 7.67** Influence of oil contamination on (**A**) Atterberg limit and (**B**) compaction curves for (1) sandy loam and (2) silty loam Basaltic residual soil (modified after Rahman et al. 2010)

### 7.5.1.1   Lime

Under natural conditions, acidic soils exhibiting a pH <~4.8 are formed on weathered acid rocks. This process occurs in a climatic regime where the amount of rainwater exceeds the amount of water lost by evapotranspiration under vegetation canopies. Soil acidification is a continuous process supported by the natural input of very dilute carbonic acid and the leaching of weathering products. However, soil acidification has increased from anthropogenic activities.

On a global scale, the acidification process has affected 10 million ha of cultivated land (Greenland et al. 1997), without considering forest or urban surfaces. In agricultural lands, the process of soil acidification is accelerated by application of large amounts of nitrogen; during mineral N uptake and transformation, the soil is enriched with an excess of $H^+$ (White 2008). Urban and industrial sources of soil acidification process are due generally to release of materials such as forms of mineral sulfur and nitrogen, which are converted to sulfuric or nitric acids, leading to acid rain and/or dry acid deposition from atmospheric origin.

Raising the pH of acidic soils through addition of lime materials is a very old procedure. Ruffen in 1882 achieved this goal by adding oyster shells to his acidic soil from the coastal plain of Virginia, USA. With time, liming became a routine procedure for altering natural or anthropogenic induced soil acidity. Examples of liming materials used in Australia and New Zealand are reviewed by White (2008), and summarized in Table 7.8. White (2008) recommended, for local conditions, raising the pH to at least 5.5 for minimizing $Al^{3+}$ toxicity to the environmental
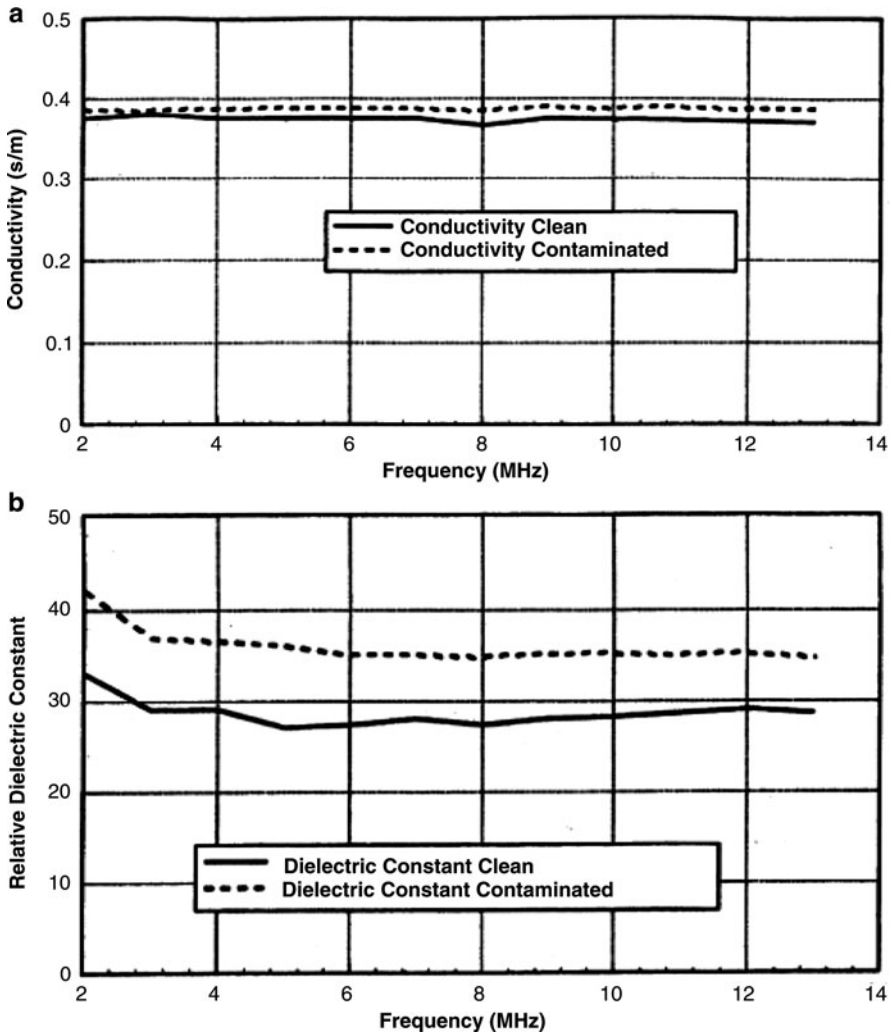
**Fig. 7.68** Changes in soil electrical properties after contamination with diesel oil: (**a**) electrical conductivity and (**b**) relative dielectric constant measured versus frequency (MHz) before and after soil contamination. Reprinted from Darayan S, Liu C, Shen LC, Shattuck D (1998) Measurement of electrical properties of contaminated soil. Geophys Prospect 46:477–488. Copyright 1998 with permission of John Wiley and Sons

vegetation. However, raising pH to values greater than 6.5 may lead to a negative effect by increasing zinc, copper, and boron deficiency in soil; these microelements are required for beneficial plant growth.

Under field conditions, the positive effect of lime addition consists of a combination of cementing and flocculation actions. Hoyt (1981) found that application of lime to two Canadian soils increased soil pH to the range 5.5–6.5, causing a

**Table 7.8** Liming materials used in Australia and New Zealand (after White [2008])

| Material and its chemical composition | Neutralizing value (NV) of commercial grade (%)[a] | Comments |
|---|---|---|
| Burnt lime, CaO | >150 | Reacts vigorously with water |
| Hydrated lime, $Ca(OH)_2$ | 120–135 | Occurs as a very fine powder; difficult to handle |
| Dolomite, $CaMg(CO_3)_2$ | 95–110 | More soluble than $CaCO_3$; contains about 11% Mg |
| Limestone, $CaCO_3$ plus impurities | 50–85 | NV depends on the concentration of impurities such as clay, silica, Fe, and Al oxides |
| Cement kiln dust, $CaCO_3$, CaO, K | 90–110 | Fine powder, byproduct of cement manufacture; often pelleted; also supplies K |

[a]Calculated relative to pure $CaCO_3$ as 100%
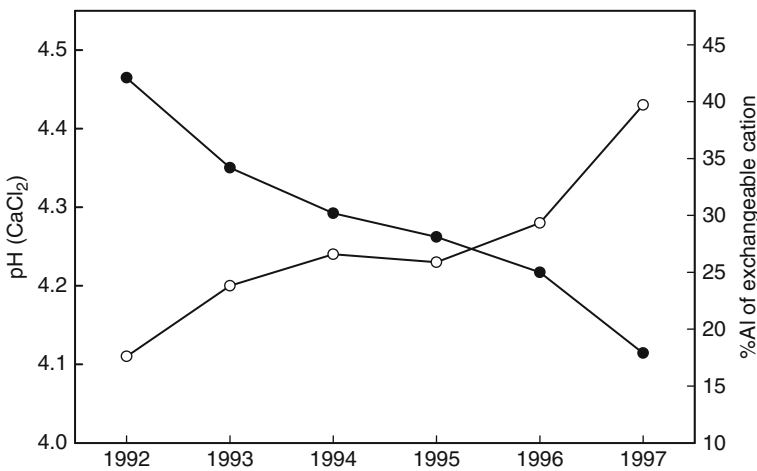


**Fig. 7.69** Time change in pH (*open circle*) and exchangeable $Al^{3+}$ (*filled circle*) in the 15–20-cm layer of an acid Kurosol initially limed to a pH of 5.5 (0–10 cm) in 1992 (after White et al. [2000]). Reprinted with permission, CSIRO Publishing, http://www.publish.csiro.au/nid/72/paper/EA 98013.htm

significant change in distribution of dry aggregates toward coarser fractions, and increasing resistance of soil to compression.

Liming is a slow release process. The time required to change the pH of an acidic soil (Kurosol) by surface application of lime materials is shown in Fig. 7.69, where the change of pH from 4.1 to 5.5 occurred only 5 years after application. The downward movement of liming products such as $OH^-$ and $HCO_3$ released from $CaCO_3$, through their diffusion or leaching, is overwhelmed by the buffering capacity of soils. As a consequence, changing soil pH by liming into the subsurface regime can be achieved only by direct subsoil application of liming materials. The slow release properties of the liming material, associated with continuous land
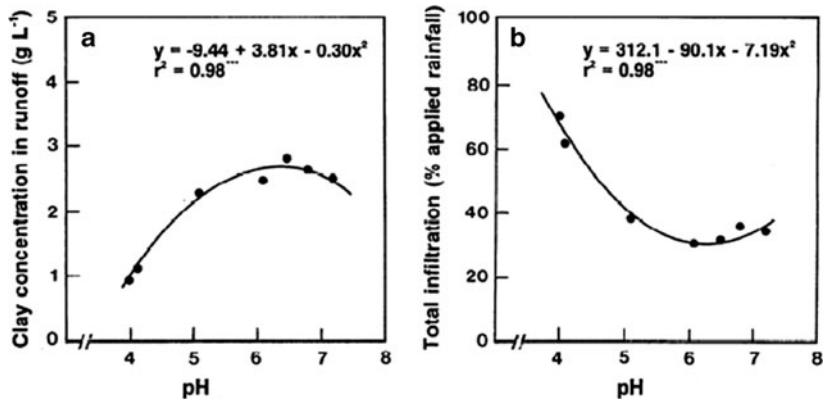
**Fig. 7.70** Relationship between pH and clay dispersion expressed as (**a**) the amount of clay concentrated in runoff and (**b**) of the total infiltration expressed as percentage of applied rainfall (after Haynes and Naidu 1998)

application of lime within a sustainable agriculture management, cause irreversible changes to soil acidity.

Increases in pH as a result of liming may cause a dispersion/flocculation process that leads to an irreversible change in soil physical properties. At low pH, acidic soils are normally flocculated because $Al^{3+}$ and $H^+$ activity in soil solution causes compression of the double layer and flocculation of clays. Liming-induced increases in pH lead to an increase in the negative charge on soil surfaces, and thus to the ratio of negative to positive charges. This in turn causes a decrease in $Al^{3+}$ activity because of aluminum precipitation as hydroxy-Al polymers. As a result, the dominant repulsive forces among particles lead to their dispersion. Under leaching, the dispersed particles formed under liming may result in a surface crust, clog the pore space, and be transported and redeposited at depth; these processes irreversibly affect water and solute transport in the soil–subsurface system (Roth and Pavan 1991; Haynes and Naidu 1998; Bednarek and Ereszka 2007).

Irreversible effects of liming on the soil structure can also be attributed to the flocculation and cementing actions of applied lime and of newly precipitated iron and aluminum oxides and hydroxides (Haynes and Naidu 1998). The relationship between pH and clay dispersion for a Brazilian Oxisol, expressed as the amount of clay concentrated in runoff and of the total infiltration expressed as percentage of applied rainfall, is shown in Fig. 7.70.

### 7.5.1.2 Gypsum

Gypsum, a hydrated calcium sulfate, is a naturally occurring mineral that may also be available as a byproduct material (e.g., phosphogypsum). Gypsum has been used on agricultural soils to increase the $Ca^{2+}$ content of acidic soils and to exchange $Na^+$ with $Ca^{2+}$ in calcareous saline-sodic soils. Gypsum solubility depends on both the

**Fig. 7.71** Average electrolyte concentration of the soil solution, where gypsum is mixed with the soil to depth of 5 mm, as a function of gypsum and water application rates (after Oster 1982)
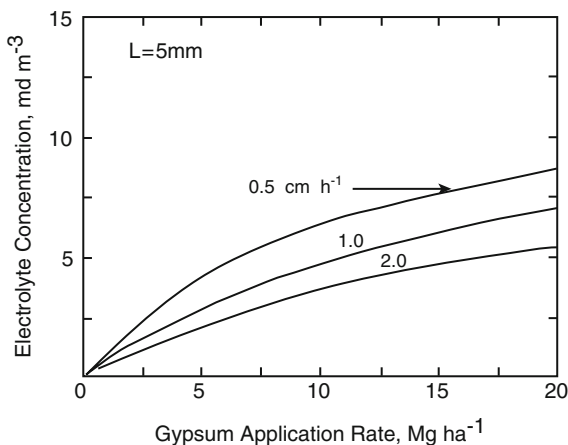


composition of soil solution and the exchange phase, and is lower when applied as mined gypsum than as a byproduct, in the widely used form phosphogypsum.

Gypsum dissolution follows first-order reaction kinetics. The electrolyte concentration of water flowing through a gypsum layer applied on soil can be described adequately by a transport equation which includes terms to account for advection, diffusion, and dissolution kinetics. The concentration of gypsum in the soil–subsurface electrolyte solution for a given rate of water application increases with gypsum application rate (Kemper et al. 1975; Oster 1982). An example of the relationship between gypsum application rate and electrolyte concentration in the soil–subsurface solution is given in Fig. 7.71.

Application of gypsum as a reclamation product to counter soil and subsurface domain acidity may, however, enhance the effect of dispersion of soil clay colloids in highly weathered acidic soils, leading to irreversible changes in the soil–subsurface system. A possible mechanism for the enhancement of clay dispersion caused by gypsum application was given by Roth and Pavan (1991). They considered that gypsum-induced clay dispersion in acidic soils is due to Al monomers and/or polymers, which act as binding agents, being displaced in the presence of $SO_4^{2-}$ from exchange sites by $Ca^{2+}$.

An alternative mechanism to $Ca^{2+}$-induced dispersion, following application of gypsum, is the specific adsorption or ligand exchange of $SO_4^{2-}$ which can change the clay particle charge characteristics (Uehara and Gillman 1981; Rao and Sridharan 1984). Additional information was obtained from soil column studies of Nishimura et al. (1999), which were designed to test the effect of gypsum application on the clay dispersion in a Japanese acidic soil. Figure 7.72 shows the breakthrough curves of ion concentration in the acidic soil column effluent, leached by an electrolyte solution containing $CaSO_4$ and a NaCl electrolyte ($mmol_c\ L^{-1}$). The retention of $SO_4^{2-}$ reached a plateau after leaching with about three pore volumes of electrolyte solutions containing $SO_4^{2-}$, independent of co-cation type. Nishimura et al. (1999) also showed that removal of $Al^{3+}$, as a binding agent of the

**Fig. 7.72** Changes in ion concentrations in effluent from the Kunigamahji soil column, CaSO$_4$ treatment (after Nishimura et al. 1999)
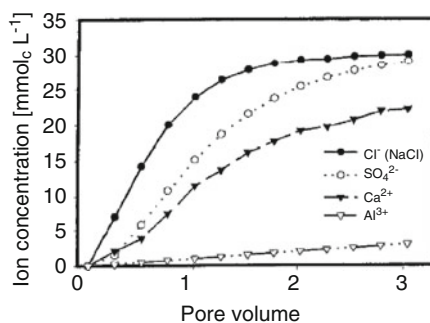
acidic soils, by Ca$^{2+}$, and the change in charge characteristic due to SO$_4^{2-}$ adsorption enhanced clay dispersion of the acidic soils following gypsum application.

The favorable effects of gypsum for reclamation of saline-sodic soils were determined in field experiments carried out as early as the beginning of the last century (e.g., Hilgard 1906; Kelley and Arany 1928), and discussed over the years in comprehensive reviews and books (e.g., US Salinity Laboratory Staff 1954; Bresler et al. 1982; Oster 1982; Shainberg and Letey 1984). Water transmission properties expressed in terms of both HC and IR may be altered by irrigation with sodic water that originates from a saline aquifer, drainage, or sewage effluents. Both HC and IR are controlled by soil–subsurface clay content and mineralogy, as well as by the Na$^+$ concentration of the incoming water. Gypsum amendments applied directly on the land surface or added to the incoming water may change and improve the water transmission properties by exchanging Na$^+$ with Ca$^{2+}$ in sodic soils, or preventing Na$^+$ adsorption on the soil solid phase caused by irrigation with sodic water.

*Hydraulic conductivity* of sodic soils is improved following gypsum application. In a laboratory column experiment, Shainberg et al. (1982) measured the hydraulic conductivity of two sodic soils having an ESP of 20, by leaching soils with distilled water to which equivalent amounts of CaCl$_2$ and gypsum were added. The effect of varying application of CaCl$_2$ and gypsum on the relative hydraulic conductivities of a noncalcareous (Golan) and calcareous (Nahal Oz) soil, as a function of cumulative effluent volume, is shown in Fig. 7.73. It can be observed that adding gypsum yielded a higher hydraulic conductivity compared to adding CaCl$_2$.

When applied in the field, gypsum dissolution in incoming water controls the efficiency of this amendment on the HC. Because of the relatively low dissolution rate of gypsum, long-term dissolution in water occurs so that HC changes are irreversible on a lifetime scale.

*Infiltration rate*, defined as the volume of water penetrating the soil–subsurface cross-section per unit surface area, is controlled by the physical nature of the upper soil layer and the possible formation of a crust (seal). Irreversible changes in soil structure may occur when clay particles become dislodged due to an increase in Na$^+$ fraction in soil and a decrease in the electrolyte level of the soil solution, or due to the impact of raindrops. Dispersion of soil clays may lead to the clogging of pores
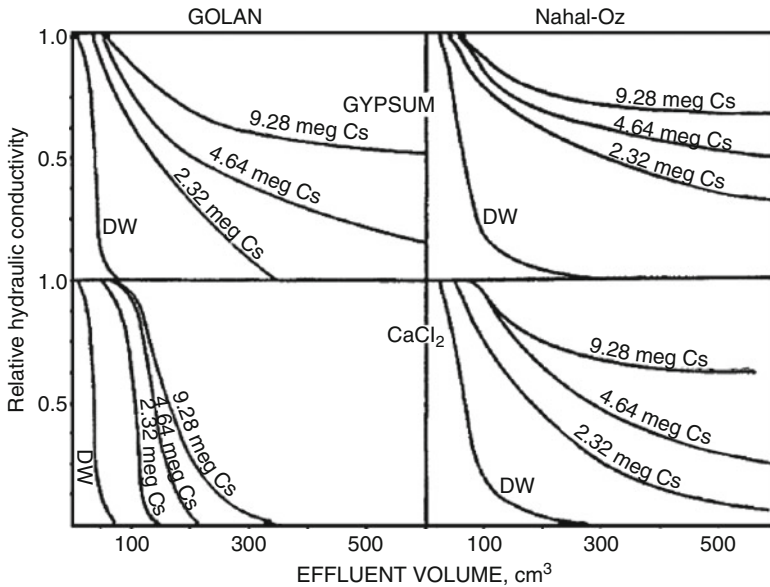
**Fig. 7.73** Effect of varying application of CaSO$_4$ and CaCl$_2$ on the relative hydraulic conductivities of Golan (noncalcareous) and Nahal Oz (calcareous) soils, as a function of cumulative effluent volume (after Shainberg et al. 1982). Copyright 1982, Soil Science Society of America. Reprinted with permission

beneath the surface, forming a layer of low permeability. Seals that form (<2 mm) have a greater density, higher shear strength, finer pores, and lower permeability than the bulk soil. Addition of gypsum to the soil surface increases electrolyte composition of the incoming water and prevents the breakdown of soil aggregates and decreases in pore size.

The effect of addition of mined gypsum and the industrial byproduct phosphogypsum on infiltration rates was studied by Levy and Sumner (1998). It was found that phosphogypsum is more effective than mined gypsum in enhancing water transmission, and that infiltration rates depend on the amount of phosphogypsum and the method of application (Fig. 7.74).

*Aggregation status* of the soil–subsurface system is a main factor in controlling water transmission properties of the soil–subsurface system. In general, the active pores conducting water are of micrometer scale and are enclosed in aggregates formed by heterogeneous conglomerates in which submicron clay particles are associated (Ahuja et al. 1989). In a laboratory study, Lebron et al. (2002) examined changes in aggregate size and geometry of three sodic soils amended with gypsum, as reflected in soil water transmission properties (Table 7.9).

All three soils, which were initially saline, exhibited lower salinity and sodicity after amendment with gypsum. An increase in ESP due to gypsum application was associated with a decrease in larger size aggregates and the saturated hydraulic conductivity (Fig. 7.75). At the soil water content of saturation, the disruption of
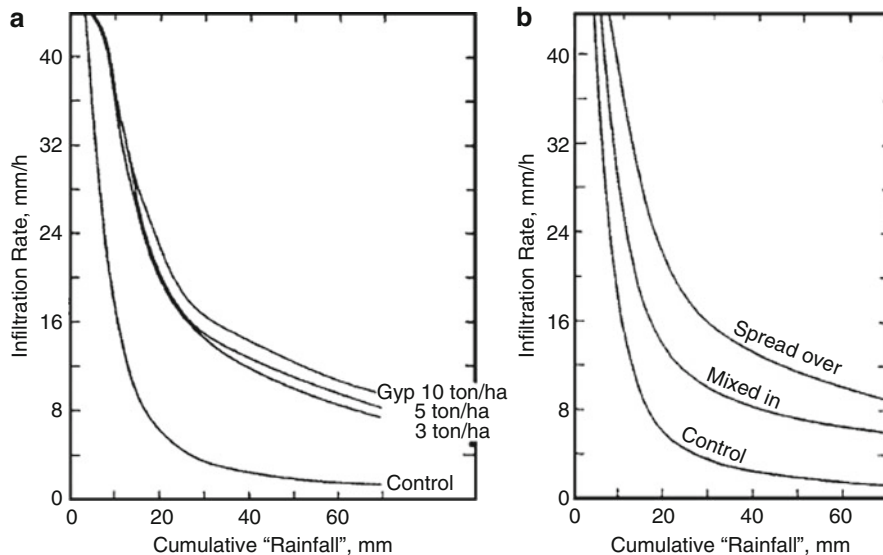
**Fig. 7.74** Infiltration rates of loess (Nahal Oz) as a function of cumulative simulated rainfall: (**a**) the effect of quantities of applied gypsum and (**b**) the effect of method of application, at a rate of 5 t ha$^{-1}$ (after Agassi et al. 1986)

**Table 7.9** Characteristics of soil used in the Lebron et al. (2002) experiment: texture, CaCO$_3$, organic matter (OM), cation exchange capacity (CEC), and exchangeable sodium percentage (ESP) of the soils in their natural conditions

| Soil type | Sand | Silt | Clay | CaCO$_3$ | OM | EC dSm$^{-1}$ | CEC | ESP | SAR | pH |
|-----------|------|------|------|----------|-----|---------------|-----|-----|-----|-----|
|           |      | %    |      |          |     |               | mmol kg$^{-1}$ |     |     |     |
| Hanford   | 78.96 | 14.78 | 6.26 | 0.07 | 0.41 | 10.44 | 59.2 | 46.6 | 45.2 | 7.06 |
| La Animas | 31.97 | 50.76 | 17.27 | 6.04 | 1.27 | 12.08 | 145 | 54.5 | 44.5 | 8.10 |
| Madera    | 52.40 | 25.74 | 22.22 | 0.06 | 0.61 | 10.57 | 150 | 45.3 | 43.0 | 7.64 |

Electrical conductivity (EC), sodium adsorption ratio (SAR), and pH were measured in the saturated paste before the start of the experiment (after Lebron et al. 2002). Copyright 2002, Soil Science Society of America. Reprinted with permission

aggregates in the soil matrix was to a certain extent irreversible (Lebron et al. 2002). Once an aggregate is broken, the individual particles migrate; and under saturated conditions, formation of new aggregates is unlikely. Thus, gypsum addition causes irreversible changes to the water transmission properties of sodic soils, by reducing breakdown of larger soil aggregates.

*Water erosion and runoff* are natural processes occurring under the impact of raindrops on geomorphologic slopes when soils have thin surface layers (seals). Under these processes, the subsurface regime is altered due to dispersion of soil particles from the upper layer to deeper soil horizons. Application of gypsum (both mined and of byproduct origin) on the soil surface may cause irreversible changes
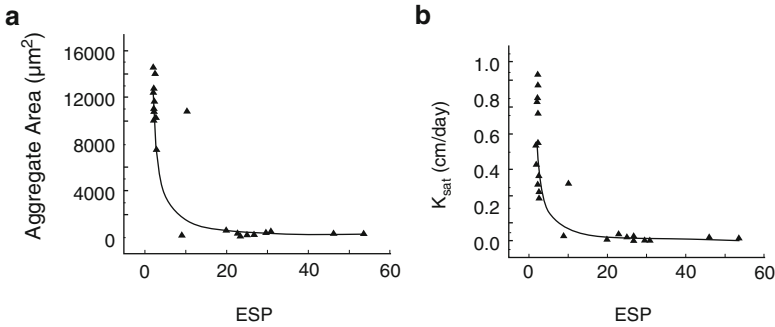
**Fig. 7.75** Effect of exchangeable sodium percentage (ESP) on soil physical properties: (**a**) area of the aggregates as a function of the ESP; (**b**) relationship between ESP and saturated hydraulic conductivity ($K_{sat}$) for Hanford, Las Animas, and Madera soils (after Lebron et al. 2002). Copyright 2002, Attributed to the Soil Science Society of America

**Fig. 7.76** Effect of rainfall, phosphogypsum treatment (PG), and slope (5 and 25%) on (**a**) infiltration rate and (**b**) soil loss from a sandy loam (Typic Rhodoxeralf) (after Warrington et al. 1989). Copyright 1989, Soil Science Society of America. Reprinted with permission
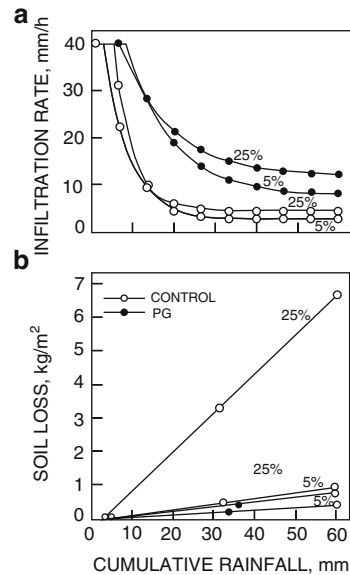


to the patterns of this process. Based on the correlation between soil erodibility and clay dispersion (Miller and Baharuddin 1986), it is expected that the use of gypsum, which favors diminished clay dispersion, will lead to a decrease in soil susceptibility to erosion by increasing the soil infiltration capacity.

We consider the rain-simulator research studies on a stable sandy loamy soil from the coastal plain of Israel to illustrate the effect of gypsum amendment on water erosion and runoff (e.g., Kazman et al. 1983; Warrington et al. 1989; Agassi et al. 1990; Agassi and Ben-Hur 1991). Figure 7.76 shows the effects of phosphogypsum, a byproduct of the phosphorus fertilizer industry, on the infiltration rate and loss of soil caused by rainfall-induced erosion. Seal formation at the soil surface

exposed to rainfall is caused by the breakdown of soil aggregates caused by raindrops, and by physicochemical dispersion of clay soil which migrates and clogs pores beneath the soil surface. The results shown in Fig. 7.76 demonstrate that phosphogypsum spread over the soil surface prevented clay dispersion, thus increasing infiltration and decreasing depth of runoff. The decrease in soil erosion and runoff intensity is explained by the increase in electrolyte concentration in both runoff and percolating water, preventing aggregate dispersion, increasing infiltration rate, maintaining or even improving the roughness of the surface, and avoiding sediment deposit.

## 7.5.2   Preventing Soil Sealing and Dispersivity

### 7.5.2.1   Organic Polymers

In general, organic polymers are applied to the soil surface to prevent a soil sealing process and clay particle dispersion and runoff caused mechanically by rain or irrigation water. Addition of organic polymers increases aggregate stability and improves water infiltration. The effects of organic polymers are, however, temporary, and beneficial changes in soil physical properties become irreversible only with continued application of those compounds. In an advanced technological society where soil changes are advantageous to the environment and human development, sustainable soil reclamation thus involves continuous application of organic polymers. As a consequence, induced soil changes from use of such chemical amendments are irreversible.

Polyacrylamides (PAM), discussed also in Chap. 6, are formed by polymerization of identical acrylamide units (homopolymer) and associated with other monomers. PAM compounds may be cationic, nonionic, or anionic (Bravenik 1994).

Nonionic PAM is used as a soil conditioner to stabilize soil aggregates and to flocculate suspended particles. This organic polymer is applied mainly on soil slopes – in large open surfaces or in irrigation furrows – to increase water infiltration by preventing soil sealing and consequently to avoid irreversible morphological changes to soil by erosion and runoff. Soil susceptibility to sealing under heavy rains or under furrow irrigation depends on a number of soil properties such as texture and mineralogy, composition of the exchangeable cations, and incoming water quality.

Impact energy from raindrops (Agassi and Ben-Hur 1992) or from surface flowing in furrow-irrigated fields (Lentz et al. 2000) causes disintegration of aggregates and clay dispersion in susceptible soils. This favors particle migration into soil pores which forms a surface thin layer seal ($<2$ mm) characterized by an increase in bulk density, higher shear strength, and lower water permeability compared to the original soil (Flanagan et al. 1997). The efficiency of PAM application on the surface of a soil, to stabilize aggregates and control runoff and erosion, was examined by addition of 10–40 kg ha$^{-1}$. An amount of 5–30 g m$^{-3}$

PAM in irrigation water was considered as an alternative method of application (Graber et al. 2006, and references therein).

The effect of PAM amendments on the cumulative runoff and sediment yield, under natural rainfall conditions, was reported by Flanagan et al. (2002); this study represents an example polymer-induced irreversible effect on soil morphology. The experiment was conducted on a highway cut-slope (created during highway construction) on a clay loam subsoil at a slope of $35°$, where an amount of 80 kg ha$^{-1}$
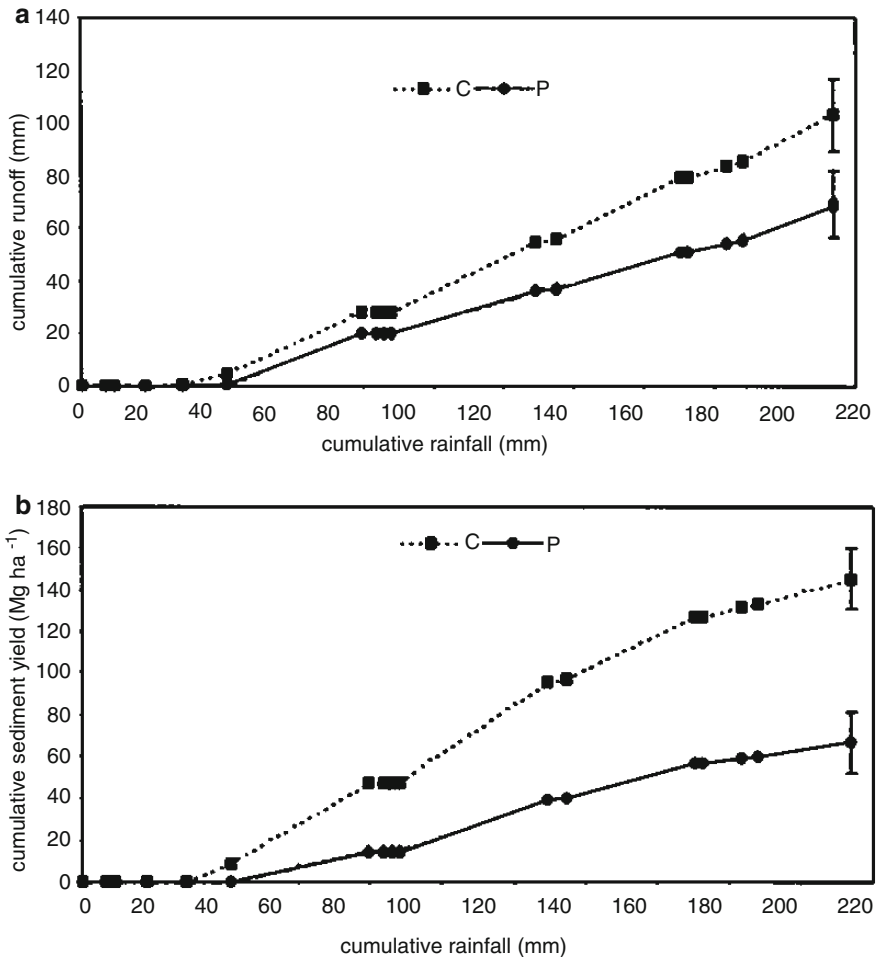


**Fig. 7.77** Polyacrylamide (PAM) effect on runoff and soil loss cumulative runoff versus (**a**) cumulative rainfall, and (**b**) sediment yield, for a natural rainfall study. *Bars* for final points indicate $P < 0.05$ confidence; C and P are untreated and treated sites, respectively (modified after Flanagan et al. 2002). Originally published as Fig. 1 in Transactions of the ASAE v45 (5):1339–1351. Reprinted with permission of the American Society of Agricultural and Biological Engineers, St. Joseph Michigan

anionic PAM was applied. Nine storm events were recorded during a period of 60 days and the effect of PAM addition was compared with untreated plots situated on the same cut-slope. PAM treatment significantly reduced cumulative runoff and soil loss (Fig. 7.77).

Furrow irrigation conducts water on the soil surface through sloped channels, which ensures water distribution in the field at a rate that matches or exceeds the infiltration capacity. Lentz et al. (2000) studied the application of water-soluble anionic PAM to furrow irrigation water during flow, with the aim of reducing sediment loss and increasing net infiltration. The efficiency of neutral, anionic, and cationic forms of PAM was tested on an irrigated silt loam soil (Portneuf). Anionic and neutral PAM were twice as effective as cationic PAM in controlling erosion and sediment transport in the new furrows. The order of effectiveness for overall soil erosion, as measured by sediment transport and loss, was anionic > neutral > cationic PAM.

General trends suggest that medium- and high-charge density anionic and neutral PAM produced the greatest increase in infiltration compared to controls. Figure 7.78 shows PAM molecular weight effects on water infiltration through
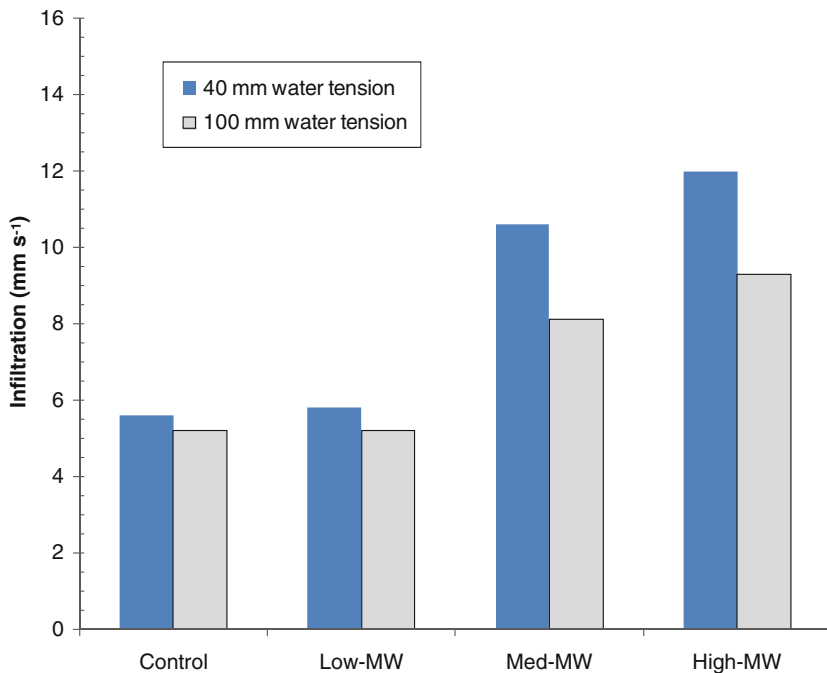


**Fig. 7.78** Polyacrylamide (PAM) molecular weight effects on water infiltration through semi-consolidated furrow depositional seals, as a function of molecular weight (MW) (after Lentz et al. 2000). Reprinted from Lentz RD, Sojka RE, Ross CW, Polymer charge and molecular weight effects on treated irrigation furrow processes. Int J Sediment Res 15:17–30, Copyright (2000), with permission from Elsevier

semi-consolidated furrow depositional seals. Lentz et al. (2000) noted that compared to control and low molecular weight treatments, the medium and high molecular weight PAM seals contained a greater number of conducting pores. PAM treatment impacted both furrow infiltration and runoff sediment amounts, transport, and redeposition on the field surface. Despite the fact that PAM impacts on furrow soils were temporary, the effect on soil morphology due to the changes in sediment erosion patterns was irreversible.

*Polysaccharides (PSD)* of anthropogenic origin form another group of organic polymers used to prevent or diminish clay particle dispersion and erosion of soils caused by aggregate stabilization and increasing infiltration rate. A laboratory study by Ben-Hur and Letey (1989) tested the effect of PSD for improving soil with low infiltration rates caused by crust formation on the surface, following mechanical aggregate dispersion induced by rainfall or irrigation water. A Haplic Durixeralf sandy loam soil (Arlington) was used in the study. The PSD employed were derivatized "*guar*" compounds (nonionic, anionic, or cationic) with differing charge density, which were applied to soil as solutes in the water used in a sprinkler infiltrometer. Figure 7.79 shows infiltration rates, as a function of cumulative water
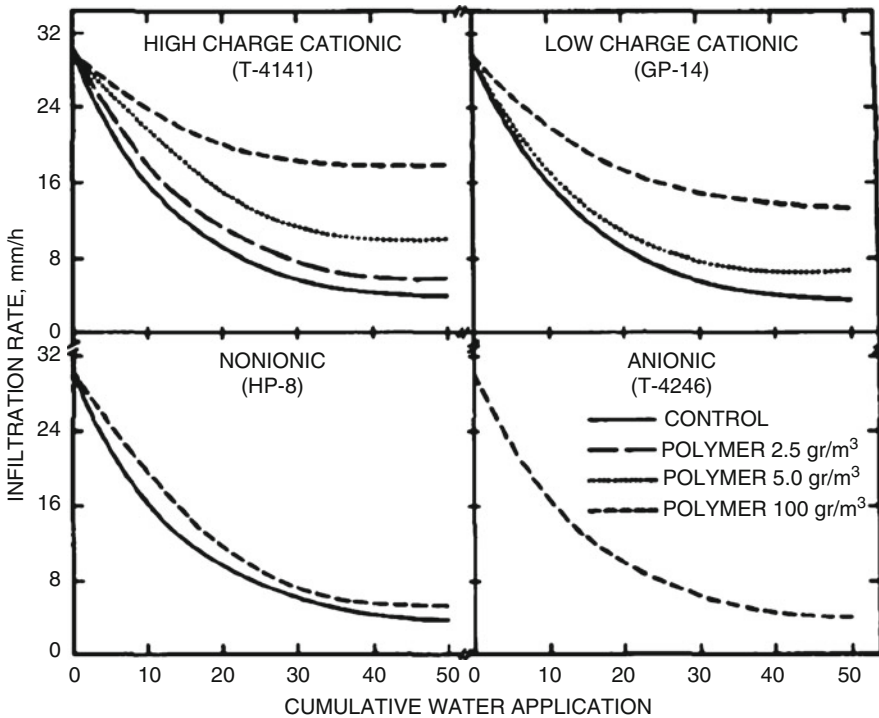


**Fig. 7.79** Infiltration rate as a function of cumulative water application for four polymer types and different concentrations in the applied water (after Ben-Hur and Letey 1989). Copyright 1989, Soil Science Society of America. Reprinted with permission

application under sprinkler conditions, as affected by the presence of the guar derivate in the incoming water.

Ben-Hur and Letey (1989) found that the type of PSD had a significant effect on changing the infiltration rate. Of the tested polymers, only the anionic compound had no effect. The final infiltration rate values of the efficient amendments were 19.0, 14.2, and 5.2 mm h$^{-1}$, compared to 4 mm h$^{-1}$ of the untreated soil. These results suggest that the electrostatic adsorption of the PSD on the negative soil clay surface was the dominant factor in providing stability to the aggregates and a change in the infiltration rate.

Application of high and low cation charge polysaccharides (HCCP and LCCP, respectively) was also studied by Ben-Hur et al. (1989), to determine changes induced by polymer application on soil infiltration rates. The effect of these derivates on preventing soil crust formation, by mechanical action of rainfall and irrigation water, was tested during wetting–drying cycles. The infiltration rates of the soil subjected to leaching with simulated regular irrigation water (EC ~ 1.0 dS m$^{-1}$; SAR 2) treated with LCCP and HCCP during the first application, and untreated (regular) water during the second and third applications are presented in Fig. 7.80. The
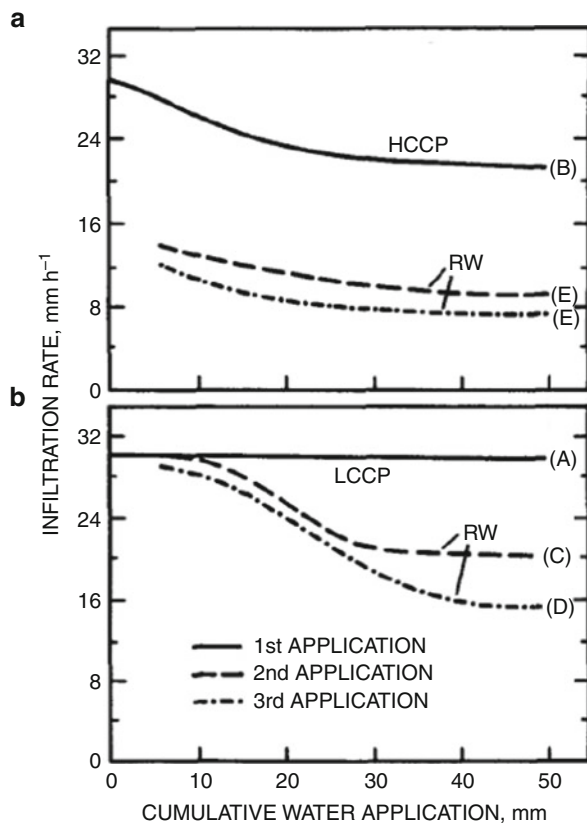


Fig. 7.80 Infiltration rate as a function of cumulative application of rain water with added polymers during the first application event (**a**) and of untreated water during subsequent application events (**b**). Different *letters in parentheses* at the ends of the *lines* indicate significant difference among the final infiltration rate values, $P < 0.05$ (after Ben-Hur et al. 1989). Copyright 1989, Soil Science Society of America. Reprinted with permission

soil infiltration rate change induced by LCCP addition to water during the first application was partially maintained during succeeding untreated water applications. Ben-Hur et al. (1989) hypothesized that this behavior was related to the ability of the derivate to provide soil aggregate stability against the energy impact of rainfall and irrigation water drops. These data supported also the hypothesis that specific PSD added to incoming water are adsorbed on soil surfaces, inducing a change in soil aggregate stability and water infiltration rate; these changes were maintained during post-treatment wetting–drying cycles.

Another essentially irreversible effect of polysaccharide application is the prevention of soil runoff that occurs as a result of seal formation at the soil surface during rainstorms. Warrington et al. (1991) reported changes in runoff pattern of soils from arid and semi-arid areas as a result of application of an anionic acid PSD of algal extracellular origin. The effects on runoff reduction of PSD applied individually or associated with electrolytes released by phosphogypsum dissolution, in three consecutive simulated rains, are shown in Fig. 7.81. A lasting and marked effect on runoff reduction in the PSD–phosphogypsum-treated soil, compared to both the untreated or only phosphogypsum-treated soils, is clearly observed.
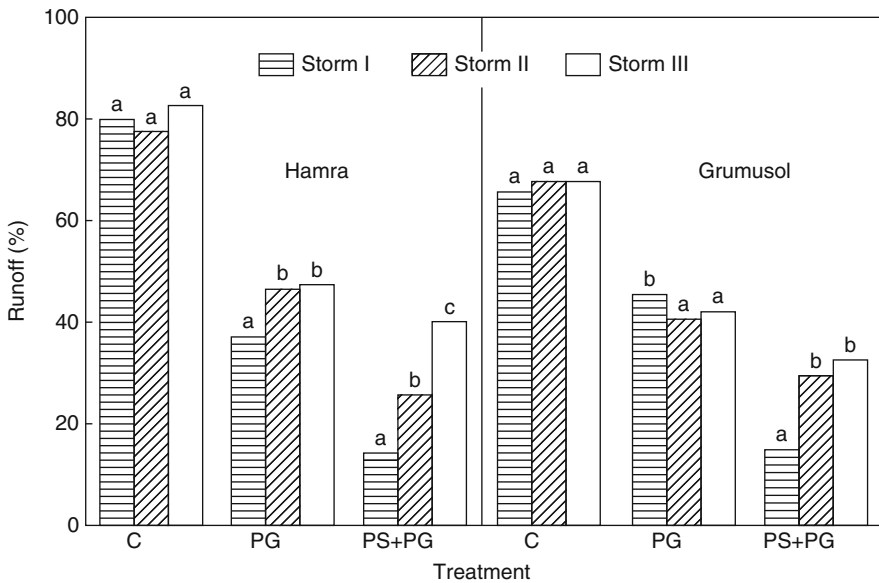


**Fig. 7.81** Application of polysaccharide (PS), phosphogypsum (PG), and polysaccharide with phosphogypsum (PS + PG) on soil vs. runoff, in comparison to untreated site (C). Percent runoff for three consecutive 60-mm rainstorms (modified after Warrington et al. 1991). Reprinted from Warrington D, Shainberg I, Levy GJ, Bar-Or Y (1991) Polysaccharide and salt effects on infiltration and soil erosion – A rainfall simulation study. Soil Technol 4:79–91, Copyright (1991), with permission from Elsevier

Fig. 7.82 Effect of alum
concentration on percentage
of soil bentonite dispersion:
(**a**) percentage of dispersion
and (**b**) density variation of
dispersed treated bentonite
(after Ouhadi and Goodarzi
2006). Reprinted from
Ouhadi VR, Goodarzi AR,
Assessment of the stability
of a dispersive soil treated
by alum. Eng Geol
85:91–101, Copyright
(2006), with permission
from Elsevier
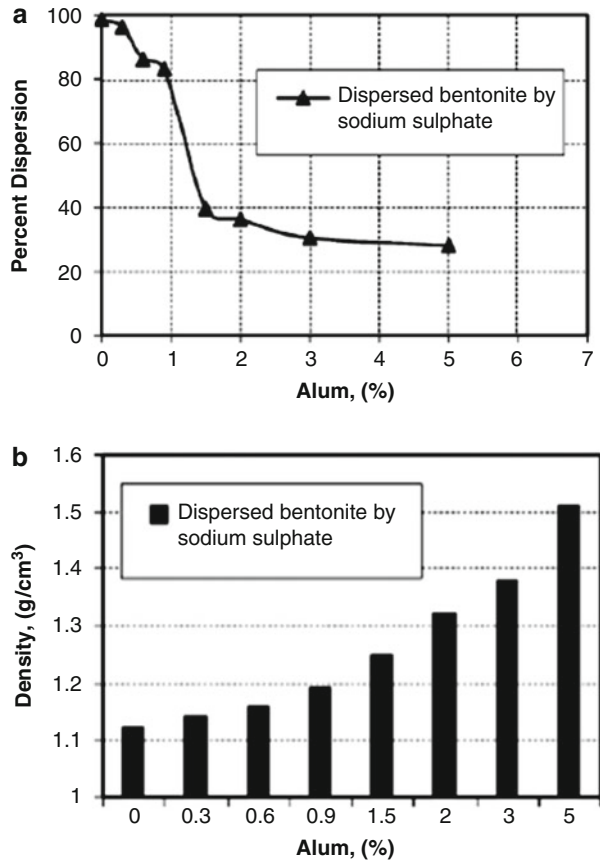
## 7.5.2.2   Alum Treatment

Dispersive soils have been found to exist in various locations under completely
different climatic conditions (Sherard et al. 1976), leading, for example, to deterio-
ration of roads or formation of piping phenomena in earth dams (Fell et al. 1992).
Soil dispersivity is determined by the amount and type of soil clay and by the
presence of sodium. Dispersive clay soils exhibiting a low permeability and
a low water velocity prevent transport of soil particles. However, once cracks
develop, dispersed soil clay particles are easily carried with water flowing through
these cracks.

   In general, soil dispersivity in agricultural lands is controlled by gypsum product
additives. However, in urban soils, alum (i.e., aluminum sulfate, $Al_2(SO_4)_3 \cdot 18H_2O$)
is also used for specific geotechnical projects. Ouhadi and Goodarzi (2006) tested
the stability of dispersive soil clays following alum treatment (Fig. 7.82). It can be
observed that the addition of 1.5% alum, for example, caused the percent dispersion

of the soil bentonite to drop to 40% (Fig. 7.82a); soil structure changed from dispersive to more flocculated and nondispersive. Alum treatment was also shown to affect the physicomechanical properties of the dispersive soil: under the application of constant stress, the density of dispersed soil bentonite increased as the percentage of alum increased (Fig. 7.82b). Ouhadi and Goodarzi (2006) attributed this behavior to a decrease in the double-layer thickness with an increase in added alum, due to the replacement of sodium ions by aluminum ions with a higher valence.

The effect of alum on the dispersivity of clay soils may be due to a pH effect, which favors interaction of clay particles and electrolyte, causing a decrease in soil dispersivity.

# References

Adams RH, Guzmán Osorio FJ, Zavala Cruz J (2008) Water repellency in oil contaminated sandy and clayey soils. Int J Environ Sci Tech 5:445–454

Agassi M, Ben-Hur M (1991) Effect of slope length, aspect and phosphogypsum on runoff and erosion from steep slopes. Aust J Soil Res 29:197–203

Agassi M, Ben-Hur M (1992) Stabilizing steep slopes with soil conditioner and plants. Soil Technol 5:249–256

Agassi M, Shainberg I, Morin J (1986) Effect of powdered phosphogypsum on the infiltration rate of sodic soils. Irrig Sci 7:53–61

Agassi M, Shainberg I, Morin J (1990) Slope, aspect and phosphogypsum effects on runoff and erosion. Soil Sci Soc Am J 54:1102–1106

Aggelides SM, Londra PA (2000) Effects of compost produced from two wastes and sewage sludge on the physical properties of a loamy and clay soil. Bioresour Technol 71:253–259

Ahuja LR, Cassel DK, Bruce RR, Barnes BB (1989) Evaluation of spatial distribution of hydraulic conductivity using effective porosity data. Soil Sci 148:404–411

Aldrich DG, Parker ER, Chapman HD (1945) Effects of several nitrogenous fertilizers and soil amendments on the physical and chemical properties of an irrigated soil. Soil Sci 59:299–312

Allred B, Brown GO (1994) Surfactant-induced reductions in soil hydraulic conductivity. Ground Water Monit Rev 14:174–184

Al-Shaieb Z, Cairns J, Puckette J (1994) Hydrogen induced diagenetic aureoles: indicators of deeper leaky reservoir. Assoc Pet Geochem Explor Bull 10:24–48

Amitay-Rosen T, Cortis A, Berkowitz B (2005) Magnetic resonance imaging and quantitative analysis of particle deposition in porous media. Environ Sci Technol 39:7208–7216

Arora HS, Coleman NT (1979) The influence of electrolyte concentration on flocculation and clay suspension. Soil Sci 127:134–139

Arye G, Tarchitzky J, Chen Y (2011) Treated wastewater effects on water repellency and soil hydraulic properties of soil aquifer treatment infiltration basins. J Hydrol 397:36–145

Assouline S, Narkis K (2011) Effect of long-term irrigation with treated wastewater on the hydraulic properties of a clayey soil. Water Resour Res 47:W08530

Bahremand MR, Afyuni M, Hajabbassi MA, Rezaeinejad Y (2003) Effect of sludge on soil physical properties. J Sci Technol Agric Nat Resources 6:1–9

Bednarek W, Ereszka R (2007) Effect of liming and fertilization with nitrogen on the physicochemical properties of soil. Agrophysica 10:523–531

Ben-Hur M, Letey J (1989) Effect of polysaccharides, clay dispersion and impact energy on water infiltration. Soil Sci Soc Am J 53:233–238

Ben-Hur M, Faris J, Malik M, Letey J (1989) Polymers as soil conditioners under consecutive irrigations and rainfall. Soil Sci Soc Am J 5:1173–1177

Bravenik FW (1994) Polyacrylamide characteristics related to soil applications. Soil Sci 158:235–242

Bresler E, McNeal BL, Carter DL (1982) Saline and sodic soils. Springer, Berlin, Germany, p 236

Burckhard SR, Pirkl D, Schafer VR, Kulakow P, Leven B (2000) A study of soil water-holding properties as affected by TPH contamination. In: Proc of the 2000 conference on Hazardous Waste Research

Calace N, Fiorentini F, Petronio BM, Pietroletti M (2001) Effects of acid rain on soil humic compounds. Talanta 54:837–846

Caravaca F, Roldán A (2003) Assessing changes in physical and biological properties in a soil contaminated by oil sludges under semiarid Mediterranean conditions. Geoderma 117:53–61

Cavallaro N, McBride MB (1984) Zinc and copper sorption and fixation by an acid soil clay. Effect of selective dissolutions. Soil Sci Soc Am J 48:1050–1054

Chen Y, Banin A (1975) Scanning electron microscope (SEM) observations on soil structure changes induced by sodium calcium exchange in relation to hydraulic conductivity. Soil Sci 120:428–436

Chenu C (1993) Clay- or sand-polysaccharide associations as models for the interface between micro-organisms and soil: water related properties and microstructure. Geoderma 56:143–156

Chenu C, Guerif J (1991) Mechanical strength of clay-minerals as influenced by an adsorbed polysaccharide. Soil Sci Soc Am J 55:1076–1080

Chenu C, Tessier D (1995) Low temperature scanning electron microscopy of clay and organic constituents and their relevance to soil microstructures. Scanning Microsc 9:989–1010

Cheshire MV, Sparling CP, Mundie CM (1984) Influence of soil type, crop and air drying on residual carbohydrate content and aggregate stability after treatment with periodate and tetraborate. Plant Soil 76:339–347

Chorum M, Murray RS, Osmund G, Rengassamy P (1994) Clay dispersion as influenced by pH and net particle charge of sodic soils. Aust J Soil Res 32:1243–1252

Cirelli FA, Ojeda C, Castro MJL, Salgot M (2009) Surfactants in sludge amended agricultural soils: a review. Environ Chem Lett 6:135–148

Conel JE, Alley RE (1985) Lisbon Valley, Utah uranium test site report. In: MJ Abrams, JE Conel, HR Lang, HN Paley (eds) The Joint NASA/Geosat Test Case Project: final report: AAPG Special Publication, pt. 2, v. 1, p. 8-1-8-158

Connaughton DF, Stedinger JR, Lion LW, Shuler MKL (1993) Description of time-varying desorption kinetics. Environ Sci Technol 27:2397–2403

Dahneke B (1975) Kinetic theory of the escape of particles from surfaces. J Colloid Interface Sci 50:89–197

Dane JH, Klute A (1977) Salt effects on the hydraulic properties of a swelling soil. Soil Sci Soc Am J 41:1043–1049

Darayan S, Liu C, Shen LC, Shattuck D (1998) Measurement of electrical properties of contaminated soil. Geophys Prospect 46:477–488

DeBano LF (2000) Water repellency in soils: a historical overview. J Hydrol 231–232:4–32

Dekker LW, Ritsema CJ (1994) How water moves in a water repellent sandy soil 1. Potential and actual water repellency. Water Resour Res 30:2507–2517

Diaz-Ravina M, Calvo de Anta R, Baath E (2007) Tolerance (PICT) of the bacterial communities to copper in vineyards soils from Spain. J Environ Qual 36:1760–1764

Doerr SH (1998) On standardising the water drop penetration time'and the molarity of an ethanol droplet techniques to classify soil hydrophobicity: a case study using medium textured soils. Earth Surf Proces Landforms 23:663–668

Doerr S, Shakesby RA, Dekker LW, Ritsema CJ (2006) Occurrence, prediction and hydrological effects of water repellency amongst major soil and land-use types in a humid temperate climate. Eur J Soil Sci 57:741–754

Donovan TJ, Friedman I, Gleason JD (1974) Recognition of petroleum-bearing traps by unusual isotopic composition of carbonate cemented surface rocks. Geology 2:351–354

Dror I, Gerstl Z, Prost R, Yaron B (2002) Abiotic behavior of entrapped petroleum products in the subsurface during leaching. Chemosphere 49:1375–1388

Epstein L, Bassein S (2001) Pesticides applications of copper on perennial crops in California, 1993–1998. J Environ Qual 30:1844–1847

Farmer VC (1978) Water on particle surfaces. In: Greenland DJ, Hayes MHB (eds) The chemistry of soil constituents. Wiley, New York

Farmer VC, Russell JD (1971) Interlayer complexes in layer silicates: the structured water in lamellar ionic solutions. Trans Faraday Soc 67:2737–2749

Feigin A Ravina I, Shalhevet J (1991) Irrigation with treated sewage effluent. Adv Ser Agric Sci, vol 17. Springer, Heidelberg

Fell R, MacGregor P, Stapledon D (1992) Geotechnical Engineering of Embankment Dams. AA Balkema, pp 675

Fine P, Yaron B (1993) Outdoor experiments on enhanced volatilization by venting of kerosene component from soil. J Contam Hydrol 12:355–374

Fine P, Graber ER, Yaron B (1997) Soil interactions with petroleum hydrocarbons: abiotic processes. Soil Technol 10:133–153

Flanagan DC, Norton LD, Shainberg I (1997) Effect of water chemistry on soil amendments on a silt loam soil Part I infiltration and runoff. Trans Am Soc Agric Eng 40:1549–1555

Flanagan DC, Chaudhari K, Norton LD (2002) Polyacrylamide soil amendment effects on runoff and sediment yield on steep slopes: Part II. Natural rainfall conditions. Trans Am Soc Agric Eng 45:1339–1351

Fox RL, Olson RA, Mazurak AP (1952) Persistence of ammonium ion and its effect upon physical and chemical properties of soil. Agron J 44:509–513

Frenkel H, Goertzen JO, Rhoades JD (1978) Effects of clay type and content, exchangeable sodium percentage, and electrolyte concentration on clay dispersion and soil hydraulic conductivity. Soil Sci Soc Am J 42:32–39

Frenkel H, Levy GJ, Fey MV (1992a) Clay dispersion and hydraulic conductivity of clay-sand mixtures as affected by the addition of various anions. Clays Clay Min 40:515–521

Frenkel H, Fey MV, Levy GJ (1992b) Organic and inorganic anion effects on reference and soil clay critical flocculation concentration. Soil Sci Soc Am J 56:1762–1766

Fu MH, Zhang ZZ, Low PF (1990) Changes in the properties of a montmorillonite-water system during the adsorption and desorption of water hysteresis. Clays Clay Miner 38:485–492

Gerstl Z, Galin T, Yaron B (1994) Mass flow of a volatile organic liquid mixture (VOLM) in soils. J Environ Qual 37:487–493

Graber ER, Fine P, Levy GJ (2006) Soil stabilization in semiarid and arid land agriculture. J Mater Civil Eng 18:190–205

Greenland DJ, Gregory PJ, Nye PH (1997) Land resources: on the edge of Malthusian precipice? Philos Trans Roy Soc, Series B-Biol Sci 352:861–867

Grolimund D, Borkovec M (2006) Release of colloidal particles in natural porous media by monovalent and divalent cations. J Contam Hydrol 87:155–175

Guidi G (1981) Relationship between organic matter of sewage sludge and physico-chemical properties of soil. In: L'Hermite PL, Ott E (eds) Treatment and use of sewage sludge. Reidel, Drodrecht, Holland, pp 530–544

Hafida Z, Caron J, Angers DA (2007) Pore occlusion by sugars and lipids as possible mechanism of aggregate stability in amended soils. Soil Sci Soc Am J 71:1831–1839

Hallett PD (2007) An introduction to soil water repellency. In: Gaskin RE (ed) Proc 8th Int Symp for Agrochem Adjuvants. Hand Multimedia, Christchurch, NZ

Hamilton AJ, Stagnitti F, Xiong X, Kreidl SL, Benke KK, Maher P (2007) Waste water irrigation: the statye of play. Vadose Zone J 6:823–840

Harrison RB, Johnson DW, Todd DE (1989) Sulfate adsorption ad desorption reversibility in a variety of forest soils. J Environ Qual 18:419–426

Haynes RJ (1984) Lime and phosphate in the soil–plant system. Adv Agron 37:249–315

Haynes RJ, Naidu R (1998) Influence of lime, fertilizer and manure applications on soil organic matter content and soil physical conditions: a review. Nutrient Cycling in Agroecosyst 51:123–137

Hilgard EW (1906) Soils-their formation, properties, composition and relation to climate and plant growth in humid and arid region. Macmillan, London

Hillel D (1971) Runoff inducement in arid lands Technical Report USDA Project No AID-SWC-36

Hoyt PB (1981) Improvements in soil tilth and rapeseed emergence by lime applications on acid soils in the Peace River region. Can J Soil Sci 61:91–98

Jamison VC (1947) Resistance of wetting in the surface of sandy soils under citrus trees in central Florida and its effect upon penetration and the efficiency of irrigation. Soil Sci Soc Am Proc 11:103–109

Jarsjö J, Destouni G, Yaron B (1994) Retention and volatilization of kerosene: Laboratory experiments on glacial and post-glacial soils. J Contam Hydrol 17:167–185

Jiang Y, Matsumoto S (1995) Change in microstructure of clogged soil in soil wastewater treatment under prolonged submergence. Soil Sci Plant Nutr 41:207–213

Katchalsky A, Curran PF (1965) Non-equilibrium thermodynamics in biophysics. Harvard University Press, Cambridge

Kazman Z, Shainberg I, Gal M (1983) Effect of low levels of exchangeable sodium and applied phosphogypsum on the infiltration rate of various soils. Soil Sci 135:184–192

Kelley WO, Arany A (1928) The chemical effect of gypsum, sulphur, iron sulphate and alum on alkali soils. Hilgardia 3:3939–3999

Kemper WD, Rosenau RC (1986) Aggregate stability and size distribution In: SSSA Methods of Soil Analysis Agronomy Monograph 9:425–442

Kemper WD, Olsen J, De Mooy CJ (1975) Dissolution rate of gypsum in flowing water. Soil Sci Soc Am Proc 39:458–463

Khaleel R, Reddy KR, Overcash MR (1981) Changes in soil physical properties due to organic waste applications: a review. J Environ Qual 10:133–141

Khan DS, Jacobson S (2008) Remote sensing and geochemistry for detecting hydrocarbon microseepages. GSA Bulletin 120:96–105, Jan/Feb 120(1–2)

Kiss S (1999) Enzymology of soils inoculated with microorganisms. Studia Universitatis Babes-Bolyai, Biologia 44:3–45

Lagaly G, Ziesmer S (2003) Colloid chemistry of clay minerals: the coagulation of montmorillonite dispersion. Adv Colloid Interface Sci 100–102:105–128

Lagerwerff JV, Nakayama FS, Frere HM (1969) Hydraulic conductivity related to porosity and swelling of soils. Soil Sci Soc Am Proc 33:3–12

Laird DA (2006) Influence of layer charge on swelling of smectites. Appl Clay Sci 34:74–87

Laird DA, Shang C, Thompson ML (1995) Hysteresis in crystalline swelling of smectites. J Colloid Interface Sci 171:240–245

Larssen T, Ludersen E, Tang DG, He Y, Gao JX, Liu HY, Duan L, Seip HM, Vogt RD, Mulder J, Shao M, Wang YH, Shang H, Zhang XS, Solberg S, Aas W, Okland T, Eilertsen O, Angell V, Liu QR, Zhao DW, Xiang RJ, Xiao JS, Luo JH (2006) Acid rain in China. Environ Sci Technol 40:418–425

Lebron I, Suarez DL, Yoshida T (2002) Gypsum effect on the aggregate size and geometry of three sodic soils under reclamation. Soil Sci Am J 66:92–98

Lentz RD, Sojka RE, Ross CW (2000) Polymer charge and molecular weight effects on treated irrigation furrow processes. Int J Sediment Res 15:17–30

Levy GJ, Sumner ME (1998) Mined and by-product gypsum as soil amendments and conditioners. In: Wallace A, Terry ER (eds) Handbook of soil conditioners. Marcel Dekker, New York, pp 445–462

Levy GJ, Fine P, Bar-Tal A (eds) (2010) Treated wastewater in agriculture: use and impacts on the soil environment and crops. Wiley-Blackwell, Oxford, UK

Likens GE, Bormann FH (1995) Biogeochemistry of a forested ecosystem, 2nd edn. Springer, New York, p 159

Lindsay BJ, Logan TL (1998) Field response of soil physical properties to sewage sludge. J Environ Qual 27:534–542

Liu M, Roy D (1995) Surfactant-induced interactions and hydraulic conductivity changes in soil. Waste Manag 15:463–470

Liu L, Song C, Yan Z, Li F (2009) Characterizing the release of different composition of dissolved organic matter in soil under acid rain leaching using three-dimensional excitation-emission matrix spectroscopy. Chemosphere 77:15–21

Lopez-Periago JE, Arias-Estevez M, Novoa-Munoz JC, Fernandez-Calvino DF, Soto B, Perez Nova C, Simal-Gandara J (2008) Copper retention kinetics in acid soils. Soil Sci Soc Am J 72:63–72

Low PF (1981) The swelling of clay III Dissociation of exchangeable cations. Soil Sci Soc Am J 45:1074–1078

Lutz JF, Pinto RA (1965) Effect of phosphorus on some physical properties of soils I Modulus of rupture. Soil Sci Soc Am Proc 29:458–460

Lutz JF, Pinto RA, Garcia-Lagos R, Hilton HG (1966) Effect of phosphorus on some physical properties of soils II Water retention. Soil Sci Soc Am Proc 30:433–437

Mace JE, Amrhein C (2001) Leaching and reclamation of soil irrigated with moderate SAR waters. Soil Sci Soc Am J 65:199–204

Magesan GN, Williamson JC, Sparling GP, Scxhipper LA, Llyod-Jones AR (1999) Hydraulic conductivity in soils irrigated with wastewaters of differing strengths: field and laboratory studies. Aust J Soil Res 37:391–402

Mainwaring KA, Morley CP, Doerr SH, Douglas P, Llewellyn CT, Llewellyn G, Matthews I, Stein BK (2004) Role of heavy polar organic compounds for water repellency of sandy soils. Environ Chem Lett 2:35–39

McBride MB (1989) Surface chemistry of soil minerals. In: Dixon JB, Weed SB (eds) Minerals in soil environments, 2nd edn. SSSA Book Series 1, Madison, WI pp 35–88

McBride MB (2001) Cupric ion activity in peat soil as a toxicity indicator for maize. J Environ Qual 30:78–84

McKinley JW, Siegrist RL (2010) Accumulation of organic matter components in soil under conditions imposed by wastewater infiltration. Soil Sci Soc Am J 74:1690–1700

McNeal BL (1968) Prediction of the effect of mixed salt solution on soil hydraulic conductivity. Proc Soil Sci Soc Am 32:190–193

McNeal BL, Coleman NT (1966) Effect of solution composition on soil hydraulic conductivity. Proc Soil Sci Soc Am 30:308–312

Metzger L, Robert M (1985) A scanning electron microscopy study of the interaction between sludge organic components and clay particles. Geoderma 35:159–167

Metzger L, Yaron B (1987) Influence of sludge organic matter on soil physical properties. Adv Soil Sci 7:141–165

Metzger L, Levanon D, Mingelgrin U (1986) Effect of sludge on soil structural stability: microbiological aspects. Soil Sci Soc Am J 51:346–351

Miller WP, Baharuddin MK (1986) Relationship of soil dispersibility to infiltration and erosion of Southeastern soils. Soil Sci 142:235–240

Miller WW, Valoras N, Letey J (1975) Movement of two nonionic surfactants in wettable and water repellent soils. Soil Sci Soc Am Proc 39:11–16

Mokni N, Olivella S, Alonso EE (2010) Swelling in clayey soils induced by the presence of salt crystals. Appl Clay Sci 47:105–112

Monteith DT, Stoddard JL, Evans CD, de Wit HA, Forsius M, Høgåsen T, Wilander A, Skjelkvåle BL, Jeffries DS, Vuorenmaa J, Keller B, Kopácek J, Vesely J (2007) Dissolved organic carbon trends resulting from changes in atmospheric deposition chemistry. Nature 450:537–540

Mooney RW, Keenan AG, Wood LA (1952) Adsorption of water vapors by montmorillonite. J Am Chem Soc 74:1371–1374

Morel JL, Guckert A (1983) Influence of limed sludge on soil organic matter and soil physical
    properties. In: Cartroux G, L'Hermite P, Suess E (eds) The influence of sewage sludge and
    activity in unsaturated porous media. Agri Sci 7:39–45
Mulder J, van Grinsven JJM, van Breemen N (1987) Impacts of acid atmospheric deposition on
    woodland soils in The Netherlands: III. Aluminum chemistry. Soil Sci Am J 51:1640–1646
Mulder J, van Breemen N, Eijck HC (1989) Depletion of soil aluminum by acid deposition and
    implication for acid neutralization. Nature 337:247–249
Mustafa MA, Letey J (1969) The effect of two nonionic surfactants on aggregate stability of soils.
    Soil Sci 107:343–347
Nishimura T, Nakano N, Miyazaki T (1999) Effects of gypsum application on dispersion of an acid
    Kunigami [Japan] mahji soil. Soil Phys Cond Plant Growth 81:15–21
Norrish K (1954) The swelling of montmorillonite. Disc Farad Soc 18:120–134
Or D, Smet BF, Wraith JM, Dechesne A, Friedman SP (2007) Physical constraints affecting
    bacterial habitats and activity in unsaturated porous media – a review. Adv Water Resour
    30:1505–1527
Oster JD (1982) Gypsum usage in irrigated agriculture: a review. Fertilizer Res 3:73–89
Oster JD, Shainberg I, Wood JD (1980) Flocculation value and gel structure of sodium/calcium
    montmorillonite and illite suspensions. Soil Sci Soc Am J 44:955–959
Ouhadi VR, Goodarzi AR (2006) Assessment of the stability of a dispersive soil treated by alum.
    Eng Geol 85:91–101
Ouhadi VR, Yong RN, Sedighi M (2006) Influence of heavy metal contaminants at variable pH
    regimes on rheological behaviour of bentonite. Appl Clay Sci 32:217–231
Pagliai M, Giddi G, LaMarca M, Giachetti M, Lucamante G (1981) Effects of sewage sludge and
    compost on soil properties and aggregation. J Environ Qual 10:556–561
Painuli DK, Abrol IP (1986) Effect of exchangeable sodium on the crusting behaviur of a sandy
    loam soil. Aust J Soil Res 24:367–376
Petrovic A, Khan SD, Chafetz HS (2008) Remote detection and geochemical studies for finding
    hydrocarbon-induced alterations in Lisbon Valley, Utah. Marine Pet Geol 25:696–705
Pilsbury AF (1947) Factors influencing infiltration rates into Yolo loam. Soil Sci 64:177–181
Powers SE, Abriola LM, Dunkin JS, Weber WJ Jr (1994) Phenomenological models for transient
    water mass transfer processes. J Contam Hydrol 16:1–33
Quirk JP (1957) Effect of electrolyte concentration on soil permeability and water entry in
    irrigated soils. Int Conf Irrig Drainage 8:115–123
Quirk JP, Schofield RK (1955) The effect of electrolyte concentration on soil permeability. Eur J
    Soil Sci 6:251–259
Rahman ZA, Hamzah U, Taha MR, Ithnain MS, Ahmad N (2010) Influence of oil contamination
    on geotechnical properties of residual basaltic soil. Am J Appl Sci 7:954–961
Rao CH, Sridharan A (1984) Mechanism of sulfate adsorption by kaolinite. Clays Clay Miner
    32:414–418
Rao PH, He M, Yang X, Zhang YC, Sun SQ, Wang JS (2006) Effect of an anionic surfactant on
    hydraulic conductivities of sodium- and calcium-saturated soils. Pedosphere 16:673–680
Reeve RC, Tamaddoni GH (1965) Effect of electrolyte concentration on laboratory permeability
    and field intake rate of a sodic soil. Soil Sci 99:261–266
Reid BJ, Jones KC, Semple KT (2000) Bioavailability of persistent organic pollutants in soils and
    sediments. Environ Pollut 108:103–122
Rengasamy P, Olsson KA (1991) Sodicity and soil structure. Aust J Soil Res 29:935–952
Reuss JO, Cosby BJ, Wright RF (1987) Chemical processes governing soil and water acidification.
    Nature 329:27–32
Roth CH, Pavan MA (1991) Effect of lime and gypsum on clay dispersion and infiltration in
    samples of a Brazilian Oxisol. Geodrma 48:351–361
Roy JL, McGill WB (2000) Investigation into mechanisms leading to the development, spread and
    persistence of soil water repellency following contamination by crude oil. Can J Soil Sci 80:
    143–152

Roy JL, McGill WB, Lowen HA, Johnson RL (2003) Relationship between water repellency and native and petroleum-derived organic carbon in soils. J Environ Qual 32:583–590

Russo D, Bresler E (1977) Analysis of the saturated-unsaturated hydraulic conductivity in a mixed sodium-calcium soil system. Soil Sci Soc Am J 41:706–710

Ryan JN, Elimelech M (1996) Colloid mobilization and transport in ground water. Colloids Surf A 107:1–56

U.S. Salinity Laboratory Staff (1954). Diagnosis and improvement of saline and alkali soils. USDA Agric. Handb. 60. U.S. Gov. Print. Office, Washington, DC.

Schofield RK, Samson HR (1954) Flocculation of kaolinite due to the attraction of oppositely charge crystal. Discuss Faraday Soc 18:135–145

Schumacher D (1996) Hydrocarbons induce alteration of soils and sediments. In Schumacher D, Abrams MAS (eds) Hydrocarbon migration and its near surface expression. AAPG Memoir 66:71–89

Schwab AP, Owensby CE, Kulyingyong (1990) Changes in soil chemical properties due to 40 years of fertilization. Soil Sci 149:35–43

Schwille F (1984) Migration of organic fluids immiscible with water in the unsaturated zone. In: Yaron GD, Heppie P (eds) Pollutants in porous media: the unsaturated zone between the soil surface and ground water, ecological studies, vol 47. Springer, New York, pp 27–48

Segal DH, Ruth MD, Merin IS, Watanabe H, Soda O, Takano O, Sano M (1984) Correlation of remotely detected mineralogy with hydrocarbon production Lisbon Valley, Utah ERIM Proc Int Symp Remote sensing for exploration geology. pp 273–292

Segal DH, Ruth MD, Merin IS (1986) Remote detection of anomalous mineralogy associated with hydrocarbon production, Lisbon Valley, Utah. Mt Geol 23:51–62

Selim HM, Gobran GR, Guan X, Clarke N (2004) Mobility of sulfate in forest soils: kinetic modeling. J Environ Qual 33:488–495

Shainberg I (1985) Soil salinity under irrigation. Springer, Heidelberg

Shainberg I, Letey J (1984) Response of soils to sodic and saline conditions. Hilgardia 52:1–57

Shainberg I, Keren R, Frenkel H (1982) Response of sodic soils to gypsum and calcium chloride application. Soil Sci Soc Am J 46:113–119

Shanmuganathan RT, Oades JM (1983) Influence of anions on dispersion and physical properties of the A horizon of a red-brown earth. Geoderma 29:257–277

Sherard JL, Dunigan LP, Decker RS (1976) Identification and nature of dispersive soils. J Geotech Eng 102:298–312

Sposito G (1992) Characterization of particle surface charge. In: Buffle J, van Leeuwen HP (eds) Environmental particles. Lewis Publ, Chelsea, MI, pp 291–314

Suarez DL, Frenkel H (1981) Cation release from Na and Ca-saturated clay sized soil fraction. Soil Sci Soc Am J 45:716–722

Suarez DL, Rhoades JD, Lavado R, Grieve CM (1984) Effect of pH on saturated hydraulic conductivity and soil dispersion. Soil Sci Soc Am J 48:50–55

Suzuki S, Prayongphan S, Ichikawa Y, Chae BG (2005) In situ observations of the swelling of bentonite aggregates in NaCl solution. Appl Clay Sci 29:89–98

Tambach T, Bolhuis PG, Hensen EJM, Smit B (2006) Hysteresis in clay swelling induced by hydrogen bonding: accurate predicting of swelling states. Langmuir 22:1223–1234

Tarchitzky J, Golobati Y, Keren R, Chen Y (1999) Wastewater effects on montmorillonite suspensions and hydraulic properties of sandy soils. Soil Sci Soc Am J 63:554–560

Tarchitzky J, Lerner O, Shani U, Arye G, Loewengart-Aycicegi A, Brener A, Chen Y (2007) Water distribution pattern in treated wastewater irrigated soils: hydrophobicity effect. Eur J Soil Sci 58:573–588

Tumeo MA (1997) A survey of the causes of surfactant-induced changes in hydraulic conductivity. Ground Water Monit Rev 17:138–144

Uehara G, Gillman G (1981) In: The mineralogy, chemistry and physics of tropical soils with variable charge, Westview Tropical Agricultural Series, Vol. 4, Chap. 3, Boulder CO

Van Breemen N, Driscoll CT, Mulder J (1984) Depletion of soil aluminium by acid deposition and implications for acid neutralization. Nature 307:599–604

Van Olphen H (1977) An introduction to clay colloid chemistry, 2nd edn. Wiley, New York

Vinten AJA, Yaron B, Nye PH (1983) Vertical transport of pesticides into soil when adsorbed on suspended particles. J Agri Food Chem 31:662–664

Wada N, Hines DR, Ahrenkiel SP (1990) X-ray-diffraction studies of hydration transitions in Na vermiculite. Phys Rev B 41:12895–12901

Wallach R, Graber ER (2007) Infiltration into effluent irrigation-induced repellent soils and the dependence of repellency on ambient relative humidity. Hydrol Proc 21:2346–2355

Wallach R, Ben-Arie O, Graber RE (2005) Soil water repellency induced by long term irrigation with treated sewage effluent. J Environ Qual 34:1910–1920

Warrington D, Shainberg I, Agassi M, Morin J (1989) Slope and phosphogypsum's effects on runoff and erosion. Soil Sci Soc Am J 53:1201–1205

Warrington D, Shainberg I, Levy GJ, Bar-Or Y (1991) Polysaccharide and salt effects on infiltration and soil erosion – a rainfall simulation study. Soil Technol 4:79–91

Wei QR, Lowery B, Peterson AE (1985) Effect of sludge application on physical properties of a silty clay loam soil. J Environ Qual 14:178–180

White RE (2008) Soil acidification: an overview for Australia and New Zealand. In: Proceedings of the conference Soil 2008 – The Living Skin of Planet Earth, pp. 218–234

White RE, Helyar KR, Ridley AM, Chen D, Heng LK, Evans J, Fisher R, Hirth JR, Mele PM, Morrison GR, Cresswell HP, Paydar Z, Dunin FX, Dove H, Simpson RJ (2000) Soil factors affecting the sustainability and productivity of perennial and annual pastures in the high rainfall zone of south-eastern Australia. Aust J Exp Agr 40:267–283

Wyszkowska J, Kucharski J, Lajszner W (2005) Enzymatic activities in different soils contaminated with copper. Polish J Environ Stud 14:659–664

Yaron B, Shainberg I (1973) Electrolytes and soil hydraulic conductivity. In: Yaron B, Danfors E, Vaadia Y (eds) Arid zone irrigation. Springer, Heidelberg, Germany, pp 189–199

Yaron B, Thomas G (1968) Soil hydraulic conductivity as affected by sodic water. Water Resour Res 4:545–552

Yaron B, Vinten AJ, Fine P, Metzger L, Mingelgrin U (1984) Effect of solid organic components of sewage on some properties of the unsaturated zone. In: Yaron B, Dagan G, Goldshmid J (eds) Pollutants in porous media. Springer, Heidelberg, pp 162–184

Yaron B, Dror I, Graber E, Jarsjo E, Fine P, Gerstl Z (1998) Behavior of volatile organic mixtures in the soil environment. In: Rubin H, Narkis N, Carberry J (eds) Soil and pollution. Springer, Berlin, pp 37–56

# Index